COST Action CA18120

Reliable roadmap for certification of
bonded primary structures

BOOKLET OF FIRST CERTBOND TRAINING SCHOOL

20th-22nd September 2021

Trieste, Italy

Editors: Chiara BEDON, José SENA CRUZ

Action Chair: Sofia TEIXEIRA DE FREITAS

Action Vice Chair: Anastasios P. VASSILOPOULOS

Training School Coordinator: Chiara BEDON

Funded by the Horizon 2020 Framework Programme of the European Union

This publication is based upon the Training School activities of COST Action CA18120 CertBond, with the financial support of COST.

This book can be cited as:

Bedon, C., Sena-Cruz, J., (eds): "Booklet of First CertBond Training School", 2021

The online version of this book (with updates and additional photos) can be found at:

https://certbond.eu/category/activities/events/training-school/

UNIVERSITÀ DEGLI STUDI DI TRIESTE

Printed by Press Service of University of Trieste

Table of Contents

About COST

The European Cooperation in Science and Technology (COST) is a funding organisation for the creation of research networks, called COST Actions. These networks offer an open space for collaboration among scientists across Europe (and beyond) and thereby give impetus to research advancements and innovation.

COST is bottom up, this means that researchers can create a network – based on their own research interests and ideas – by submitting a proposal to the COST Open Call. The proposal can be in any science field. COST Actions are highly interdisciplinary and open. It is possible to join ongoing Actions, which therefore keep expanding over the funding period of four years. They are multi-stakeholder, often involving the private sector, policymakers as well as civil society.

Since 1971, COST receives EU funding under the various research and innovation framework programmes, such as Horizon 2020.

COST funding intends to complement national research funds, as they are exclusively dedicated to cover collaboration activities, such as workshops, conferences, working group meetings, training schools, short-term scientific missions, and dissemination and communication activities. For more information, please go to the Funding section of the COST website (https://www.cost.eu/).

The COST Association places emphasis on actively involving researchers from less research-intensive COST Countries (Inclusiveness Target Countries, ITC[1]). Researchers from Near Neighbour Countries and International Partner Countries can also take part in COST Actions, based on mutual benefit. For more information, please visit the global networking page (https://www.cost.eu/).

[1] Albania, Bosnia and Herzegovina, Bulgaria, Croatia, Cyprus, Czech Republic, Estonia, Macedonia, Hungary, Latvia, Lithuania, Luxembourg, Malta, Montenegro, Poland, Portugal, Romania, Serbia, Slovakia, Slovenia, Turkey

COST Action CA18120

With the increasing pressure to meet unprecedented levels of eco-efficiency, aircraft industry aims for superlight structures and towards this aim, composites are replacing the conventional Aluminium. The same trend is being followed by civil, automotive, wind energy, naval and offshore industry, in which the combination (or replacement) of steel with composites can increase the strength-to-weight ratio. However, the joining design is not following this transition. Currently, composites are being assembled using fasteners. This represents a huge weight penalty for composites, since holes cut through the load carrying fibres and destroy the load path.

Adhesive bonding is the most promising joining technology in terms of weight and performance. However, its lack of acceptance is limiting its application to secondary structures, whose failure is not detrimental for the structural safety. In primary (critical-load-bearing) structures, fasteners are always included along bondlines, as “back-up” in case the bond fails. The main reasons for this lack of acceptance are the limited knowledge of their key manufacturing parameters, non-destructive inspection techniques, damage tolerance methodology and reliable diagnosis and prognosis of their structural integrity.

The Action aims to deliver a reliable roadmap for enabling certification of primary bonded composite structures. Despite the motivation being aircraft structures, which is believed to have the most demanding certification, it will directly involve other application fields in which similar needs are required. This Action will tackle the scientific challenges in the different stages of the life-cycle of a bonded structure through the synergy of multi-disciplinary fields and knowledge transfer.

General information

Start of Action: 04/04/2019
End of Action: 03/04/2023

Main Contacts

Sofia TEIXEIRA DE FREITAS
Action Chair

Anastasios P. VASSILOPOULOS
Action Vice Chair

Jose SENA CRUZ
Science Communication Manager

E-Mail: certbond@tudelft.nl
Action website: https://certbond.eu/
Domain website: https://www.cost.eu/actions/CA18120

Action Management Committee

Action Chair	Sofia TEIXEIRA DE FREITAS (s.teixeiradefreitas@tudelft.nl)
Action Vice Chair	Anastasios P. VASSILOPOULOS (anastasios.vassilopoulos@epfl.ch)

WG 1 - Adhesive and interface chemistry	Ana MARQUES (ana.marques@tecnico.ulisboa.pt)
WG 2 - Design phase	Konstantinos TSERPES (kitserpes@upatras.gr)
WG 3 - Manufacturing phase	Nicolas CUVILLIER (nicolas.cuvillier@safrangroup.com)
WG 4 - In-service life phase	Wieslaw OSTACHOWICZ (wieslaw@imp.gda.pl)
WG 5 - Disassembly phase	Laurent BERTHE (laurent.berthe@ensam.eu)
WG 6 - Certification	Thomas KRUSE-STRACK (thomas.kruse-strack@airbus.com)

Grant Holder Scientific Representative	Sofia TEIXEIRA DE FREITAS (s.teixeiradefreitas@tudelft.nl)
Science Communication Manager	Jose SENA CRUZ (jsena@civil.uminho.pt)
STSM Coordinator	Loucas PAPADAKIS (l.papadakis@frederick.ac.cy)
ITC Conference Manager	Loucas PAPADAKIS (l.papadakis@frederick.ac.cy)
Training School Coordinator	Chiara BEDON (chiara.bedon@dia.units.it)
Database Coordinator	Michal BUDZIK (mibu@eng.au.dk)

Action Working Groups

WG 1 - Adhesive and interface chemistry
Leader: Ana MARQUES
Vice-leader: Åsa LUNDEVALL

- Evaluate current common practice in industry: adhesive chemistries and surface treatment processes for bonded joints.
- Collect the requirements and needs of the stakeholders and certification agencies, in terms of regulations (REACH).
- Propose novel non-toxic and environmentally friendly surface treatment processes and adhesive chemistries.
- Evaluate the quality of the new proposed eco-friendly solutions.

WG 2 - Design phase
Leader: Konstantinos TSERPES
Vice-leader: Norbert BLANCO

- Explore new design concepts (geometrical configurations and new crack arresting design features).
- Compare testing procedures for bondline characterization and models validation (under static, fatigue and impact loading, creep phenomena, imperfect bonding and environmental effects).
- Evaluate different design methodologies for the structural behaviour and progressive damage analysis of adhesively bonded structures.

WG 3 - Manufacturing phase
Leader: Nicolas CUVILLIER
Vice-leader: Rūta RIMAŠAUSKIENĖ

- Specify and select the key-parameters that influence the manufacturing process on an industrial scale.
- Evaluate destructive and non-destructive testing for quality control of manufacturing process.
- Propose novel embedded sensing solutions for the evaluation of adhesion strength.
- Evaluate of the effect of different manufacturing defects on the bondline performance.

WG 4 - In-service life phase
Leader: Wieslaw OSTACHOWICZ
Vice-leader: Theodoros LOUTAS

- Propose diagnostic tools for the structural integrity assessment of the bonded structure.
- Propose prognostic tools for the remaining useful life of the bonded structure.
- Develop guidelines towards bonded repairs application.

WG 5 - Disassembly phase
Leader: Laurent BERTHE

- Description of the state-of-the-art about disassembly technologies.
- Evaluation of the technologies and selection of the most promising technology.

WG 6 - Certification
Leader: Thomas KRUSE-STRACK
Vice-leader: Ranko PETKOVIC

- Define common nomenclature for all WG's activities and deliverables.
- Integrate the outcomes and build the roadmap.
- Establish contact with relevant certification bodies and large industry manufacturers in naval, civil, offshore, automotive and wind energy and disseminate the progress of the Action and the roadmap.

First CertBond Training School

The goal of first CertBond Training School is to connect the young generation of early-stage scientists and offer network opportunities with international experts in the field of bonding and adhesives.

A very intensive three-day school able to connect international researchers and experts from several Countries, and a great way to restart networking face-to-face after a long period.

The CertBond Training School (University of Trieste, Italy; 20th-22nd September 2021) is planned to include:

- Frontal lectures from international experts in the area of adhesives
- Workshop sessions to give voice to CertBond Trainees
- A "Best Poster" competition for the CertBond Trainees
- (virtual) Technical visits to laboratories and facilities
- And all around in a series of networking and social events able to enforce their interaction

Local Organizing Committee & Staff

Dr. Chiara BEDON
Assistant Professor of Structural Engineering

Prof. Vanni LUGHI
Associate Professor of Science and Technology of Materials

Prof. Salvatore NOÈ
Associate Professor of Structural Engineering

Dr. Marco FASAN
Post-Doctoral Fellow
in Structural Engineering

Ms. Alessia BEZ
Research Fellow
in Structural Engineering

Mr. Emanuele RIZZI
Research Fellow
in Structural Engineering

Participants

Mohammad Ayad	*France*
Kaleeswaran Balasubramaniam	*Poland*
Pier Giovanni Benzo	*Portugal*
Afonso Carlos Bonina de Mesquita	*Portugal*
Cristina Busuioc	*Romania*
Jagoda Cupac	*Germany*
Maxime Guerbois	*France*
Julian Hänig	*Germany*
Oguzcan Inal	*United Kingdom*
Eliana Inca Cabrera	*Portugal*
Alina Joachim	*Germany*
Damjan Klobčar	*Slovenia*
Christiane Kothe	*Germany*
Gregorio Mariggiò	*Italy*
Silvana Mattei	*Italy*
Lukas Münch	*Germany*
Faidra Oikonomopoulou	*Netherlands*
Kosmas Papadopoulos	*Greece*
Nikola Perković	*Croatia*
Danica Simic	*Serbia*
Shishir Kumar Singh	*Poland*
Nataša Tomić	*Serbia*
Uroš Trdan	*Slovenia*
Selen Unaldi	*France*
Efstratios Volakos	*United Kingdom*
Michaela Zdražilová	*Czech Republic*
Markéta Zikmundová	*Czech Republic*

About Trieste

Trieste is a city and seaport in the north-eastern part of Italy, right next to Slovenia. It is located at the head of the Gulf of Trieste on the Adriatic Sea with a population of around 200,000. It is the capital of the autonomous Friuli Venezia Giulia Region that enjoys a special status and constitution granted by the Italian government. Popular tourist destination, Trieste was one of the oldest parts of the Habsburg Monarchy, belonging to it from 1382 until 1918.

The city is home to **University of Trieste** and many other scientific centers, like **ICTP** (Abdus Salam International Centre for Theoretical Physics), **SISSA** (International School for Advanced Studies), and **ELETTRA SINCROTRONE** (a multidisciplinary international research center specialized in generating high quality synchrotron and free-electron laser light and applying it in materials and life sciences).






Venue

University of Trieste – Department of Engineering and Architecture
Piazzale Europa 1 (main campus)
34127 Trieste
ITALY

Main location for the Training School
Building C7 – Room A "LICIO GIORGIERI" (ground level)

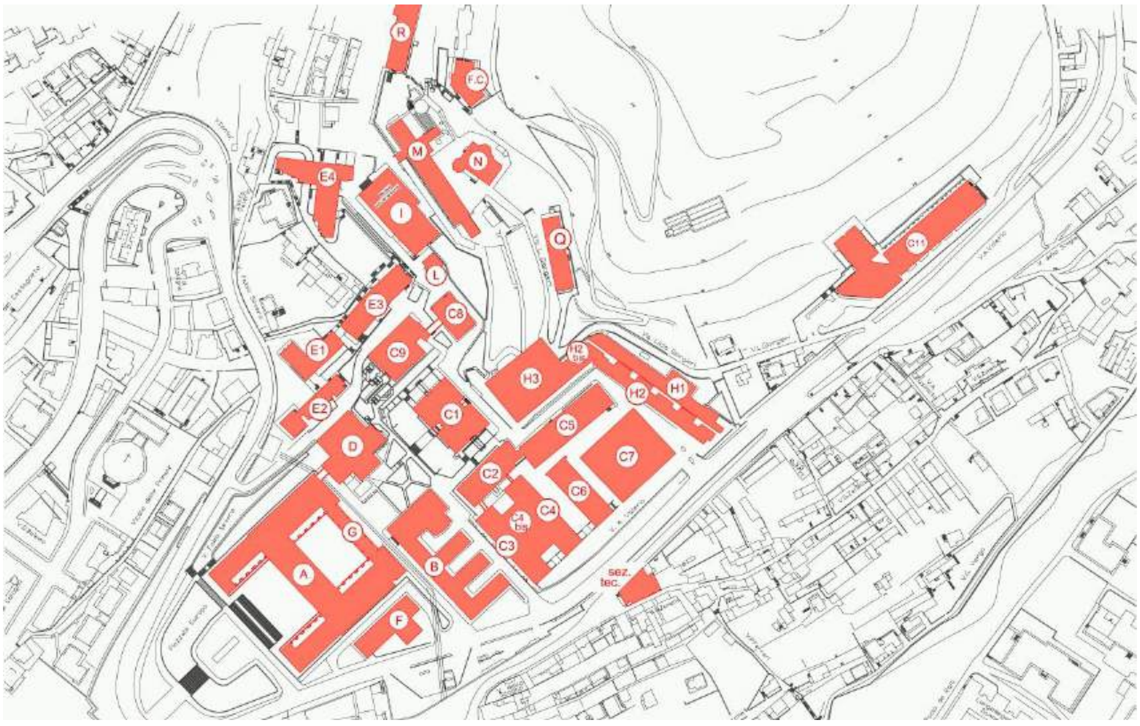


AULA LICIO GIORGIERI

Hybrid Event

The CertBond Training School is organized as face-to-face networking event, under a rigid respect of preventive measures against Covid-19 pandemic.

The University of Trieste, through the most suitable and effective methods, informs anyone having access to the university facilities about the provisions taken by the Authorities regarding the containment measures for the Covid-19 emergency. Detailed information can be found in the specific section on the University website (https://www.units.it/en/about/emergency-covid-19-guidelines-Updates), that also contains governmental and regional records (in Italian), as well as internal guidelines and provisions adopted by the University Bodies.

Anyway, all the lectures, technical visits, workshop presentations of the CertBond Training School are also shared online with the support of video-conference systems and MS Teams.

20th September 2021:

https://teams.microsoft.com/l/meetup-join/19%3a491917769d464fe296966f08ba9aad9e%40thread.tacv2/1631280714168?context=%7b%22Tid%22%3a%22a54b3635-128c-460f-b967-6ded8df82e75%22%2c%22Oid%22%3a%229d4dd650-dd14-42da-8d38-42068b6800c2%22%7d

21st September 2021:

https://teams.microsoft.com/l/meetup-join/19%3a491917769d464fe296966f08ba9aad9e%40thread.tacv2/1631280781318?context=%7b%22Tid%22%3a%22a54b3635-128c-460f-b967-6ded8df82e75%22%2c%22Oid%22%3a%229d4dd650-dd14-42da-8d38-42068b6800c2%22%7d

22nd September 2021:

https://teams.microsoft.com/l/meetup-join/19%3a491917769d464fe296966f08ba9aad9e%40thread.tacv2/1631280828862?context=%7b%22Tid%22%3a%22a54b3635-128c-460f-b967-6ded8df82e75%22%2c%22Oid%22%3a%229d4dd650-dd14-42da-8d38-42068b6800c2%22%7d

Detailed agenda

20th September 2021		
9:30	**Registration @ Building C7 – Room "A"**	
9:45	Welcome	CertBond
10:15	Practical lecture: *"A GLANCE AT BIOBASED AND LOW ENVIRONMENTAL IMPACT COATINGS AND BINDERS"*	S. Caillol
11:15	**Coffee break & Posters**	
11:30	WG1 lecture *"ADHESIVE BONDING"*	E. Stammen
12:15	WG4 lecture *"NON–DESTRUCTIVE ASSESSMENT OF STRUCTURAL INTEGRITY AND FAILURES FOR LIGHTWEIGHT MATERIALS"*	W. Ostachowicz (online)
13:00	**Lunch break**	
14:30	Workshop of CertBond Trainees (part I)	Pag.44
16:00	**Coffee break & Posters**	
16:15	Workshop of CertBond Trainees (part II)	Pag.44
17:30	End of day 1	CertBond

21st September 2021		
9:15	**Registration @ Building C7 – Room "A"**	
09:30	WG5 lecture: *"LASER ADHESION TESTS VIA SHOCK WAVES"*	S. Unaldi
10:15	**Coffee break & Posters**	
10:30	Practical lecture: *"ADHESIVE BONDING IN GLASS CONSTRUCTION"*	C. Louter, C. Kothe
11:30	Virtual LAB visits	UniTS DIA
12:45	**Lunch Break**	
14:30	WG3 lecture: *"AN INDUSTRIAL POINT OF VIEW ON BONDING"*	N. Cuvillier
15:15	WG2 lecture: *"A CRITICAL REVIEW ON TEST METHODS AND SIMULATION MODELS FOR THE CHARACTERIZATION OF ADHESIVE JOINTS"*	K. Tserpes

21st September 2021		
16:00	**Coffee break & Posters**	
16:15	Talk with experts & Networking *Feedback and discussion with trainers about ongoing research projects and studies*	CertBond, Trainers & Trainees
17:30	End of day 2	CertBond

22nd September 2021		
9:15	**Registration @ Building C7 – Room "A"**	
9:20	Technical visit @ ELETTRA SINCROTRONE (virtual)	
10:00	**Coffee break & Posters**	
10:15	Workshop of CertBond Trainees (part III)	Pag.44
12:30	Closure of Training School & Best Poster announcement	CertBond
12:45	**Lunch break / End of Training School**	

Trainers

Prof. Sylvain CAILLOL
Centre National de la Recherche Scientifique (CNRS) Paris
France
sylvain.caillol@enscm.fr

Sylvain Caillol is Research Director with *CNRS*. He received his PhD degree in 2001 from the University of Bordeaux. Then he joined Rhodia Company and headed the Polymer Research Department in the Research Center of Aubervilliers. In 2007 he joined the CNRS at the University of Montpellier and started a research activity dedicated to Green Chemistry and Biobased Polymers. He is co-author of more than 200 articles, patents and book chapters. He won the Green Materials Prize in 2018 and 2020.

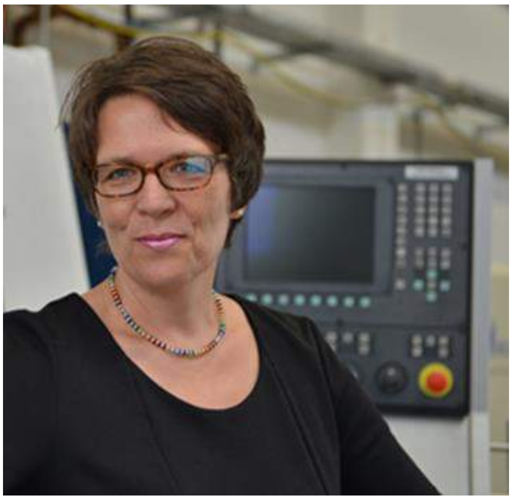

Dr. Elisabeth STAMMEN
Technische Universität Braunschweig
Germany
e.stammen@tu-braunschweig.de

Elisabeth Stammen got a degree in Chemistry in 1994 at Aachen University, Germany. Since 2002 she is research fellow and since 2014 head of department "Adhesive Bonding" at the Institute of Joining and Welding (ifs), Technical University Braunschweig, Germany. Fields of Research are adhesive bonding in automotive, transportation, aerospace and construction, in fuel cells and batteries, surface pre-treatment of polymers and metals, aging behaviour of adhesives and aging test methods and quality of adhesive bonds and bonding processes.

Prof. Wieslaw OSTACHOWICZ
Polish Academy of Sciences
Poland
wieslaw@imp.gda.pl

Prof. Ostachowicz specializes in several important sub-disciplines, like structural health monitoring techniques, vibration control, structural dynamics, composite structures, smart materials and structures, damage assessment of structures. He participated in the investigation of 24 international research projects as a coordinator, leader of WP, or main contractor. Presently prof Ostachowicz is involved in work (as editor/associate editor) for various international journals.
He has received several prestigious awards and distinctions, among others Medal of O.C. Zienkiewicz (2013), Dragon–STAR Innovation Award (1st place) as confirmation of cooperation between Poland (Polish Academy of Sciences) and China (Hohai University and The Hong Kong Polytechnic University), 2015, and SHM Life Achievements Award (sponsored by Boeing Co.), Stanford University, USA (2019).

Ms. Selen Unaldi
Arts et Métiers Paris Tech, ENSAM
France
selen.unaldi@ensam.eu

Selen earned the Bachelor of Science Degree in Physics at METU, Turkey. Finished her master studies at Université Paris Saclay in physics. Currently, Selene is involved in her PhD degree at Arts et Métiers Paris Tech, ENSAM, which is entitled as " Adhesion test and stripping process of paint using Shock Produced by Laser Plasma: Application to Aeronautical parts " under the frame work of Clean Sky 2 Vulcan Project.

Prof. Christian LOUTER
Technische Universität Dresden
Germany
christian.louter@tu-dresden.de

Christian Louter is full Professor and Director at the Institute of Building Construction, Faculty of Civil Engineering, TU Dresden. He obtained his PhD in 2011 on the topic of structural glass design at the TU Delft in the Netherlands. From 2010, Christian worked as a post-doctoral researcher at the Steel Structures Laboratory at the EPFL in Switzerland.
In 2015, Christian returned to the Netherlands to work as an Assistant Professor of Structural Design at the TU Delft, before joining TU Dresden in 2019. Next to his research and teaching activities, Christian is Director of an accredited test & certification laboratory, an organiser of the international Challenging Glass conference series, an Editor-in-Chief of the Glass Structures & Engineering journal (Springer) and member of several (inter)national committees.

Dr. Christiane KOTHE
Technische Universität Dresden
Germany
christiane.kothe@tu-dresden.de

Christiane Kothe is a Chemist and Research Associate at the Institute of Building Construction, Faculty of Civil Engineering, TU Dresden since 2008. There she received her PhD in 2013 for her work on surface modification methods for improving adhesive joints. In the associated Friedrich Siemens Laboratory, she is responsible for the investigation of polymer materials and substrate surfaces with spectroscopic methods, thermal analysis and microscopy.
Christiane works on a variety of research projects related to bonding and surface treatment. She also supports the accredited test & certification laboratory in questions about adhesive joints, material properties, aging behaviour and surface characteristics. In addition, she supervises student work and holds adhesive-related lectures and training courses.

Dr. Nicolas CUVILLIER
Safran Composites
France
nicolas.cuvillier@safrangroup.com

Nicolas Cuvillier is presently Research Leader for “New materials, functionalisation of CRFP and assemblies” at Safran Composites, the Safran corporate research center on composite materials. After a PhD in physical-chemistry, he has worked for Arianegroup for about nine years on the development of solid propellant and leaded the chemistry and formulation team (40 researchers). Since 2014, at Safran Composites, he has developed a strong expertise on “bonded assemblies” through several projects covering all the aspect of bonding (adhesive formulation, surface preparation, NDT) with a special interest on Laser Surface preparation.

Prof. Konstantinos TSERPES
University of Patras
Greece
kitserpes@upatras.gr

Konstantinos Tserpes is an Associate Professor in the Department of Mechanical Engineering & Aeronautics. He is a member of the Laboratory of Technology & Strength of Materials.
His expertise is in the area of strength of materials. Since 1999 he has participated in more than 20 EC funded research projects in the area of Aeronautics.
In the last 10 years, he has participated in 7 EC funded projects in the area of adhesive joints. He has published more than 80 papers in journals, more than 100 papers in conference proceedings, 10 chapters in books and he has co-edited 5 international books. Currently, he is a member of the Board of Directors of the European Aeronautics Science Network. He is the leader of Certbond’s Working Group 2.

Summary of lectures

A glance at biobased and low environmental impact coatings and binders

S. Caillol

Polymers hold a very important place in chemistry with a worldwide production of about 400Mt in 2020 and applications in all economic sectors, from basic materials for construction or furniture, to the cutting-edge sectors of aerospace or construction and health. Thus, half of the molecules produced by the petrochemical industry - foremost among which is ethylene (160 Mt/year) - are ultimately found in polymers. Green Chemistry, owing to the concept proposed in 1998 by Anastas et al.[1], is a chemistry response to the challenges of reducing the environmental impact of our society. This remarkable place of polymers in chemistry is found naturally in green chemistry, and essentially through the use of renewable resources for the development of agro-resourced or bio-sourced polymers.

The objective of using renewable resources is not only motivated by the reduction of dependence on fossil resources and consequently of greenhouse gas emissions at the end of life, but also by the search for new features. Likewise, the reduction of impacts, in particular through the use of less hazardous monomers, is a strong driver for the development of renewable resources (Figure 1).

Among renewable resources, our team has studied the use of vegetable oils for the development of monomers and polymers. In order to improve the thermomechanical properties of polymers from renewable resources, we have also functionalized natural phenols[2], such as tannins, vanillin[3], eugenol or cardanol to develop various polymers, phenolics, polyepoxides, polyacrylates or polyurethanes. Polyurethane is currently one of the most commonly used polymers in the world for various applications such as rigid and flexible foams, coatings, elastomers, adhesives and sealants. However, isocyanate precursors are very harmful. Thus, in recent years, much research work has been carried out for the design of isocyanate-free polyurethanes (NIPU) s resulting from the reaction between five-membered cyclic carbonates and amines leading to polyhydroxyurethanes (PHU). However, this reaction has a drawback: the low reactivity of the aminolysis of the cyclic carbonate. Our work first made it possible to propose complete reactivity studies in order to determine the influence of the structure of the reactants[4]. Second, we proposed innovative solutions to allow the development at room temperature of a range of PHUs materials, foams and PHU-hybrids (epoxy, acrylate, silicone, etc.) with increased adhesion properties to meet the properties thermo-mechanics required by potential applications.

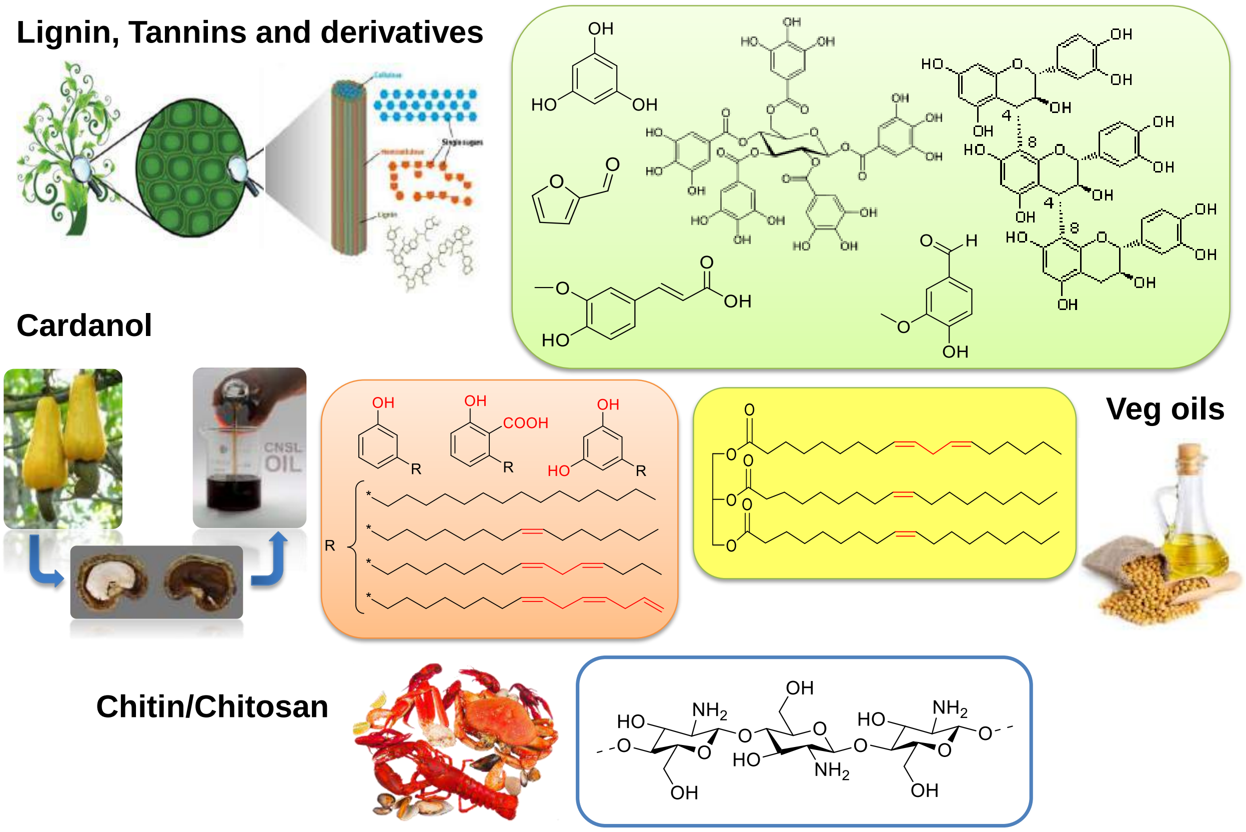

Figure 1. *Renewable resources for sustainable polymers and coatings.*

References

1. Anastas, P. T.; Warner, J. C. Green Chemistry: Theory and Practice, Oxford University Press: New York, 1998.
2. Biobased phenol and furan derivatives coupling for the synthesis of functional monomers, M Decostanzi, R Auvergne, B Boutevin, S Caillol, Green Chemistry, 2019, 21, 724-747
3. Vanillin production from lignin and its use as a renewable chemical (perspective), M Fache B Boutevin, S Caillol; ACS Sustainable Chemistry & Engineering, 2016, 4, 35−46
4. A Perspective Approach to Sustainable Routes for Non-Isocyanate Polyurethanes, A Cornille, R Auvergne, O Figovsky, B Boutevin, S Caillol, European Polymer Journal, 2017, 87, 535-552

Adhesive bonding in glass construction

C. Louter, C. Kothe

Introduction

This contribution and the associated lecture focuses on adhesive bonding in glass construction. A short introduction into glass bonding is provided in the next sections, whereas the lecture will include further examples of glass bonding both in practice and in research.

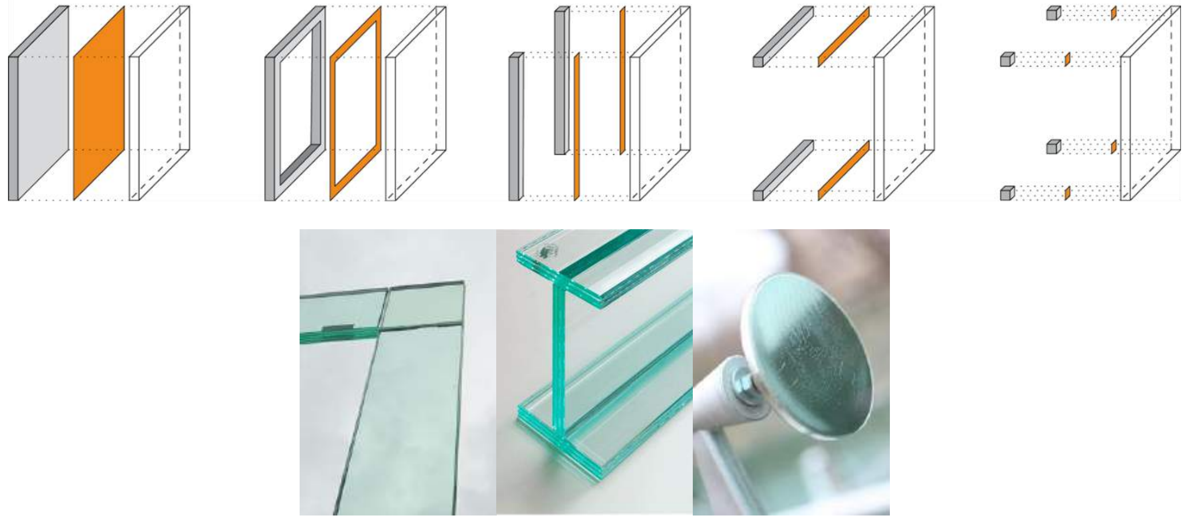

Figure 1. *Examples of adhesive bonds in glass construction; e.g. area, linear and point bonds.*

Glass as a substrate

Flat glass for the building industry is primarily produced using the float glass process. Molten glass with a temperature of 1,050 °C flows into the float chamber. There it floats as a ribbon of glass on liquid tin. This results in glass panes with parallel, flat surfaces and a completely distortion-free transparency. On the side facing the tin bath, tin ions diffuse into the glass surface in exchange with alkali ions. However, this ion incorporation is not homogeneous, so that the surface properties are very difficult to control. Bonding is therefore primarily carried out on the atmospheric side of the glass.

The silicate in the glass surface reacts quickly with the surrounding air humidity. A chemisorbed layer of silanol groups results that adsorbs more water. This surface moisture can hardly be removed permanently, as it is constantly formed due to the humidity. In terms of glass bonding, this surface acts like a barrier. As a result, it is difficult for the adhesive to approach the glass surface and build up adhesive forces.

Adhesive connections

The state of the art for bonded glass constructions in civil engineering is currently structural sealant glazing (SSG). In these systems, the glazing is connected to a support frame or an adapter profile made of stainless steel and anodized or coated aluminium using linear bonding. The European guideline ETAG 002 describes the structure, the materials that can be used and the experimental investigations which are required for the approval of SSG façades. In terms of this guideline, the selection of possible adhesives is limited to silicones. These are adhesives for which reliable test results and many years of experience are available. Silicones have very good adhesion to the glass surface and are highly resistant to environmental influences. However, the low stiffness, the low strength and the black colour of the adhesives are disadvantageous.

In particular, transparent or higher modulus adhesives open up new fields of glass bonding applications. Such new developments are, for example, glass hybrid components. The planar or linear adhesive connections of glass with ductile materials increase its load-bearing and residual behaviour. Material combinations with steel, aluminium, wood, glass fibre reinforced plastics and even reinforced concrete have been investigated. Adhesive point fixings are also possible and have already been implemented in glass façades. These connections avoid drilling or clamping the glass. The glass surface looks very homogeneous and the stresses in the point fixings are evenly distributed.

Adhesive connections in glass construction also comprises laminated glass and insulating glass units. Laminated glass consists of at least two glass panes and a polymer interlayer. The standard material is polyvinyl butyral and, for photovoltaic modules, ethylene vinyl acetate. Further interlayers are polyurethane, polymethylmethacrylate, ionomers and casting resins. The edge seal of insulating glass units is based on a sealing and a linear bond made with polysulphide or silicone.

Adhesive selection

The selection criteria for an adhesive should take into account the properties and surface conditions of the substrates, the strength requirements for the construction, the expected environmental influences, the structural design of the adhesive connection and the acting types of stress.

In addition, considerations about the manufacturing process of the adhesive connection should be included. The processing time as well as the type of dosage and adhesive application are important here.

Furthermore, an assessment of the adhesives with regard to their tendency to creep and their relaxation behaviour under permanent loads is necessary so that their suitability for bonds with dead load transfer can be determined.

The durability and resistance of adhesives and, as a result, that of the adhesive connection are influenced by environmental factors such as temperature, humidity, corrosive substances and radiation. There are extensive tests for artificial aging in ETAG 002 and other standards, especially for adhesive connections in glass construction.

In addition to these mentioned measurable factors, other aspects such as the visual appearance and aesthetics are also important.

Surface pre-treatment

The surface quality of the substrate is decisive for the build-up of adhesive forces and for the long-term stability and strength of the bonded connection. Special pre-treatments lead to better wettability of the surface and create energetically active centers which interact with the adhesive. The type of the surface pre-treatment depends on the substrate material and the adhesive, on the current condition of the surfaces and on the requirements for the bonded construction. The surface treatment is divided into three process steps: preparation, pre-treatment and post-treatment.

In the first step, the substrates are adjusted in order to obtain an even, tension-free joint for the bond. In addition, large impurities, unwanted coatings and greases are removed. This is followed by surface pre-treatment. In addition to mechanical processes that remove parts of the substrate surface and thus change the roughness, physical-chemical processes are used. Plasma application, flame treatment or sandblast coating, all of which work with silane-containing raw materials, produce salinized surfaces with excellent wetting and adhesive properties. Subsequent post-treatment of the activated or coated surfaces is necessary because their increased surface energy makes them particularly sensitive to undesired contamination from the surrounding atmosphere and to deactivating post-reactions.

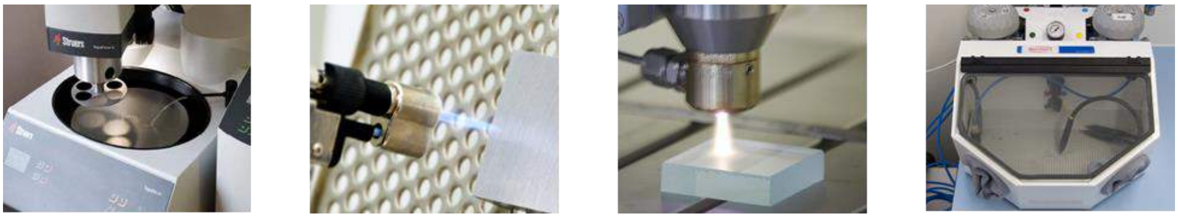

Figure 2. *Surface pre-treatment techniques; e.g. grinding, flame silicating, plasma and sandblast.*

WG1 lecture: Adhesive bonding

E. Stammen

Driven by the need to improve fuel economy and to reduce carbon emissions, manufacturers reduce vehicle weights by increasing the use of light-weight materials like magnesium, carbon fiber reinforced plastics and high strength steel. Especially multi-material structures demand joining technologies to enable commercially feasible and high-volume manufacturing processes. Together with welding and soldering, adhesive bonding is one of the materially jointed connections. In such joints, the force is transmitted over the entire joint area. This results in a more favourable uniform stress distribution than in the case of frictional and positive connections. Adhesive bonding is capable of permanently bonding different materials, even in thin material thicknesses, without negative influences, e.g. thermal, on the substrate microstructure. The uniform stress distribution along the bonded area enables to have a higher stiffness and load transmission, reducing the weight and thus the cost.

In contrast, the temperature dependence of many adhesive properties, the aging behaviour and the often more complex manufacturing process are problematic for the application or implementation of adhesive bonding. In addition, quality assurance of the entire bonding process chain is of particular importance [1].

Despite all this, adhesive bonding is often the only possible joining method, as it offers solutions for a wide range of applications due to the diverse base chemistry available and the broad spectrum of properties of the adhesives.

<u>Adhesives – Mechanisms and examples</u>

The various adhesive systems can be classified in many different ways; according to the origin of the raw materials, the chemical basis or the reaction mechanisms. A general classification into physically setting and chemically reacting systems is shown in Figure 1 [2].

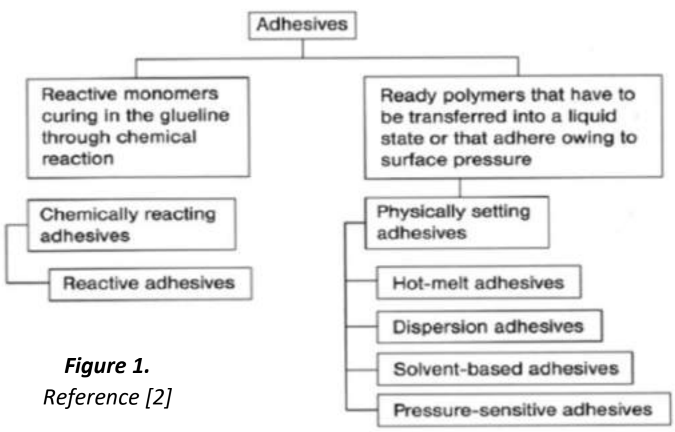

Figure 1.
Reference [2]

The chemically reacting systems can be distinguished on the basis of the polymer reaction. Possible reactions are polymerisation, polyaddition and polycondensation.

Cyanoacrylates, so-called super glues, methyl methacrylates or anaerobic adhesives are among the well-known polymerisation adhesives. Polyurethanes and epoxy resins belong to the group of polyaddition adhesives, while silicones and phenolic resins are polycondensation adhesives. The three reaction mechanisms are shown schematically in Figure 2.

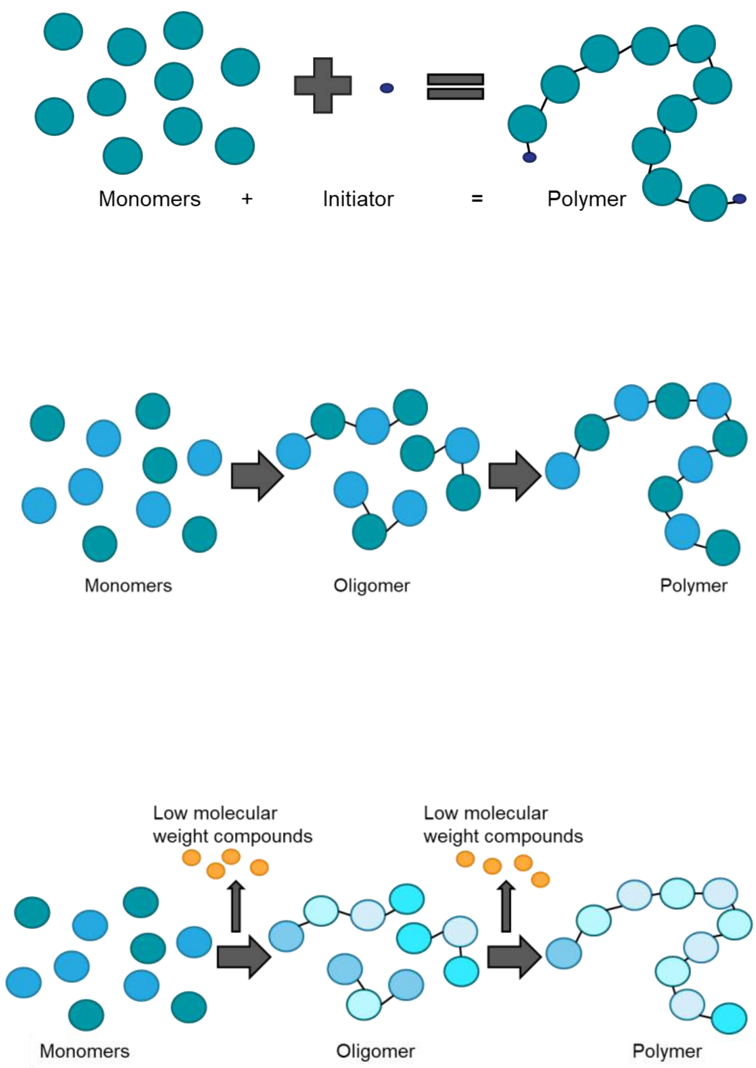

Polymerisation

Polyaddition

Polycondenation

Figure 2

In polymerisation reactions, the stoichiometry of the components is less important; the reaction starts with an initiator. In polyaddition, the monomers react stoichiometrically with each other; errors in the mixing ratio have the effect of lower strengths, among other things. Polycondensation reactions are similarly sensitive; here it is important to allow the escaping cleavage product to escape via the porous substrate, for example.

<u>Surfaces and pre-treatment</u>

Adhesion (of polymers) is practically only determined by intermolecular binding forces. These binding forces (adhesion) are small compared to main valence bonds (cohesion). There is no general theory of adhesion. Adhesion must be seen as the effect of many individual interactions!

In order to achieve good adhesion on a surface, wetting of the substrate is of great importance. If the surface tension of an adhesive is lower than the surface energy of the substrate, the adhesive can wet the surface (at a suitable viscosity). Most of the time it is necessary not only to clean the surface but also to pre-treat it, Figure 3. A wide variety of processes are available for this purpose, which are used depending on the substrate or technological necessity in order to achieve a reproducible surface. The aim is not only to improve adhesion but also to increase ageing resistance [3].

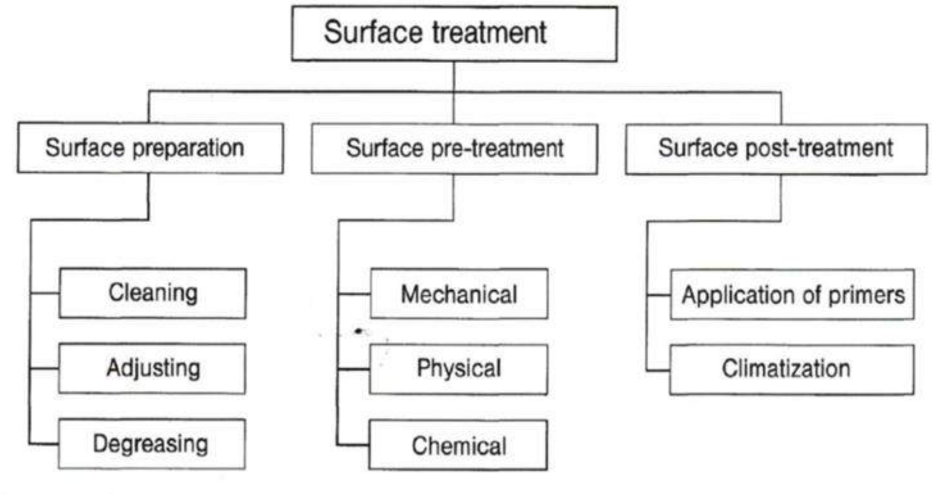

Figure 3. *Reference [2].*

In recent years, the trend has been towards environmentally friendly processes in the field of pre-treatment. The same trend can be seen in adhesives, where more and more bio-based products are being found. Adhesive technology is thus making an active contribution to reducing carbon dioxide.

References

1. DIN 2304-1 (German Standard) : Adhesive bonding technology - Quality requirements for bonding processes - Part 1: Bonding process chain, https://dx.doi.org/10.31030/3138880
2. Gerd Habenicht: Applied Adhesive Bonding, WILEY-VCH 2006, ISBN 978-3-527-32014-1
3. Ana C. Marques et al. : Review on Adhesives and Surface Treatments for Structural Applications: Recent Developments on Sustainability and Implementation for Metal and Composite Substrates, Materials 2020, 13(24), 5590, https://www.mdpi.com/1996-1944/13/24/5590
4. Solange Magalhães et al. : Brief Overview on Bio-Based Adhesives and Sealants ; Polymers 2019, 11, 1685; https://www.mdpi.com/2073-4360/11/10/1685

WG2 lecture: A critical review on test methods and simulation models for the characterization of adhesive joints

K. Tserpes

In the framework of the COST Action CertBond (Reliable roadmap for certification of bonded primary structures), a wide group of researchers from 27 European Countries have had the opportunity to work on the topic of certification of bonded joints for primary structural applications from different engineering sectors such as the aerospace, automotive, civil engineering, wind energy and marine sectors. In the frame of Working Group 2, test methods and simulated models are listed and critically reviewed on the basis of their application to the certification of adhesive joints.

Testing mechanical performance of adhesively bonded composite joints in engineering applications: an overview

The first part of the present lecture presents the commonly used experimental methods for the investigation of mechanical performance of adhesively bonded joints in the aerospace, wind energy, automotive and civil engineering sectors. In these sectors, due to their excellent intrinsic properties, composite materials are often used along with conventional materials such as steel, concrete and aluminium. In this context, and due to the limitations that the traditional joining techniques present, adhesive joints are an excellent alternative. However, standardized experimental procedures are not always applicable for testing representative adhesive joints in these industries. Lack of relevant regulations across the different fields is often overcome by the academia and companies' own regulations and standards. Additional costs are thus mitigated to the industrial sectors in relation with the certification process which effectively can deprive even the biggest companies from promoting adhesive bonding. To ensure continuous growth of the adhesive bonding field the new international standards, focusing on actual adhesive joints' performance rather than on specific application of adhesive joints are necessary.

References

1. Michal K. Budzik, Markus Wolfahrt, Paulo Reis, Marcin Kozłowski, José Sena-Cruz, Loucas Papadakis, Mohamed Nasr Saleh, Klara V. Machalicka, Sofia Teixeira de Freitas & Anastasios P. Vassilopoulos (2021) Testing mechanical performance of adhesively bonded composite joints in engineering applications: an overview, The Journal of Adhesion, DOI:10.1080/00218464.2021.1953479

Failure theories and simulation models

Virtual testing and optimization are basic tools in the certification process of adhesive joints. The second part of the present lecture discusses the most important failure theories and simulation models that have been developed for adhesive joints. Nine different models/theories are presented: the Classical Analytical Methods, the Process Zone Methods, Linear Elastic Fracture Mechanics (LEFM), the Virtual Crack Closure Technique (VCCT), the Stress Singularity Approach, Finite Fracture Mechanics (FFM), the Cohesive Zone Method (CZM), the Progressive Damage Modeling method and the Probabilistic methods. Also, at the end of the section, the modelling of temperature effects on adhesive joints are addressed. For each model/theory, information on the methodology, the required input, the main results, the advantages and disadvantages and the applications are given.

References

1. Konstantinos Tserpes, Alberto Barroso-Caro, Paolo Andrea Carraro, Vinicius Carrillo Beber, Ioannis Floros, Wojciech Gamon, Marcin Kozłowski, Fabio Santandrea, Moslem Shahverdi, Davor Skejić, Chiara Bedon & Vlatka Rajčić (2021) A review on failure theories and simulation models for adhesive joints, The Journal of Adhesion, DOI: 10.1080/00218464.2021.1941903

WG3 lecture: An industrial point of view on bonding

N. Cuvillier

As a part of the CertBond training school (Trieste, September 2021), this presentation has for objective to review some basics on structural bondings, with an industrial (and moreover aeronautical) point of view.

This lecture is not focused on bonding theoretical principles (that can be easily found in many books or web resources) but has the complementary objective to give some "ticks and tips" on bonding, based on the return of experiment of industrial users.

Technically, the advantages of a bonded joint when compared to a more "classical" mechanical assembly are now well established. To be short, one can say that a bonded join is lighter (one replaces metallic parts by a thin layer of organic "resin"), stronger (no holes in the parts => no degradation of the mechanical properties, no stress concentration) and cheaper (much less operations to do for the assembly). Although these advantages, the use of bonding remains limited, especially in the aeronautical domain, due in particular to concern on the capacity to assure a reliable adhesion in an industrial environment. This concern is reinforced by the certification constraints that practically forbid the use of bonded joint in a lot of situations.

In this talk, we will try to cover the full life cycle of a bonded joint in order to give to the students some tricks and tips that will help us to build a reliable and reproducible bonded assembly.

Schematically, the bonding process could be described using the following diagram, that shows the major steps between the initial parts (+ the adhesive) and the final assembly, ready to "fly".

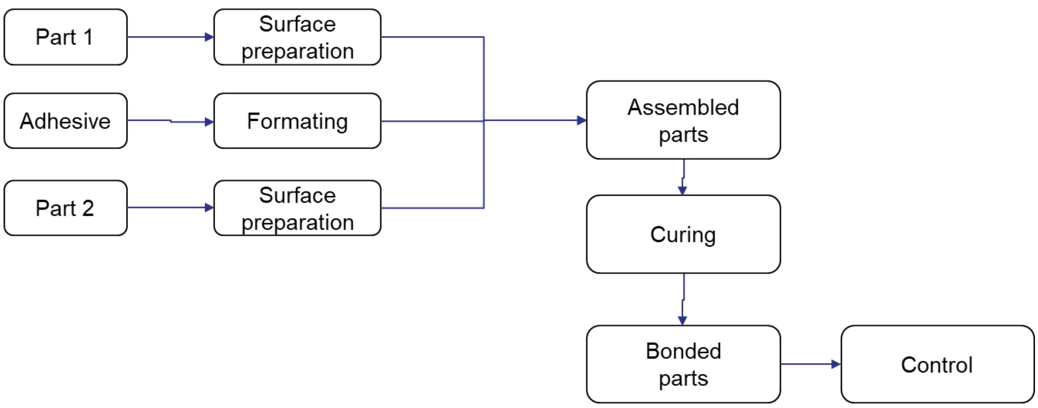

In the aeronautic domain, structural adhesive is almost synonym of Epoxy structural adhesive (except for some specific applications, e.g. high temperature). Suppliers propose a lot of different adhesive formulation that are always "excellent", "high strength, "good". Despite these commercial presentations, it is a critical to choose the right adhesive for each application and we will propose a general method to reduce the risk during this phase.

In conjunction to choose of the right adhesive, the selection of the right surface preparation for each of the parts to be assembled could be event more crucial on the reliability of the assembly. If a non-adapted adhesive could decrease the assembly's performances below the objective, a "bad" surface preparation could lead to catastrophic event, with almost zero mechanical strength. Therefore, we will present some classical processes for the surface preparation of both metallic and composite surfaces but also some more details on promising methods based on laser irradiation.

We will then cover the following steps of the process, mainly the curing of the adhesive and the control of the final assembled parts.

Finally, we will present some recent work on the automation of the bonding that could be a powerful way to improve the reproducibility and the reliability of an adhesive joint. One should keep in mind that despite its “high tech” image, the bonding in the aeronautic field remains mainly manual and “artisanal”.

Within all the information’s, one hopes that more and more bonded joints will fly in the next years.

WG4 lecture: Non–destructive assessment of structural integrity and failures for lightweight materials

W. Ostachowicz

Issues and Challenges

The subject of the lecture will be issues and challenges of non–destructive assessment of structural integrity and failures for lightweight materials. As is well known, such a need results from the necessity to monitor the condition of joints in composite structures as well as during repairs of damaged structures. Composite patches are becoming more and more common.

In the initial part of the lecture, motivations and research objectives will be presented. For the most part, the lecture will show the methods of inspection of composite structure joints. The methods of surface assessment before joining will be highlighted, and then the quality assessment methods for structural joints.

Various methods for detecting mechanical, thermal, moisture, material ageing and other damage will also be described. In the main part of the presentation, various methods of NDT (non-destructive testing) and SHM (structural health monitoring) will be discussed.

As potential sources of risks to the proper functioning of joints in composite structures, the dominant ones were selected. Moreover, the above-mentioned sources of risks have been divided into two groups.

The first group of threats includes possible sources of weak bonds that appear in the manufacturing process. There are:

- moisture
- anti-adhesive agent (release agent)
- errors in bonding
- finger print

On the other hand, the second group of threats includes possible sources of weak bonds that appear in the servicing process. There are:

- moisture
- fuel
- hydraulic fluid (skydrol)
- de-icer
- thermal degradation
- errors in bonding
- finger print

The presentation covers investigated cases for study of the adhesive bond quality of polymer reinforced carbon fibres (CFRP), in example:

- active thermography using ultrasonic excitation
- THz / GHz reflectometry
- nonlinear ultrasound
- LASAT technique
- laser ultrasound
- active thermography using optical excitation
- laser scanning vibrometry

- electromechanical impedance
- vibrothermography
- ultrasonic frequency analysis

The presentation also covers investigated cases for study of the surface of polymer reinforced carbon fibres samples (CFRP), in example:

- X-ray fluorescence spectroscopy
- reflectometry/ellipsometry
- infrared spectroscopy
- laser scanning vibrometry
- optically stimulated electron emission
- active thermography
- aerosol wetting test
- laser induced breakdown spectroscopy
- THz / GHz reflectometry
- optical fibre sensors
- electrochemical impedance spectroscopy
- electromechanical impedance
- dual-band active thermography
- vibrothermography
- THz technology
- optical coherence tomography
- nuclear magnetic resonance
- electronic nose technology

The descriptions of research methods presented in the lecture were taken from the experiences of research teams carrying out two research projects of the European Union. The first was the ENCOMB project, 7th Framework Programme (2010-2014), titled *Extended Non-Destructive Testing of Composite Bonds*. The second project was the ComBoNDT project, Horizon 2020 Programme (2015-2018), titled: *Quality assurance concepts for adhesive bonding of aircraft composite structures by advanced NDT*. In addition, a number of research results have been used in the preparation of the lecture, which have been investigated over the last ten years in the Mechanics of Intelligent Structures Department, at the Institute of Fluid-Flow Machinery, Polish Academy of Sciences in Gdansk, Poland.

References

1. Cavalcanti W., Brune K., Noeske M., Tserpes K., Ostachowicz W., Schalag M., Adhesive Bonding of Aircraft Composite Structures, Springer, ISBN 978-3-319-92809-8
2. Dugnani R, Zhuang Y, Kopsaftopoulos F et al (2016) Adhesive bond-line degradation detection via a cross-correlation electromechanical impedance–based approach. Struct Health Monit 15(6):650–667
3. Dugnani R, Chang F-K (2017) Analytical model of lap-joint adhesive with embedded piezoelectric transducer for weak bond detection. J Intell Mater Syst Struct 28(1):124–140
4. Malinowski P, Wandowski T, Ostachowicz W (2015) The use of electromechanical impedance conductance signatures for detection of weak adhesive bonds of carbon fibre–reinforced polymer. Struct Health Monit 14(4):332–344.

WG5 lecture: Laser adhesion test via shock waves

S. Unaldi

As known, aeronautical industry started to increase the use composite materials within their aircrafts which is due to their strength to weight ratio (leads to less fuel consumption) and corrosion properties. For example, for Airbus A380 composite part of the aircraft is 25%, for A350 it's around 52%. Even though there are assembly techniques, they are not well adapted for the composites such as Carbon Fiber Reinforced Polymer (CFRP) use and as a result, industrials ending up having extra costs and larger production time. With the usage of adhesive bonding, 12% of the aircraft weight can be reduced. Using a glue can be an option to bond composite parts together, however, there is no Non-Destructive Technology (NDT) which is capable of testing the mechanical strength of bonds. Laser Shock Wave adhesion test (LASAT) is a promising method for this kind of problem. This technique allows the generation of high tensile stresses within the tested material, which can debond or not the interface according to its strength [1].

The main phenomena for LASAT tests is that when a high intensity pulsed laser source (1J, 10 ns) is focused on a target, high pressure plasma (GPa range) is generated and a shock wave is induced inside the specimen. For applications, a confined regime with water is preferred (Fig. 1) because generated pressure on the target is two times longer and four times higher compared to non-confined regime [2,3,4].

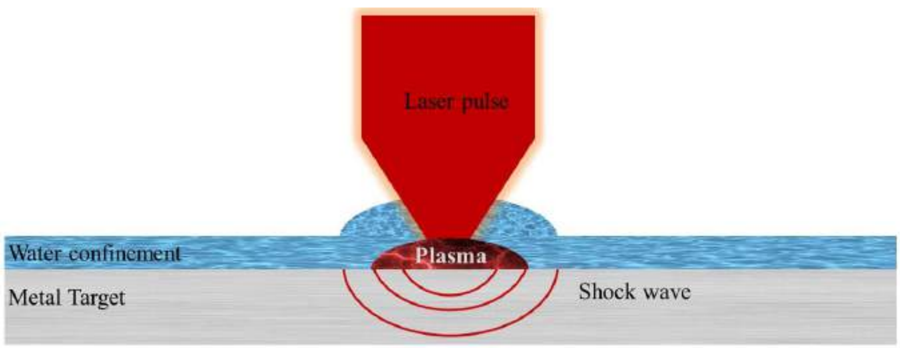

Figure 1. *Principle Laser Shock wave creation phenomena with a confinement.*

By changing laser parameters such as using two beams as a double or symmetrical configuration, the optimization is done to test different bonded composites.

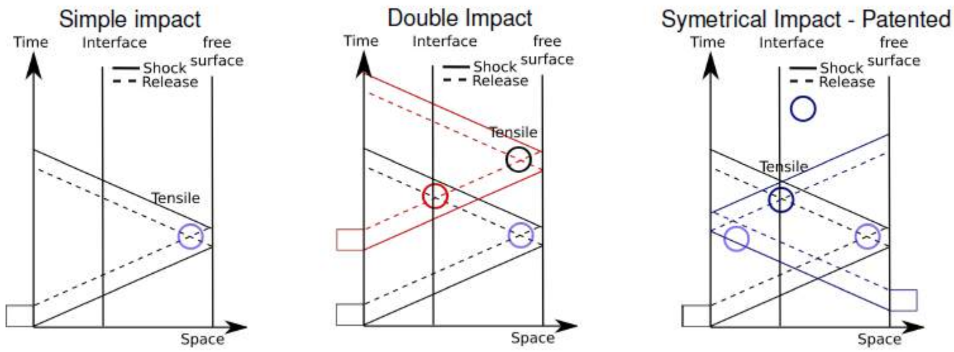

Figure 2. *Space-Time Diagrams for different impact scenarios.*

Laser Adhesion Tests has been applied on external aircraft coatings (paints) which consist of structural primer (epoxy), exterior primer (optional, epoxy) and a top coat (base coat+clear coat-polyurethane) as shown in Figure 3. In addition to bonded structures testing on composite materials, it is used to test paint adhesion levels as function of applied surface treatment, thickness or thermal/humid ageing both on composite and aluminum based specimens.

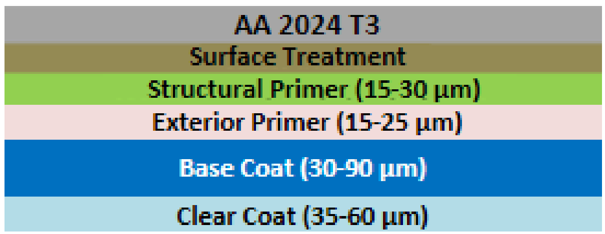

Figure 3. *Typical External Aircraft Coating of an AA 2024-T3 sample.*

Since laser shock process is high strain rate of deformation, it is difficult to observe all kind of phenomenon during laser shock propagation. Therefore, numerical method coupled with experimental data using the explicit code LS-DYNA, which has been used to optimize the experimental paint striping/ paint adhesion test. To that scope, the material mode for the AA2024-T3 and the Epoxy has been validated using mono-shots on the stack of Aluminum + Epoxy. The validated material model used in the graphical optimization tool that interfaces perfectly with LS-DYNA (LS-OPT) to get the best laser parameters which gives the biggest traction stress at the interface. We demonstrated that using optimized delay between the two laser beams for a defined configuration, the stress at the interface is bigger than using single beam, instantaneous laser beams as shown in Figure 4a, while the propagation of axial stresses are shown in Figure 4b.

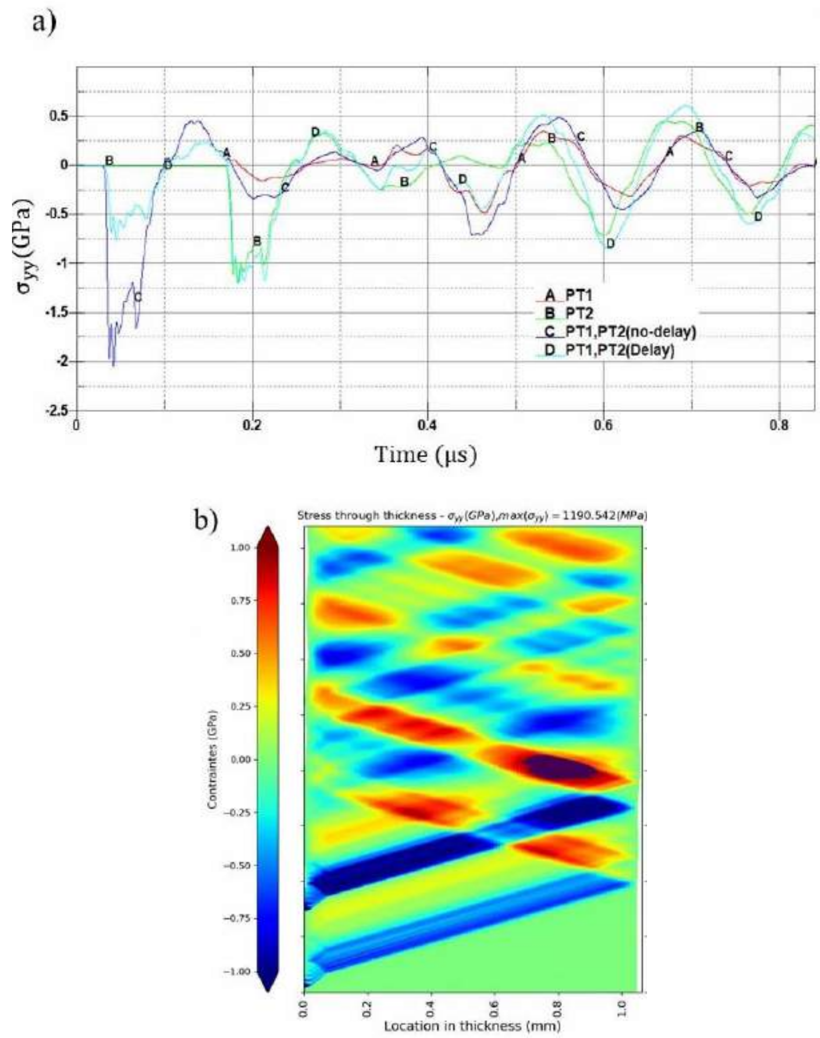

Figure 4. *(a) PT1=0.24GW/cm² and PT2=0.52 GW/cm², 4mm Focal Spot,48 µm of Epoxy, Aluminum pure (scotch) of 28 µm. (b) Stress level σ_{yy} (vertical axis) during the wave propagation through the target thickness (horizontal axis) and during the laser shock.*

References

1. Romain Ecault. *Etude expérimentale et numérique du comportement dynamique de composites aéronautiques sous choc laser*. Optimisation du test d'adhérence par ondes de choc sur les assemblages composites collés. PhD thesis, Ecole Nationale Supérieure de Mécanique et d'A érotechique, 2013
2. J.A. Fox, Effect of water and paint coatings on laser irradiated targets*, Applied Physics Letters* 24 (1974) 461–464.arXiv:http://dx.doi.org/110.1063/1.1655012
3. N. C. Anderholm, Laser-generated stress waves, Applied Physics Letters 16 (3) (1970) 113–115. arXiv:https://doi.org/10.1063/1.1653116,doi:10.1063/1.1653116.URLhttps://doi.org/10.1063/1.1653116
4. R. Fabbro, J. Fournier, P. Ballard, D. Devaux, J. Virmont, Physical study of laser-produced plasma in confined geometry, Journal of AppliedPhysics 68 (2) (1990)

Workshop of CertBond Trainees

Scientific Committee

Dr. Sofia TEIXEIRA DE FREITAS
Delft University of Technology
Netherlands

Dr. Anastasios P. VASSILOPOULOS
Ecole Polytechnique Fédérale de Lausanne
Switzerland

Dr. Chiara BEDON
University of Trieste
Italy

Prof. Jose SENA CRUZ
University of Minho
Portugal

Dr. Loucas PAPADAKIS
Frederick University
Cyprus

Prof. Ana MARQUES
Instituto Superior Técnico, Universidade de Lisboa,
Portugal

Dr. Michal BUDZIK
Aarhus University
Denmark

Mr. Thomas KRUSE-STRACK
Airbus Operations GmbH
Germany

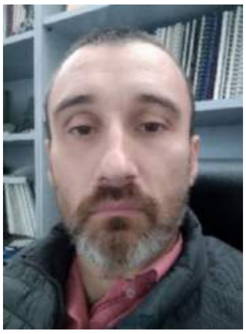

Dr. Laurent BERTHE
CNRS Paris
France

Workshop agenda

	20th September 2021	
14:30	Opening	CertBond
14:35	*IN SEARCH OF THE HOLY GRAIL OF ADHESIVES FOR CAST GLASS STRUCTURES: TWO CONTRADICTORY CASE STUDIES, THE CRYSTAL HOUSES FAÇADE IN AMSTERDAM AND A SMALL GLASS PAVILION IN GREENLAND*	F. Oikonomopoulou *(online)*
14:45	*STRUCTURAL PERFORMANCE OF EMBEDDED LIQUID-LAMINATED GLASS CONNECTIONS*	E. Volakos *(online)*
14:55	*EPOXY-PVB COMPOSITE BINDER REINFORCED WITH NANOSTRUCTURES OF* WS_2	D. Bajić *(online)*
15:05	*ADHESION CAPABILITY OF ECO-EPOXY ADHESIVES YNTHESIZED BY THE ADDITION OF MODIFIED TANNIC ACID*	N. Tomic *(online)*
15:15	*NONDESTRUCTIVE ANALYSIS OF DEBONDING IN A HONEYCOMB COMPOSITE SANDWICH PANEL*	K. Balasubramaniam
15:25	*VITROCERAMIC COATINGS BONDED TO METALLIC IMPLANTS FOR DENTAL AND ORTHOPAEDIC APPLICATIONS*	C. Busuioc
15:35	*A LIGHTWEIGHT FLOOR SYSTEM BASED ON SANDWICH PANEL*	P.G. Benzo
15:45	*INFLUENCE OF ELEVATED TEMPERATURE ON GLUED-IN STEEL RODS FOR CLT ELEMENT*	N. Perković
15:55	*THE APPLICATION OF ADHESIVES FOR CONNECTING STRUCTURAL GLASS STRIPS TO EXISTING TIMBER JOISTS*	Z. Unuk
16:05	**Coffee break**	
16:15	*STRUCTURAL GLASS FACADES SUBJECTED TO SEISMIC LOADING*	A. Mesquita
16:25	*FINITE ELEMENT ANALYSIS OF POINT FIXED LAMINATED GLASS PANELS UNDER DISTRIBUTED LOAD: A COMPARISON BETWEEN MECHANICAL AND BONDED FIXING SOLUTION*	E. Inca
16:35	*TESTS OF THE EMBEDDED LAMINATED CONNECTION FOR GLASS STRUCTURES*	M. Zdražilová
16:45	*MECHANICAL PROPERTIES OF GLASS-METAL ADHESIVE CONNECTION UNDER ELEVATED TEMPERATURE*	M. Zikmundová
16:55	*DEVELOPMENT OF STRUCTURAL CONNNECTION JOINTS FOR ADHESIVELY BONDED GLASS–PLASTIC-COMPOSITE PANELS*	J. Hänig
17:05	Discussion	All
17:30	End of day 1	CertBond

22nd September 2021		
10:15	Opening	CertBond
10:20	*POST-TENSIONED GLASS BEAMS WITH ADHESIVELY BONDED TENDONS*	J. Cupac
10:30	*ADHESIVE SELECTION FOR THE REALIZATION OF A BONDED EDGE SEAL FOR FLUID FILLED IGU’S*	A. Joachim
10:40	*ON THE IMPROVEMENT OF ADHESION BETWEEN GLASS AND POLYMERIC MATERIALS*	G. Mariggiò
10:50	*EFFECTS OF TEMPERATURE AND PEEL-RATE ON FRACTURE ENERGY IN THE PEELING PROCESS OF A COMMERCIAL SAFETY FILM BY CONSIDERING A VARIABLE PEEL-ANGLE* θ	S. Mattei
11:00	*PROPAGATION SIMULATION OF MULTIPLE CRACKS IN ADHESIVELY BONDED COMPOSITE JOINTS*	L. Münch
11:10	*NUMERICAL SIMULATION OF LASER SHOCK PAINT STRIPPING ON AIRCRAFT ALUMINUM SUBSTRATES*	K. Papadopoulos
11:20	*ADHESION TESTS AND LASER STRIPPING PROCESS OF PAINT USING SHOCK WAVES: APPLICATION TO AERONAUTICAL PARTS IN AL ALLOYS AND CFRP*	S. Unaldi
11:30	*DATA FUSION BASED DAMAGE STUDY USING ELECTROMECHANICAL IMPEDANCE METHOD*	S. Kumar Singh
11:40	*DYNAMICAL MECHANICAL ANALYSIS AND FRACTURE TOUGHNESS OF CARBON REINFORCED EPOXY COMPOSITES*	U. Trdan
11:50	*INTERLEAVING THERMOPLASTIC NON-WOVEN VEILS TO ENHANCE THE STRUCTURAL BEHAVIOUR OF CO-CURED COMPOSITE JOINTS*	O. Inal
12:00	*A PARAMETRIC STUDY OF FRICTION RIVETING ON THE DISIMILAR JOINT FORMATION AND STRENGTH*	D. Klobčar
12:10	Discussion	All
12:30	Closure of Training School & Best Poster announcement	CertBond
12:45	**Lunch break / End of Training School**	

Posters

NONDESTRUCTIVE ANALYSIS OF DEBONDING IN A HONEYCOMB COMPOSITE SANDWICH PANEL

CertBond
COST Action CA18120

Kaleeswaran Balasubramaniam[1*], Shirsendu Sikdar[2], Pawel H. Malinowski[1]
[1]Institute of Fluid Flow Macinery PAS, Gdansk, Poland. [2]Ghent University, Ghent, Belgium

INTRODUCTION

In the study, we focused on using nondestructive debonding detection strategies in honeycomb sandwich composite structures (HCS).The sandwich panels consists of CFRP facets and Aluminium core. Two different sized debondings were identified inside the panels using NDT applications.

RESULTS

Sample HCS studied

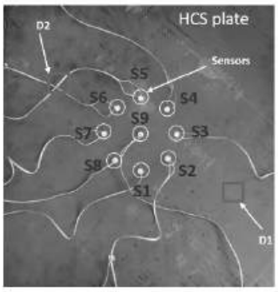

Guided waves from LDV

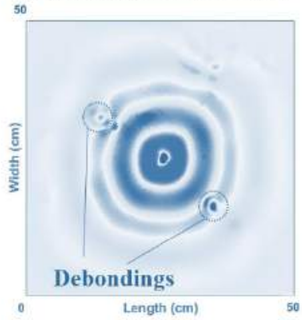

Guided waves from FEM

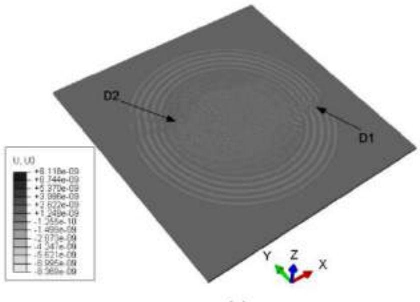

Signal analysis

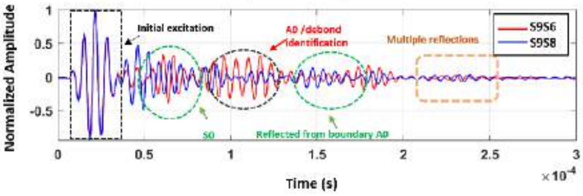

Signal processing with RMSD

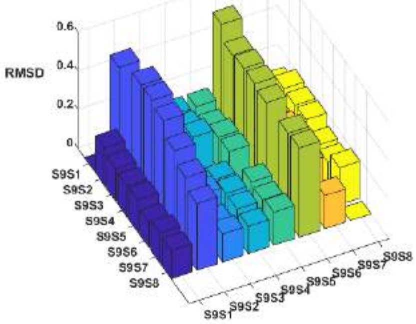

CONCLUSION

The poster shows NDT guided wave analysis of debonding identification inside HCS. Future works depends on localisation and damage severity analysis of the HCS using SHM applications.

Acknowledgements : National Science Centre, Poland: SONTA BIS – 2016/22/E/ST8/00068; Flanders research foundation Belgium – FWO.3E0.2019.0102.01; TASK CI, Gdansk for computational resources.

Funded by the Horizon 2020 Framework Programme of the European Union

cost
EUROPEAN COOPERATION IN SCIENCE & TECHNOLOGY

A LIGHTWEIGHT FLOOR SYSTEM BASED ON SANDWICH PANEL

Pier Giovanni Benzo
Supervisors: José Sena Cruz / João M Pereira

❑ MOTIVATION

The aim of this research is the development of a lightweight floor system based on sandwich panel for applications in the rehabilitation of degraded floor in exiting building and modular construction (see Fig.1).

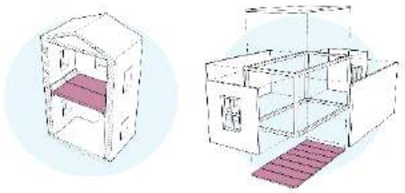

Fig. 1 Existing building floor rehabilitation and modular construction.

❑ ADHESIVELY BONDED CONNECTION

The adhesive must ensure (see Fig.2):

- Load transfer from the face sheets to the webs
- Long-term deformation in fulfillment of the serviceability limit state for floor in residential building
- Chemical compatibility with the PUR foam
- Curing temperature compatible with the foaming process of PUR
- Curing time compatible with the production line cycle of sandwich panels

From preliminary lap shear tests Epoxy resin adhesive showed higher ultimate strength compared to Reactive/Modified Acrylic and polyurethane (PUR) based adhesive.

❑ SANDWICH FLOOR PANELS

Three prototypes were preliminary designed to meet the structural safety, thermal and acoustic requirements. All of the prototypes involve the use of steel face sheets and different web core system (see Fig.3).

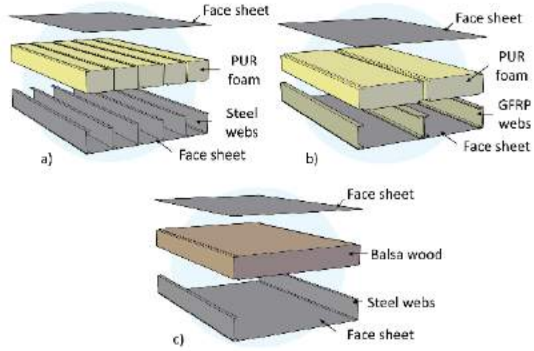

Fig. 3 Layout of a) steel + PUR core system, b) GFRP + PUR and c) steel + balsa wood

❑ CONCLUSIONS AND FUTURE WORK

Prototypes of the steel – PUR foam web core solutions will be manufactured to test the strength of the connections.

❑ ACKNOWLEDGEMENTS

Research project Lightslab – (POCI-01-0247-FEDER-033865), co-funded by the European Regional Development Fund (FEDER)

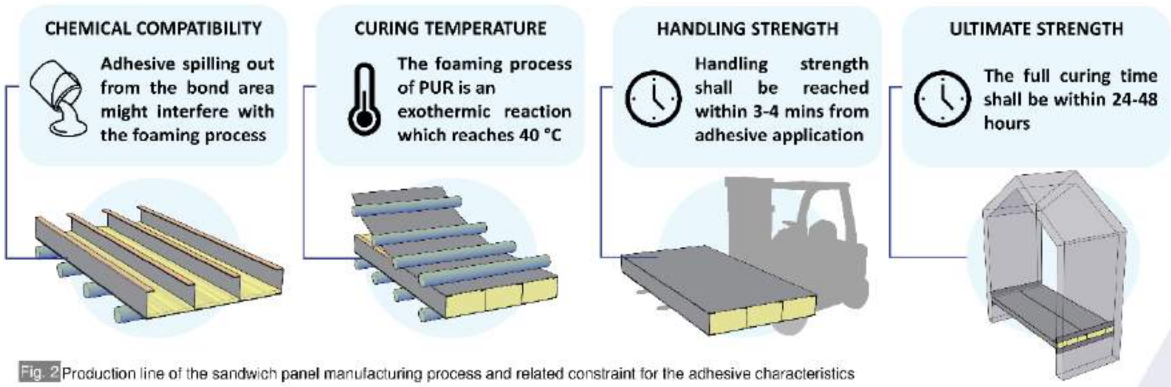

Fig. 2 Production line of the sandwich panel manufacturing process and related constraint for the adhesive characteristics

Funded by the Horizon 2020 Framework Programme of the European Union
COST EUROPEAN COOPERATION IN SCIENCE & TECHNOLOGY

STRUCTURAL GLASS FACADES SUBJECTED TO SEISMIC LOADING

Sandra Jordão (Coordinator of GF SEISMIC Project) ;
Eliana Inca (PhD Student) ;
Afonso Mesquita (Researcher)

CertBond
COST Action CA18120

UNIVERSIDADE D COIMBRA
isise Institute for Sustainability and Innovation in Structural Engineering

1. Motivation, objectives and methodology

Structural glass facades **[Fig. 1]** correspond to a commonly used typology but which may be quite susceptible to the **seismic action** **[Fig. 2]**. Present code provisions do not cover all necessary aspects of this topic and as a consequence the industry of this sector pays a significative tool. The present project aims at contributing to tackle this predicament by preparing tailored **design formulation**, **constructive guidelines** and also **retrofitting recommendations**. The focus will be on **point fixed facades** [Fig. 1], which are the most affected by the seismic load. In the first phase, the parametric variation will encompass the **type of bolt** (**countersunk**, **embedded** and **adhesive** or **bonded**) [Fig. 3] and the **lamination interlayer** (**PVB**, **EVASAFE** and **Sentryglas®**).

Fig. 1 – Examples of glass facades with spiders in point fixed bolted panels

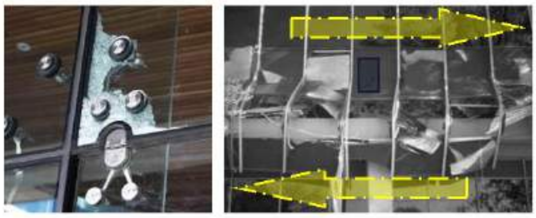

Fig. 2 – Glazing damage during an earthquake

Fig. 3 – Isolated glass panel with 4 stainless steel bolts

The foreseen new analytical design formulation will be duly validated by numerical models calibrated with experimental results of a sector of a full scale facade (with 9 panels). Due to the inherent complexity of seismic analysis of the sector of the facade (**Phase 2**), the work will consider an initial phase were the panel and joints are considered individually (**Phase 1**) [Fig. 4]. This will allow for a step by step analysis which will yield key information on the structural behaviour of the panel and local phenomena, and will allow for detailed step by step numerical modelling of all the key structural features up to the final facade.

2. Phase 1 - Experimental analysis of individual panels subjected to wind load

The present full-scale models of individual glass panels are being considered to fully characterize its own behaviour and study local phenomena at the respective joints, diagonals and central point [Fig. 5].

Fig. 4 – Layout and measuring devices : LVDTs and Strain gauges

Displacement – position Line I - I

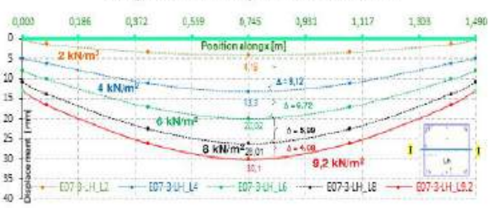

Tension lines

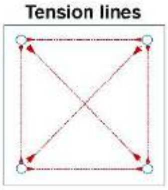

Load – Stress relation

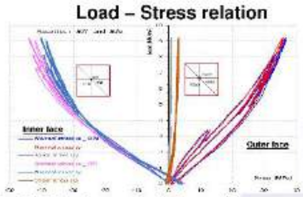

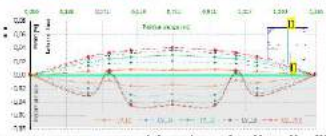

Vertical strain – position curves superposition (y axis, line II - II)

Fig. 5 – Main results regarding the structural behaviour of the individual panels (Phase 1)

Funded by the Horizon 2020 Framework Programme of the European Union
cost EUROPEAN COOPERATION IN SCIENCE & TECHNOLOGY
FCT Fundação para a Ciência e a Tecnologia
Sponsoring Companies:
Sika Portugal
vidromax
b-face
Pentagonal
CRUZFOITO
MARTIFER GROUP
BUILDING FACADE CONSULTANTS & ENGINEERING

VITROCERAMIC COATINGS BONDED TO METALLIC IMPLANTS FOR DENTAL AND ORTHOPAEDIC APPLICATIONS

CertBond
COST Action CA18120

Cristina Busuioc, Izabela Constantinoiu, Dana Miu, Sorin-Ion Jinga

In the framework of "bonded structures" concept, we propose the development of mineral thin films through physical or chemical approaches, with the aim of improving the biological response of metallic implantable devices by controlling the biochemical processes occurred at the interface between the living tissue and artificial bone substitute. It is obvious that the targeted application is dedicated to the tissue engineering and regenerative medicine fields, namely repair of bone defects, regeneration of diseased tissues or replacement of lost parts from the skeletal system.

Looking for potential solutions as response to the large variety of clinical issues, we have explored the vitroceramic area of inorganic materials, which provides, through its glassy and crystalline phases, suitable features for the imposed standards within the domain of hard tissue engineering. Thus, the vitreous matrix ensues a rapid and tunable interaction with the body fluids, while the different families of crystalline domains enhances the mechanical characteristics and biocompatibility factors.

SiO_2–P_2O_5–CaO–CaF_2
SiO_2–P_2O_5–CaO–MgO–ZnO–CaF_2

SiO_2–P_2O_5–CaO–MgO–ZnO
SiO_2–P_2O_5–CaO–SrO–ZnO

SiO_2–P_2O_5–CaO–MgO–Na_2O
SiO_2–P_2O_5–CaO–MgO–SrO–Na_2O
SiO_2–P_2O_5–CaO–MgO–CeO_2–Na_2O

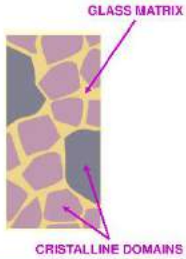

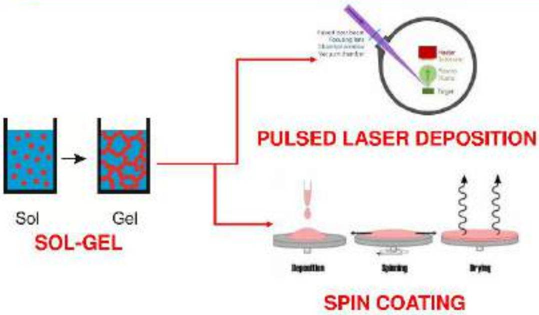

In this context, we present several oxide systems that were studied from the material design to the functionality assessment, the synthesis being carried out through laser ablation on a wet-chemistry prepared target or spin coating combined with a sol-gel approach. The resulting layer-on-substrate bonded structures were characterized from compositional, structural and morphological point of view by X-ray diffraction, Fourier-transform infrared spectroscopy, scanning and transmission electron microscopy, energy-dispersive X-ray spectroscopy and selected area electron diffraction. Moreover, the *in vitro* investigations revealed the bioactivity, biocompatibility and sometimes antibacterial characteristics of the obtained coated metallic implants.

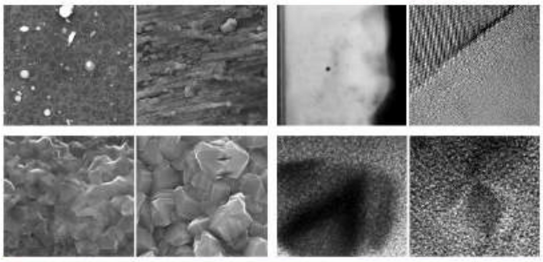

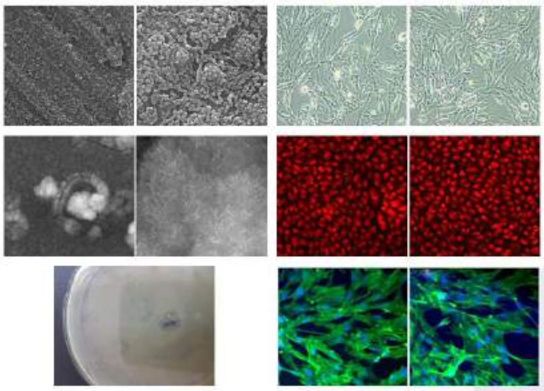

Concluding, the results indicated the growth of nanostructured vitroceramic thin films of few hundreds of nanometers thickness, with an excellent bioactive behaviour after 28 days of testing, as well as good biological effect on the selected cell cultures, which confirms the suitability of such bonded structures for medical applications.

Funded by the Horizon 2020 Framework Programme of the European Union

cost
EUROPEAN COOPERATION IN SCIENCE & TECHNOLOGY

Corresponding author: Cristina BUSUIOC
E-mail: cristina.busuioc@upb.ro
jinga_cristina@yahoo.co.uk

POST-TENSIONED GLASS BEAMS WITH ADHESIVELY BONDED TENDONS

Jagoda Cupać, PhD[1,2]

Supervisors: Prof. Dr. ir. Christian Louter[1]
Prof. Dr. Alain Nussbaumer[2]

[1] Institute of Building Construction
Technische Universität Dresden

[2] Resilient Steel Structures Laboratory
École Polytechnique Fédérale de Lausanne

CertBond
COST Action CA18120

Post-tensioned glass beams are hybrid structural components comprising glass beams reinforced and pre-stressed with ductile tendons to **enhance the load-bearing capacity and post-fracture behaviour of glass**. This novel beam system increases material efficiency and safety of glass beams, while preserving a high level of transparency. **Three variations** of the system – **AS, MD, AMD** - with single or double stainless steel tendon, with and without the application of adhesive, were designed and investigated in an extensive **experimental study**, accompanied by **numerical modeling** and **analytical interpretation of results**. The research has demonstrated that the **adhesive plays an integral role** in transferring the post-tensioning loads into the glass, securing lateral stability and enhancing the residual load-bearing capacity in the event of glass fracture. **A demonstrator – 6m long glass bench ATLAS** - was designed, fabricated and installed at the EPFL campus in Lausanne, sponsored by industrial partners, and presented at the international fair *glasstec 2018*.

EXPERIMENTAL PROGRAMME
Cross-sections of investigated glass beam typology

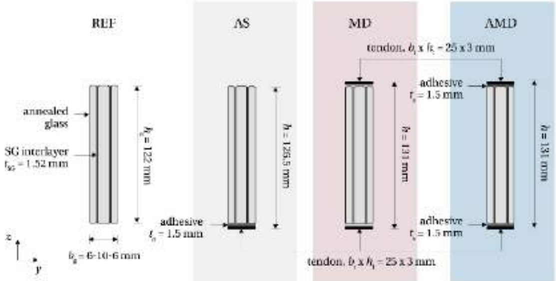

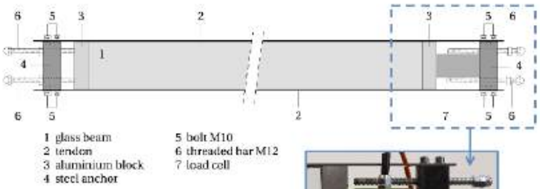

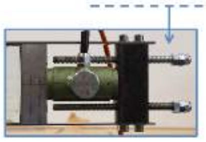

POST-TENSIONING SETUP

COMPARATIVE TEST ANALYSIS
Four-point bending tests on 1.5m long beam specimens

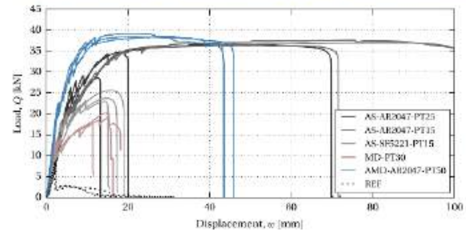

Series	Q_{in} [kN]	Q_{max} [kN]	Q_{in}/Q_{max} [%]
REF	8.64	2.63	31
AS-SF5221-PT15	14.38	24.14	172
AS-AR2047-PT15	16.96	**36.99**	220
AS-AR2047-PT25	**20.80**	33.33	166
MD-PT30	13.25	19.18	145
AMD-AR2047-PT50	**20.03**	**38.76**	194

BEAM TYPE – ADHESIVE – PRE-LOAD [kN] APPLIED THROUGH THE TENDON(S)

- 1.5 – 2.4x higher initial fracture load Q_{in} when compared to reference glass beams (REF)
- Up to 15x higher ultimate failure load Q_{max}
- Superior performance of bonded series - composite action, lateral stability, full flexural capacity, structural integrity in post-fracture state

DEMONSTRATOR I 6m long glass bench supported by UHPFRC blocks

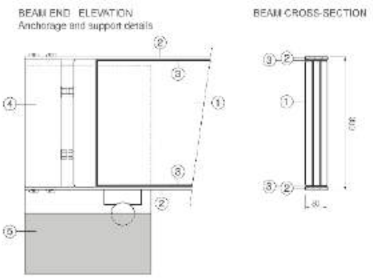

1 – LAMINATED GLASS BEAM; 2 - STAINLESS STEEL TENDON; 3 – ADHESIVE 4 – ANCHORAGE; 5 – UHPFRC SUPPORT

Cupać, J., Nussbaumer, A., and Louter, C. (2021). **Post-tensioning of glass beams: Analytical determination of the allowable pre-load**. Glass Structures & Engineering. https://doi.org/10.1007/s40940-021-00150-0

Cupać, J., Nussbaumer, A., and Louter, C. (2021). **Flexural behaviour of post-tensioned glass beams: Experimental and analytical study of three beam typologies**. Composite Structures 255. https://doi.org/10.1016/j.compstruct.2020.112971

Funded by the Horizon 2020 Framework Programme of the European Union

cost
EUROPEAN COOPERATION IN SCIENCE & TECHNOLOGY

EPFL

TECHNISCHE UNIVERSITÄT DRESDEN

APPLICATION OF LASER SHOCK PEENING ON HIGH ELASTIC LIMIT STEELS FOR POWER TRANSMISSION COMPONENTS

Maxime Guerbois

Supervisors: Laurent Berthe & Véronique Favier

CertBond
COST Action CA18120

Context & Goals:

Objective: Improving the gears life cycle for naval and aeronautics industries

As the immobilisation of vehicles is an issue, dealing with the ageing of the gears, and being able to realise maintenance on the vehicle itself is one of the main concern of this project.

The treatment method needs to be applicable in production and in maintenance

- Laser Shock Peening (LSP) is used as a mean to improve fatigue life by introducing high level of residual stresses and improving the corrosion behaviour of treated pieces.[1,2]
- The transport of the beam by optical fiber is required to reach reduced access areas.

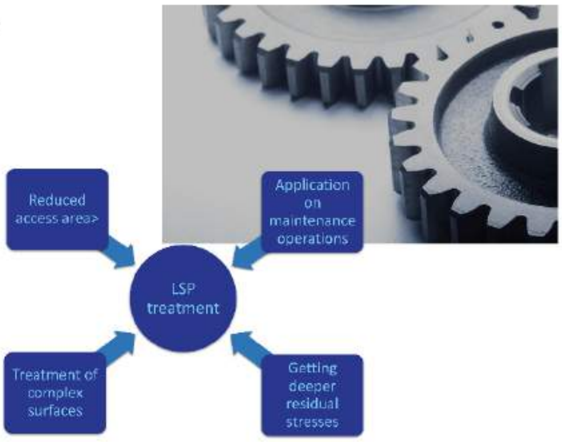

Laser Shock Peening process

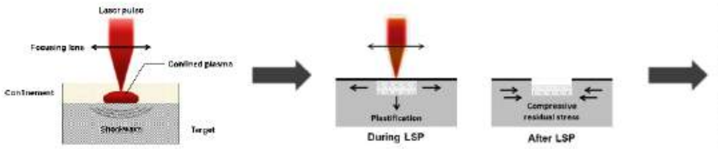

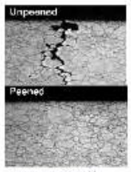

Figure taken from [1]

Sample after LSP treatment

- The plasma produced on the surface by the impulsion produces a pressure over 1 GPa during its release.
- This impulsion leads to the introduction of deep and high compressive residual stress in the treated piece, compared to conventional peening.
- Prevents the cracks on the surface.
- Using low energy and small spot size, it is possible to transport the beam through optical fiber.

LSP treatment parameters

All the LSP treatment were realised at the Héphaistos facility at PIMM Laboratory.

- λ = 532 nm
- Spot size = 1 mm, (order of magnitude)
- Frequency : 2 Hz
- Pulse duration : 7 ns
- Overlapping : 80% - 85% (order of magnitude)
- Intensity : 12-16 GW/cm² (order of magnitude)
- Targets : 16NCD13 blocks (60x60x20 mm)
- Surface treated : 20x20 mm²

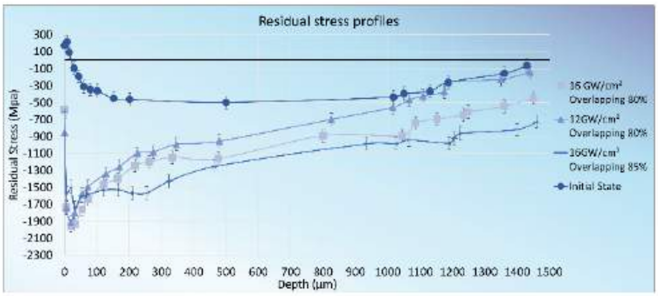

Results

- The highest compression is obtained for a 20 µm depth, with 2GPa.
- The higher the overlap is, the higher the compressive residual stress is.
- Residual stress can be observed over more than 1 mm below the surface.
- The Average Roughness is 1.4 µm on the treated specimen. This is 0.9 µm higher than before LSP.
- The surface ablation of 25 µm is a real issue for now, as it is radically changing the geometry of the specimen.

Funded by the Horizon 2020 Framework Programme of the European Union

COST
EUROPEAN COOPERATION IN SCIENCE & TECHNOLOGY

References

[1] Yuji Sano, Koichi Akita, Kiyotaka Masaki, Yasuo Ochi, Igor Altenberger, and Berthold Scholtes. Laser peening without coating as a surface enhancement technology. Pulse, 100 (40):250mJ, 2006.
[2] Fabbro, R., et al. "Physics and applications of laser-shock processing." *Journal of laser applications* 10.6 (1998): 265-279.

DEVELOPMENT OF STRUCTURAL CONNNECTION JOINTS FOR ADHESIVELY BONDED GLASS–PLASTIC-COMPOSITE PANELS

Julian Hänig

Supervisors: Christian Louter / Bernhard Weller

CertBond
COST Action CA18120

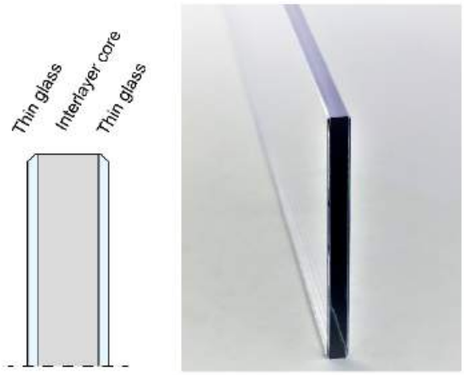

Figure 1: Glass–plastic-composite panel structure (build-up and view)

Motivation

All-glass systems such as mobile glass partition walls and glass doors set high requirements for transparency, lightness and durability. The interconnection between the panels is conventionally performed by eye-catching fittings and clamping details. Innovative glass–plastic-composite panels (Figure 1) consist of adhesively bonded thin glass cover layers by a thick polymer Polymethylmethacrylate (PMMA) interlayer core. The composites show high-performance load-bearing behaviour, durability and exhibit full transparency at low self-weight. Additionally, the novel composite assembly allows for a direct connection into the mechanically processed PMMA interlayer core.

Novel glass construction with glass–plastic-composite panels utilize the low panel self-weight and require small as well as unobtrusive connections to fulfil the desired maximum transparency. Therefore, integrated structural connection joints with transparent structural adhesives are under development and tested with a focus on applications in all-glass systems for the building industry.

Connection Design

The adhesive connection joint was designed for a minimized size and directly integrated into the PMMA interlayer core using transparent adhesives. Thus, the increased fracture toughness of the PMMA compared to glass provides improved resistance to fracture and a reduction in glass stress concentrations.

Figure 2 provides an overview of the component design with associated dimensions. The stainless-steel insert consists of an exterior block serving as a representation of connection hardware with an insert tab that is adhesively bonded to the milled PMMA interlayer core. The adhesive joint was designed with a gap of 0.5–1 mm for the application of structural adhesives.

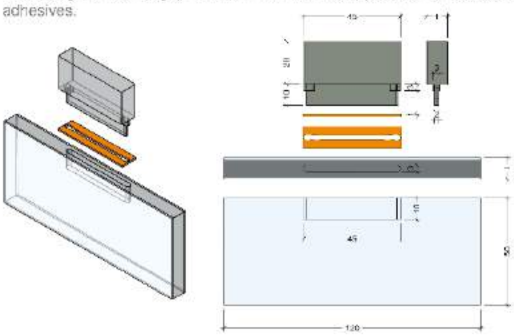

Figure 2: Connection design of the structural connection joint

Adhesive Selection + Experimental Testing

A preliminary study of 14 structural adhesives, consisting of polyurethanes, acrylates, epoxides and silicones, was conducted to assess compatibility with the desired adhesive joint. To compliment the desire for a less obtrusive connection, a colourless transparent appearance was a crucial initial parameter in assessing the success of the adhesive. Other parameters included viscosity, applicability for small gap sizes of 0,5–1 mm, adhesion, shrinkage and imperfections after application. A reduced pool of viable adhesives was tested in UV-ageing and climate testing to assess long-term aesthetic stability.

Based on the aforementioned evaluation criteria 3 structural adhesives with varying stiffnesses were selected for mechanical testing:

- 2-C epoxy (Huntsman Araldite® 2020) – E = 2468 N/mm²
- UV curing acrylate (DELO® Photobond ® GB368) – E = 900 N/mm²
- 2-C polyurethane (technicoll® 9430-1) – E = 25 N/mm²

The connections for glass–plastic-composite panels were experimentally tested with the final adhesive selection. Five test specimens each test series in thicknesses of t = 8 and 12 mm with 1 mm annealed thin glass (ANG) were tested for short term load-bearing behaviour under pure tensile and pure shear force in custom made test rigs.

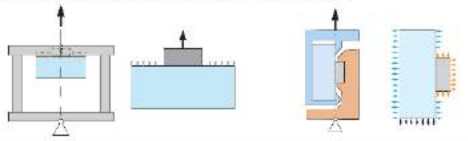

Summary + Conclusions

The tested connection joints showed significant differences in their load-bearing behaviour that was mainly dependent on the flexibility and strength of the adhesive. The more stiff adhesive connections with epoxy and acrylate showed substrate failure and exceled in connection application. The final failure of the stiff adhesive connections highly exceeds the initial glass defect and leads to desirable ductility. The flexible polyurethane adhesive displayed the lowest connection performance with early cohesive as well as adhesive failure at insufficient load levels. The thicker build-up showed higher resistance to initial glass defect due to lower glass stresses. In conclusion, the designed connections provide suitable levels of force transfer given the size of connections and show ductility offered by the polymeric PMMA interlayer core. This allows for a suitable hardware design in all-glass systems. Further investigations examine the connection performance using panels with stronger glass faces made of chemically strengthened glass (CSG).

Funded by the Horizon 2020 Framework Programme of the European Union

cost EUROPEAN COOPERATION IN SCIENCE & TECHNOLOGY

TECHNISCHE UNIVERSITÄT DRESDEN

BAUKO

INTERLEAVING THERMOPLASTIC NON-WOVEN VEILS TO ENHANCE THE STRUCTURAL BEHAVIOUR OF CO-CURED COMPOSITE JOINTS

CertBond
COST Action CA18120

Oğuzcan İnal

Supervisors: Prasad Potluri, Constantinos Soutis, Kali-Babu Katnam

The University of Manchester, UK

WHY COMPOSITE BONDED JOINTS?

- Lighter structure
- Comparatively uniform stress/load transfer
- No need to drill holes (No damage to the composite laminate)

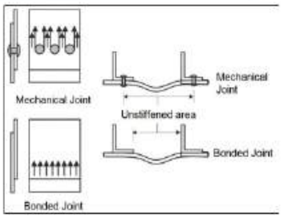

Figure 1: Load transfer map of composite joints [1].

WHY CO-CURING?

- No surface preparation required.
- One-step manufacturing (simultaneous bonding and curing).
- <u>However, co-cured joints have low fracture resistance!</u>

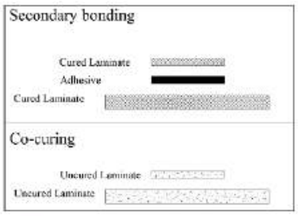

Figure 2: Commonly used bonding strategies.

HOW TO ENHANCE FRACTURE PROPERTIES?

- Interleaving thermoplastic non-woven veils to the interlaminar regions of CFRP laminates [2].

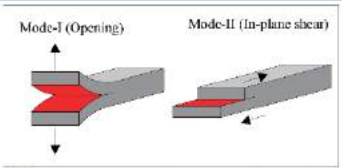

10 g/m² Polyphenylene sulphide (PPS) microfibre non-woven veil

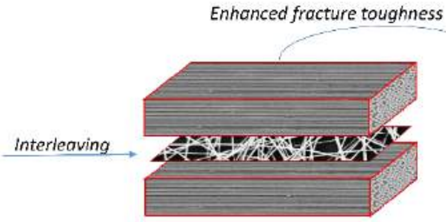

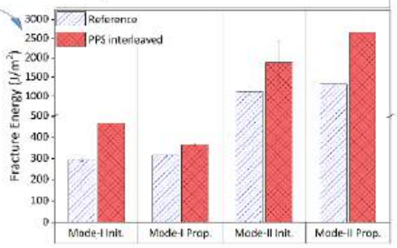

CAN IMPROVED FRACTURE TOUGHNESS BE TRANSLATED TO SKIN-STIFFENER CO-CURED JOINTS?

- One-layer of PPS microfibre non-woven veil at the skin-stiffener interface significantly improves the failure load.

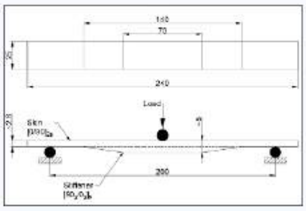

Quasi-static three-point bending testing of cross-ply skin-stiffener co-cured CFRP joint

Skin-stiffener debonding / final failure

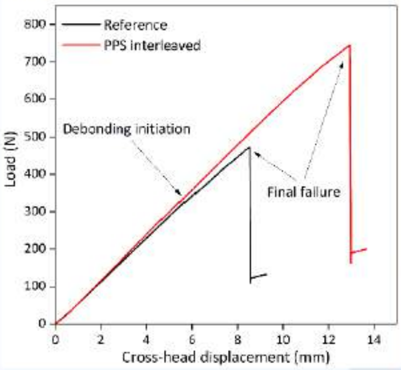

Funded by the Horizon 2020 Framework Programme of the European Union

cost
EUROPEAN COOPERATION IN SCIENCE & TECHNOLOGY

References:

1-Campbell Jr, F.C., Manufacturing processes for advanced composites. 2003: Elsevier.

2-İnal, O., Akbolat, M. Ç., Soutis, C., & Katnam, K. B. (2021). Toughening mechanisms in cost-effective carbon-epoxy laminates with thermoplastic veils: Mode-I and in-situ SEM fracture characterisation. International Journal of Lightweight Materials and Manufacture, 4(1), 50-61.

FINITE ELEMENT ANALYSIS OF POINT FIXED LAMINATED GLASS PANELS UNDER DISTRIBUTED LOAD: A COMPARISON BETWEEN MECHANICAL AND BONDED FIXING SOLUTION

CertBond
COST Action CA18120

Eliana Inca (PhD Student); Sandra Jordão (Coordinator of GF SEISMIC Project) ;
Chiara Bedon (Co-Supervisor); Afonso Mesquita (Researcher)

Motivation, Objectives & Methodologies

Pointed Fixed Laminated Glass System are typically used on contemporary building's façade as an architectural statement of transparency, allowing to reach lighter and spacious facilities [Fig. 1]. The fixing elements are characterized by **stainless steel bolts**, that are mechanically attached or bonded to the glass surface [Fig. 1]. However, despite the exponential growth of glass façade construction industry, **design codes** for glass elements are still **under development**.

The numerical analysis here presented, was developed with the aim of **characterize the structural behavior** of Bolted Pointed Fixed Laminated Glass Panels (**PFLGP**), subjected to orthogonal distributed load, e.g., Wind Load. The study focused on the **methodologies to numerically modelled** the articulated bolts and its interaction with the Laminated Glass Panels (LGP), benchmarked with an ongoing **experimental campaign** [Fig. 3]. The first stage was the characterization of the lamination material, considering three different interlayers: PVB, EVA and SentryGlas® [Fig. 2] [Fig. 4]. Next, the characterization of PFLGPs and the correspondent finite element numerical models [Fig. 5], were developed, aiming to compare the performance of three different fixing methods: i) Mechanical (Countersunk bolts), ii) Laminated (Embedded) and iii) Bonded bolts.

Fig. 1 – Examples of glass façades and utilization of spiders in point fixed bolted panels

Fig. 2 – Experimental campaign Simple Supported Laminated Glass Panels

Fig. 3 – Layout of Experimental Campaign for PFGFS, different bolt fixings and interlayers

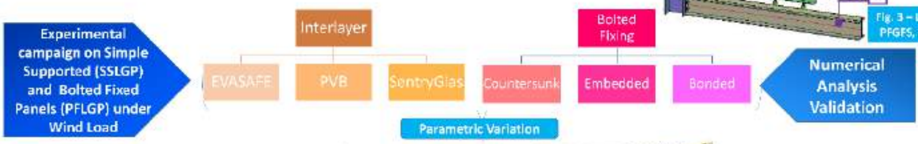

Fig. 4– Workflow

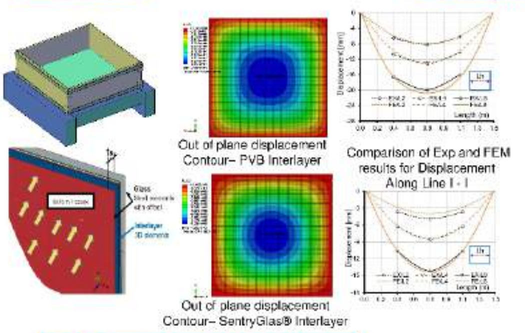

Fig. 5– Numerical Analysis and Results for SSLGP

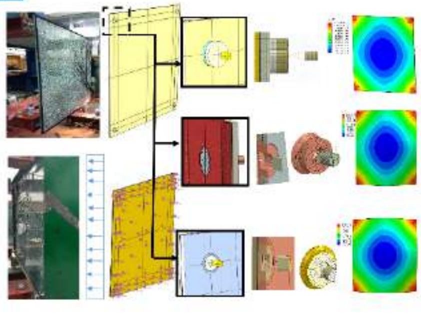

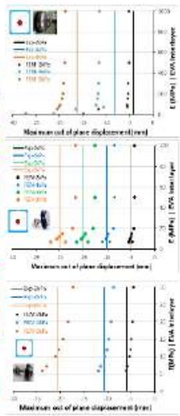

Fig. 6– Numerical Analysis and Results for PFLGP

Outcomes

The methodologies to develop Numerical models for Countersunk, Embedded and Bonded stainless-steel articulated point fixings for Laminated Glass Panels (PFLGP) [Fig. 3], used for facade systems, were presented. The numerical models allow to compare the performance for bonded and classical mechanical fixing solutions, while characterizing the most important parameters for the PFGFS [Fig. 6], in terms of Interaction properties and interlayer material. The results from the numerical models were benchmark with experimental test results from GF-Seismic research project.

Funded by the Horizon 2020 Framework Programme of the European Union

Sponsoring Companies:

ADHESIVE SELECTION FOR THE REALIZATION OF A BONDED EDGE SEAL FOR FLUID FILLED IGU's

CertBond
COST Action CA18120

Alina Joachim

Supervisors: Christian Louter / Bernhard Weller

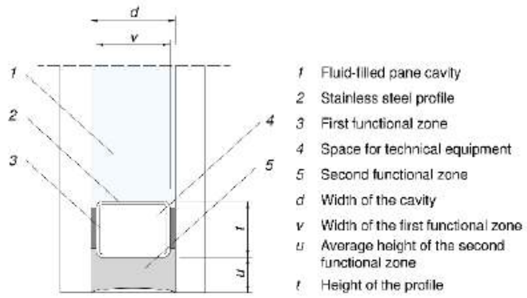

Figure 1: Design of the structrurally bonded edge seal for fluid-filled IGU

Motivation

Modern architecture strives for a maximum degree of transparency. Especially in office buildings, the number of all-glass façades is constantly increasing. Multi-pane insulating glass units (IGUs) are used. The principle of a IGU is based on the good thermal insulation of the gas-filled cavity. However, in the case of long-lasting and large temperature differences, heat exchange takes place even in high-efficient IGUs. The idea of filling the cavity with a fluid is based on the high thermal conductivity of a circulating fluid. Compared to air, water reacts about ten times more sensitively to temperature changes and can therefore be quickly adapted to building conditions and requirements. The temperature in the interior can be kept constant by heating or cooling the fluid in the cavity.

Structural-sealant glazings are used in modern façade designs to replace external clamps and create a homogeneous glass surface. The current research project *fluidIGU* is working on the development of a structurally bonded edge seal that can withstand the high hydrostatic loads and is also resistant to the ageing caused by permanent contact with fluids. The aim is to create a façade element in full floor-to-ceiling size with the height of 3000 mm.

Structurally Bonded Edge Seal Design

The design of the novel edge seal is based on the principle of a conventional edge seal of gas-filled IGUs. Two functional zones are used. The first functional zone is located between the spacer and the glass and is responsible for the sealing. The second zone on the outside of the spacer takes all structural loads from the hydrostatic pressure in the cavity, the wind and the live loads.

This leads to the following structurally bonded edge seal design for the fluid-filled IGU (compare Figure 1):

- Hollow stainless-steel profile as a spacer
- $v = t = 15$ mm installation space for technical equipment
- Water-ethylene glycol mixture (70:30) as a fluid (ethylene glycol prevents the growth of algae and serves as an antifreeze)
- Optimal thickness of the first functional zone $d_{zone\,1} = 4$ mm (determined by numerical analysis)
- Total cavity width $d_{total} = 23$ mm

Test Program for Material Selection

For the preselection of the adhesives for both functional zones, the following requirements have to be fulfilled by the adhesives:

Adhesive for First Functional Zone

- High adhesion to glass and to stainless steel
- Desired adhesive joint dimensions can be realized
- High resistance to water and ethylene glycol
- Impermeability to the fluid
- Viscosity >10 000 mPa·s

Adhesive for Second Functional Zone

- Two-component curing
- Desired adhesive joint dimensions can be realized
- Valid European Technical Approval (ETA) according to ETAG 002-1
- Design stress resistance $\sigma_d > 0.20$ MPa

Based on the preselection requirements 14 commercial available adhesives were tested in small-scale tests for their suitability for the first functional zone and 5 adhesives for the second functional zone. According to uniaxial tensile tests performed at the TU Dresden, all tested adhesives show elastic behavior and a tensile strength of 1–10 N/mm² with an average elongation at break of 70–300 %.

Experimental tests of the test program presented below are currently running. With progressing test program, adhesives are eliminated based on the results obtained.

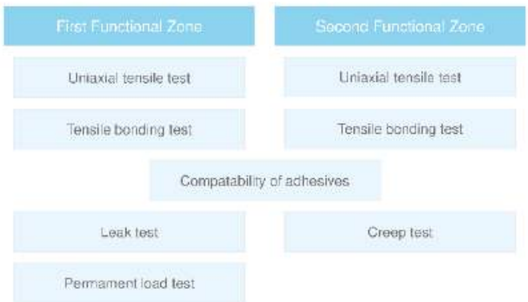

Funded by the Horizon 2020 Framework Programme of the European Union

cost EUROPEAN COOPERATION IN SCIENCE & TECHNOLOGY

TECHNISCHE UNIVERSITÄT DRESDEN

BAUKO

A PARAMETRIC STUDY OF FRICTION RIVETING ON THE DISIMILAR JOINT FORMATION AND STRENGTH

CertBond
COST Action CA18120

Damjan Klobčar[1], Haidi Škrabar[1], Franci Pušavec[1], Drago Bračun [1], Aljaž Ščetinec[1], Ivan Jurič[2], Ivica Garašič[2], Zoran Kožuh[2]

1 Faculty of Mechanical Engineering, University of Ljubljana, Slovenia, *correspondence: damjan.klobcar@fs.uni-lj.si
2Faculty of Mechanical Engineering and Naval Architecture, University of Zagreb, Croatia

ABSTRACT

Similar or dissimilar materials in aerospace applications can be joined using friction. In this way a certain CRM components of titanium alloys, stainless steel and magnesium alloys can be replaced by aluminium alloys or composites. Such replacement can reduce the weight of aerospace component and substantially reduce the fuel consumption and CO_2 emissions. The present work shows the effect of friction riveting parameters on the anchoring effect and joint strength. The materials used are aluminium alloy 2024 and polyethermide. After the riveting the joints were examined by X-ray, which showed an insight into the joint geometry and anchoring shape of the rivet. Part of the joints were tested with pull-out test and from the rest macro-sections were prepared. Samples produced with higher mechanical energy achieved greater anchoring depths of rivets into the polymetric base plates and consequently higher pull-out forces. It was established that the most important parameters are friction force and time of the first phase of friction riveting process. Higher energy input in the first phase is reflected in higher rivet deformation i.e. higher anchoring effect.

Keywords: friction riveting, reduction of CRM's, aluminium alloy 2024, polyethermide, pull-out test, NDT

MATERIALS AND METHODS

The subject of the study were rivets made of aluminum rods (Fig. 1) grade 2024-T351 in the polythermide (PEI) base material (24x24x14 mm). Rivets were made with a CNC Doosan NX 6500 II Aluminum rods (Fig. 1) were clamped in the machine at the thinner section.
Additionally, Fig. 1 shows friction riveting process.

Rivet formation was section in two phases where each of the phases had different combination of the feed speed Vf, and penetration depth **Z**.

1. Aluminum rod made contact with the base material and heating due friction initiated followed by the insertion of the rod in the base material
2. Increase of feed speed and insertion depth followed by stopped rotation and consolidation.

Figure 1: Aluminum rivet dimension and riveting process.

Process parameters

Spindle speed was a constant at 20000 min^{-1}. Z in the first phase was 5 mm, 9 mm and 10 mm while Vf was either 100 mm/min or 200 mm/min. In the second phase Z was 10 mm, 15 mm, 19 mm or 20 mm. While Vf was 900 mm/min, 1200 mm/min, 1800 mm/min or 2000 m/min. Parameters for each rivet are shown in the table 1.

Sample nr.	Phase 1		Phase 2	
	Z [mm]	Vf [mm/min]	Z [mm]	Vf [mm/min]
1	5	100	10	1200
2	5	200	15	2000
3	10	200	20	1200
4	10	200	20	1800
5	10	200	20	900
6	9	200	20	900
7	9	200	19	900

Destructive and non-destructive testing

To determine the quality of friction rivets, they was examined by means of X-ray tomography and pull-out test. X-ray tomography showed an insight into the joint geometry and anchoring shape of the rivet. Part of the joints were tested with a pull-out test. From the remainder macro-sections were prepared.

Modelling of the process

Heat input (E_M) was modelled by calculation of mechanical energy, as shown in the Equation 1

$$E_M = E_{T1} + E_{T2} = \int T1 \times \omega \times dt + \int T2 \times \omega \times dt \ [J] \quad \text{Eq. 1}$$

Where E_{T1} And E_{T2} represent energy input through torque (T) and angular velocity (ω) in the first and second phase of river formation.

The volumetric ratio [0-1] (Eq. 2) establishes a simplified quotient between the volume of the plastically deformed rivet and the volume of polymer offering mechanical resistance to a rivet pull-out action. The volumetric ratio (VR) is determined by Equation 2. Equation components are explained with the assist of the Fig. 2. H is the penetration depth, B the deformed tip height, W the maximum deformed width of the rivet tip and D the original rivet diameter

$$VR = \frac{(W^2 - D^2) \cdot D_p}{H \cdot W^2} \ [/] \quad \text{Eq. 2}$$

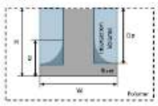

Figure 2: Volumetric ratio and interaction volume in a friction rivet

RESULTS

X-ray tomography

Dimensions of all rivets are shown in the Fig 3, along with the corresponding volumetric ratio. Example of rivet dimensions measurement is shown in Fig 4.

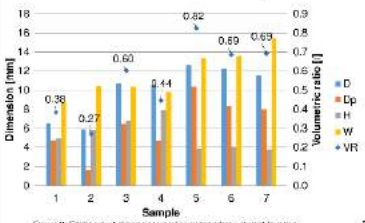

Figure 3: Friction rivet dimensions and corresponding volumetric ratios

Figure 3: Friction rivet dimensions measurement.

X-ray Tomography

Figure 5 shows X-ray tomography images of all rivets. In addition to dimensions measurements, each image was examined for possible defects in the joint. Three different joint shapes were recognized: anchor (5, 6, 7), bell with decreasing diameter (3), bell with highest diameter at the end of rivet.

1

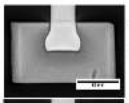

- Bell-shaped rivet No fractures
- Low penetration depth

2

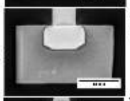

- Bell-shaped rivet
- No fractions
- Lack of polymer above the bell to hold the rivet in place

3

- Bell-shaped rivet with decreasing diameter towards the bottom
- No fractions
- High depth of penetration

4

- Bell-shaped rivet with decreasing diameter towards the bottom
- No fractions
- High depth of penetration

5

- Anchor-shaped rived
- Fractions in the rivet
- High depth of penetration and diameter of the rivet
- Defects in the interaction volume of the polymer

6

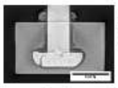

- Anchor-shaped rivet
- Fractions in the rivet
- High depth of penetration and diameter of the rivet

7

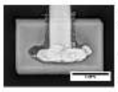

- Anchor-shaped rivet
- Great fractions in the rivet
- Aluminum crumpled in the interaction volume
- Additional defects in the interaction volume

Figure 5: X-ray tomography of manufactured friction rivets

Pull-out test results

Pull-out test results are shown in the Fig 7, which does not include samples 3, 4, and 6, since those samples failed in the base material of the rivet. Three different failure modes observed (Figure 6):

a)

- Samples 1 and 2 (low depth of penetration)
- Failure occurs in the polymer base material. **This failure mode can be observed at friction rivets with low depth of penetration.**

b)

- Samples 5 and 7
- Failure happens in the deformed section of the aluminum rivet. Fraction of the polymer from the interaction volume breaks at non deformed section of the rivet. **Highest pull-out force was observed here.**

c)

- Samples 3, 4, 6
- Failure in the base material of the rivet.

Figure 6: Macrographs of friction rivets after pull-out test

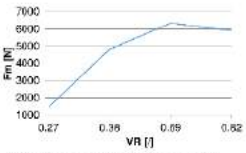

Figure 7: Pull-out force in relation to the volumetric ratio

CONCLUSIONS

1. Recognized joint shapes:
   - Bell shape with decreasing diameter.
   - Bell shape with highest diameter at the end of the rivet.
   - Anchor shape.
2. Pull-out force increases with increasing VR. With increasing VR over 0,69 the pullout force shows decreasing trend
3. Three different failure modes at pull-out test:
   - Failure in the polymer base material.
   - Failure in the deformed section of the aluminum rivet.
   - Failure in the undeformed section of the aluminum rivet.
4. Two additional possible defects were recognized:
   - Crumpling of the aluminum rivet inside the polymer base material.
   - Defects in the interaction volume.

Funded by the Horizon 2020 Framework Programme of the European Union

cost
EUROPEAN COOPERATION IN SCIENCE & TECHNOLOGY

LAVAR

FSB

On the improvement of adhesion between glass and polymeric materials

Gregorio Mariggiò, Sara Dalle Vacche

Supervisors: Mauro Corrado, Roberta Bongiovanni, Christian Louter

CertBond
COST Action CA18120

Objective

The goal of this research is to improve the adhesion between UV-curable polymers and glass and demonstrate, using two examples, how a strong and reliable adhesion can lead to the development of stronger, more durable, and lighter load-bearing glass structures. The adhesion-promoting properties of silane coupling agents with polymers are used to create strong bonds between 3D printed materials and glass to develop lighter and more reliable composite materials, as well as to provide durable connections between glass and a coating developed by the authors to prevent stress corrosion.

Silanization

Glass surface modification by immersion in water solution of the silane (0.2 % vol): Creation of strong and durable Si-O-Si bridging bonds between glass and polymers.

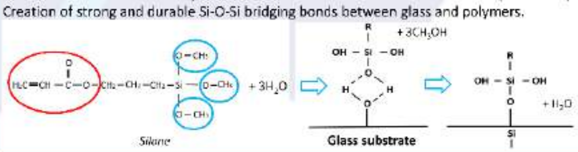

Glass stress corrosion mechanism

Decrease of the bending strength during aging under load, favored by the presence of water:

- related to the sub-critical growth of micrometric surface defects and cracks
- rupture of silicon-oxygen bonds
- activation energy provided by external stress

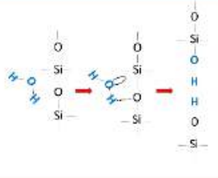

Development of a functional coating for inhibiting stress corrosion

Requirements:
Hydrophobicity,
Low permeability to water
Good adhesion to glass

Main challenge and approach:
Hydrophobicity and **adhesion** are competing properties: need for a compositional profile from the air side to the substrate. External surface (exposed to the environment) enriched with fluorinated moieties, acrylated silane to improve adhesion at the surface in contact with glass.

I. Preparation of coated glass samples

II. Evaluation of the adhesion between coating and glass

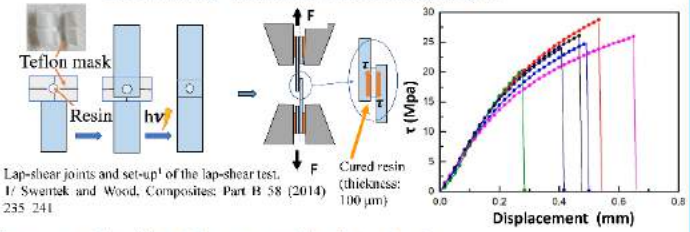

Lap-shear joints and set-up[1] of the lap-shear test.
1/ Swentek and Wood, Composites: Part B 58 (2014) 235–241

III. Evaluation of the effectiveness and durability of the coating and the adhesive bond

1. **Mechanical ageing**, accomplished by subjecting coated samples to cyclic loads;
2. **Natural weathering**, performed by exposing coated samples to atmospheric agents;
3. **Artificial weathering**, carried out by exposing coated specimens to fluorescent UV lamps, heat and water.

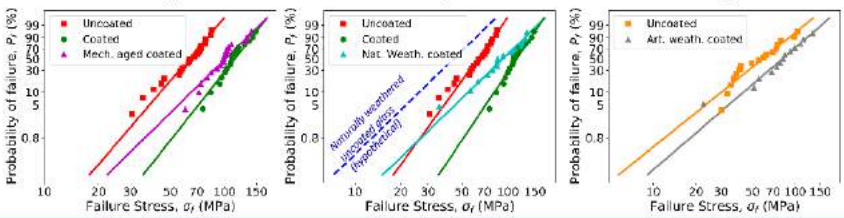

Enhancement of the adhesive strength of 3D-printed materials to glass

Sandwich panels consisting of two outer thin glasses and an inner additively manufactured polymeric core can replace conventional façade glazing[2] because of their superior strength-to-weight ratio, which reduces manufacturing costs and emissions. However, the structural integrity and full exploitation of the bending strength of composites depend on the reliability, strength and durability of the bond between polymer and glass. The employment of silane coupling agents allows to create covalent bonds between glass and UV-curable polymers, resulting in:

- Very high adhesive strength $\tau \approx 40$ MPa
- Transparent and nanometer-thick adhesive layer
- Printing of the polymeric core directly on the silanized glass
- Fully automatable production of the glass-polymer composite

2/ Kothe, Bodenko, Nicklisch, Louter. Civil Engineering Design. 2021; 3: 35–42

Lap-shear test results

Sample	Adhesive strength τ (Mpa)	Failure
1	48,99	Stock break
2	52,15	Adhesive
3	39,22	Adhesive
4	39,60	Adhesive
5	56,00	Stock break
6	42,22	Stock break
7	47,84	Stock break
8	53,27	Stock break
9	47,97	Adhesive
10	53,13	Stock break
11	36,65	Adhesive

Adhesive Strength $\tau = 43{,}12 \pm 6.61$ MPa

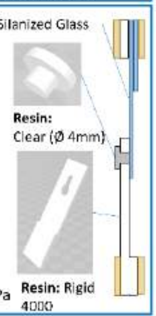

Research products

- S. Dalle Vacche, G. Mariggiò, A. Vitale, R. Bongiovanni, M. Corrado: Compositionally Graded Hydrophobic UV-Cured Coatings for the Prevention of Glass Stress Corrosion. Coatings 9:7, 2019.
- G. Mariggiò, S. Dalle Vacche, R. Bongiovanni, C. Louter, M. Corrado: Enhancing the design bending strength of new and aged glass with a functional coating. Glass Structures & Engineering, 5:135, 2020.
- G. Mariggiò, S. Dalle Vacche, R. Bongiovanni, C. Louter, M. Corrado: A durable coating for an improved glass bending strength under long-term loads. Glass Structures & Engineering, 2021. (in press)

Funded by the Horizon 2020 Framework Programme of the European Union

COST
EUROPEAN COOPERATION IN SCIENCE & TECHNOLOGY

Effects of temperature and peel-rate on fracture energy in the peeling process of a commercial safety film by considering a variable peel-angle θ

CertBond
COST Action CA18120

Silvana Mattei, Luca Cozzarini

Supervisors: Chiara Bedon

Abstract The use of protective films on glass elements is common also in the civil engineering field but the literature is lacking in definition of the advantages in using protective films on glass impact. The aim of this research is to provide a complete characterization of the adhesive layer at the interface by using in combination experimental tests, theoretical assessment and numerical parametric studies in Abaqus/Simulia. The adhesion strength can be used as a critical parameter in the definition of delamination. In particular, it has been studied how the influence of temperature and aging time can influence the characteristics of these materials.

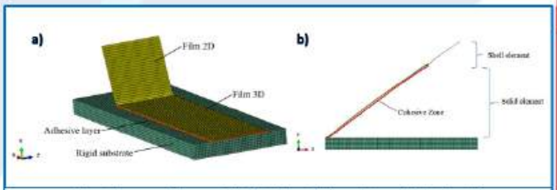

Fig.1 Fracture Energy FE Model: 3d view (a) and 2d view (b).

Introduction In addition to the energy saving features, many experimental studies have shown how the use of films can increase the performance of glass, both in terms of resistance and in terms of safety especially in case of impulsive and unpredictable nature events (e.g., Smith and Brokaw [1]). The numerical ABAQUS model (as shown in Fig.1) has been used to assess the adhesion energy and to develop a consistent cohesive zone law (Fig.2) for the specific protective film (as reported in Fig.3) in a peeling configuration in order to investigated fracture behaviour by properly reproducing experimental setup.

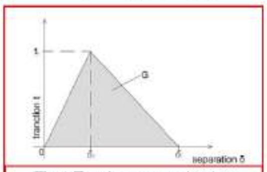

Fig.2 Traction-separation law.

Materials and Methods The experimental program can be divided in two main parts based on the nature of the involved experiments. The first part concerned the characterization of materials making up the film, with DSC and IR Spectroscopy analyses (Fig.4), and its mechanical behaviour while the second dealt with the numerical characterization of adhesive layer. Moreover, a theoretical approach, based on Kinloch discussion [2], was introduced to consider the peel angle variation from an initial 90-degree configuration (i.e., Fig.5).

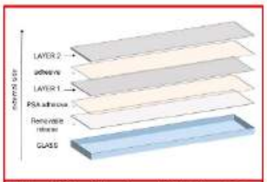

Fig.3 Stratification detail of safety film on glass substrate.

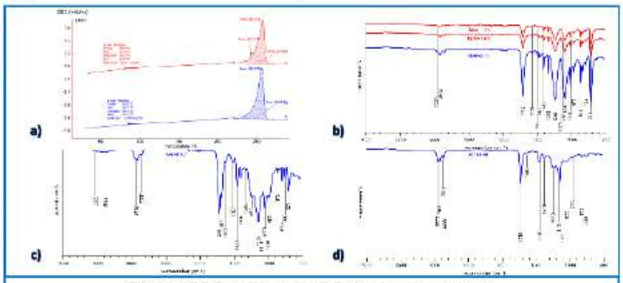

Fig.4 (a) DSC and (b, c, d) IR Spectroscopy analyses.

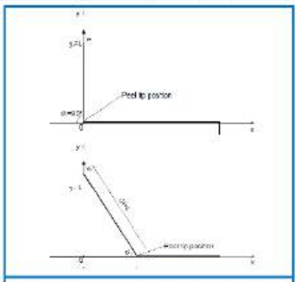

Fig.5 Schematic geometry of peel-test.

Results and conclusion Generally, the temperature, such as peel-rate, is known to significantly influence the mechanical behaviour of polymers. Firstly, it is important to note that although the temperature range explored in this work is below the glass transition temperature (T_g) of the material, the influence of temperature on PET tensile properties has not be neglected in order to properly model the material in FE software. Finally, 54 parametric numerical analyses - eleven samples in function of temperature, ageing time and peeling rate - show a good agreement between the shape of each pair of outputs (numerical and theoretical according to a modified Kinloch approach), as shown in Fig.6, but the effect of the variable peel-angle and the influence of little impurities or inclusion lead to an underestimation for FE simulations.

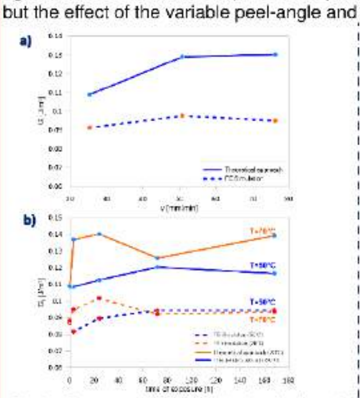

Fig.6 Fracture energy calculated by the theoretical approach and by ABAQUS simulations as functions of (a) peel-rate and (b) temperature.

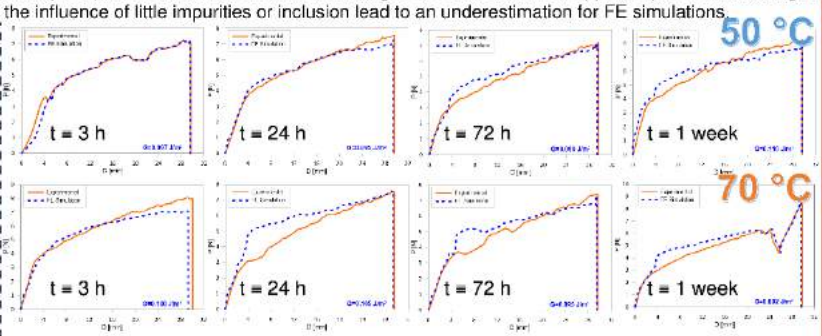

Fig.7 For simplicity, for one specimen of each aged sample, a comparison between experimental curves and numerical simulations is reported: peel force F versus vertical displacement D for various prescribed aging conditions, according to BS EN ISO 9142:2003.

References [1] J.L. Smith, J.T. Brokaw:2000. "Explosive tests for the evaluation of the glass fragment mitigation characteristics of MSC Specialty Films Inc. security window film." Applied Research Associates, Vicksburg, Miss.

[2] A.J. Kinloch , C.C. Lau, J.G. Williams:1994. The peeling of flexible laminates. Int. J. Fract. 66: 45-70.

Funded by the Horizon 2020 Framework Programme of the European Union

COST EUROPEAN COOPERATION IN SCIENCE & TECHNOLOGY

UNIVERSITÀ DEGLI STUDI DI TRIESTE

dipartimento di ingegneria e architettura

PROPAGATION SIMULATION OF MULTIPLE CRACKS IN ADHESIVELY BONDED COMPOSITE JOINTS

CertBond
COST Action CA18120

Lukas Münch

Supervisor: Prof. Dr.-Ing. Peter Middendorf

Background of the Institute

Previously developed simulation method for crack propagation in a single plane

- Extension of Cohesive Zone Model
  - Additional fatigue damage variable
- Adaption of Paris' Law
  - Mixed mode ratio dependent Paris' Law
- Crack Tip Degradation Approach
  - Apply fatigue degradation to crack tip elements
- Integration into Abaqus Explicit
  - Load envelop and correlation of time with cycles

- Local neighbor depended crack front calculations

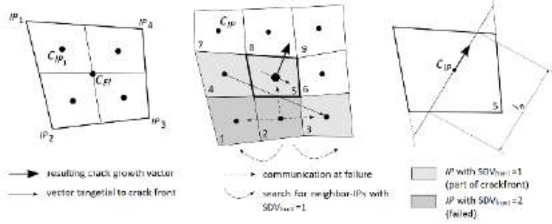

Knowledge Gap

- Extension of method to 3D
  - Will allow for more modelling freedom and therefore potential use cases of the simulation method

- Implementation of multiple crack fronts in the propagation simulation
  - In order to model complex crack initiation scenarios such as impact damage

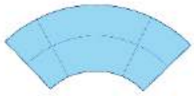

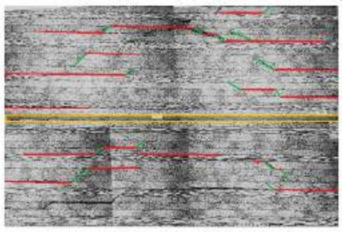

Results

- Adaptation from Abaqus 6.14 to Abaqus 2019
  - Here the previously validated could be matched closely

- Mathematical adaptation of the preprocessor and material model to allow for distorted elements
  - The simulation method can handle distorted elements for low angle deviations
  - For larger distortions some development still needs to be conducted

- The preprocessor can handle multiple instances with the user defined material model.
  - Multiple crack fronts can propagate simultaneously within the simulation

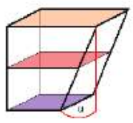

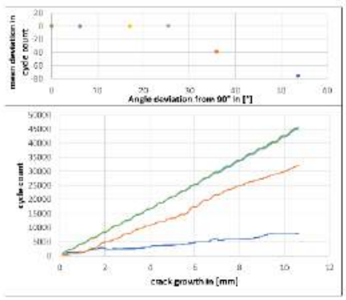

Outlook

- Material characterization for delamination failure
- Validation of model for interlaminar failure
- Simulation of crack propagation with complex crack initiation

Lukas Münch
Lukas.muench@ifb.uni-stuttgart.de
Tel.: +49 (0) 711 685-60532

University of Stuttgart
Institute of Aircraft Design
Pfaffenwaldring 31, 70569 Stuttgart

Funded by the Horizon 2020 Framework Programme of the European Union

COST EUROPEAN COOPERATION IN SCIENCE & TECHNOLOGY

University of Stuttgart

JoinDT

In search of the holy grail of adhesives for cast glass structures: Two contradictory case studies, the Crystal Houses façade in Amsterdam and a small glass pavilion in Greenland

CertBond
COST Action CA18120

Dr. Faidra Oikonomopoulou

Research team (TUD): Telesilla Bristogianni, dr. Fred Veer

Architects: MVRDV (Crystal Houses, NL), Konstantin Arkitekter (Glass pavilion, GL)

Crystal Houses – The challenge: A fully transparent, self-supporting façade of extreme dimensional accuracy


The completed façade

Quick facts:
Cast glass structure dimensions: 10x12 m
Typical glass block unit: 105/210x210x65 mm
Location: Amsterdam, NL
(access by road, electricity provided)
Climate: Moderate maritime
Budget for construction: high
Building crew: highly-skilled team
Status of construction: Completed (2016)

Adhesive requirements:
Structural performance
- good short & long term compressive behaviour
- establish high bond strength with glass
- provide a rigid structure
- good resistance to weathering
- good aging behaviour

Visual performance
- completely transparent/colourless
- should not discolour when exposed to sunlight

Ease-of-assembly
- fast fixing & curing time
- have no emissions of noxious or poisonous
- chemicals during processing and curing

Selected Adhesive:
Delo Photobond 4468
(colourless, one-component, UV-curing acrylate)
- Setting time (100% strength): 60-120s under UV light
- Application thickness: 0.25 mm

Main challenges during construction:
Virtually zero adhesive thickness (0.25 mm) required resulting in:
- extreme precision in construction / inability to accommodate dimensional tolerances.
- need of post-processing of the bricks (increasing the cost)
- need of highly-skilled building crew
- need for homogeneous spread of adhesive / relatively slow construction

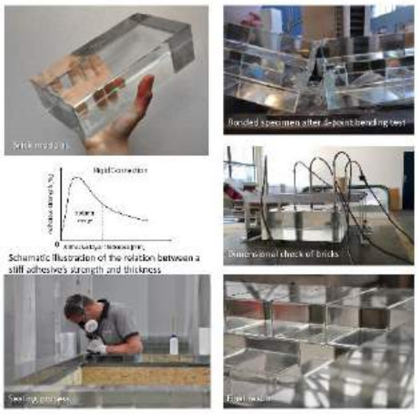

Schematic illustration of the relation between a stiff adhesive's strength and thickness
Bonded specimen after 4-point bending test
Dimensional check of bricks

A glass pavilion in Greenland – The challenge: A transparent, self-supporting structure in an extreme, remote location


3D-visual representation of the pavilion in Greenland by Konstantin Arkitekter

Quick facts:
Cast glass structure dimensions: 3m x 2.5 m
Typical glass block unit: 246 x 116 x 53 mm
Location: Arctic Circle, Greenland
(no access by road, no electricity)
Climate: Tundra/Polar
Budget for construction: low
Building crew: amateur/volunteering team
Status of construction: under construction (2021)

Adhesive requirements

Structural performance:
- tensile strength 1-10 MPa
- service T as low as -30°C
- elongation at break: 15 – 50%

Visual performance:
- transparent or light in colour
- can be easily spread

Ease-of-assembly:
- fast fixing & curing time
- thickness should accommodate dim. tolerances

Selected adhesives:
3M™ Scotch-Weld™ Polyurethane Adhesive DP610 (colourless) for the 9 lower layers
- setting time: 10min, ≈ 2h for 100% strength
- application thickness: 1-2 mm

DOWSIL™ EA-3838 (white) for the upper layers
- setting time ≈ 20min, ≈ 24-48h for 100% strength
- application thickness: 2-3 mm

Main challenges during construction:
No access to electricity and highly-skilled crew, and cold climate resulting in:
- need of an easy and fast construction that can be made locally
- need of an adhesive that can accommodate size deviations and eliminate any need for post-processing of the bricks
- need of battery gun for sealing and for the application of DOWSIL
- particular caution on sealing in order to resist water ingress / frost

Funded by the Horizon 2020 Framework Programme of the European Union

cost
EUROPEAN COOPERATION IN SCIENCE & TECHNOLOGY

NUMERICAL SIMULATION OF LASER SHOCK PAINT STRIPPING ON AIRCRAFT ALUMINUM SUBSTRATES

Kosmas Papadopoulos

Supervisor: Assoc. Prof. Konstantinos Tserpes

CertBond
COST Action CA18120

Paint stripping on aircrafts

The paint stripping process uses a hazardous chemical with an important environmental impact followed by a plastic media blasting, which damages the substrate's material surface. It is, therefore, important to develop more environmentally friendly methods for laser stripping which do not damage the substrate.

Laser shock-based paint stripping*

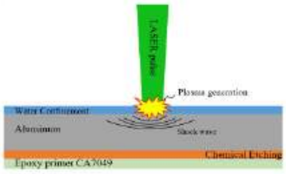

Experimental Setup

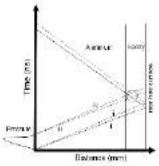

Shock wave propagation

Finite element model

An explicit 3D FE model has been developed in the **LS-Dyna** software to simulate the laser shock paint stripping on aircraft aluminum substrates.

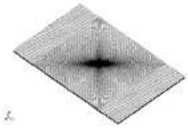

3D Model

3D Model (zoom)

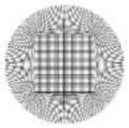

Loading Area

Material	LS - DYNA Material Model
Aluminum	MAT15_JOHNSON_COOK
Epoxy	MAT_10_ELASTIC_PLASTIC_HYDRO
Interface	MAT_138_COHESIVE_MIXED_MODE

Table 1. Material modeling.

Material	Range	Reference
Aluminum thickness	0.7 – 1.2 mm	0.97 mm
Epoxy thickness	25 – 150 μm	25 μm
Laser spot diameter	2.5 – 5.0 mm	4 mm
G_{IC} and G_{IIC}	Division factor: 1.25, 1.50, 1.75, 2.0	1018.52 J/m² and 783.41 J/m²
P_{max} for 1.75 GW/cm²	2300 MPa – 2650MPa	2639 MPa

Table 2. Parameter's range of the parametric study and reference parameters.

Model validation against tests*

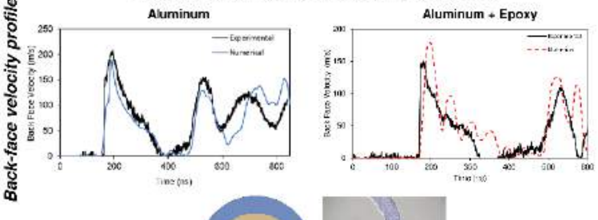

stripping pattern

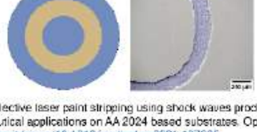

*S. Unaldi et al. (2021). Towards selective laser paint stripping using shock waves produced by laser-plasma interaction for aeronautical applications on AA 2024 based substrates. Optics & Laser Technology 141, 107095. https://doi.org/10.1016/j.optlastec.2021.107095

Results

Distribution of normal stress during wave propagation

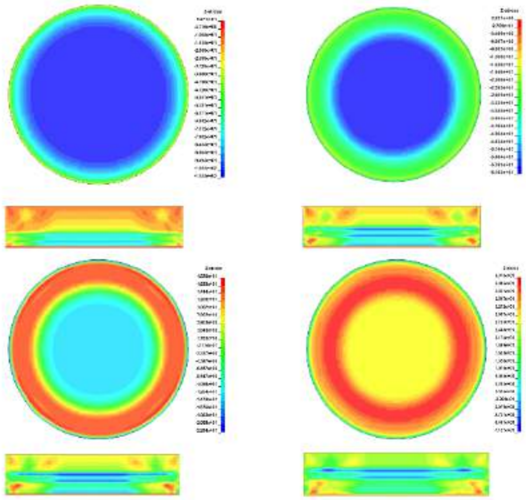

Corona effect

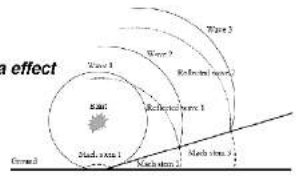

Effect of substrate thickness on the stripping pattern

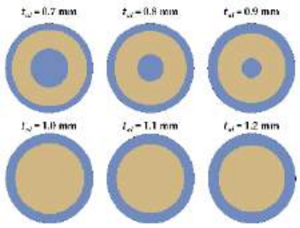

Findings of the parametric study:

- With increasing the aluminum thickness, a transition from the annular to the solid stripping pattern takes place. For values of aluminum thickness smaller than 1 mm, an incomplete stripping is predicted.
- With increasing the epoxy thickness, a transition from a solid circular to an annular stripping pattern takes place. For the values of 0.075 mm and 0.1 mm, an incomplete stripping is predicted.
- The laser spot's diameter significantly affects the stripping propagation and the final stripping pattern. For values larger than 4.0 mm, an incomplete strip-ping is predicted.
- G_{IC} affects the first stages of stripping evolution, while G_{IIC} does not affect stripping evolution.
- With increasing the maximum applied pressure, a transition from the annular to the solid stripping pattern takes place. For values smaller than 2500 MPa, an incomplete stripping (annular) is predicted.

Funded by the Horizon 2020 Framework Programme of the European Union

cost EUROPEAN COOPERATION IN SCIENCE & TECHNOLOGY

Laboratory of Technology & Strength of Materials
Department of Mechanical Engineering & Aeronautics
University of Patras

UNIVERSITY OF PATRAS
ΠΑΝΕΠΙΣΤΗΜΙΟ ΠΑΤΡΩΝ

Influence of elevated temperature on glued-in steel rods for CLT elements

CertBond
COST Action CA18120

Nikola Perković

Supervisor : Vlatka Rajčić

Abstract

Structural bonding technology has proven to be an economically and attractive connection process in timber engineering. Connections and reinforcements with glued-in rods have been used for many years. Glued-in rods (GiR) are an effective way to connect timber elements from both load-bearing capacity/stiffness and aesthetic points of view. The load-bearing capacity of GiR is significantly influenced by the temperature of the adhesive. Although GiR are widely used in timber structures, there are still no unified European test standards, product standards, or design equations for such connections. This work presents an experimental program for obtaining pull-out strength for GiR inserted to Cross Laminated Timber (CLT) when subjected to both ambient and elevated temperatures. Within the experimental investigation, the total number of 36 specimens were tested at ambient temperature and 10 specimens at elevated temperature. Results obtained from both tests are shown, discussed, and compared in this work.

Introduction

Glued-in rods (GiR) are an effective way of producing stiff, high-capacity connections in timber structures. GiR are used for column foundations, moment-resisting connections in beams and frame corners, as shear connectors, and for strengthening structural elements when extensively loaded perpendicular to the grain and in shear. The main advantages of glued-in rods are high load transition, good application in combination with prefabrication for fast installation. In addition, the aesthetic appearance of the finished joint also plays an important role. GiR are often used as a connection method in structures that are landmarks and testimonials to the achievements of structural engineering like exhibition halls, long-span buildings, and timber bridges. Examples of such structures with GiR connections are shown below - Figure 1.

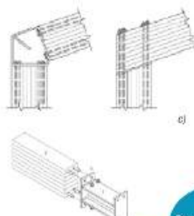

a) b) c)

Figure 1: a) Glued-in rods as a connection method in long – span timber structure – Metropol Parasol in Seville, Spain; b) Neumatt Bridge, Switzerland – joints in the timber truss were made using GSA® technology developed by neue Holzbau AG; c) Application of GiR in moment resistant joints

Great experience has been gathered in the repair and strengthening of beams made of solid timber, both softwood and hardwood, and in connecting concrete slabs to floor beams. Examples are notched beams or beams with holes, curved or tapered beams, and contact zones/supports with high compression stress perpendicular to the grain as shown in Figure 2.

Figure 2: Application of GiR in strengthening timber structural elements [1]

Test methods

The tests in pull – compression (also known as the push-pull method) are widely accepted because of their simplicity, low cost, and comparability with other dowel-type fasteners. The tests are often performed as a push-pull test as it is characterized in EN 1382:1999. Failure modes like the tensile failure are excluded by this test setup and also the splitting of the specimen is detained by friction between the timber and the steel plate. Shear failure along the rod in the adhesive layer or the timber surrounding the rod can occur mostly combined as well as yielding of the rod. Figure 3 illustrates the test setup. The load is transferred from the rod in axial tension to the adhesive and the timber by mechanical interlock.

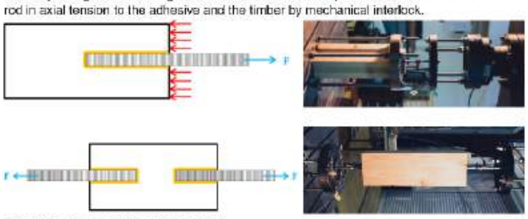

Figure 3: Pull – compression (above) and pull – pull setup

Materials and laboratory tests

The timber members, where the rods were glued-in, were made either of cross-laminated timber with lamellas of a grade CL24h. All timber specimens were equal in their dimensions with the length of 400 mm, the height of 160 mm, and the width of 90 mm.

Table 1: CLT panel

Nominal thickness [mm]	Designation	Layers	Grade
90	L3s	3	C24

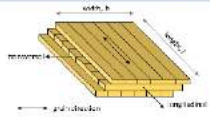

The purpose of the research was to estimate the load-carrying capacity of GiR and to estimate the type of failure. Therefore, the rods had to be designed to remain in the elastic range at failure. Accordingly, steel bars with metric threads M10 with strength grade 8.8 (characteristic tensile strength fub of 800 N/mm2 and characteristic yield strength fyb of 640 N/mm2) were used. In the laboratory tests, two-component epoxy-based adhesive (EPOCON '88) by Croatian producer KGK was used. The modulus of elasticity of the adhesive in tension at 20 °C is 29,5 MPa.

Test protocols

Figure 4 : Thermal chamber and test setup

Results – ambient temperature

The possible failure modes at ambient temperature that can occur are summarized in Figure 5.

Figure 5 : Possible failure modes: yielding of the rod, bond failure or cohesive failure in the wood near the bond line, splitting failure of the wood (only for pull-compression method)

Results obtained from the experimental investigation of the CLT specimens are shown in Figure 6. It is visible from the figures that pull–out forces vary from 25,64 kN to 33,87 kN for the pull–compression test setup.

Figure 6: Pull out forces obtained from the pull compression test method for GiR set in CLT (left), Shear failures (right) – ambient temperature (Rajčić et al. 2016)

Results – elevated temperature

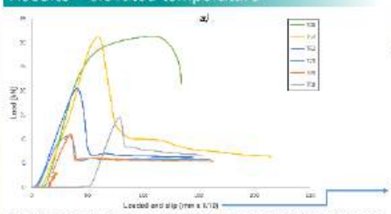

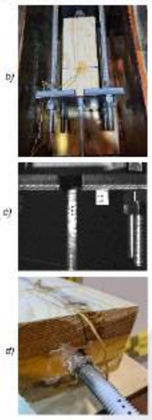

b) c) d)

Figure 7: a) Load vs. slip curves; b) general view of the specimen in the thermal chamber; c) video extensometer; d) failure mode

Conclusion

The experimental study exhibit a failure of the connection in the wood in the vicinity of the wood–adhesive interface. The experimental results revealed a significant decrease in the stiffness of the connection for temperatures above 60 C° (Figure 7). The diameter of the bar does not affect the resistance of such joints. the diameter of the bar does not affect the resistance of such joints.

Funded by the Horizon 2020 Framework Programme of the European Union

COST EUROPEAN COOPERATION IN SCIENCE & TECHNOLOGY

Epoxy-PVB composite binder reinforced with nanostructures of WS_2

CertBond
COST Action CA18120

Danica Bajić, Milica Marjanović, Bojana Fidanovski
Military Technical Institute, Belgrade, SERBIA

OBJECTIVE

The aim of this research was to examine the possibility of reinforcing a polymeric binding system epoxy/PVB with small concentrations of WS_2 nanostructures (inorganic fullerene-like nanoparticles, IF, and nanotubes, INT) for the possible implementation as a binder in composite structures for aircrafts construction and other demanding applications, and as a bonding interface for various types of materials.

Poly(vinyl butyral), PVB, is a thermoplastic elastomer often used as a good impregnating matrix, with good adhesion properties. It is usually added to brittle resins, such as phenolic or epoxy, in order to enhance their toughness and ductility. So far, IF-WS_2 and INT-WS_2 have shown outstanding mechanical resistance themselves, but also as reinforcing fillers in polymer matrices.

MATERIALS AND METHODS

- PVB powder Mowital B30H (Kuraray GmbH),
- Epoxy resin (Hexion aero),
- IF-WS_2 and INT-WS_2 (NanoLub, ApNano Israel),
- ethanol 96%.

PVB

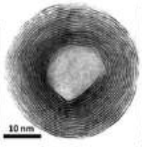

IF- WS_2

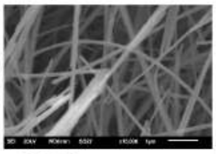

INT- WS_2

Ultrasonication

PVB was dissolved in ethanol in which IF-WS_2 or INT-WS_2 were ultrasonically dispersed; then this solution was mixed with epoxy resin component A, and after homogenization component B was added and mixed. The mixture was cast into flat moulds and dried until ethanol evaporated. Thick film samples were obtained and specimens for mechanical tests and other analyses were cut out. Also, sample PVB/epoxy without WS_2 was made.

Nanostructures were observed using SEM microscopy to analyze their morphology and size before the incorporation in the composite binder and after composite preparation and curing, in order to determine the uniformity of their dispersion in it.

FTIR technique was used to confirm the reaction between PVB and epoxy, as well as to confirm the chemical inertness of the nanofiller with the resin system.

DSC was used to determine the glass transition temperature of the composite and increased thermal resistance was observed with IF-WS_2.

The tensile test was performed and it showed that IF could not have positive effect on the tensile strength, due to their shape, except on the ductility, i.e. on the increase of the elongation at break (for 64%); so with their addition other tensile strength parameters decreased. On the other hand, INT had a positive effect: they caused a significant increase in elongation at break (for 96%) and increase in the absorbed deformation energy U_T.

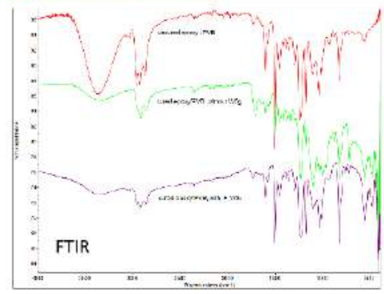

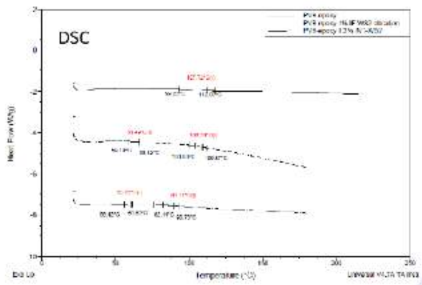

Sample	F_{max} [kN]	R_m [MPa]	E [GPa]	ε [%]	U_T [MJ/m^3]
without WS_2	170.250	14.853	48.533	0.137	1.647
IF-WS_2 1 mas.%	127.125	9.113	16.078	0.225	1.480
INT-WS_2 0.3mas.%	128.200	9.562	14.167	0.269	1.743

CONCLUSION

The new composite binding system was successfully reinforced with IF and INT-WS_2m, so it might be applied in laminated composites and as a bond for structures and materials for demanding exploitation conditions, such as: aerospace, nautical, automotive and construction, sports and protective equipment, etc.

Funded by the Horizon 2020 Framework Programme of the European Union

COST EUROPEAN COOPERATION IN SCIENCE & TECHNOLOGY

Acknowledgement:
This research was supported by Ministry of education, science and technological development of the Republic of Serbia, grant No. 451-03-9/2021-14/200325, and by COST Action 18120, CERTBOND.

Data fusion based damage study using Electromechanical Impedance Method

Shishir Kumar Singh

Supervisors: Paweł H. Malinowski

CertBond

COST Action CA18120

Applications

✓ There is a search of effective damage identifcation solutions for light weight structures (e.g. aeroplane fuselage, wind turbine blades) to prevent failures. One of the promising method is the EMI method.

Introduction

✓ The electrical impedance of the bonded PZT transducer is equal to the voltage (V) applied to the PZT transducer divided by the current passing through the PZT

$$Z(\omega) = \frac{V}{I}$$

✓ Due to mechanical coupling the electrical response contains information about mechanical condition of the structure.

✓ The EMI method employs high frequencies range in assessing the local structural response by application of statistical indices.

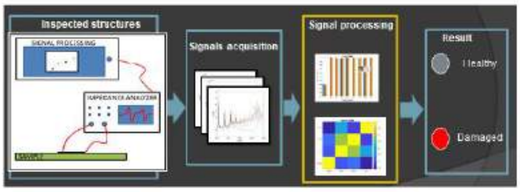

Sample for investigation

✓ Sensor network diagram of Al plate used for damage detection in data fusion technique. Damage severity study based on different size of drilled hole (1) 5 mm and enlarged (2) 8 mm hole in the Al plate. The impedance (Z), admittance (Y), Conductance (G) and resistance (R) EMI data used for the data fusion in damage detection of hole severity.

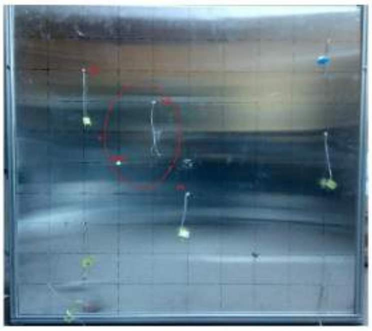

Methodology

✓ Data-driven data fusion based damage detection using PCA and self organizing map (SOM).

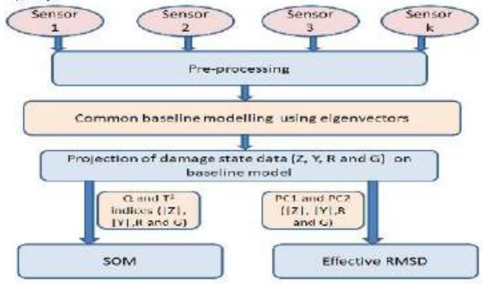

Results

✓ A comparative study of RMSD and PCA based fused RMSD for a) 5mm, b) 8 mm and c) P1 fused RMSD for 5 mm hole and 8 mm hole.

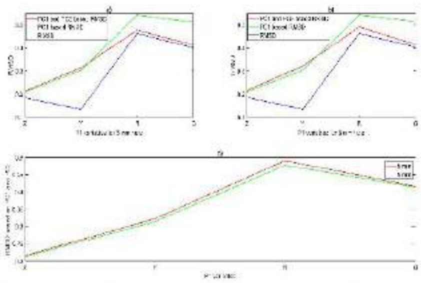

The most common PCA based damage detection indices are Q index and the Hotellings T² index.

✓ Q index used to analyze the variability of projected data in the residual subspace

✓ T² index used to analyze the variability of projected data in the new space of the principle components.

Classification of damages using the Q index

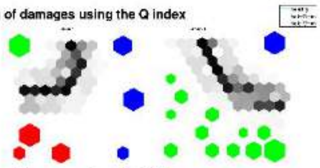

Classification of damages using the Q index

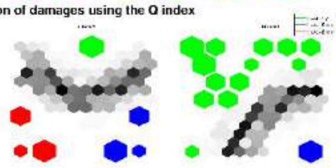

Classification of damages using the Q index

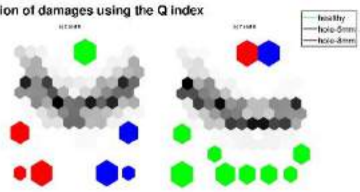

Funded by the Horizon 2020 Framework Programme of the European Union

cost

EUROPEAN COOPERATION IN SCIENCE & TECHNOLOGY

ADHESION CAPABILITY OF ECO-EPOXY ADHESIVES SYNTHESIZED BY THE ADDITION OF MODIFIED TANNIC ACID

Nataša Z. Tomić, Mohamed Nasr Saleh, Sofia Teixeira de Freitas, Andreja Živković, Marija Vuksanović, Aleksandar Marinković

CertBond
COST Action CA18120

Introduction

The aim of this study is to investigate the interface adhesion of novel eco-epoxy adhesives by the addition of two types of modified tannic acid: (A) glycidyl ether and (B) glycidyl phosphate ester of TA, which are used as a bio-based replacement of the BPA-based epoxy component. The majority of structural epoxy adhesives, used in aerospace, contain a BPA component, and thus the adhesion effects were analyzed on two different substrates: aluminum (Al) and carbon fiber reinforced polymer (CFRP), which are used for lightweight structures. Methods used for characterization were the microhardness testing method, the bell peel test (BPT), and microstructural analysis of fractured surfaces. In addition, proving that the microhardness testing method of the interface adhesion is a reliable and fast testing method will enable its use as qualitative indicator in adhesive selection.

TA modification

The chemical structure of both types of adhesive components obtained by the modification of TA are presented in Scheme 1.

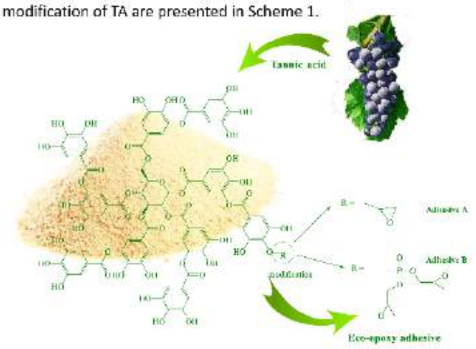

Scheme 1. Chemical structure of modified tannic acid for the aim of obtaining eco-epoxy components

Results and discussion

Figure 1 shows the values of the adhesion parameter b as a function of the replaced epoxy BPA component. An increase of the adhesion parameter b with the increase of TA content indicated an increase of adhesion with Al adherend. The adhesion parameter b, for adhesive B with 15 wt.% of replacement, was 41.6% higher than for adhesive A and 153.4% higher than the REF.

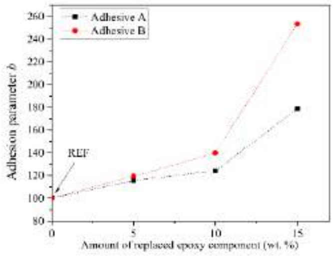

Figure 1. Adhesion parameter b determined using the Chen–Gao model [1,2]

A consequence of the increase in the peel load of adhesive B was the higher percentage of CF than for REF and A. Adhesive B showed slightly different fracture behavior. Two regions of unstable forces can be noticed, which are related to the higher percentage of CF and to the crack, jumping from the interface to within the adhesive and vice-versa.

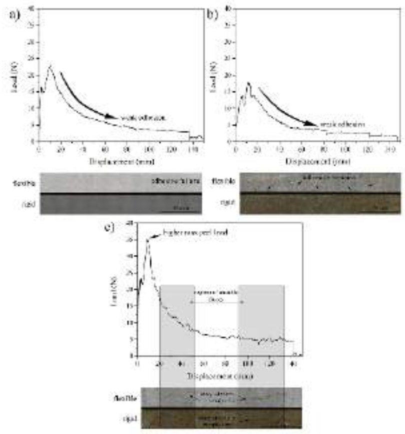

Figure 2. Examples of load–displacement graphs of the bell peel test (BPT) on Al for adhesives a) REF, b) A, and c) B

The obtained results from Figure 3 indicated that the fast and easy method for assessment of the adhesion quality, using the adhesion parameter b, may be used to predict the differences between the selected adhesives for the same adherend material.

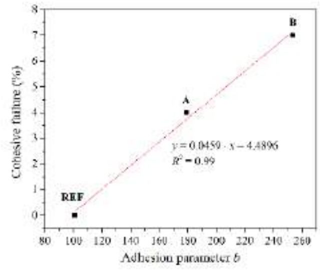

Figure 3. Correlation between the cohesive failure and the adhesion parameter b for adhesives REF, A, and B on Al adherends

Conclusions

The synthesized epoxy ester phosphate derivate of TA (adhesive B) showed enhanced interfacial adhesion on both Al and CFRP, and their high potential as a replacement of the BPA component (DGEBA) was emphasized. Industrial application of obtained eco-epoxy adhesives might consider bonding of secondary/non-structural elements of lightweight structures.

Acknowledgments: This study was funded by Cost Action CA18120 within the Horizon 2020 Framework Program, grant number ECOST-STSM-Request-CA18120-45546 and by the Ministry of Education, Science and Technological Development of the Republic of Serbia (Contract No. 451-03-68/2020-14/200135).

Funded by the Horizon 2020 Framework Programme of the European Union

COST EUROPEAN COOPERATION IN SCIENCE & TECHNOLOGY

References

[1] Chen, M.; Gao, J. Mod. Phys. Lett. B 2000, 14, 103–108.

[2] Tomić, N.; Saleh, M.N.; Teixeira de Freitas, S.; Živković, A.; Vuksanović, M.; Poulis, J.A.; Marinković, A. Polymers. 2020, 12, 1541.

DYNAMICAL MECHANICAL ANALYSIS AND FRACTURE TOUGHNESS OF CARBON REINFORCED EPOXY COMPOSITES

CertBond
COST Action CA18120

Z. Bergant[1], A. Savin[2], R. Šturm[1], U. Trdan[1,*]
[1]Faculty of Mechanical Engineering, University of Ljubljana, Slovenia
[2]Nondestructive Testing Department, National Institute of R&D for Technical Physics, Romania
*correspondence: uros.trdan@fs.uni-lj.si

ABSTRACT
The objective of this research is to evaluate the mechanical properties of a cross-ply and quasi-isotropic symmetrical plain weave carbon-epoxy laminate produced with a vacuum bagging method and a autoclave processing method for a given set of epoxy/carbon fabrics types. Autoclave processed laminates exhibit higher static strengths, higher moduli in tension, compression and bending, but lower Charpy impact toughness. New findings about materials properties were deducted from dynamic multi-frequency tests between 1 to 50 Hz where it was found that the activation energy is 1.8 times higher in autoclave processed specimens. Moreover, autoclave laminates have, on an average 1.7-times lower damping ratio in the glassy plateau region and a 3-times lower peak damping ratio in the glass transition region than wet-layup specimens.

SAMPLE PREPARATION

The subject of the study were **eight-ply $[0]_8$** laminate composite and an **eight-ply laminate composite** with the stacking sequence (45/0/45/0/0/45/0/45) or **$[(45/0)_2]_s$** produced from orthotropic (cross-ply, or 0/90) woven -> **Fig. 1.**

Wet-layup method with vacuum bagging

- **8 plies** of dry plain weave **carbon fabrics Sigratex® CW200-PL1/1** (7 µm fibers (200 tex) of **500 × 500 mm²** impregnated with epoxy-resin **MGS® 285** (Rm=70-80 MPa, E=3–3.3 GPa, A= 5–6%, ρ=1.19 g/cm³)
- **Peel ply** on the top of the impregnated fabrics + polyester-based 2.5 mm thick non-woven absorber for removing the excess resin after the vacuum
- The **total production time was 50 min**, followed by **24 hours of initial curing** at room temperature. Then, the plate was subjected to **post-curing at 60 °C for 6 hours.**

Fig. 1. Biaxial woven laminates

Autoclave prepreg processing

- **8 plies** of plain weave **prepreg** material **CC202 ET 445** (7 µm fibers (200 tex)
- **Peel ply** on the top of the laminate + 3 mm thick non-woven absorber for even distribution of vacuum pressure over the plate and inserted into the autoclave.
- **A vacuum level of 30 kPa** was established and the **pressure of 400 kPa.**
- The heating rate of **3°C/min** and the holding time of **100 minutes at 130°C** was used (Fig. 2).

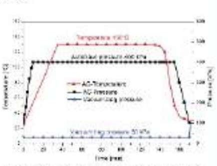

Fig. 2. The autoclave manufacturing cycle

MACROSTRUCTURE AND FIBRE VOLUME FRACTION *(according to ASTM D2584)*

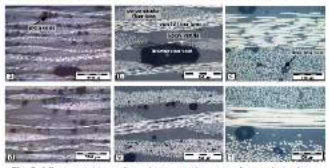

Fig. 3. Microstructures of wet lay-up and vacuum-bagged specimens.

***Wet-layup & vacuum-bagged*:**
- **Highly porous** laminates
- Overall **thickness of 2.8 mm**
- **32% fibre volume content**
- **Void content: 4.8–6.8 %**
- 3 void groups:
  - **Interlaminar** voids (>500 um)
  - **Resin** voids (10–100 µm)
  - **Fibre-tow** voids (30–50 µm)

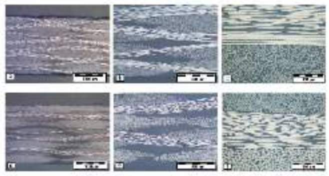

Fig. 4. Microstructures of autoclave processed composites

***Autoclave-prepreg*:**
- **NON-porous, Void FREE microstructure**
- Overall thickness of 2.05 mm
- **44% fibre volume content**
- **Higher fiber density & smaller resin-rich areas**

TENSILE, COMPRESSIVE & FLEXURAL TESTING

- **Smaller E** and **strengths** with the **wet-layup laminates.**
- The **wet-laminated $[0]_8$** laminate **reached only 76%** of the **tensile**, **58%** of **compressive** and **68%** of **flexural strength** of **$[0]_8$ autoclave prepreg laminate** *(Fig. 5(a-c-e)).*
- **The elastic moduli, strengths and ultimate strains decrease in quasi-isotropic $[(45/0)_2]_s$ stacking sequence in comparison with $[0]_8$ layup.**
- In this case, the **wet-laminated $[(45/0)_2]_s$ laminate reached 72 %** of the **tensile**, **59% of compressive** and **74 %** of **flexural strength** of **$[(45/0)_2]_s$ autoclave-prepreg laminate**, *(Fig. 5(b-d-f)).*

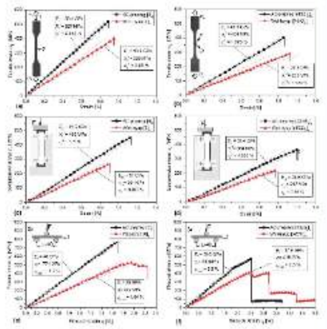

Fig. 5. Stress-strain; (a,b) tension, (c,d) compression, (e,f) flexural tests.

DYNAMICAL MECHANICAL ANALYSES (DMA)

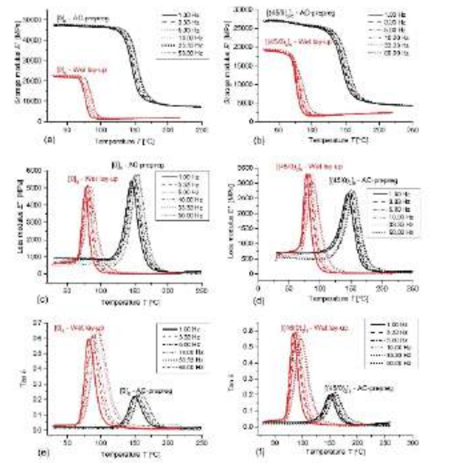

Fig. 6. Storage modulus $E'(T)$, loss modulus $E''(T)$, $\tan\delta(T)$ at testing frequencies 1, 3.33, 5, 10 and 50 Hz.

- The **storage modulus** E' **varies significantly** with the **manufacturing technology** *(Fig. 6a-b).*
- **Increase** in **storage modulus of autoclaved prepreg laminates -> higher fibre content** (rule of mixture) and a **decrease with the** incorporation of ±45° **plies in $[(45/0)_2]_s$** stacking sequence
- **Autoclave-processed** specimens have **lower damping tanδ throughout the entire temperature range,** with **much lower peak-damping than wet-layup specimen** (0.2 vs. 0.6), *Fig. 6c-d.*

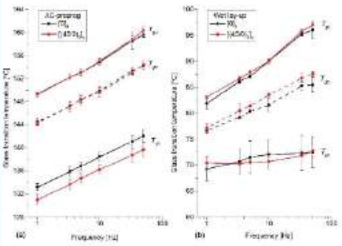

Fig. 7. Glass transition temperature as a function of testing

- **The glass transition temperatures T_{gA}** (from storage modulus), T_{gB} (from loss modulus curve) and T_{gC} (from tan δ curve) **increases with frequency of testing.**
- T_g **increased** between **2-14°C** ***(wet layup)*** and **8-11°C** ***(autoclave prepreg)***
- T_{gA} of the **wet layup laminate** is the **same as of epoxy** MGS 285 ->**70.2°C**

CHARPY IMPACT TOUGHNESS

- **Higher impact energies** with **wet lay-up specimens** (effect of epoxy resin with lower T_g)
- **Obvious effect** of the **stacking sequence** and **production** process-> **higher toughness** with **quasi-isotropic $[(45/0)_2]_s$ & wet-lay-up**
- With additional/newly prepared **$[\pm45]_8$** specimens the **highest impact energy** has been absorbed & **samples** were **visually undamaged.**

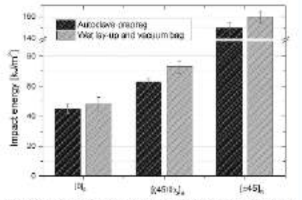

Fig. 8. Charpy un-notched impact energy; flatwise test (ISO 179-2:1997)

CONCLUSIONS

- The **autoclave processed** ToraycarET445 **laminate** exhibit **significantly higher tensile, compressive and flexural strength** (between 24-42 %) **than wet lay-up** laminate specimens.
- Contrary, **autoclaved laminate** exhibit **lower Charpy impact fracture energy**, due to increased higher brittleness of epoxy system in prepreg, **with higher T_g transition**. The **incorporation of ±45° plies increases the fracture energy** regardless of the manufacturing technology used.
- **DMA multi-frequency analyses** between 30-220°C **confirm** the **storage modulus glass transition influence by the frequency of the test**. Frequency **increase from 1 Hz to 50 Hz**. **increases** the glass transition temperature-***Tg*, up to 14 °C**. **Energy loss** through damping tanδ **is significantly higher** (*over complete T and f range*) in **wet lay-up specimens** due to lower fibre content.

Funded by the Horizon 2020 Framework Programme of the European Union

cost
EUROPEAN COOPERATION IN SCIENCE & TECHNOLOGY

Department for Materials Science and Technology

University of Ljubljana
Faculty of Mechanical Engineering

Adhesion tests and laser stripping process of paint using shock waves: Application to Aeronautical Parts in Al alloys and CFRP

Selen UNALDI
Processes and Engineering in Mechanics and Materials,ENSAM, Paris
Supervisors: Laurent Berthe, Emmanuel Richaud & Matthieu Gervais
In collaboration with Patras University

CertBond
COST Action CA18120

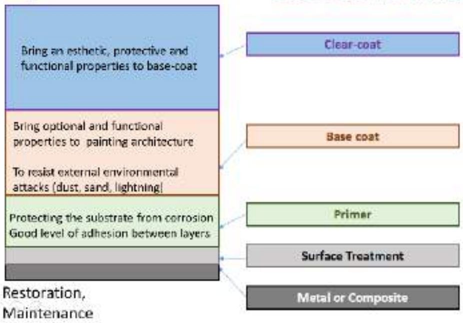

- Restoration,
- Maintenance
- Routine inspection during their life time

Clean Sky Vulcan Project

GOALS

- Development of an industrial laser stripping process which is able to remove selectively the top coat of an aircraft paint system by keeping the substrate health
- Environmental Friendly
- Universal solution that is applicable for both composites and metals

Concept & Approach

- The tensile location can be shifted by changing laser parameters (duration, pulse configuration)
- If the tensile stresses created by the shock waves are lower than the failure stress of the material, no mechanical damage is obtained. For the case of spallation, the tensile stress levels which are created via shock waves are higher than the material's tensile stress [2].

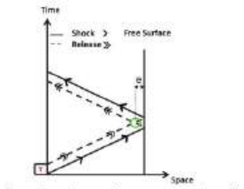

Space-time diagram for a mono pulse impact

Background & Specifications

Chemical Stripping	• Sensitive areas should be protected during the operation • Waste chemical disposal after the operation
Media Blasting	• Not Selective • Treatment of dust during blasting • Treatment of media after stripping
Laser Stripping	• No use of chemical products • Process can be monitored • Lower investment cost

Process Parameters

- ❑ Pulse Duration: 8-25 ns
- ❑ Wavelength: 532-1064 nm
- ❑ Energy: 0.2-50 Joules
- ❑ Repetition Rate: 1-20 Hz
- ❑ Spot Diameter: mm
- ❑ Power Density: 1-10 GW/cm²
- ❑ Pressure: 1-8 GPa

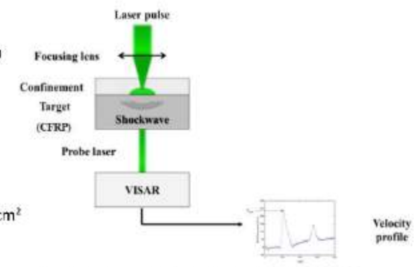

Schematic Representation of VISAR Diagnostic *(Le Bras, 2019)* [1].

Samples & Methodology

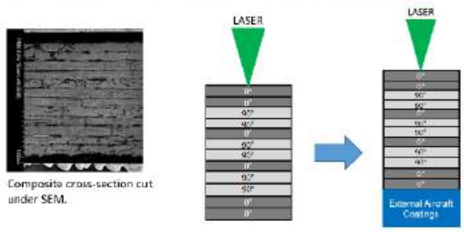

Composite cross-section cut under SEM.

First, debonding threshold calculated via VISAR for base materials
Then, stripping threshold for the paint is calculated for CFRP+External aircraft coatings to verify base material's health as function of different spot sizes.

Results & Discussion

VISAR Analysis

Evaluation of the Removal Threshold

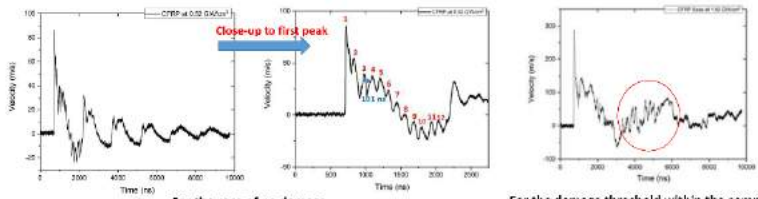

For the case of no damage

For the damage threshold within the composite

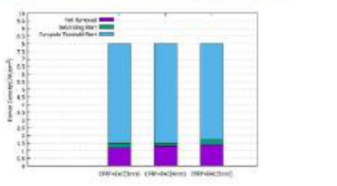

Strippiing Threshold Evaluation as function of spot diameter

- With VISAR Diagnostics, we were able to monitor the shock wave propagation within plies. Number of peaks corresponds to the number of plies. It was also monitorable to detect the damage threshold within the composite from the change of the wave propagation.
- The damage threshold for the base material is higher (1.62 GW/cm²) than the stripping threshold for the external aircraft stripping threshold (1.5 GW/cm² for 3 & 4mm spot sizes) which means that without damageing the substrate, we can have a stripping on the composite+EAC with these configuration.
- The stripping rate is calculated as 0.7 m²/h for the composite+eac which is in the framework of the project.

Funded by the Horizon 2020 Framework Programme of the European Union

COST
EUROPEAN COOPERATION IN SCIENCE & TECHNOLOGY

REFERENCES

[1] Le Bras, A. Rondepierre, R. Seddik, M. Scius-Bertrand, Y. Rouchausse, L. Videau, B. Fayolle, M. Gervais, L. Morin, S. Valadon, R. Ecault, D. Furfari, L. Berthe, Laser shock peening: toward the use of pliable solid polymers for confinement, Metals 9 (793) (2019) 1–13

[2] Unaldi, S.; Papadopoulos, K.; Rondepierre, A.; Rouchausse, Y.; Karanika, A.; Deliane, F.; Tserpes, K.; Floros, G.; Richaud, E.; Berthe, L. Towards selective laser paint stripping using shock waves produced by laser – Plasma interaction for aeronautical applications on AA 2024 based Substrates. Opt. Laser Technol. 2021, 141, 107095

THE APPLICATION OF ADHESIVES FOR CONNECTING STRUCTURAL GLASS STRIPS TO EXISTING TIMBER JOISTS

CertBond
COST Action CA18120

Žiga Unuk - University of Maribor, Faculty of Civil Engineering, Transportation Engineering and Architecture

Introduction

Strengthening procedures often impair the original appearance of timber floors. An example of such a procedure is applying tensile strengthening elements made of steel or various polymers. This study proposes using structural glass strips as a transparent tensile reinforcement.

Materials and methods

Two methods of connecting the structural glass strips to the timber joists were considered. The first method was direct adhesive bonding, whereas the second method employed a newly developed timber–glass point joint, consisting of self-tapping screws, an aluminium insertion, and an epoxy resin-based adhesive. First, the two connection methods were tested on a small scale regarding their shear load-bearing capacity and load-slip behaviour. Finally, the two connection methods were tested on old timber joists strengthened with CLT panels and structural glass strips under four-point bending conditions over a span of 4.5 m.

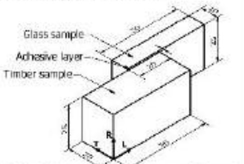

Fig. 1. Adhesive bonding specimen configuration

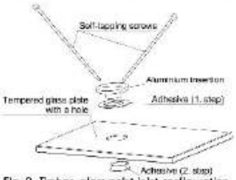

Fig. 2. Timber–glass point joint configuration

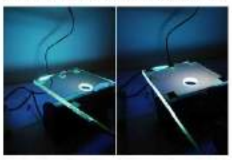

Fig. 3. Ultraviolet light shining on the air (left) and tin side (right) of the glass strips

Results

The results comprise small scale shear loading test results and four-point bending test results.

Fig. 4. Bonded specimen shear test

Fig. 5. Bonded specimen failure types

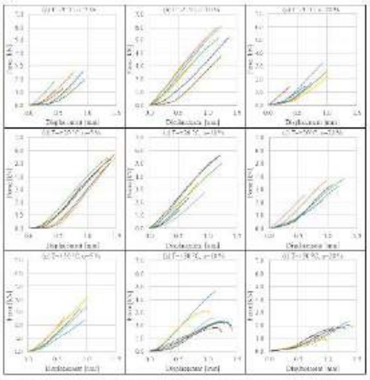

Fig. 6. Load-displacement curves for the shear specimens and for different environmental conditions

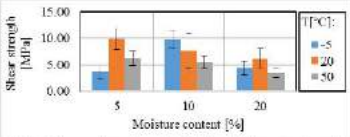

Fig. 7. Average shear strength of the bonded shear specimens in relation to different test temperatures and timber moisture contents (with error bars representing standard deviation)

Fig. 8. Timber–glass point joint

Fig. 9. Timber–glass point joint shear test

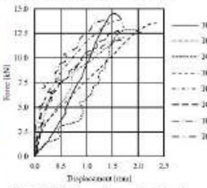

Fig. 10. Timber–glass point joint shear test Load-displacement curves

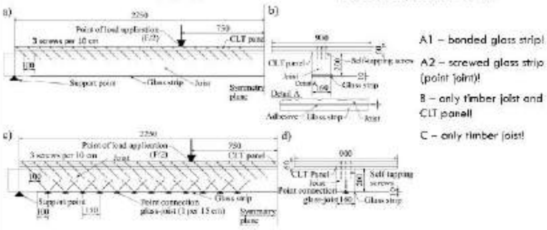

Fig. 11. a) Configuration A1 – longitudinal section; b) configuration A1 – cross-section; c) configuration A2 – longitudinal section; d) configuration A2 – cross-section

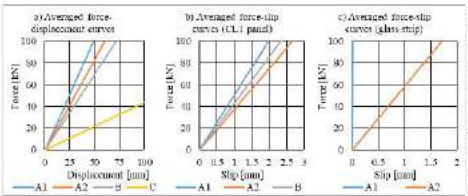

Fig. 12. Four-point bending test averaged force-displacement (a), force-slip (CLT – b, glass strip – c) curves for different joist configurations

Conclusions

The performed experiments on small shear specimen under different environmental conditions indicate the suitability of the chosen rapid-setting thixotropic epoxy adhesive for bonding glass to timber.

The point joint represents an alternative to classic adhesive bonding, when reversibility is an important factor.

The results of the four-point bending experiments show that the structural glass strips significantly increased the bending stiffness of the tested timber joist configurations and, in some cases, also resulted in higher load-bearing capacities.

The screwed glass strip is structurally less efficient than the bonded glass strip, but it is superior in terms of non-invasiveness and reversibility, which is essential for applications on the wooden built heritage.

Additional information:

- Unuk, Žiga, et al. "Evaluation of a structural epoxy adhesive for timber-glass bonds under shear loading and different environmental conditions." International Journal of Adhesion and Adhesives 95 (2019): 102425.
- Unuk, Žiga, et al. "Novel composite connection for timber–glass composite structures." Archives of Civil and Mechanical Engineering 20.1 (2020): 1-16.
- Unuk, Žiga, et al. "Strengthening of old timber floor joists with cross-laminated timber panels and tempered glass strips." Construction and Building Materials 298 (2021): 123841.

Acknowledgments

The author acknowledges the financial support from the Slovenian Research Agency (research core funding No. P2-0129).

Funded by the Horizon 2020 Framework Programme of the European Union

COST EUROPEAN COOPERATION IN SCIENCE & TECHNOLOGY

STRUCUTRAL PERFORMANCE OF EMBEDDED LIQUID-LAMINATED GLASS CONNECTIONS

CertBond
COST Action CA18120

PhD candidate: Stratis Volakos
Supervisor: Prof. Mauro Overend

Abstract

Embedded laminated glass connections consist of a metallic insert embedded within a laminated glass unit by means of transparent polymeric foil interlayers. The connection is assembled via the standard autoclave lamination process where the heating/cooling of materials with different coefficients of thermal expansion can lead to residual stresses [1] thus reducing the connection strength.

In this work, a variant of this connection is investigated, consisting of a thin steel insert encapsulated by a transparent cold-poured resin to eliminate the unfavourable residual stresses. In particular, the connection mechanical response is assessed via numerical (FE) analyses and pull-out tests performed at different displacement rates (1 & 10 mm/min) to examine the effect of the viscoelastic resin behaviour.

① Failure Mechanisms

Test Set-up

Steel failure (high strain-rate)

Glass failure (low strain-rate)

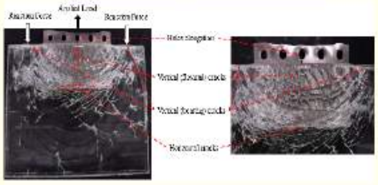

② Load-Displacement behaviour

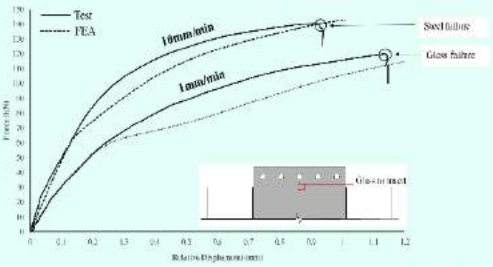

High strain-rate tested specimens exhibit higher strength and stiffness

③ Load-Transfer Mechanisms

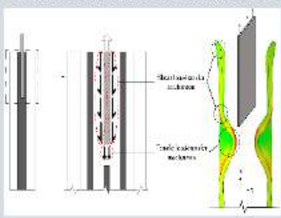

1) Shear mechanism: Shear stresses in the interlayer
2) Tensile mechanism: Tensile stresses in the interlayer

④ Glass stress state

Tensile Mechanism

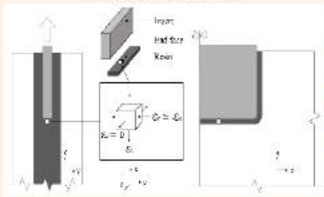

Stress concentration

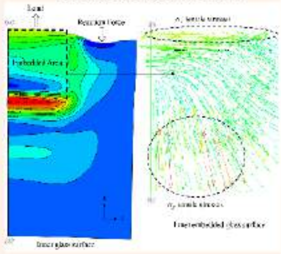

- Resin highly confined

⑤ Contactless Configuration

Load-Displacement behaviour

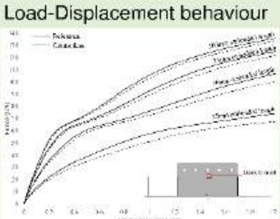

Stress concentration

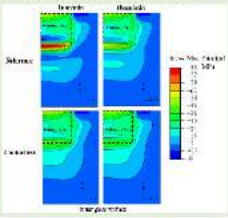

Conclusions: The tests showed that the stiffness, the load-bearing capacity and the failure mode of the connection are significantly affected by the imposed strain rate. The FE results indicate that the resulting stress state within the connection is a consequence of two load-transfer mechanisms and that the relative contribution of each mechanism depends on the relative stiffnesses of the constituent materials. In this regard, a modified embedded connection (contactless) configuration was proposed that significantly reduces the glass stress concentration without compromising the pull-out stiffness of the connection or its aesthetic qualities.

References : [1] Santarsiero, M., Bedon, C., Louter, C.: Experimental and numerical analysis of thick embedded laminated glass connections. Composite Structures, 242-256 (2018)

Funded by the Horizon 2020 Framework Programme of the European Union
COST EUROPEAN COOPERATION IN SCIENCE & TECHNOLOGY

TESTS OF THE EMBEDDED LAMINATED CONNECTION FOR GLASS STRUCTURES

CertBond
COST Action CA18120

Michaela Zdražilová
Supervisors: Zdeněk Sokol / Martina Eliášová

FACULTY OF CIVIL ENGINEERING CTU IN PRAGUE

INTRODUCTION

Laminated connection belongs to the most progressive ways of glass components connecting. Despite being widely used, the design procedure is mostly based on experiments. Within the ongoing research at the Faculty of Civil Engineering of CTU in Prague, two series of small scale experiments focusing on characteristics of the embedded laminated connection under the short-term tensile and eccentric shear loads were performed.

TESTING PROCEDURE

For both sets of samples, the testing process:

- included numerous loading and unloading cycles;
- after each increase or decrease cycle, the load was kept on a constant value for 1 minute;
- the load was cyclically increasing until the collapse.

A special frame with detachable bottom part was used to apply the tensile load. The samples were placed on a steel bed with two cylindrical supports and plastic pads.

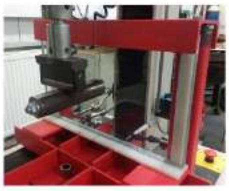

For the eccentric shear load tests, the glass pane was vertically clamped to a steel frame with a detachable upper part. To create the eccentric shear force load, a special steel tool was put on the bolt screweded in the steel element.

CONCLUSION

The experiment revealed the dominant mode of failure and described the behaviour of this fixing system under two different types of loading. However, further research consisting of full scale tests and numerical modelling should be performed.

ACKNOWLEDGEMENTS

This experiment was prepared with a support of the grant Hidden Connection of Laminated Glass Panes No. TH 03010175 of the Technology Agency of the Czech Republic (TACR), SGS of the Czech Technical University SGS19/150/OHK1/3T/11 and with a cooperation of OGB s.r.o.

DESCRIPTION OF THE SAMPLES

Laminated connection:

- the same manufacturing process as for the standard laminated glass panes;
- combines mechanical and adhesive systems;
- the steel element (bolt) is embedded between two glass panes;
- the adhesive interlayer is represented by two layers of foil.

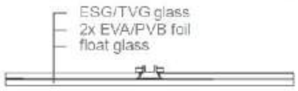

All the samples were checked before the experiment. Defects do not influence the performance of the connection, but they might be unacceptable for the aesthetical reasons.

The samples may suffer from:

- bubbles surrounding the edges of the steel element;
- bigger bubbles in the area of the steel element;
- combination.

COURSE OF THE TESTS

The course of both types of tests was essentially the same:

1. Small bubbles appeared in the area of the connection.
2. Their number was increasing with the increasing load.
3. After reaching a certain point, they started to merge into bigger bubbles.
4. The bubbles eventually covered the whole area of the connection exposed to tension.
5. In some cases, bubbles appeared out of the connection as well.
6. The connection failed due to reaching the tensile resistance limit of the glass pane. No delamination occured.

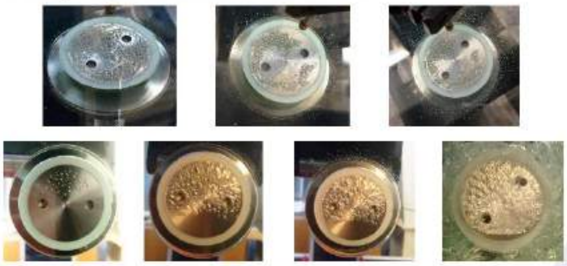

Funded by the Horizon 2020 Framework Programme of the European Union

cost
EUROPEAN COOPERATION IN SCIENCE & TECHNOLOGY

MECHANICAL PROPERTIES OF GLASS-METAL ADHESIVE CONNECTION UNDER ELEVATED TEMPERATURE

Markéta Zikmundová
Supervisor: Martina Eliášová

CTU CZECH TECHNICAL UNIVERSITY IN PRAGUE

CertBond
COST Action CA18120

INTRODUCTION

- Adhesive bonding is commonly used in automotive and aerospace industry.
- Nowadays, adhesives are more used in civil engineering, especially for facade application as a modern type of connection.
- There is not enough knowledge about adhesives with higher strength and stiffness, especially about their behaviour at elevated temperature.

EXPERIMENTAL PROGRAMME

- Specimens as double lap shear joints.
- A float glass plate in the middle,
- Two different external metal sheets:
  - Zn-electroplated steel, roughened surface,
  - Aluminium, roughened surface.
- Two component acrylate was used as an adhesive bond.
- Joint thickness of 1 mm.

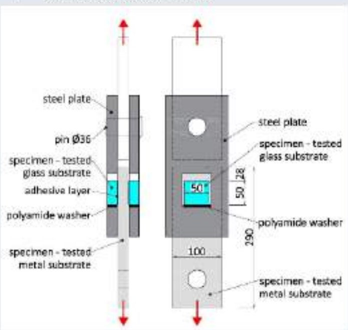

- Different temperatures during the test:
  - Room temperature,
  - Elevated temperature 60 °C,
  - Elevated temperature 80 °C.

RESULTS

- Shear strength reduction on 63.7 % (60 °C) and 36.5 % (80 °C).
- Decrease of the initial stiffness and a bigger elongation with elevated temperature.

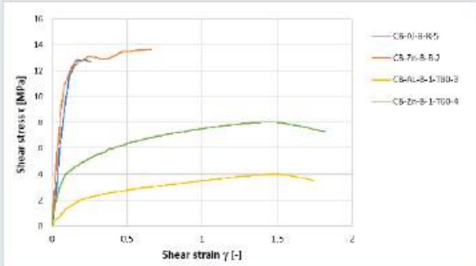

- Fracture of glass at the room temperature, at 60 °C combination failure mode with dominant cohesive mode of failure, at 80 °C failure of adhesion on the glass surface.

Temperature	Substrate	Average shear strength τ [MPa]	Standard deviation [MPa]	Failure mode	Ratio τ_i/τ_{ref}
22 °C	Zn-electroplated steel	12,356	1,407	A-C-S	100,0%
22 °C	Aluminum	11,267	2,152	S	91,2%
60 °C	Zn-electroplated steel	7,867	0,879	A-C-S	63,7%
80 °C	Aluminum	4,507	0,414	A	36,5%

Specimen at 22 °C (left), specimen at 60 °C (middle), specimen at 80 °C (right)

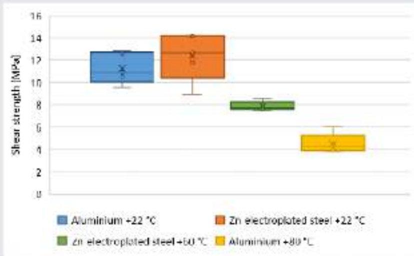

CONCLUSION

- Lower stiffness and strength with higher temperature.
- Low adhesion to glass for high temperature.

ACKNOWLEDGEMENT

This work was supported by the Czech Science Foundation [grant number GA18-10907S]; and the Student grant competition of CTU [grant number SGS18/169/OHK1/3T/11].

Funded by the Horizon 2020 Framework Programme of the European Union

cost EUROPEAN COOPERATION IN SCIENCE & TECHNOLOGY

Keynote Lectures

CertBond
COST Action CA18120

Date: 22-23 September 2021
Place: University of Trieste, Trieste, Italy

A Glance at biobased and low environmental impact coatings and binders

Dr Sylvain CAILLOL
Sylvain.Caillol@enscm.fr

Montpellier, FRANCE

cnrs
enscm CHIMIE Montpellier
UNIVERSITÉ MONTPELLIER
ICGM Institut Charles Gerhardt Montpellier
INSTITUT CARNOT CHIMIE BALARD

MONTPELLIER, FRANCE

- Famous region for summer activities…

CHEMISTRY IN MONTPELLIER, FRANCE

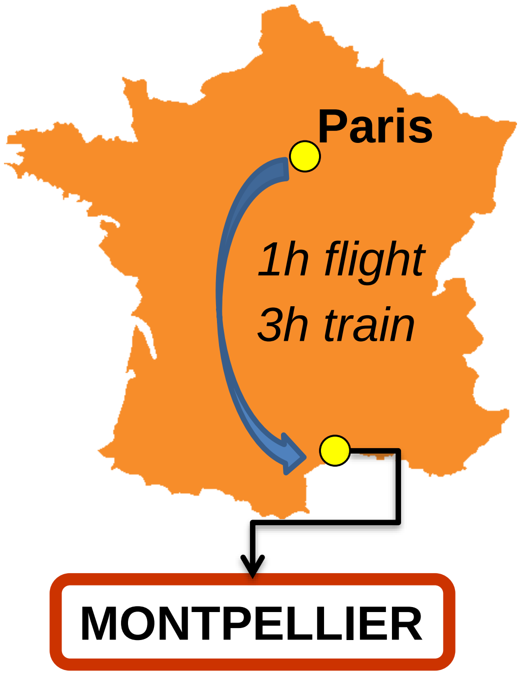

CHEMISTRY Dpt
- **1,000 scholars**
- **3,000 students**
- 600 publications / year
- 30 international patents / year

Chemistry Institute

- **Polymer team** of the Chemistry Institute **ICGM**
- ***Green Chemistry and Polymers***

Green Chemistry and Polymers

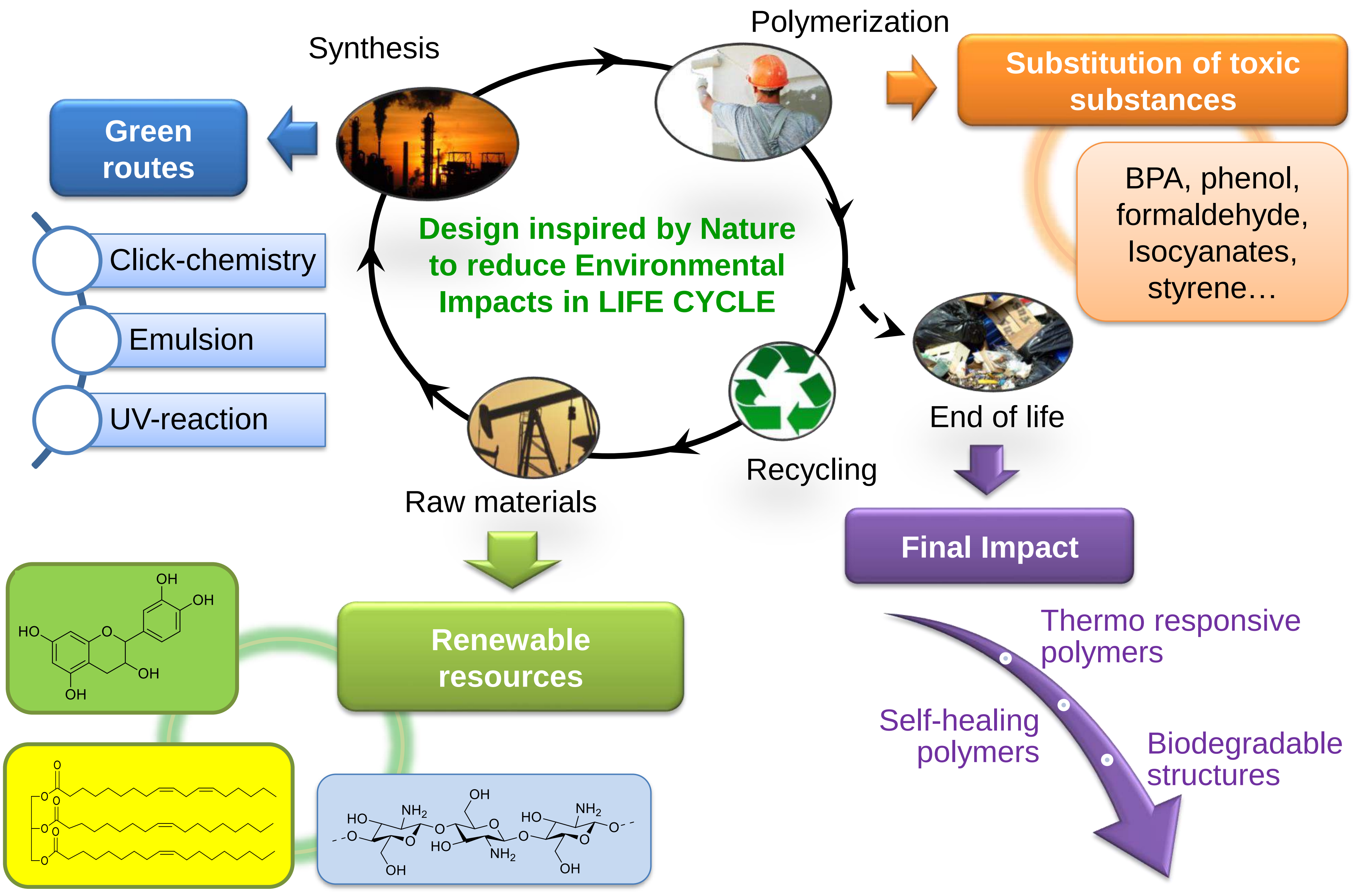

Green Chemistry and Polymers

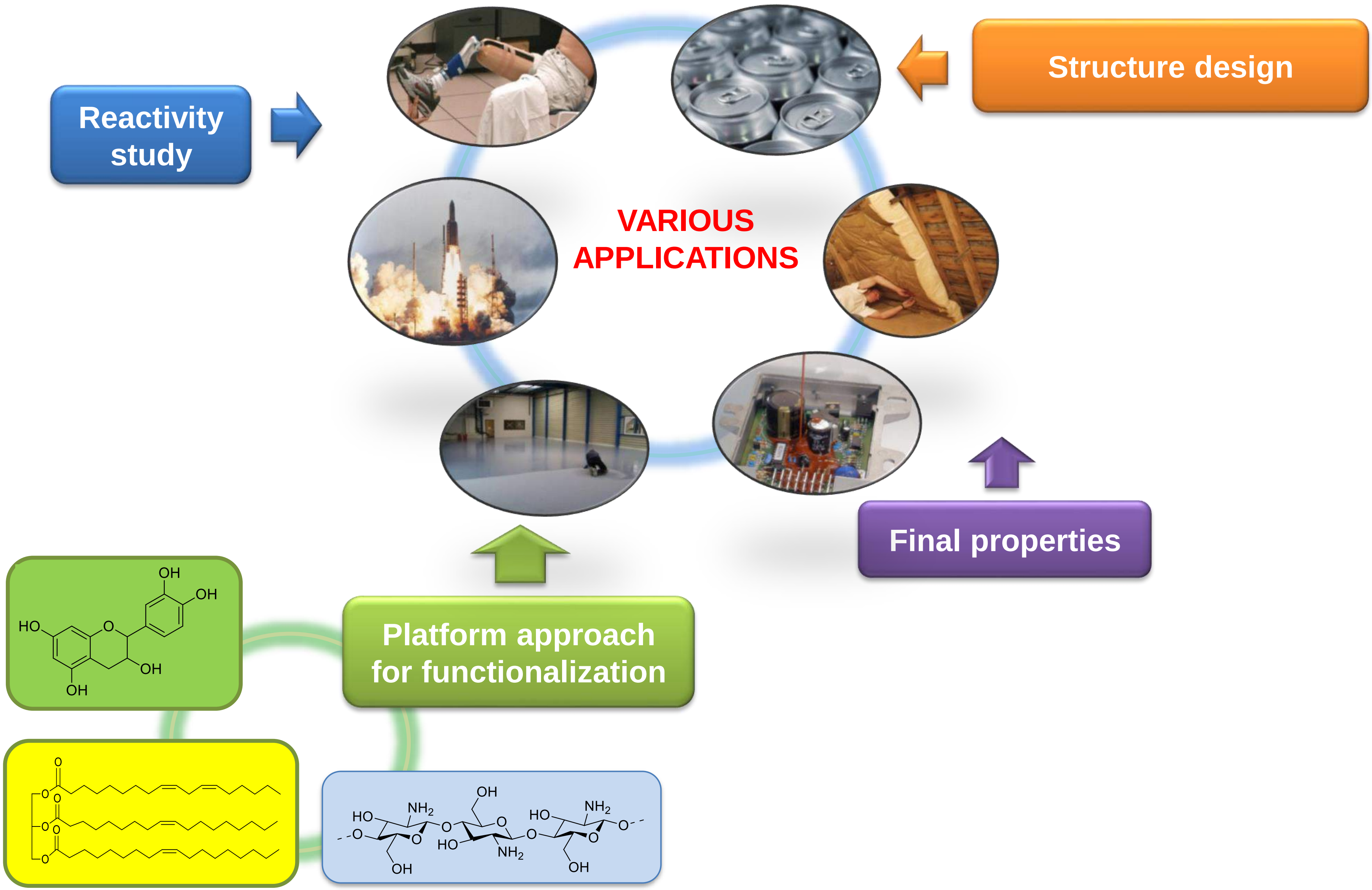

Functionalization of renewable resources

Lignin, Tannins and derivatives

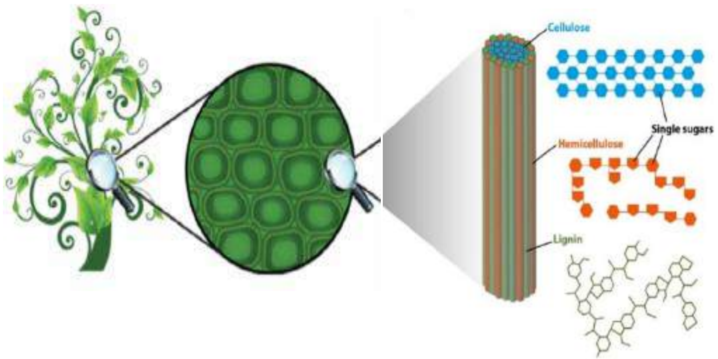

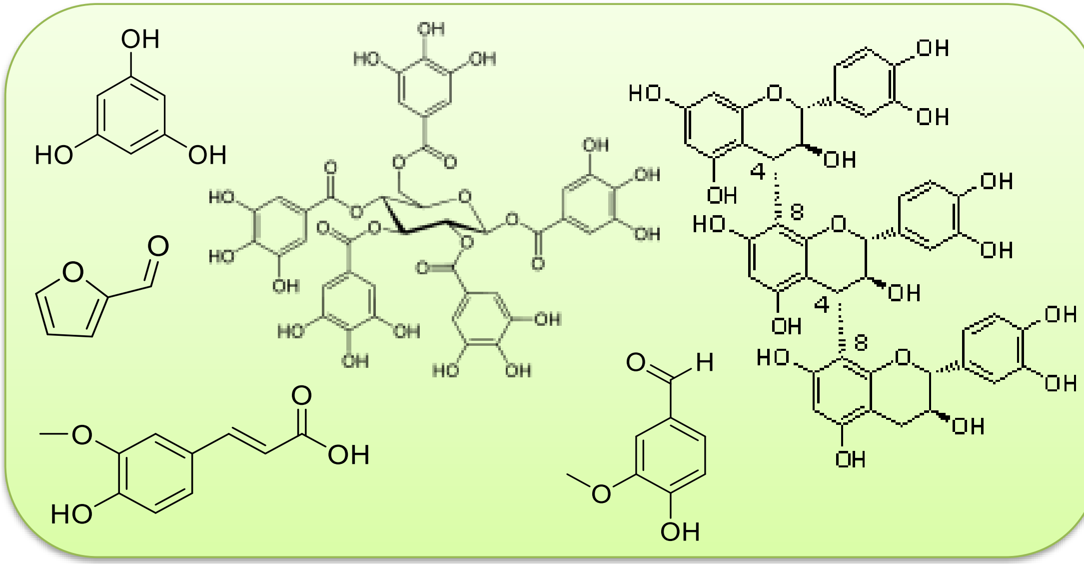

Cardanol

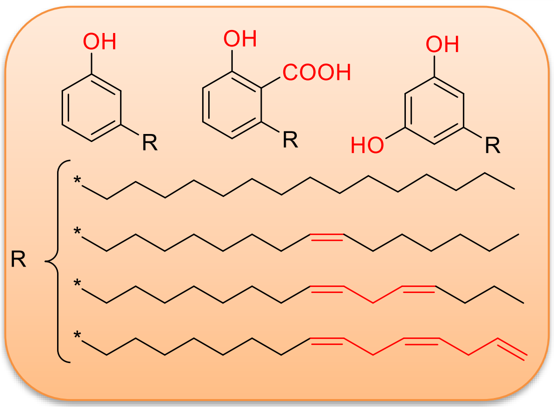

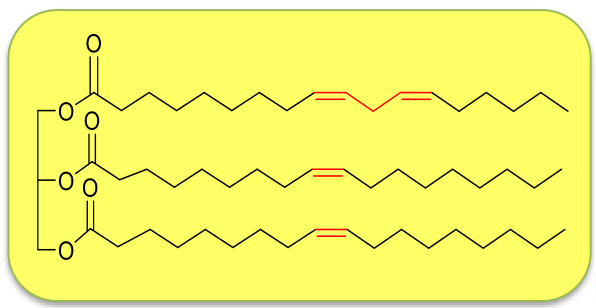

Veg oils

Chitin/Chitosan

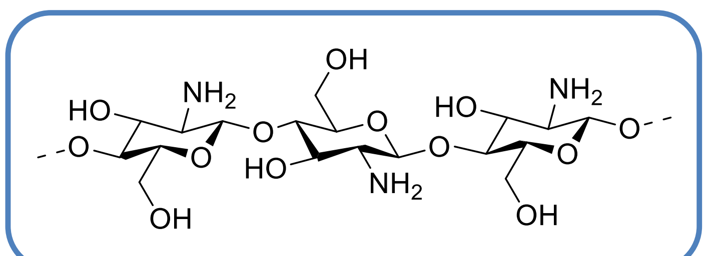

BIOBASED AROMATICS: WHY ?

Aromatics: From oil to biomass

- **Renewable sources** to reduce fossil footprint
- **Volatility** of oil price → biomass as more stable supplies ?
- Development of shale gas (USA…)
  → Tensions over **naphta cut and aromatics availability**

  - **BIOBASED MONOMERS AND POLYMERS**

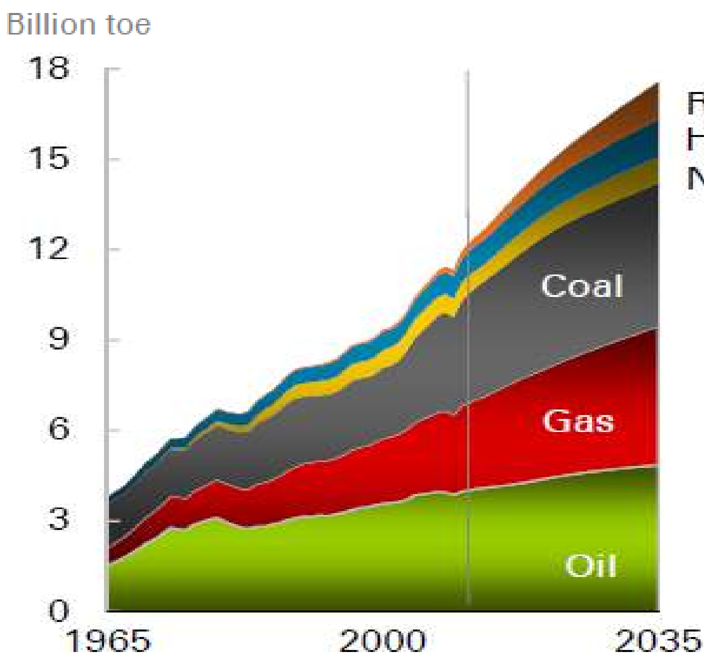

Aromatic polymers

- Needed for high **thermo-mechanical properties**
- Most of the time **thermosets** – no recycling

REAL STAKES FOR THE DEVELOPMENT OF BIOBASED AROMATIC MONOMERS AND POLYMERS

Sources; SRI Consulting, Platts Special Report; The shale revolution and its impacts on aromatics supply, pricing and trade flows. 2013, European Bioplastics

Substitution of harmful aromatic monomers

- **Bisphenol A**: 4Mt/y - various applications

BPA : CMR Repr. Cat. 2, Endocrine disruptor

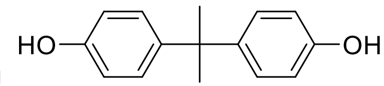

Forbidden in France since January 2015 (food contact)

Mimics estradiol
Low-dose effects !!

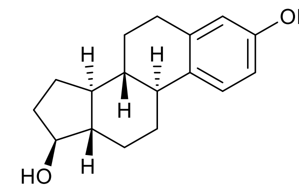

⇒ **Used in 90% polyepoxide networks – 2Mt/y**

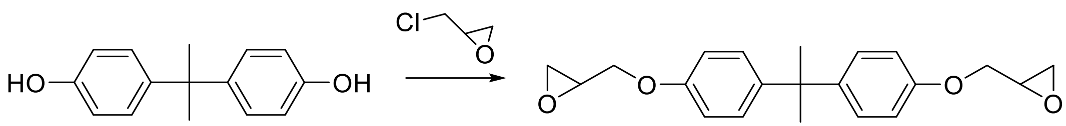

Bisphenol A (BPA)

BADGE
(BPA diglycidyl ether)

- and also:

Phenol, styrene, isocyanates….

⇒ **TARGETS**

- **Biobased non-toxic aromatic monomers for polymer synthesis**

Structure / toxicity relationship

- **Bisphenol A**: endocrine disruption effect

BPA : CMR Repr. Cat. 2, Endocrine disruptor

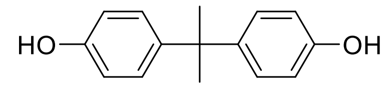

Regulates activity

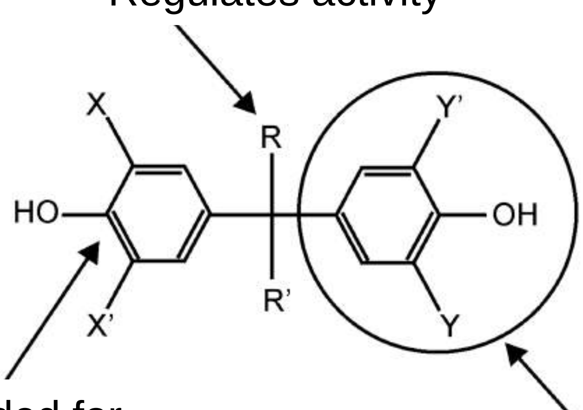

Needed for estrogenic activity

Increases activity

Creates H bonds

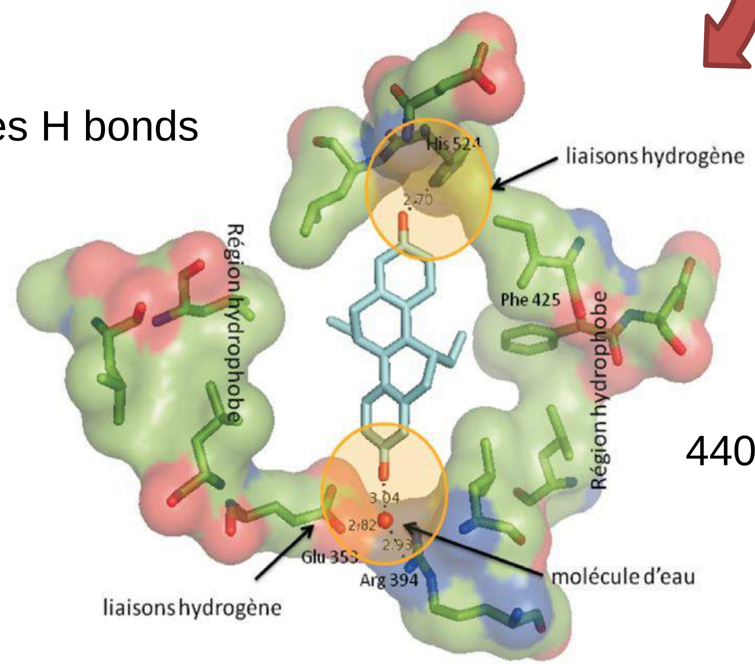

440Å^3

Activity reduced with:
- Longer or shorter molecules
- X, X', Y, Y' ≠ H

Hydrophobic pocket of Erα (estradiol) receptor

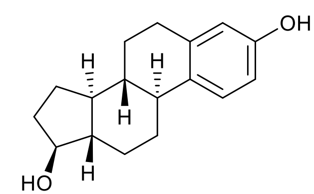

Expertise Collective INSERM, Reproduction et Environnement, 2011, ISBN 978-2-85598-891-

Biobased is not harmless

Tannins

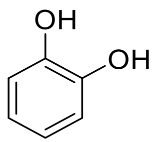

Catechol

CMR

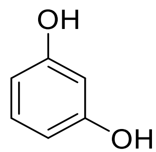

Resorcinol

CMR

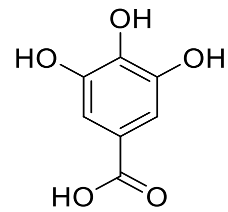

Gallic acid

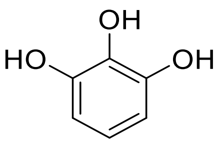

Pyrogallol

CMR

Cashew Nut Shell Liquid

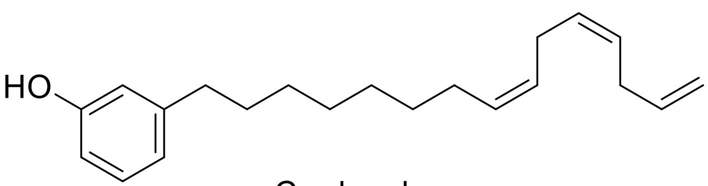

Cardanol

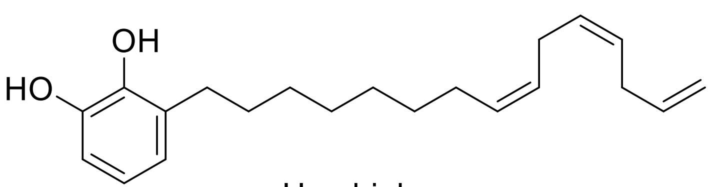

Urushiol

Sensitizer

Biobased doesn’t necessary mean « no impact ! »

- **Petrochemical vs biobased materials**

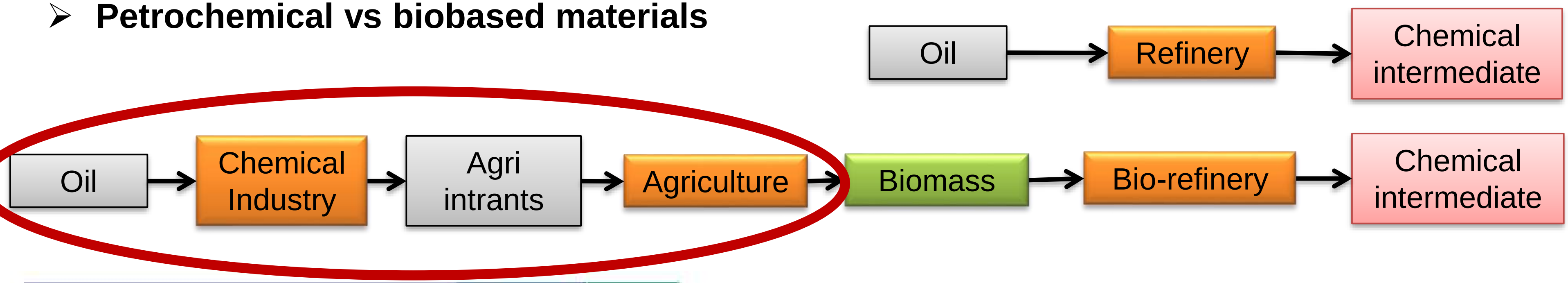

Material	Green Design Rank	LCA Rank
PLA (NatureWorks)	1	6
PHA (Utilizing Stover)	2	4
PHA (General)	2	8
PLA (General)	4	9
High Density Polyethylene	5	2
Polyethylene Terephthalate	6	10
Low Density Polyethylene	7	3
Bio-polyethylene Terephthalate	8	12
Polypropylene	9	1
General Purpose Polystyrene	10	5
Polyvinyl chloride	11	7
Polycarbonate	12	11

Which renewable resources ?

- **Careful choice** of low impact and non-toxic renewable resources
- Cultures with reduced inputs
- **By-products !!**
- **Wood ➔ lignin and tannins derivatives**
- **Robust processes** to avoid purification **(networks!)**

Tabone, Environ. Sci. Technol. 2010, 44, 8264–8269

From natural phenols to biobased networks and coatings

Lignin derivatives

Lignin → **Vanillin**

Depolymerization

15-30% of dry weight lignocellulosic biomass
2nd largest molecule on earth after cellulose
1st most abundant source of phenols > 300bt/y
50Mt/year extracted from paper pulp

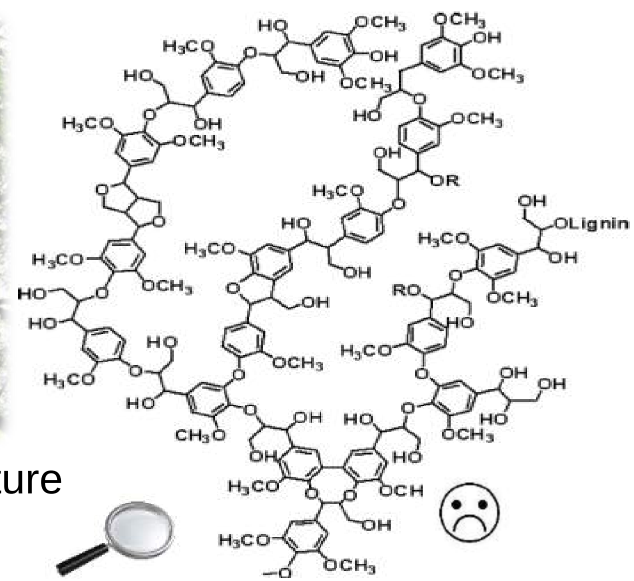

- Complex structure
- High Mn
- Insolubility
- Diversity (species, time of year, extraction process…)
- **Mostly used as it in materials or after partial functionalization**

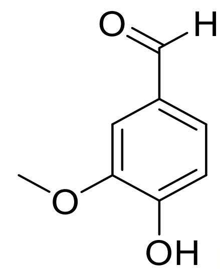

- Innocuity
- Aromatic structure
- Reactive functions
- Industrial production process from wood[1]
- **DIFUNCTIONAL**

[1] Borregaard Company

Example of Vanillin platform

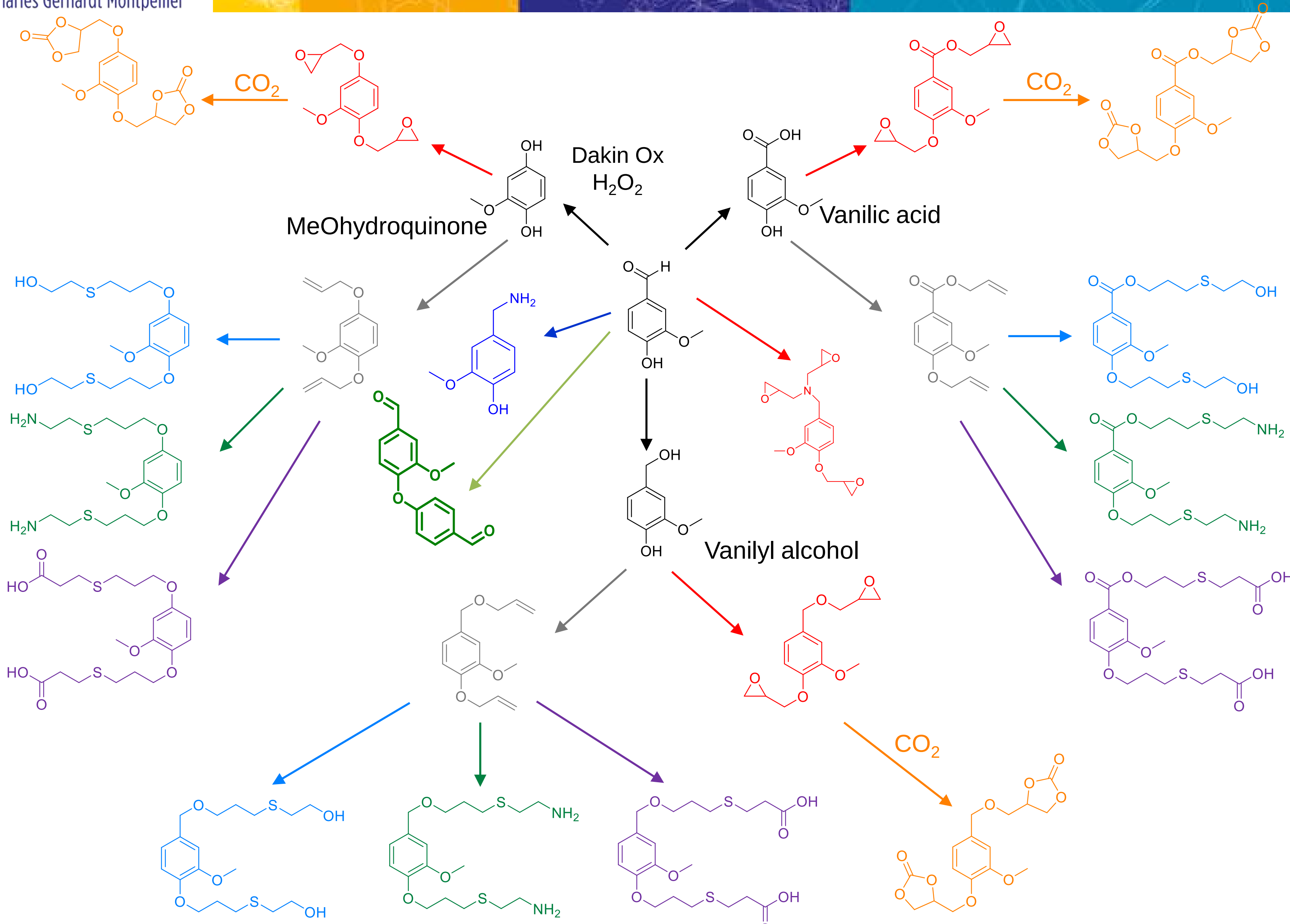

Fache, Caillol et al., **Green Chemistry**, 2014, **16**, 1987-1998

Vanillin-based epoxy polymers

Biobased and aromatic diepoxy monomers from vanillin:

- Use of common industrial hardener : iPDA
- Comparison to existing systems for the synthesis of polyepoxide networks
  - Substitution of BPA diglycidyl ether (BADGE) ?

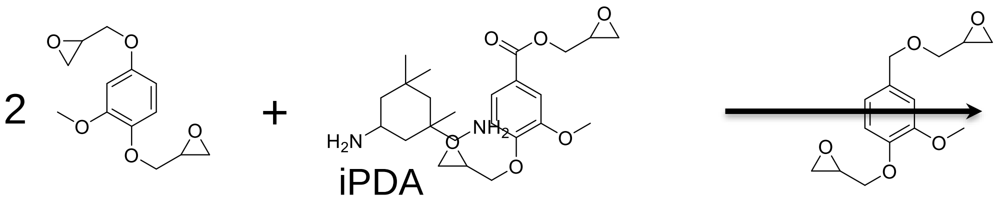

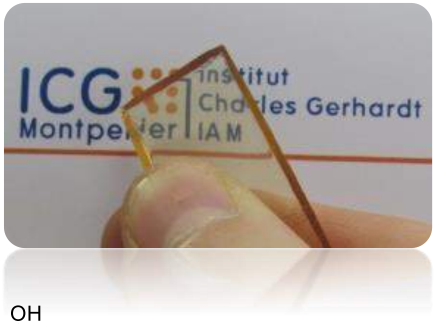

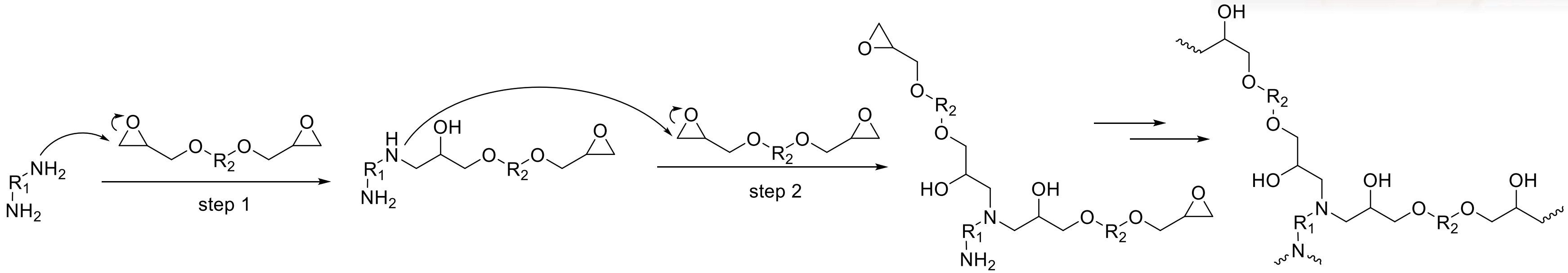

Fache, Caillol et al., **Europ Pol J.**, 2015, **67**, 527-538

Tg of epoxy networks

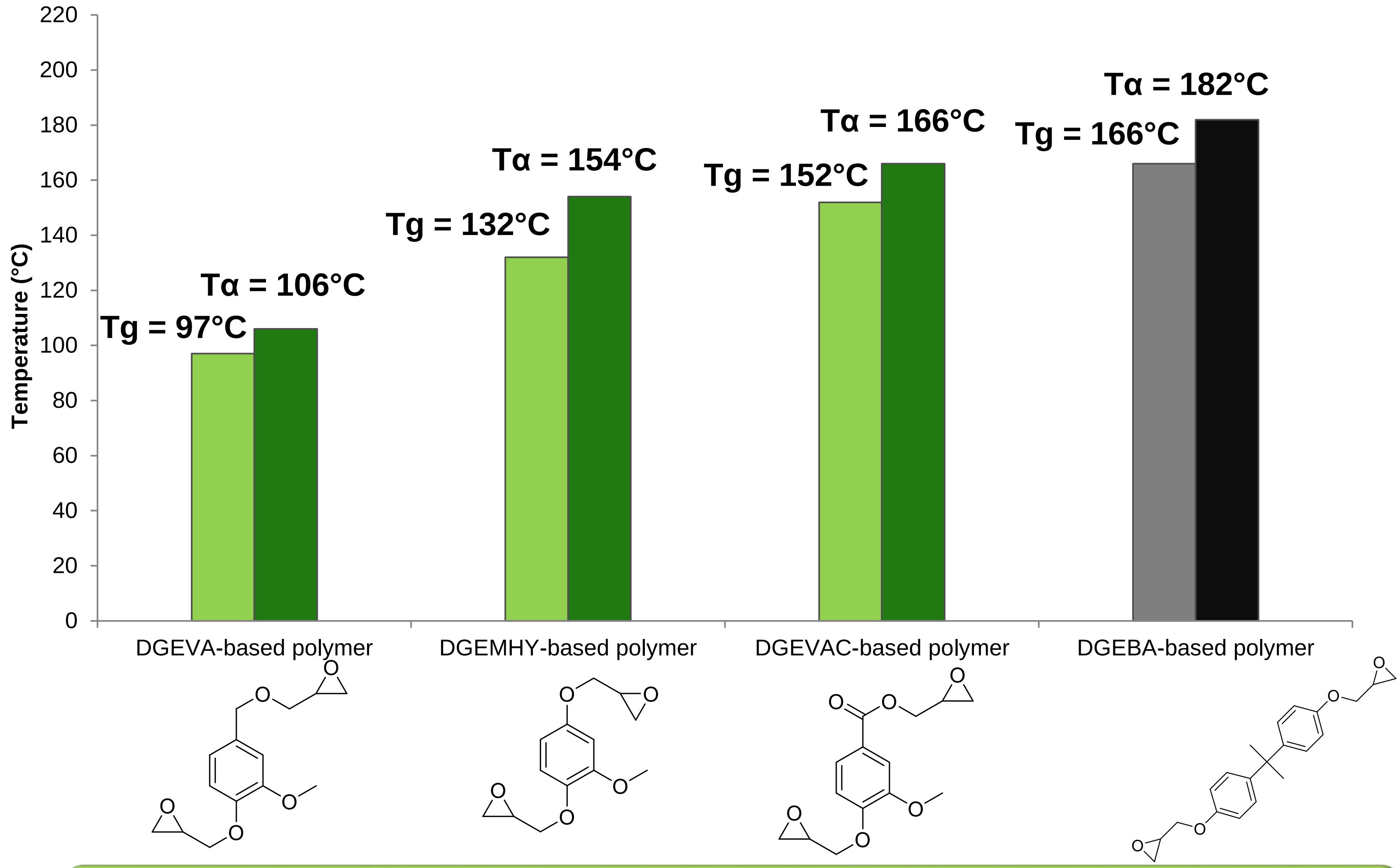

- **Good thermo-mechanical properties, close to BADGE-based materials.**
- **Tunability through the structure of the monomer used.**

Fache, Caillol et al., **Europ Pol J.**, 2015, **67**, 527-538

Structure-property relationships

DGEVA

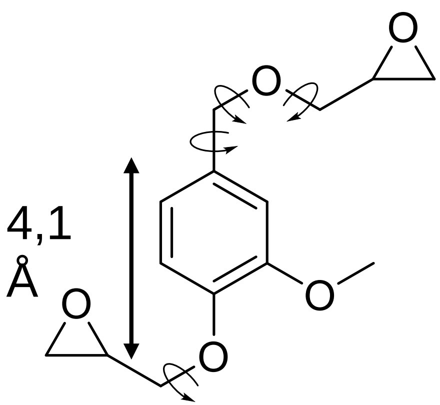

T_g = 97°C
T_α = 106°C

DGEMHY

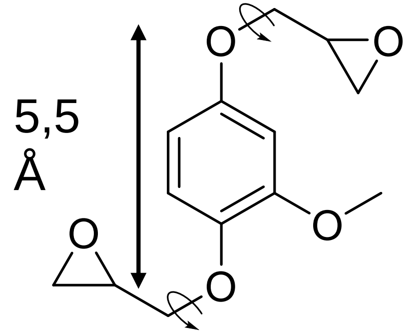

T_g = 132°C
T_α = 154°C

DGEVAC

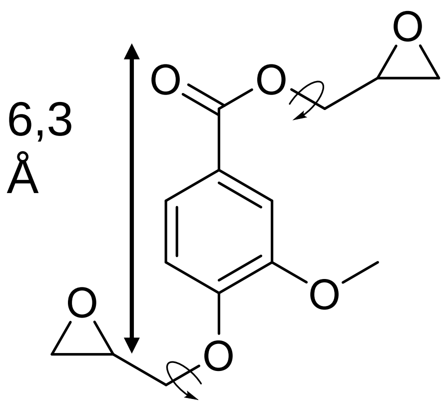

T_g = 152°C
T_α = 166°C

- Size of rigid segments
- Rotations possible

Similar properties compared to networks from BADGE
Possibility to tune properties with structure of monomers

Fache, Caillol et al., **Europ Pol J.**, 2015, **67**, 527-538

Structure-properties

Reactivity

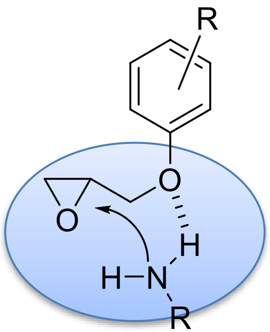

- Reactivity of amines governed by favourable positions due to **H-Bonds**[1]

- **Higher reactivity** of external, ether epoxides, compare to external then internal ones

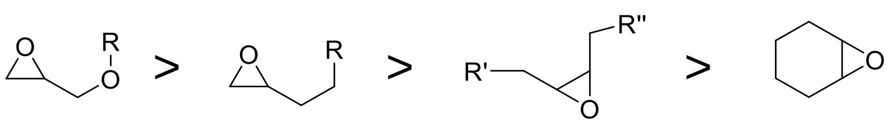

Tg value

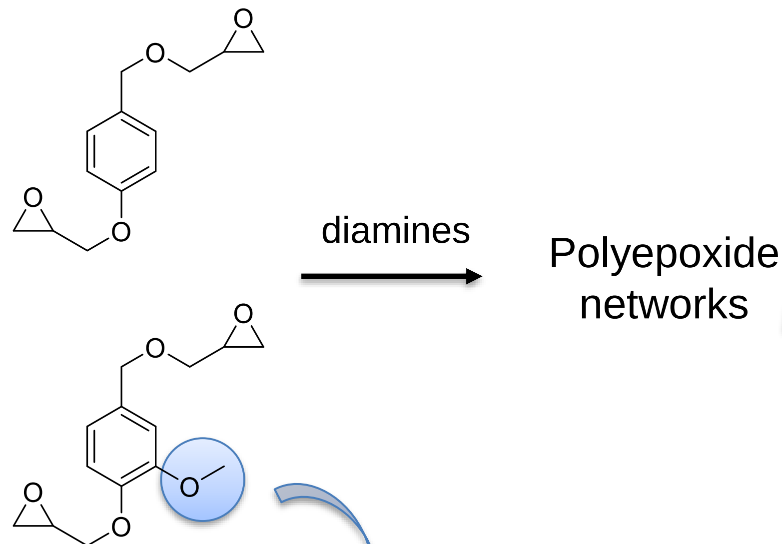

- **MeOH buky groups reduce Tg** of polymers obtained thereof by 23°C [2,3]

1. A Cupples, H Lee, D Stoffey, Advances in Chemistry Series, 1970, 92, 173-207
2. D Hernandez, Master Thesis, Rowan University, USA, 2015
3. D. Hernandez, J. J. La Scala, J. F. Stanzione, et al. ACS Sustainable Chem. Eng., 2016, 4, 4328–4339.

Real life ?

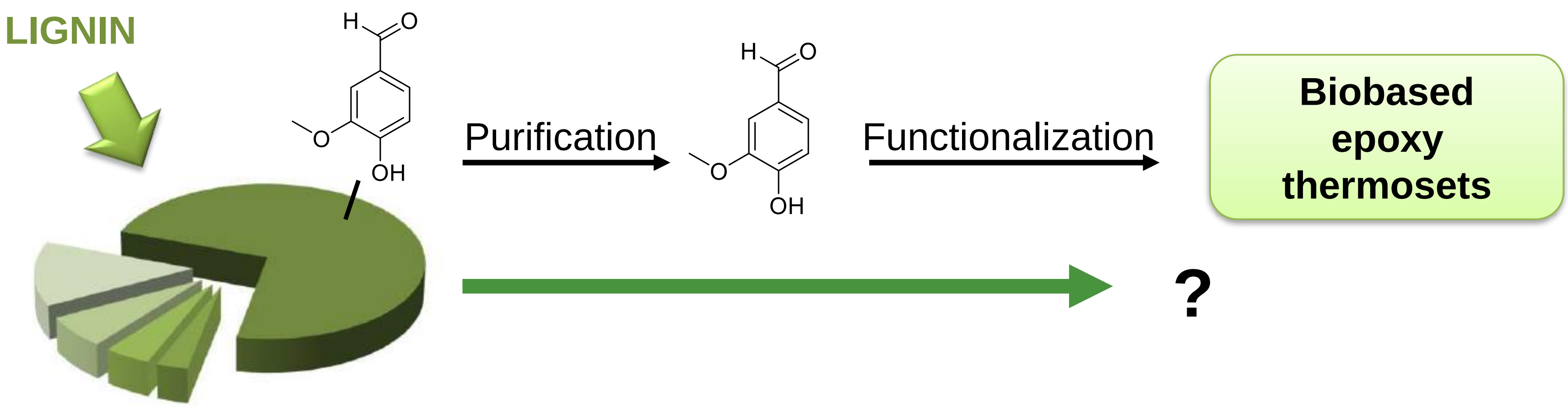

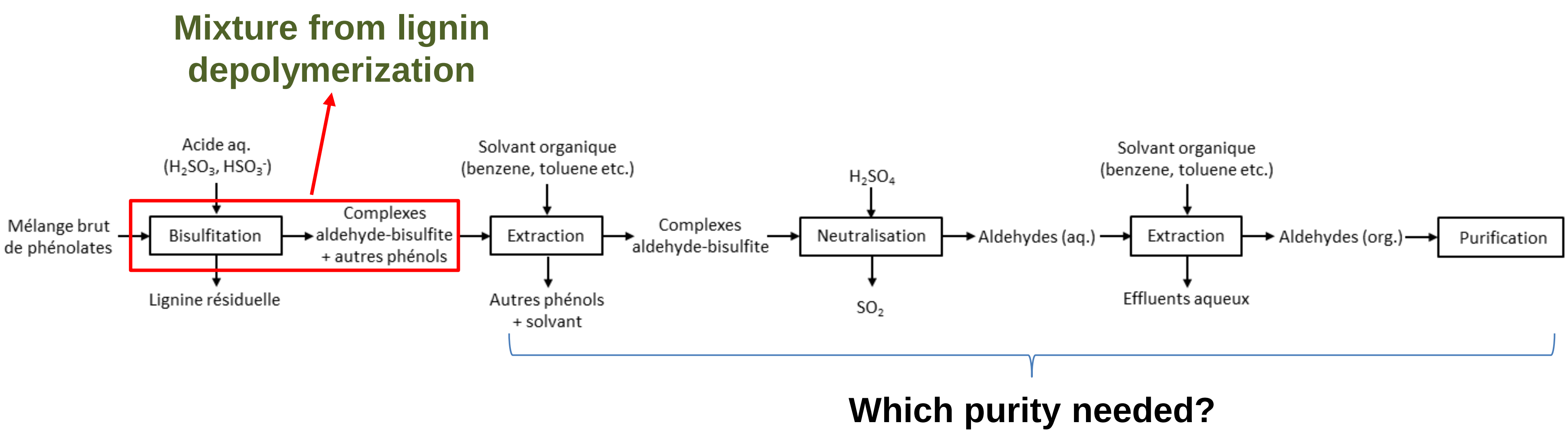

Fache, Caillol et al., **Green Chemistry**, 2016, **18**, 712-725

Epoxy networks from model mixtures

LIGNIN

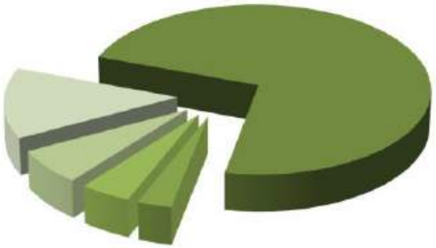

Biobased epoxy thermosets

Mixture from lignin depolymerization

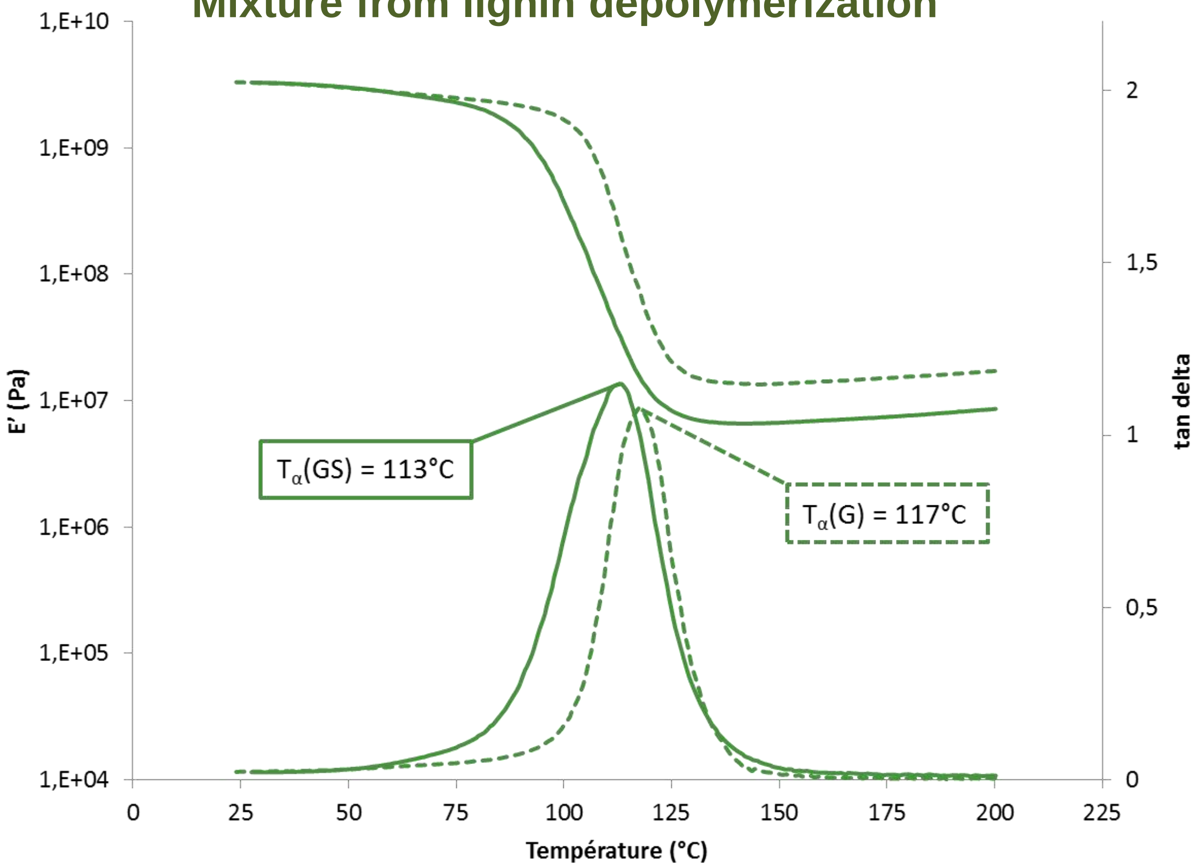

Tα # 115°C

Char @ 600°C : 20%

Fache, Caillol et al., **Green Chemistry**, 2016, **18**, 712-725

From natural phenols to biobased epoxy networks

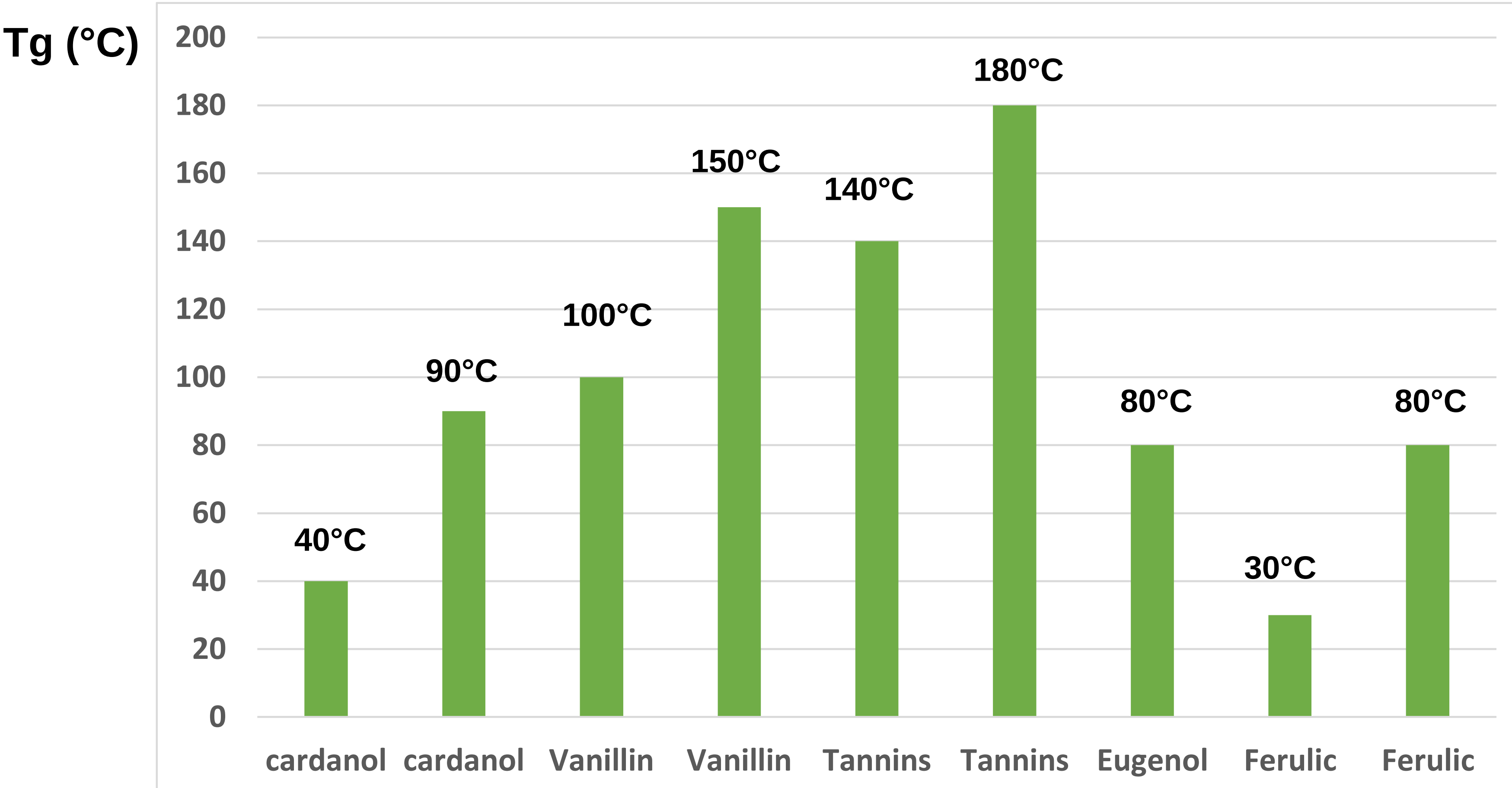

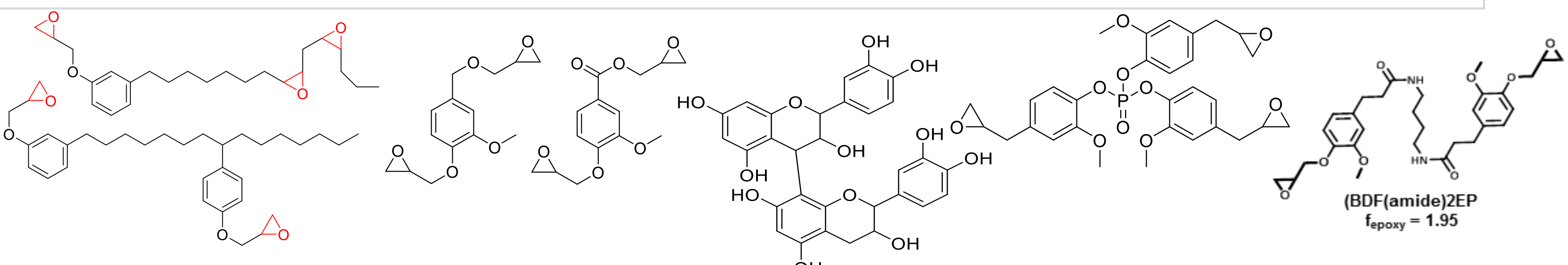

ChemI Rev, 2014, **114**, 1082–1115

Amination of epoxide: toward green amines

- **Direct amination** of glycidyl ether with aqueous ammonia solution
- Obtention of **a hydroxyl amine**

DGEBA (n = 0)

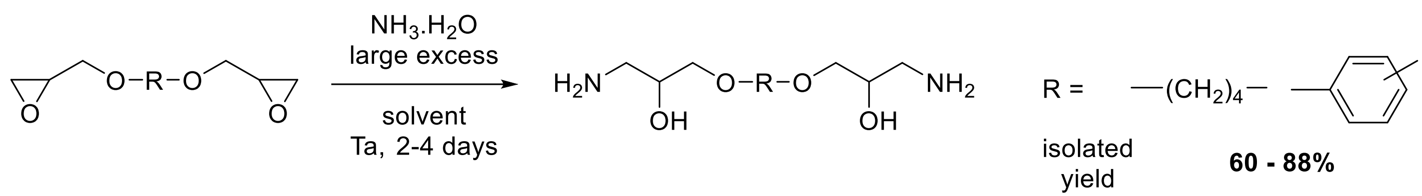

Solvent = acetone, methanol or dioxane

Targets

- Green reaction conditions
- Application to bio-based monomers
- Use of new amine in epoxy thermoset system
- Study of the reactivity of β-hydroxylamine

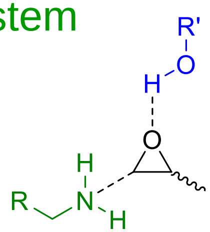

a) Y. Iwakura, S.-I Izawa, F. Hayano, K. Kurita, Die Makromolekulare Chemie, **1967**, *104*, 66-76
b) X. Xu, R. Wang, L. Ling, J. O. Burgess, Journal of Polymer Science: Part A: Polymer Chemistry, **2007**, *45*, 99-110

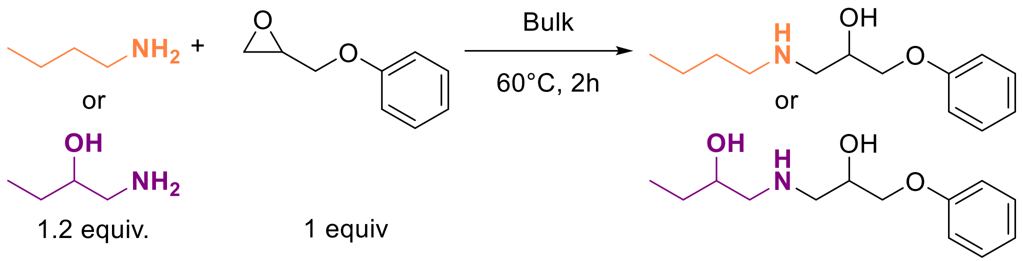

- **Hydrogen bonds ?**

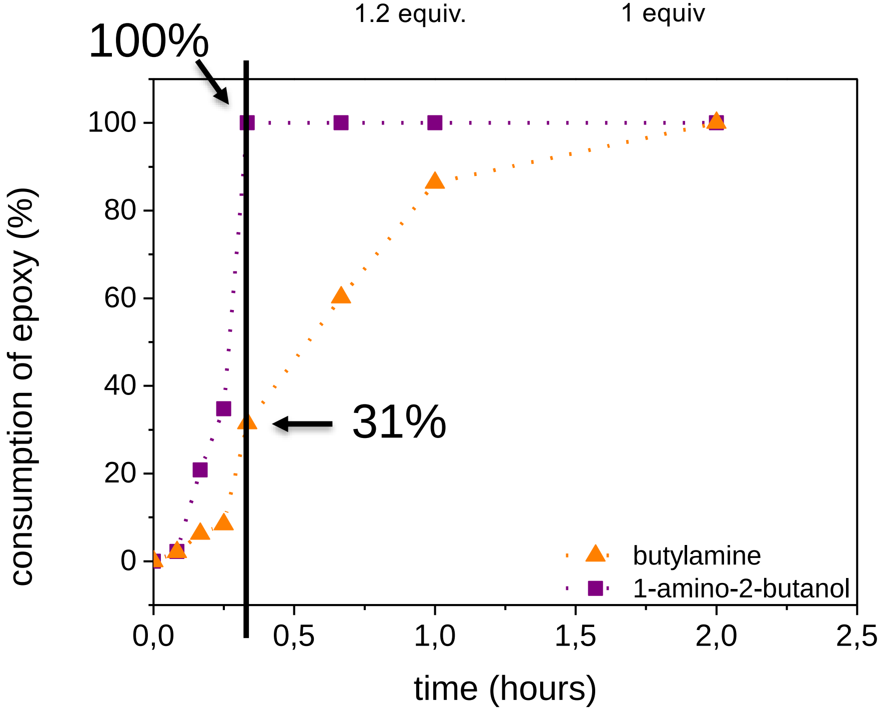

✓ **Positive effect of β-hydroxyl group on amine reactivity**

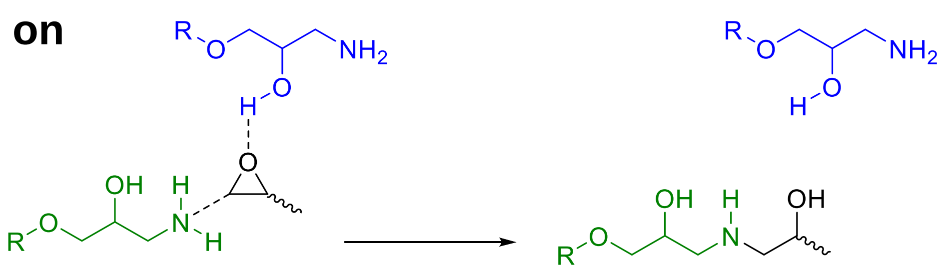

Mora, Caillol et al.,
Green Chemistry, 2018, **20**, 4075-4084

Synthesis of two bio-based amines

- Improvement of this methodology
  - Microwaves irradiations: reduction of heating-time
  - Use of 2-MeTHF, bio-based and nontoxic solvent
  - Functionalization of vanillin-based epoxy monomer

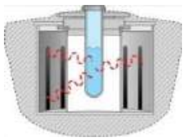

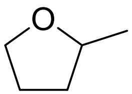

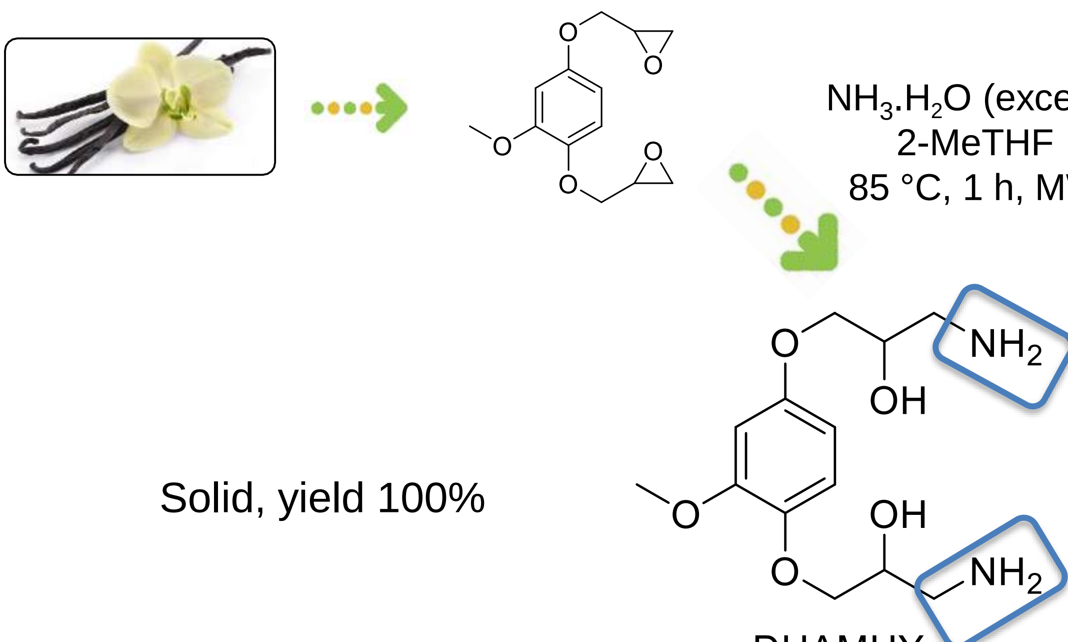

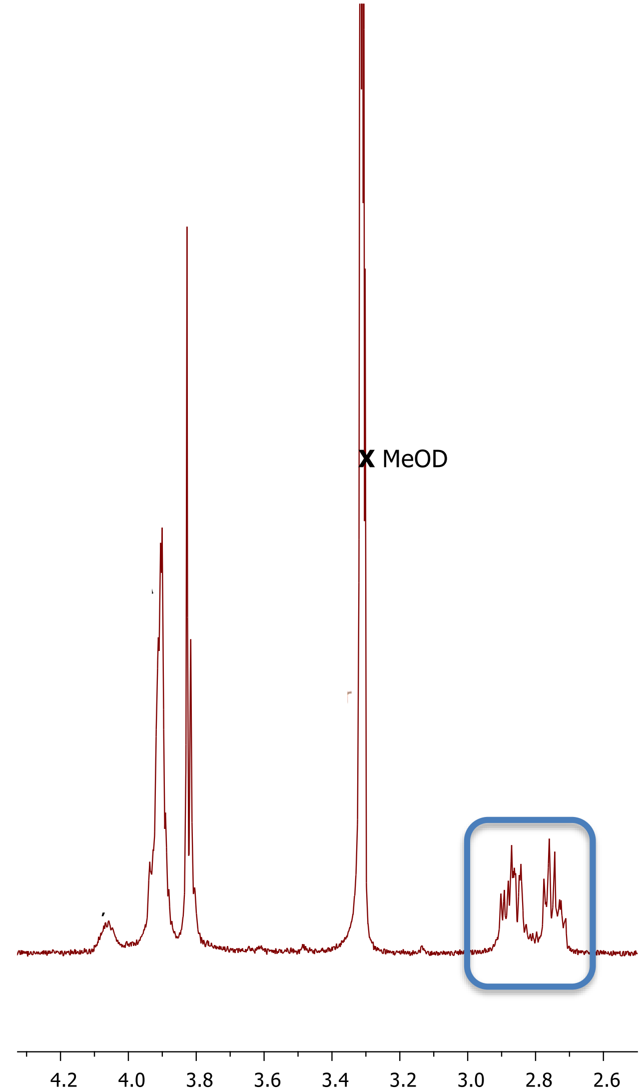

Mora, Caillol et al.,
Green Chemistry, 2018, **20**, 4075-4084

- Improvement of this methodology

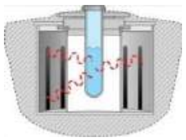

  - Microwaves irradiations: reduction of heating-time
  - Use of 2-MeTHF, bio-based and nontoxic solvent

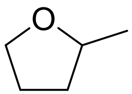

  - Functionalization of vanillin-based epoxy monomer

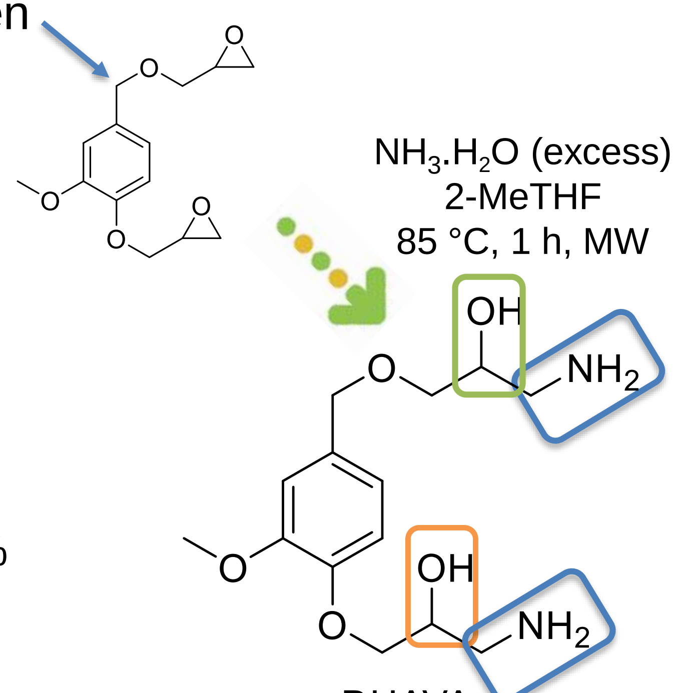

DHAVA

Liquid, yield 100%

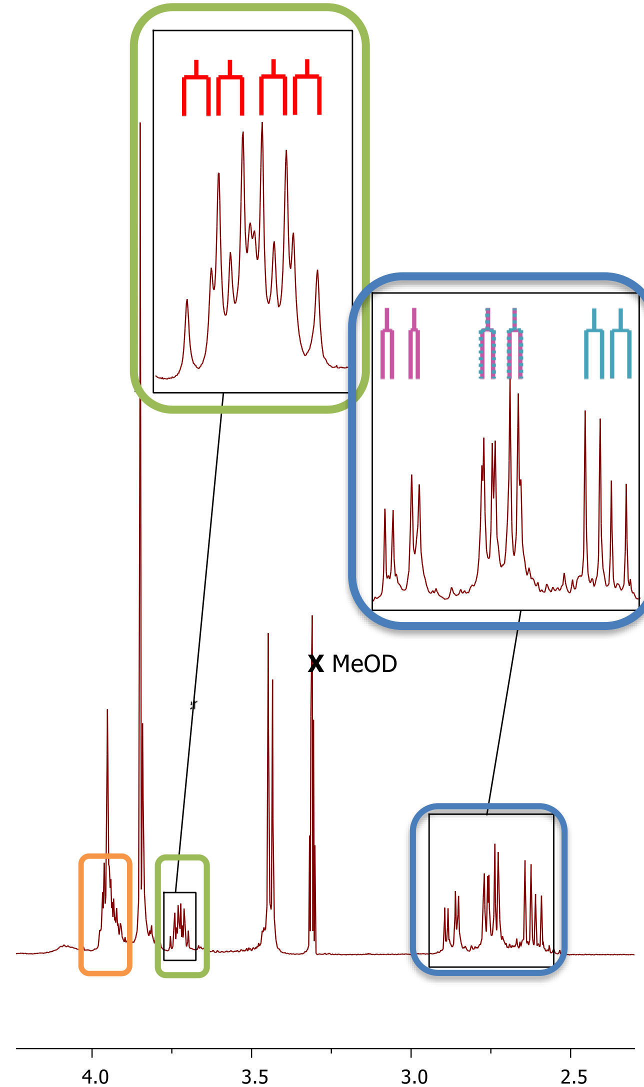

Mora, Caillol et al.,
Green Chemistry, 2018, **20**, 4075-4084

Synthesis of epoxy networks

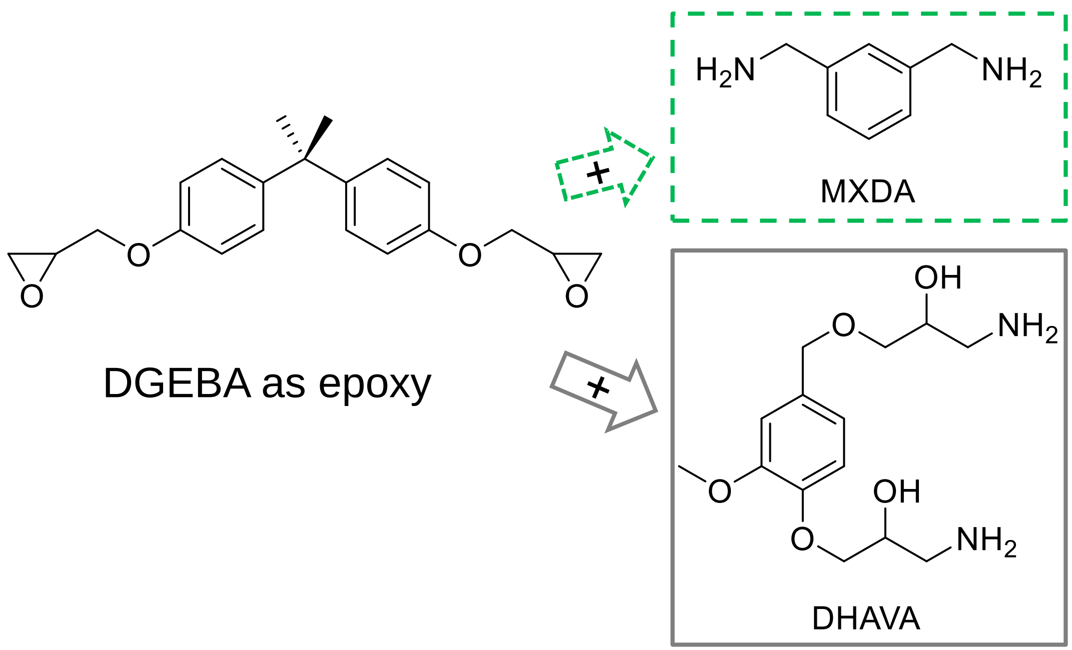

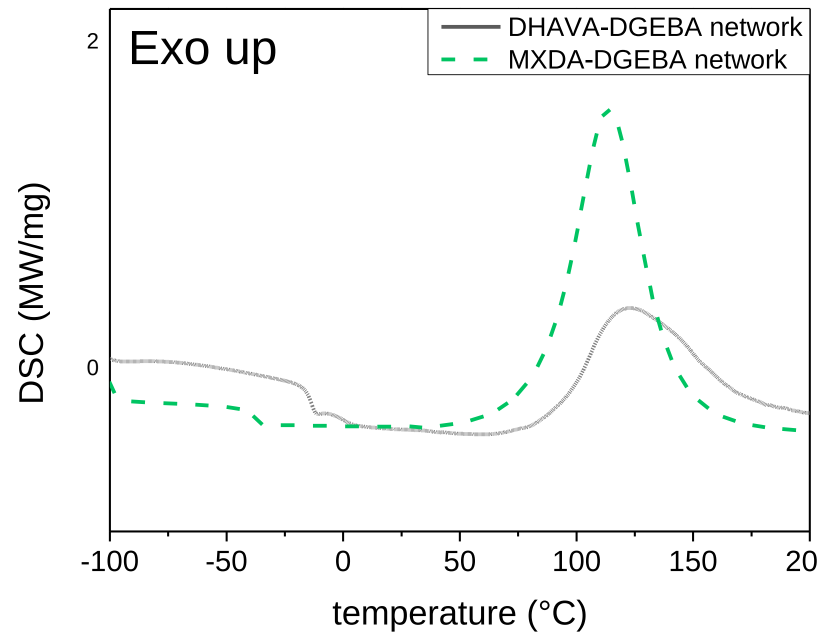

- T_{onset} are very close
  - ➢ 93 °C for DHAVA and 86 °C for MXDA
- The measured enthalpy of the DHAVA-DGEBA network is lower
  - ➢ ΔH ≈ 6 J/mol for DHAVA and ΔH ≈ 84 J/mol for MXDA
  - ➢ Can be advantageous for industrial applications

✓ High reactivity for the β-hydroxylamine DHAVA

Mora, Caillol et al.,
Green Chemistry, 2018, **20**, 4075-4084

Synthesis of epoxy networks

1 monomer = 1 thermoset !

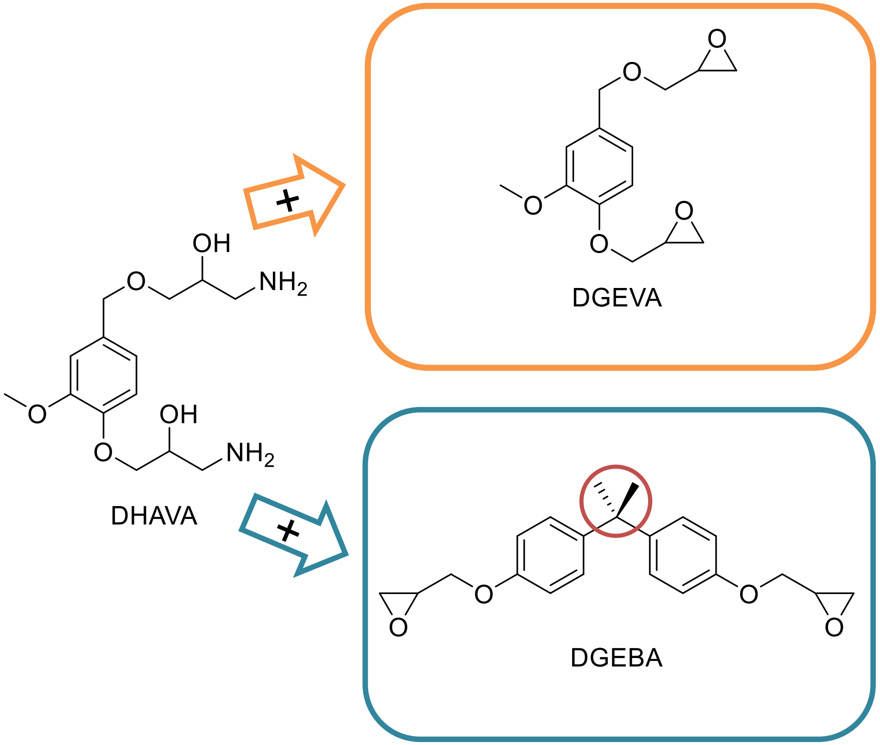

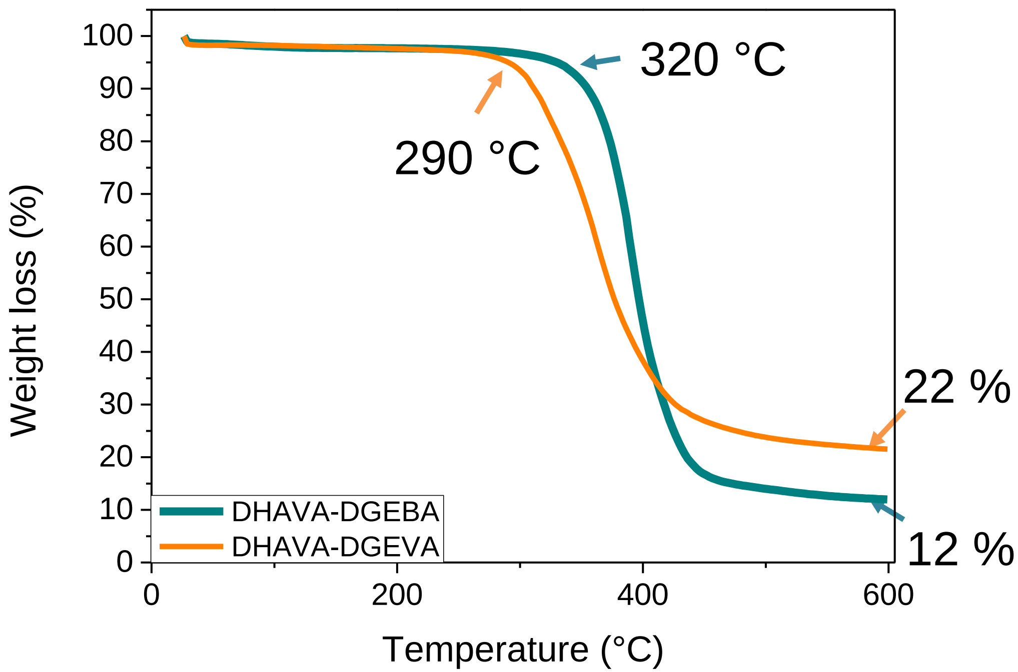

$T_{5\%}$: the higher aromaticity of DGEBA confers higher thermal stability to the thermoset

Residual mass at 600 °C: higher thermal stability over time = the absence of the *gem* dimethyl bridge on DGEVA

Mora, Caillol et al.,
Green Chemistry, 2018, **20**, 4075-4084

Synthesis of epoxy networks

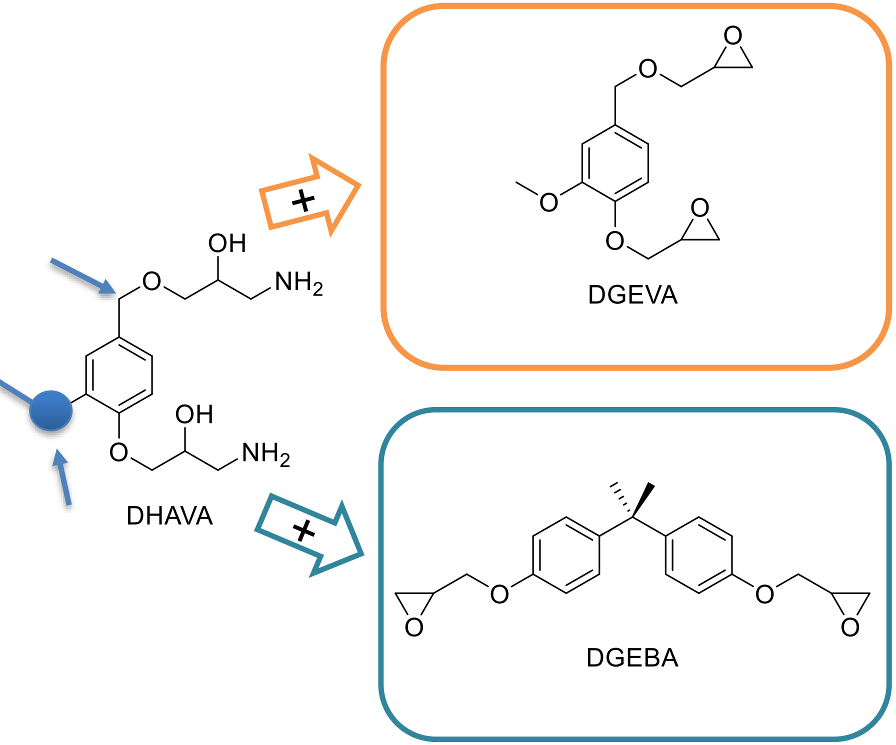

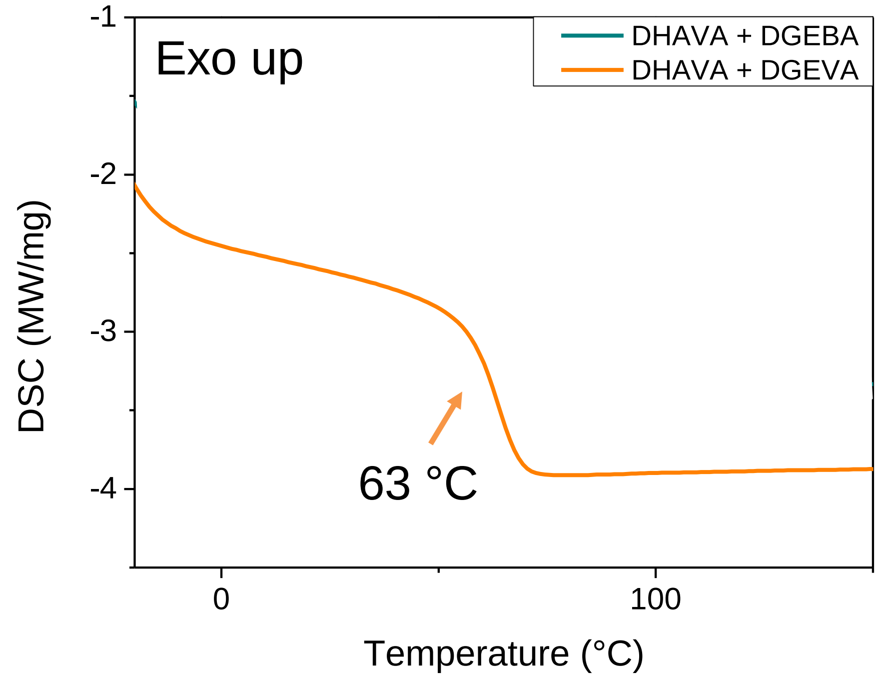

Methoxy [a] and methylene groups behave as spacers and lower the Tg

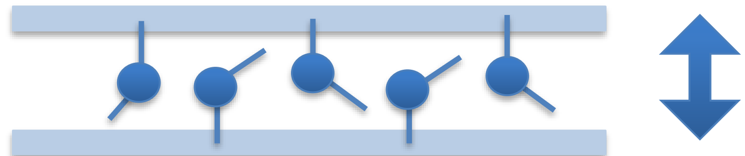

Mora, Caillol et al.,
Green Chemistry, 2018, **20**, 4075-4084

a) E. D. Hernandez, A. W. Bassett, J. M. Sadler, J. J. La Scala and J. F. Stanzione, ACS Sustainable Chem. Eng., 2016, 4, 4328–4339.

Synthesis of epoxy networks

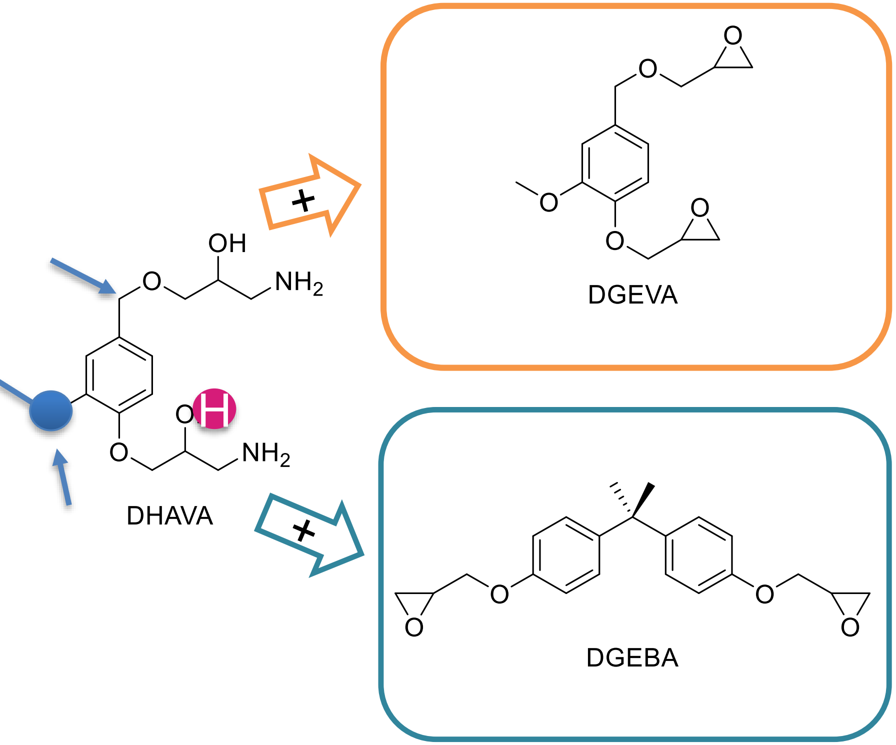

Higher Young modulus = high rigidity

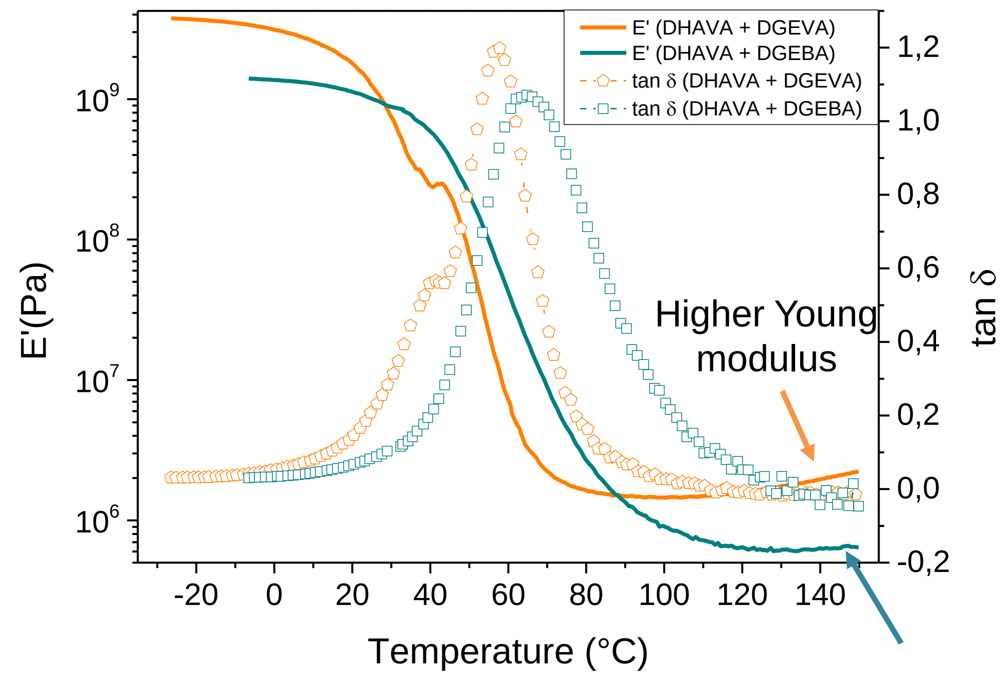

Network	DHAVA-DGEBA	DHAVA-DGEVA
Swelling index	134%	5%

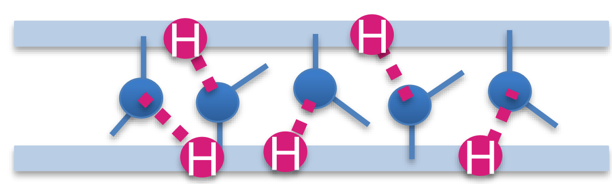

Hydrogen bonds

✓ The methoxy moieties may increase stiffness because of hydrogen bonding

Mora, Caillol et al., **Green Chemistry**, 2018, **20**, 4075-4084

Context

Elaboration of ablative phenol-formaldehyde resol resins for aerospace industry

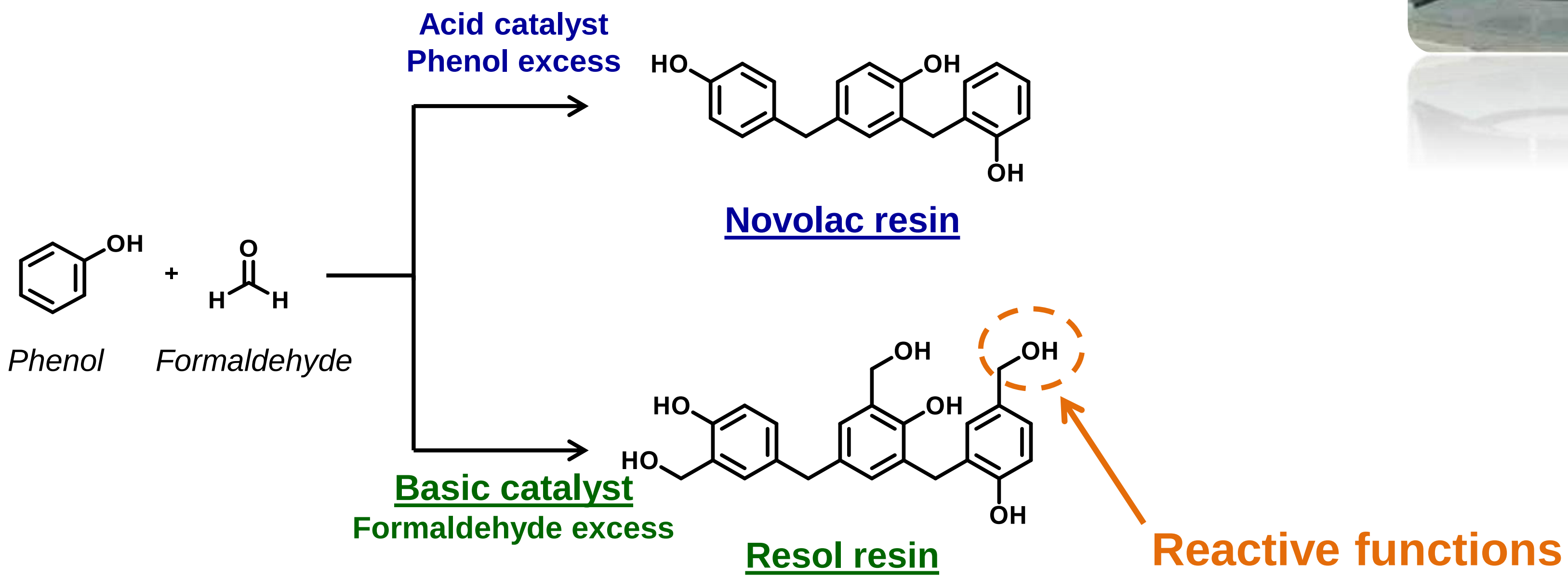

Resin polymerizable in several steps [cat. basic]

Context

Elaboration of ablative phenol-formaldehyde resol resins for aerospace industry

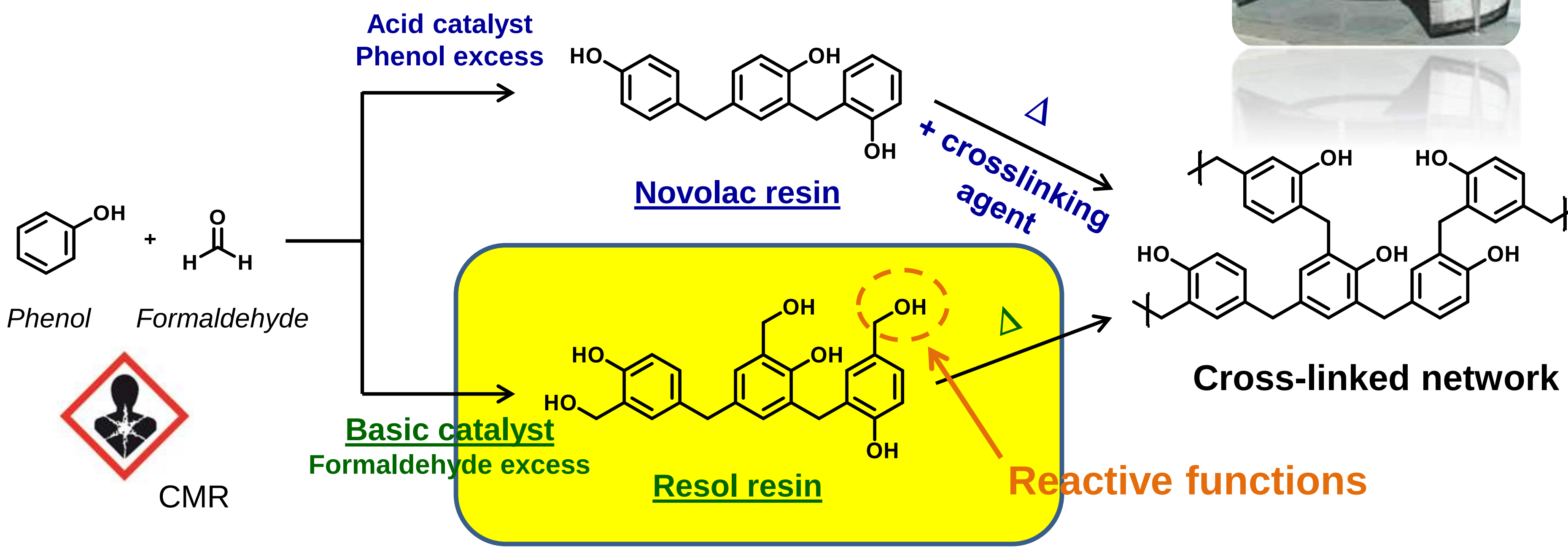

Resin polymerizable in several steps [cat. basic]

Which biobased aldehydes?

Biobased aldehyde reactants

Furfural 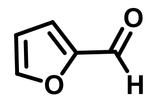

Glyoxal 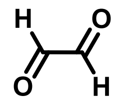

Reactive aldehydes[1,2] but **CMR 2**

Dimethoxyethanal 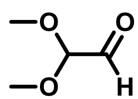

Not CMR but **low reactivity**[3]

Vanilline 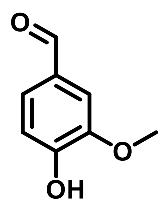

Non toxic [food ingredient]

Available resource [lignin]

Aromatic aldehyde [high density of aromatic]

No information in literature on reactivity in basic media

[1] C. Lacoste; M. C. Basso; A. Pizzi; M. P. Laborie; D. Garcia; A. Celzard, *Industrial Crops and Products,* **2013**, *45*, 401.
[2] L. H. Brown, *J. Ind. Eng. Chem.,* **1952**, *44*, 2673.
[3] A. Despres; A. Pizzi; C. Vu; H. Pasch, *J. Appl. Polym. Sci.,* **2008**, *110*, 3908.

Reactivity of vanillin derived aldehydes

- **No information in literature on reactivity of vanilin derivatives in basic media**
- **Theoretical study of reactivity of aldehyde functions**

Hammett constants[1] **: σ** $\Longrightarrow$ Study of electronic effect of substituents R

For each substituant :

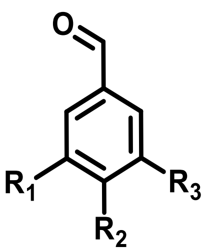

$\sigma>0$: *Electro-attracting* effect on aldehyde function

$\sigma<0$: *Electro-donating* effect on aldehyde function

R	σ_{meta}	σ_{para}
H	0	0
OH	0,12	-0,37
O^-	-0,47	-0,81
OMe	0,12	-0,27
CHO	0,35	0,42

Sum of effects of all substituents :

$$\boxed{\Sigma\sigma = \sigma\,(R_1)_{meta} + \sigma\,(R_2)_{para} + \sigma\,(R_3)_{meta}}$$

Σσ↗ : Electrophilic reactivity of aldehyde ↗[2]

[1] C. Hansch; A. Leo; R. W. Taft, *Chem. Rev.*, **1991**, *91*, 165.
[2] E. F. Pratt; E. Werble, *J. Am. Chem. Soc.*, **1950**, *72*, 4638.

Reactivity of vanillin derived aldehydes

Institut Charles Gerhardt Montpellier

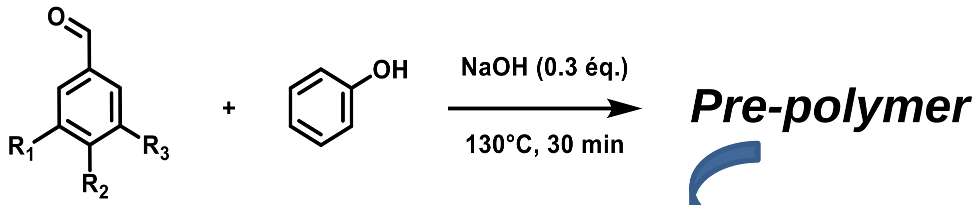

Reactivity at 15mn by ^{1}H NMR

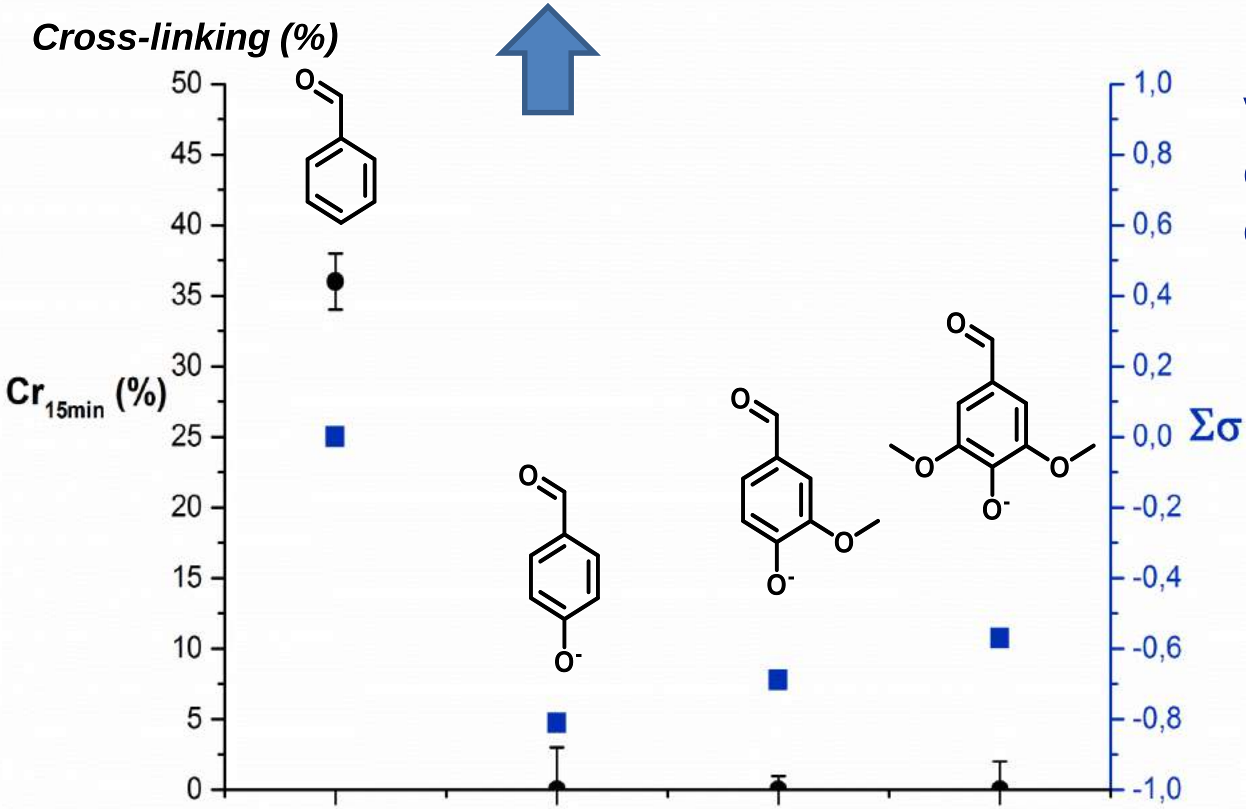

Very low reactivity confirmed by Hammett constants

R	σ_{meta}	σ_{para}
H	0	0
OH	0,12	-0,37
O^-	-0,47	-0,81
OMe	0,12	-0,27
CHO	0,35	0,42

Need to protect hydroxy functions to avoid formation of hydroxylate

Reactivity of vanillin derived aldehydes

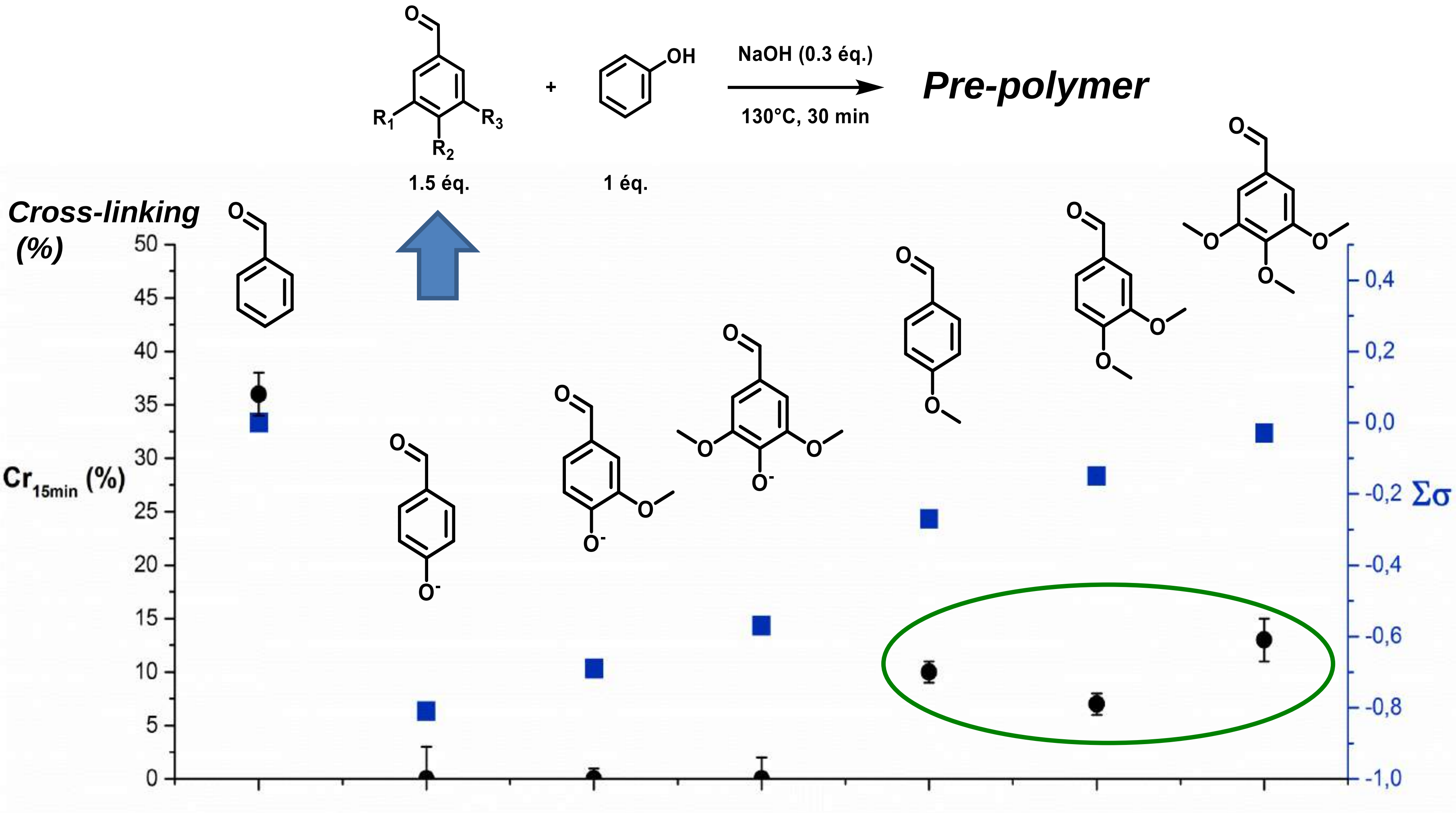

Significative increase of reactivity

Reactivity of vanillin derived aldehydes

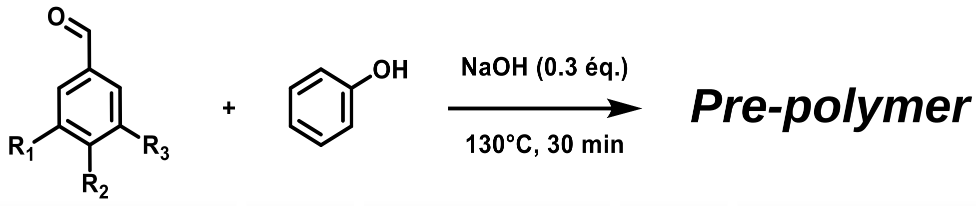

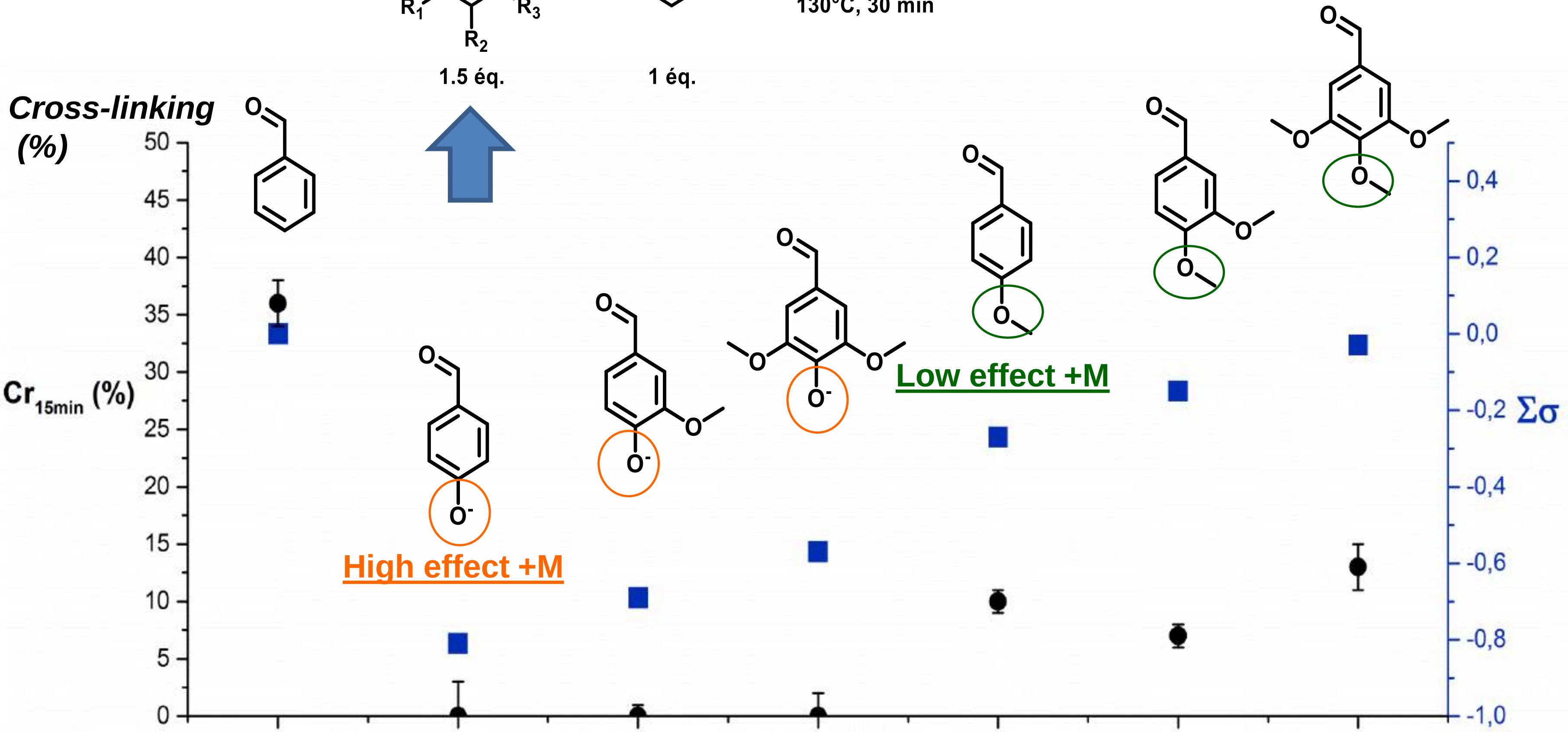

Significative increase of reactivity

- Despite lower electro-donating effects
- Still low conversion
- And low thermal stability

Functionalization to increase reactivity

Grafting of aromatic aldehyde groups

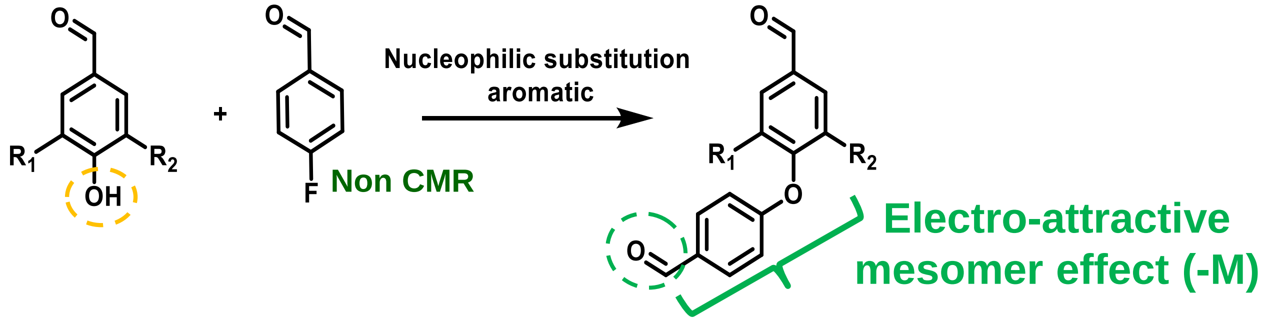

Foyer, Caillol et al.,
Eur. Pol. J., 2016, **74**, 296-309
Eur. Pol. J., 2016, **77**, 65-74

Functionalization to increase reactivity

Institut Charles Gerhardt Montpellier

Grafting of aromatic aldehyde groups

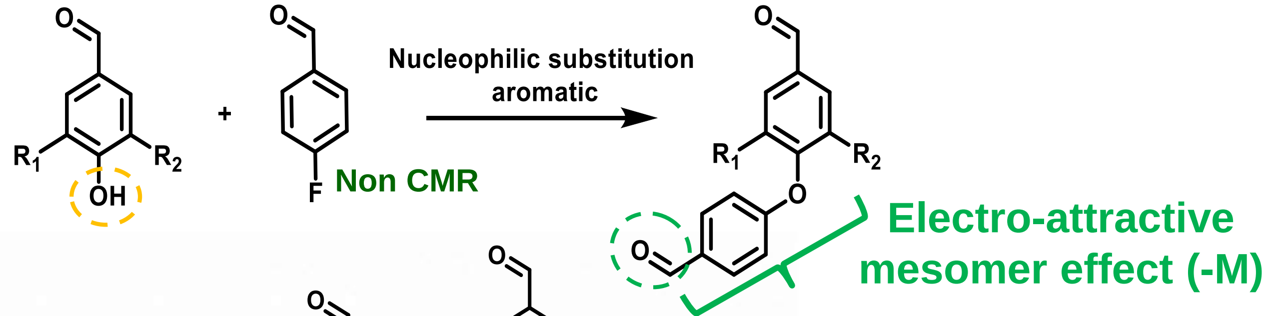

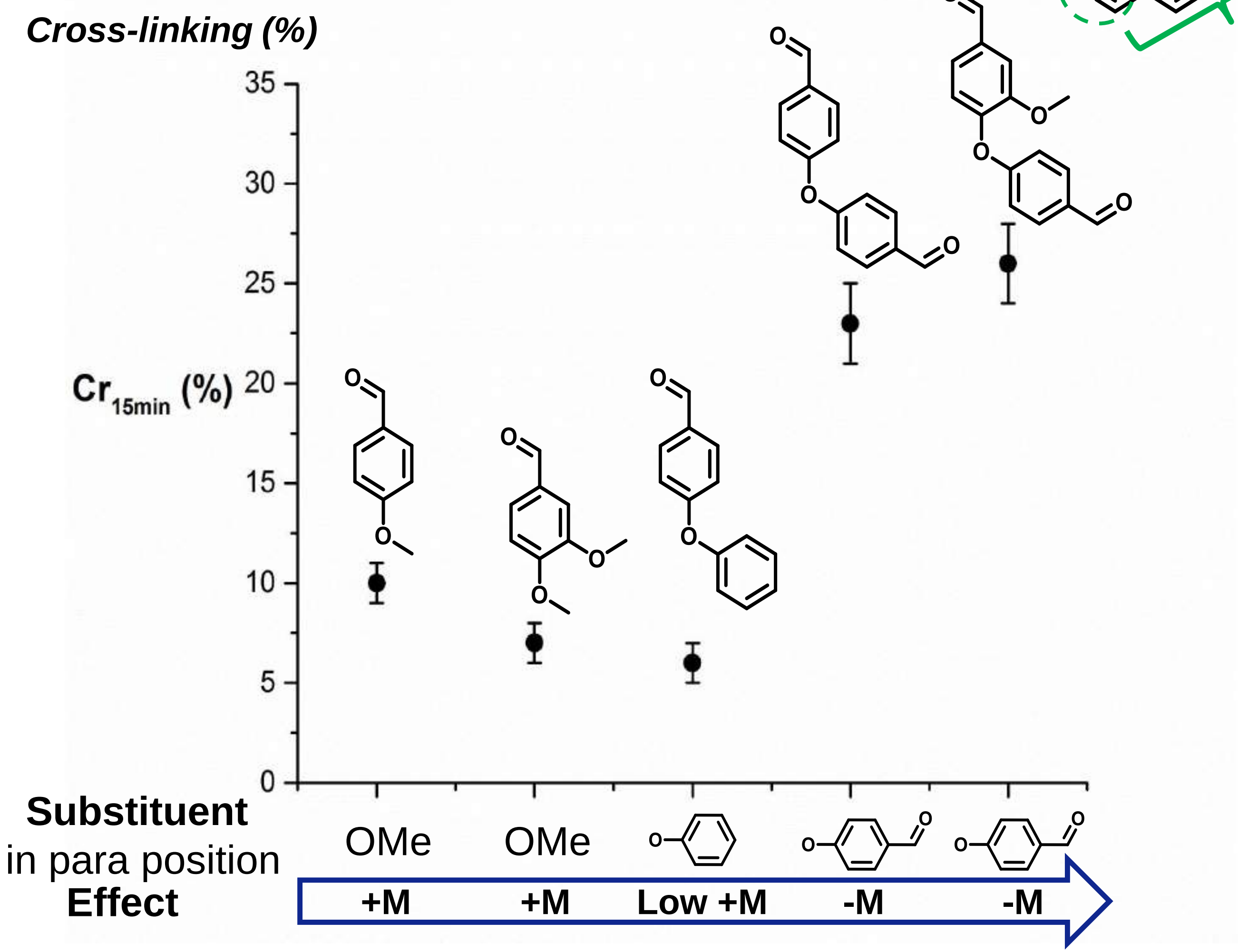

Foyer, Caillol et al.,
Eur. Pol. J., 2016, **74**, 296-309
Eur. Pol. J., 2016, **77**, 65-74

Functionalization to increase reactivity

Grafting of aromatic aldehyde groups

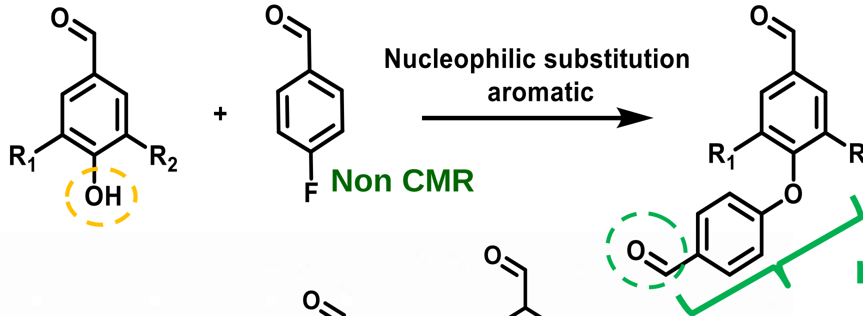

Electro-attractive mesomer effect (-M)

Cross-linking (%)

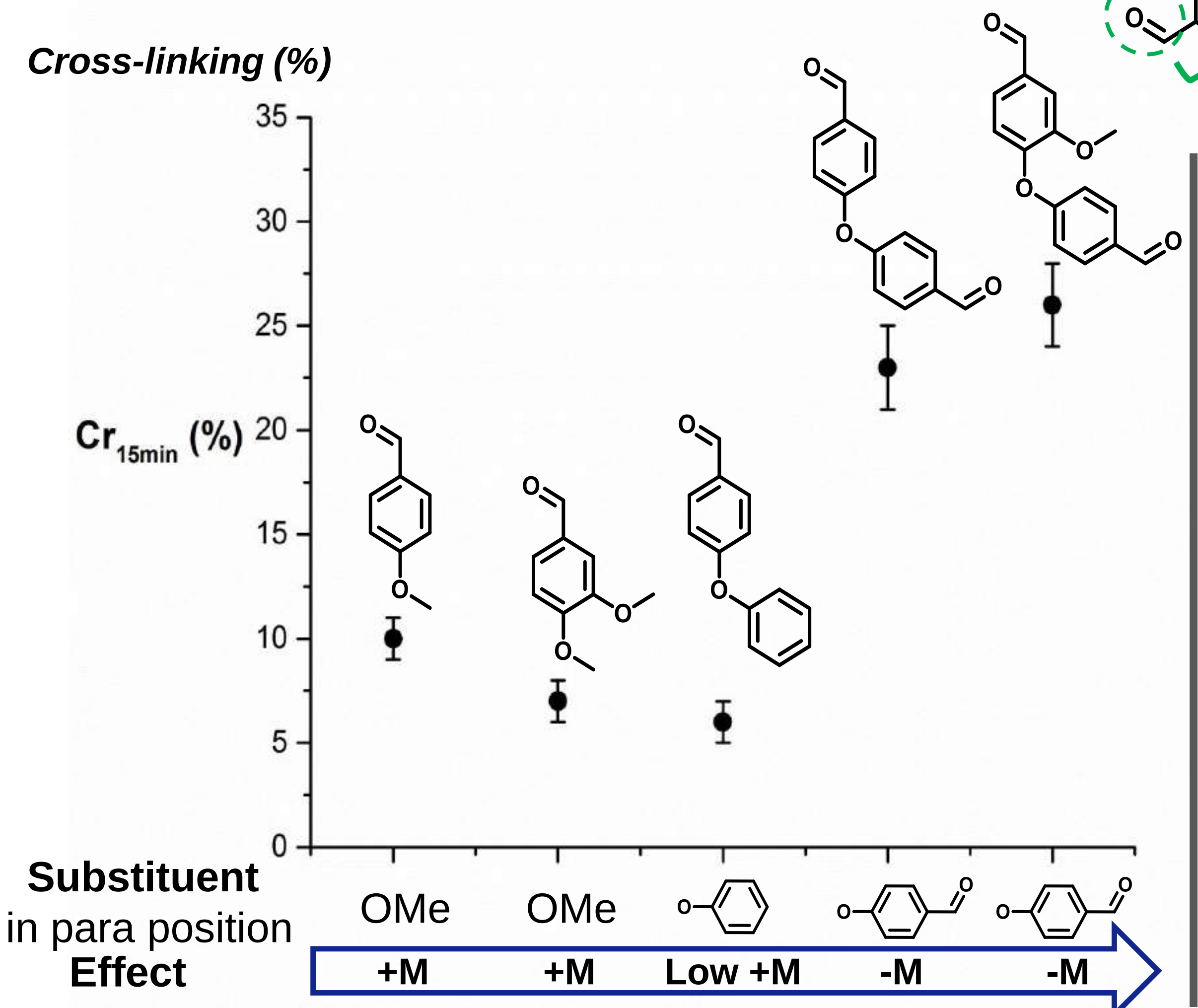

Steric hindrance of phenoxy group

Significative increase of reactivity by functionalization with group -M

Aldehydes:
Biobased, Reactive, Aromatic and Difunctional

Foyer, Caillol et al.,
Eur. Pol. J., 2016, **74**, 296-309
Eur. Pol. J., 2016, **77**, 65-74

Thermal resistance: Char content

Determination of char (coke) content of formadehyde free resins [TGA under N_2] ***:***

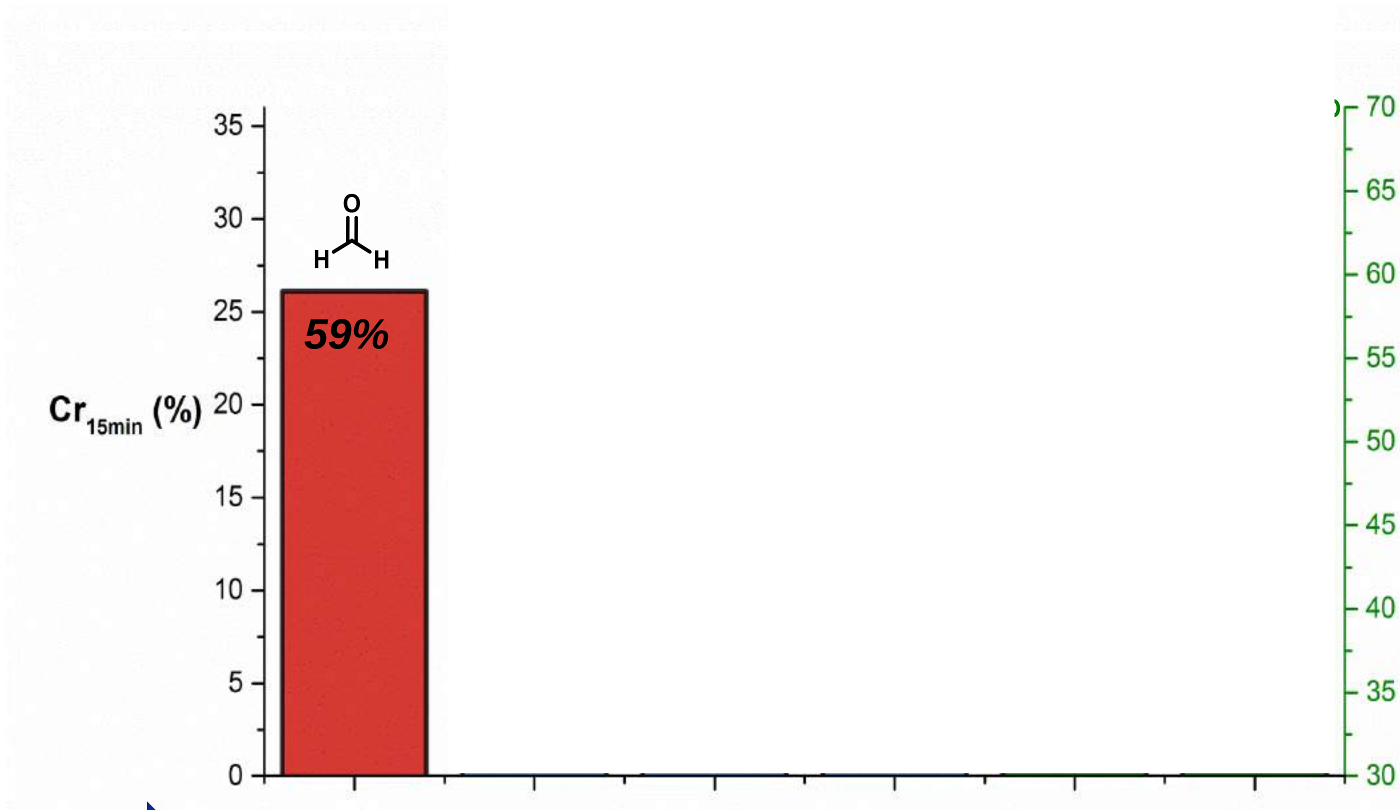

Target reached

(≥ 59%)

Char content (%)

900°C

Strategy validated: **Biobased precursors allow substitution of formaldehyde**

Herakles Patent, WO116697A1, 2016 ; Herakles Patent, WO116699A1, 2016; Herakles Patent pending FR 1560070, 2015

Foyer, Caillol et al.,
Eur. Pol. J., 2016, **74**, 296-309
Eur. Pol. J., 2016, **77**, 65-74

Particle board adhesives

Maritime pine bark tannins

Natural extract

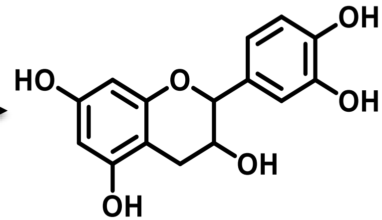

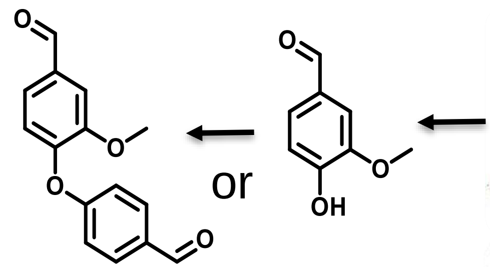

Wood lignin

20% w/w

Water/EtOH

10% solids with dry industrial wood chips
Panels hot pressed at **220 °C** - 7.5min with a pressure cycle of 28kgcm^3/15kgcm^3/5 kgcm^3 for 2min/2.5min/3min.

European Standard EN319 : 1993
Determination of tensile strength perpendicular to the plane of the board
0.47MPa > 0.35MPa

Polymers suitable for particle board adhesive

Collaboration
Pr Antonio Pizzi
ENSTIB

Pizzi, Caillol et al., **Int J Adhesion and Adhesives,** 2016, **10**, 239-248

Curing of Acrylic polymer with biobased aromatic cross-linker

Example of standard curing :

Polyacrylate

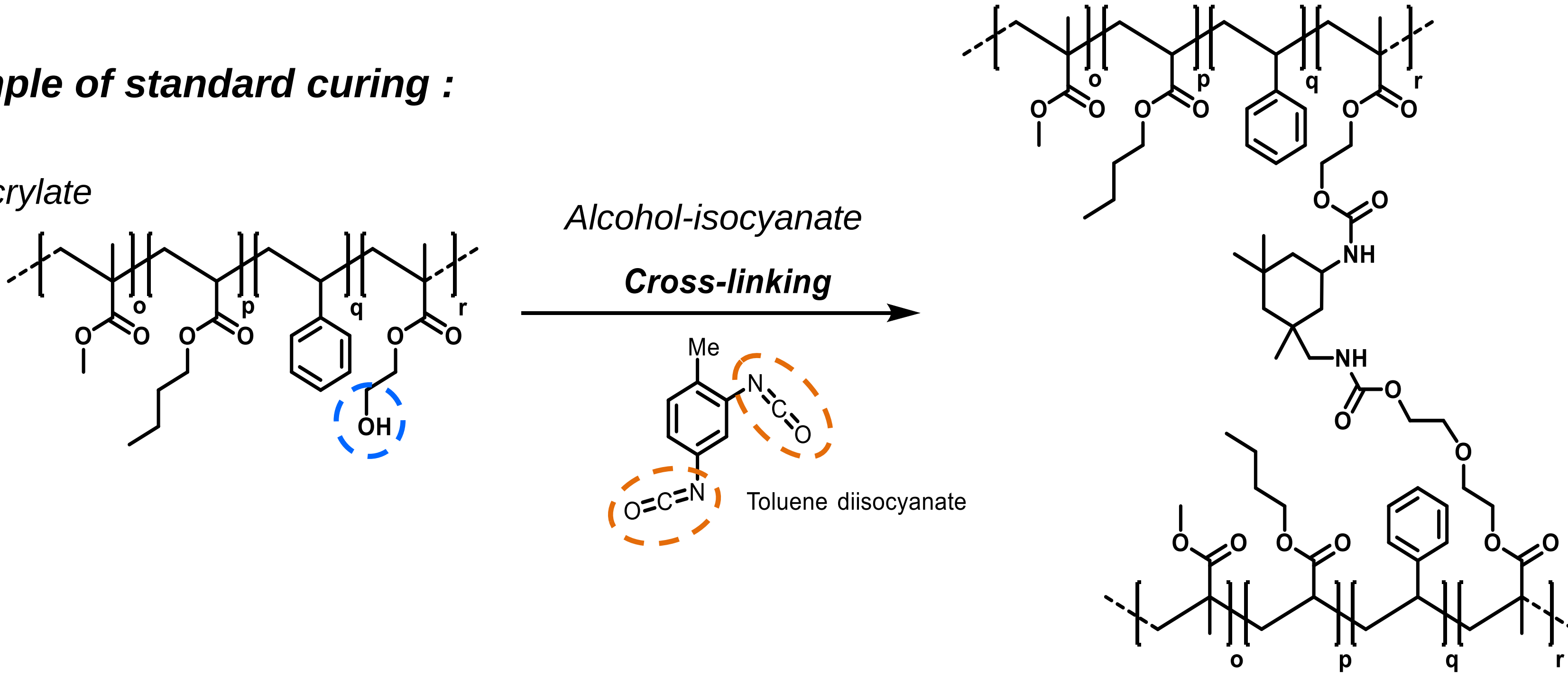

Cross-linked coating

<u>High performance properties:</u>

- ***durability***
- ***thermal stability***
- ***solvent and water resistance***
- ***mechanical strength***
- ***stain protection***

Curing of Acrylic polymer with biobased aromatic cross-linker

Toxicity issues

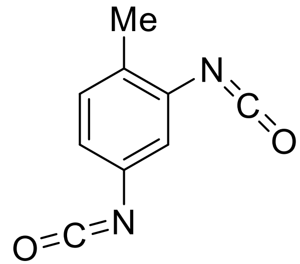

TDI classified CMR
(Carcinogenic Mutagenic Reprotoxic)

Phenolic hardener

Need of alternative aromatic cross-linking systems <u>without toxic hardener</u>

Aldehyde-functional styrenic monomer

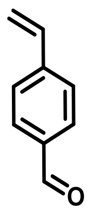

Vinylbenzaldehyde (VBA)

Not classified as CMR

Copolymerization

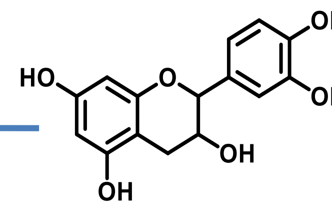

Catechin

Biobased and non-toxic crosslinker from wood tannins

Aldehyde functional copolymer

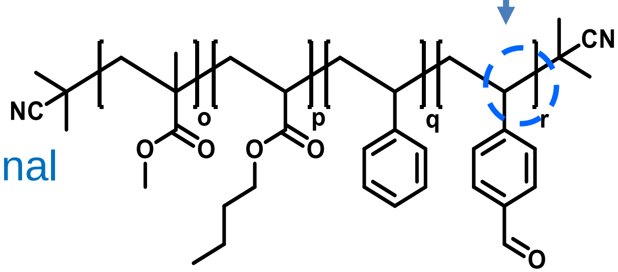

Cross-linking

Cross-linked coating

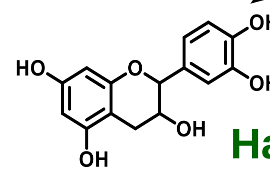

Hardener

<u>Advantage</u>: Aromatic composition ***Thermal stability and rigidity***

Synthesis and polymerization of aldehyde monomer

- **Synthesis of aldehyde monomer[1]**

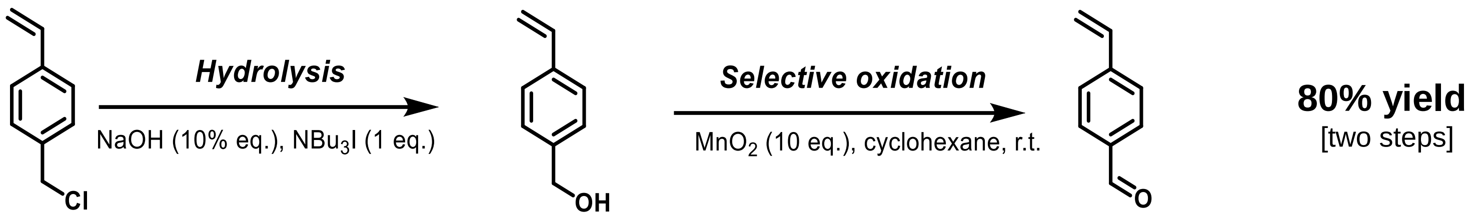

Vinylbenzylchloride   Vinylbenzylalcohol   **Vinylbenzylaldehyde VBA**

- **Copolymerization of the aldehyde monomer**

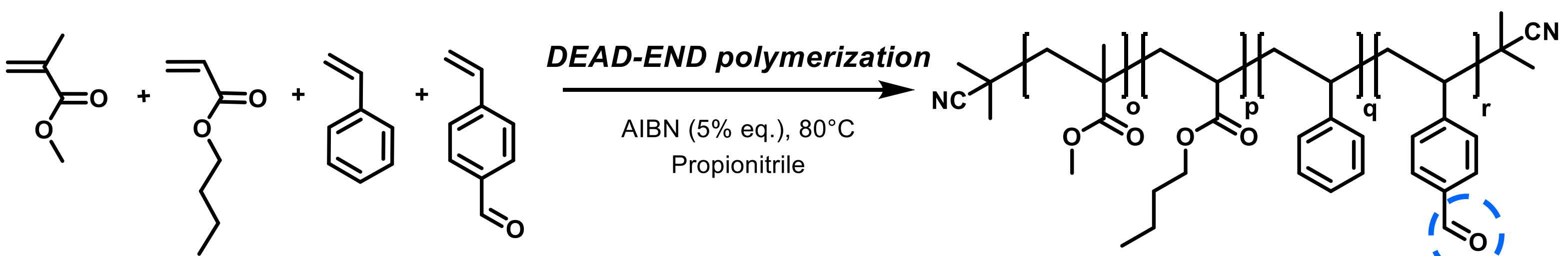

MMA   **ABu**   **S**   **VBA**

VBA concentrations: 0, 2, 4 and 6%w

▸ New (meth)acrylic-styrenic oligomers with aldehyde functional groups for coating applications

Foyer, Caillol et al., **Progress in Organic Coatings**, **2015**, 84, 1-8,

Cross-linking of aldehyde copolymer with:

- resorcinol (as a model)
- catechin

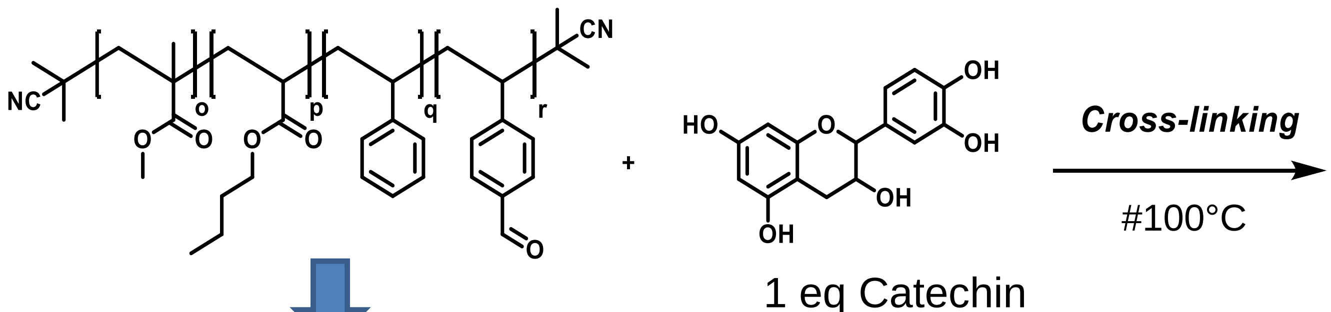

Copolymer	$\overline{\text{Mn}}$ (g/mol)	Tg (°C)
COP-0%	7,600	65
COP-2%	5,000	68
COP-4%	7,550	67
COP-6%	5,050	72
COP-6% LTg	8,600	50

Cross-linked coating

- Formulations casted on steel plates with a 50 µm film thickness (bar-coater)

Foyer, Caillol et al., **Progress in Organic Coatings**, **2015**, 84, 1-8,

Coating characterizations

ALDEHYDE MONOMER CONTENT

For all cross-linked coatings:

Gel content (%)

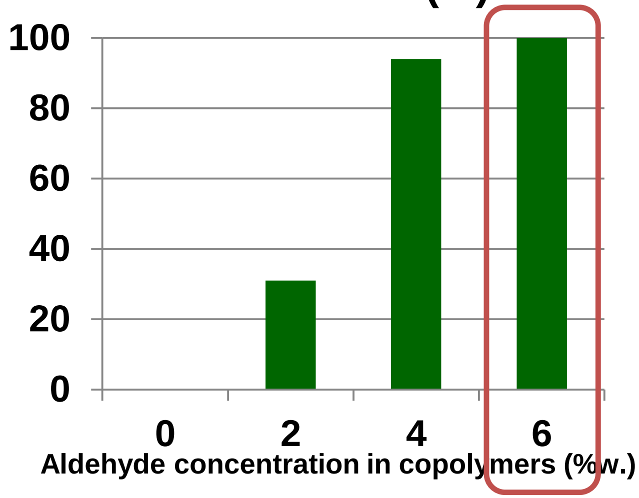

Swelling index (%)

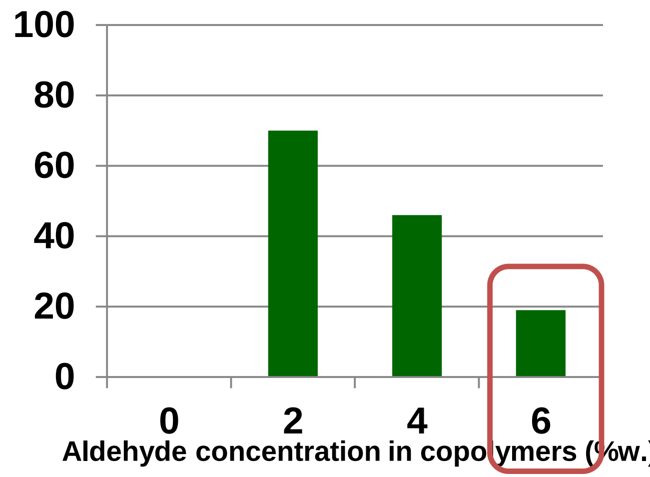

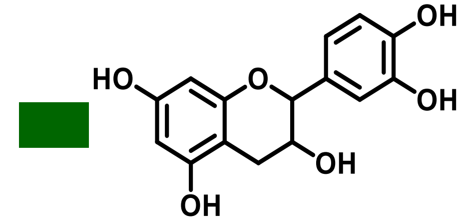

- **Thermal stability properties:**

For all cross-linked coatings,

$Td_{10\%} \approx$ 350°C

- **Aldehyde function concentration ↗**

Cross-linking degree ↗

6%w aldehyde function = best concentration

Foyer, Caillol et al., **Progress in Organic Coatings**, **2015**, 84, 1-8,

Coating characterizations

Falling ball test

Impact resistance results (cm)

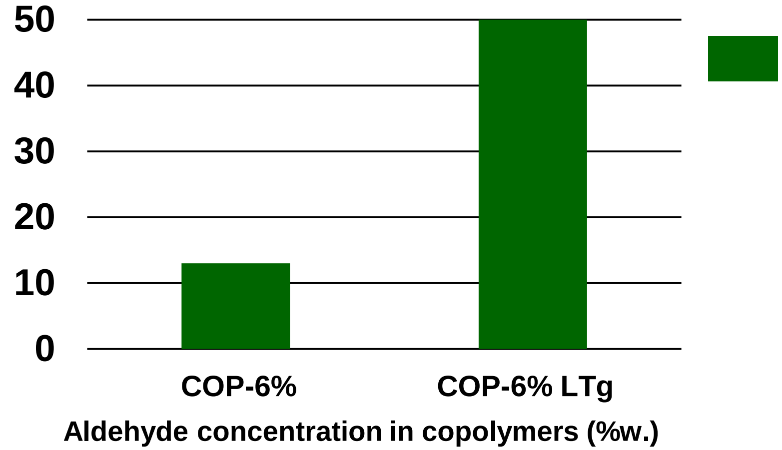

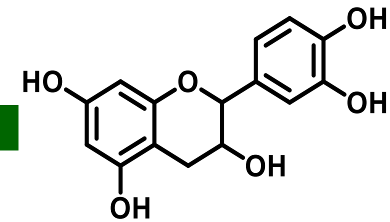

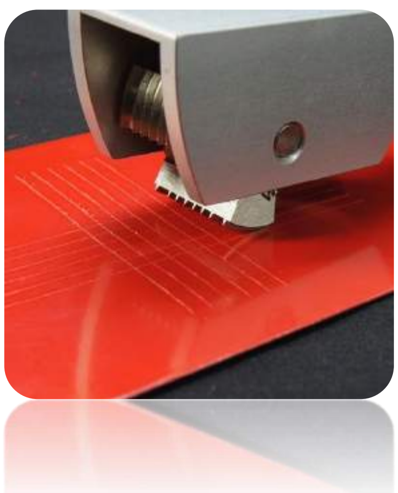

Cross cut adhesion = 1

- **Coating with high mechanical resistance suitable for industrial applications**

Foyer, Caillol et al., **Progress in Organic Coatings**, **2015**, 84, 1-8,

Non isocyanate Polyurethanes

PUs : 6th polymer in the world, 18Mt/y

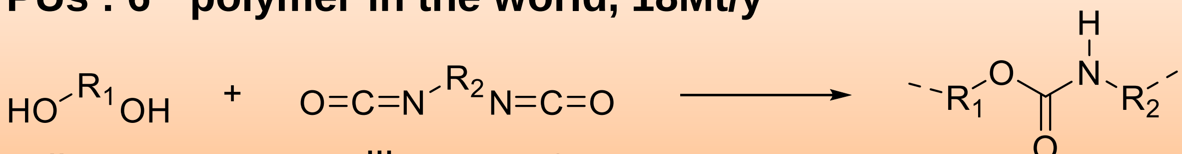

diols

diisocyanates

Polyurethanes



ISSUES

- Aromatic isocyanates are **harmful** reactants
- **TDI** and **MDI** (CMR)

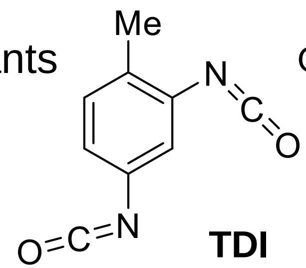

TDI

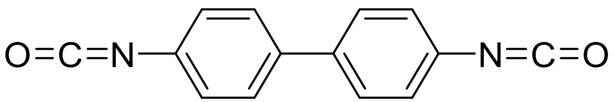

MDI

Synthesis of **non-isocyanate PUs**

Non isocyanate Polyurethanes

PUs : 6th polymer in the world, 18Mt/y

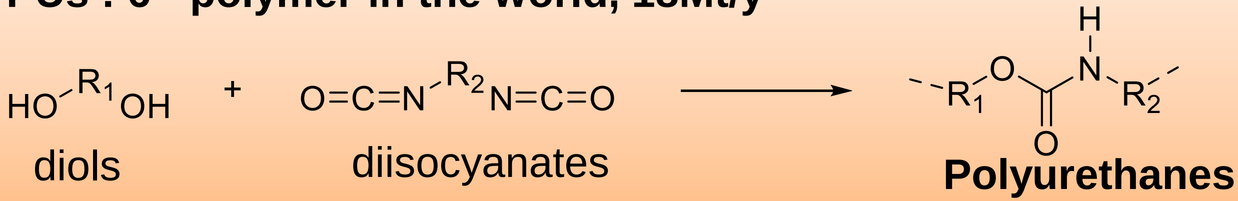

ISSUES

- Aromatic isocyanates are **harmful** reactants
- **TDI** and **MDI** (CMR)

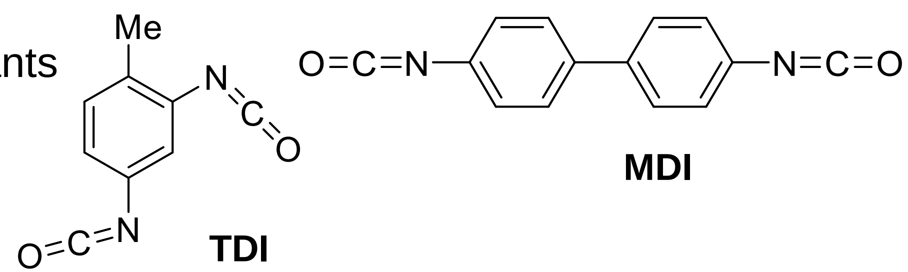

Synthesis of **non-isocyanate PUs**

Synthesis of **Polyhydroxyurethanes (PHUs)** by reaction between **cyclic carbonates** and **amines**

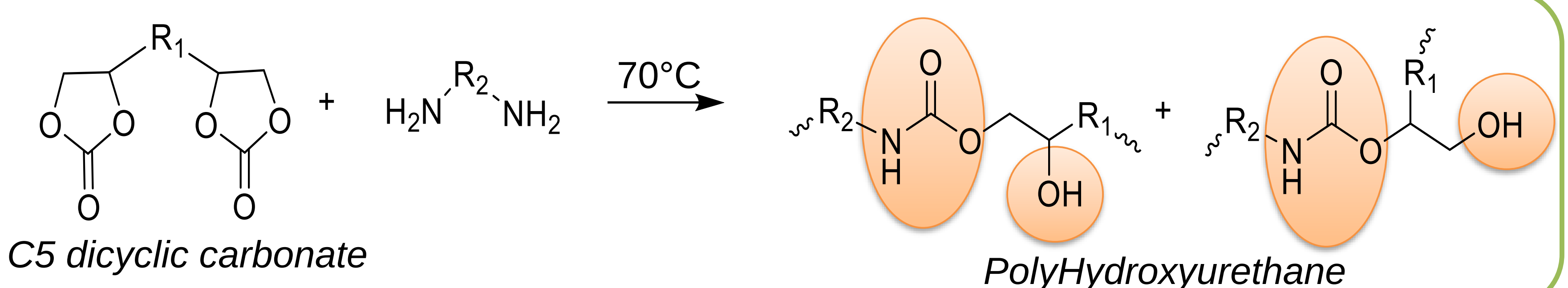

From cyclocarbonates to PHUs

Carbonation of oxiranes with CO_2

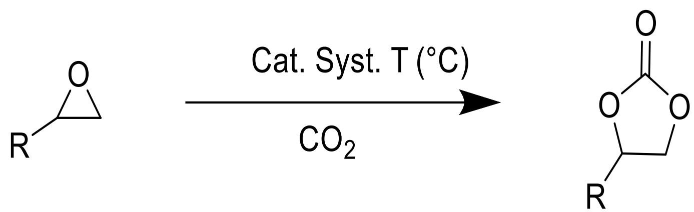

(Trans)esterification with glycerol carbonate

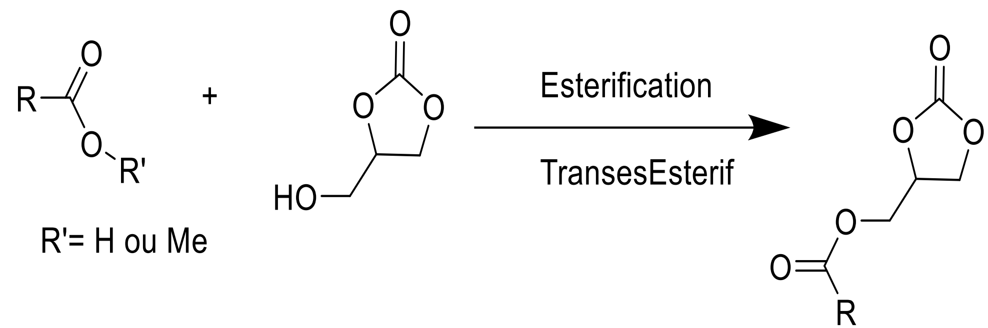

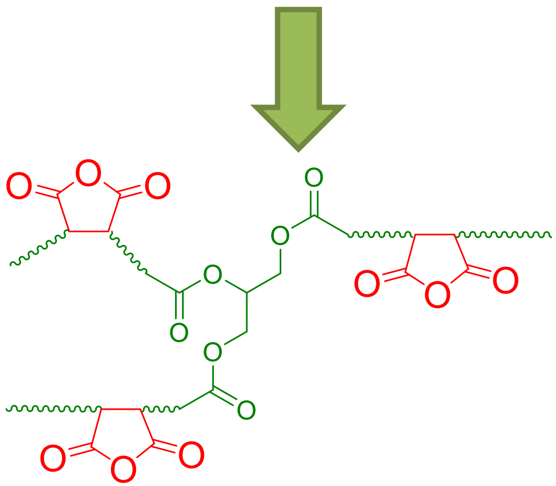

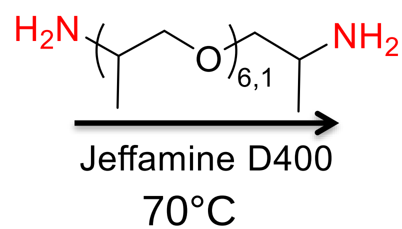

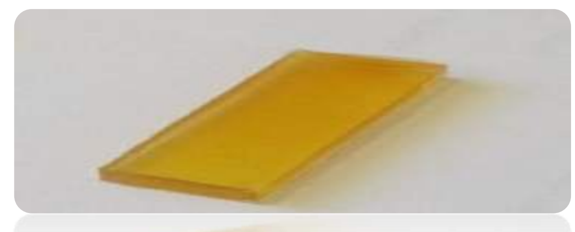

Non-isocyanate Polyhydroxyurethane

- **Access to biobased non-isocyanate polyurethanes**
- **Various properties and applications owing to the structure of carbonates and amines**

Cornille, Caillol et al.,
European Polymer Journal, 2017, **87**, 535-552
European Polymer Journal, 2016, **84**, 404-420

Adhesive Properties of PHU Materials

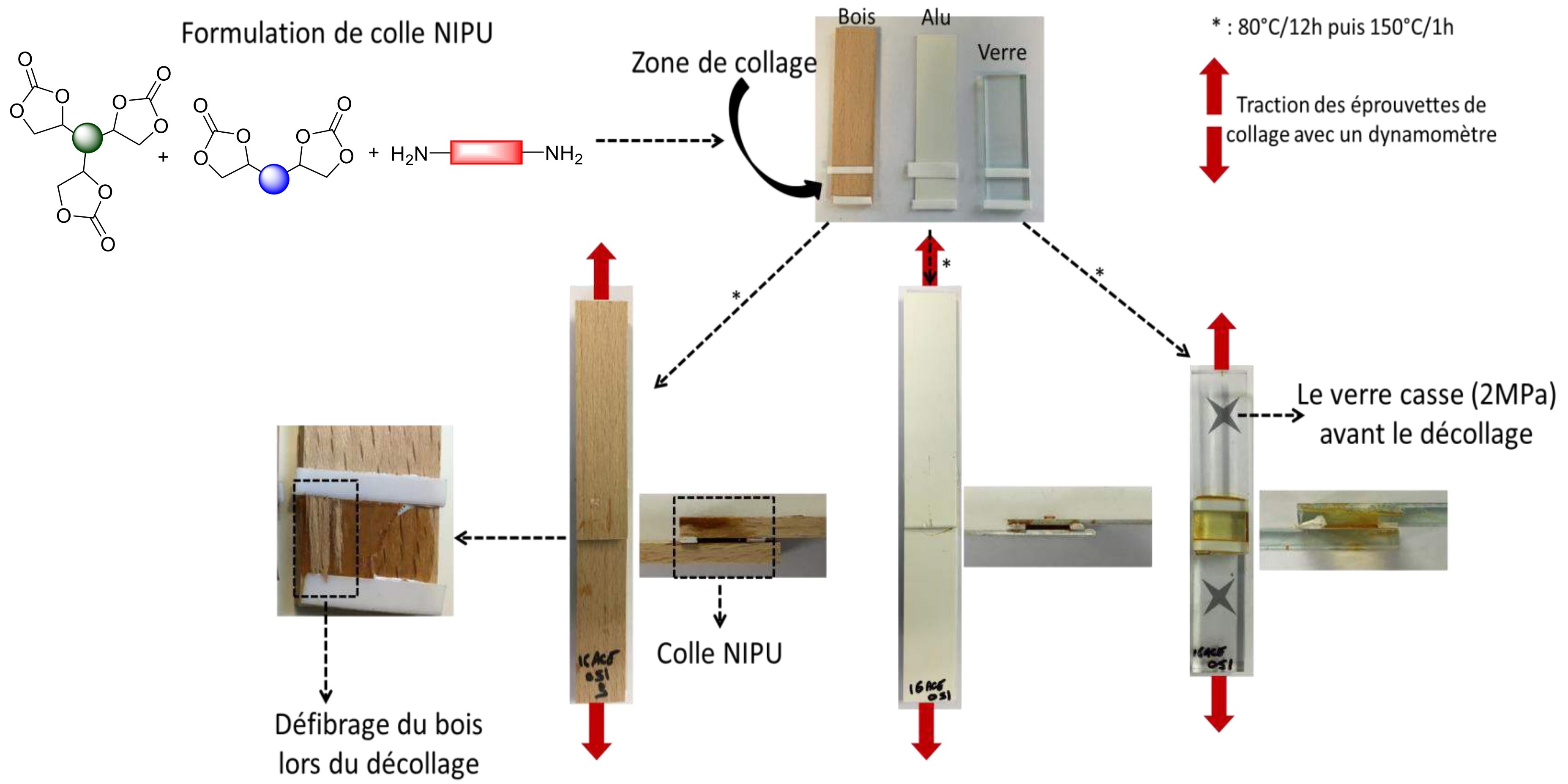

Excellent adhesive properties of PHU on the 3 tested substrates

Adhesive Properties of PHU Materials

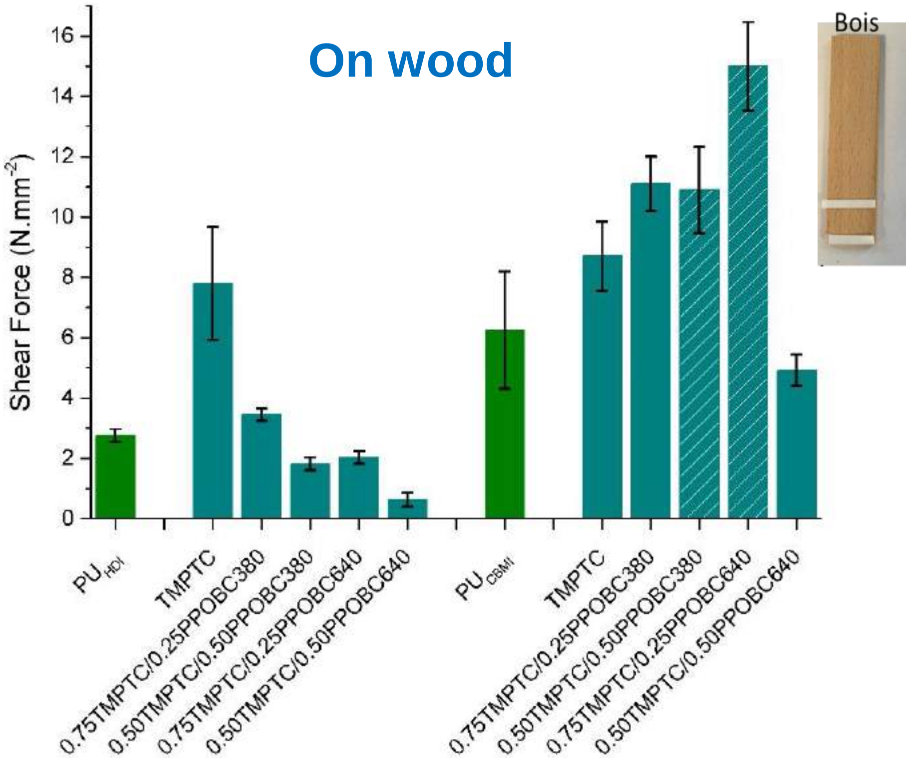

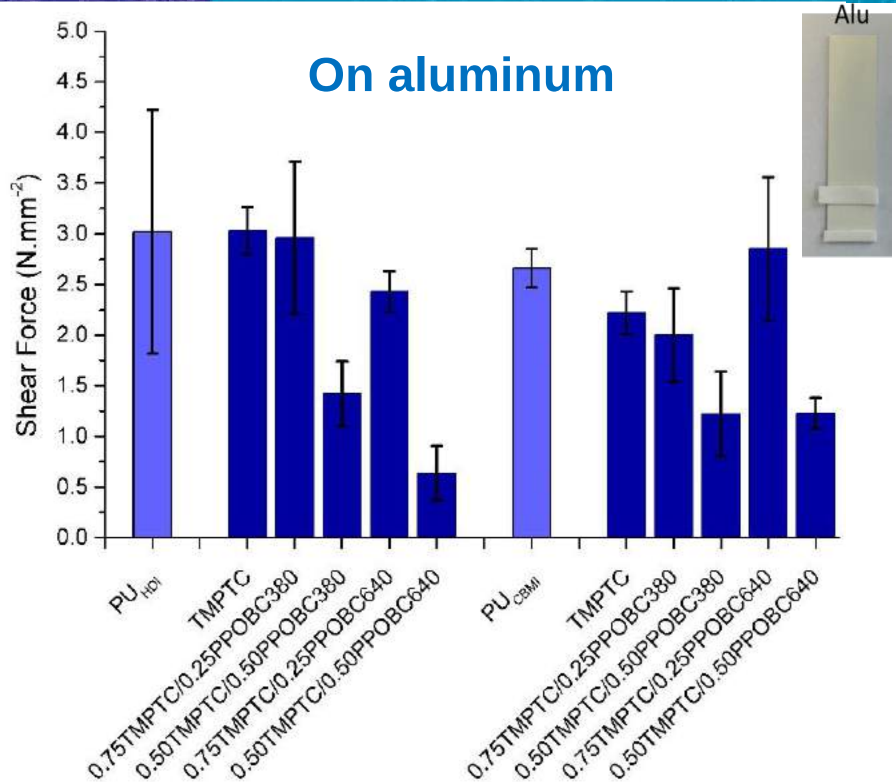

Best adhesive property of PHU compare to PU on wood ➔ Creation of H bonds between OH of PHU and wood

Failure mechanism
PU ➔ Adhesive failure
PHU ➔ Cohesive failure

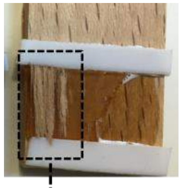

Défibrage du bois

Similar adhesive property of PHU compare to PU on Aluminum

Failure mechanism:
PU and PHU: Adhesive failure

Synthesis of C5, C6 and CS cyclic carbonates

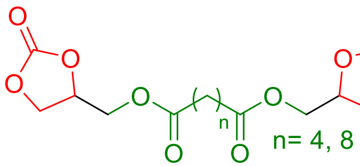

DCadp (n=4)

DCseb (n=8)

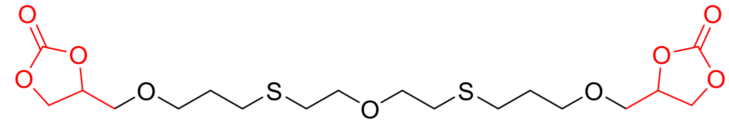

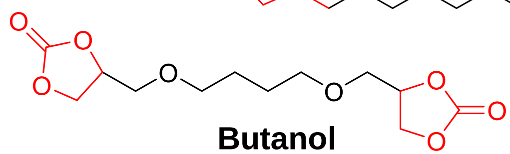

Butanol

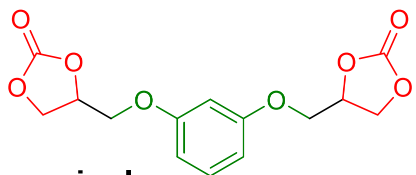

Resorcinol

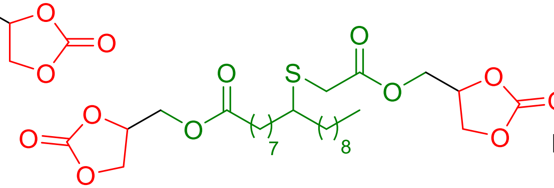

DColq

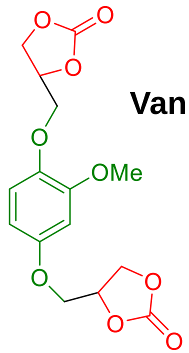

Vanillin derived

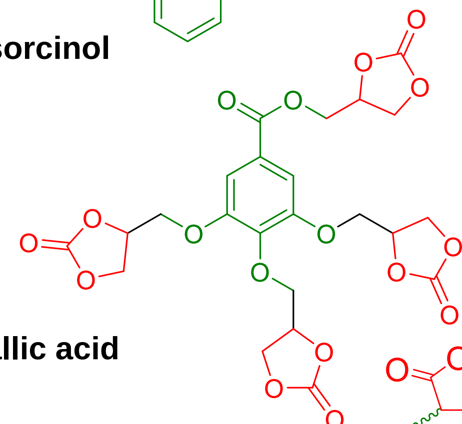

Gallic acid

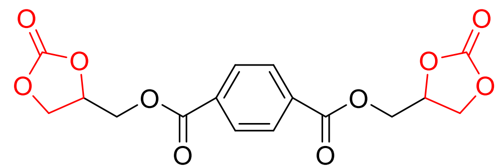

DCter

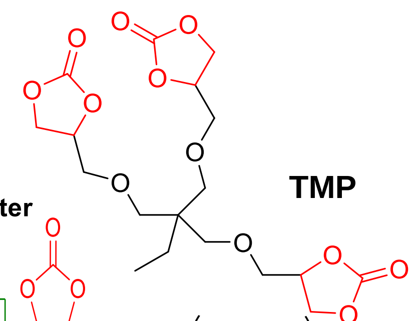

TMP

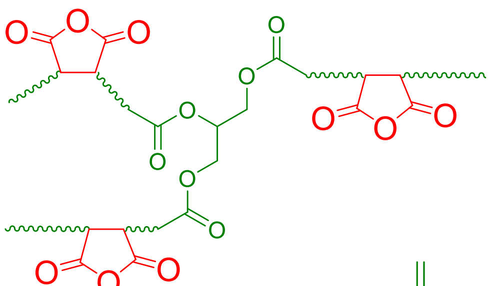

Vegetable Oil

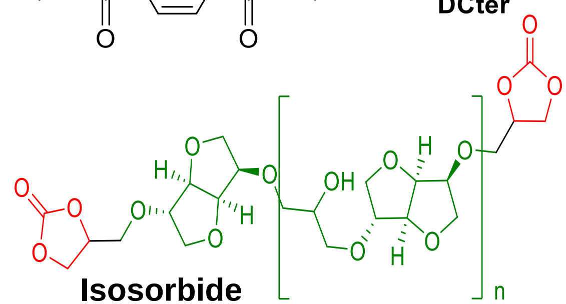

Isosorbide

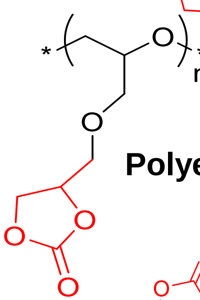

Polyether

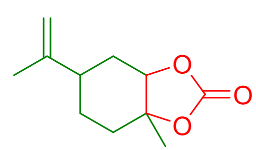

limonene

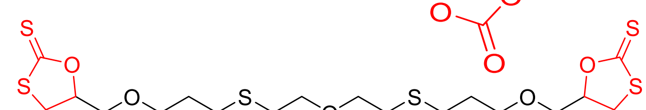

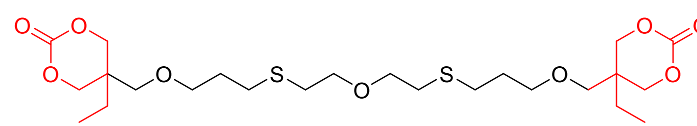

Caillol et al.,
Polymer International, 2012, **61**, 1666-1674
Polymer International, 2012, **61**, 918–925
Reactive and Functional Polymers, 2013, **73**, 588-594.
Polymer Chemistry, 2011, **2**, 2661-2667
J. Pol. Sci. Part A: Polymer Chem., 2011, **49**, 2677–2684
Lipid Technology, 2014, **26**, 35-38

From PHU materials to new properties

➔ Tg of PHUs synthesized with various diamines

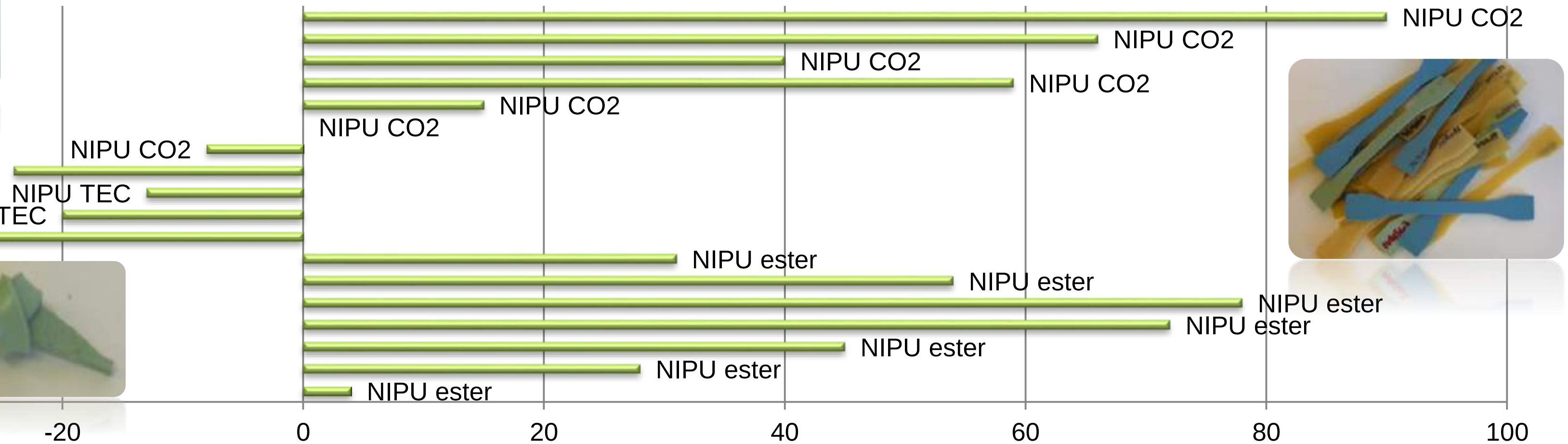

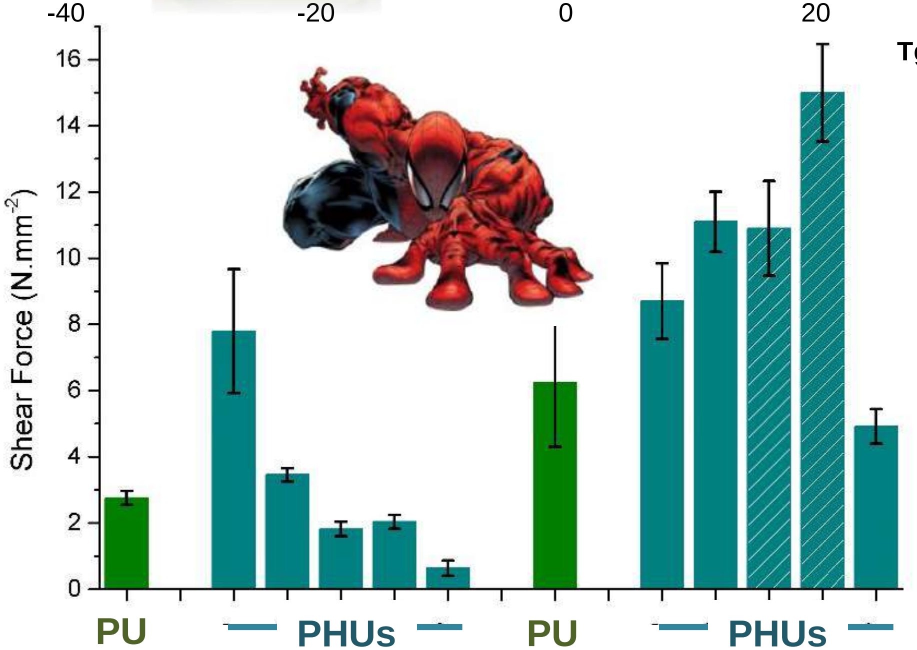

- **Promising adhesive properties of PHU** compare to PU

➔ Creation of H bonds between OH of PHU and wood

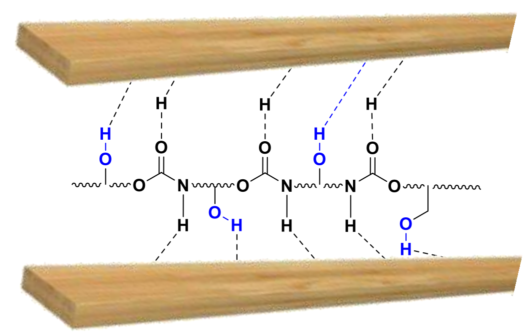

Cornille, Caillol et al., **European Polymer Journal**, 2016, **84**, 404-420

Toward reversible PHUs

Synthesis of cleavable cyclic carbonate

Diels-Alder bis cyclic carbonate

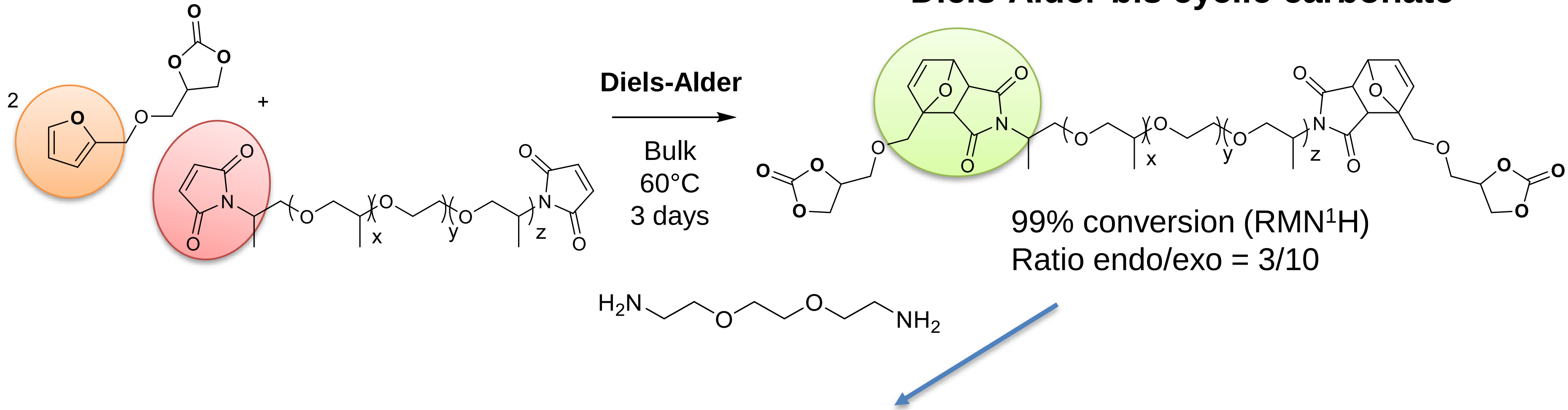

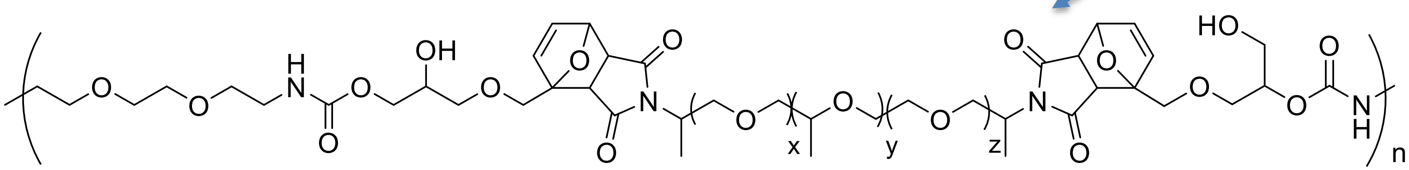

Reversible PHU

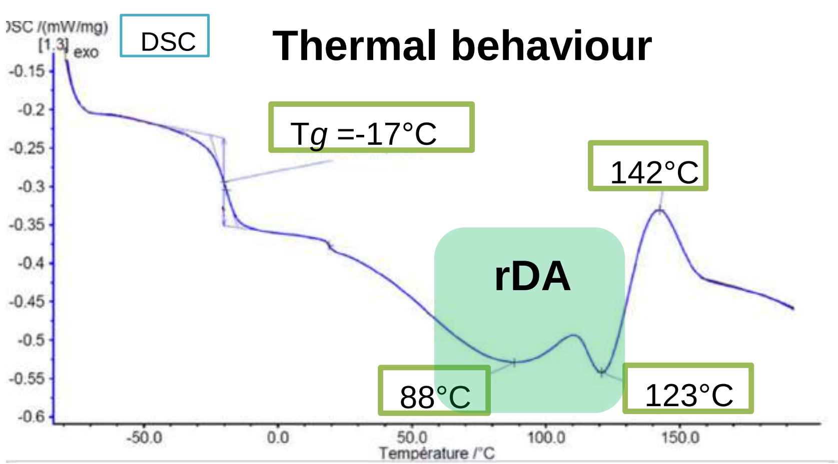

Thermal behaviour

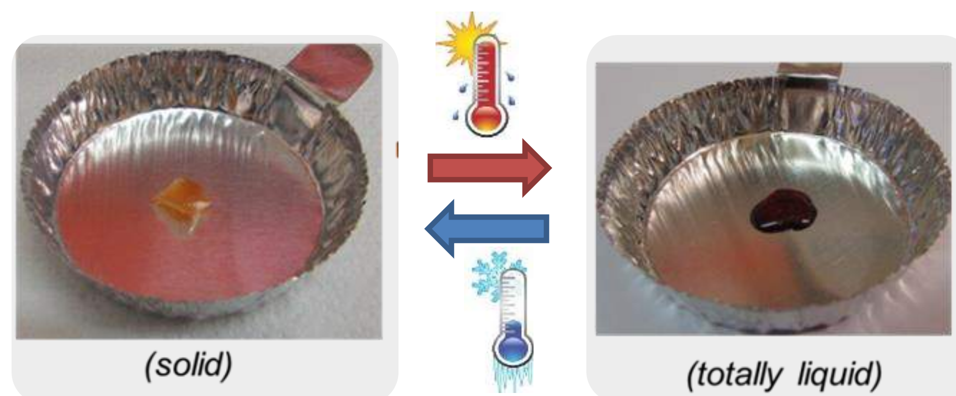

Dolci, Caillol et al., **Polymer Chemistry**, 2015, **6**, 7851-7861

Toward reversible PHUs

Before (25°C)

PHU-2G

0,75DA-tc/0,25PPG-dc/1,0EDR148

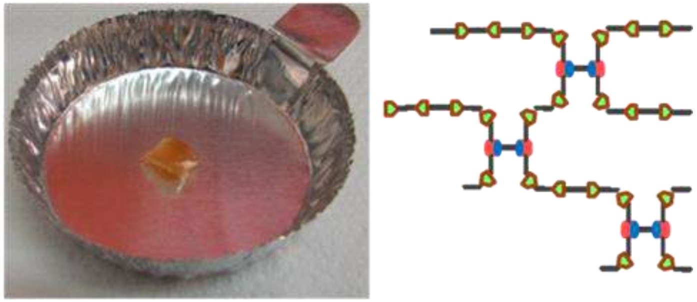

(solid)

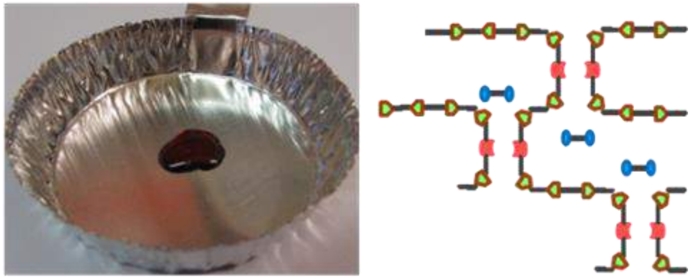

(totally liquid)

After thermal treatment (140°C, 2h)

DEBONDING

Dolci, Caillol et al., **Polymer Chemistry**, 2015, **6**, 7851-7861

Strategy: PHU cross-linking

Strategy:
Radical copolymerization of **GCMA** in styrene-acrylic polymers; *cross-linking with diamines*.
Substitution of de 2-ethyl-hexyle acrylate (HEA) / *isocyanate* system

GCMA

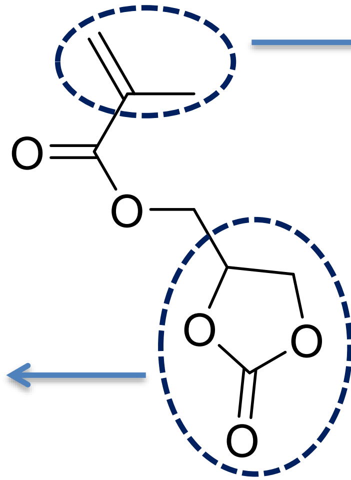

Free radical polymerization

Cross-linking with diamines

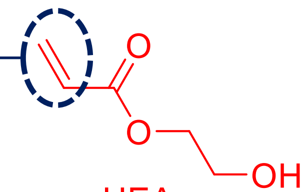

HEA

Cross-linking with poyisocyanates

Synthesis

GMA

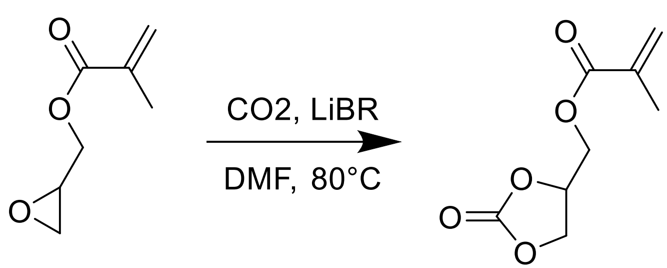

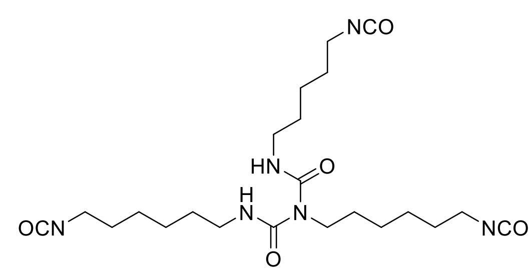

Camara, Caillol et al., **Polym. Chem. 2013**, 4, 4545-4561

Study

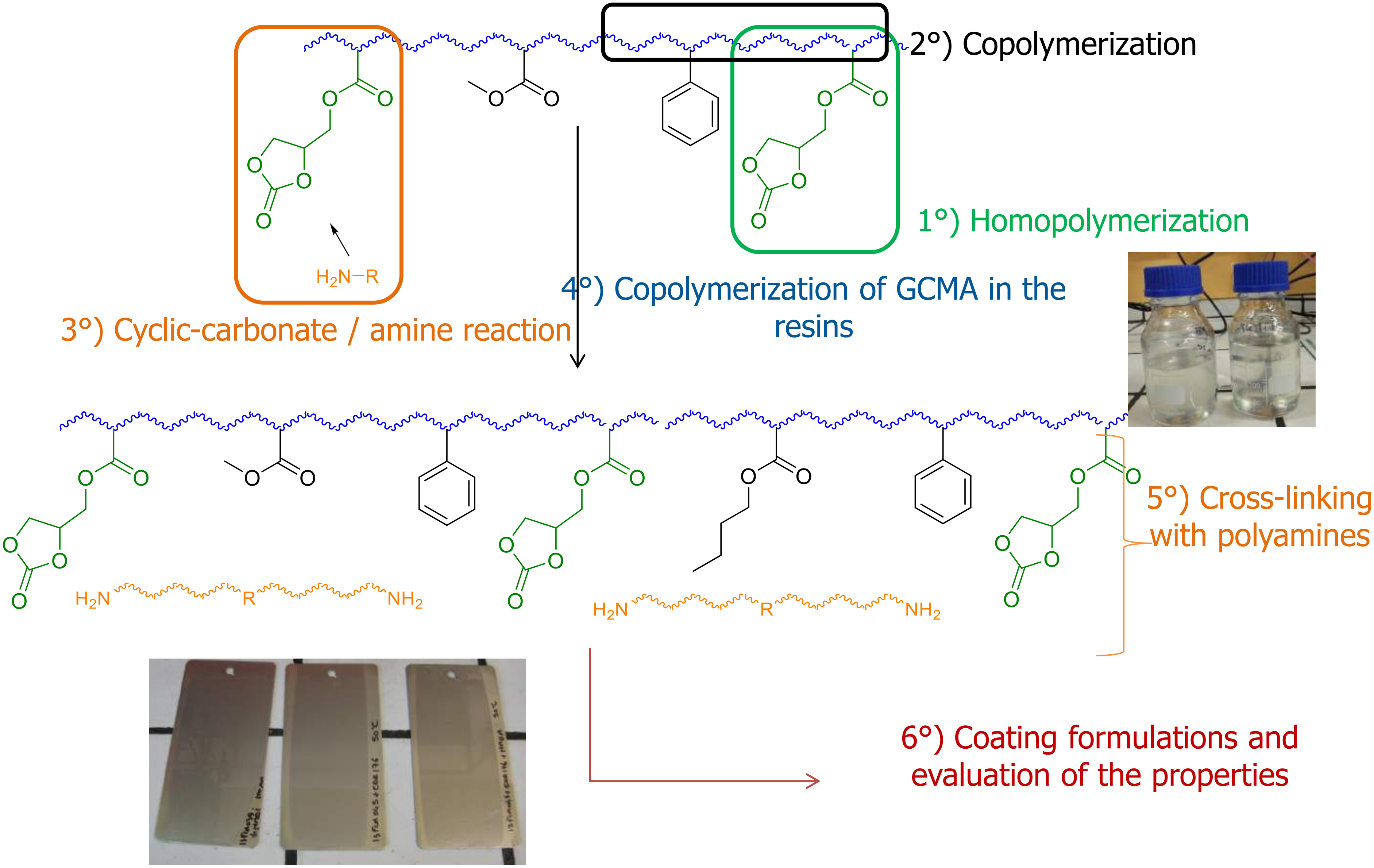
2°) Copolymerization
1°) Homopolymerization
H_2N-R
3°) Cyclic-carbonate / amine reaction
4°) Copolymerization of GCMA in the resins
5°) Cross-linking with polyamines
H_2N R NH_2
H_2N R NH_2
6°) Coating formulations and evaluation of the properties

Polymer characterization

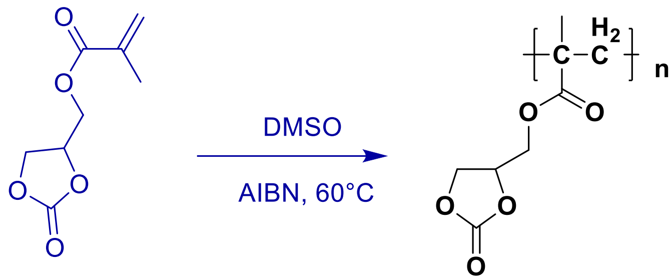

- **Tg # 120°C**
- **Détermination of ratio** $\frac{k_p^{\ 2}}{k_{te}}$

NMR→ln[Mo]/[M]

Tobolsky equation :

$$\ln[M]_0/[M]_t = 2\,kp/\sqrt{kte} \times \sqrt{\frac{f}{kd} \times \sqrt{[I_2]}} \times (1-\exp(-kdt/2))$$

Polymer characterization

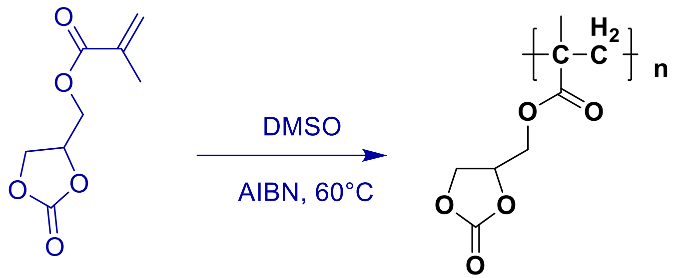

- Tg # 120°C
- Détermination of ratio $\frac{k_p^{\,2}}{k_{te}}$

NMR→ln[Mo]/[M]

Tobolsky equation :

$$\ln[M]_0/[M]_t = 2\,kp/\sqrt{kte} \times \sqrt{\frac{f}{kd}} \times \sqrt{[I_2]} \times (1-\exp(-kdt/2))$$

- **GCMA is more reactive than MMA and GMA** (in DMSO at 60°C)

Literature : Acrylic cyclic-carbonate monomers polymerize more rapidly than classical acrylic monomers, in photopolymerisation.

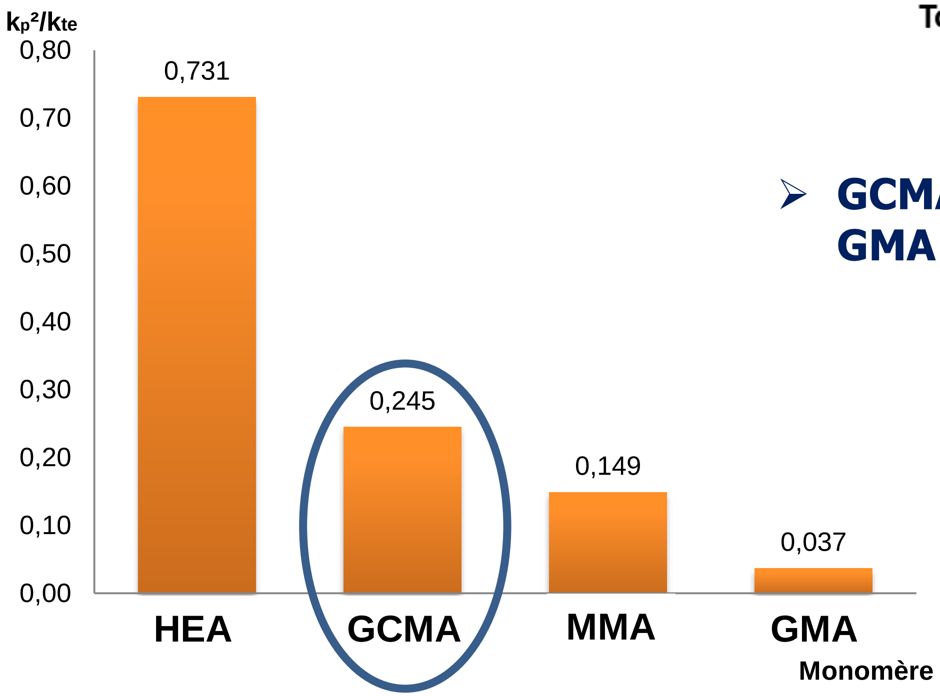

Berchtold, K. A.; Nie, J.; Stansbury, J. W.; Bowman, C. N. *Macromolecules (Washington, DC, U. S.)* **2008,** 41, 9035-9043.
Kilambi, H.; Stansbury, J. W.; Bowman, C. N. *J. Polym. Sci., Part A: Polym. Chem.* **2008,** 46, 3452-3458.
Decker, C.; Moussa, K. *Makromol. Chem.* **1991,** 192, 507-22

European Polymer Journal, 2014, 61, 133–144

Paint formulation

REFERENCE: Acrylic copolymer (HEA)

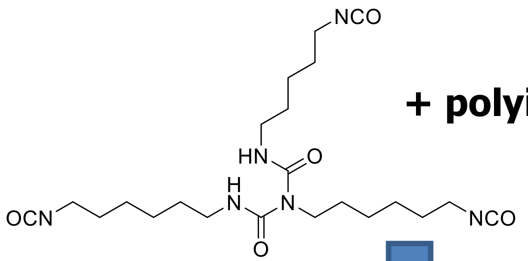

+ polyisocyanate

24 hours RT 1 hour 80°C

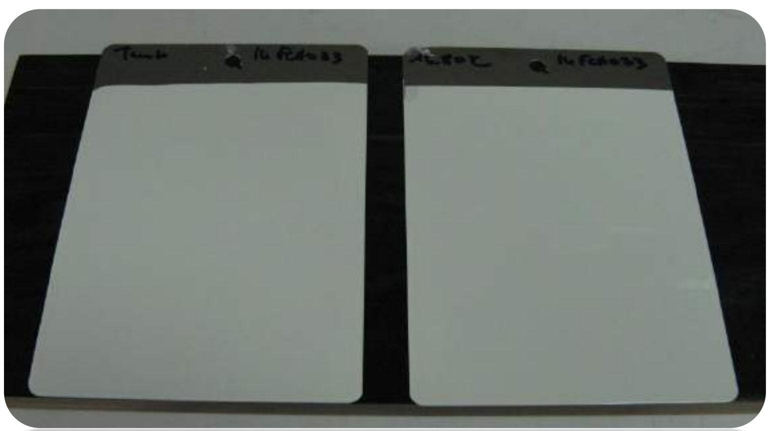

Copolymer MAGC

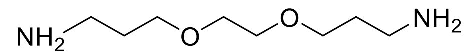

EDR 176

+ diamine

24 hours RT 1 hour 80°C

1 and 2 same aspect than the reference

Property	Comparison to the reference
Gloss (60°/20°)	**Similar**
Adhesion (cross cut)	**Similar**
Solvant resistance (MEK)	**Similar**
Persoz hardness	**Similar**

Camara, Caillol et al., **European Polymer Journal**, **2014**, 61, 133–144

Varnish formulation

REFERENCE: Acrylic copolymer (HEA)

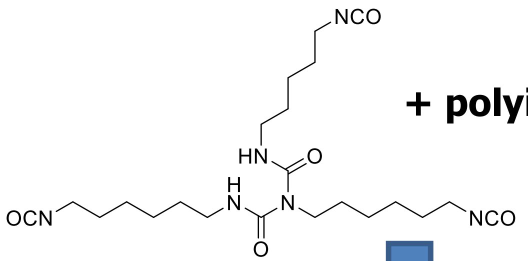

+ polyisocyanate

24 hours RT **1 hour 80°C**

Camara, Caillol et al., **European Polymer Journal**, **2014**, 61, 133–144

Copolymer MAGC

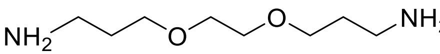

EDR 176

+ diamine

24 hours RT **1 hour 80°C**

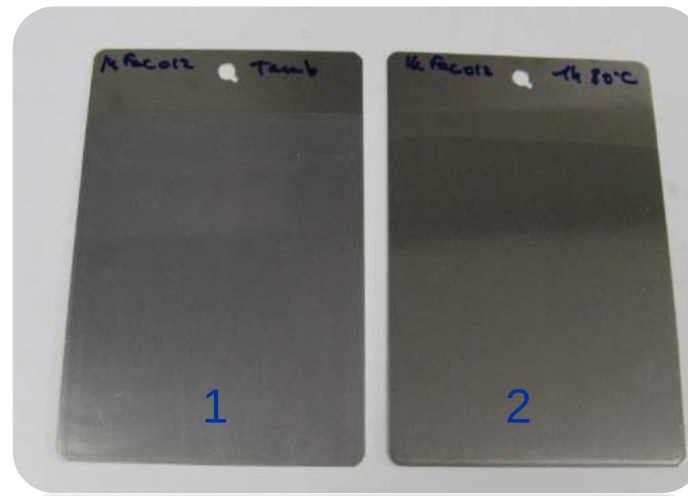

1- Whitening after drying at RT
2- Same after 1 hour curing

Improvements:
- Polyamine structure
- Cyclic-carbonate content in the polymer

Biobased polymer latexes

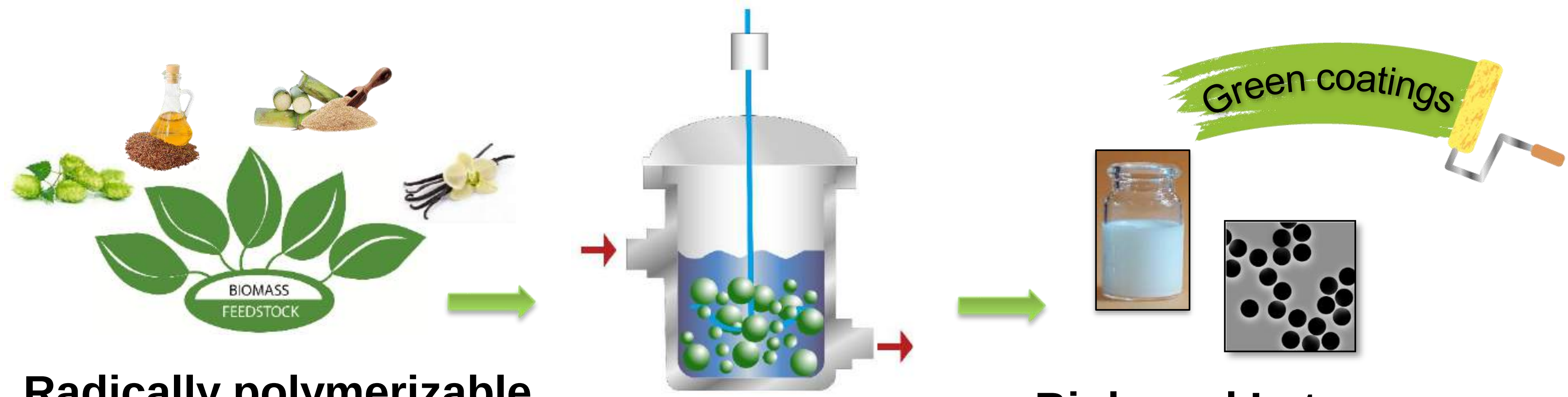

Radically polymerizable Biobased monomers

Radical Emulsion Polymerization

Biobased Latexes

- **Water: Innocuous and nonflammable solvent**
- **Reduction of reaction medium viscosity**
- **Improves heat transfer (easier reaction temperature control)**

Emulsion Polymerization for waterborne binders and coatings

Mixture of monomers

(meth)acrylates

Styrene

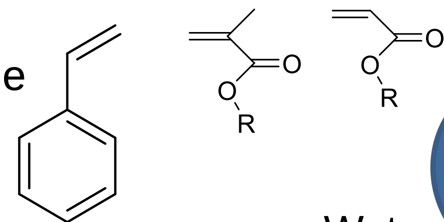

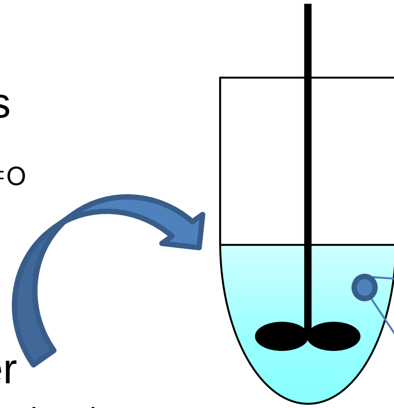

Water
Surfactant
Initiator

Emulsion radical polymerization

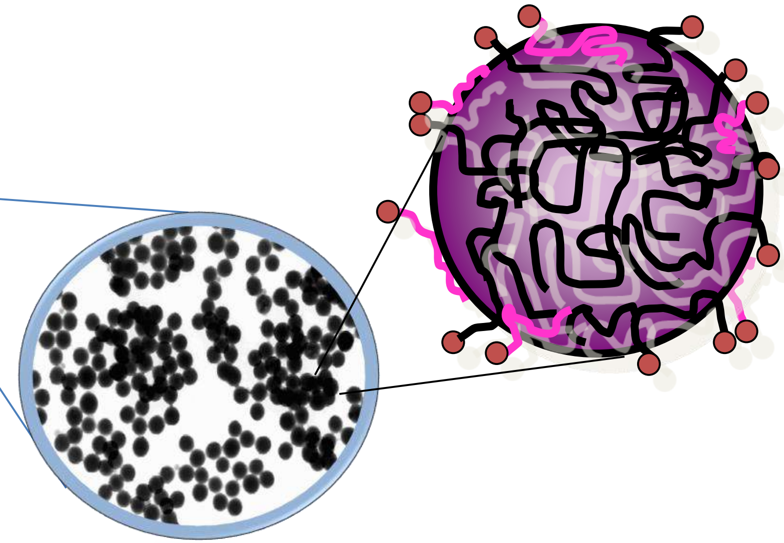

Substitution of mixture of comonomers by cardanol

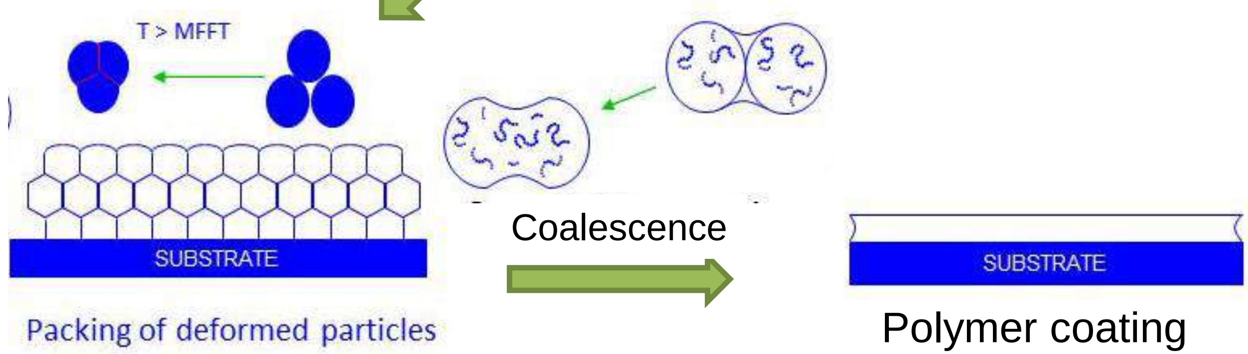

Ratio of **monomers** for a **Tg** of polymer suitable for **film forming**

Eugenol

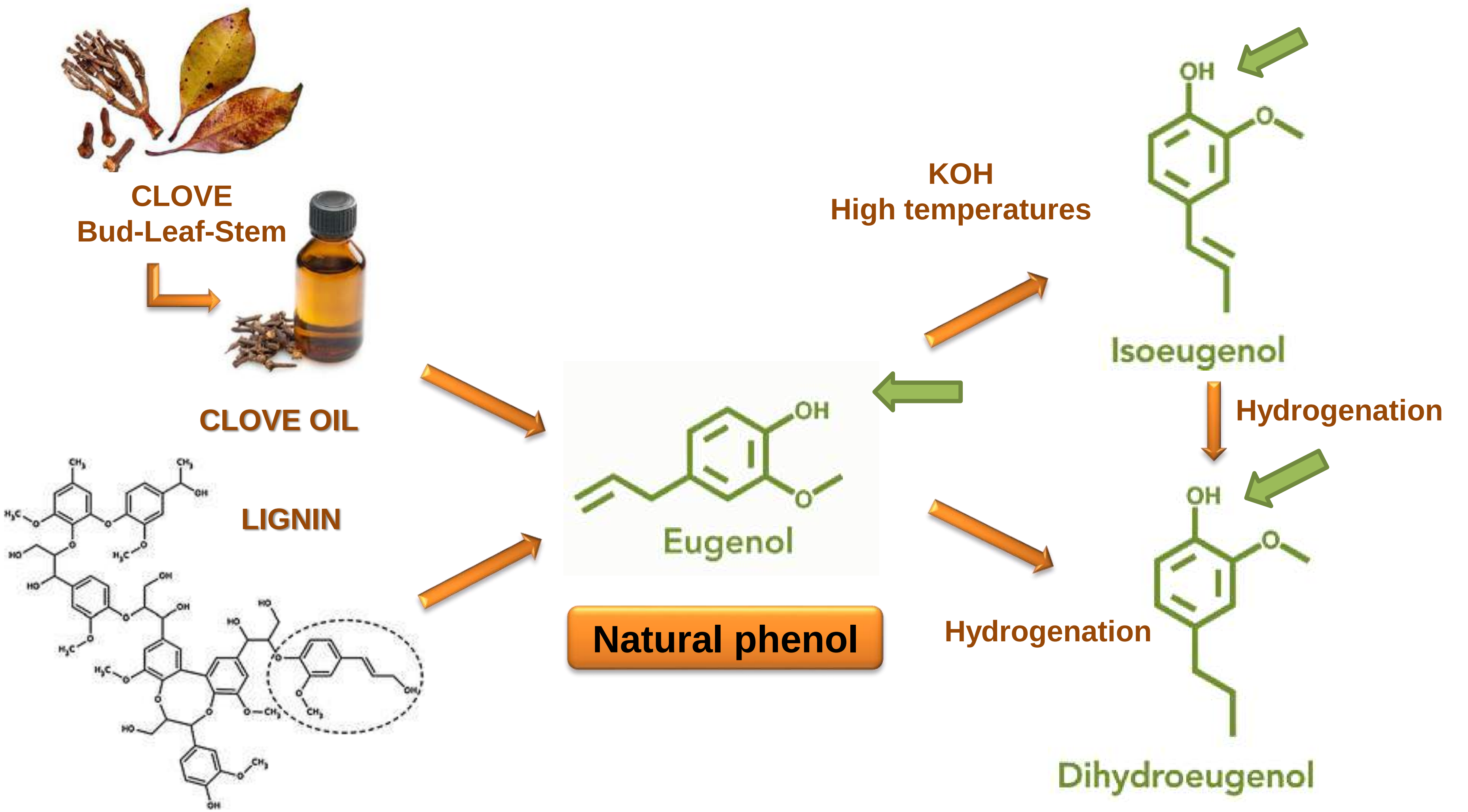
CLOVE
Bud-Leaf-Stem
CLOVE OIL
LIGNIN
Eugenol
Natural phenol
KOH
High temperatures
Isoeugenol
Hydrogenation
Hydrogenation
Dihydroeugenol
OH
O

Synthesis of Eugenol-based monomers

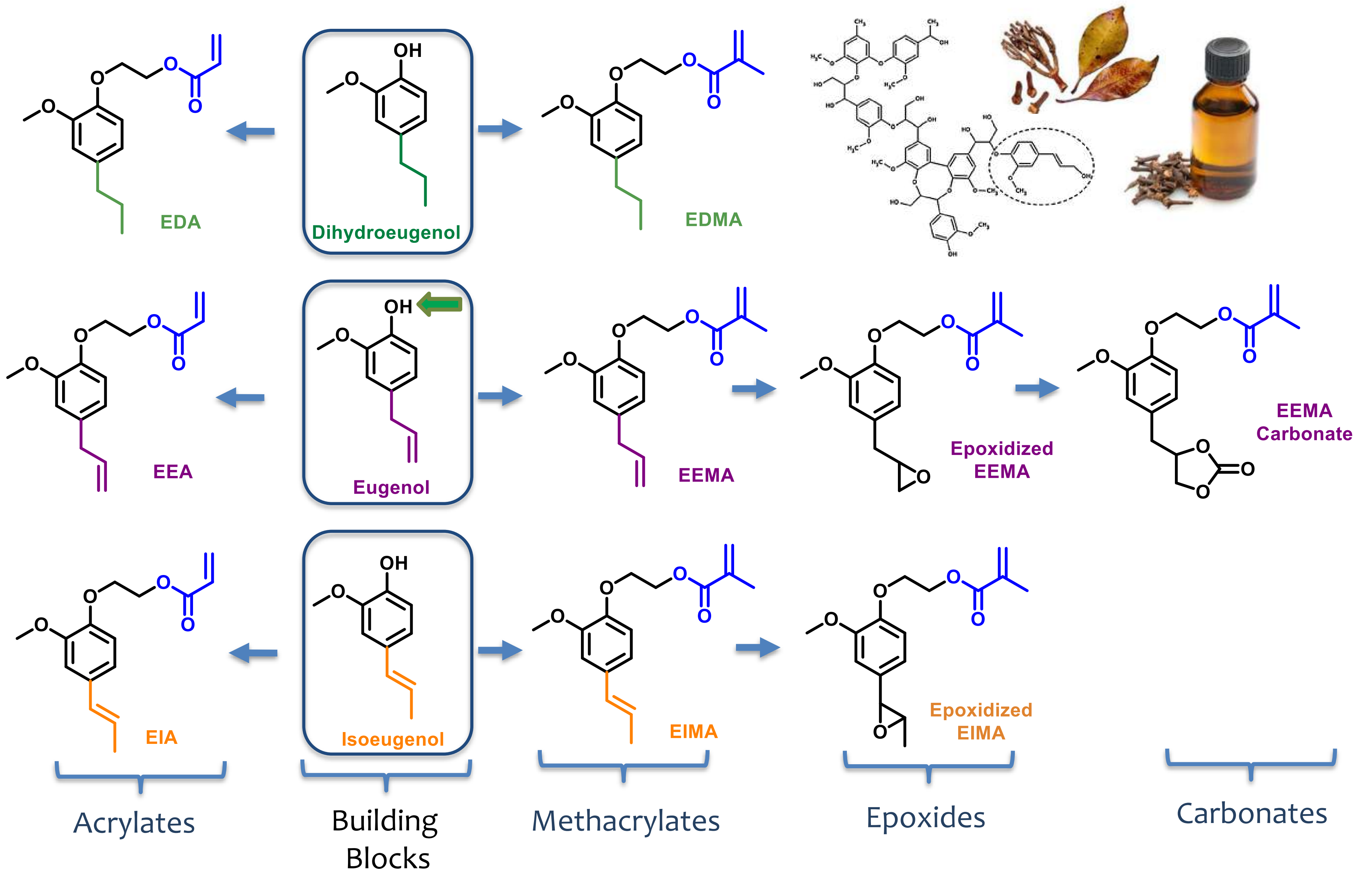

Molina-Gutiérrez, Caillol, et al. , **Macromol Chem Phys,** 2019, **220**

Synthesis of Eugenol-based monomers

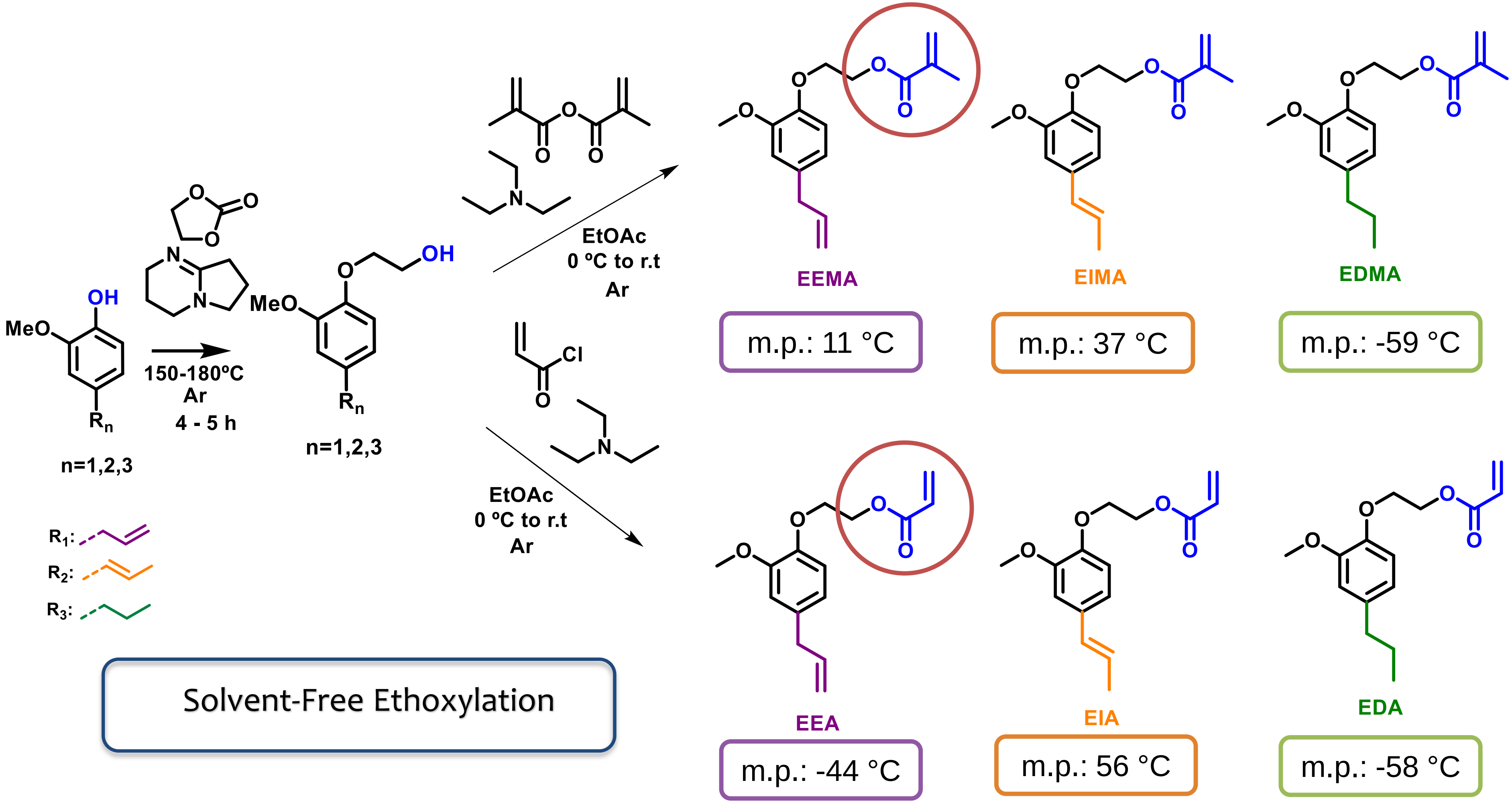

Solvent-Free Ethoxylation

Molina-Gutiérrez, Caillol, et al. , **Macromol Chem Phys,** 2019, **220**

Miniemulsion Homopolymerization

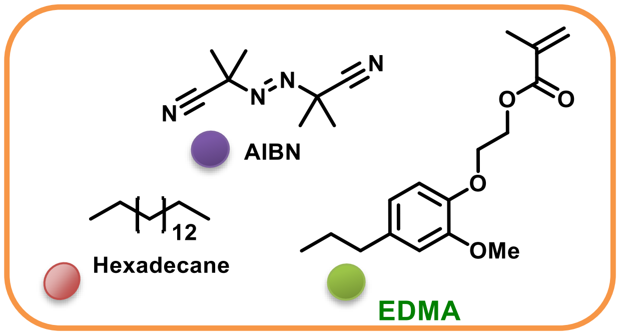

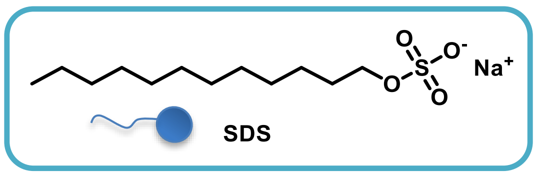

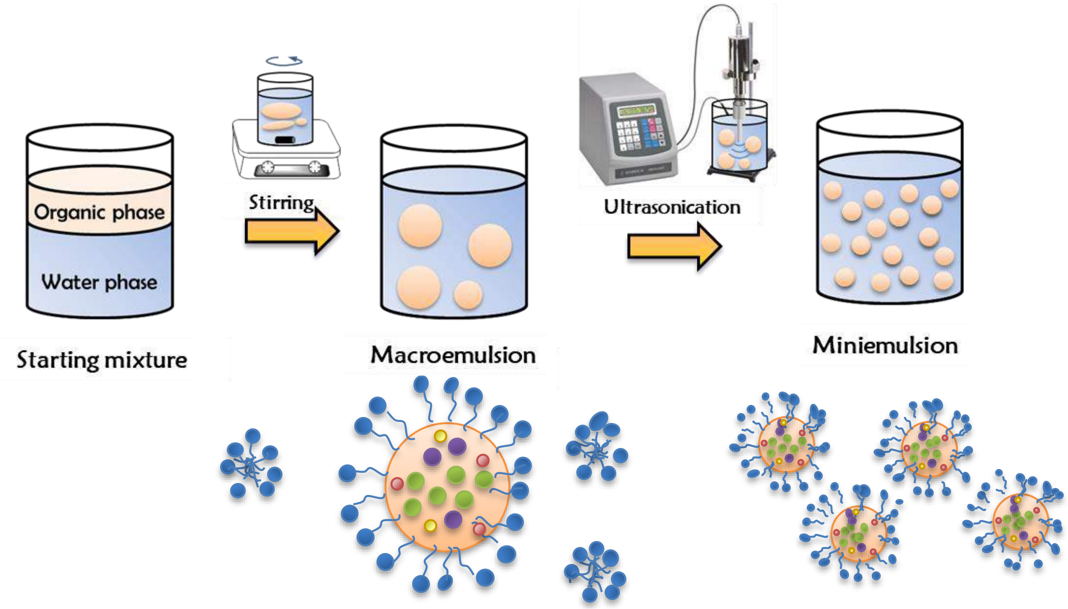

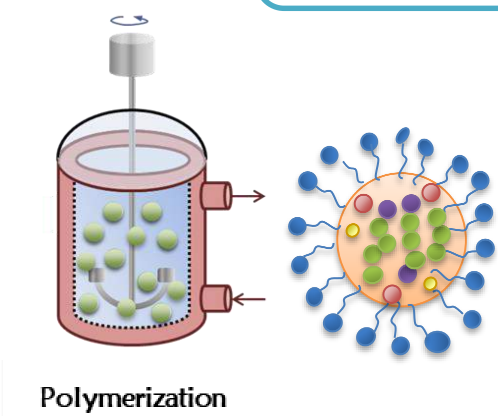

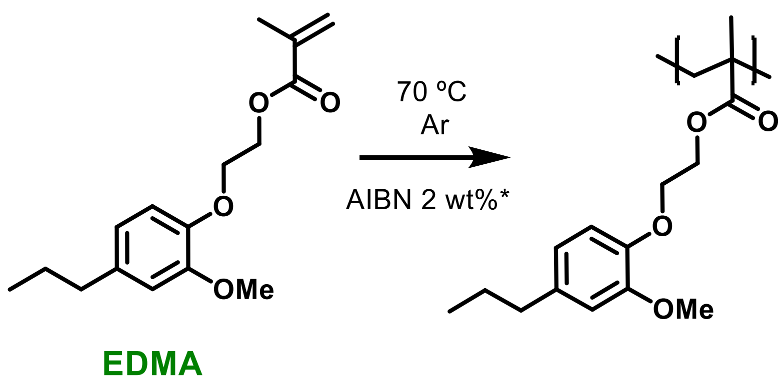

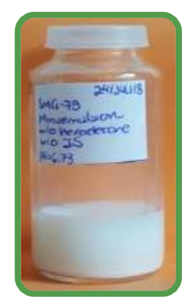

Monomer conversion > 97%

115 nm / T_g : 30°C

12.5 wt% solids

*wt% based on monomer

Direct Emulsion Homopolymerization

- Thermal Initiation

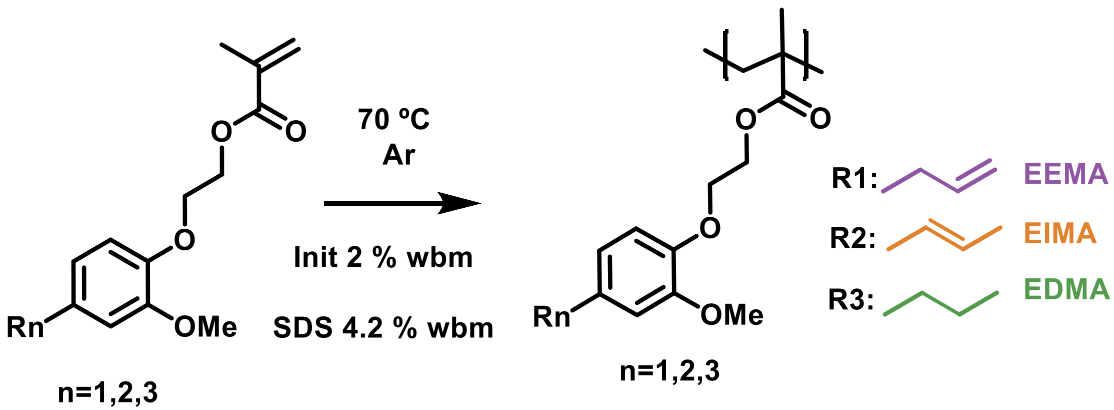

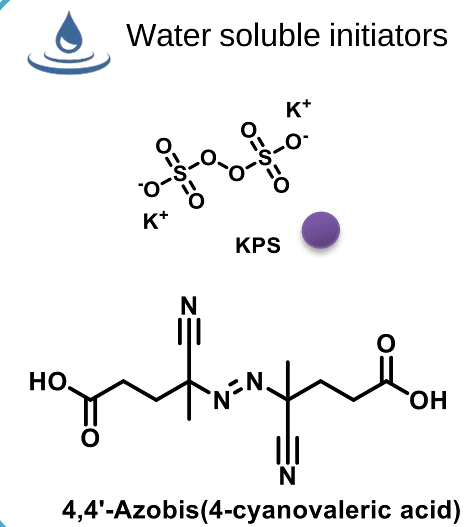

12.5 wt% solids / % wbm weight based on monomer

Monomer conv > 97%

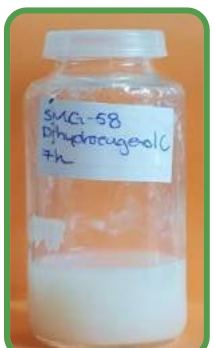

EDMA

Colloidal Stability ✓

Gel Content: 1 %
D_i: 63 nm
T_g : 26°C
pH: 8.9

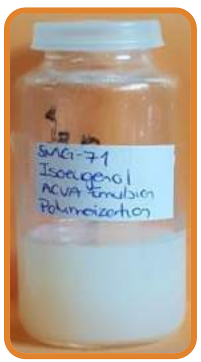

EIMA

Colloidal Stability ✓

Gel Content: 74 %
D_i: 45 nm
T_g : 63°C
pH: 6.4

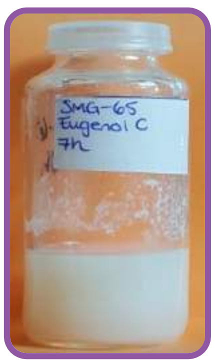

EEMA

Colloidal Stability ✓

Gel Content: 98 %
D_i: 57 nm
T_g : 27 °C
pH: 8.5

Molina-Gutiérrez, Caillol, et al. , **Indus. Eng. Chem. Res.**, 2019, **58**, 21155

PSA Application

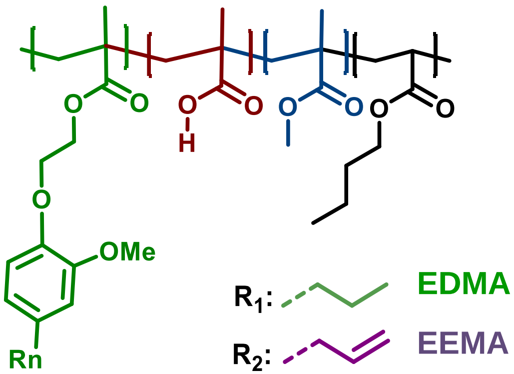

MMA 12% wbm

MMA 6% wbm – EDMA 6% wbm

EDMA 12% wbm

EDMA 11% wbm – EEMA 1% wbm

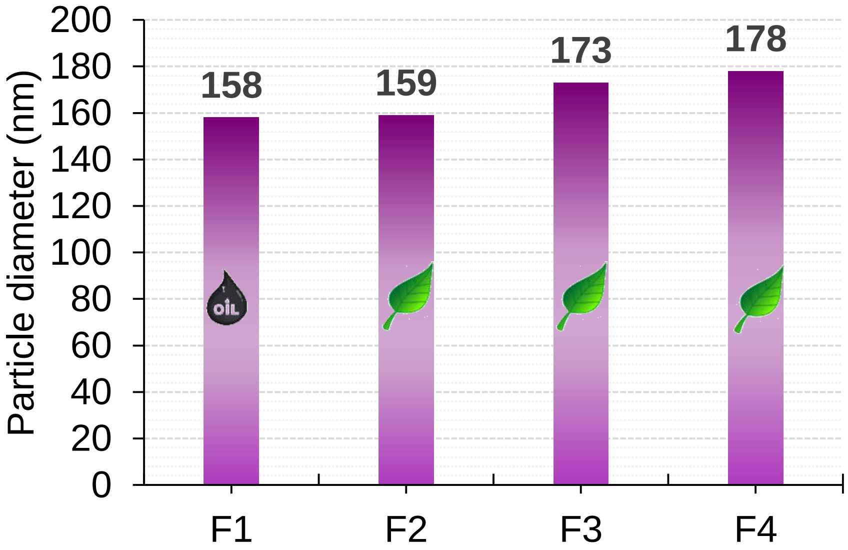

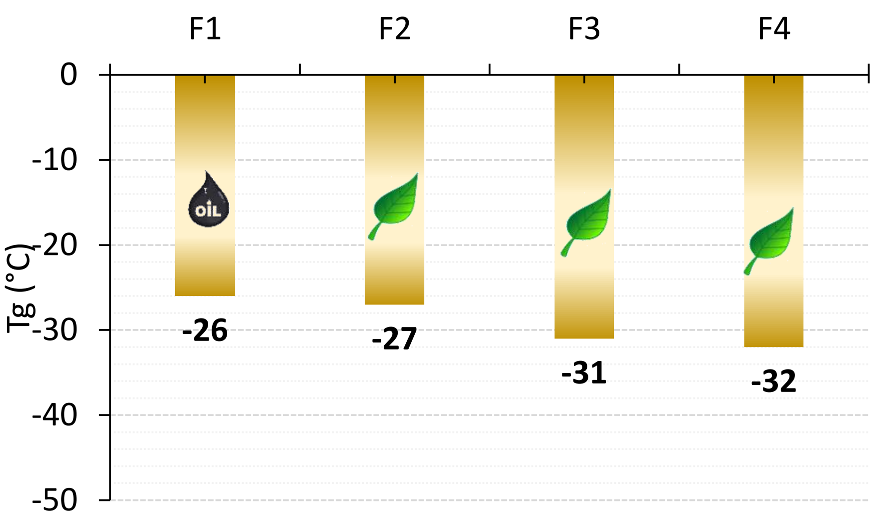

Molina-Gutiérrez, Caillol, et al. , Biomacromolecules, **2020,** 21, 4514

PSA Application

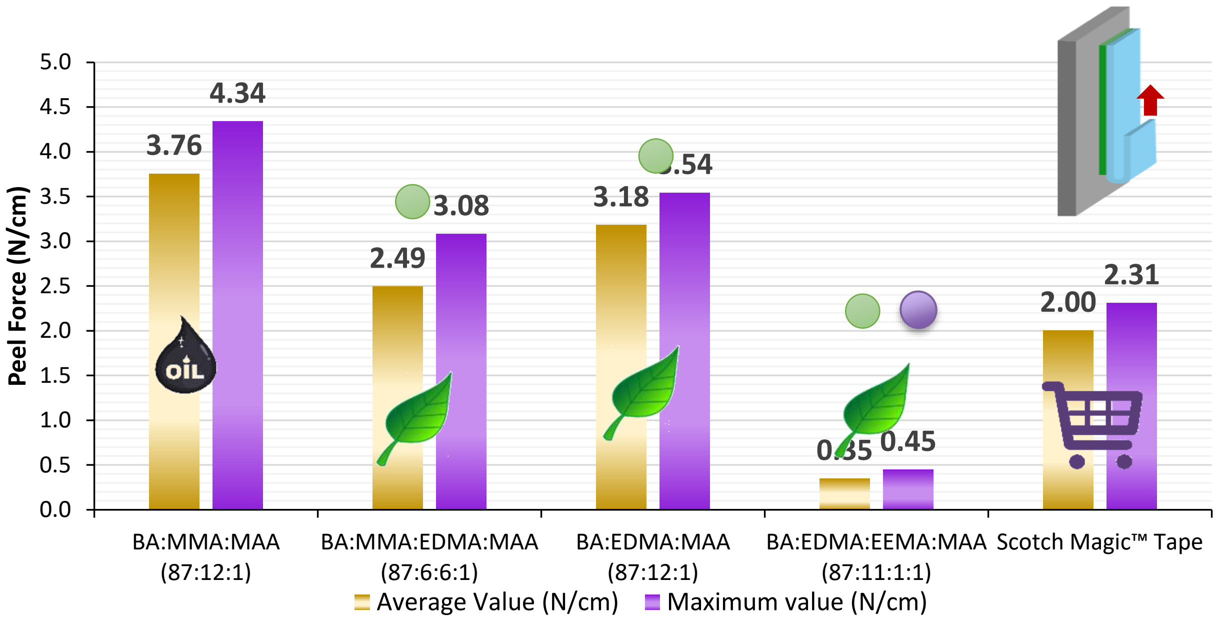

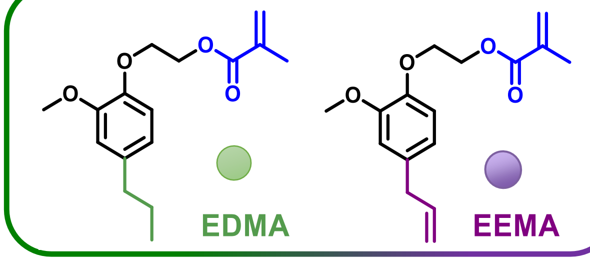

- Peel force decreases with biobased monomer
- EEMA → Noticeable decrease of peel force

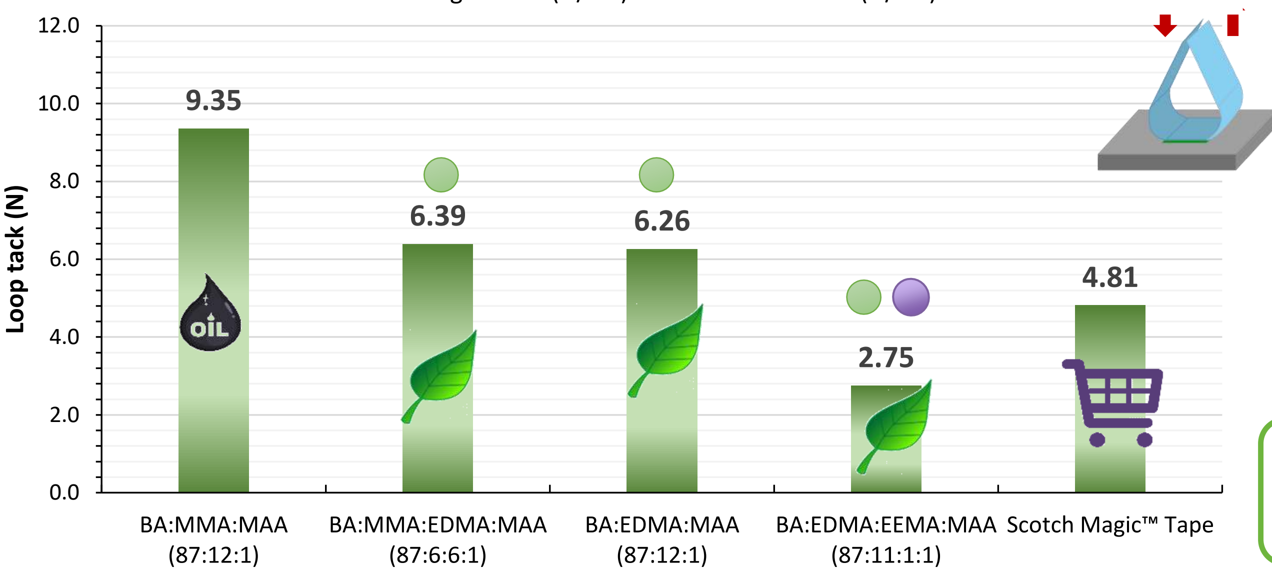

- Tack force decreases with biobased monomer
- EEMA → Noticeable decrease of tack force

Comparable with commercial formulation

Molina-Gutiérrez, Caillol, et al. , Biomacromolecules, **2020,** 21, 4514

From Cashew to Cardanol

Institut Charles Gerhardt Montpellier

Cashew tree

Cashew nut and fruit

Raw Cashew nut

Cashew Nut Shell
(80-75 wt%)

Cashew apple

Cashew nut
(20-25 wt%)

Cashew nuts world production
2014 : 3,700 kt
2015 : 4,275 kt

Main producing countries of cashew nuts in 2015

Country	*Prod (t)*
Nigeria	922,000
India	772,000
Viet-Nam	590,000
Côte d'Ivoire	570,000
Benin	226,000
Philippines	188,000

Source: FOOD AND AGRICULTURE ORGANIZATION OF THE UNITED NATIONS STATISTICS DIVISION

From Cashew to Cardanol

Cashew Nut Shell

Cashew Nut Shell Liquid (20-40 wt%)

Prod
1 Mt/y
world

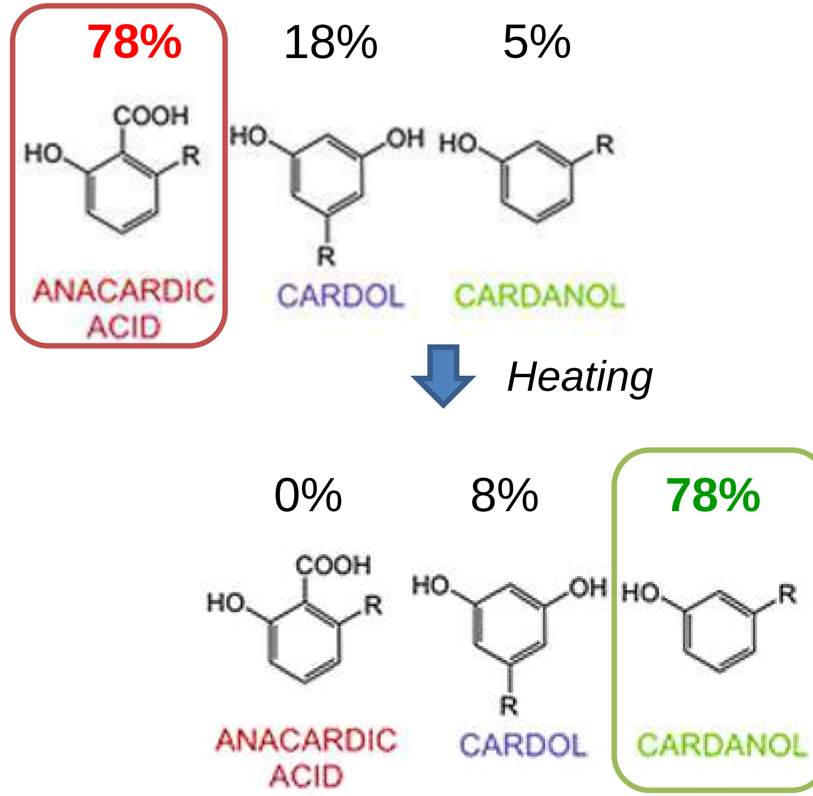

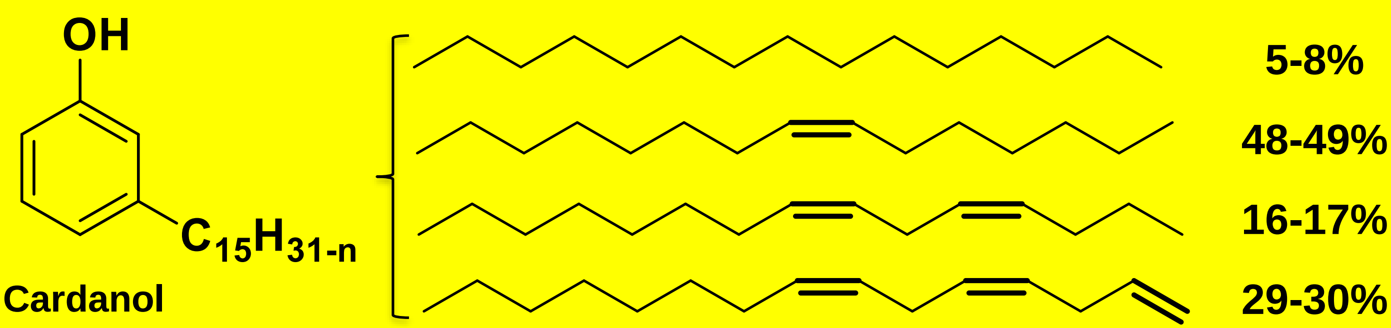

Institut Charles Gerhardt Montpellier

Examples of Cardanol Platform

Cashew Nutshell Liquid

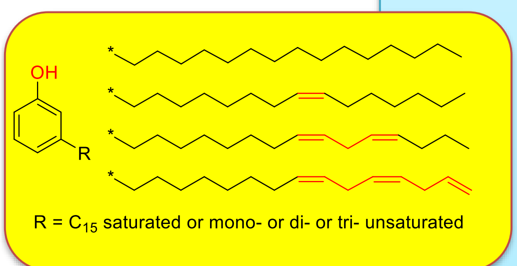

Caillol et al.
Green Materials, 2015, **3**, 1-29
COGSC, 2018, **14**, 26-32

Linseed fibers and Cardanol vinyl ester composites

***EJLST, 2014**, 116, 928–939; **2015**, 71, 248-258*

PVC Plasticizer

Indus Crops Prod, **2019**, 130, 1-8

Cardanol-nonanal resole resins

***EJLST, 2018**, 120, 1800175*

Cardanol surfactants

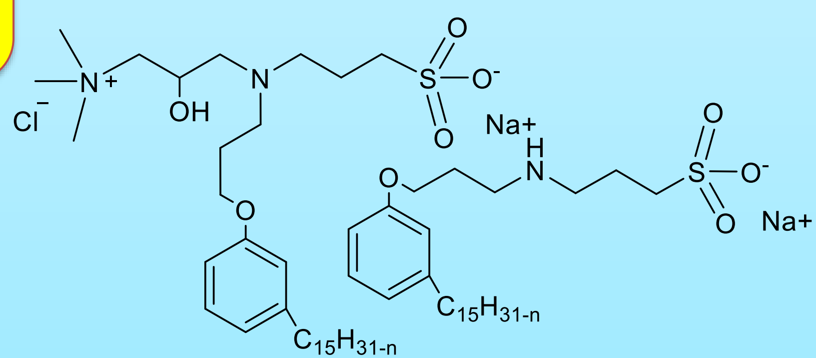

***Green Materials, 2017**, 5, 144–152*

From cardanol to methacrylated monomers

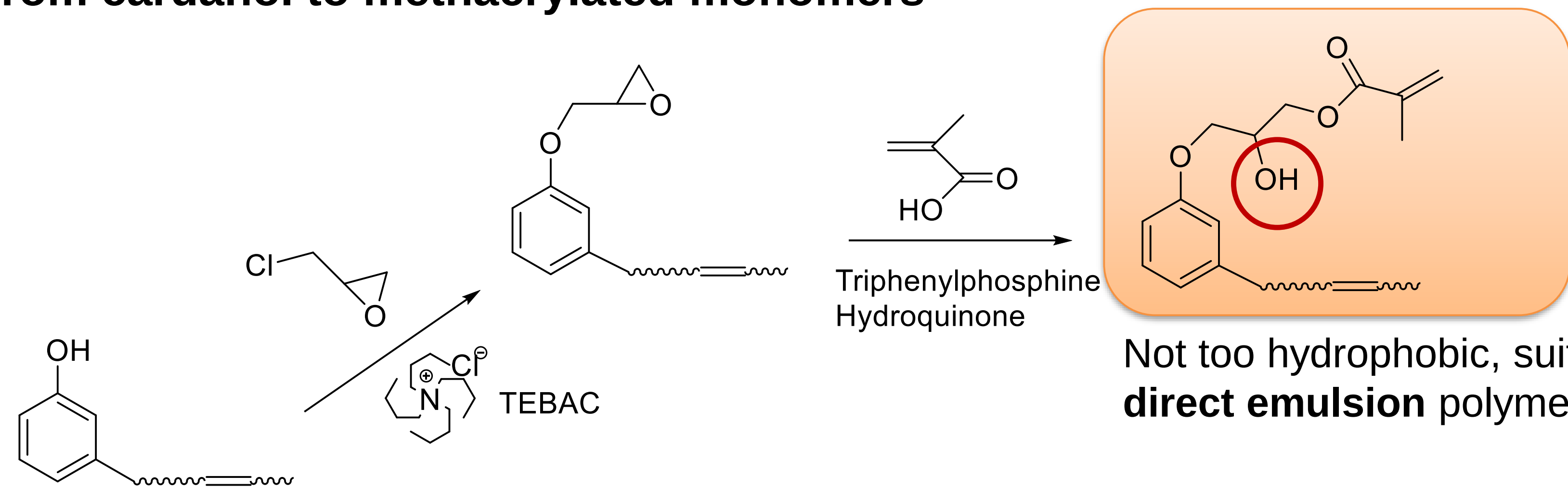

Not too hydrophobic, suitable for **direct emulsion** polymerization

Homo- and co-polymerization with MMA
Low Tg of polymers due to dangling chain

Caillol et al., **European Polymer Journal**, 2017, **93**, 785-794
Caillol et al., **Polymer Chemistry**, 2018, **9**, 2468-2477

Emulsion and Mini-emulsion polymerization

Direct Emulsion Polymerization

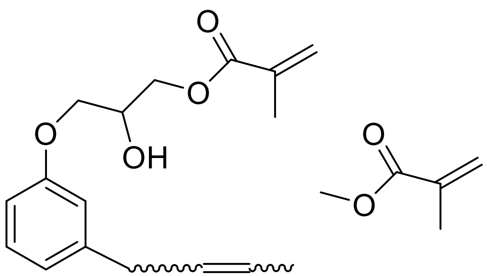

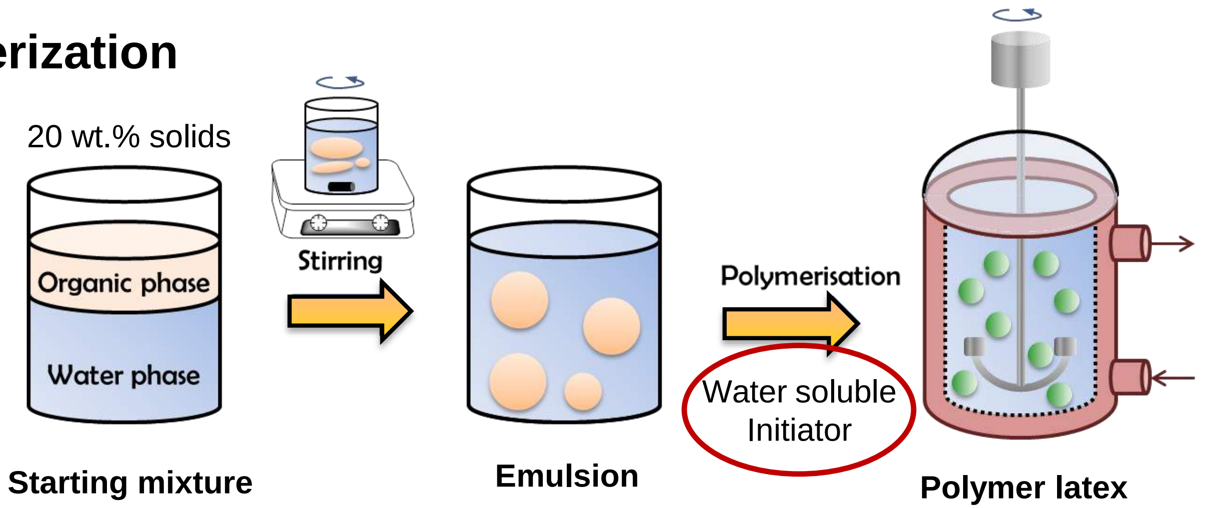

Mini Emulsion Polymerization

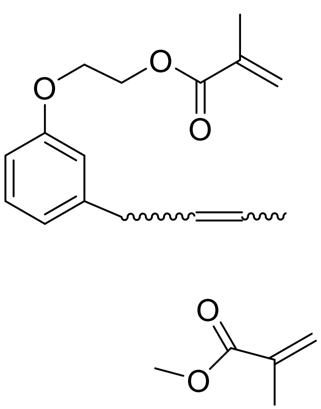

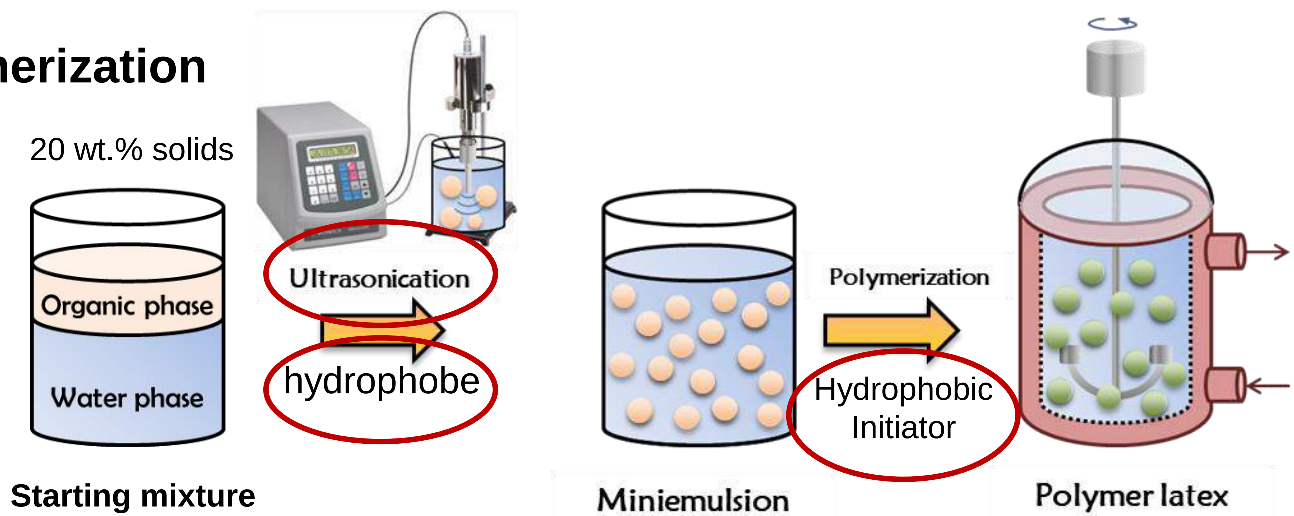

Cardanol-based emulsion polymerization

Emulsion Co-polymerization with MMA

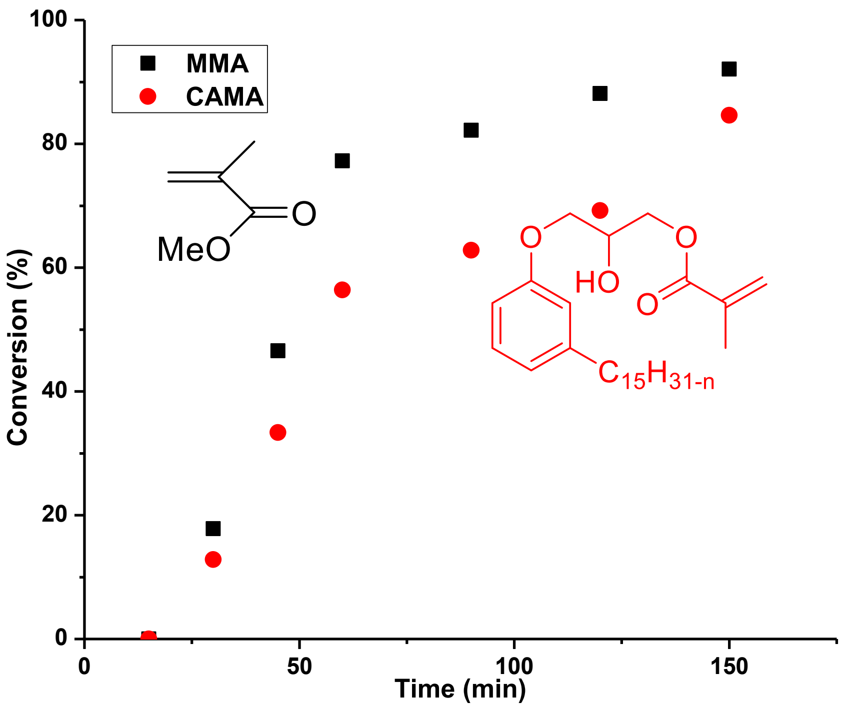

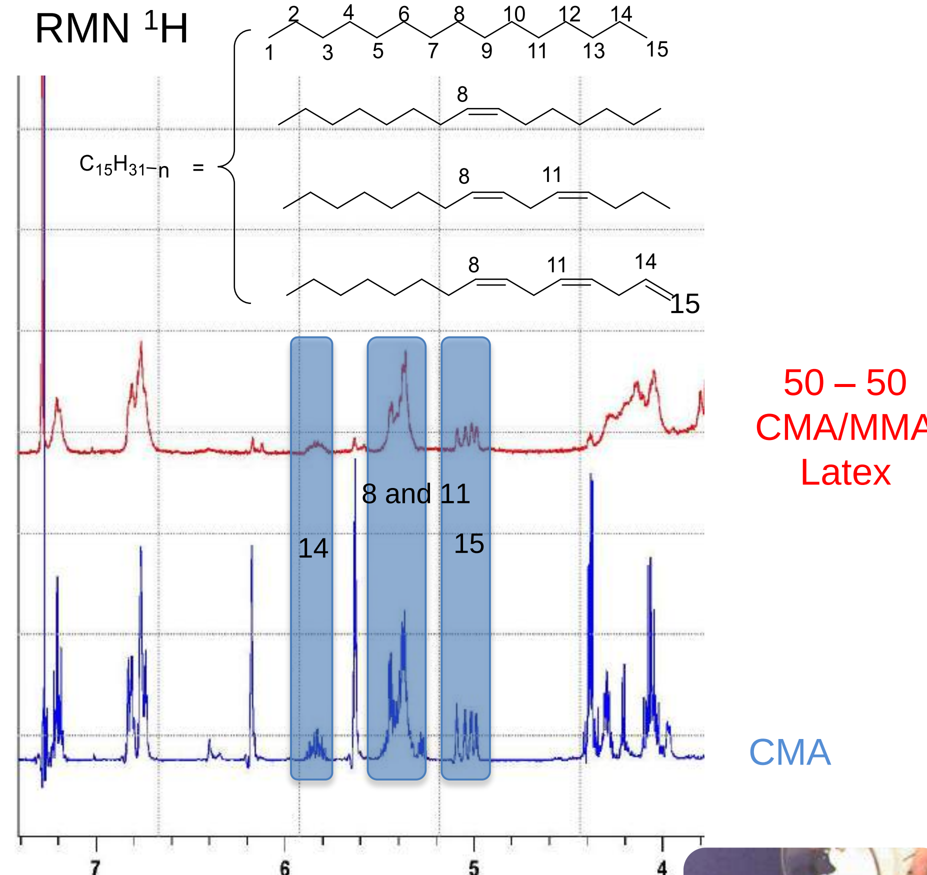

- **Similar reactivity** of both monomers
- **Particle sizes # 60nm**
- **Tg # 20°C**
- Double bonds or cardanol are **not reactive** during polymerization
    - ➢ Available for **cross-linking**

Caillol et al., **European Polymer Journal**, 2017, **93**, 785-794
Caillol et al., **Polymer Chemistry**, 2018, **9**, 2468-2477

Mini-emulsion polymerization

Mini-Emulsion Co-polymerization with MMA

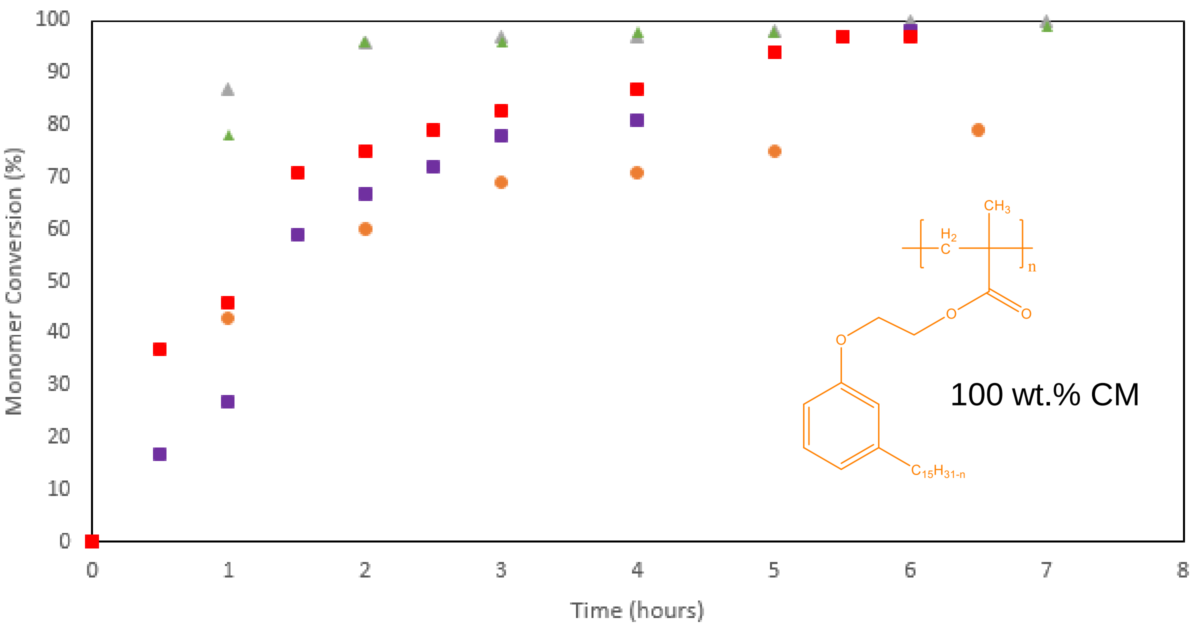

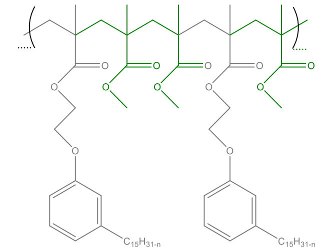

25 wt.% CM

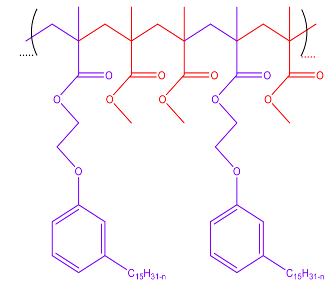

75 wt.% CM

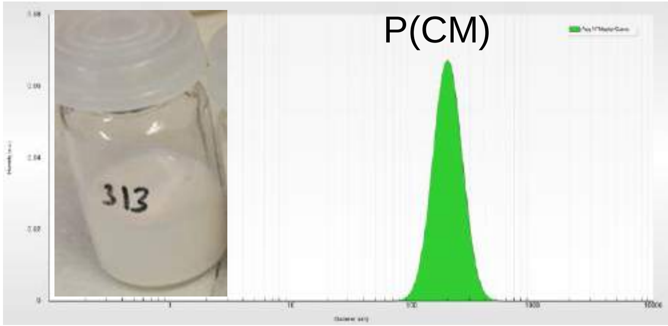

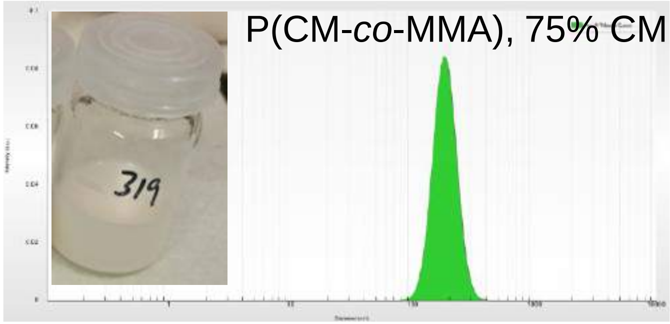

- **Similar reactivity** of both monomers
- Particle sizes # **180-200nm**
- Tg from 0 to 75°C
- Double bonds or cardanol are **not reactive** during polymerization

Caillol et al., **European Polymer Journal**, 2017, **93**, 785-794

Cardanol-based water coatings

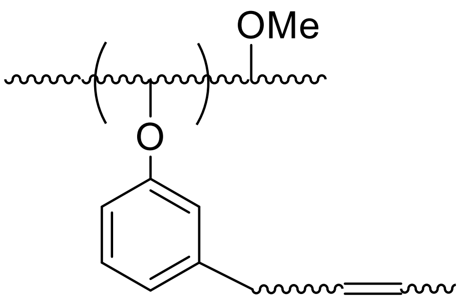

Biobased nanolatex

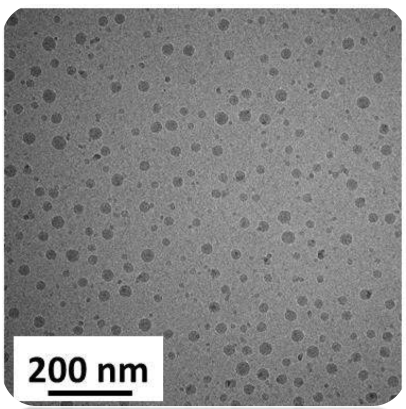

Gel content # 10%

Film formation

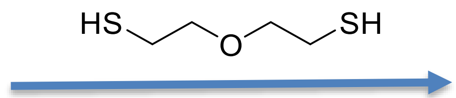

UV 1800W - 200-600 nm

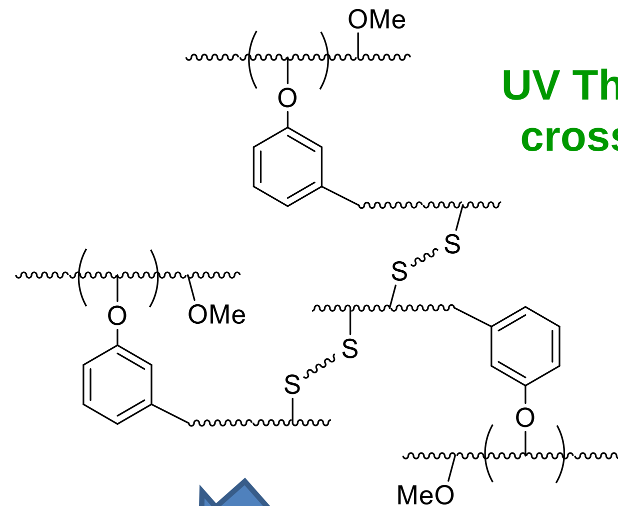

UV Thiol-Ene crosslinking

Crosslinked biobased coatings

Gel content # 90%

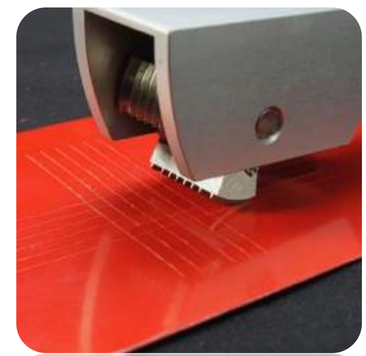

Cross cut adhesion = 1

▶ **Cross-linking degree ↗**
IMPACT RESISTANCE ↗

Caillol et al., **European Polymer Journal**, 2017, **93**, 785-794

Ferulic acid

Beetroot

Wheat or rice bran

Bagasse

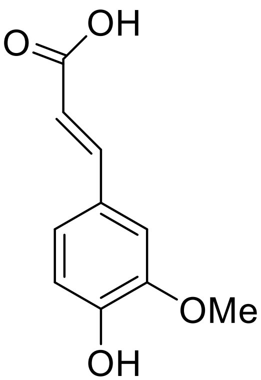

Ferulic acid

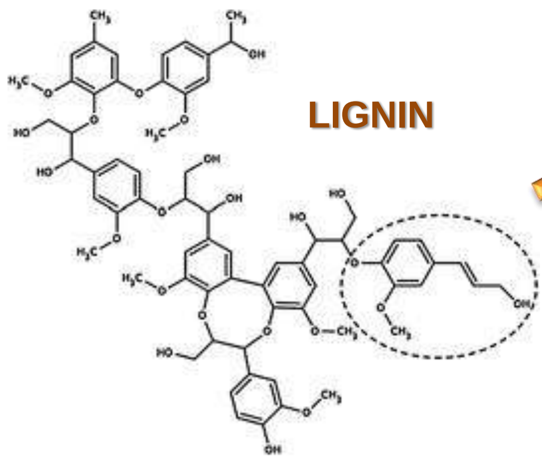

LIGNIN

Collaboration
Prof Masami Kamigaito
Prof Kotaro Satoh
Nagoya University

H Takeshima, K Satoh, M Kamigaito, **Macromolecules**, 2017, **50**, 4206−4216

Core-shell ferulic-based latex

Styrene

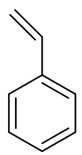

Bu Acrylate

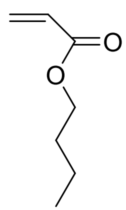

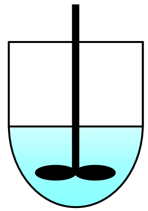

Copolym

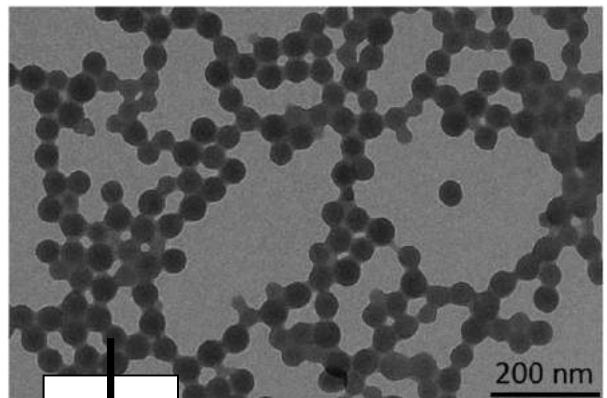

Seed latex
Particle size: **50nm**
Tg = **70°C**

Collaboration
Prof Masami Kamigaito
Prof Kotaro Satoh
Nagoya University

1. Shell-polym
2. Phenol deprotec

Ferulic-based monomer

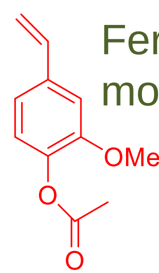

Core-shell latex
Particle size: 90nm
Tg = 70, 116°C

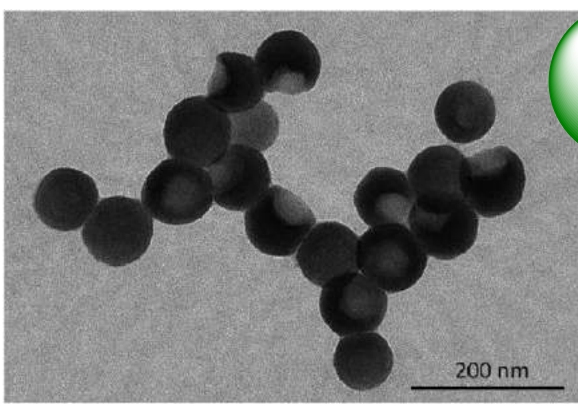

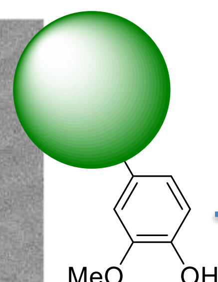

Film forming

Glyoxal addition

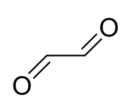

Cross-linked Network
(phenol-aldehyde)

Li, Satoh, Kamigaito, Caillol et al., **Polymer Chemistry**, 2019, **10**, 3116–3126

Conclusion: from biosourced monomers and polymers to materials

- **Natural phenols**: interesting building blocks for monomer synthesis for various polymers such as polyepoxides, polyurethanes, vinyl esters, polyacrylates…
- **Aromatic ring**: confers interesting reactivity and high mechanical or thermal properties
- **Safer chemicals**: replacement of isocyanates, styrene, BPA, DINP…

- Some of our **achievements**

Sport floor coating

Prosthetic socket

Doming

Composite matrix

ACKNOWLEDGEMENTS

ICGM - IAM
Gabriel Foyer (PhD)
Maxence Fache (PhD)
Dr Vincent Besse
Adrien Cornille (PhD)
Jennifer Wing-Sze Li
Romain Tavernier (PhD)
Dr Lerys Granado
Dr Mélanie Decostanzi
Dr Claire Negrell
Dr Patrick Lacroix-Desmazes
Hon Prof Bernard Boutevin
Dr Vincent Ladmiral

LCPO Bordeaux
Prof Stéphane Carlotti
Prof Henri Cramail

Univ Lille
Prof Serge Bourbigot
Prof Gaelle Fontaine

NCL Pune (Ind)
Prof Prakash Wadgaonkar

Nagoya University
Prof Masami Kamigaito
Prof Kotaro Satoh

Sylvain.Caillol@enscm.fr

CertBond
COST Action CA18120

Adhesive bonding

Introduction, Chemistry and Pre-treatments

Elisabeth Stammen, ifs, TU Braunschweig, Germany
e.stammen@tu-braunschweig.de

Institute of Joining and Welding

COST EUROPEAN COOPERATION IN SCIENCE & TECHNOLOGY

Funded by the Horizon 2020 Framework Programme of the European Union

Outline

- Introduction
- Adhesives – Mechanisms and examples
- Surfaces and pre-treatment

Introduction

CertBond
COST Action CA18120

COST
EUROPEAN COOPERATION IN SCIENCE & TECHNOLOGY

Funded by the Horizon 2020 Framework Programme of the European Union

Adhesive Bonding…a new age?

CertBond
COST Action CA18120

What is an adhesive?

The definition of an adhesive according to DIN 2304-1 (2020):

"Bonding of joined parts via **adhesion** (surface adhesion) and **cohesion** (internal strength) with a non-metallic substance (adhesive)”

Adhesion and Cohesion

Cohesion	Adhesion
The effect of attractive forces between atoms or molecules within a substance.	Effect of attractive forces between different substances.

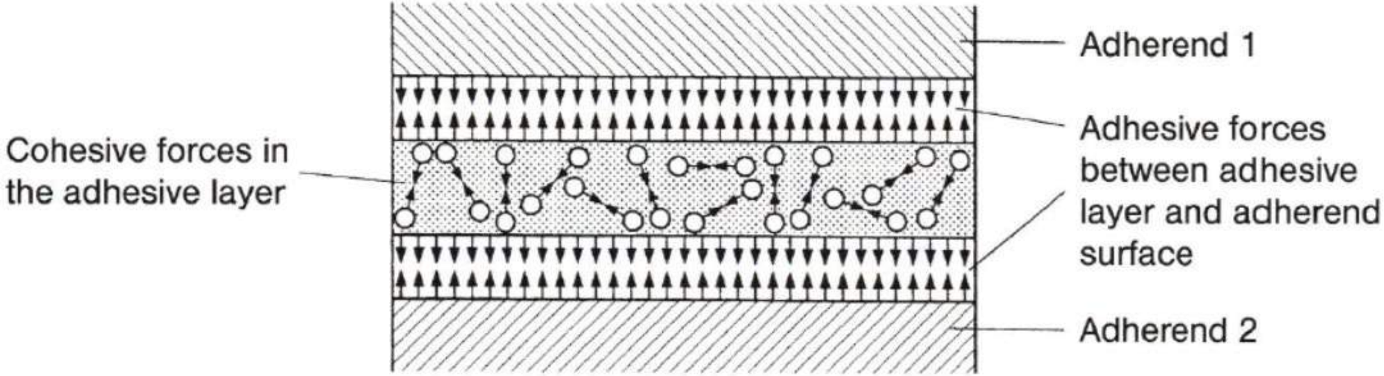

Source: Habenicht

Adhesion and cohesion are decisively determined by the binding forces!

Adhesive Bonding…pro's

CertBond
COST Action CA18120

- Uniform stress distribution perpendicular to the loading direction
- Possibility of joining very thin parts
- High fatigue strength
- Low thermal stress (only with cold-curing adhesives)
- No thermal influence on the microstructure
- No thermally induced component distortion
- Joining option for very heat-sensitive materials
- Bonding option for different material combinations
- Possibility of bonding metals with different electrochemical properties
- Joining of sensitive materials (e.g. glass)
- High vibration damping

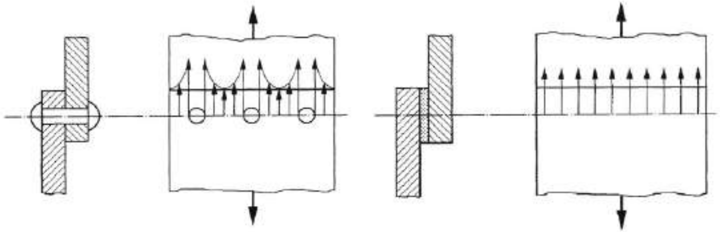

Weight saving &
lightweight construction

Source: Habenicht

Adhesive Bonding…con‘s

CertBond
COST Action CA18120

- Difficult process integration
- Viscous media (no initial strength)
- Long process times (curing)
- Resistance to ageing
- Monitoring difficult
- Change of properties
- Infiltration
- Testing
- "Kissing bonds”
- Properties of bonds dependent on temperature

Combination of disadvantages → limited use in aviation

Adhesive Bonding…influences

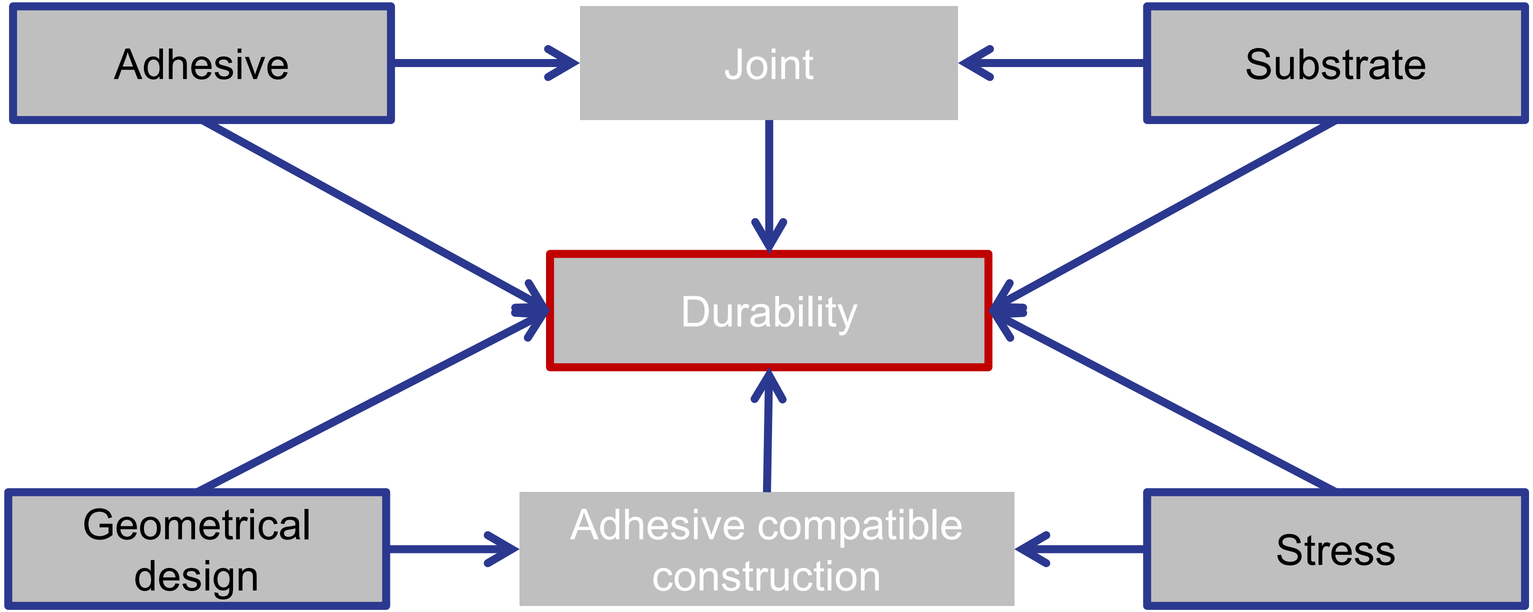

Adhesive Bonding…focus of lecture

CertBond
COST Action CA18120

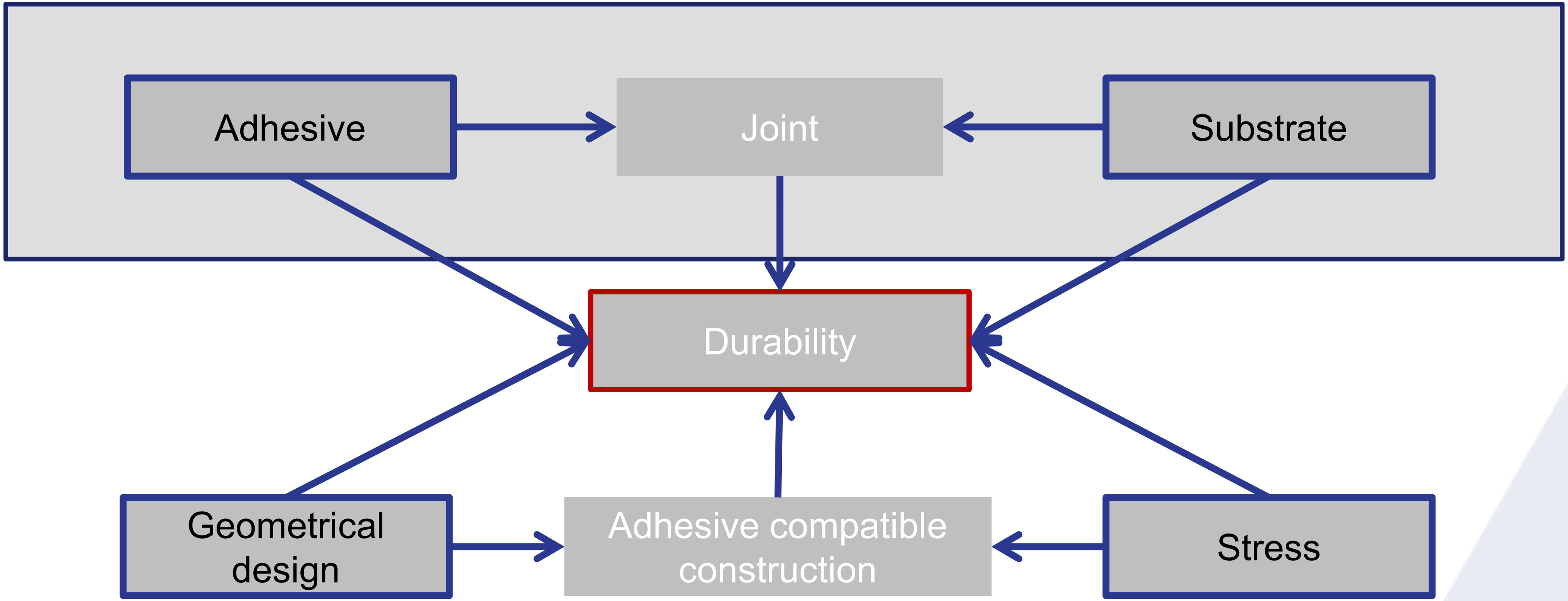

Adhesives – Mechanism and Examples

CertBond
COST Action CA18120

cost
EUROPEAN COOPERATION IN SCIENCE & TECHNOLOGY

Funded by the Horizon 2020 Framework Programme of the European Union

Adhesive – A general classification

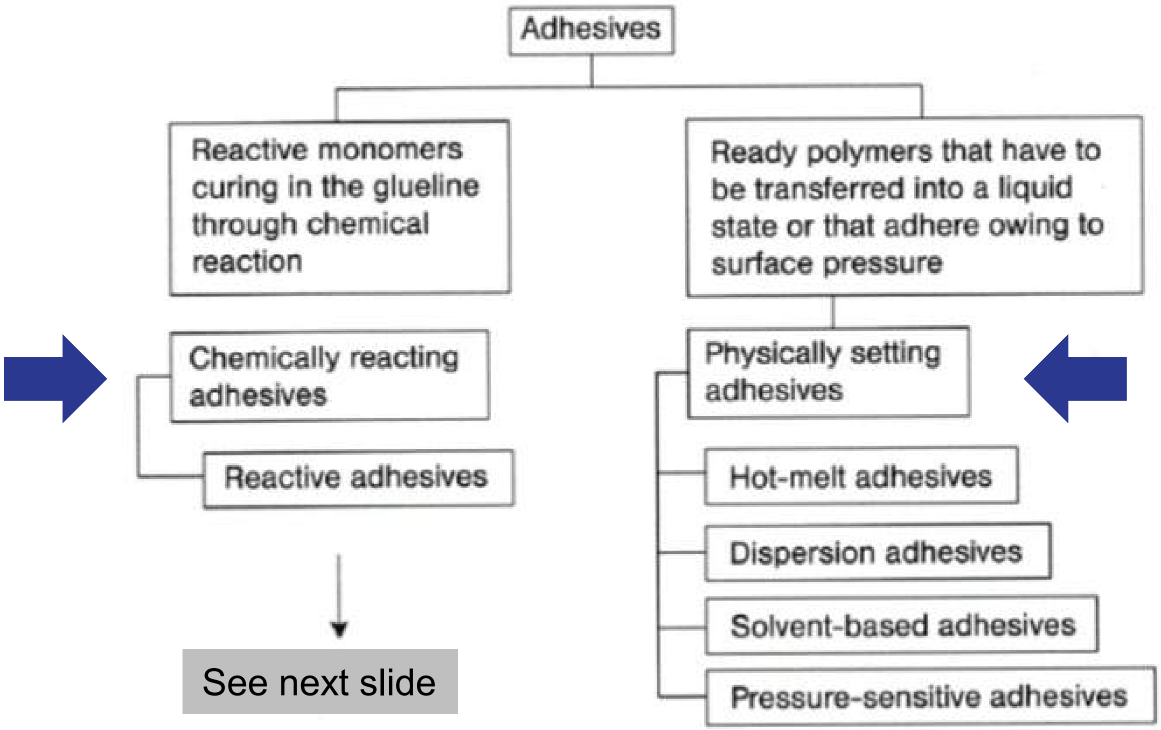

Source: Habenicht

Chemical reactive adhesives

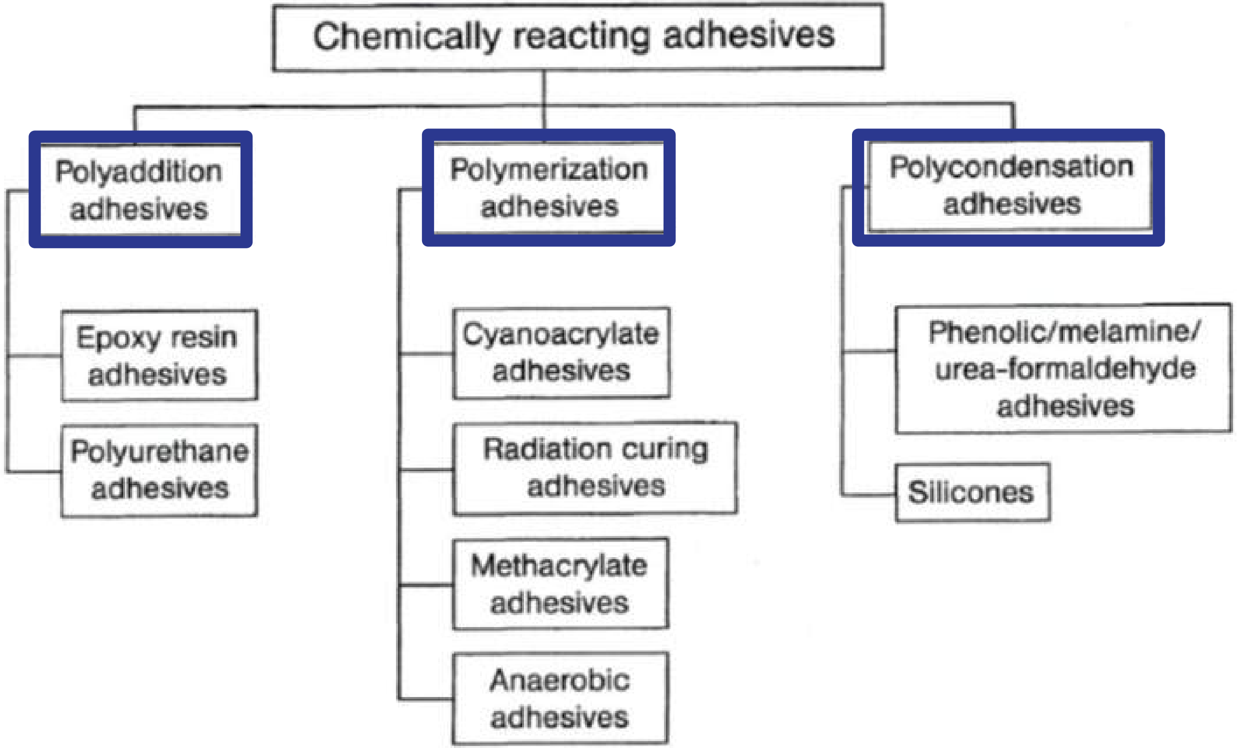

Source: Habenicht

Functional groups

A functional group is a group of atoms in a molecule that shows characteristic properties and reactions and that essentially determines the behaviour of the molecule.
Several identical or different functional groups can be present in a molecule at the same time.

Functional Groups*	Formula	Example
Hydroxyl	-OH	Alcohol
Amino	$-NH_2$	Aminoacid
Carbonyl	-COOH	Aceticacid
Aldehyde	-CHO	Formaldehyde
Isocyanate	-N=C=O	Methylisocyanate
Vinyl	$-CH=CH_2$	Vinylchloride
Epoxy	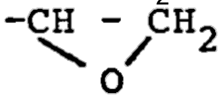	Epoxyresin

*not exclusive

General reaction mechanisms

- Polymersiation
- Polyaddition
- Polycondensation

Polymerisation

CertBond
COST Action CA18120

- Reaction of low-molecular substances with the opening of multiple bonds or ring structures to form macromolecules (requires C=C double bonds).
- Initiation (also called chain start or primary reaction): The reaction(s) that set the chain reaction and thus the formation of polymers in motion.
- Growth reaction (also called build-up or propagation reaction or propagation): Here the molecular chains become longer and longer (run length approx. 0.1 mm)
- Chain termination: Reactions that lead to the termination of the chain reaction.
- As a rule, thermoplastics are formed.
- No stoichiometric mixing of the components is necessary.

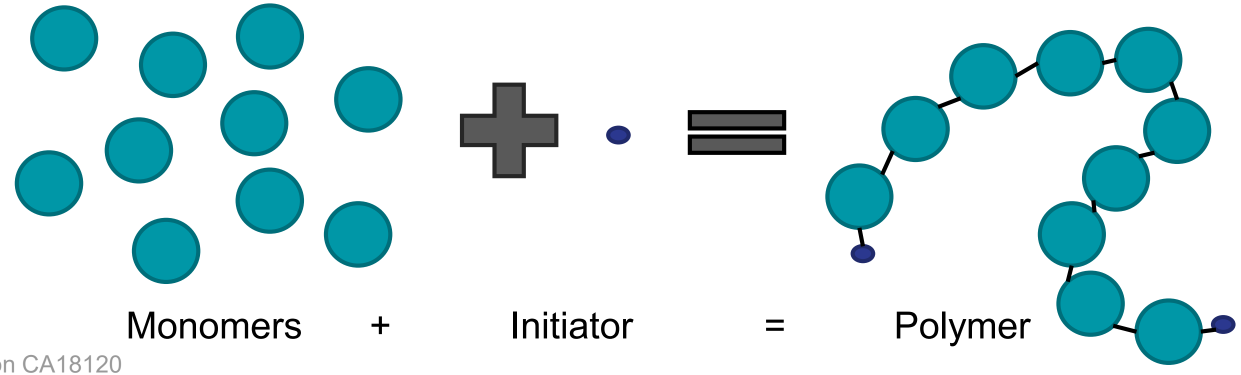

Polyaddition

- Reaction of polyfunctional monomers with different reactive groups with migration of hydrogen atoms.
- No initiator
- First linking of individual groups, then linking of groups to form long polymer chains → Step-growth reaction
- 2C and 1C possible
- Mandatory stoichiometric

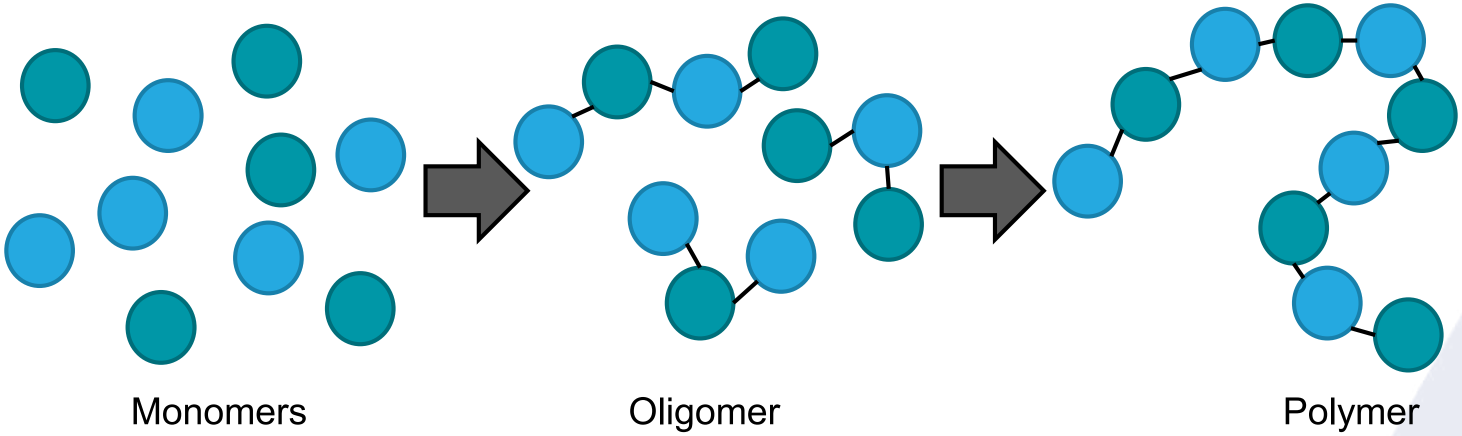

Polycondensation

- Similar to polyaddition, but formation of one low-molecular-weight compound per linked bond.
- Step growth reaction
- Porosity possible due to deposition (Low molecular weight compounds)

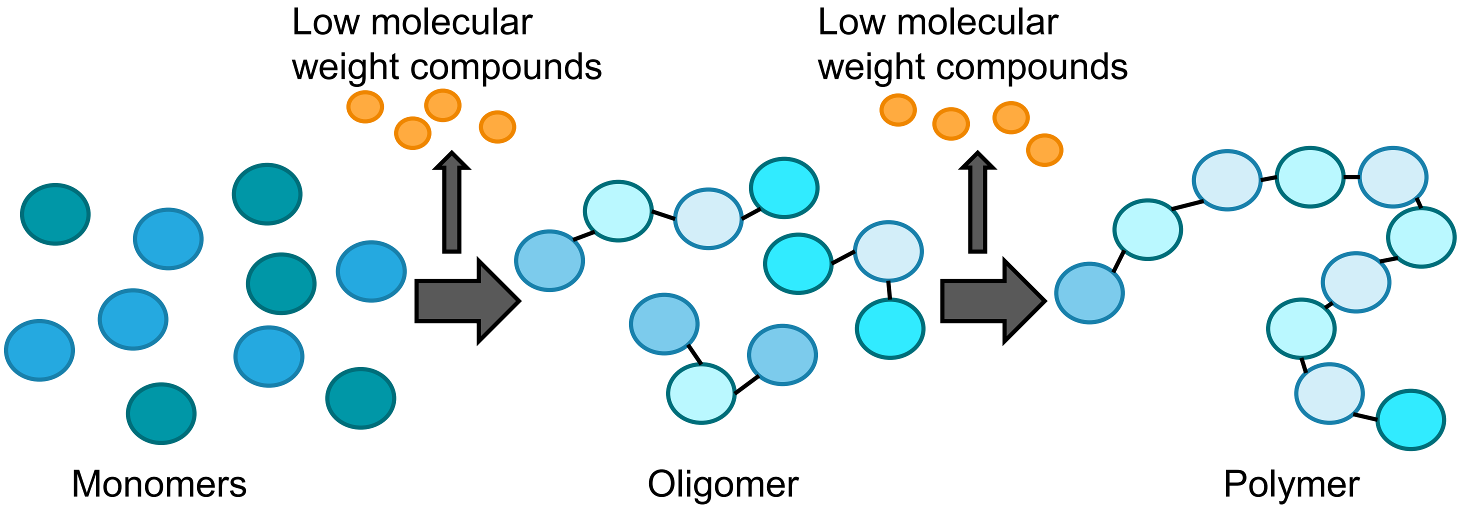

Examples

- Polymerisation

1C Polymerisation: Cyanoacrylate

- Linear chain growth → thermoplastic adhesive
  - Moderate temperature resistance (approx. 80°C)
  - Moderate media resistance (e.g. in water: substitute absorption)
  - Low adhesive layer thickness (100 - 200 µm)
  - Small bonding surface
  - Brittle
  - Very fast curing (→ super glue)
  - Reaction with moisture (rel. humidity min. 30..40%)

- Examples of applications:
  - Bonding of elastomers
  - Bonding of plastics

Source: Cyberbond Europe GmbH

1C Polymerisation: Cyanoacrylate

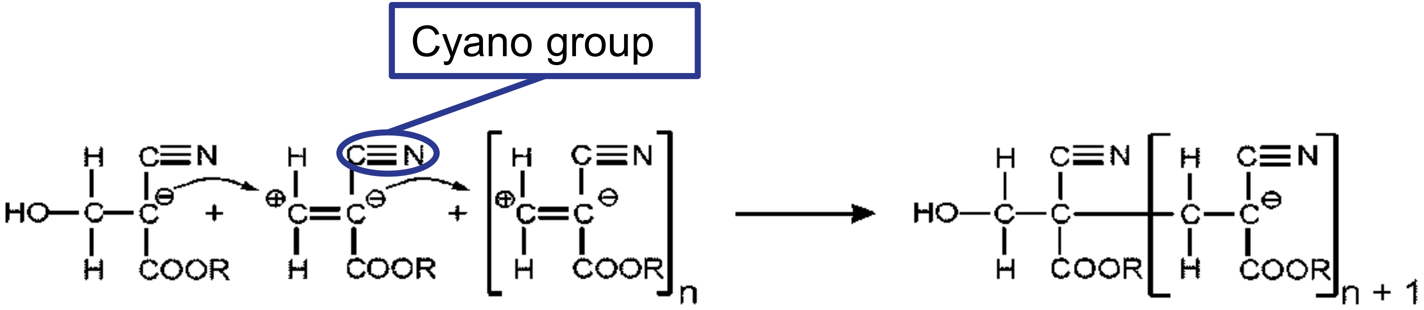

- Chain initiator: OH^- -Ions (as a rule: from humidity or activator)
- Does not stick to acidic surfaces (e.g. ceramics): H_3O^+ surplus → no OH^--ions to start the reaction
- The chain grows by adding further monomers to the already activated adduct
- Chain break: meet a second chain or another OH^--ion (limited chain length → thin adhesive layers)

1C Polymerisation: Anaerobic

- 1C polymerisation adhesives that cure in the absence of oxygen

  → Adhesives remain in a liquid state as long as they are in contact with oxygen ("liquid plastics")

- After bringing the metallic joining partners together, the stabilising oxygen is shielded → Curing reaction starts

- Low activation energy → Curing at room temperature

- Metal ions for curing necessary → at least one metallic joining part or activator required

Source: Cyberbond Europe GmbH

1C Polymerisation: Anaerobic

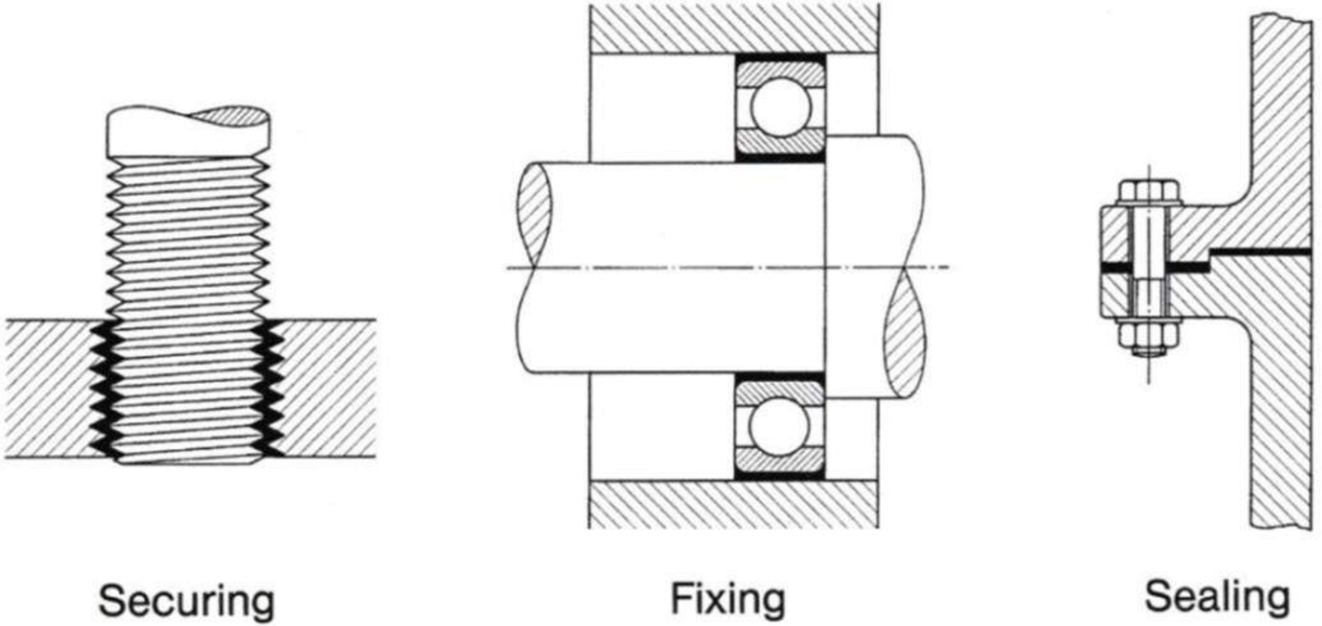

Source: Habenicht

1C Polymerisation: Anaerobic

- Starting products**:** Monomers derived from methacrylic acid by esterification of tetraethylene glycol

- Example: Tetraethylene glycol dimethacrylate (TEGMA)

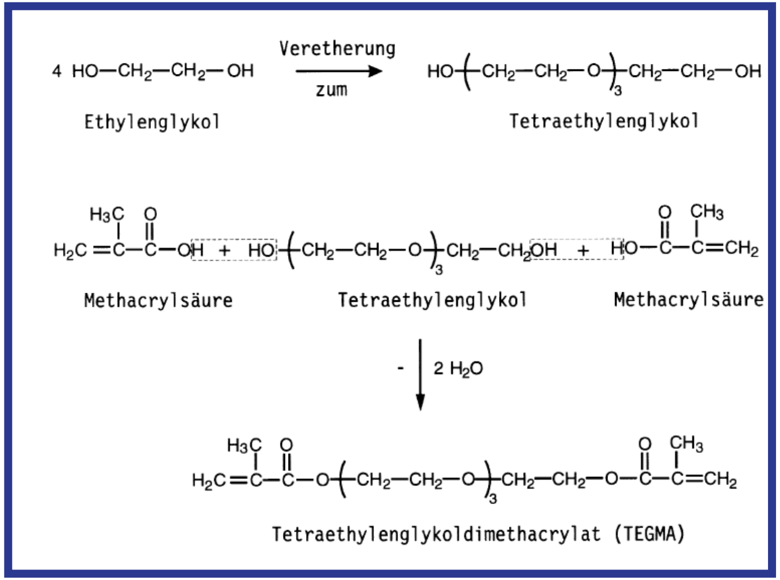

„Liquid plastic“

1C Polymerisation: Anaerobic

- Question: Why does the adhesive remain liquid when oxygen is present?
  - TEGMA radicals are continuously formed in small quantities with the hydroperoxide (by UV radiation/ temperature).
  - TEGMA radicals have high reactivity to oxygen: reaction to peroxide-containing TEGMA radicals: Impeding polymerisation

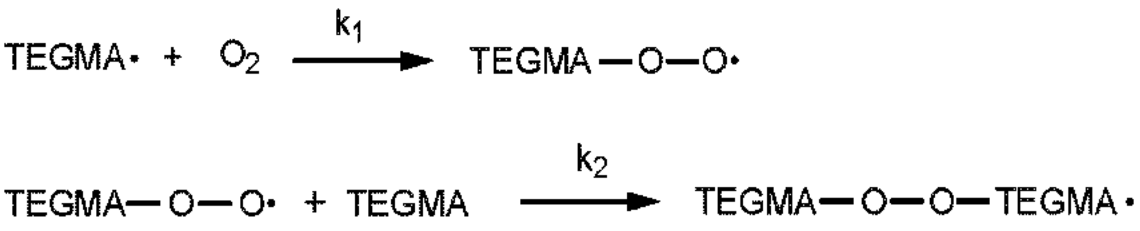

k_1, k_2 - Reaction rate constants

Reaction constant k1>>k2: Reaction stops at this stage and polymerisation does not take place

1C Polymerisation: Anaerobic

- Two-step curing reaction

1.: Formation of radicals by metal ions

Metal ions must be present!

2.: Chain growth under oxygen exclusion

No oxygen must be allowed to get into the adhesive!

1C Polymerisation: Anaerobic

- Radical-forming substance: Dimethylbenzyl-hydroperoxide

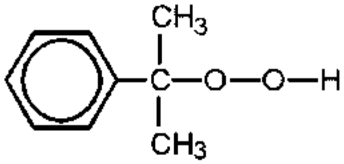

- Metal ion-catalysed decomposition of hydroperoxide as a source for the formation of free radicals

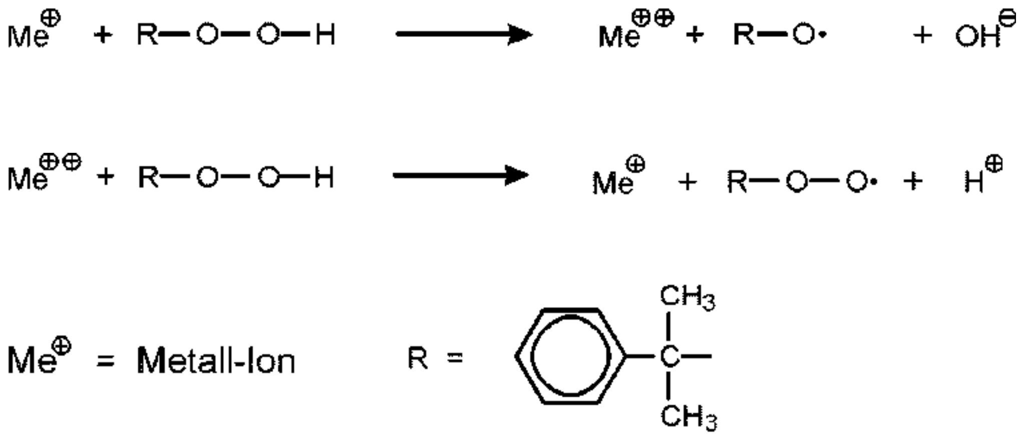

Speed of formation of the radicals: <u>metal-dependent</u>

Total duration of adhesive curing: <u>metal-dependent</u>

1C Polymerisation: Anaerobic

CertBond
COST Action CA18120

Free radical

TEGMA

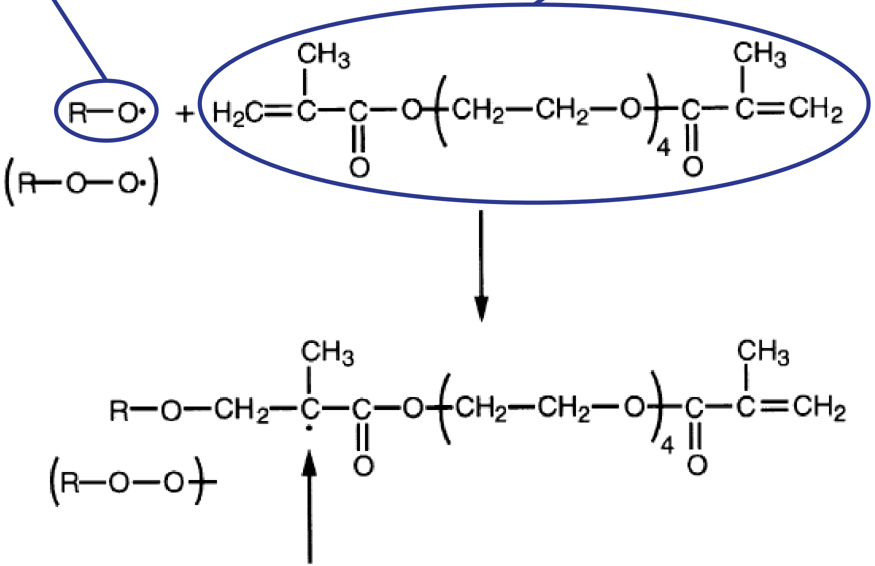

Here accumulation of further oxygen molecules

Breaking the double bonds in the TEGMA

Chain growth through polymerisation

Attention!

Polymer chains are only formed when no oxygen molecules are present!

1C Polymerisation: Light curing

Energy emission after conversion of electrical energy into radiation by the radiation source

↓

E-radiation curing.
Energy absorption by the monomer molecules

UV radiation curing: photoinitiators

↓

Photochemical primary reaction

Formation of free radicals

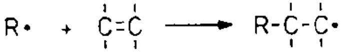

↓

Initiation of the reactive system through the formation of monomer molecules

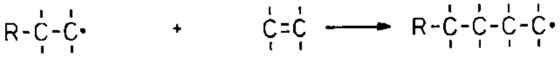

↓

Formation of chain start molecules

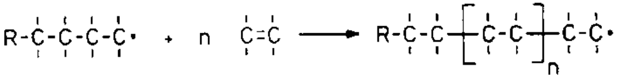

↓

Chain growth (formation of the cross-linked adhesive layer)

↓

Chain termination by recombination or radical molecules

Source: Internet

1C Polymerisation: Light curing

CertBond
COST Action CA18120

- Radical formation through photocleavage**:**

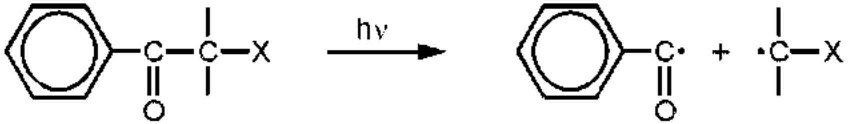

- Radical formation through hydrogen splitting (H-abtractors):

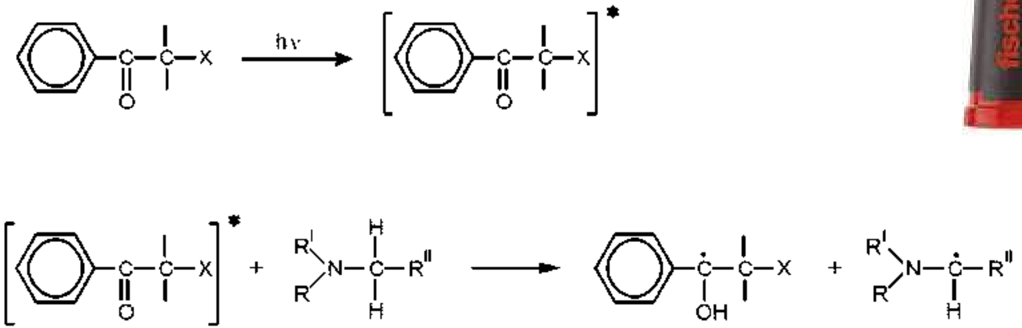

tertiary amine

Source: Internet

2C Polymerisation: MMA

- Initiator decomposition through accelerator:

Accelerators: tertiary aromatic amines $(R_x)_3N$, e.g. dimethyl-p-toluidine

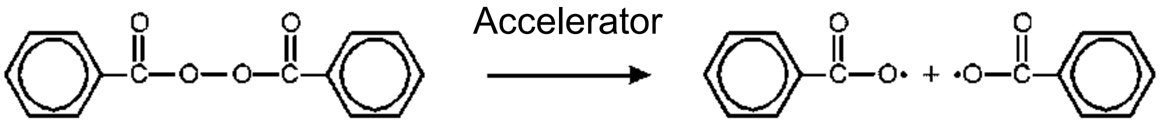

Dibenzoylperoxid

- Radical chain polymerisation of the MMA (methyl methacrylate) monomer:

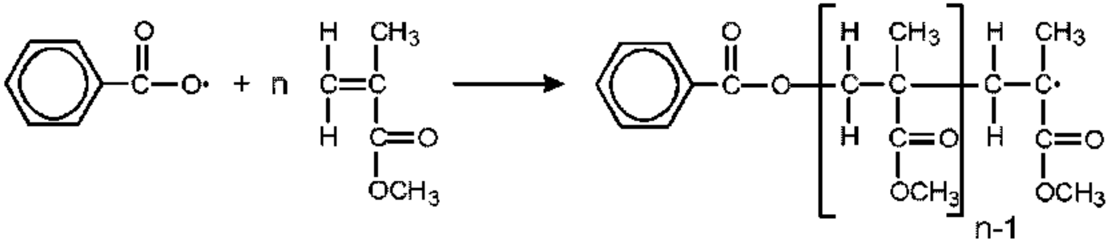

2C Polymerisation: MMA

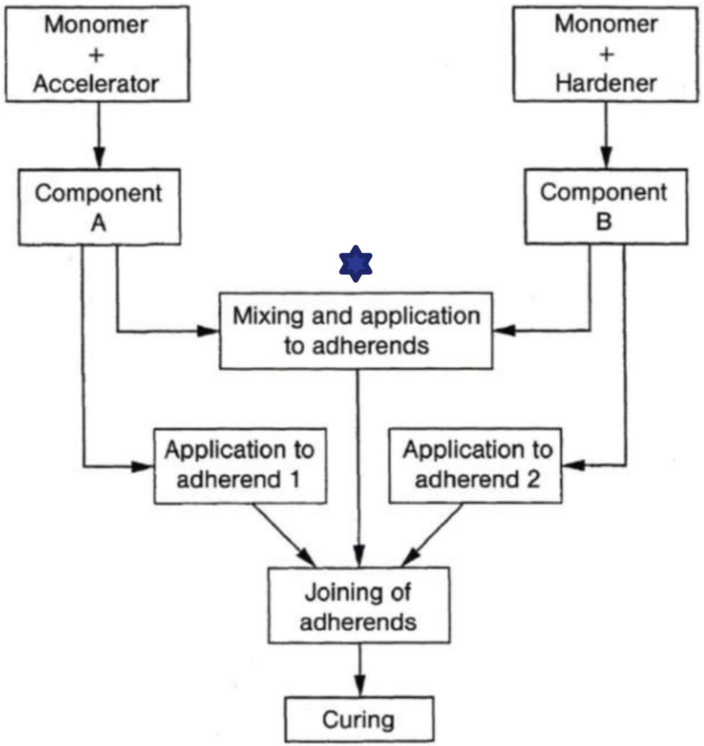

Source: Habenicht + UHU GmbH & Co. KG

Examples

- Polyaddition

Polyaddition: Epoxide

DEGBA

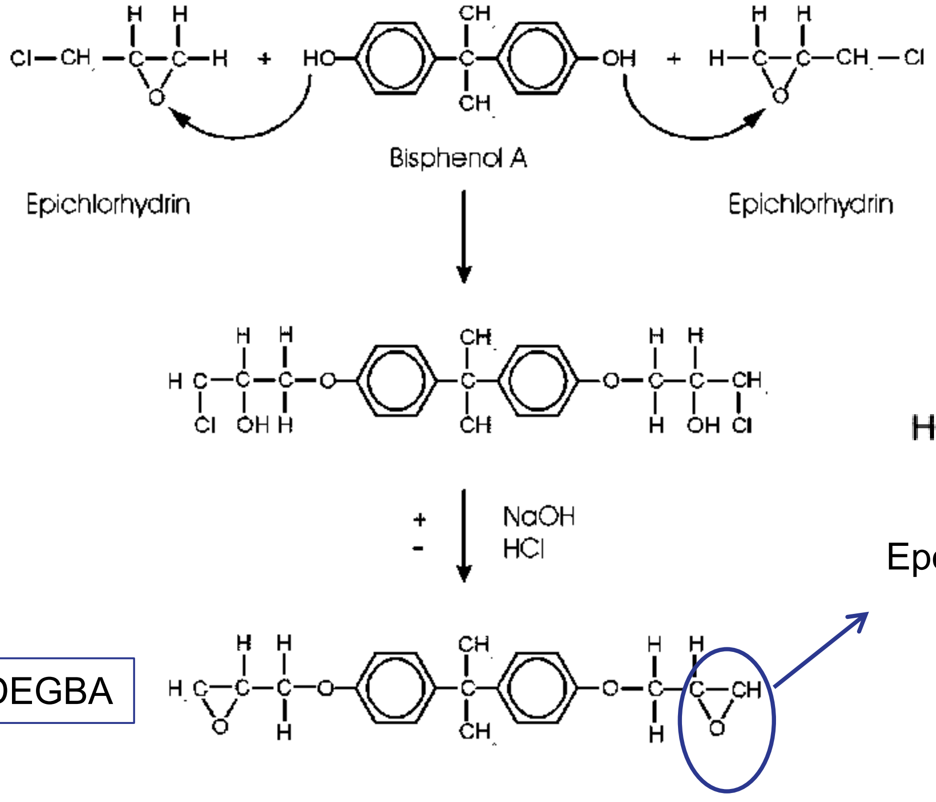

Diglycidylether von Bisphenol A (D G E B A)

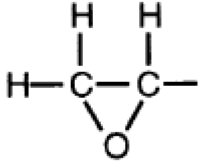

Epoxy-Group

Source: Internet

Polyaddition: Epoxide

CertBond
COST Action CA18120

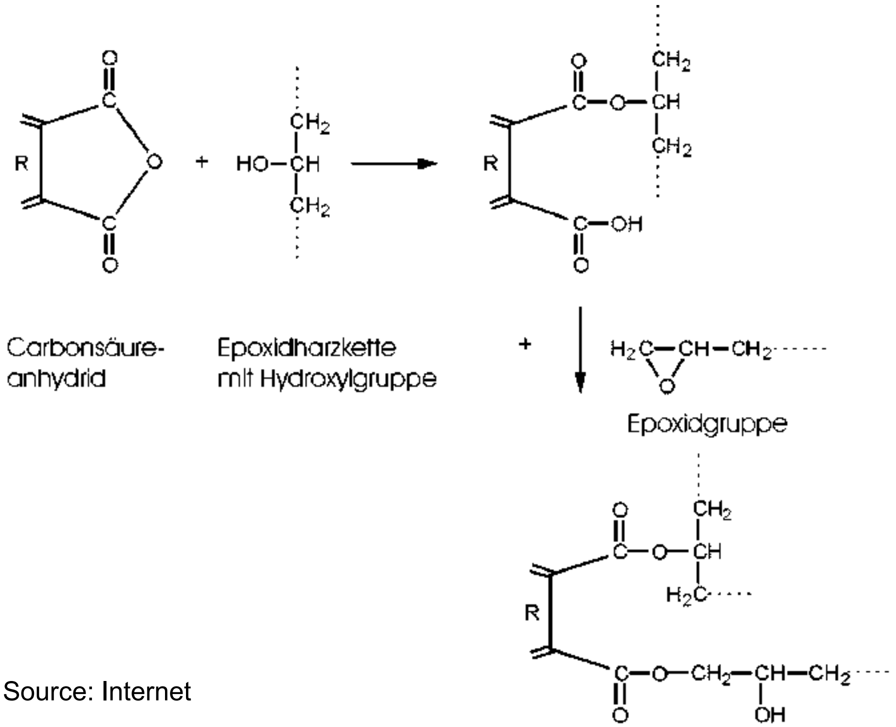

Source: Internet

Polyaddition: Epoxide

CertBond
COST Action CA18120

Curing agents for several applications and specifications, e.g.:

- Aliphatic amine, aromatic amine
- Polyamine-epoxyresin-adduct
- Polymercaptane
- Anhydrite
- Latent hardener, e.g. DICY (Dicyandiamide)
- Light curing, UV curing agents, e.g. onium-salts

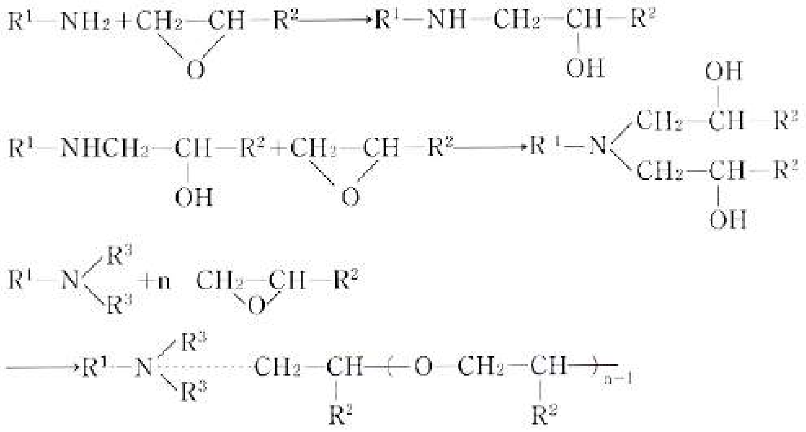

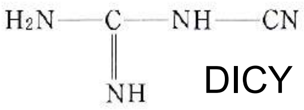

DICY

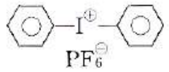

Diphenyliodonium hexafluorophosphate

1C/2C Polyaddition: Epoxide

- **General description**
  - Solvent-free adhesive (2C: resin (component A) and hardener (component B), 1C: with latent hardener)
  - Cures at room temperature (2C) or elevated temperatures (1C, 2C) to a duromer
- **Typical properties of the cured adhesive**
  - High strength
  - Generally brittle with low elongation at break (toughend products also available)
  - Use of the cured adhesive possible up to 200 °C
  - Good resistance to physical (e.g. sunlight) or chemical influences (moisture, cleaning agents, chemicals, etc.)

2C Polyaddition: Polyurethane

CertBond
COST Action CA18120

- Solvent-free two-component adhesive (2C) consisting of resin (component A) and hardener (component B). Resin and hardener are supplied in separate or individual containers and must be mixed for processing.
- Cure at room temperature or elevated temperatures
- Curing depending on the adhesive to an elastomer

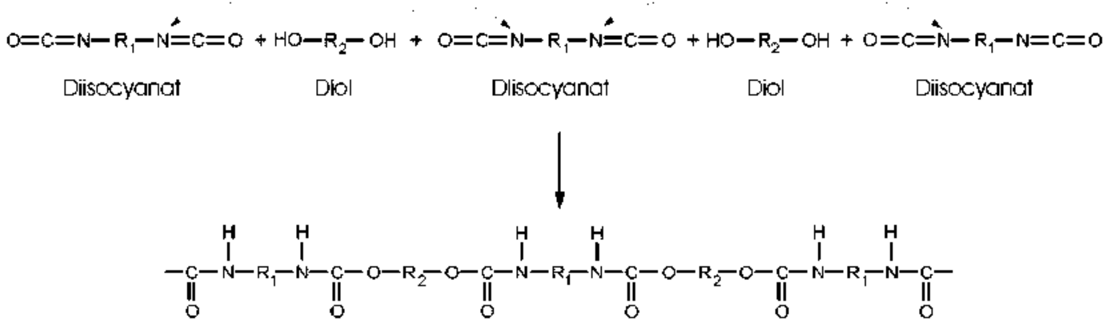

Polyisocyanate + Polyole → Polyurethane

Diisocyanate

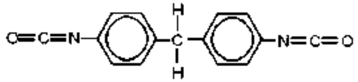

Diphenylmethan - 4,4'-diisocyanat (M D I)

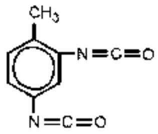

2,4 - Toluoldiisocyanat (TDI)

2C Polyaddition: Polyurethane

Characteristics of the cured adhesive

- Rubber to hard elastic, medium elasticity at break
- Medium to high strength
- Temperature range from -40 °C to approx. 110 °C
- Adhesion without primer sometimes problematic
- UV-sensitive
- Repair bonding on the cutted bead possible
- Can be painted over even in hardened state
- Lower resistance to physical and chemical stress than epoxies

Source: Weiss

1C Polyaddition: Polyurethane

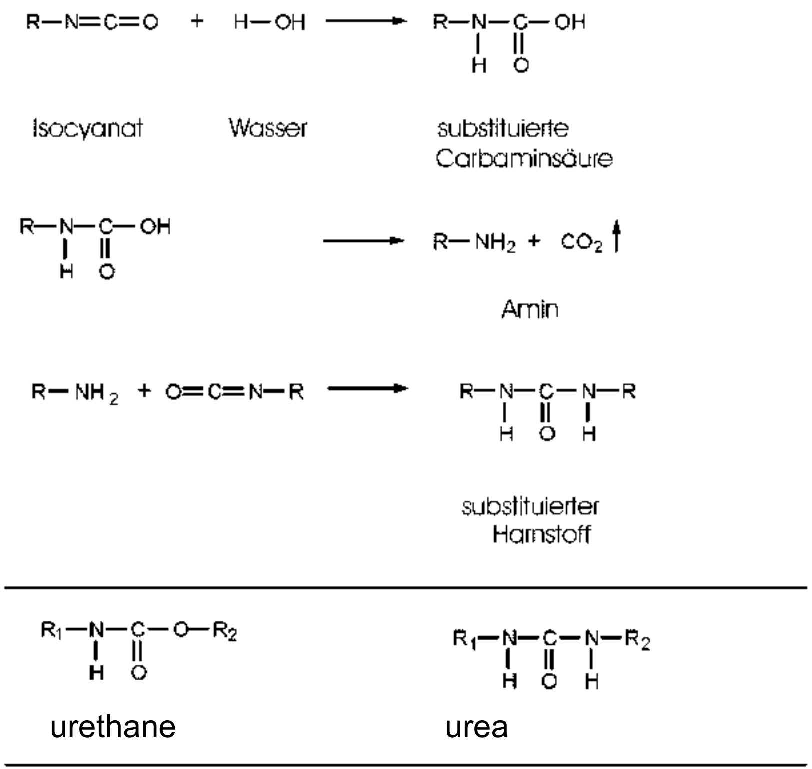

Curing by water from the air:

- Observe ambient conditions (temperature & humidity)
- Foaming possible (CO_2 formation)
- Limited bonding areas (apply in lines)

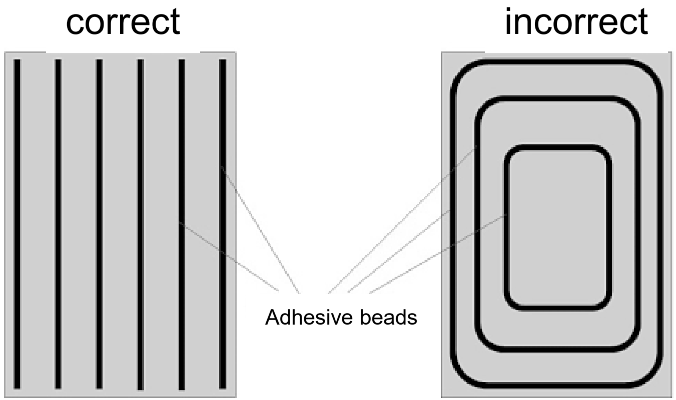

1C/2C Polyaddition: Polyurethane

„Booster“ Applications

Source: Sika Deutschland GmbH

Examples

- Polycondensation

Polycondensation: Phenol-Formaldehyde-Resin

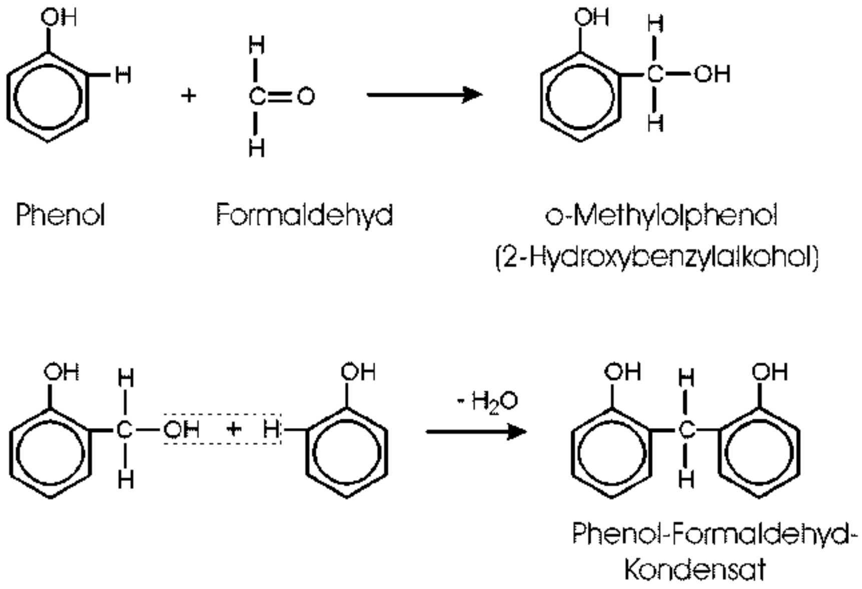

The linking of the two phenol molecules takes place after the splitting off of an H_2O molecule via a methane bridge ($-CH_2-$).

Polycondensation: 1C Silicone

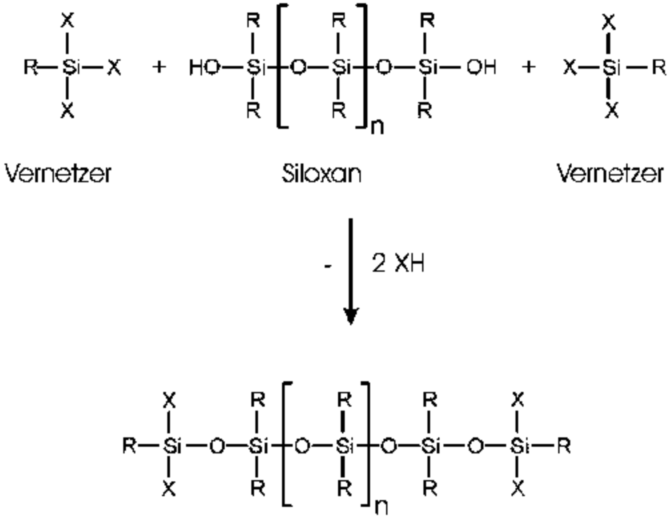

blocked siloxane

Prevention of premature polymer formation

Setting process

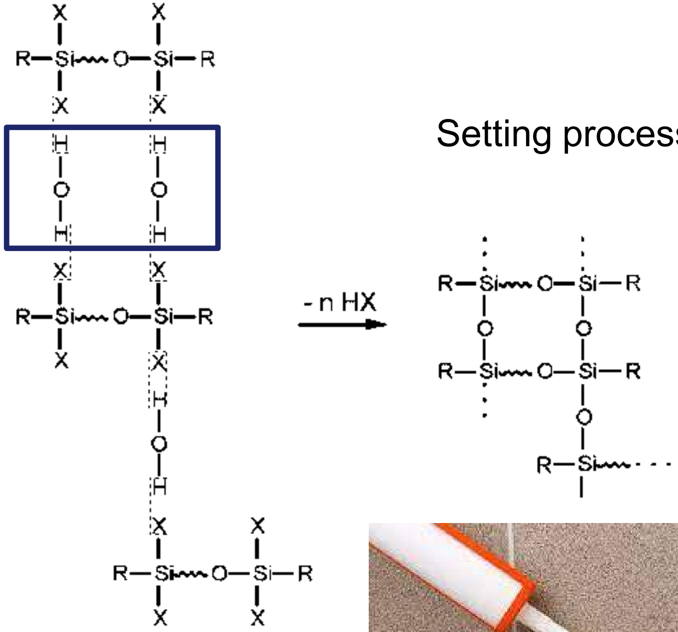

Source: Internet

Polycondensation: 2C Silicone

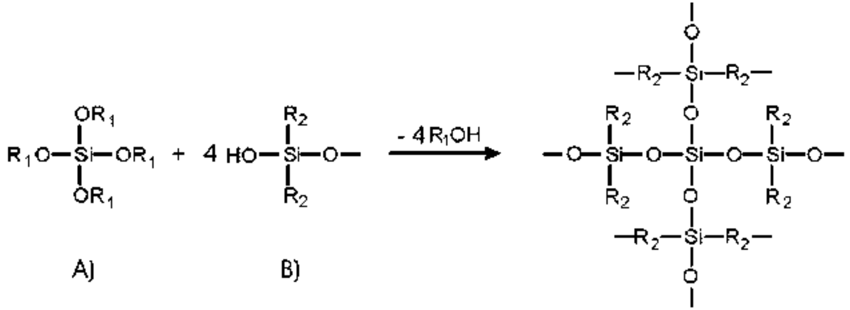

Condensation crosslinking of
A) silicic acid ester and
B) hydroxypolysiloxane

For comparison, 2C silicone as an addition reaction:

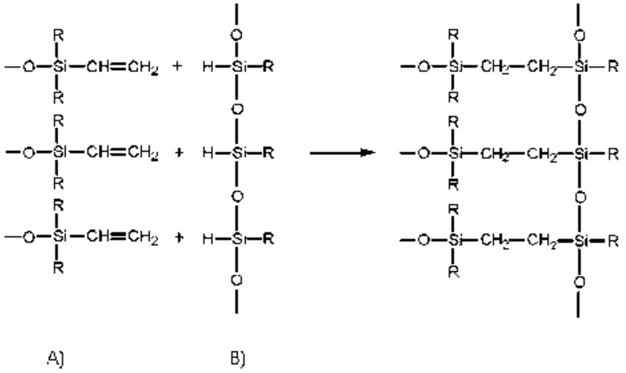

Addition crosslinking of
A) siloxane with vinyl group and
B) siloxane with Si-H bonds

Adhesive – A general classification

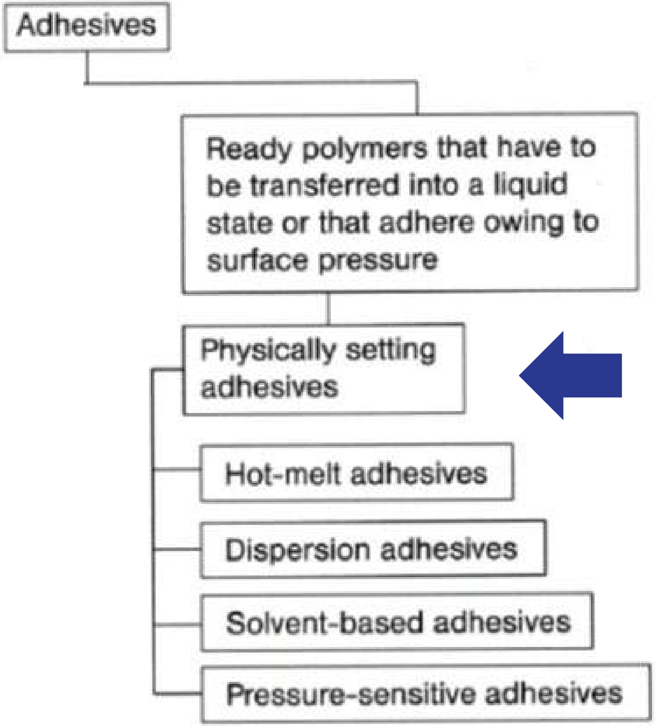

Source: Habenicht

Physical

Polymer	Liquefy	Setting	Adhesive
Thermoplastic	Melting	Solidifying	Hotmelt adhesives
Thermoplastic	Dissolving	Evaporation of the solvent	Solvent adhesives
Thermoplastic	Permanently plastic Soft Sticky		Pressure sensitive adhesives
Thermoplastic droplets in solvent		Gelation due to reduction of solvent content	Plastisols

Hotmelts

- Adhesive is a polymer
- Heating up to or beyond the melting range
- Application of the melt to the part to be joined
- Wetting of the part to be joined
- Joining
- Solidification of the adhesive
- Formation of the adhesive layer

Source: Internet

- Polyvinyl-acetate (PVAC, T_m~ 70..210 °C)
- Ethylene-vinyl-acetate-copolymers (EVAC, T_m ~150 °C)
- Polyamide (PA, T_m= 220 °C)
- Polyethylene terephthalate (PET, Tm: 250 °C)
- Polyolefin →Polyethylene (PE, T_m~ 140..210 °C)
  →Polypropylene (PP, T_m~ 160 °C)
- Polyetheretherketone (PEEK, T_m ~ 335 °C)

Hotmelts

CertBond
COST Action CA18120

Properties of the setting adhesive

- Free of solvents and monomers (individual building blocks of plastics)
- Medium to high strength in the bonded joint, flexibility depending on the thermoplastic
- Continuous use temperature is below the softening temperature
- Swelling problems, tends to creep

Attention

The parts to be bonded must be acclimatised before bonding. Especially important when bonding metallic parts (high thermal conductivity): Danger of shock-like setting.

Solvent based/ water based adhesives

A solution is a homogeneous mixture consisting of one or more dissolved substances and a solvent.

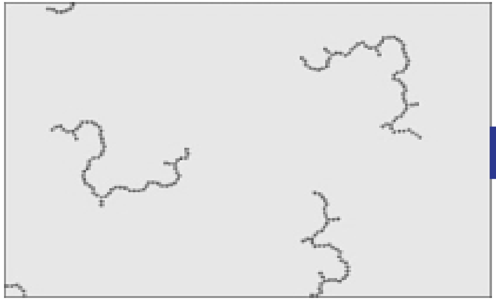

- Thermoplastic, dissolved in organic solvent
- Setting takes place through evaporation of the solvent

A dispersion is a heterogeneous mixture of at least two substances that do not or hardly dissolve in each other.

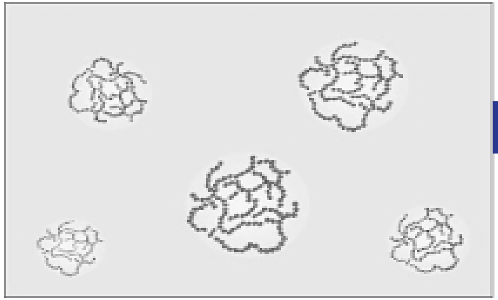

- Polymer particles distributed (dispersed) in water
- Setting to thermoplastic or elastomer

Due to the absence of organic solvents, dispersion adhesives are traded as an environmentally friendly alternative to solvent adhesives!

Pressure sensitive adhesives

Base polymers

Various rubber polymers
e.g. CR, NBR, SBR, acrylates, silicone

Coating types

Solvent adhesives
Hotmelt adhesives

- Radiation crosslinking
- Electron beam crosslinking
- UV crosslinking

PSA = Pressure-Sensitive Adhesives

Source: Internet

Pressure sensitive adhesives

CertBond
COST Action CA18120

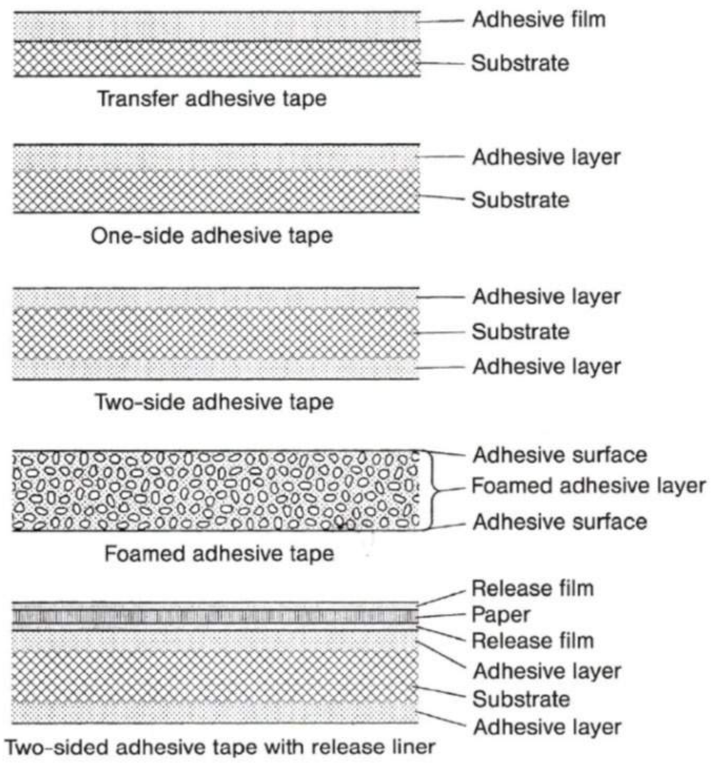

Source: Habenicht

Plastisole

Base polymers

PVC
Acrylates

Plasticiser

Tricresyl-phosphate
various phthalates

Tying

at 150 °C - 180 °C by swelling of the base polymer and accumulation of the plasticiser molecules

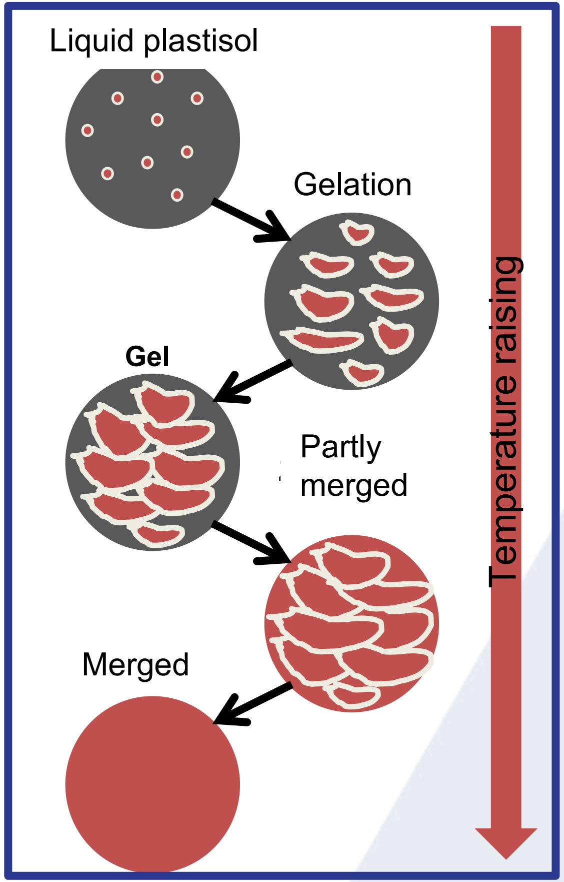

Surfaces and pre-treatment

CertBond
COST Action CA18120

cost
EUROPEAN COOPERATION IN SCIENCE & TECHNOLOGY

Funded by the Horizon 2020 Framework Programme of the European Union

Bonding – In general

- Adhesion (of polymers) is practically only determined by intermolecular binding forces.
- These binding forces (adhesion) are small compared to main valence bonds (cohesion).
- There is no general theory of adhesion.
- Adhesion must be seen as the effect of many individual interactions!

Source: Internet

Types of bonding

Major valence bonds (chemical bond)	Secondary valence bonds (intermolecular bonds)	
Homeopolar bond (covalent bond) 0,1-0,2 nm; 60-700 kJ/mol	**Van der Waals bonds** Dipole forces (Keesom-energy) 0,3-0,5 nm; 50-60 kJ/mol	**Hydrogen bonds** 0,3-0,5 nm; <50 kJ/mol
Heteropolar bond (ionic bond) 0,1-0,2 nm; 600-1000 kJ/mol	Induction forces Debye energy 0,3-0,5 nm; 2-10 kJ/mol	
Metallic bond	Dispersion forces (London energy) 0,3-0,5 nm; 5-10 kJ/mol	

Black: bindings relevant in bondings

Surface of a metal

CertBond
COST Action CA18120

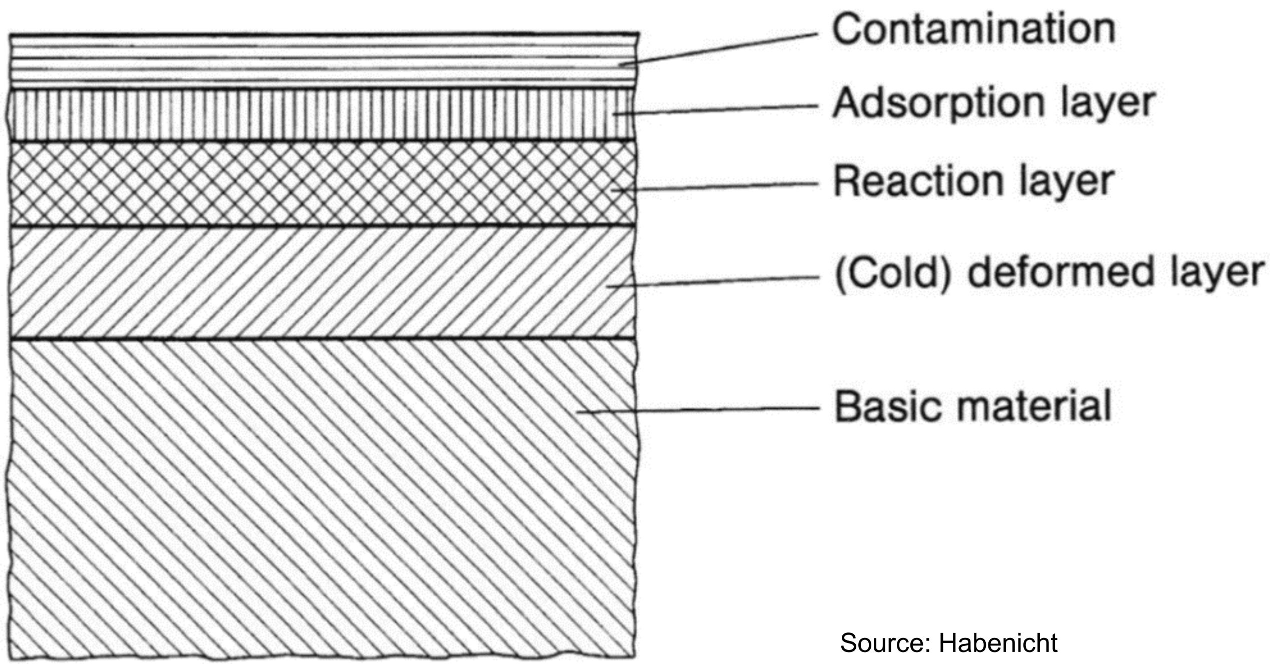

Source: Habenicht

The surface and the structure of the surface layers have a direct influence on the bondability of the materials!

Wetting

Wetting is crucial for adhesion!

Range of the forces ~ 1/10 nm

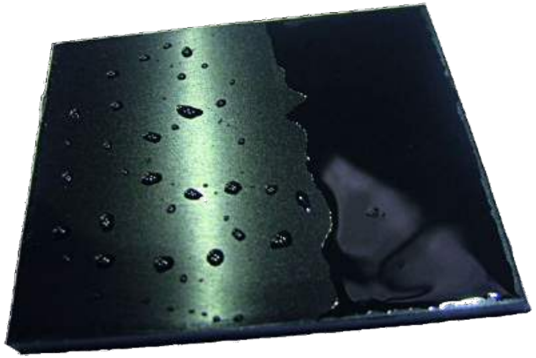

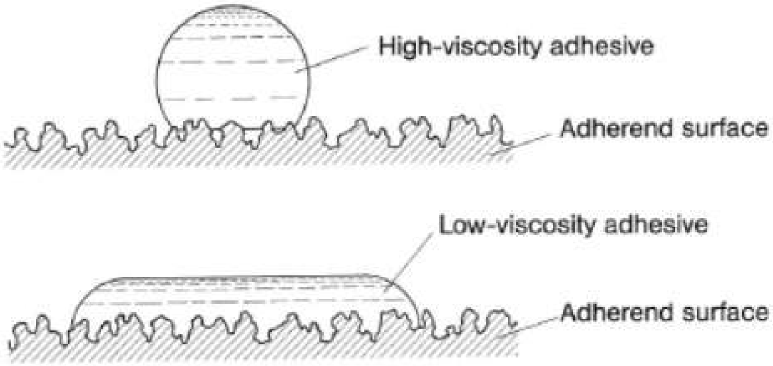

Wetting behavior of a high-viscosity and a low-viscosity adhesive.

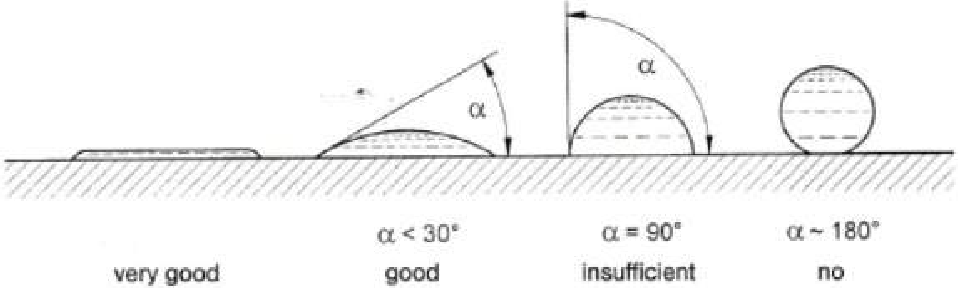

Wetting

Source: Habenicht

Young/ Dupre formula

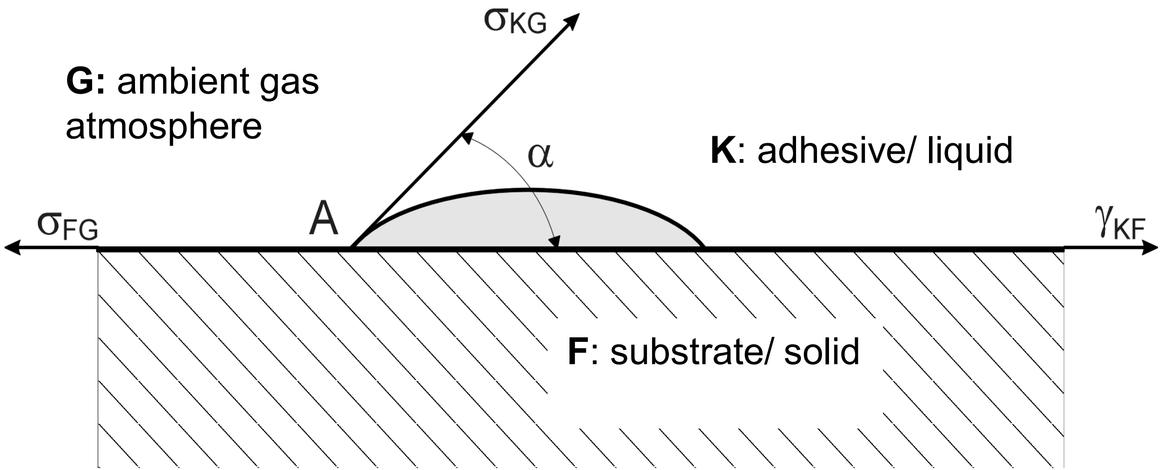

Young's equation: $\sigma_{FG} = \gamma_{KF} + \sigma_{KG} \cos \alpha$

Dupré equation: $W_a = \sigma_{KG} + \sigma_{FG} - \gamma_{KF}$

α	Wetting angle
σ_{FG}	Surface tension of the joined part
σ_{KG}	Surface tension of the liquid adhesive
γ_{KF}	Interfacial tension between the surface of the part to be joined and the liquid adhesive
W_a	Work of adhesion

Surface energy

- According to Dupré's equation, the surface energy of the parts to be joined has a direct influence on the work of adhesion:
- High surface energy of the joined part → high work of adhesion → Surface energy of the joined part should be higher than that of the adhesive

Material	Surface energy [mJm^{-2}]	Material	Surface energy [mJm^{-2}]
Polytetrafluorethylene	18,5	Water	72,8
Silicone	24	Aluminium	1200
Polypropylene	29	Lead	610
Polyethylene	31	Chromium	2400
Polyamide 6.6	46	Iron	2550
Epoxy resin	47	Gold	1550
Polyamide	49...57	Glass	290

Pre-treaments - Processes

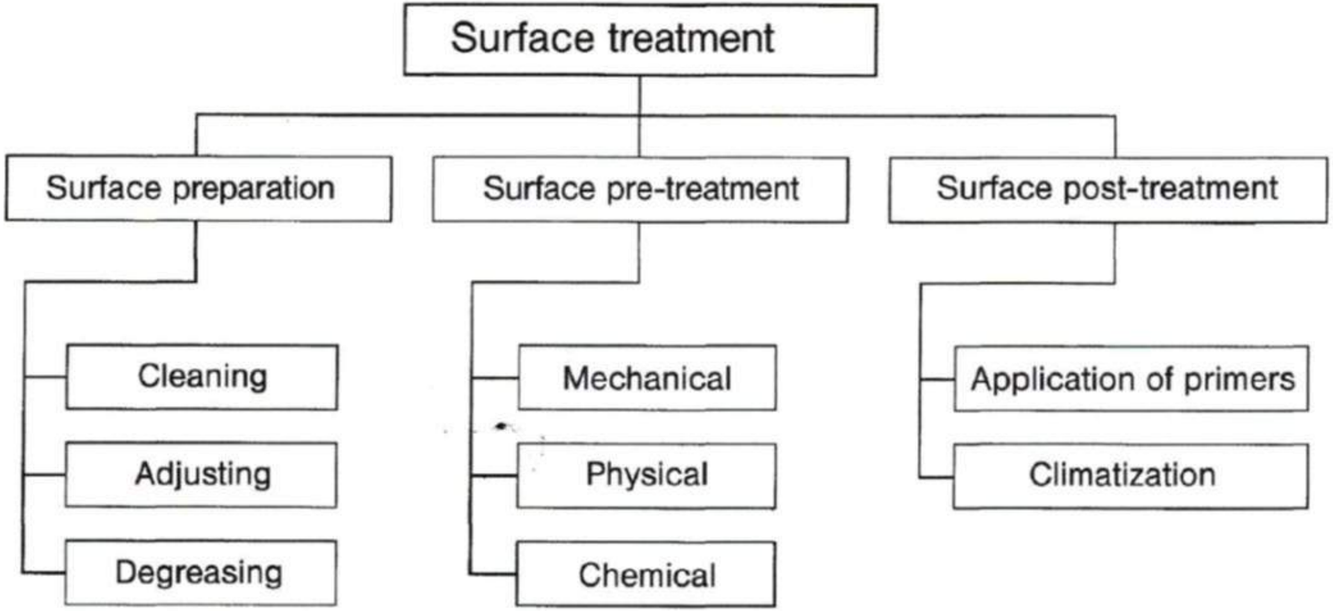

Source: Habenicht

Surface pre-treament

Tasks

- Improve adhesion (adhesion promoter)
- Increase ageing resistance
- Preserve surface condition (primer)

The surface pretreatment must provide a reproducible surface for the bonding process

Primer

Adaptation of the joining part surfaces to the adhesive matrix

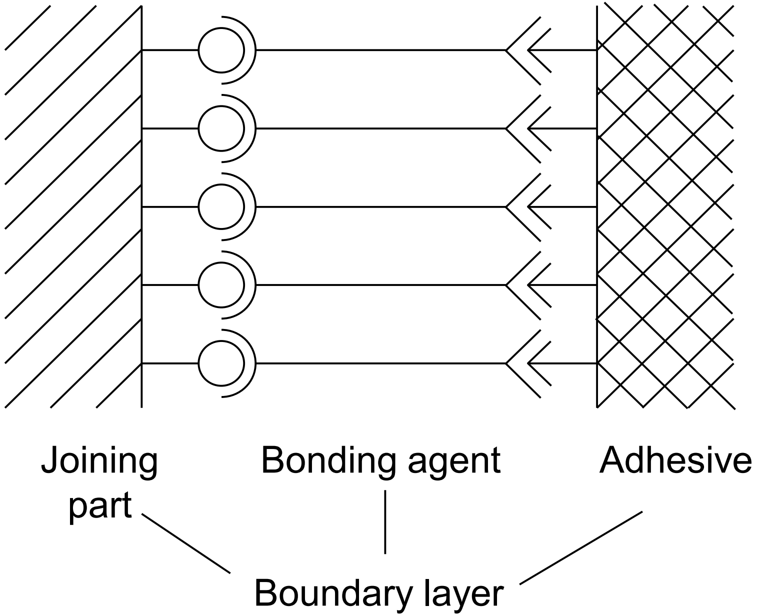

Examples:

- Silane coupling agent
- Zirconaluminate adhesion promoter
- Bonding agents based on epoxy-functional anthraquinone compounds
- Amines

Characteristic for the adhesion promoters is a bifunctionality of the molecular structure, which does not lead to any intramolecular reactions of the monomers or prepolymers.

Well done

Bondline
0.2 mm x
Ø70 mm

[DP760, pre-treatment: sand blasting]

Source: 3M
Worldrecord 2012

…but adhesives can do much better!

Literature

- Ana C. Marques et al.: Review on Adhesives and Surface Treatments for Structural Applications: Recent Developments on Sustainability and Implementation for Metal and Composite Substrates, *Materials* **2020**, *13*(24), 5590, DOI: 10.3390/ma13245590

- DIN 2304-1 (German Standard) : Adhesive bonding technology - Quality requirements for bonding processes - Part 1: Bonding process chain

- Gerd Habenicht: Applied Adhesive Bonding, WILEY-VCH 2006, ISBN 978-3-527-32014-1

Acknowledgment

This STSM was developed under the COST Action CA18120 (CERTBOND) and supported by COST (European Cooperation in Science and Technology).

Funded by the Horizon 2020 Framework Programme of the European Union

CertBond
COST Action CA18120

Thank You!

www.certbond.eu

Content of this lecture:
Lectures @
Institute of Joining and Welding
(ifs), TU Braunschweig

Pictures:
Internet, Company
Homepages, ifs

For private use only

cost
EUROPEAN COOPERATION
IN SCIENCE & TECHNOLOGY

Funded by the Horizon 2020 Framework Programme
of the European Union

Institute of Joining
and Welding

ifs

Non–destructive assessment of structural integrity and failures for lightweight materials

Issues and Challenges

Wiesław Ostachowicz

Polish Academy of Sciences, Institute of Fluid-Flow Machinery
Department of Mechanics of Intelligent Structures
Gdańsk, Poland

CertBond
COST Action CA18120

EUROPEAN COOPERATION IN SCIENCE & TECHNOLOGY

Funded by the Horizon 2020 Framework Programme of the European Union

Outline

- INTRODUCTION
- MOTIVATION AND RESEARCH OBJECTIVES
- INSPECTIONS OF COMPOSITE STRUCTURES
  - NDT/SHM methods for surface assessment
  - NDT/SHM methods for structural joints
  - NDT/SHM methods for damage detection
- CONCLUSIONS

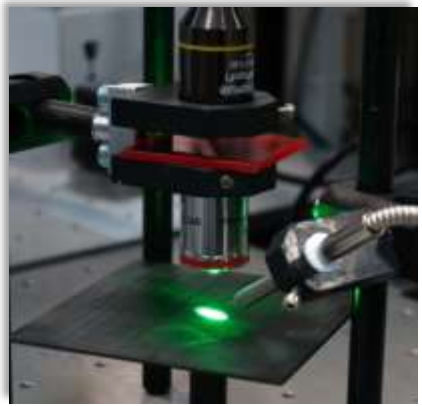

Motivation

- Composite materials are increasingly used in aviation construction.
- Boeing 787 and Airbus A350XWB – carbon composites pose over 50%.
- Aircraft still use significant amounts of rivets, even for fuselages made of composite materials.
- Airbus A380 - 3 mln rivets (merely in wings 1,5 mln).
- Eiffle Tower - 2,5 mln rivets.
- Composite patches are becoming more and more common.
- Effective surface assessment methods are needed, for assessment of adhesive bonds and fault detection.

Sources:
http://www.hexcel.com/solutions/aerospace/
http://www.corrosion-doctors.org/Landmarks/Eiffel.htm
http://www.answers.com/Q/How_many_rivets_in_an_airbus_a380_aircrafts
http://www.theguardian.com/business/2006/feb/23/theairlineindustry.travelnews
http://www.amrdec.army.mil/amrdec/pif/composites.html

Motivation

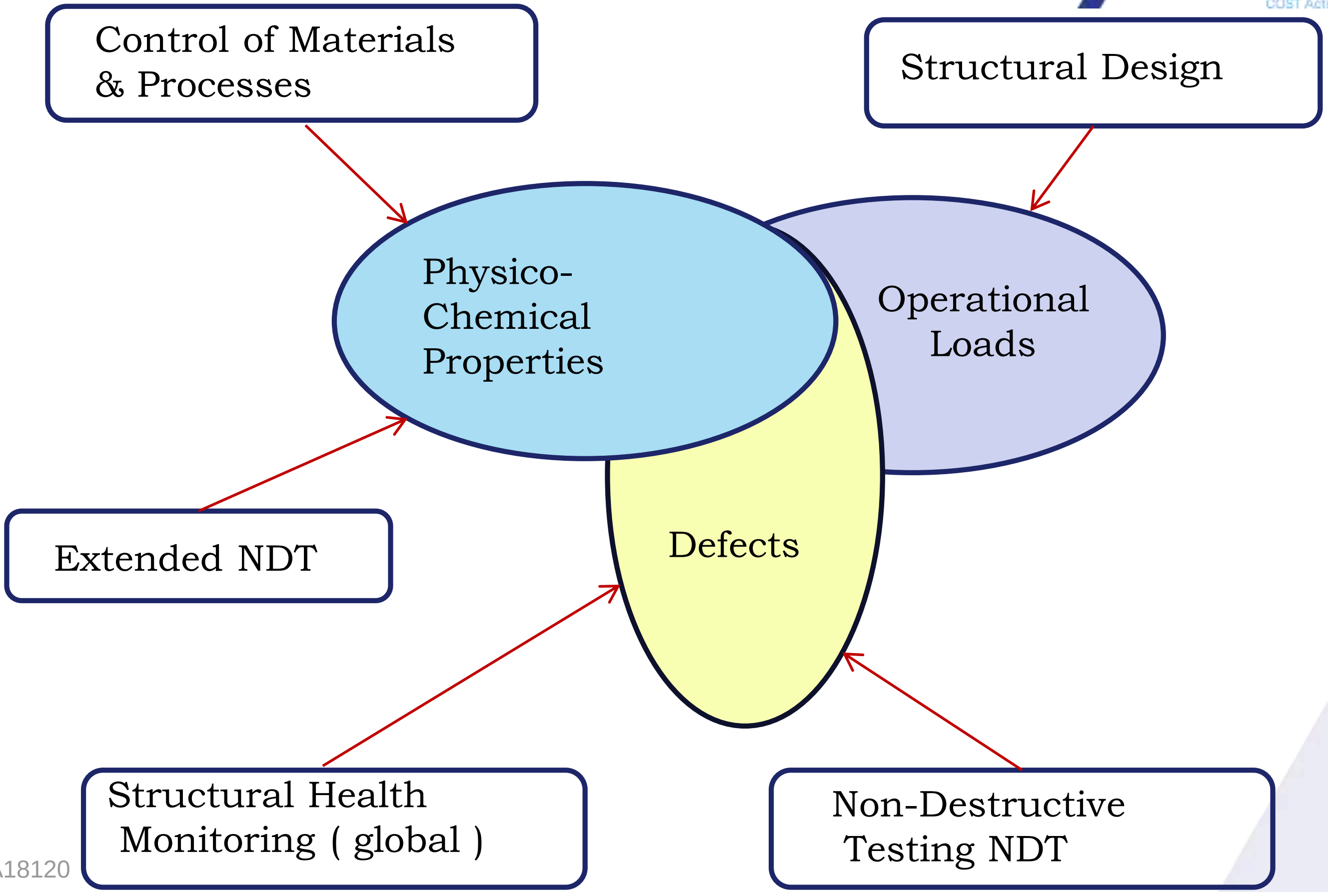
Control of Materials & Processes
Structural Design
Physico-Chemical Properties
Operational Loads
Extended NDT
Defects
Structural Health Monitoring (global)
Non-Destructive Testing NDT

Research Objectives

- Evaluation of surface condition before bonding
- Evaluation of the bonded joint condition
- Damage detection

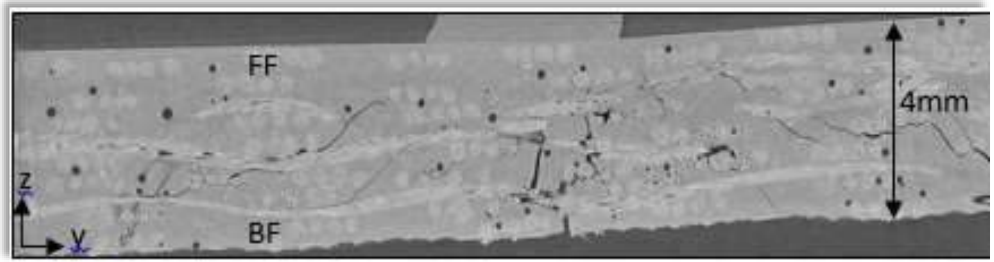

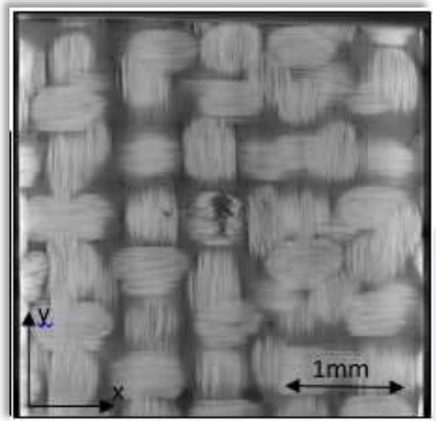

Sources:
P. Malinowski *et al. Composite bonds assessment using EMI technique.* Proceedings of 9th IWSHM, Sep. 10-12, 2013, Stanford, California, USA.
P. Malinowski *et al., Assessment of damage in `green` composites.* Proceedings of SPIE 2017

Investigated Cases

- Study of the surface of polymer reinforced carbon fibres samples (CFRP)

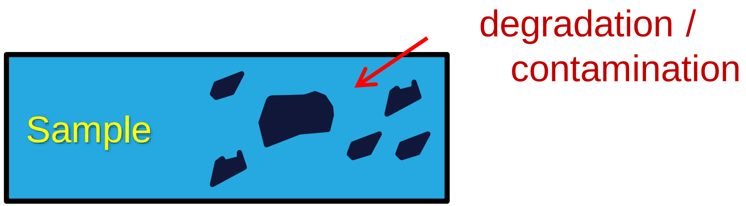

- Investigations of condition for CFRP bonds

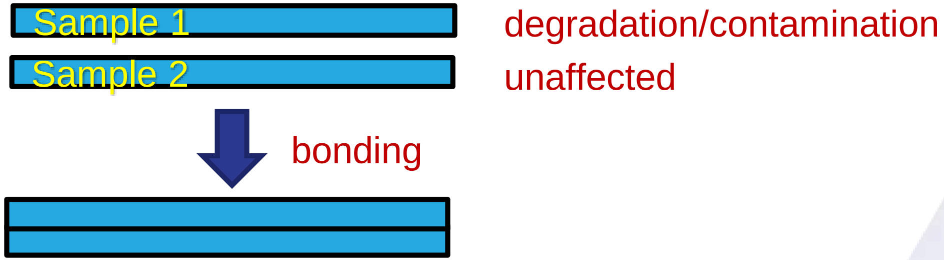

- Delaminations, cracks

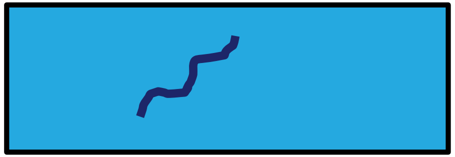

Motovation

CertBond
COST Action CA18120

Adhesive bond quality	METHOD
	Active thermography using ultrasonic excitation
	THz / GHz reflectometry
	Nonlinear ultrasound
	LASAT technique
	Laser ultrasound
	Active thermography using optical excitation
	Laser scanning vibrometry
	Electromechanical impedance
	Vibrothermography
	Ultrasonic frequency analysis
	Active thermography (for Tg analysis)

ENCOMB | 7th Framework Programme | *Extended Non-Destructive Testing of Composite Bonds*

Adherend surface quality	METHOD
	X-ray fluorescence spectroscopy
	Reflectometry/Ellipsometry
	Infrared Spectroscopy
	Laser scanning vibrometry
	Optically stimulated electron emission
	Active thermography (for Tg analysis)
	Aerosol wetting test
	Laser induced breakdown spectroscopy
	THz / GHz reflectometry
	Optical fibre sensors
	Electrochemical impedance spectroscopy
	Electromechanical impedance
	Dual-band active thermography
	Vibrothermography
	THz technology
	Optical coherence tomography
	Nuclear magnetic resonance
	Electronic nose technology

General Overview on SHM and NDT methods

Most common NDT methods
Ultrasonic inspection
Dye penetration test
Laser excited ultrasounds
X-ray radioscopy
Strain gauges
Other ……………………..

Most common Extended NDT methods
Electromechanical impedance [EMI]
Active thermography using optical excitation
Active thermography using ultrasound excitation
Laser Doppler vibrometer
THz technology
Other ……………………..

Most common SHM methods
Vibration based methods
Guided wave methods
Fiber optics techniques
Acoustic emission
Comparative vacuum monitoring
Electromagnetic layer
Other ……………………..

General Problems | Areas of Interest

General Problems
Sensors (type, …..)
Location of sensors
Implementations
Measurements
Modelling of structures
Signal processing
Visualization
Other ……………………

Areas of Interest
Sensors
Models
Signal processing
Temperature
Damping
Moisture
Chemical contamination
Nonlinear properties
Other …………………

Investigated Methods

CertBond
COST Action CA18120

Electromechanical Impedance

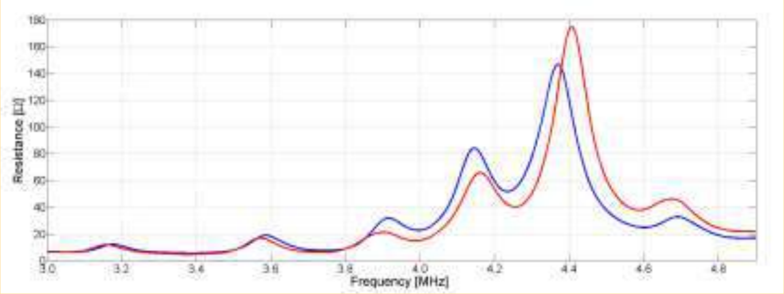

Frequency range: 4 Hz – 5 MHz

Laser Fluorescence

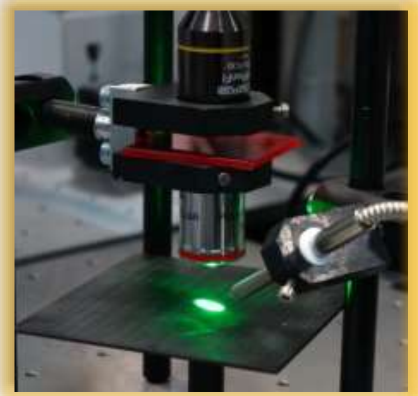

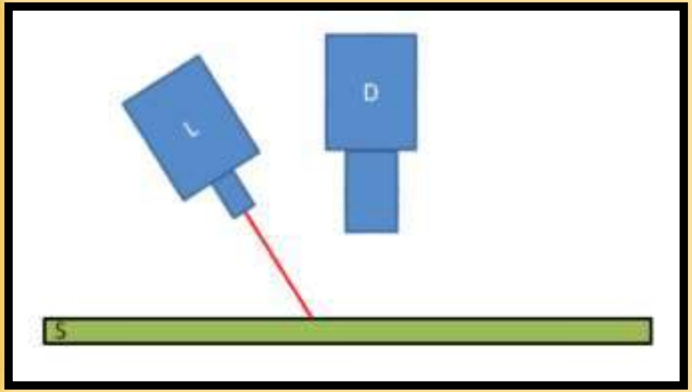

Laboratory: Institute of Fluid-Flow Machinery, PAS, Gdansk, Poland

Investigated Methods

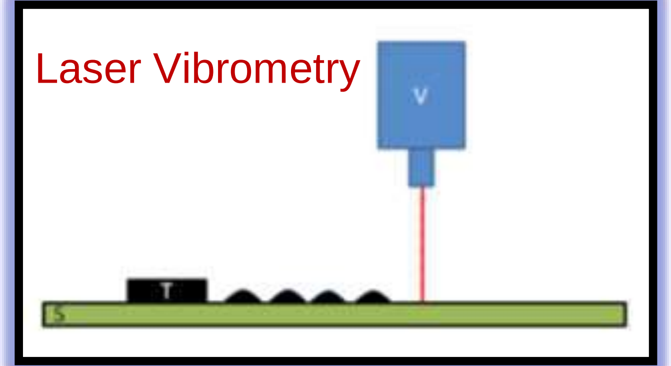

Laboratory: Institute of Fluid-Flow Machinery, PAS, Gdansk, Poland

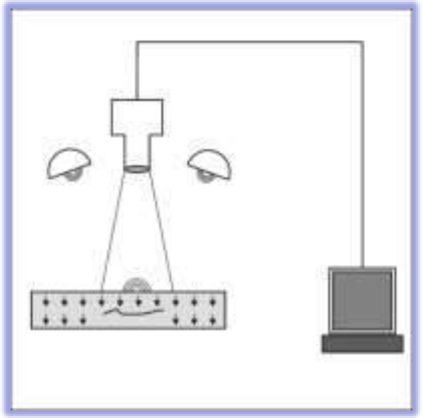

Investigated Methods

Terahertz spectroscopy

THz

γ-rays X-rays UV visible lt. IR Microwave Radio

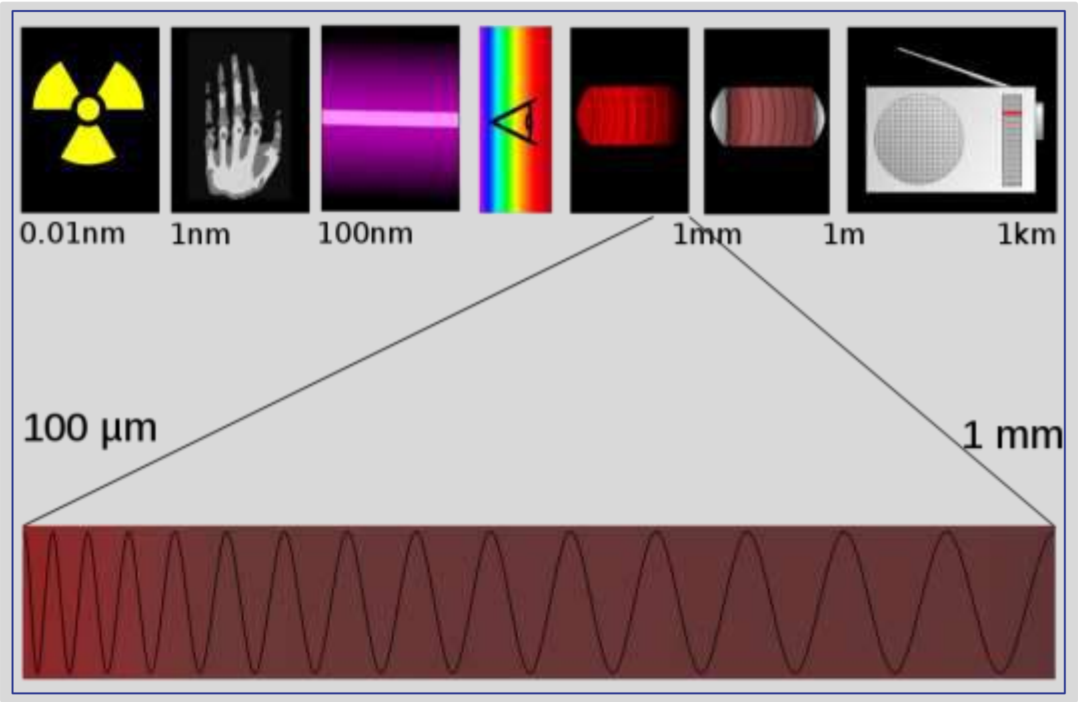

Teraview THz time domain spectrometer

Gantry unit for large sample scanning

Frequency range:
~0.1 – 4 THz

Transmission mode

Reflection mode

Source: http://en.wikipedia.org/wiki/File:Spectre_Terahertz.svg

THz Laboratory

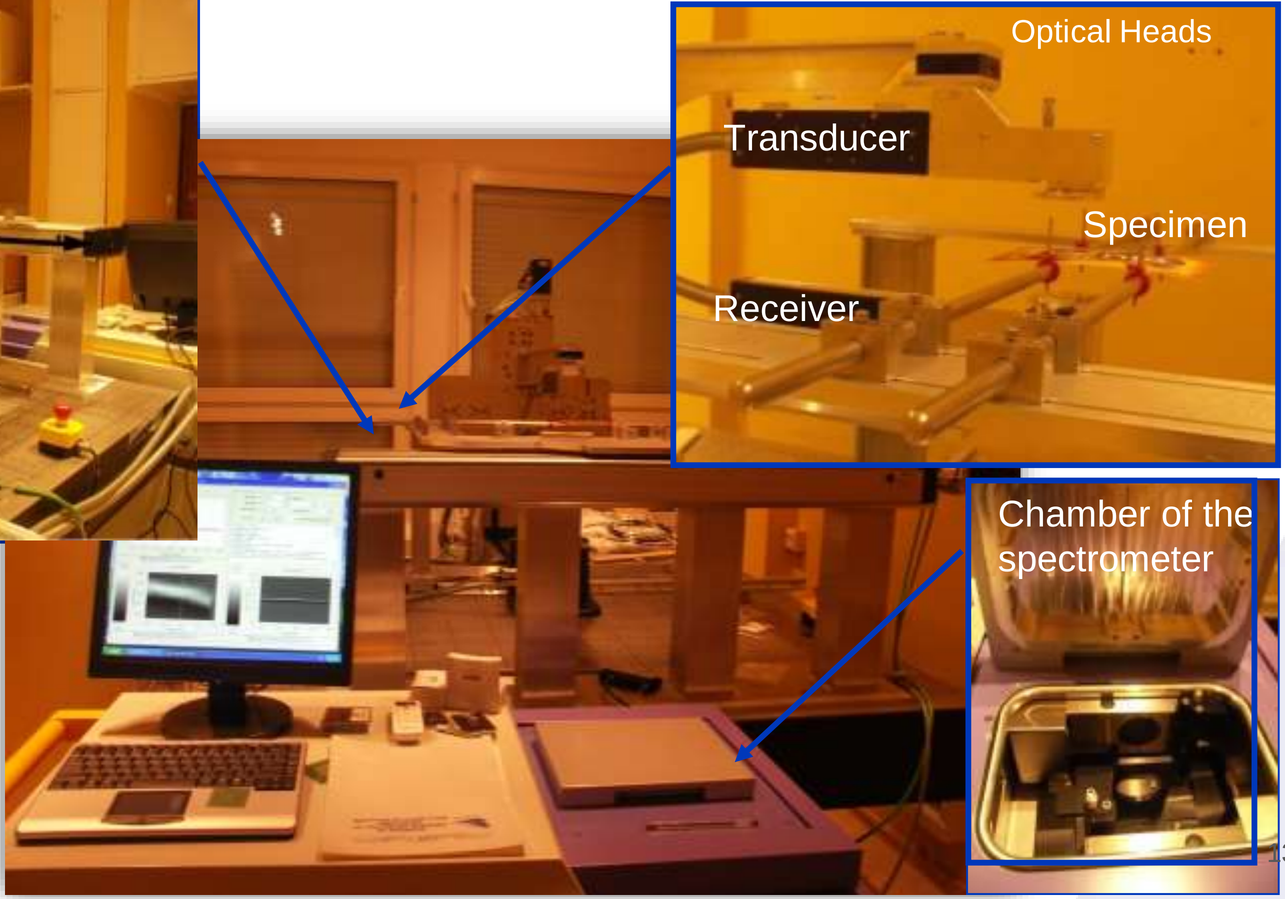

Laboratory: Institute of Fluid-Flow Machinery, PAS, Gdansk, Poland

CertBond
COST Action CA18120

INSPECTION OF COMPOSITE STRUCTURES

NDT/SHM Methods for Surface Assessment

cost
EUROPEAN COOPERATION IN SCIENCE & TECHNOLOGY

Funded by the Horizon 2020 Framework Programme of the European Union

EMI Method for Moisture Detection

CertBond
COST Action CA18120

Electro-mechanical impedance technique

Laboratory: Institute of Fluid-Flow Machinery, PAS, Gdansk, Poland

HIOKI IM3570 – Impedance Analyzer

- Frequency range: 4 Hz – 5 MHz
- Frequency accuracy : ± 0.01 %
- Voltage:
  - 5 mV - 5 V up to 1 MHz
  - 10 mV - 1 V up to 5 MHz
- Impedance range: 0 – 1 GΩ

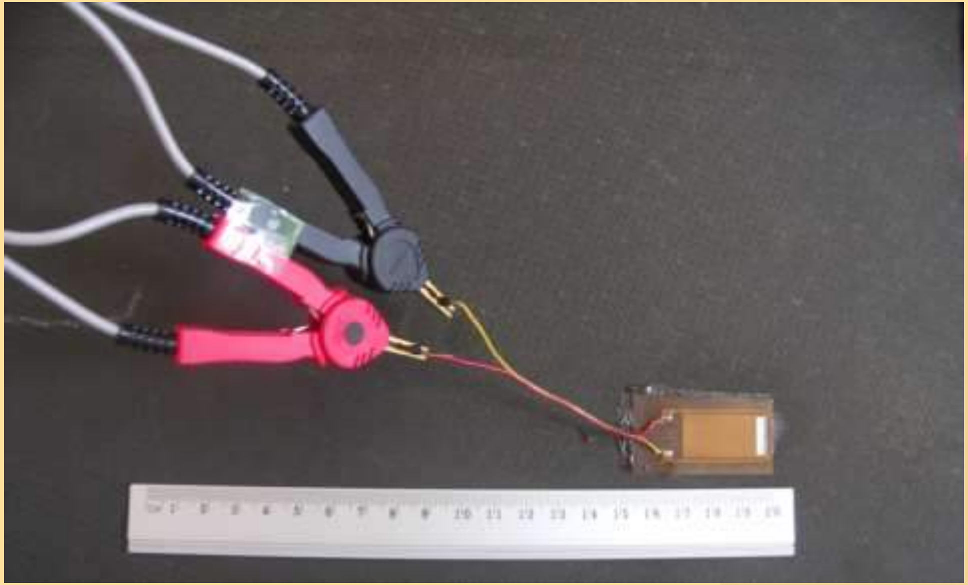

EMI Method for Moisture Detection

Electro-mechanical impedance technique

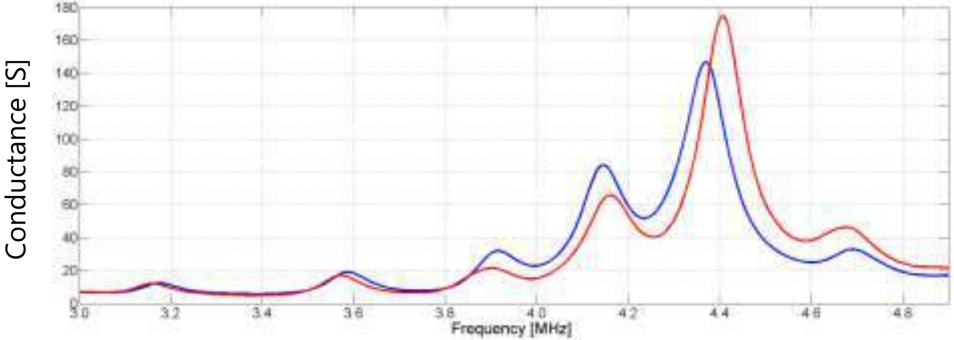

Registered response – impedance spectrum

Root Mean Square Deviation was chosen to quantitatively assess the samples

$$RMSD_{\%} = \sqrt{\frac{\sum_i (y_i - x_i)^2}{\sum_i x_i^2}} \times 100$$

x – conductance for reference sample measurement

y – conductance for tested sample measurement

Electrical impedance of a piezoelectric sensor is measured. Due to mechanical coupling the electrical response contains information about mechanical vibration of the structure.

Laboratory: Institute of Fluid-Flow Machinery, PAS, Gdansk, Poland

EMI Method for Moisture Detection

- Carbon Fiber sample from Augusta Westland AW-139 helicopter
- made out of 3 carbon-epoxy pre-pregs [-45^0/45^0/0^0] + of one layer 0.14 mm for surface quality improvement
- total thickness 1.5 mm
- piezoelectric CERAMTEC transducer made out of Sonox P502 (diameter 10mm) attached and covered by silicone

CFRP sample

Attached piezoelectric transducer isolated by silicone layer

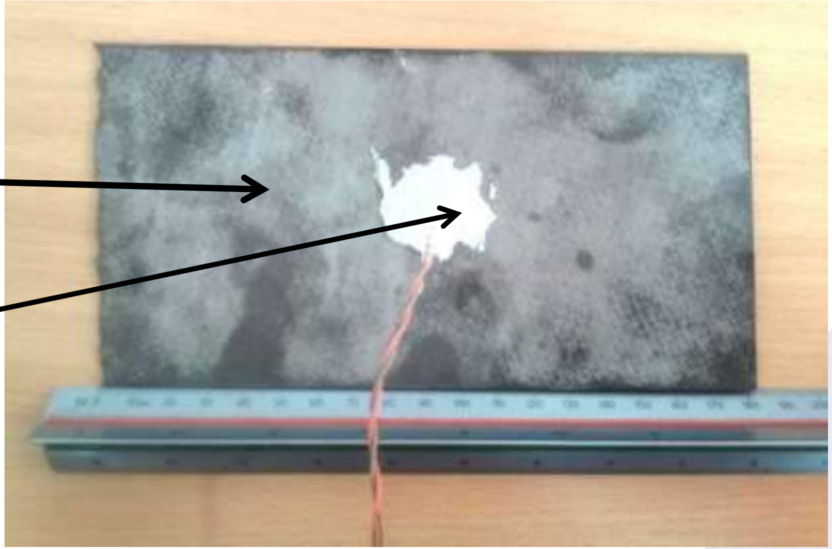

Sample has been immersed in water

Source: T. Wandowski, P. Malinowski, L. Skarbek, W. Ostachowicz, *Moisture detection in carbon fiber reinforced polymer composites using electromechanical impedance technique*, Proceedings of the Institution of Mechanical Engineers, Part C: Journal of Mechanical Engineering Science 230: 331-336, 2016.

EMI Method for Moisture Detection

CertBond
COST Action CA18120

Absorption after thirteen days

Mass of CFRP sample with moisture	
Mass [g]	Weight increase [%]
36.74	2.72

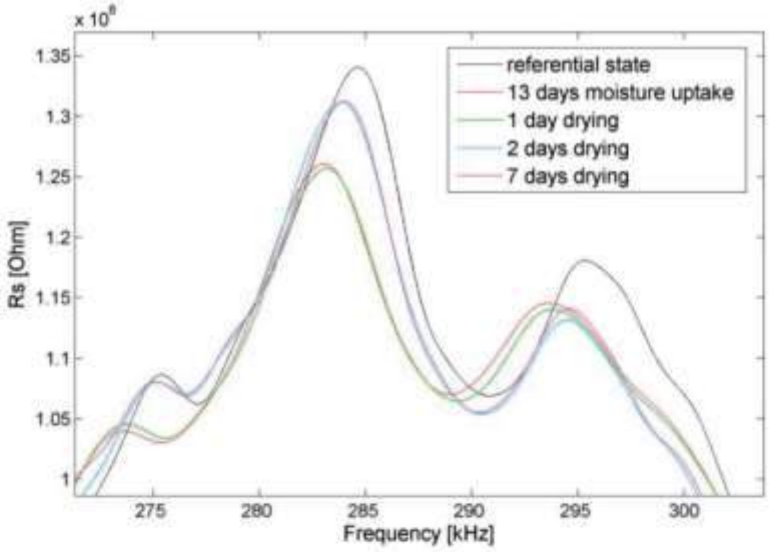

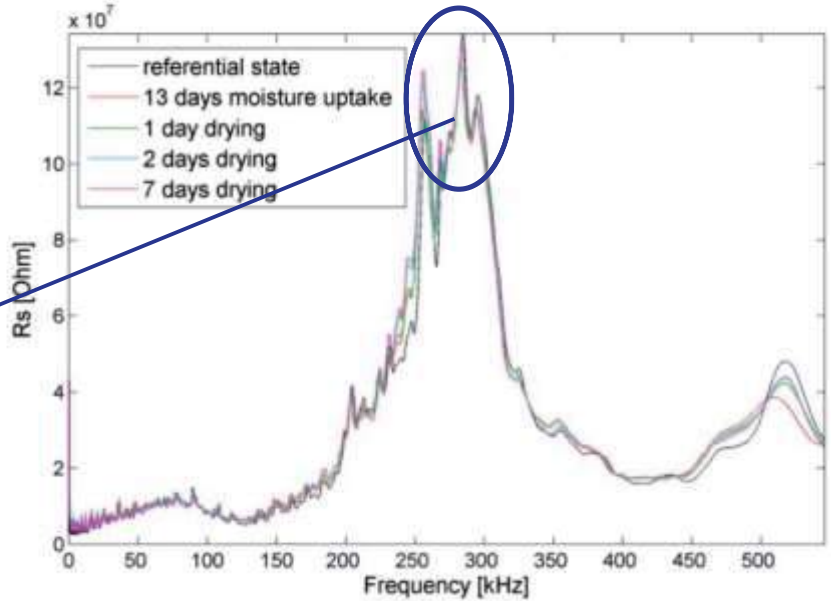

There are some changes in the spectra barely visible in this wide frequency range.
The closer look reveals the frequency shift to the left and amplitude drop due to moisture.

Source: T. Wandowski, P. Malinowski, L. Skarbek, W. Ostachowicz, *Moisture detection in carbon fiber reinforced polymer composites using electromechanical impedance technique*, Proceedings of the Institution of Mechanical Engineers, Part C: Journal of Mechanical Engineering Science 230: 331-336, 2016.

EMI Method for Moisture Detection

CertBond
COST Action CA18120

Deviation Index for drying process monitoring

$$DI = \sum \left| \frac{R_W(i) - R_D(i)}{R_D(i)} \right|$$

R_W – i-th sample of resistance for wet sample

R_D – i-th sample of resistance for dry sample

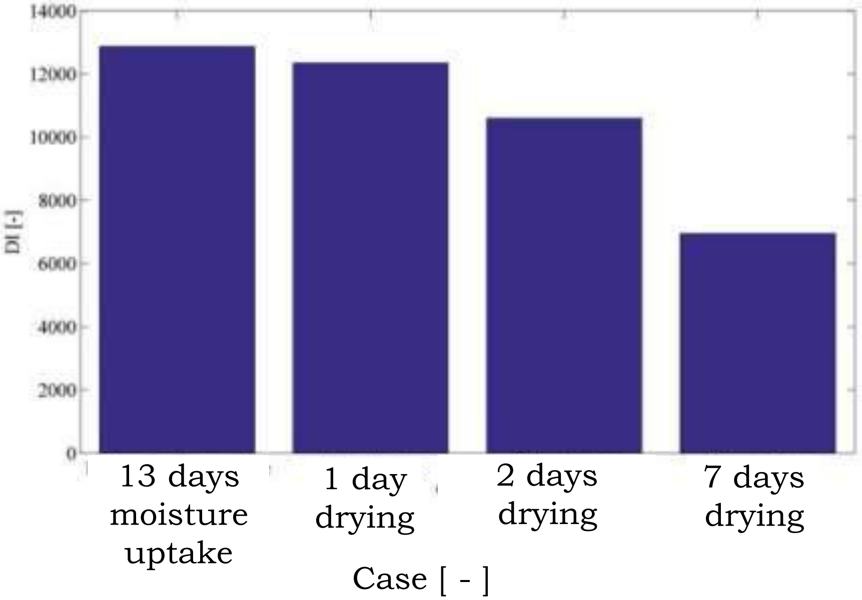

Source: T. Wandowski, P. Malinowski, L. Skarbek, W. Ostachowicz, *Moisture detection in carbon fiber reinforced polymer composites using electromechanical impedance technique*, Proceedings of the Institution of Mechanical Engineers, Part C: Journal of Mechanical Engineering Science 230: 331-336, 2016.

Moisture, initial stresses, thermal, icing, …

EMI – Electromechanical Impedance Results

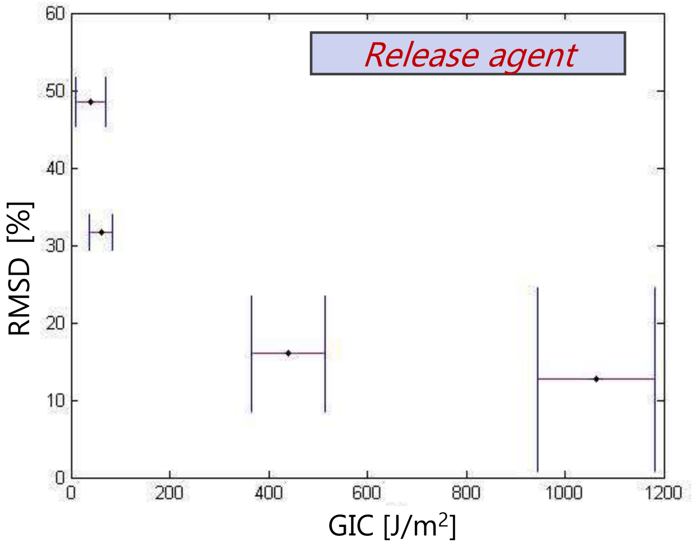

Sample	G_{IC} [J/m²]	RMSD
Reference	1072.72	0.00 %
2.1 at% of Si	1062.75	12.66 %
6.5 at% of Si	439.2	15.99 %
8.2 at% of Si	60.8	31.67 %
10.1 at% of Si	40.4	48.48 %

Source: P. Malinowski, K.I. Tserpes, T. Wandowski, L. Skarbek, W. Ostachowicz, *Composite Bonds Assessment using EMI Technique*, Proc. of. IWSHM 2013.

Moisture, initial stresses, thermal, icing, …

EMI – Electromechanical Impedance Results

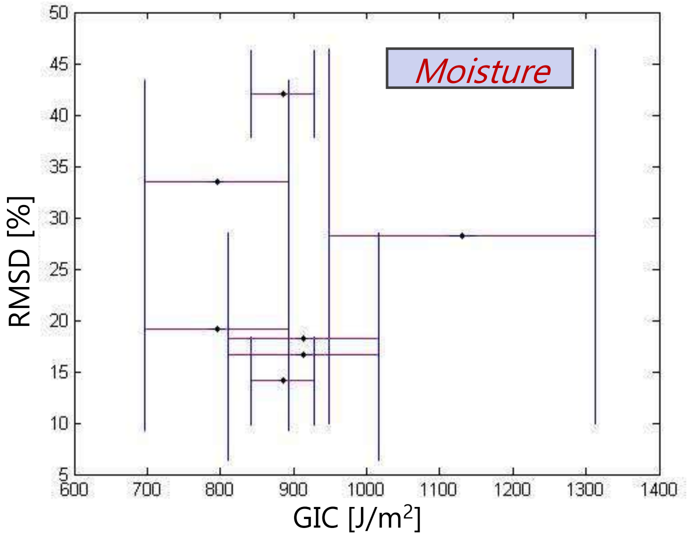

Sample	G_{IC} [J/m²]	RMSD
0.45 WT%	1129.95	-
0.45 WT%	1129.95	28.17 %
0.80 WT%	914.44	16.68 %
0.80 WT%	914.44	18.24 %
1.13 WT%	795.31	19.14 %
1.13 WT%	795.31	33.46 %
1.25 WT%	885.17	14.08 %
1.25 WT%	885.17	42.06 %

Source: P. Malinowski, K.I. Tserpes, T. Wandowski, L. Skarbek, W. Ostachowicz, *Composite Bonds Assessment using EMI Technique*, Proc. of. IWSHM 2013.

Terahertz method

Teraview THz time domain spectrometer

Gantry unit for large sample scanning.

Frequency range: ~0.1 – 4 THz.

Transmission mode.

Reflection mode.

Example of registered signal

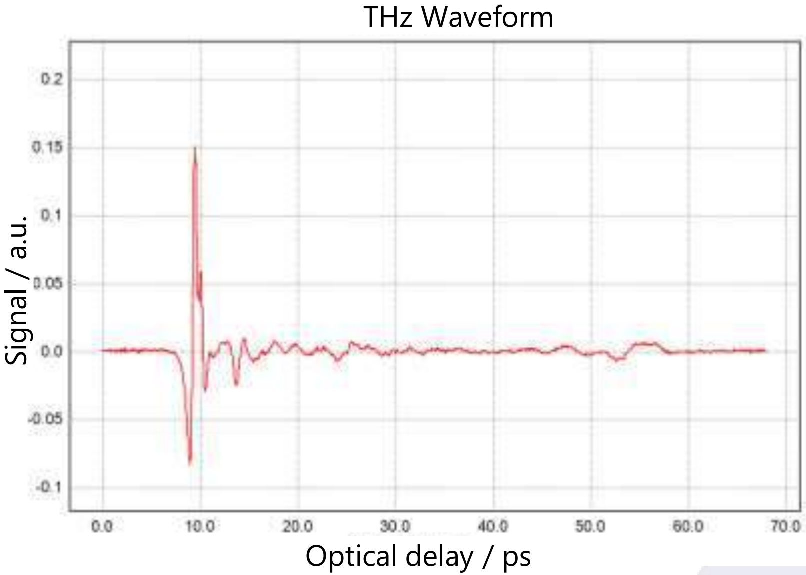

Laboratory: Institute of Fluid-Flow Machinery, PAS, Gdansk, Poland

Terahertz Applications

Teflon insert
in GFRP

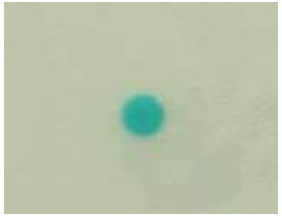

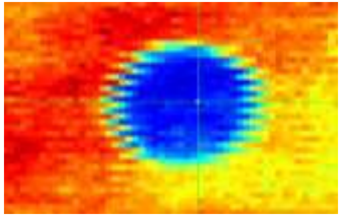

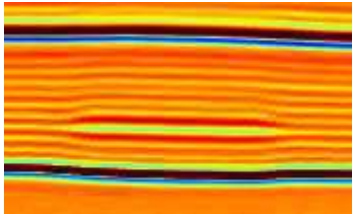

Impact
in GFRP

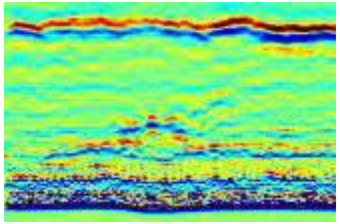

Delamination
in GFRP

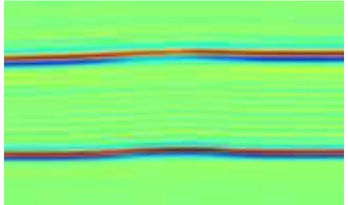

Moisture on CFRP

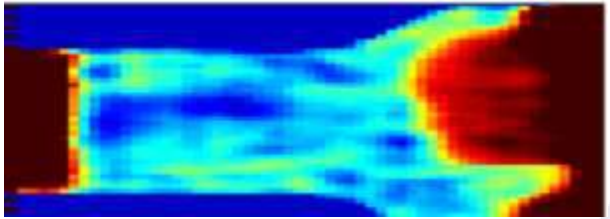

Electronic component
- transistor

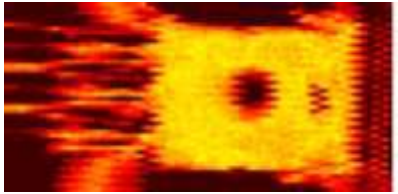

Terahertz Method for Moisture Detection

Transmission measurement

Surface water contamination (100-300 µm)

Amplitude dropped twice due to water

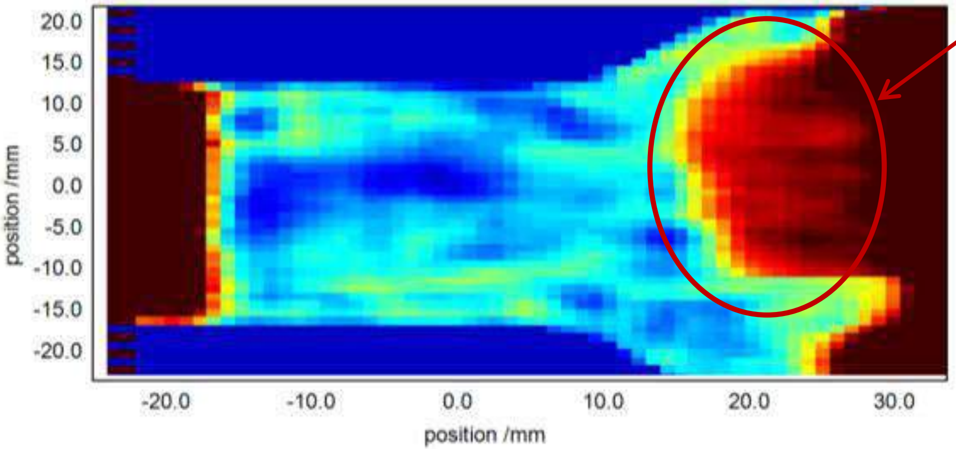

Source: P. Malinowski, N. Palka, S. Opoka, T. Wandowski, W. Ostachowicz, *Moisture detection in composites by terahertz spectroscopy*, Proceedings of DAMAS 2015 Conference.

THz Spectroscopy – Thermal Degradation of GFRP

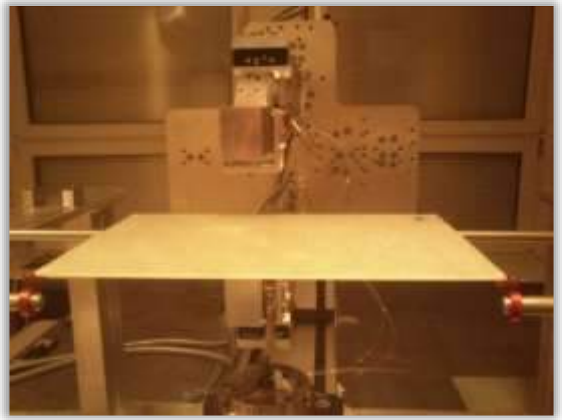

Heating of samples

State	T[°C]	t[h]
1	100	1
2	100	20
3	100	24
4	100	68
5	120	22
6	140	22
7	160	22
8	180	1

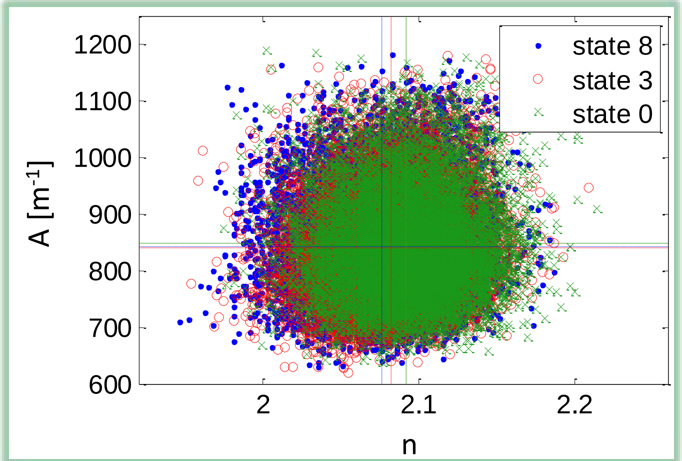

Changes in refractive index (n) and absorption (A) for the selected heating steps

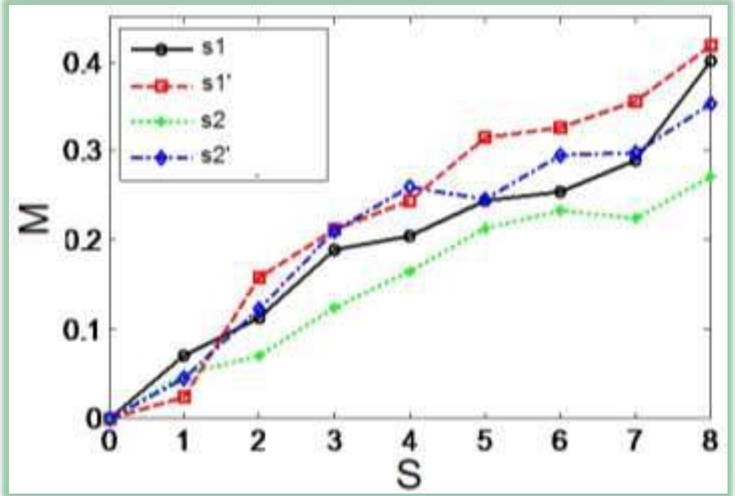

Mahalanobis distance between the reference state and a further step of heating (for two samples s-1 and s-2)

Source: M. Radzieński, M. Mieloszyk, E.K. Rahani, T. Kundu, W. Ostachowicz, *Heat induced damage detection in composite materials by terahertz radiation*, Proceedings of SPIE 2015 Conference.

Damage Detection Using – THz Technique

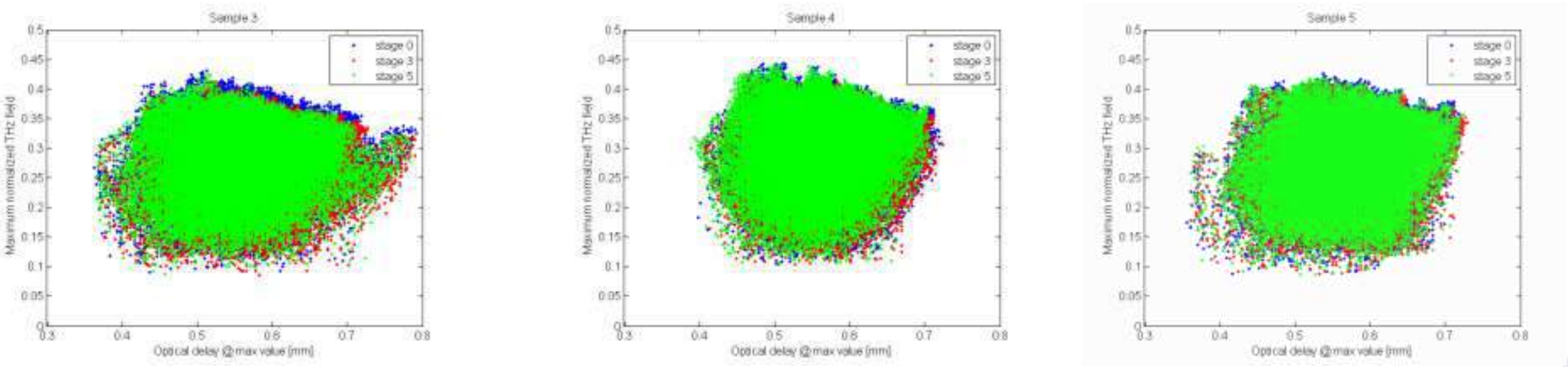

Normalized peak values and the time of arrival of the peak (referred as optical delay) are plotted along the two axes. Three colors are used to plot the points that correspond to three states or stages of heating – 0, 3 and 5. Three plots correspond to three samples – 3, 4 and 5.

Source: M. Radzieński, M. Mieloszyk, E.K. Rahani, T. Kundu, W. Ostachowicz, *Heat induced damage detection in composite materials by terahertz radiation*, Proceedings of SPIE 2015 Conference.

Damage Detection Using – THz Technique

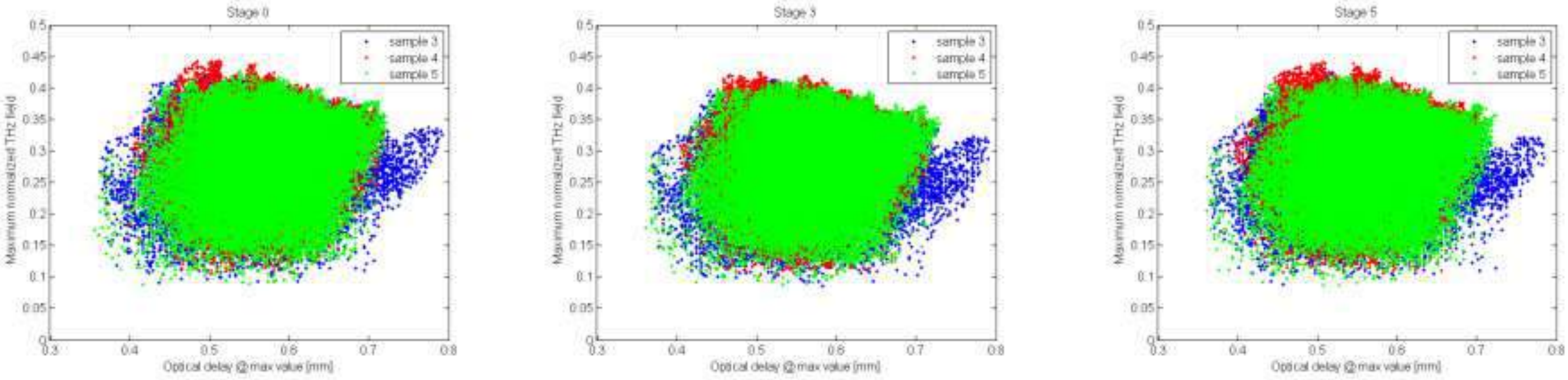

Normalized peak values and the time of arrival of the peak (referred as optical delay) are plotted along the two axes. Three colors are used to plot the points that correspond to three samples – 3, 4 and 5. Three plots correspond to three states or stages of heating – 0, 3 and 5.

Source: M. Radzieński, M. Mieloszyk, E.K. Rahani, T. Kundu, W. Ostachowicz, *Heat induced damage detection in composite materials by terahertz radiation*, Proceedings of SPIE 2015 Conference.

Damage Detection Using – THz Technique

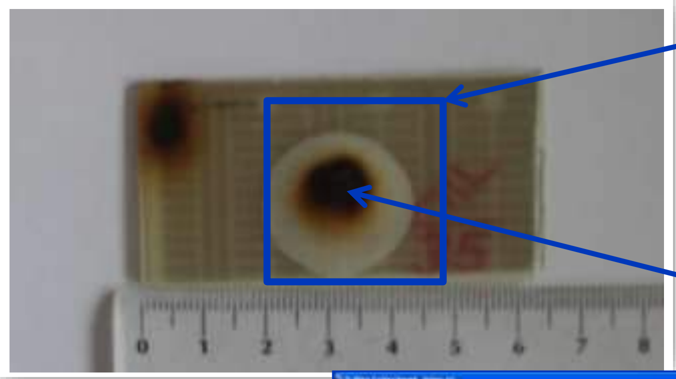

Scan area

Thermal delamination

Specimen – laminate FR4 (reinforced by glass fibres) with thermal delamination

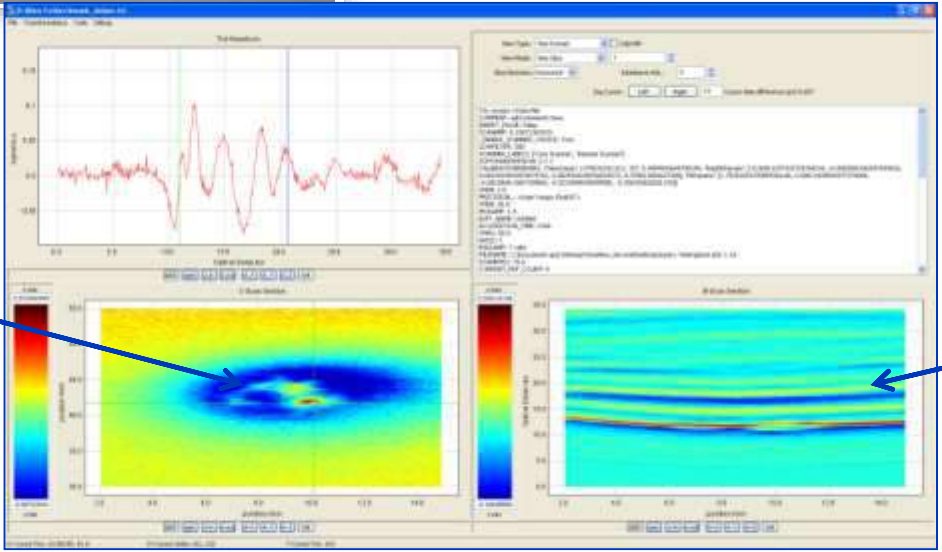

Thermal delamination

View to composite layers and debondings

Laboratory: Institute of Fluid-Flow Machinery, PAS, Gdansk, Poland

Damage Detection Using – THz Technique

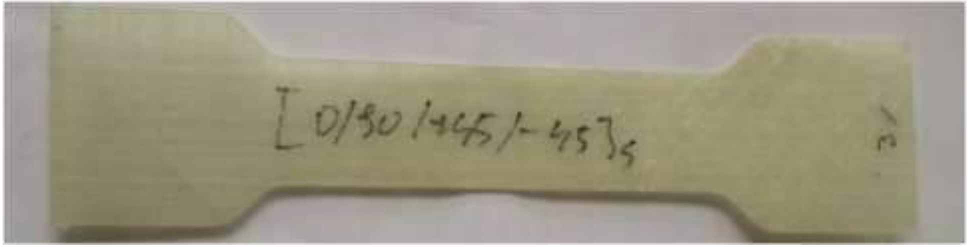

Photograph of one of the 3 specimens tested

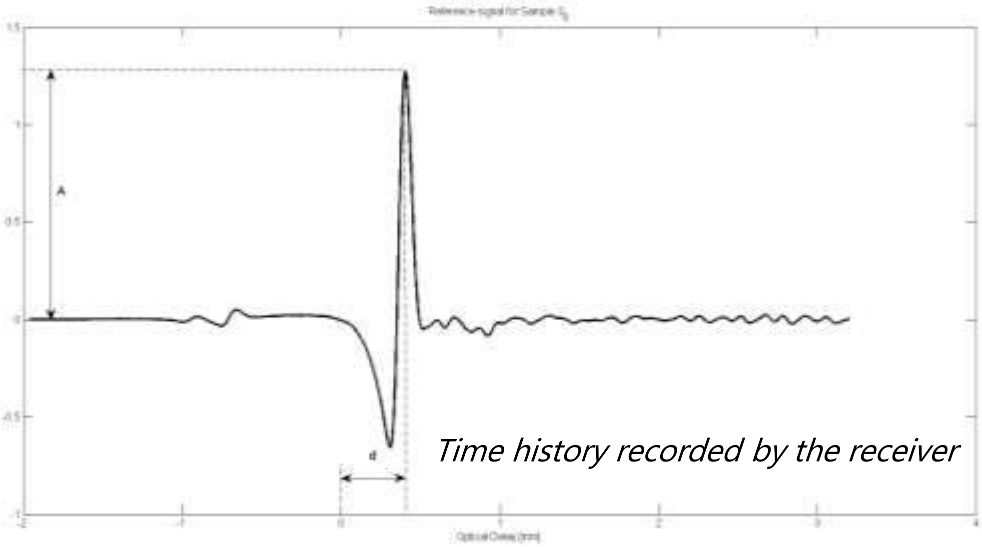

Time history recorded by the receiver

Photograph showing the specimen mounted on the THz machine

Laboratory: Institute of Fluid-Flow Machinery, PAS, Gdansk, Poland

Damage Detection Using – THz Technique

Specimens at states 0, 1 and 2 (varying from left to right in the top photo) and at states 0 and 4 (varying from left to right in the bottom photo).
Note the color changes due to heating.

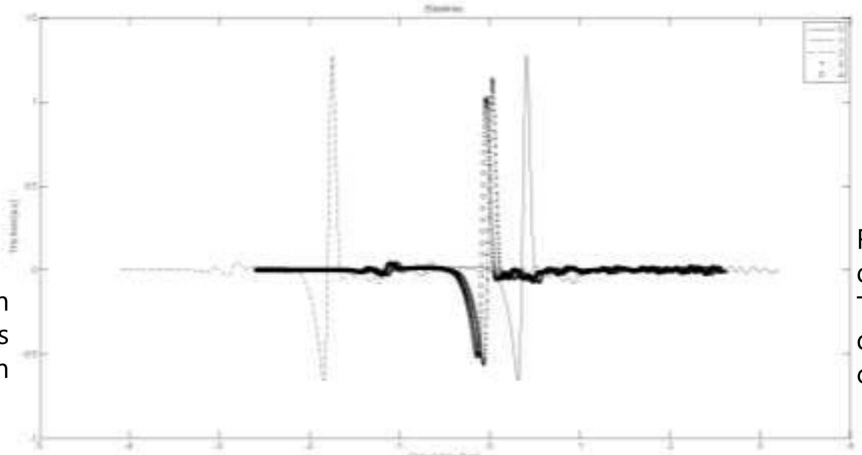

Reference signals recorded at different times – for all these signals T-ray passes through air. These differences are due to machine calibration problem.

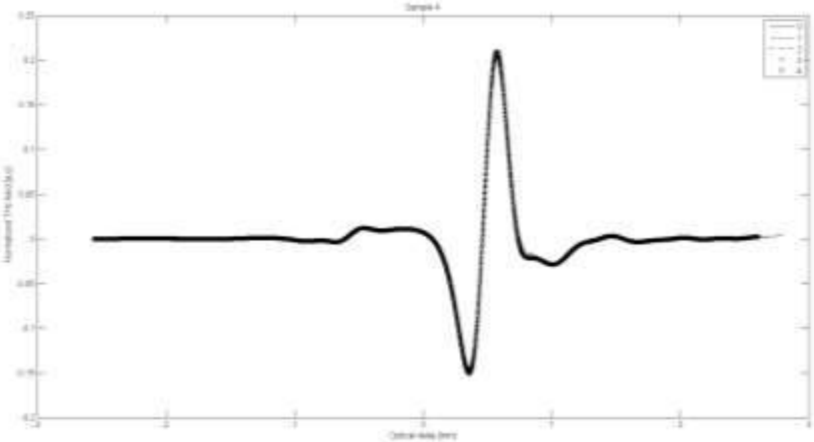

Five different signals are transformed into one signal after appropriate time shift and multiplication by the scaling factors.

Laboratory: Institute of Fluid-Flow Machinery, PAS, Gdansk, Poland

Investigated Methods

Laser Fluorescence

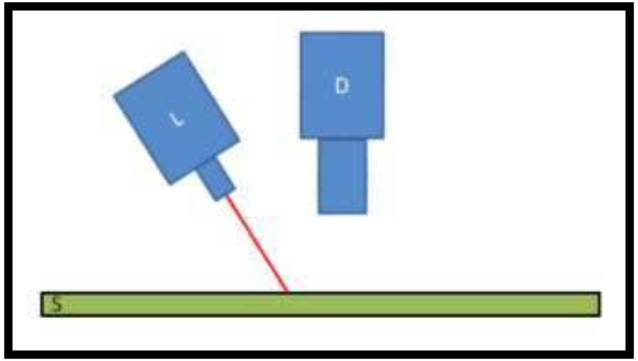

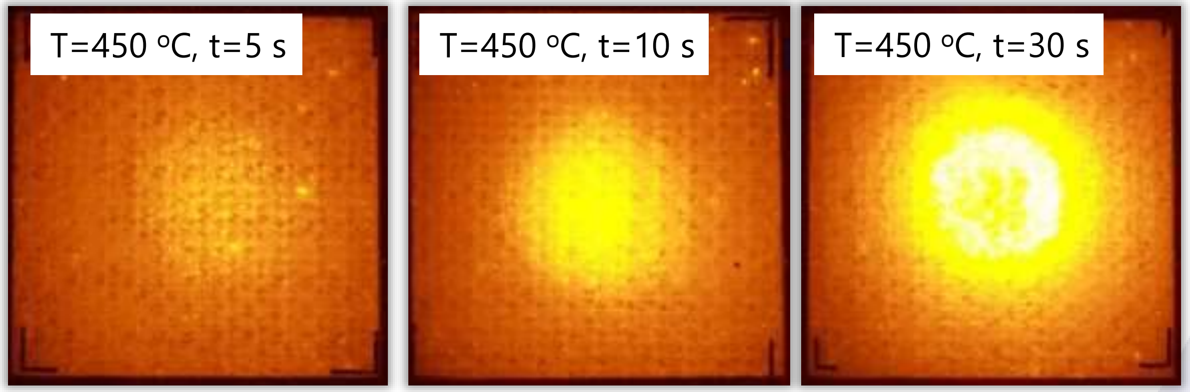

Distributions of fluorescence intensity at different times of exposure to high temperatures

Source: P. Malinowski, M. Sawczak, T. Wandowski, M. Radzieński, W. Ostachowicz, *Composites Surface State Assessment by LIF Method , Proc. 7th International Symposium on NDT in Aerospace 2015.*

Laser Induced Fluorescence Method – Thermal Degradation of Composite Materials

Distributions of fluorescence intensity at different times of exposure to high temperatures

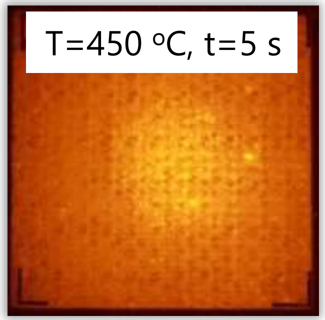

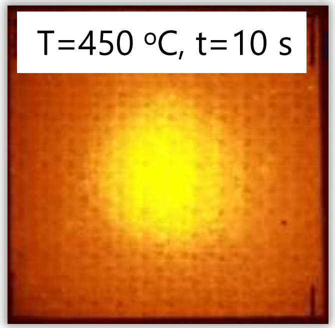

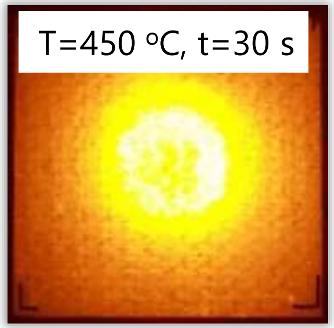

Integral of area bellow the intensity curve

Intensity of fluorescence vs. the time of exposure (amplitude for 585 nm)

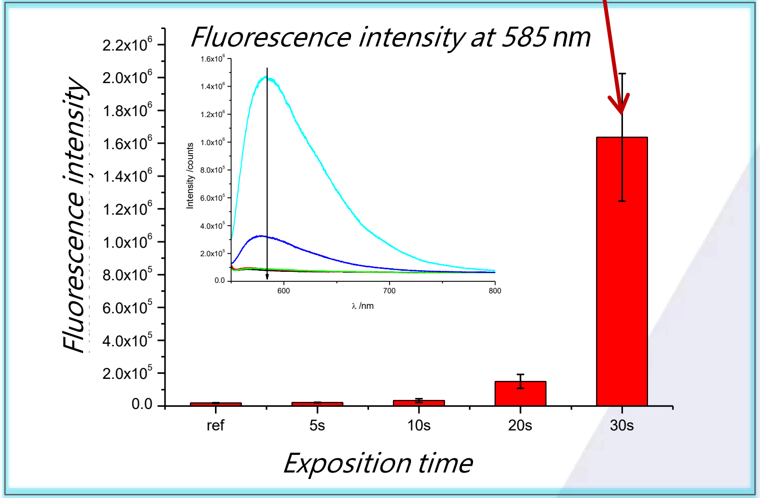

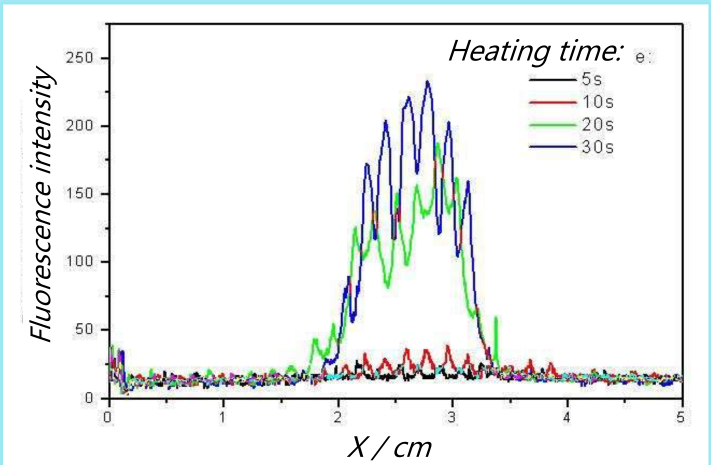

Dependence of fluorescence intensity distribution vs. the time of exposure

Source: P. Malinowski, M. Sawczak, T. Wandowski, M. Radzienski, W. Ostachowicz, *Composites Surface State Assessment by LIF Method , Proc. 7th International Symposium on NDT in Aerospace 2015.*

Laser Induced Fluorescence Method – Thermal Degradation of Composite Materials

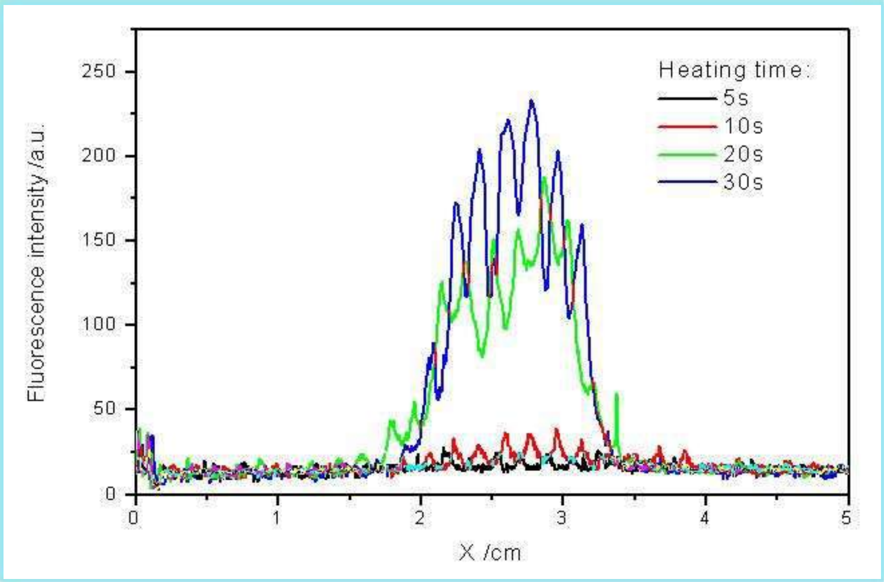

Dependence of fluorescence intensity distribution vs. the time of exposure

Integral of area bellow the intensity curve

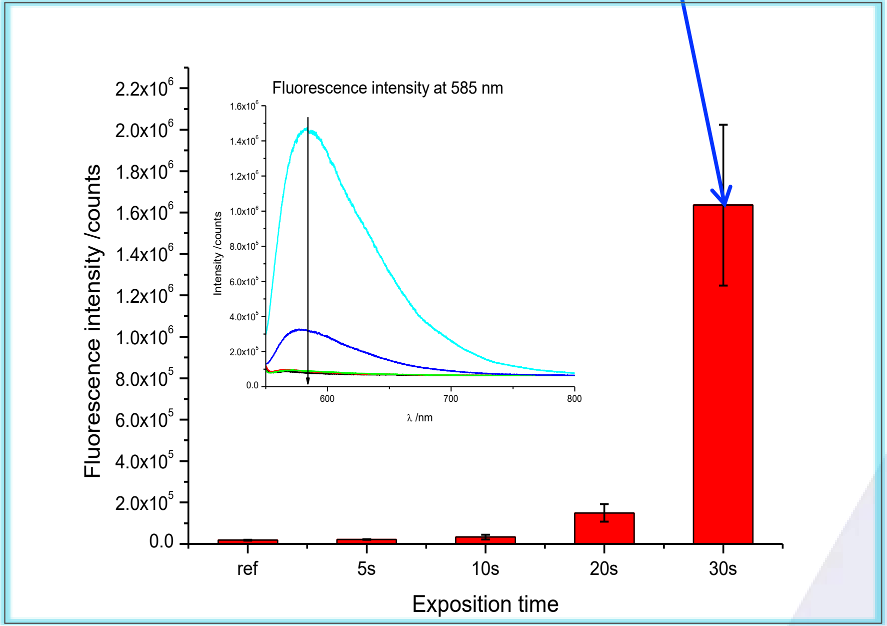

Intensity of fluorescence vs. the time of exposure (amplitude for 585 nm)

Source: P. Malinowski, M. Sawczak, T. Wandowski, M. Radzieński, W. Ostachowicz, *Composites Surface State Assessment by LIF Method, Proc. 7th International Symposium on NDT in Aerospace 2015.*

Laser Fluorescence Method – Detection of Chemical Contamination in Composite Specimen

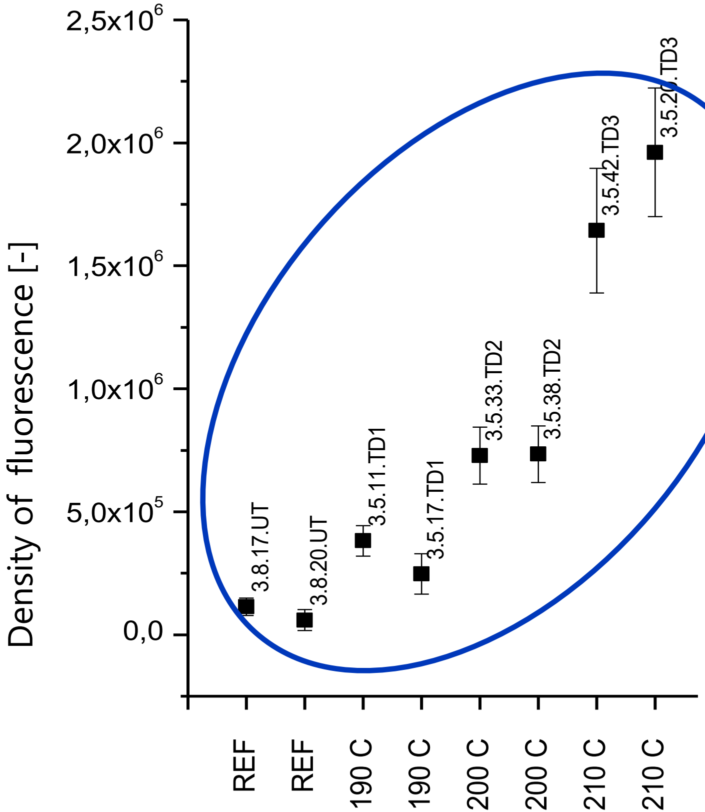

Selected Results of Research

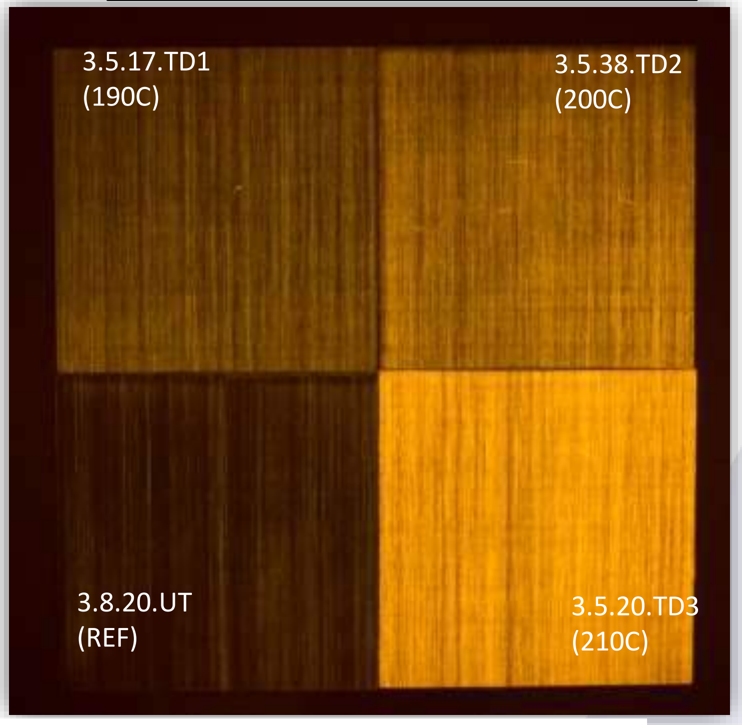

An increase of density of fluorescence vs. temperature of a composite

<u>Source</u>: P. Malinowski, M. Sawczak, T. Wandowski, W. Ostachowicz, A. Cenian, *Characterisation of CFRP surface contamination by laser induced fluorescence*, Proc SPIE 9064, 90640E, 2014.

Thermography – Detection of Water Drop

Vibrothermography

4-layer GFRP specimen

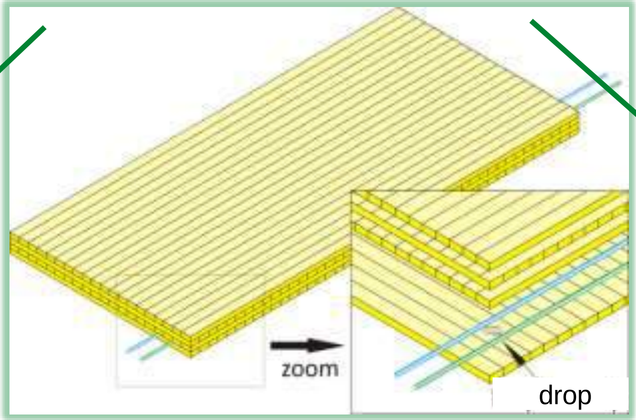

pulse thermography

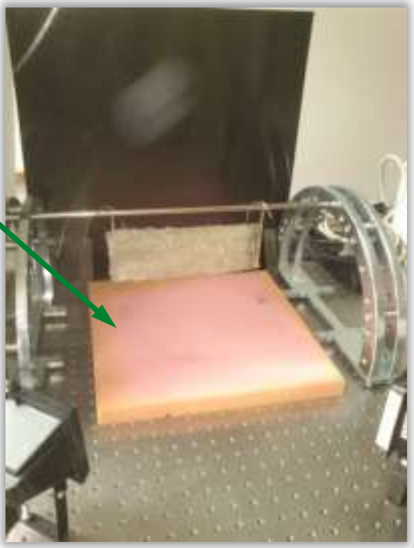

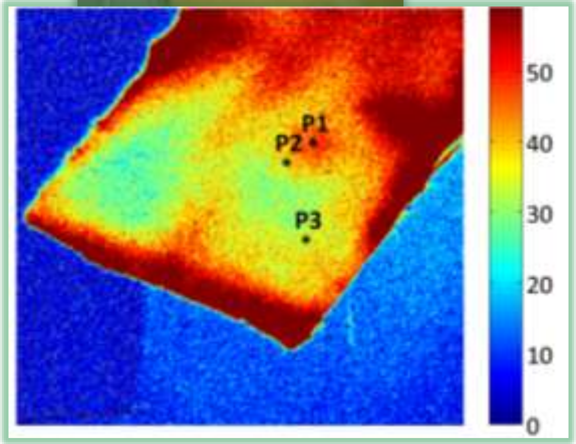

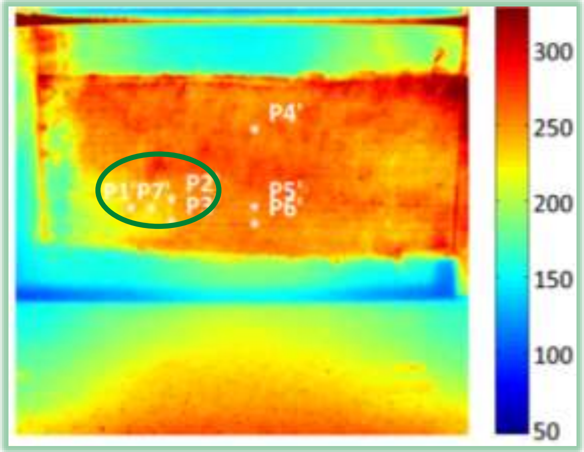

P1, P1′ – drop of water
P2,P3,P7′, P4′ – composite
P2′,P3′,P5′,P6′ – optical fibre

Source: K. Majewska, M. Mieloszyk, W. Ostachowicz, *Glass fibre composite elements with embedded fibre Bragg grating sensors inspected by thermography techniques*, e-journal of NDT, ISSN 1435-4934, 2016.

INSPECTION OF COMPOSITE STRUCTURES

NDT/SHM Methods for Structural Joints

CertBond
COST Action CA18120

cost
EUROPEAN COOPERATION IN SCIENCE & TECHNOLOGY
Funded by the Horizon 2020 Framework Programme of the European Union

Adhesive Bonds Assessment

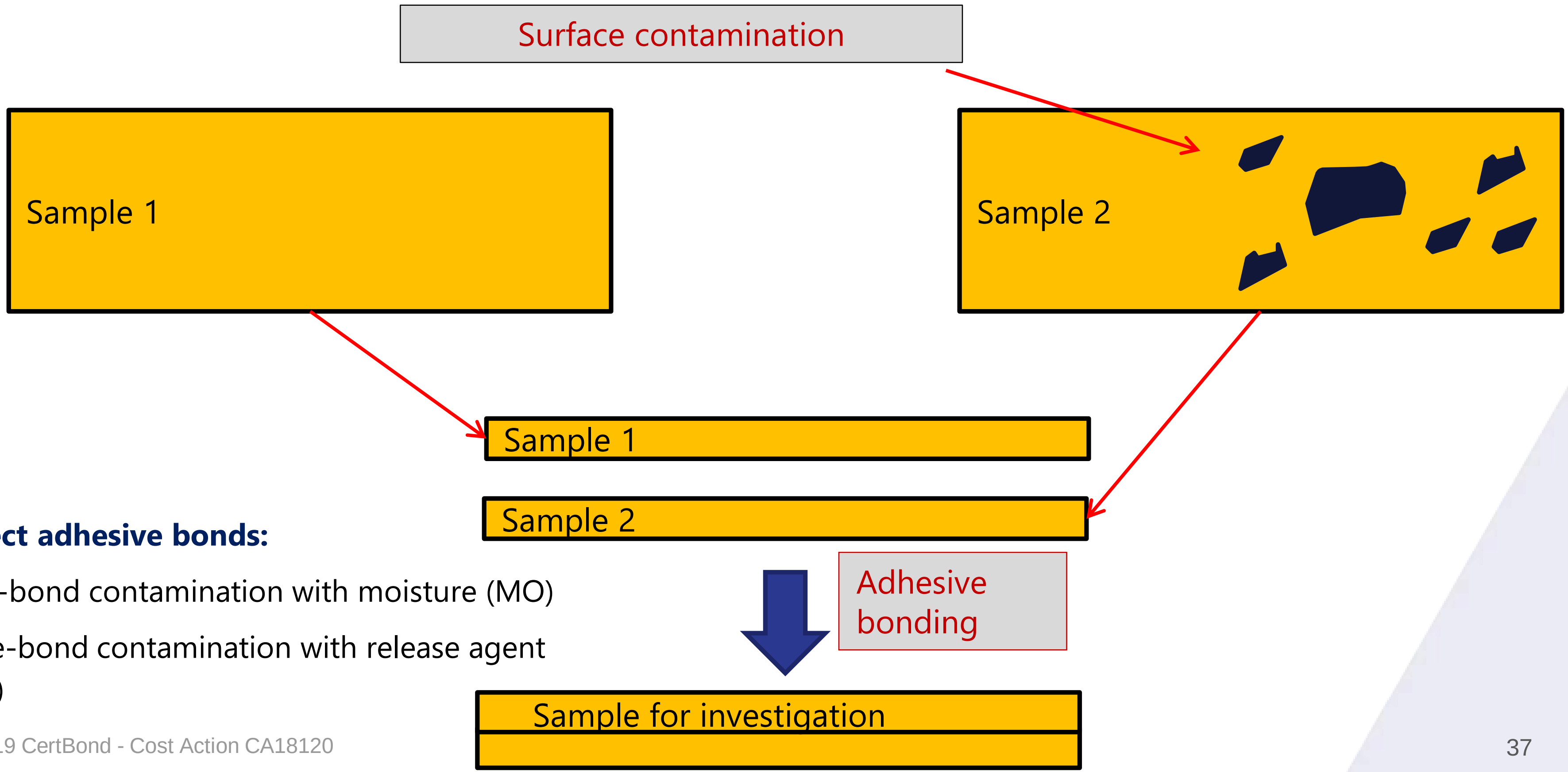

Imperfect adhesive bonds:

1. Pre-bond contamination with moisture (MO)
2. Pre-bond contamination with release agent (RE)

Adhesive Bonds Assessment

<u>Imperfect adhesive bonds:</u>

Poorly cured adhesive

Adhesive bonding

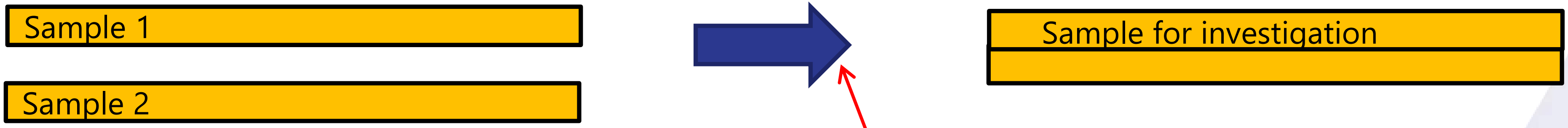

poor curing with too low temperature

Possible Sources of Weak Bonds

Sources	Manufacturing	Services
moisture	X	X
anti-adhesive agent (release agent)	X	
fuel		X
hydraulic fluid (skydrol)		X
de-icer		X
thermal degradation		X
improper adhesive curing		
errors in bonding	X	X
finger print	X	X

Introduction and Motivation

CertBond
COST Action CA18120

Contamination influence on the adhesive bond

Normal bond:
Jumping from one interface to the other

Bond contaminated with release agent:
Adhesive failure

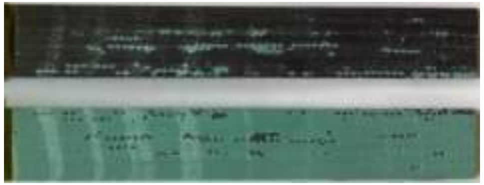

Thermal degradation:
Adhesive failure

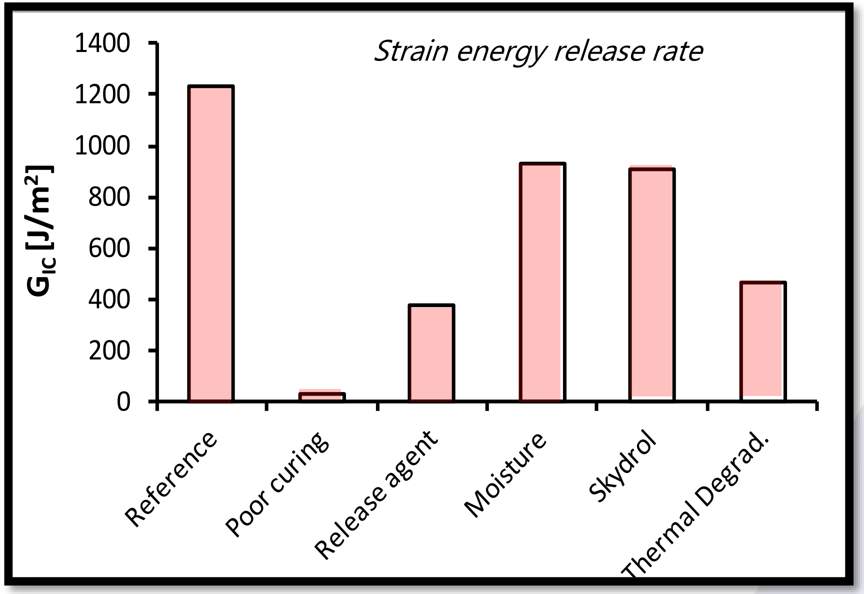

1. Markatos D., Tserpes K.I. , Rau E., Pantelakis Sp. **2013**. *Degradation of Mode-I fracture toughness of CFRP bonded joints due to moisture and release agent and moisture pre-bond contamination*. The Journal of Adhesion, doi: 10.1080/00218464.2013.770720.
2. Markatos, D.N, Tserpes, K.I., Rau, E., Markus, S., Ehrhart, B., Pantelakis, Sp. **2013**. *The effects of manufacturing-induced and in-service related bonding quality reduction on the mode-I fracture toughness of composite bonded joints for aeronautical use*. Composites Part B: Engineering 45, 556-564.
3. Malinowski P., Tserpes K.I., Wandowski T., Skarbek L., Ostachowicz W. **2013**. *Composite bonds assessment using EMI technique*. Proceedings of 9th IWSHM, September 10-12, 2013, Stanford, California, USA, pp. 2407-2414.

Investigated Methods

Electromechanical Impedance

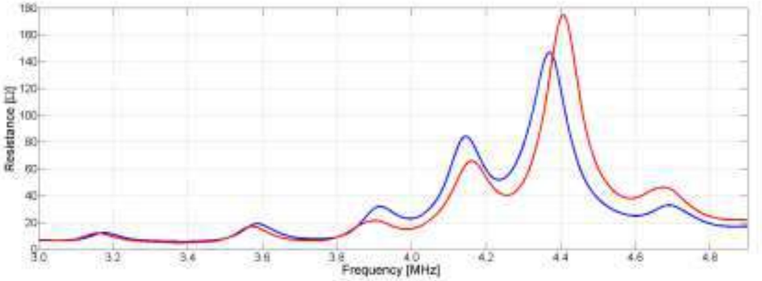

Frequency range: 4 Hz – 5 MHz

The most popular signal processing approach is to extract:

1. Resistance
2. Conductance

and compare it with a numerical index such as RMS, CC, …

$$Y = G + iB$$

$$Z = R + iX$$

$$|Y| = \frac{1}{|Z|}$$

Laboratory: Institute of Fluid-Flow Machinery, PAS, Gdansk, Poland

where: Y - admittance, G – conductance, B – susceptance

Proposed Numerical Processing Approach for EMI

CertBond
COST Action CA18120

Proposed a 2D approach analysing the curves on a complex plane

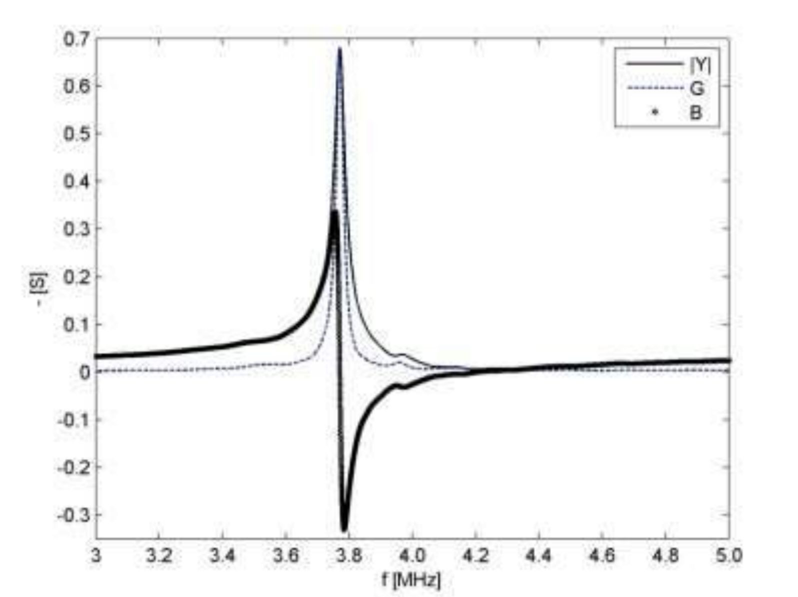

Representation on a complex plane

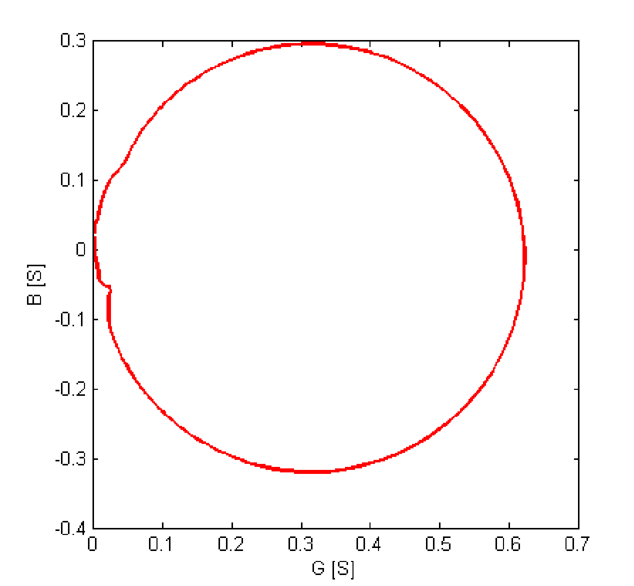

$$Y = G + iB$$

where: Y - admittance, G – conductance, B – susceptance

Source: P. Malinowski P., T. Wandowski, Ostachowicz W., *Study on adhesive bonds influence on EMI signatures*, Proc. of IWSHM 2015

Assessment of Curves Similarity

CertBond
COST Action CA18120

Frechet distance:

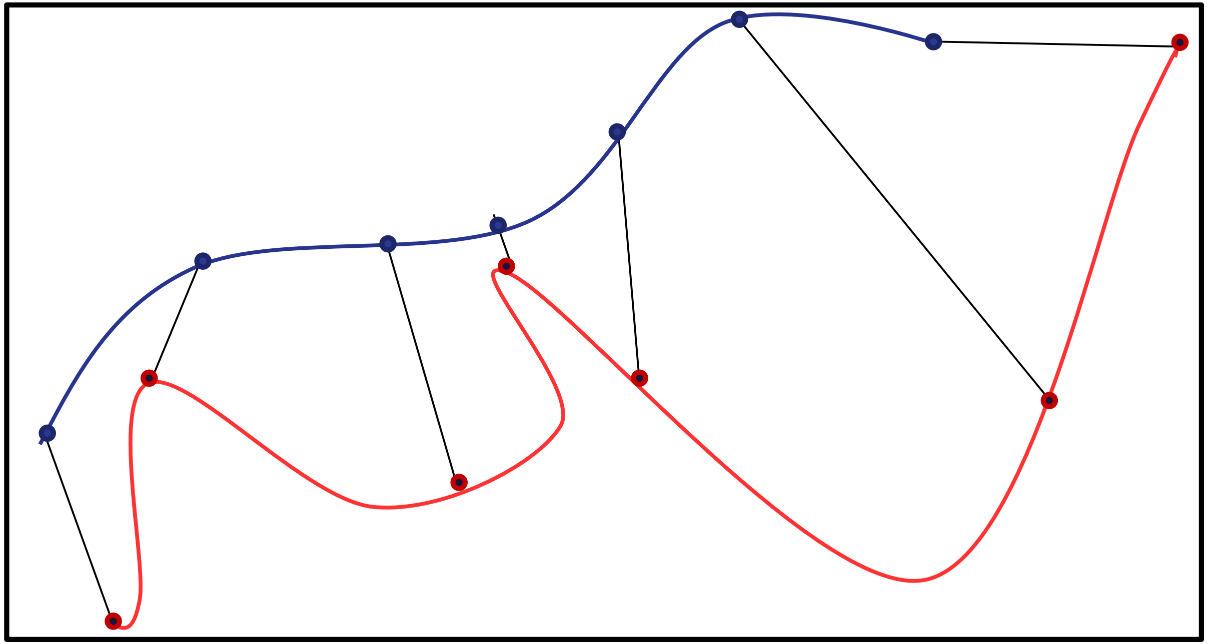

The minimum cord-length sufficient to join a point traveling forward along blue and one traveling forward along red curve, although the rate of travel for either point may not necessarily be uniform.

Sources:

1. Zachary Danziger, http://www.mathworks.com/matlabcentral/fileexchange/31922-discrete-frechet-distance
2. Tristan Ursell, http://www.mathworks.com/matlabcentral/fileexchange/41956-frechet-distance-calculator

Adhesive Bond Assessment - Results

CertBond
COST Action CA18120

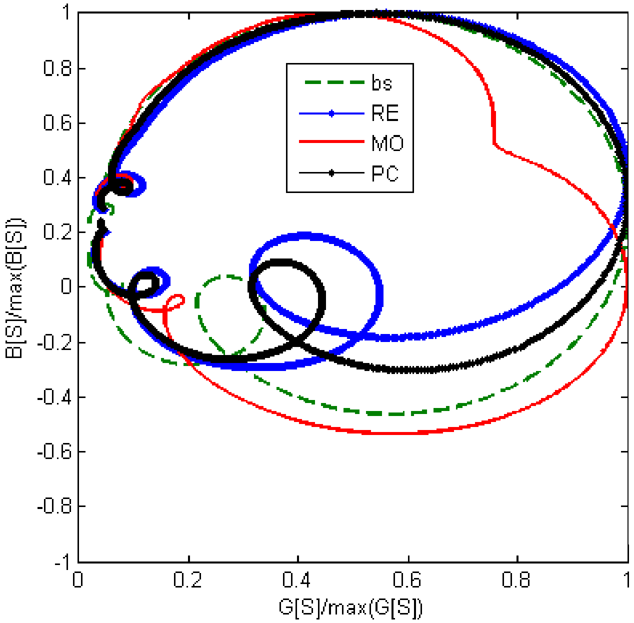

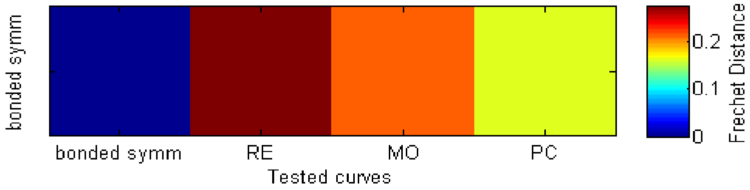

Adhesively bonded two 1.5 mm-thick CFRP samples with prebond contamination or improper curing of one of the samples.

RE – release agent contamination

MO – moisture contamination

PC – poor curing at 120^{0}C

Bonded symmetric (***bs***) sample cured at 180 ^{0}C

Source: P. Malinowski P., T. Wandowski, Ostachowicz W., *Study on adhesive bonds influence on EMI signatures*, Proc. of IWSHM 2015

EMI Method – Diagnostics of Adhesive Joint

CertBond
COST Action CA18120

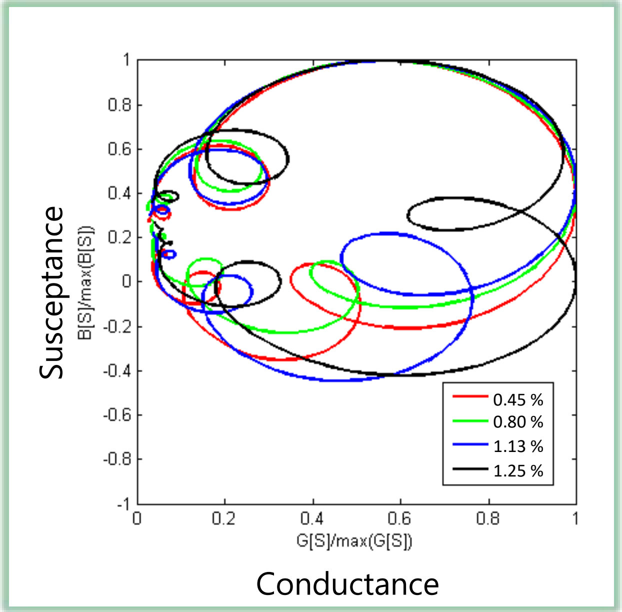

A comparison between curves using the so-called Frechet distance

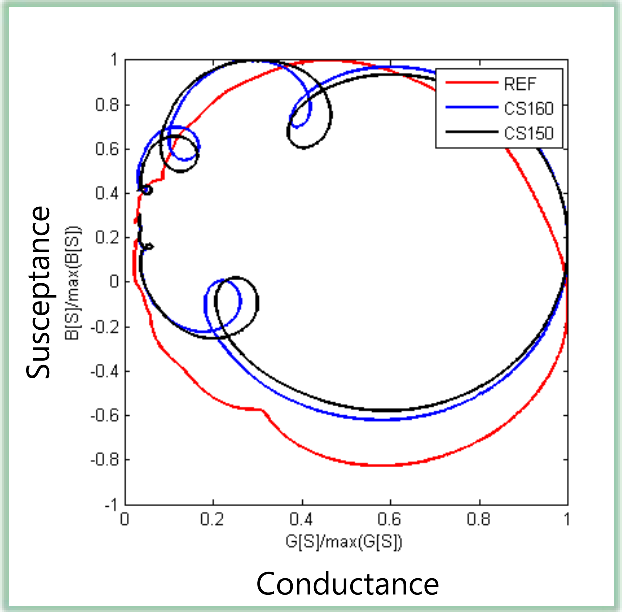

Moisture contaminated adhesive bond

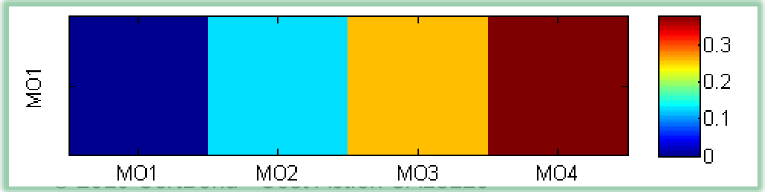

Adhesive lowered curing temperature

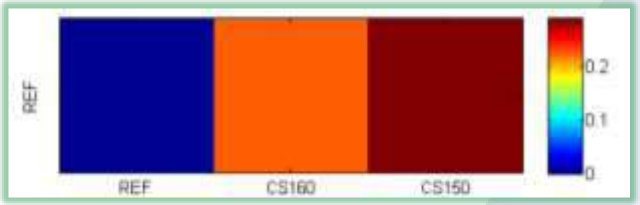

Source: P. Malinowski P., T. Wandowski, Ostachowicz W., *Study on adhesive bonds influence on EMI signatures*, Proc. of IWSHM 2015

EMI - Selected Results of Research

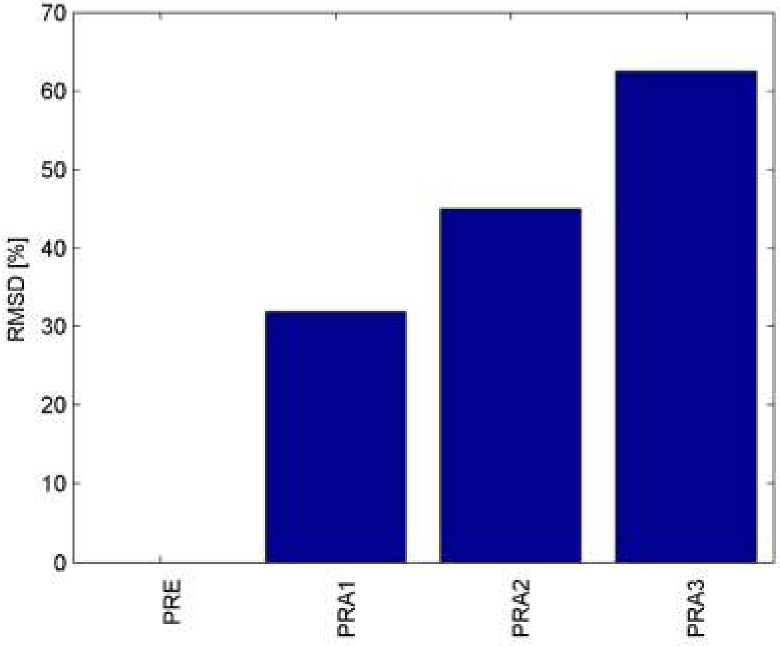

Electromechanical Impedance
(assessment of weak adhesive joint)

Symbol	Description	Contamination
PRE	Reference measurement	absence
PRA1	Anti-adhesive agent, level 1	3.2 (+/- 0.2) at.% Si
PRA2	Anti-adhesive agent, level 2	5.1 (+/- 0.7) at.% Si
PRA3	Anti-adhesive agent, level 3	6.2 (+/- 0.3) at.% Si

Source: P. H. Malinowski, R. Ecault, T. Wandowski, W. M. Ostachowicz, *Evaluation of adhesively bonded composites by nondestructive techniques*, Proc. of SPIE 10170, 101700B, 2017.

EMI - Results for Pre-bond Thermal Treatment

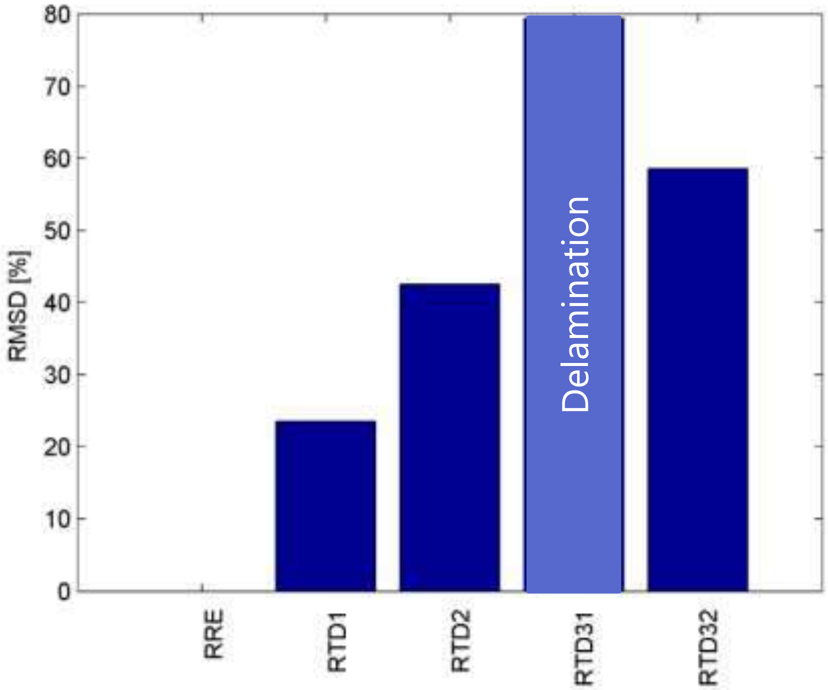

- According to US test RTD31 has a delamination, most probably caused by the heating.
- The results for the highest level of thermal treatment (280°C) were separated.
- Samples: RRE2, RTD12, RTD22, RTD33 rejected due to different spectra shape.

Source: P. H. Malinowski, R. Ecault, T. Wandowski, W. M. Ostachowicz, *Evaluation of adhesively bonded composites by nondestructive*

EMI - Disbond size estimation

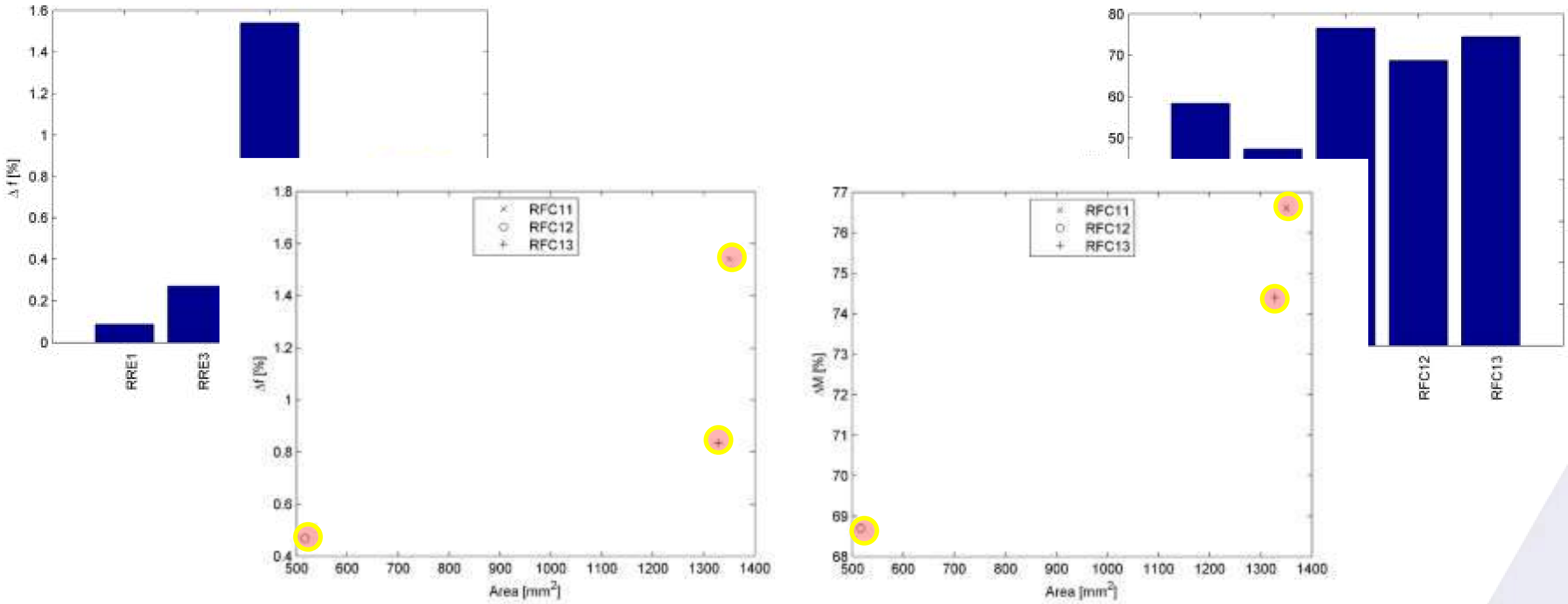

- Changes of conductance maximum (location and magnitude) in relation to unbonded sensors

Source: P. H. Malinowski, R. Ecault, T. Wandowski, W. M. Ostachowicz, *Evaluation of adhesively bonded composites by nondestructive techniques*, Proc. of SPIE 10170, 101700B, 2017.

LDV (Laser Doppler Vibrometry)

LDV (Laser Doppler Vibrometry) method for adhesive bonds

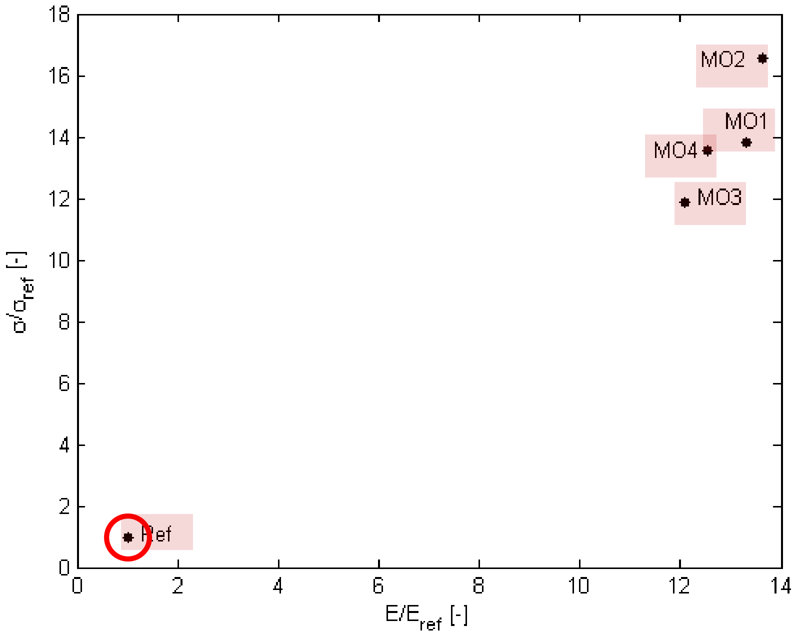

Pre-bond contamination with moisture

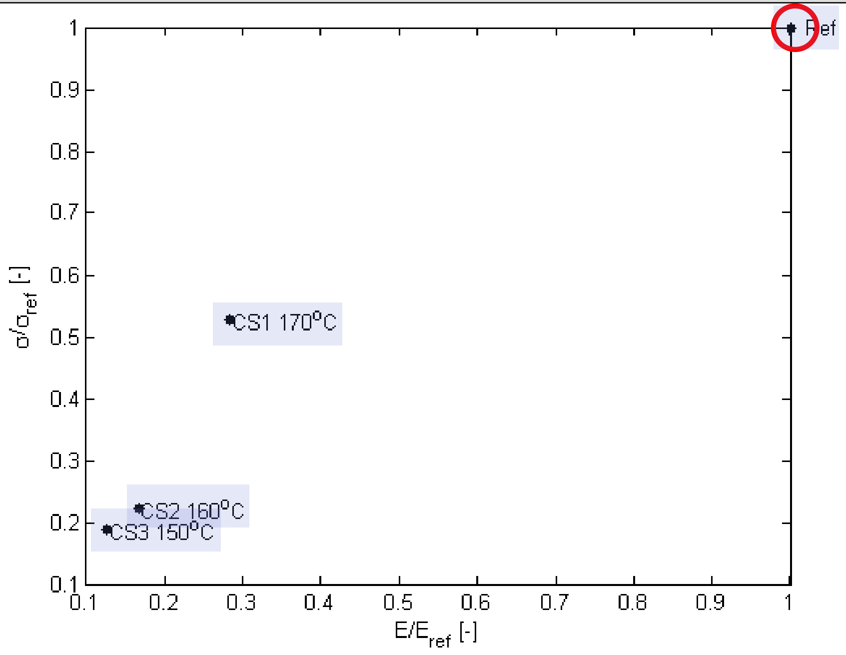

Poor curing of adhesive

E – mean out–of–plane vibration energy

σ – standard deviation of E

ENCOMB | 7th Framework Programme *Extended Non-Destructive Testing of Composite Bonds*

Adhesive Bonds Assessment | THz

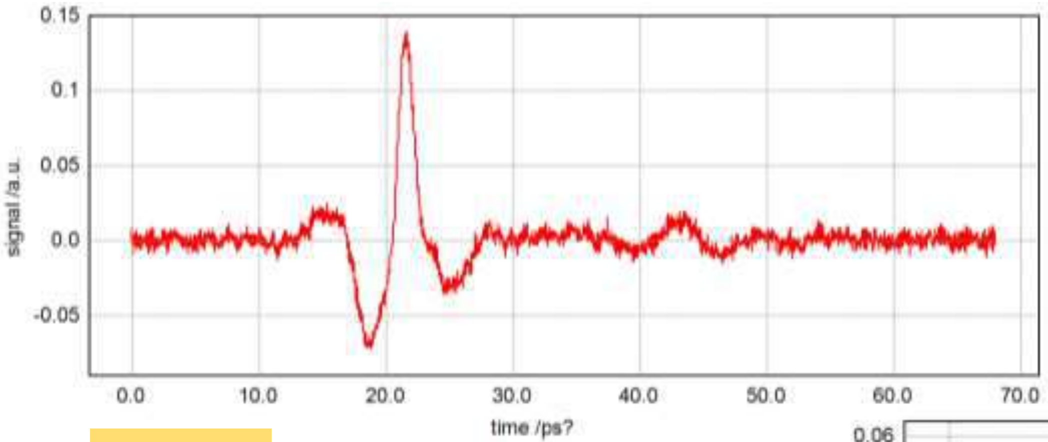

Dry case

Results | Moisture at the interface

Transmission study – thick layer

Moisture case

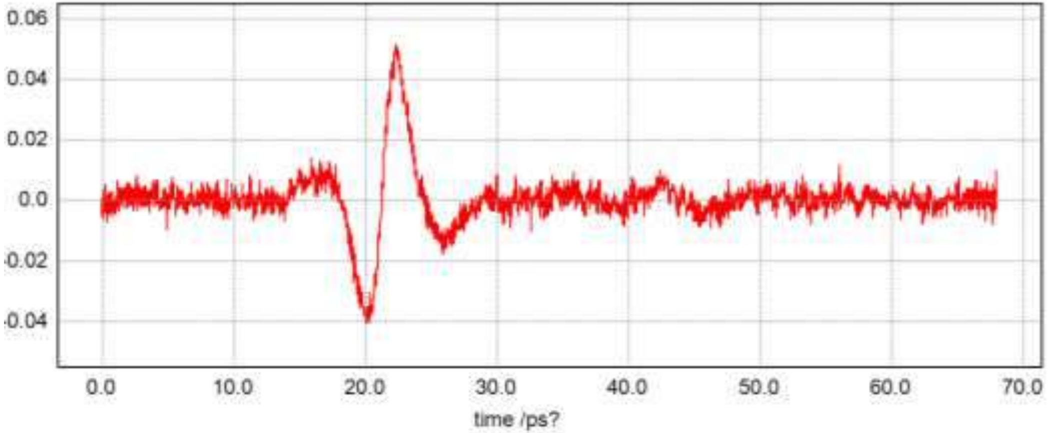

The thick layer (100-300 μm) causes significant attenuation.
Three times reduction of pulse amplitude is visible.

Source: P. Malinowski, N. Palka, S. Opoka, T. Wandowski, W. Ostachowicz, *Moisture detection in composites by terahertz spectroscopy*, Proceedings of DAMAS 2015 Conference.

Adhesive Bonds Assessment | THz

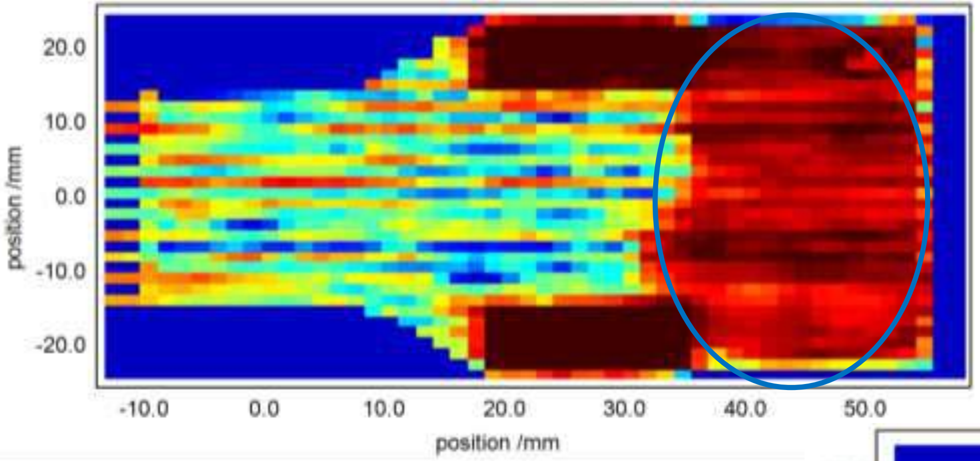

Results | Moisture at the interface

Transmission study – thick layer

Max in time domain

Max in frequency domain

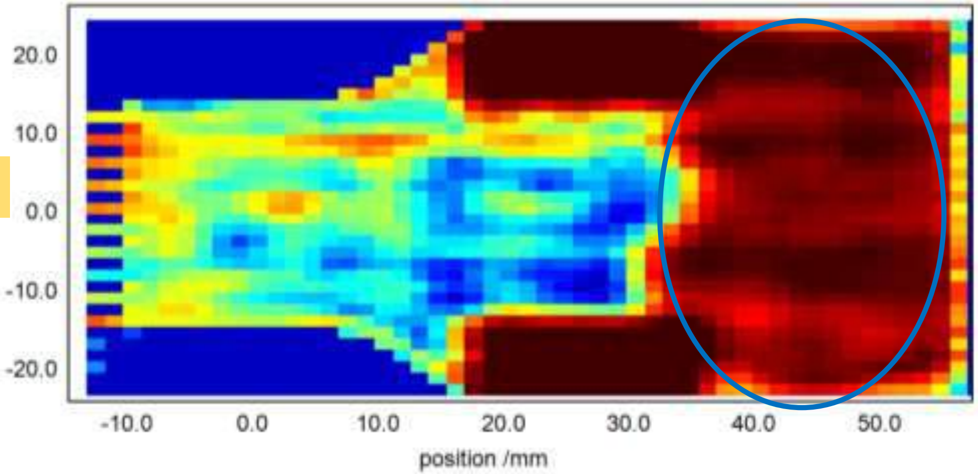

Source: P. Malinowski, N. Palka, S. Opoka, T. Wandowski, W. Ostachowicz, *Moisture detection in composites by terahertz spectroscopy*, Proceedings of DAMAS 2015 Conference.

Sizing of the disbonds with ultrasonics

CertBond
COST Action CA18120

Defect Detection

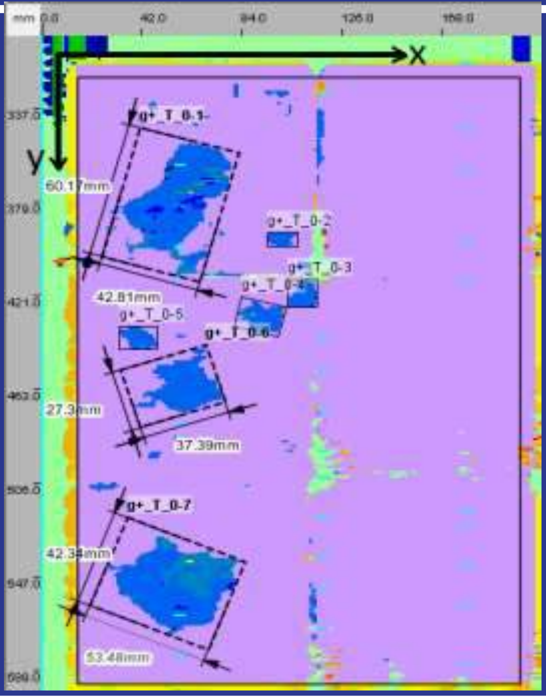

Names (centers)	Area (mm^2)	Outline (mm^2)	Length (mm)	Mean (µs)
g+_T_0-1 (X=43, Y=62)	1328.0	2575.6	60.2	1.08
g+_T_0-2 (X=92, Y=81)	57.0	78.0	13.0	1.08
g+_T_0-3 (X=98, Y=7)	115.0	144.0	12.0	1.09
g+_T_0-4 (X=80, Y=20)	174.0	260.2	19.2	1.12
g+_T_0-5 (X=28, Y=27)	108.0	160.0	16.0	1.08
g+_T_0-6 (X=49, Y=49)	517.0	1020.9	37.4	1.07
g+_T_0-7 (X=44, Y=44)	1350.0	2264.3	53.5	1.12

Source: Malinowski P., Ecault R., Wandowski T., Ostachowicz W., *Evaluation of adhesively bonded composites by nondestructive techniques*, SPIE Smart Structures/NDE, March 25-29, 2017

INSPECTION OF COMPOSITE STRUCTURES

NDT/SHM Methods for Damage Detection

CertBond
COST Action CA18120

cost
EUROPEAN COOPERATION IN SCIENCE & TECHNOLOGY

Funded by the Horizon 2020 Framework Programme of the European Union

Electromechanical Impedance

A stand for electromechanical impedance tests with AD5933 system

IMPEDADANCE ANALYZER AD 5933
ANALOGUE DEVICES

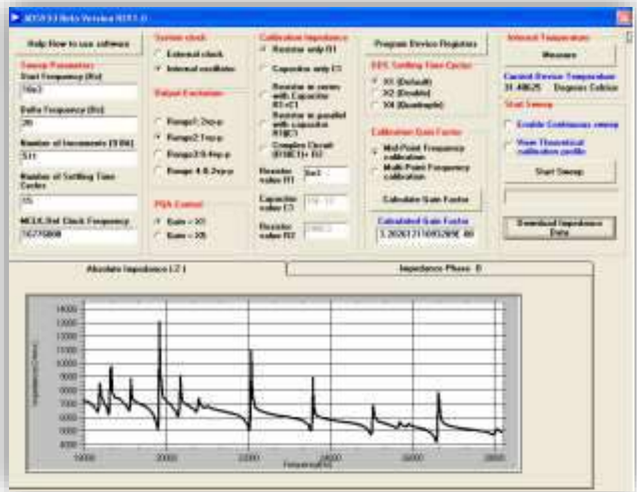

A computer programme for configuration of the AD5933 system and selected tests

An electronic devices for the AD5933 system

<u>Laboratory</u>: Institute of Fluid-Flow Machinery, PAS, Gdansk, Poland

EMI - Investigated Methods

CertBond
COST Action CA18120

Electromechanical Impedance

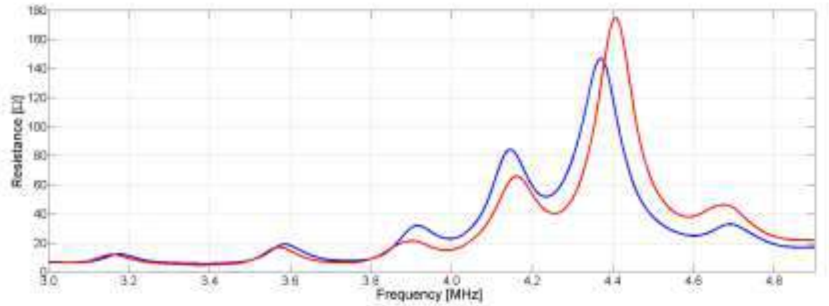

Frequency range: 4 Hz – 5 MHz

Measurements were taken for CFRP sample with dimensions:

100 mm × 100 mm × 3.5 mm at:

- ✓ referential state, temperature T=22°C
- ✓ referential state, T=24°C
- ✓ damage state – delamination **D1**, T=22°C
- ✓ damage state –delamination **D2**, T=22°C

<u>Laboratory</u>: Institute of Fluid-Flow Machinery, PAS, Gdansk, Poland

EMI FOR DELAMINATION DETECTION

CertBond
COST Action CA18120

delamination **D2**

delamination **D1**

CFRP sample dimensions:

100 mm × 100 mm × 3.5 mm

<u>Laboratory</u>: Institute of Fluid-Flow Machinery, PAS, Gdansk, Poland

EMI Temperature Compensation

CertBond
COST Action CA18120

Temperature compensation for CFRP sample with delaminations

600 mm × 200 mm × 3.5 mm

- ✓ Dimensions:
  600 mm × 200 mm × 3.5 mm
- ✓ Varying temperature
- ✓ Delaminations with different size

Temperature influenced signal shifting in order to minimize CCD.

$$CCD = 1 - \sum_{i=1}^{n} \frac{\left[R(i)_R - \bar{R}_R\right]\left[R(i)_D - \bar{R}_D\right]}{\sigma_R \sigma_D}$$

$R(i)_R$ - resistance for referential case

$R(i)_D$ - resistance for damage or temperature influenced case

$\bar{R}_R$, $\bar{R}_D$ - mean values

σ_R , σ_D - standard deviations

Laboratory: Institute of Fluid-Flow Machinery, PAS, Gdansk, Poland

EMI - Selected Results of Research

CertBond
COST Action CA18120

Electromechanical Impedance (detection of delamination)

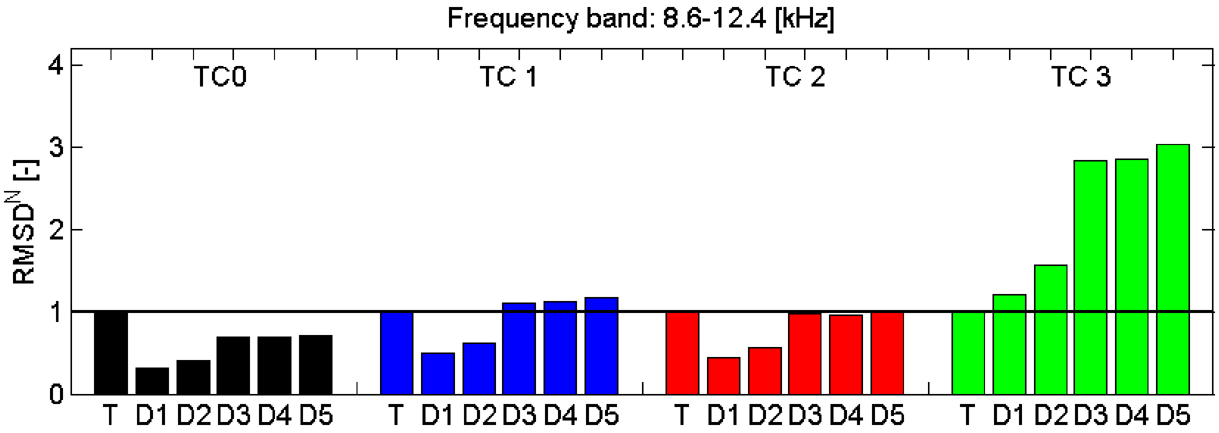

Source: Wandowski T, Malinowski PH, Ostachowicz WM. *Temperature and damage influence on electromechanical impedance method used for carbon fibre–reinforced polymer panels*. Journal of Intelligent Material Systems and Structures, 2017; 28 (6): 782-798.

EMI | Method – Damage Detection

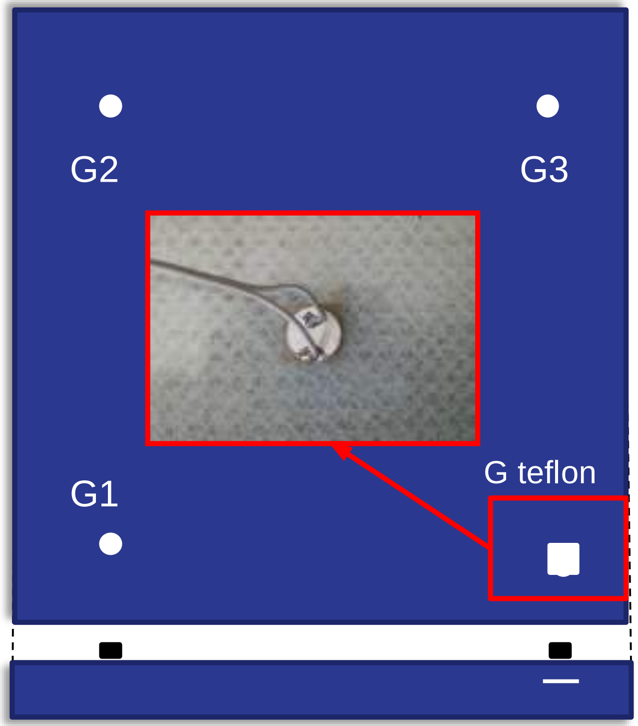

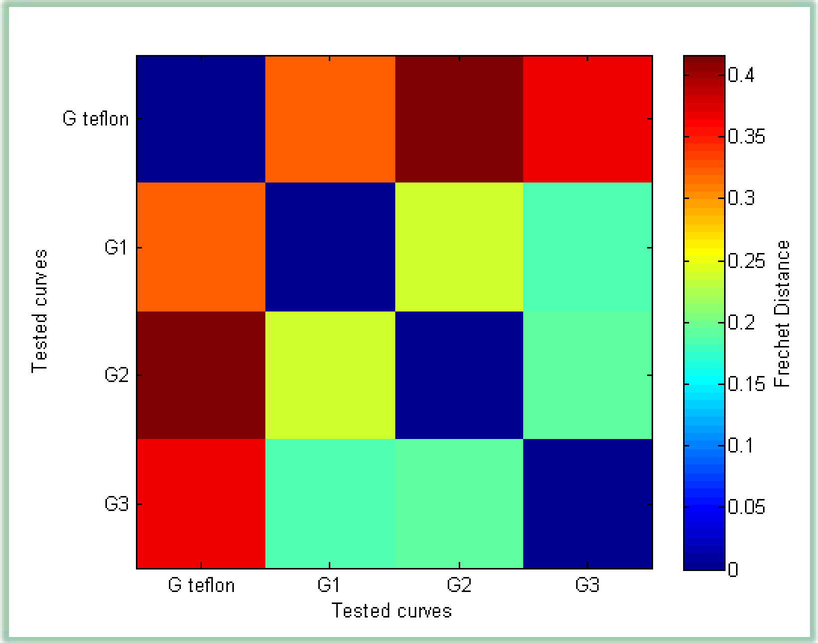

Larger differences in the presence of damage than between measurements G1, G2 and G3

- 3,0 mm thickness, position of layers [0/90/0/90]s
- composite with carbon reinforcement 500 mm × 500 mm
- damage (delamination) – teflon spacer between 2 and layer 3

Source: P. Malinowski P., T. Wandowski, Ostachowicz W., *Study on adhesive bonds influence on EMI signatures*, Proc. of IWSHM 2015

EMI Method - Tests for Damaged Beams

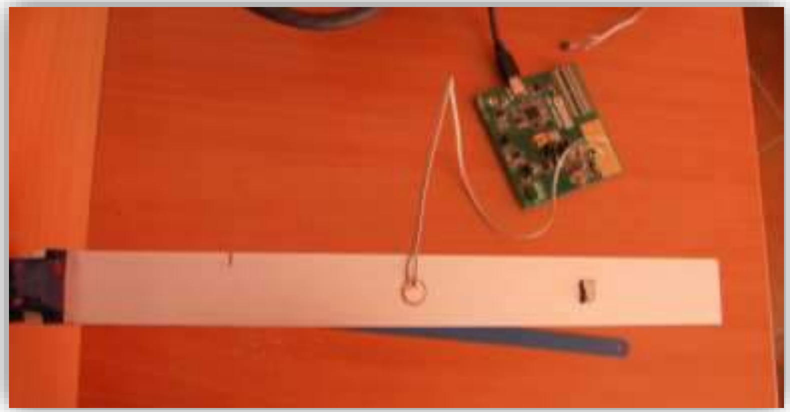

A cantilever aluminium beam with a notch and additional mass

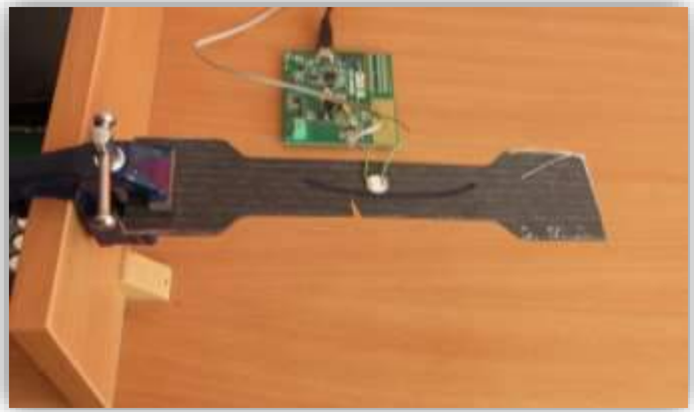

A cantilever composite beam reinforced by carbon fibres with a notch

An aluminium beam clamped in both ends (without damages)

Laboratory: Institute of Fluid-Flow Machinery, PAS, Gdansk, Poland

Research aims

1. Detect the weak bond

2. Assess the bond quality

- The performance of adhesive bonds depends on the physico-chemical properties of the adherend surfaces.
- The weak bond can be caused by surface contamination of the adherend sufaces.
- The contamination leading to weak bonds may have various origin (moisture, release agent, hydraulic fluid, poor curing of adhesive, ...).

Investigated weak bonds scenarios

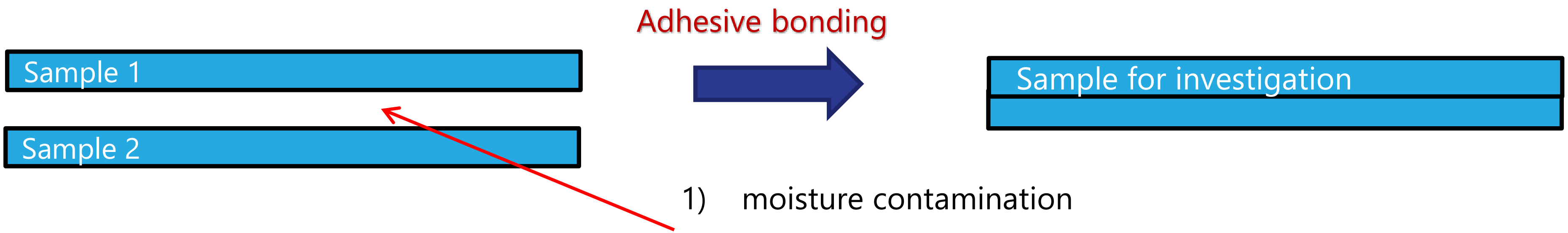

1) moisture contamination

2) release agent contamination

1. Moisture

Methods tested: Electromechanical impedance, Active thermography, Laser ultrasonics, Ultrasound frequency analysis

2. Release agent (resulting in Si contamination of the surface)

Methods tested: Electromechanical impedance, Ultrasonic arrays, Laser ultrasonics, Laser Shock Adhesion Test, Ultrasound frequency analysis

Varying contamination influence

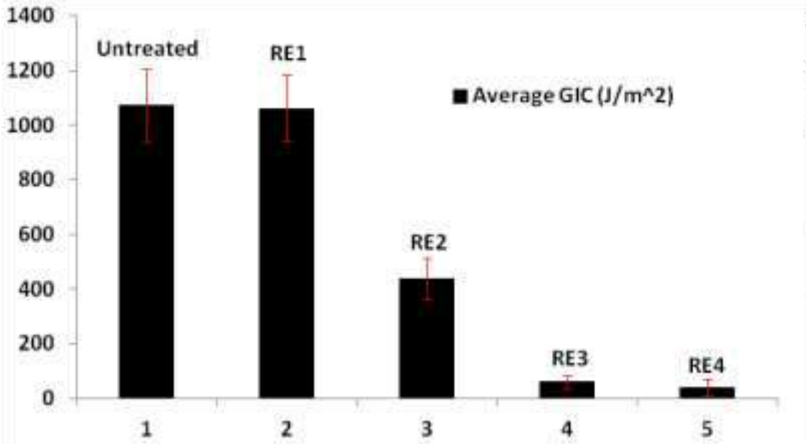

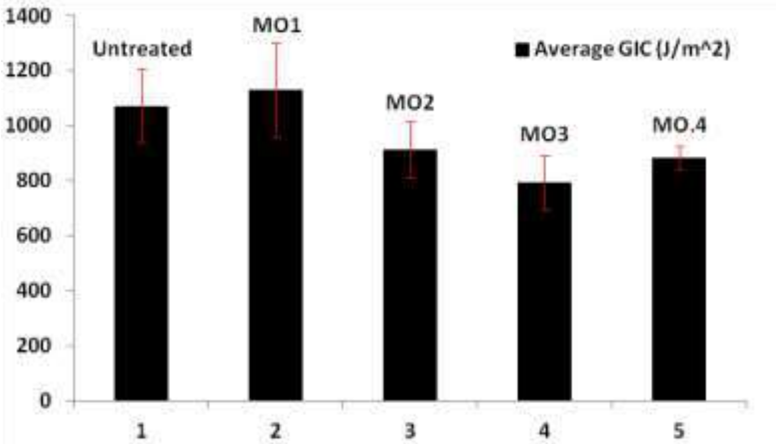

Sample	Symbol	Average GIC [J/m2]
Untreated		1072.72
2.1 at% of Si	RE1	1062.75
6.5 at% of Si	RE2	439.2
8.2 at% of Si	RE3	60.8
10.1 at% of Si	RE4	40.4
0.45 WT%	MO1	1129.95
0.80 WT%	MO2	914.44
1.13 WT%	MO3	795.31
1.25 WT%	MO4	885.17

Source: Markatos, D., Tserpes, K.I., Rau, E., Pantelakis, Sp. (2012) *Degradation of mode I fracture behavior of composite bonded joints due to moisture and release agent pre-bond contamination.* The Journal of Adhesion, DOI: 10.1080/00218464.2013.770720

Active thermography with optical heating technique

CertBond
COST Action CA18120

Principle of the optical heating technique

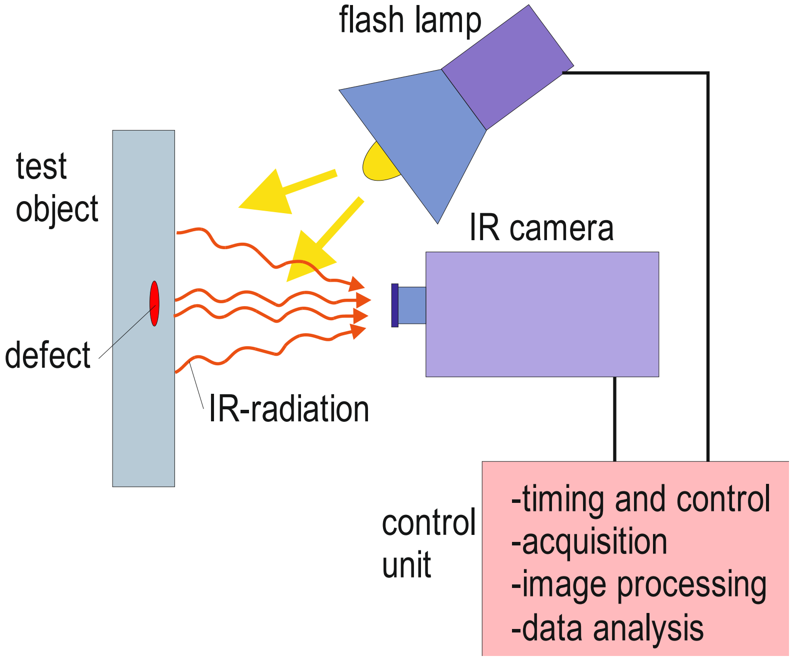

Specimen heated at surface by pulsed optical excitation.

Heat is propagating into the material.

The instationary heat diffusion is depending on the effusivity of the material:

E= $\sqrt{\lambda}\,\rho\, c$

where:

E – effusivity

λ – heat density

ρ – volumic mass

c – specific heat capacity

ENCOMB | 7th Framework Programme *Extended Non-Destructive Testing of Composite Bonds*

Fraunhofer IZFP

Source: Ehrhart B., Netzelmann U., Walle G., et all, *Extended NDT Methods for Evaluation of CFRP Adhesive Bonds*, International Workshop on Aero Structures, October 9-11, 2013, Milano, Italy, (presented by W. Ostachowicz)

LAser Shock Adhesion Test (LASAT)

CertBond
COST Action CA18120

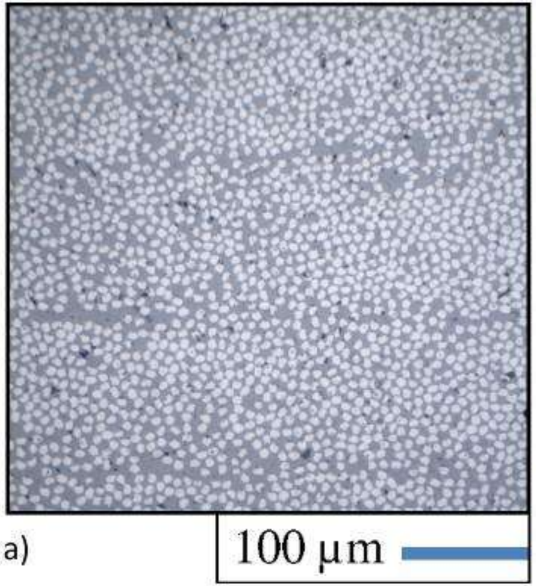

a)

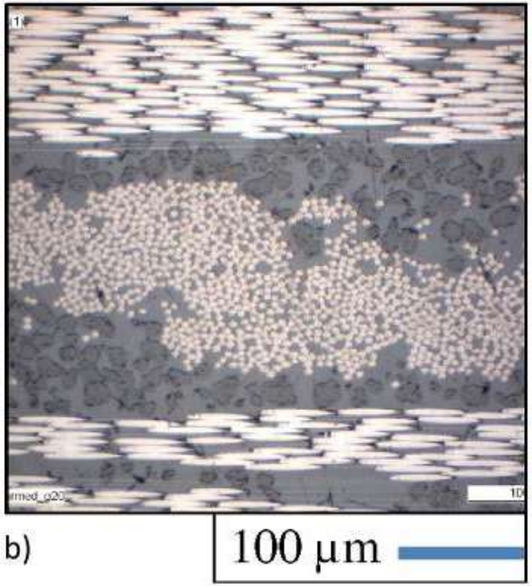

b)

Studied materials

T800/M21 unidirectional composite qualified by aeronautical companies as an enhanced version of T300/914, thermoplastic nodules are added in the M21 matrix in order to increase the shock resistance of the material. The pre-impregnated plies are thicker (about 250 µm).

T300/914 unidirectional composite material composed of several pre-impregnated plies of carbon fibers and epoxy matrix (approximately 150 µm thick)

Source: Malinowski P., Ecault R., Boustie M., Touchard F., Berthe L., Ostachowicz W., *Damage detection method for composites based on laser vibrometers*, 5th International Symposium on NDT in Aerospace, November 13-15, 2013, Singapore (presented by W. Ostachowicz)

LAser Shock Adhesion Test (LASAT)

A dynamic tensile loading due to shock wave propagation

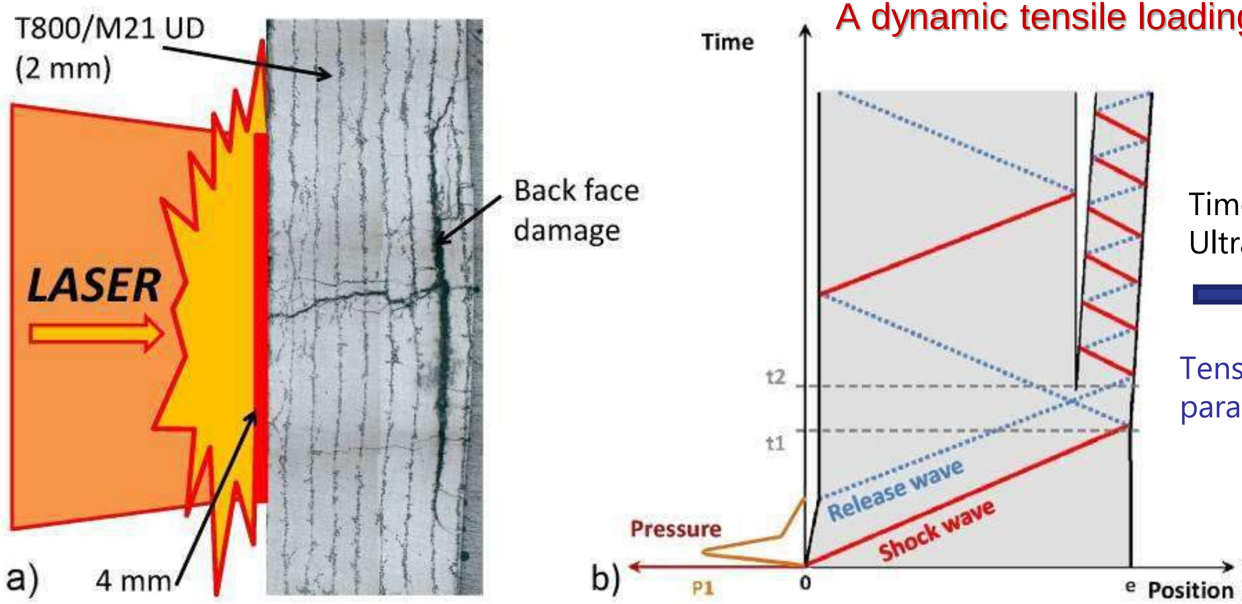

Time-resolved diag. Velocimetry
Ultrasonic (Post mortem observations)

Tensile stress controlled by the laser parameters and CFRP assembly

The laser source used in this study generates laser gaussian pulses whose FWHM is about 25 ns and whose beam energy can be adjusted in the range: 0J – 25J. This laser source is generally used to test thick samples (millimeters) and can create sizeable inside damage (millimeters) in case of composite materials.

Source: Malinowski P., Ecault R., Boustie M., Touchard F., Berthe L., Ostachowicz W., *Damage detection method for composites based on laser vibrometers*, 5th International Symposium on NDT in Aerospace, November 13-15, 2013, Singapore (presented by W. Ostachowicz)

LAser Shock Adhesion Test (LASAT)

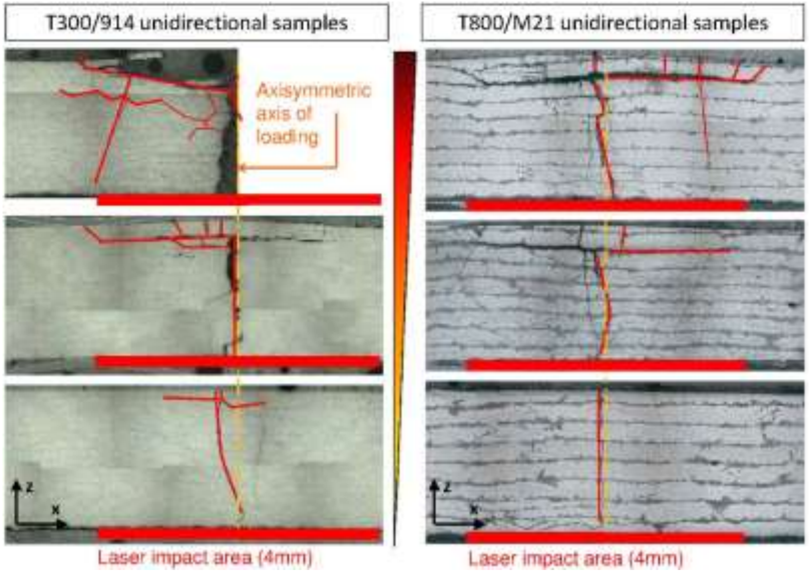

Results – micrographies

- Damage is located close to the back face, around 250 μm deep.
- Long transverse cracks due to the flexural component of the loading
- The laser irradiation is also responsible for the delamination which can be observed on almost all the micrographies.
- The T800/M21 material seems stronger.

Source: Malinowski P., Ecault R., Boustie M., Touchard F., Berthe L., Ostachowicz W., *Damage detection method for composites based on laser vibrometers*, 5th International Symposium on NDT in Aerospace, November 13-15, 2013, Singapore (presented by W. Ostachowicz)

DAMAGE LOCALIZATION APPROACH

Results – T300/914

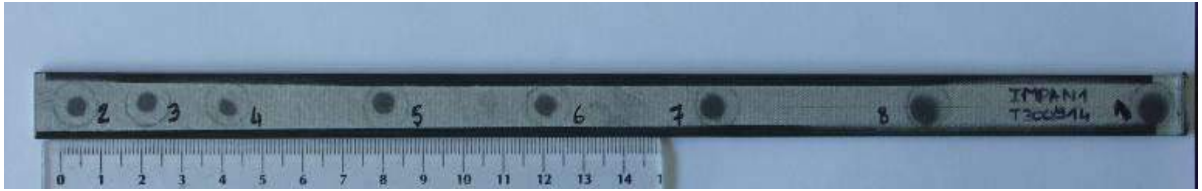

Energy based index is calculated for each signal *S* registred in *N* mesh points:

Shot number	Spot diameter (mm)	Pulse duration (ns)	Energy (J)	Intensity (GW/cm^2)
1	4.2	29.6	18.62	4.54
2	4.2	29.6	1.40	0.34
3	4.2	29.6	1.73	0.42
4	4.2	29.6	2.49	0.61
5	4.2	29.6	2.50	0.61
6	4.2	28.8	3.40	0.85
7	4.2	29.4	7.36	1.81
8	4.2	29.8	14.06	3.41

$$E_i = \log_{10}\sqrt{\frac{1}{N}\sum_{j=1}^{N} S_{ij}^2}$$

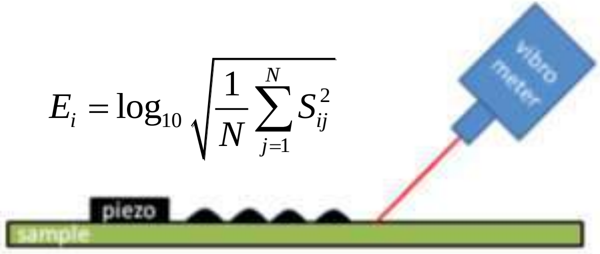

Source: P. Malinowski P., Ostachowicz W., Touhard F., Boustie M., Chocinski-Arnault L., Gonzales P., Berthe L., et al. *Study of plant fibre composites with damage induced by laser and mechanical impacts*, Composites Part B: Engineering 152, 209-219, 2018.

NDT Results – T300/914

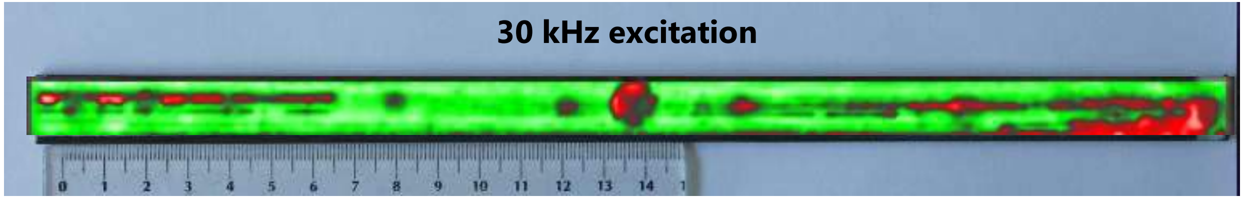

- Wave source – piezoelectric disc was between damage 6 and 7.
- Measurements showed deviation in both directions (leftward and right ward from the piezoelectric transducer) along the specimen.
- Local circular increase in wave energy indicates the laser caused defects.
- Straight line of higher damage index indicates damaged fibres.
- Defects that are farther away from the piezo disc are not detected so well due to wave attenuation.
- Moreover, the wave in order to reach this region has to travel the region of remaining defects.

Source: P. Malinowski P., Ostachowicz W., Touhard F., Boustie M., Chocinski-Arnault L., Gonzales P., Berthe L., et al. *Study of plant fibre composites with damage induced by laser and mechanical impacts*, Composites Part B: Engineering 152, 209-219, 2018.

Results – T800/M21

Shot number	Spot diameter (mm)	Pulse duration (ns)	Energy (J)	Intensity (GW/cm²)
2	**4**	**28.20**	10.43	2.94
3	**4**	**27.23**	5.14	1.50
4	**4**	**28.02**	2.38	0.68
5	**4**	**27.95**	10.12	2.88
6	**4**	**26.41**	2.68	0.81
7	**4**	**29.54**	0.94	0.25
8	**4**	**26.03**	0.97	0.30

I ≥ 2.8 GW/cm² **I = 1.5 GW/cm²** **I ≤ 0.8 GW/cm²**

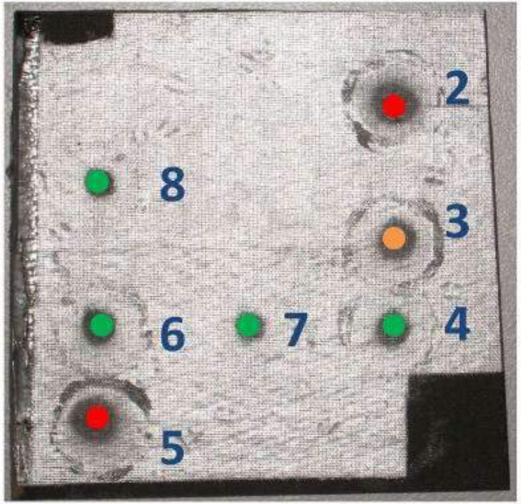

- The sample was shocked in 8 different positions.
- Severe damage occurred only at three locations, numbered 2, 3 and 5.
- At the remaining locations the damage threshold was not exceeded.
- The sample was painted afterwards to perform a blind NDT test.

Source: P. Malinowski P., Ostachowicz W., Touhard F., Boustie M., Chocinski-Arnault L., Gonzales P., Berthe L., et al. *Study of plant fibre composites with damage induced by laser and mechanical impacts*, Composites Part B: Engineering 152, 209-219, 2018.

Ultrasonic Frequency Analysis

The challenge is the testing of adhesive bonding on CFRP-structures. In this regard conventional testing methods reach their limits.
The basic idea is to take a closer look at the signal of an ultrasonic inspection, particularly at the frequency spectrum.

Thus, a weak bond should have an effect to parts of the frequency spectrum.

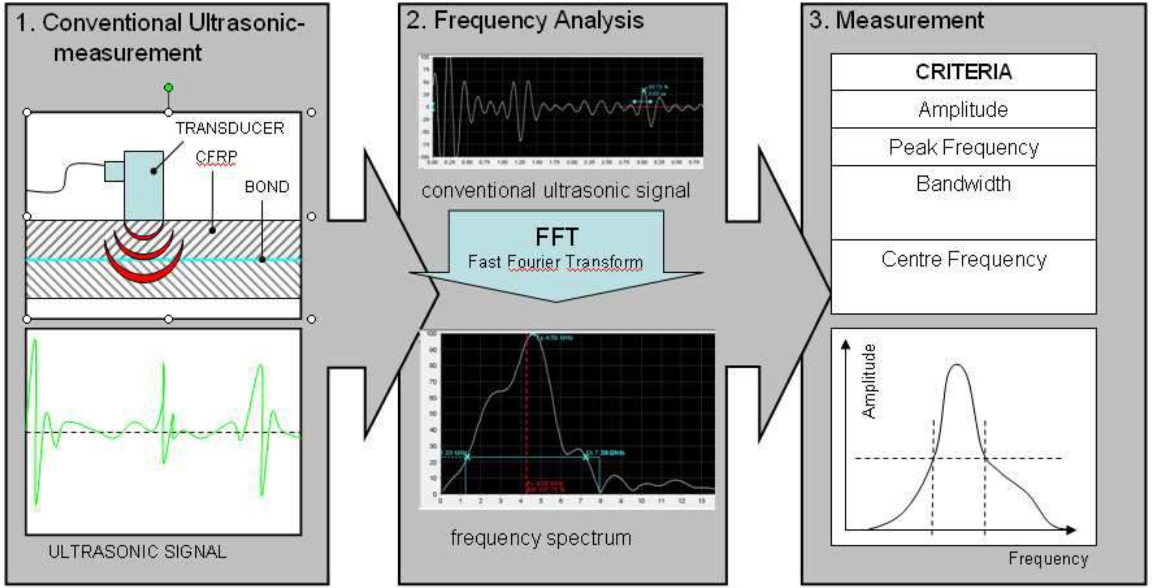

- The starting situation is a conventional ultrasonic signal.
- In the next step the frequency spectra is determined by means of a fast Fourier transformation.
- By comparing a proper bonded reference area and a testing specimen, it should be possible to find changes in the strength behavior that can indicate a so-called weak bond.

ENCOMB | 7th Framework Programme *Extended Non-Destructive Testing of Composite Bonds*

Source: Heichler G., Ossiander G., *Extended NDT Methods for Evaluation of CFRP Adhesive Bonds*, International Workshop on Aero Structures, October 9-11, 2013, Milano, Italy, (presented by W. Ostachowicz)

Ultrasonic Frequency Analysis Results

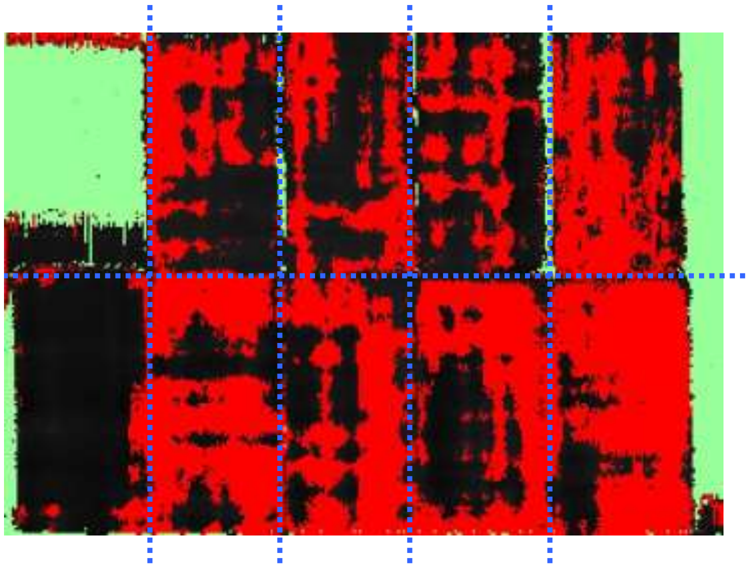

- First tests have shown, that there is a significant change of the bandwidth of the frequency spectra in parts of the weak bonded samples.
- Up to now the testing method is very sensitive to influences from the CFRP material (moisture, surface roughness, thickness of the bond line).
- Another challenge would be a differentiation between the degrees of contamination.

UT – untreated

RE – release agent

MO – moisture

- Indication

ENCOMB | 7th Framework Programme *Extended Non-Destructive Testing of Composite Bonds*

Source: Heichler G., Ossiander G., *Extended NDT Methods for Evaluation of CFRP Adhesive Bonds*, International Workshop on Aero Structures, October 9-11, 2013, Milano, Italy (presented by W. Ostachowicz).

Surface Acoustic Waves

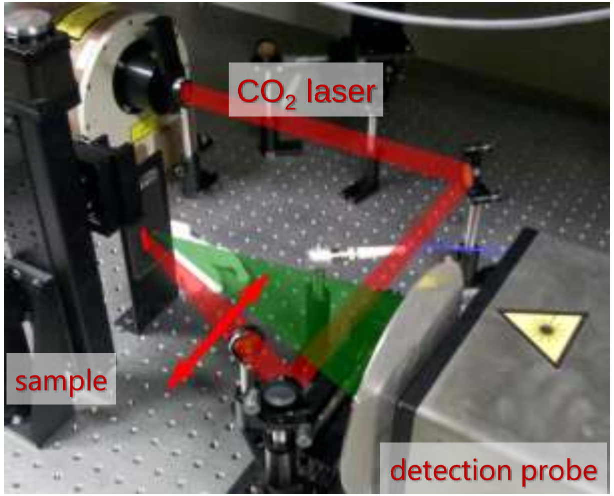

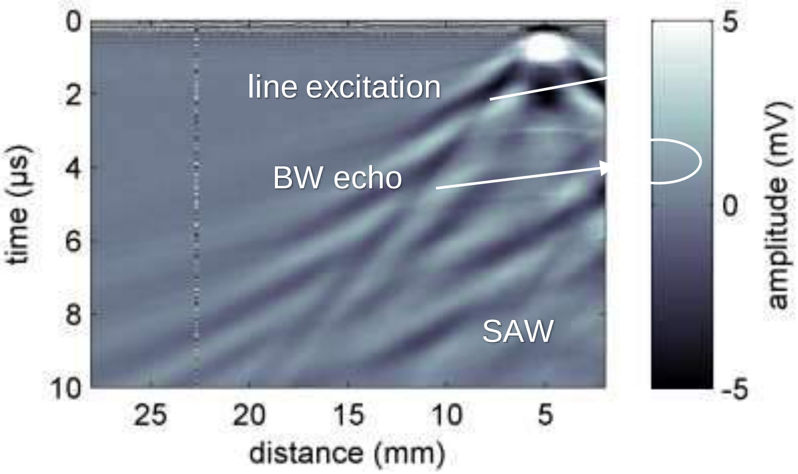

CertBond
COST Action CA18120

<u>CFRP bond characterisation using surface acoustic waves</u>:

- SAW penetration depth ~ λ:
  Interaction with bonding layer.
- Single line excitation:
  Cylindrical lens → broadband SAW generation.
- Multiple line excitation:
  Spatial light modulator (SLM) or intensity mask → single wavelength generation.
- Further investigations.

ENCOMB | 7th Framework Programme
Extended Non-Destructive Testing of Composite Bonds

RECENDT
RESEARCH CENTER NON DESTRUCTIVE TESTING

<u>Source</u>: Seyrkammer R., Galos R., Reitinger B., et. al., *Extended NDT Methods for Evaluation of CFRP Adhesive Bonds*, International Workshop on Aero Structures, October 9-11, 2013, Milano, Italy (presented by <u>W. Ostachowicz</u>)

ARRAY TECHNIQUES

CertBond
COST Action CA18120

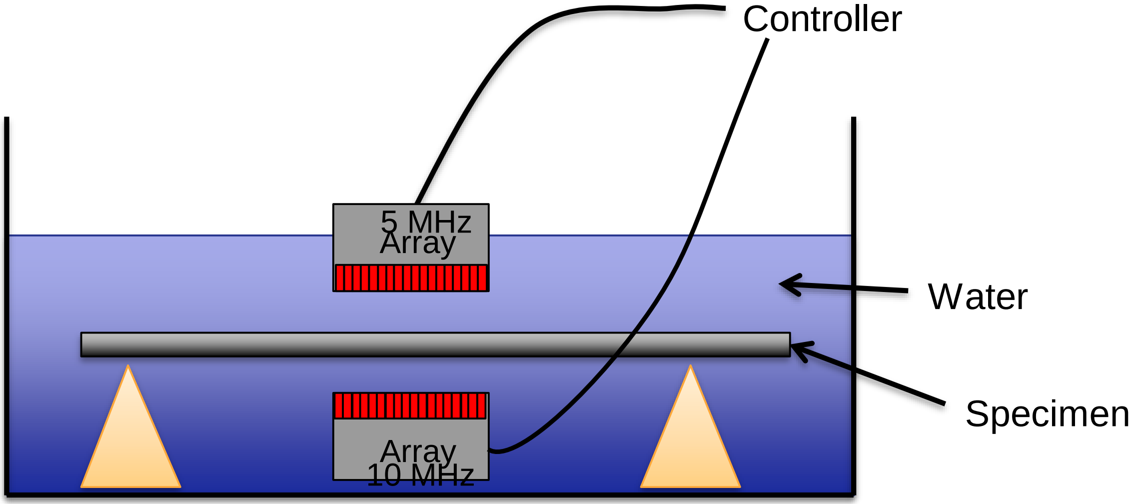

- Ultrasonic phased arrays can be used to inspect components.
- From a single sided measurement backscattered energy determines amplitude.
- Through transmission can be used to measure nonlinearity in a system with arrays at 2 frequencies.
- Both approaches studied with the configuration below.

ENCOMB | 7th Framework Programme
Extended Non-Destructive Testing of Composite Bonds

University of BRISTOL

Source: Croxford A., Sapountzi K., Neild S., *Extended NDT Methods for Evaluation of CFRP Adhesive Bonds*, International Workshop on Aero Structures, October 9-11, 2013, Milano, Italy (presented by W. Ostachowicz)

Acknowledgment

This STSM was developed under the COST Action CA18120 (CERTBOND) and supported by COST (European Cooperation in Science and Technology).

Funded by the Horizon 2020 Framework Programme of the European Union

Thank You!

www.certbond.eu

EUROPEAN COOPERATION IN SCIENCE & TECHNOLOGY

Funded by the Horizon 2020 Framework Programme of the European Union

CertBond
COST Action CA18120

Adhesion Tests via Laser Shock Waves (LASAT)

Selen Ünaldı & Mohammad AYAD

PIMM, UMR8006 ENSAM, CNRS, CNAM, 151 bd de l'Hôpital, 75013 Paris, France

Under supervision of Laurent Berthe

cost
EUROPEAN COOPERATION
IN SCIENCE & TECHNOLOGY

Funded by the Horizon 2020 Framework Programme
of the European Union

Figure 1: Aloha airlines flight 243 incident, flight suffered an extensive damage but landed safely

Explosive decompression caused by maintenance problems

Maintenance & Routine Inspection during their life time for structural bonding health- LASAT

Outline

CertBond
COST Action CA18120

- Background & Specifications
- Laser Shock Phenomena
- Experimental Results
- Technology Readiness Levels (TRL) Assesments
- Numerical Results
- Conclusion & Perspectives

CertBond
COST Action CA18120

Background & Specifications

EUROPEAN COOPERATION IN SCIENCE & TECHNOLOGY
Funded by the Horizon 2020 Framework Programme of the European Union

Structural Bonding

CertBond
COST Action CA18120

Figure 2: Manufacturing and inspection processes

Use of CFRP is increased in aeronautical industry

Airbus A380 composite part of the aircraft is 25%, for A350 it’s around 52%

With the usage of adhesive bonding, 12% of the aircraft weight can be reduced

Weak bond detection for CFRP

Figure 2: Manufacturing and inspection processes

Issues

- How to be sure about the properties during the manufacturing & use?
- How to quantify the structure of composite materials?
- Current NDTs are not proof mechanical tests for bonds so we need LASAT!

Shock Wave Creation Phenomena in Water Confinement Regime

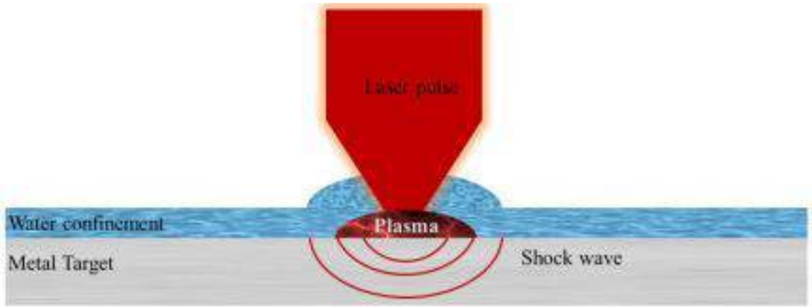

Figure 3: Shock Wave Creation Phenomena

Process Parameters

- Pulse Duration: 8-25 ns
- Wavelength: 532-1064 nm
- Energy: 0.2-50 Joules
- Repetition Rate: 1-20 Hz
- Spot Diameter: mm
- Power Density: 1-10 GW/cm^2
- Pressure: 1-8 GPa

Why confined regime?

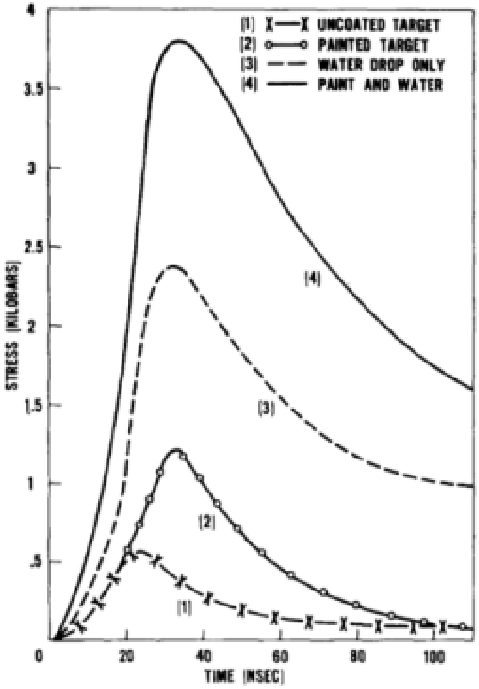

Figure 4: Stress wave histories in 1. 0 mm aluminum targets for various coatings.
Retrieved from: Fox (1974), Effect of water and paint coatings on laser-irradiated targets

ADVANTAGES

- Pressure x4 higher than in direct regime
- Loading x2 longer
- Easy to apply
- Cheap

ISSUES

- Needs a protective layer/ablator layer
- Breakdown plasma in confined material layer (screens a notable amount of the incident laser pulse)
- Difficult to use in specific processes (need of a solid confinement)

Shock Wave Propagation Space-Time Diagrams

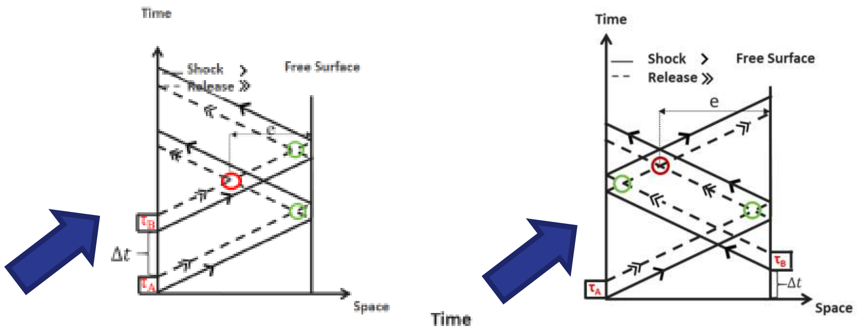

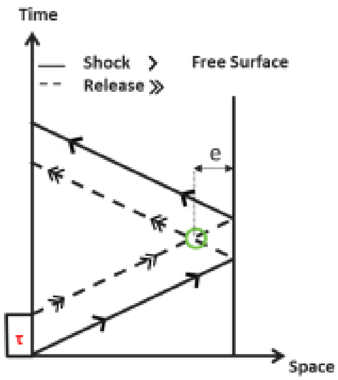

(a) Mono Impact

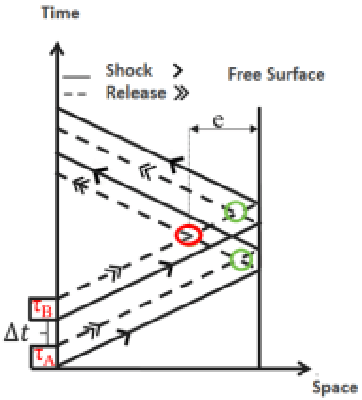

(b) Double Impact

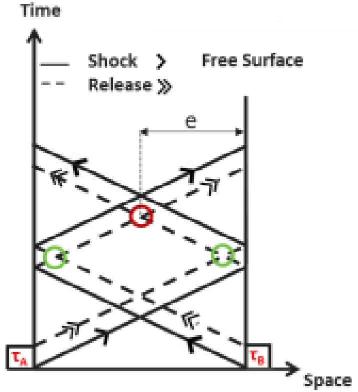

(c) Symmetrical Impact

Figure 5: Space-time diagrams for different scenarios**.**

- The front of the shock wave is solid lines & release wave which sets the material back to its initial state is dotted lines
- Upon crossing the initial release wave, the reflected shock wave generates a tensile stress
- The tensile stress location can be shifted by playing with the laser parameters (need of simulation to optimize many different parameters such as pulse duration, applied power densities, used focal spots)

How does it work?

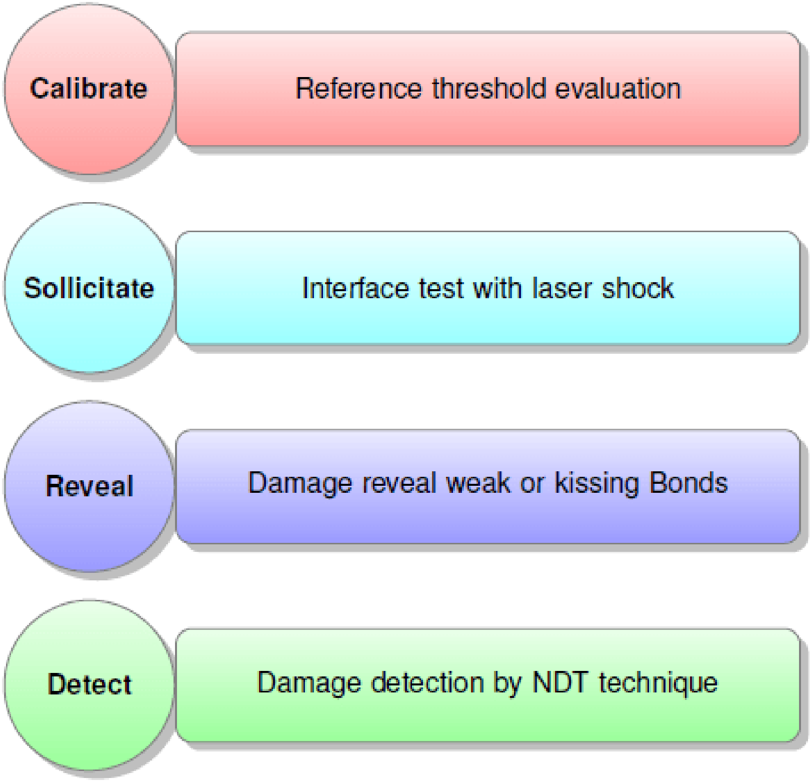

LASAT enables the generation of high tensile stresses within the material, which can debond or not depending on its strength.

- **Damage Creation for weak bond via LASAT**
- **No Damage Creation for correct bond (correct bond defined by the company/project)**

Sollicitate, Reveal, Detect : Shock laser + US C-scan - PhD R.Ecault

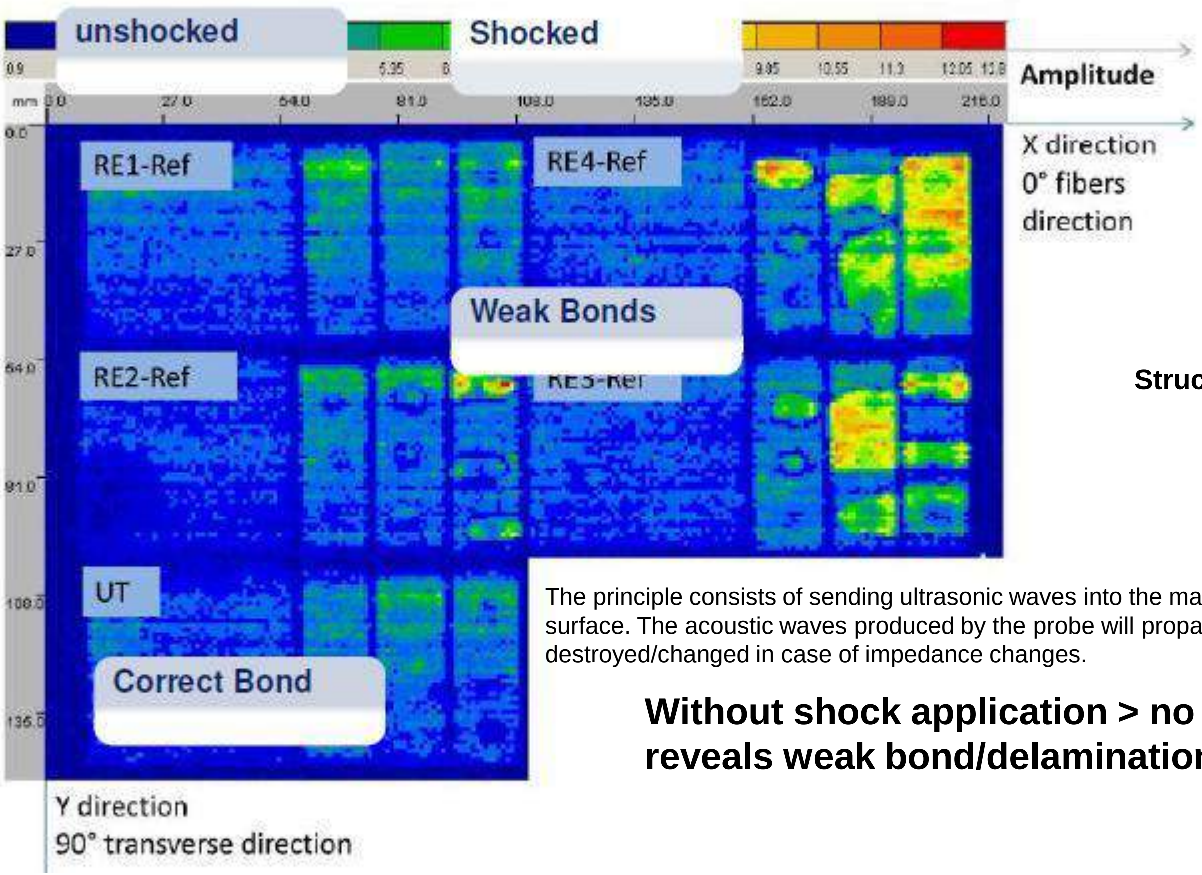

Figure 7: C-Scan Result

Structural Bonding Applications (mm scale)

The principle consists of sending ultrasonic waves into the matter through an emitter placed on the surface. The acoustic waves produced by the probe will propagate through the sample and be destroyed/changed in case of impedance changes.

Without shock application > no weak bond detection >LASAT reveals weak bond/delamination!

LASAT on External Aircraft Coatings?- PhD S. Ünaldı

- Lasat technique also applied on External Aircraft Coatings (paint) side of aircrafts. Different type & thicknesses of layers and applied thermal ageing conditions are investigated **(µm scale).**

Figure 8: Example of EAC with a laser

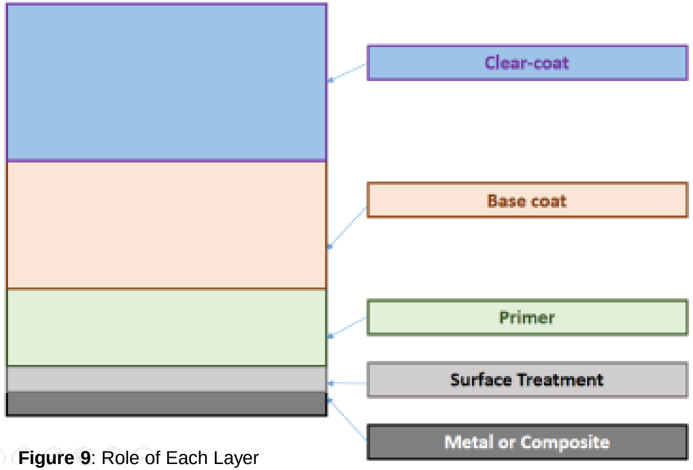

Figure 9: Role of Each Layer

Figure 10: Example of a coated sample

Primer: (Chemical Family-Epoxy)

- Protecting the substrate from corrosion
- Present a good level of adhesion between layers

Base Coat: (Chemical Family-Polyurethane)

- Bring optional and functional properties to painting architecture
- To resist external environmental attacks (dust, sand, lightning strike)

Clear Coat: (Chemical Family -Mainly Polyurethane)

- Bring an esthetic, protective and functional properties to base-coat

ISSUES


Material
under
Shock
Laser
Interaction
Damaging
Laser
Adhesion Test
Laser
technologie
Interface
Adhesion
NDT
Modeling

RESULTS

Funded by the Horizon 2020 Framework Programme
of the European Union

EU Projects to NDT Assesments

CertBond
COST Action CA18120

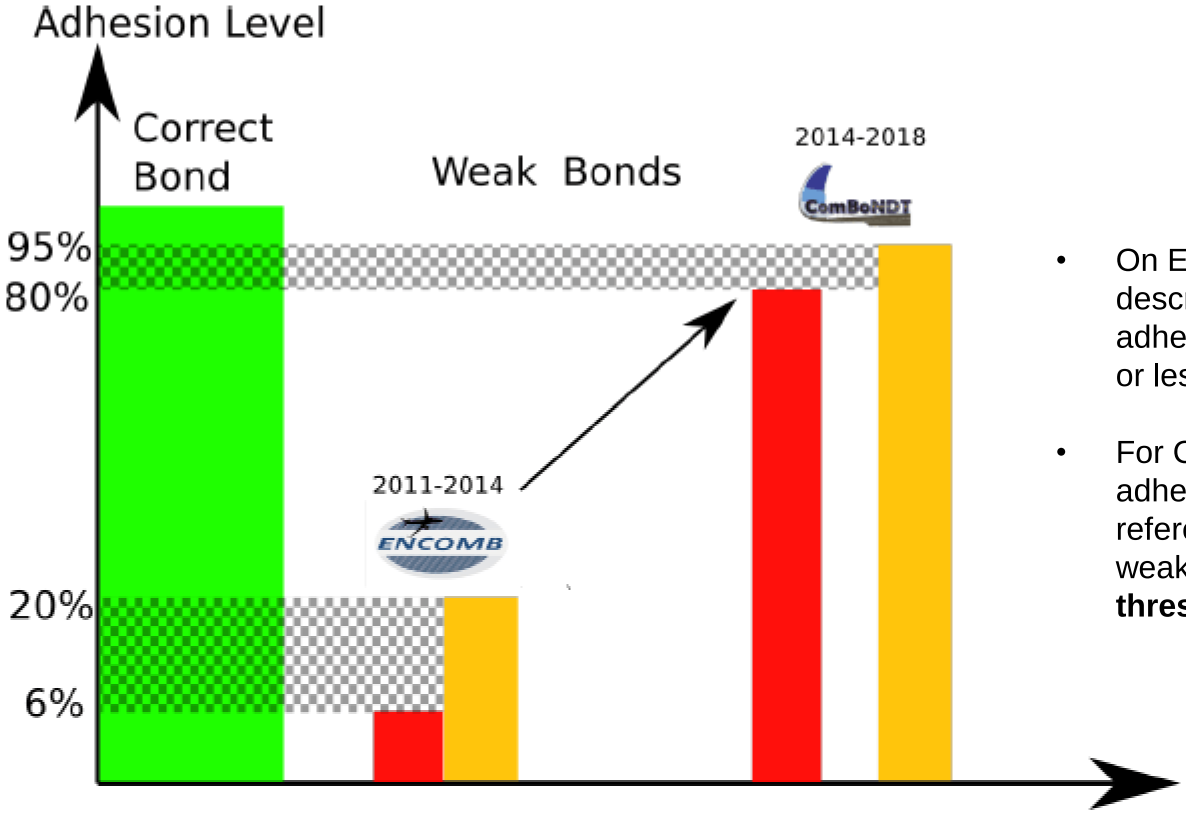

Figure 11: ENCOMB and ComBoNDT Projects.

- On Encomb, weak bonds were described as bond with an adherence level equivalent to 20% or less of a reference bond.
- For ComBoNDT, bonds with an adherence level of 80% of a reference ones are considered as weak bonds (**the weak bond threshold has been increased**)

EU Projects to NDT Assesments

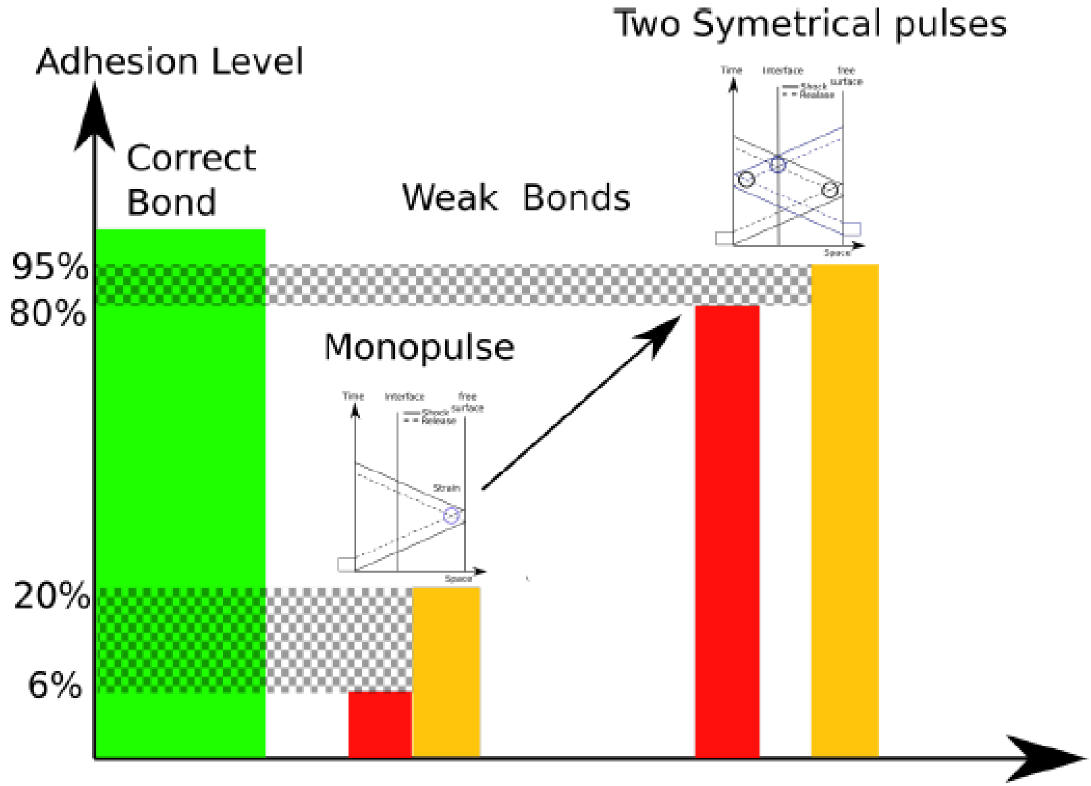

- ENCOMB- mono impact, very weak production scenarios
- Combondt- symmetrical impact, weak and extended production scenarios to increase TRL
- Two scenarios are common between ComBoNDT and ENCOMB: the release agent and moisture contamination

Figure 12: ENCOMB and ComCoNDT with pulse scenarios

Contamination Scenarios-PhD M. Sagnard

Project defined two sets of contaminants, the one mainly found on production lines and the one typical from repair lines for the ENCOMB project.

Finger print: finger print residues can be left on the part during its manipulation.

Contamination

De-icing fluid: To prevent the wings from freezing, a de-icing fluid is applied on their surfaces. This fluid can penetrate through voids and leave residues deep inside of the structure.

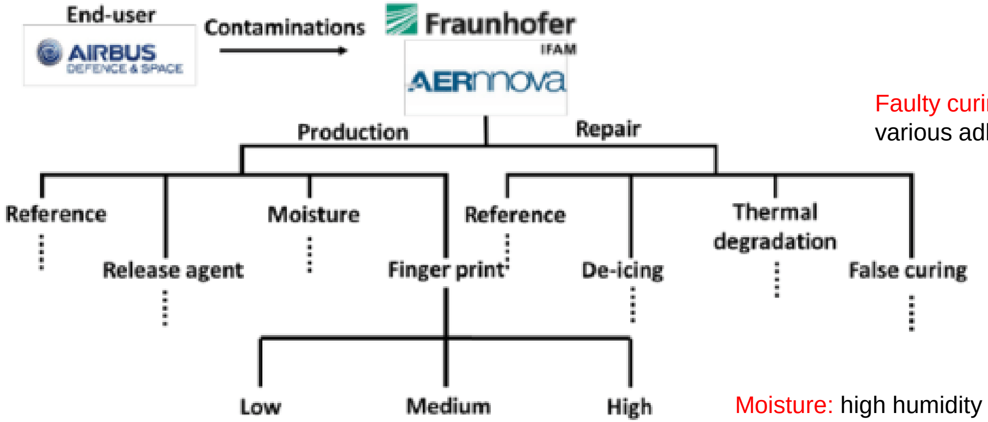

Faulty curing: epoxy curing may not always be homogeneous which might lead to various adherence levels on a same surface.

Moisture: high humidity levels may be reached in the production line leading to water take-up. This water is later released during the curing process, weakening the bond strength.

Figure 13: Contamination Scenarios.

Retrieved from: Maxime Sagnard. Detection of Weak Bonds in Bond CFRP Assemblies using Symmetrical LAser Shock Adhesion Test (S-LASAT). PhD thesis, 2019. Thèse de doctorat dirigée par Berthe, Laurent Mécanique-matériaux (AM) Paris, ENSAM 2019

Release Agent Detection Sensibility- PhD M. Sagnard

Release agent: to ease up the de-moulding process of composite panel, a solution, release agent, is sprayed onto the mould before the part is cured. After the whole process, and the part removed from the mould, some traces of this solution can be found on the surface of the sample if not cleaned properly.

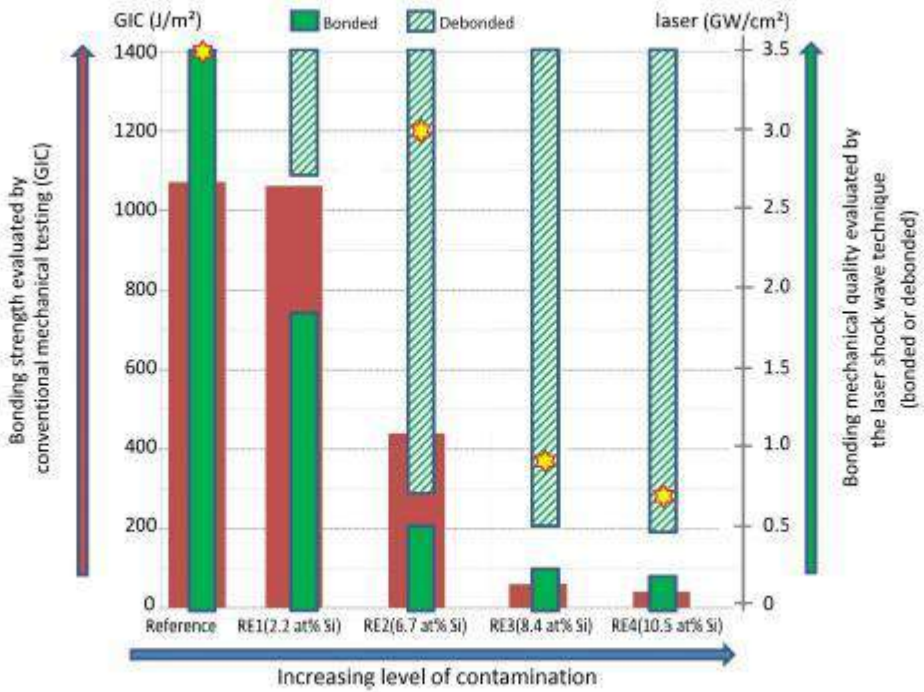

Figure 14: Levels of contamination.

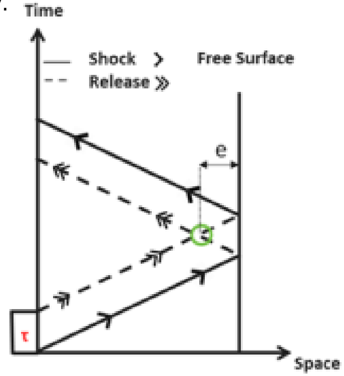

- Damage threshold value decreases with release agent level contamination
- No threshold for Correct Bond (too high to detect)

Retrieved from: Maxime Sagnard. Detection of Weak Bonds in Bond CFRP Assemblies using Symmetrical LAser Shock Adhesion Test (S-LASAT). PhD thesis, 2019. Thèse de doctorat dirigée par Berthe, Laurent Mécanique-matériaux (AM) Paris, ENSAM 2019

Release Agent Detection Sensibility- PhD M. Sagnard

CertBond
COST Action CA18120

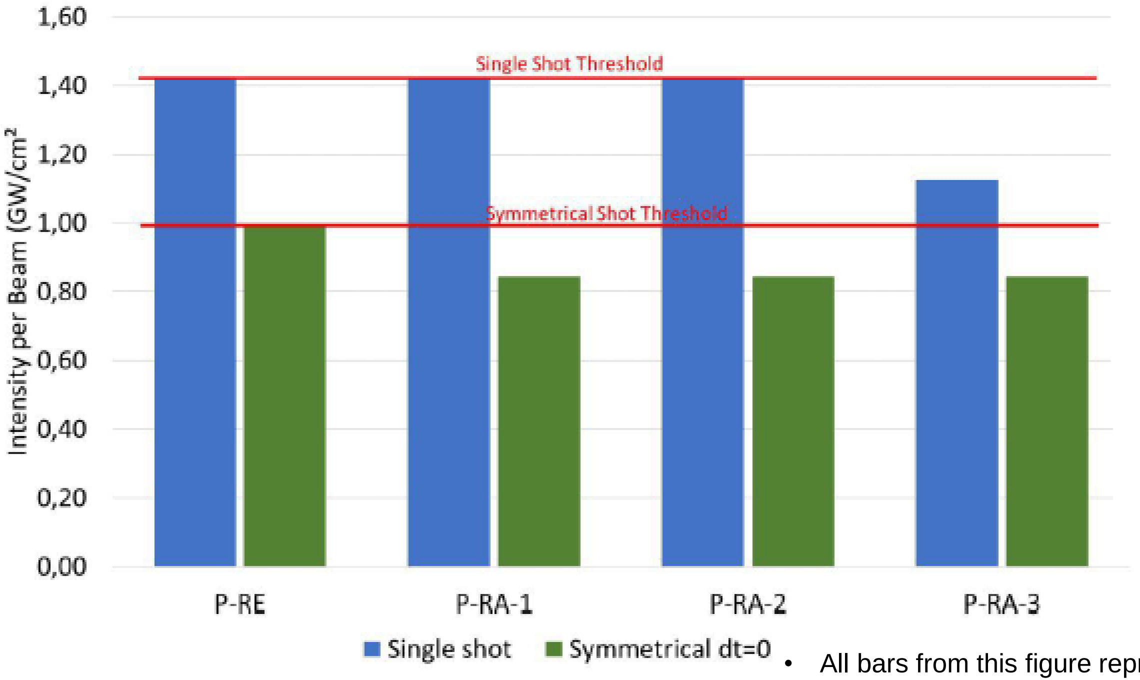

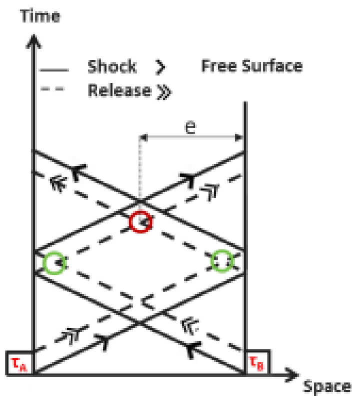

Figure 15: Release Agent Detection Sensibility.

Retrieved from: Maxime Sagnard. Detection of Weak Bonds in Bond CFRP Assemblies using Symmetrical LAser Shock Adhesion Test (S-LASAT). PhD thesis, 2019. Thèse de doctorat dirigée par Berthe, Laurent Mécanique-matériaux (AM) Paris, ENSAM 2019

- All bars from this figure represent the bond threshold
- Impossible to to generate a debonding without damaging the CFRP – mono impact
- Detection of all levels of contamination -symmetrical

LASAT- External Aircraft Coatings / Different Primer Thicknesses

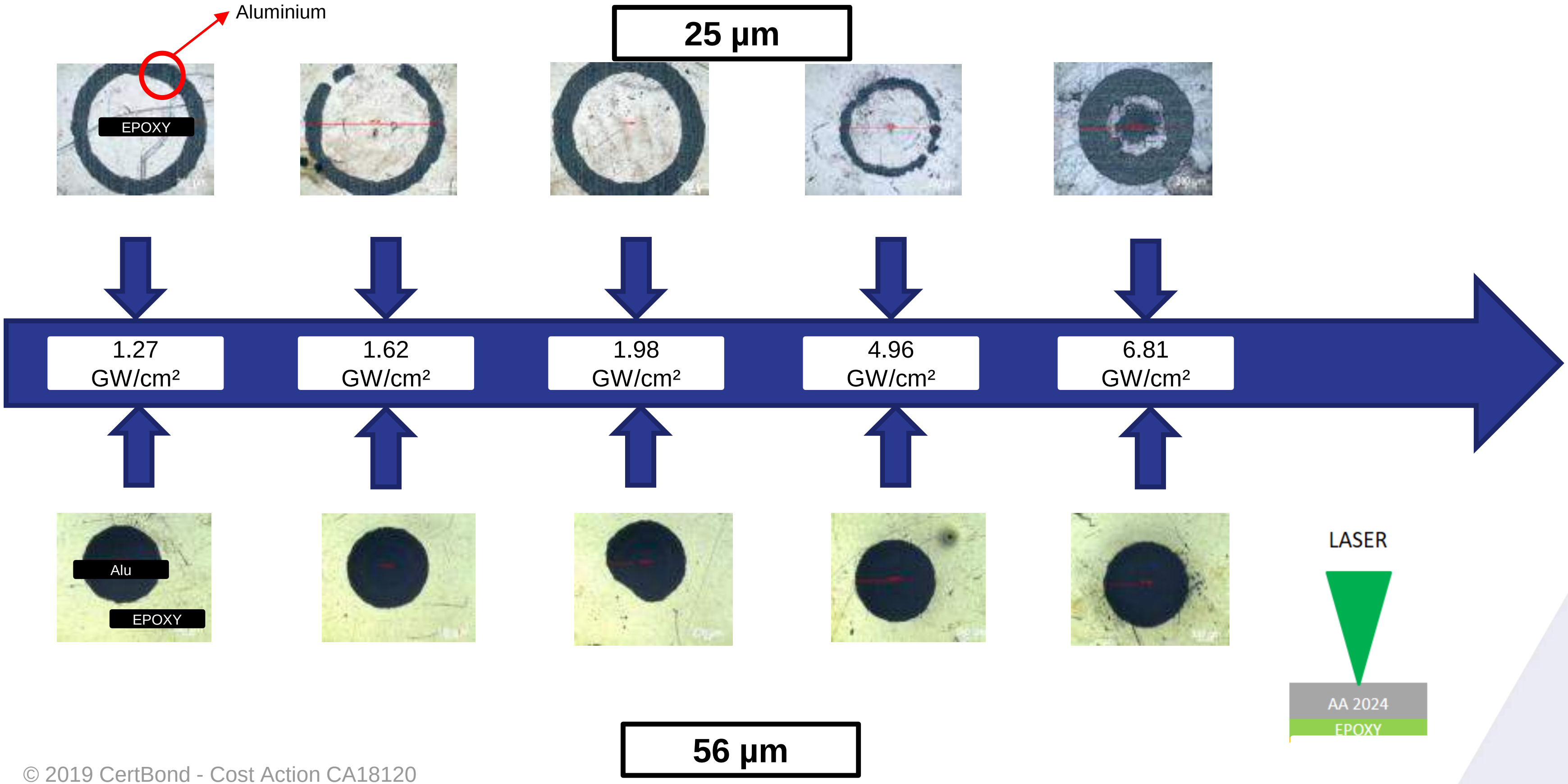

Figure 16: Adhesion levels as function of different epoxy thicknesses under optical microscope

LASAT- External Aircraft Coatings / Numerical Work

The predicted initiation and propagation of failure of the cohesive zone for the cases of I= 1.75 GW/cm² and I=8.23 GW/cm² is depicted.

For the lower intensity/pressure, “damage ring” is formed while for the higher intensity the entire circular area fails

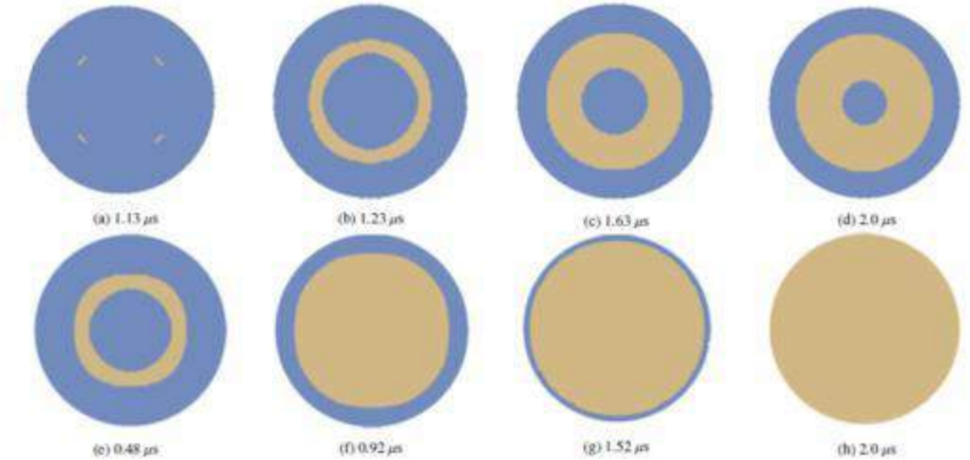

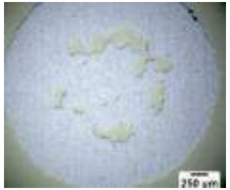

Figure 17: Predicted initiation and propagation of failure of the cohesive zone for the cases of (a) I= 1.75 GW/cm² and (b) I=8.23 GW/cm² This finding is a first verification of the model’s capability to simulate laser shock-induced stripping.

In collaboration with Patras University (for more, see Kosmas Papadopoulos’s poster)

Retrieved from: S. Unaldi, K. Papadopoulos, A. Rondepierre, Y. Rouchausse, A. Karanika, F. Deliane, K. Tser-pes, G. Floros, E. Richaud, and L. Berthe. Towards selective laser paint stripping using shockwaves produced by laser-plasma interaction for aeronautical applications on aa 2024 based substrates. 2021

LASAT- External Aircraft Coatings / Thermal Ageing of Primer

Because of their activity in the air, the external parts of the aircraft are exposed to a high degree of sunlight. In order to simulate the natural exposure conditions of the external parts of the aircraft, thermal ageing conditions applied. To do this, samples of AA2024+epoxy are inserted into ventilated ovens heated between 60 and 120°C.

Samples	Conditions	Duration
AA 2024+Epoxy	Thermal Ageing (180°C)	1h 1h30 4h
AA 2024+Epoxy	Thermal Ageing (150°C)	24h 48h 72h 100h
AA 2024+Epoxy	Thermal Ageing (120°C)	7 days 21 days
AA 2024+Epoxy	Thermal Ageing (60°C)	7 days

Table 1: Thermal ageing conditions with their respective durations.

When epoxy resin networks undergo a temperature increase, the major changes observed are the formation of carbonyl and amide products. It loses some of its mechanical properties - shear strength decreases.

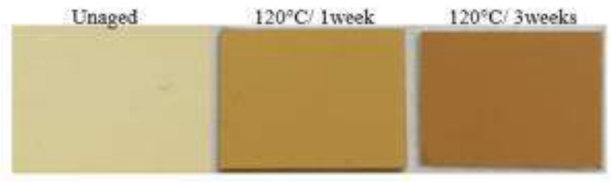

Figure 18: Ageing evaluation

LASAT- External Aircraft Coatings / General View

1) Thickness and Type Variation

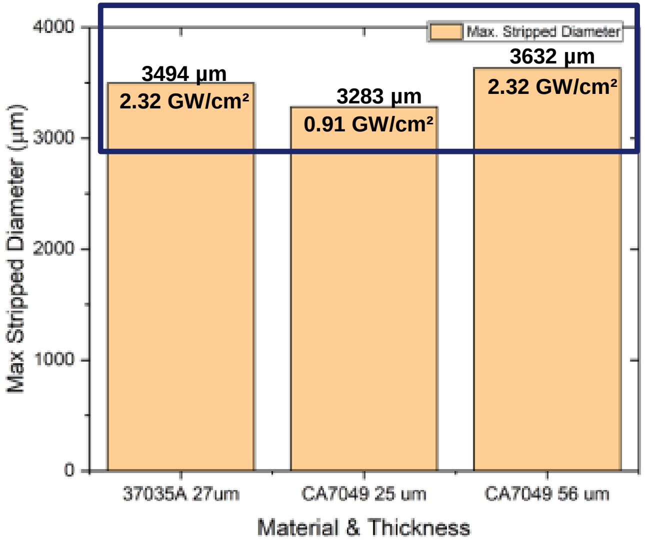

Figure 19: Effect of epoxy thickness & type variation.

2) Thermal Ageing Variation

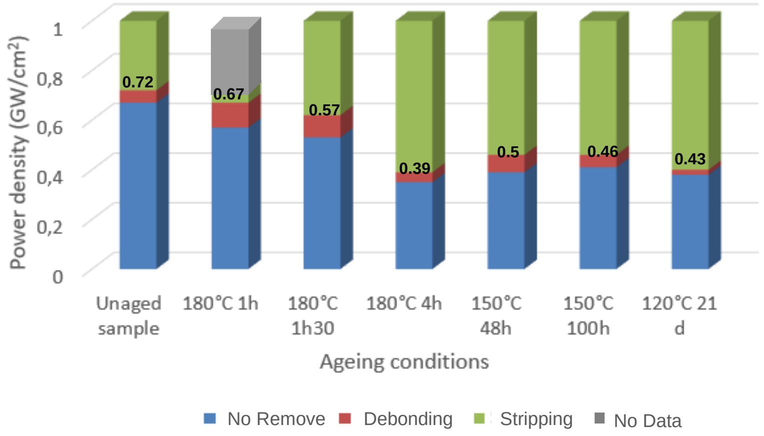

Figure 20: Effect of thermal ageing variation.

TRL Assesments

Funded by the Horizon 2020 Framework Programme
of the European Union

INDUSTRIAL CONSTRAINS

Laser Parameters

- Top Hat Shaped Laser (extra diagnostic)
- Laser Stability
- Min 6 Joules of Energy with defined spot sizes (mm)

Material Related

- Several meters long parts to treat
- Thickness variation

Enviromental Constrains

- Repair 1 day to 2 weeks : Parked plane costs a lot
- Temperature (15 -27°C) – humidity (20 – 70%)
- No water as a confinement

SOLID CONFINEMENT

Commercial polymers

Coroplast

Acrylate Pressure Sensitive Adhesive

- Controled formulation
- Different controlled thicknesses

Polymer synthesis

Gelest   DOW CORNING

Silicone radical polymerization

- Controled tack and cross-linking
- Controled thickness to some extent

PROS OF POLYMER CONFINEMENT

- Adaptation to complex surfaces
- Flexible properties

WHICH PROPERTIES?

- Transparent in IR/VIS
- High temperature resistance
- Easy bonding/debonding
- Generated pressure up to 4 GPa

PRESSURE COMPARISON- PhD C. Le Bras

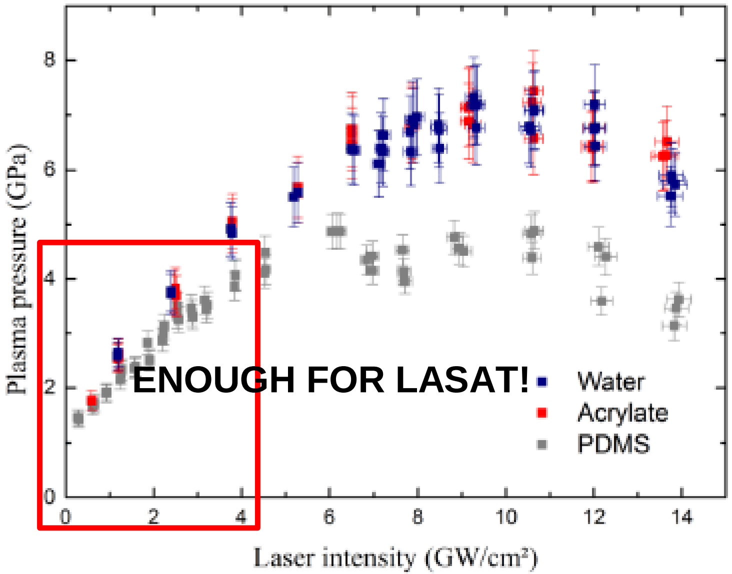

Same pressure as water – acrylate

Glass as a confinement

Transparent Acrylate Tape

Figure 21: Effect of confinment on obtained pressure. **Retrieved from:** Le Bras(2019), Metals, 9(7), 793

SPOT SIZE – WITH & WITHOUT DOE

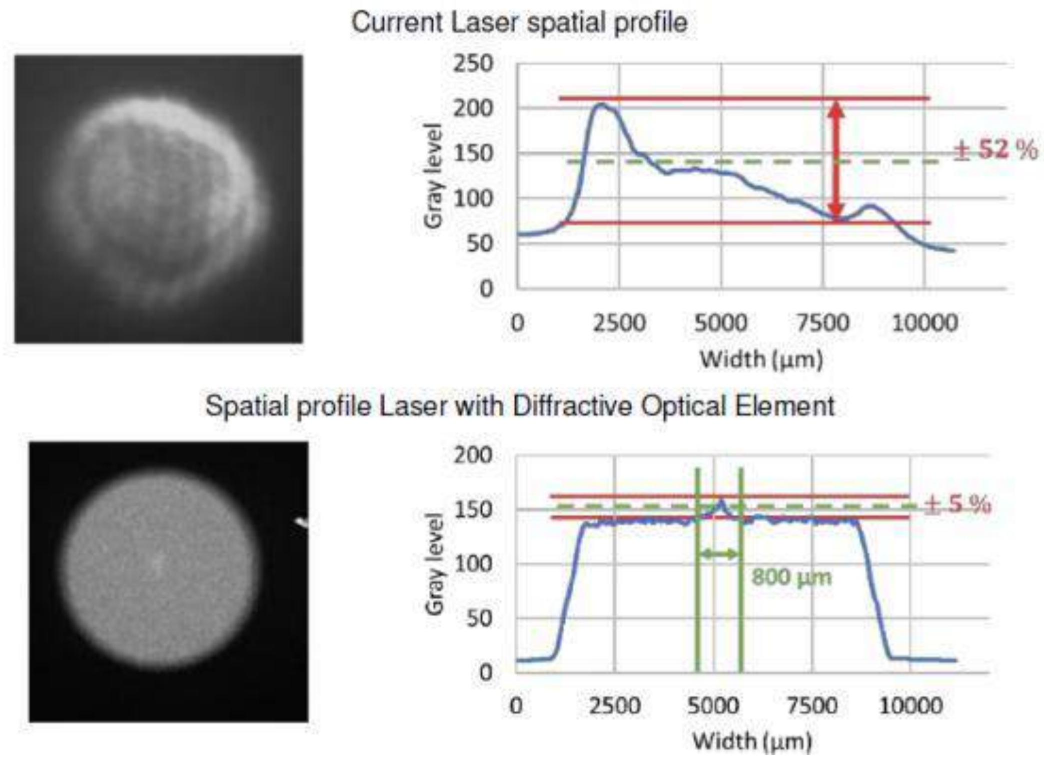

Figure 22: Laser Spot Spatial with/without DOE

DEMONSTRATION/VALIDATION- PhD M.Sagnard

CertBond
COST Action CA18120

Repair Panel

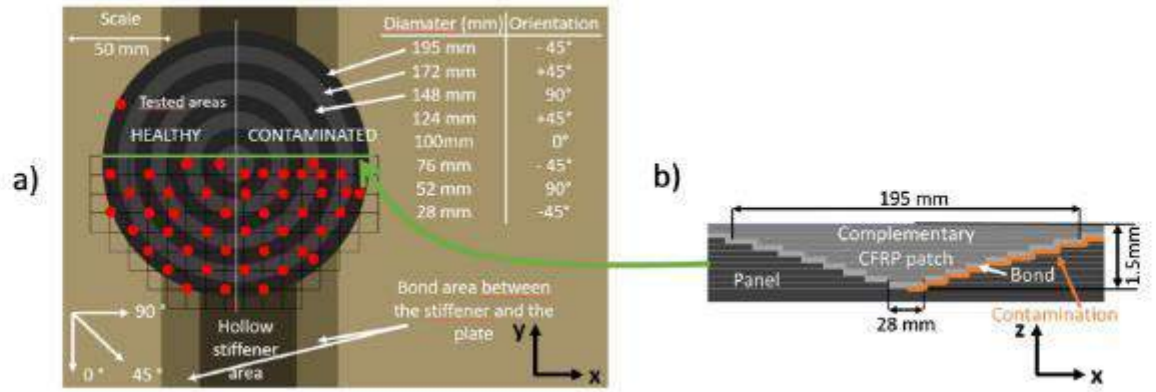

Figure 22: Repair Panel

Panel	Area	SYMMETRICAL SHOT SETUP: S-LASAT threshold I_t (intensity per beam)	Total number of shots at 80% of I_t	Number of opened bonds	SINGLE SHOT SETUP: LASAT threshold I_t (total intensity)	Total number of single shots at 80% of I_t	Number of opened bonds
Production	Healthy	0.85GW/cm²	32	0			
	Contaminated		21	21			
Repair	Healthy	0.72GW/cm²	8	0	0.84GW/cm²	7	0
	Contaminated		8	8		10	2
		Success rate: 100%			Success rate: 20%		

Retrieved from: Maxime Sagnard. Detection of Weak Bonds in Bond CFRP Assemblies using Symmetrical LAser Shock Adhesion Test (S-LASAT). PhD thesis, 2019. Thèse de doctorat dirigée par Berthe, Laurent Mécanique-matériaux (AM) Paris, ENSAM 2019

Numerical Results

Funded by the Horizon 2020 Framework Programme
of the European Union

Numerical modeling using LS-DYNA

CertBond
COST Action CA18120

Selective Laser Paint Stripping

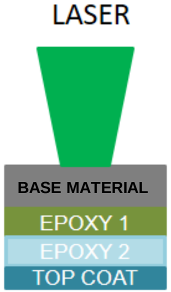

Laser Paint Stripping from Specimen Side

OPENED UP A NEW PERSPECTIVE

Laser Paint Adhesion Tests

- Different Thickness
- Surface Treatment
- Thermal Ageing

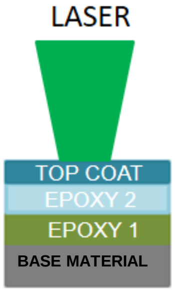

Laser Paint Stripping from Paint Side

NUMERICAL OPTIMIZATION IS ONGOING

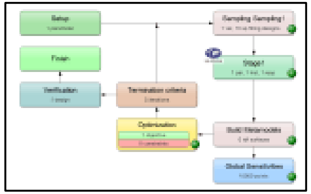

Numerical modeling using LS-DYNA

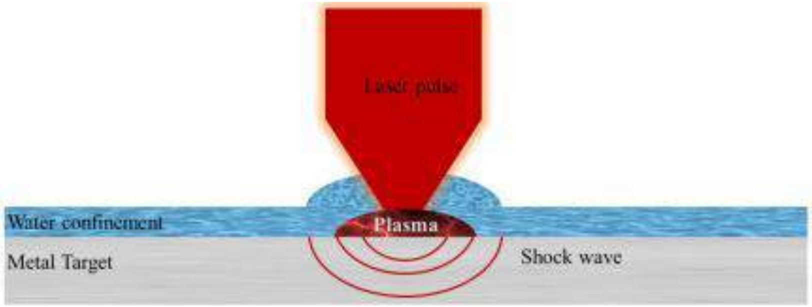

Figure 23: Shock Wave Creation Phenomena

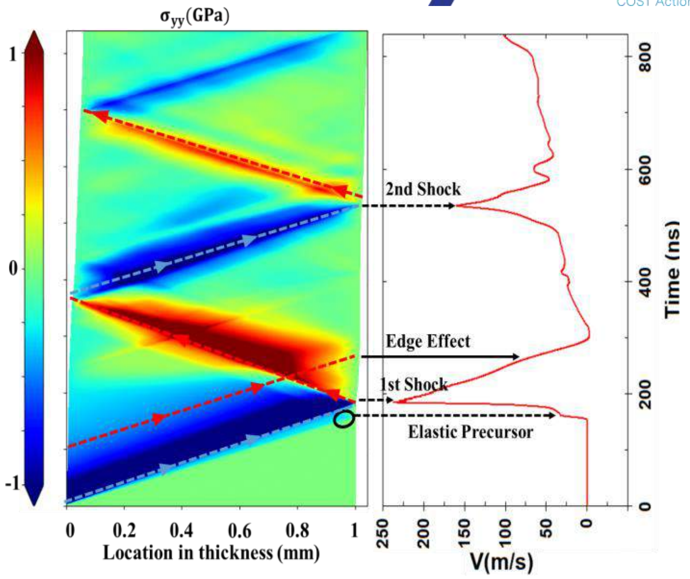

Figure 24: Stress level (vertical axis) during the wave propagation through the target thickness(horizontal axis) and during the laser shock with the associated BFV profile under 3.3GW/cm² laser intensity and 3 mmfocal spot.

Héphaïstos Laser Facility

VISAR pure-AL + Material model

↓

Boundary conditions → Boundary conditions + New material ⇒ Material model

Numerical modeling using LS-DYNA

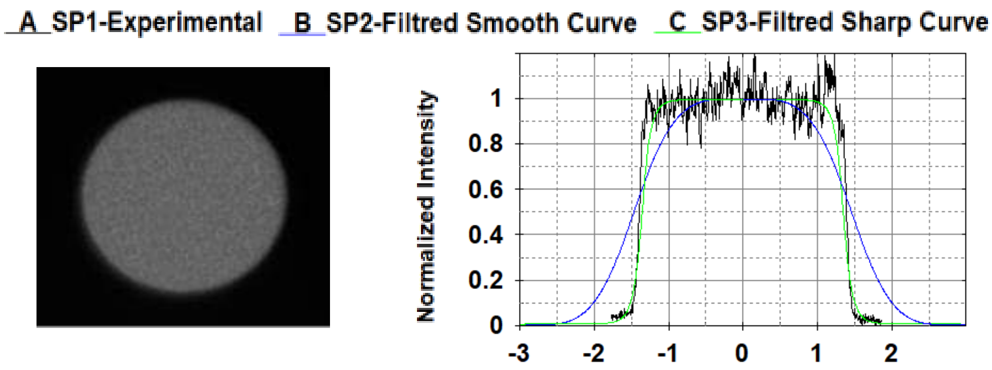

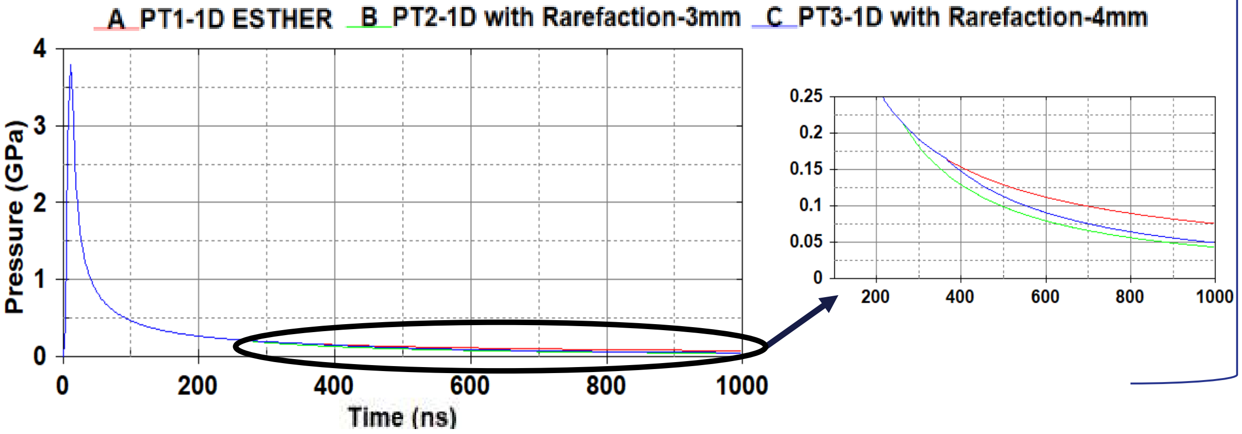

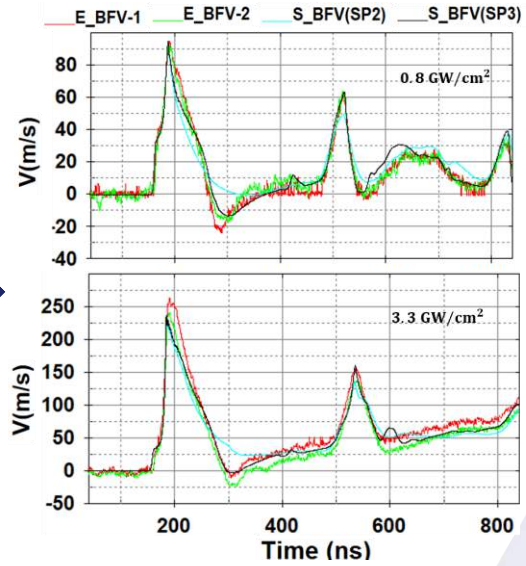

Numerical modeling using LS-DYNA

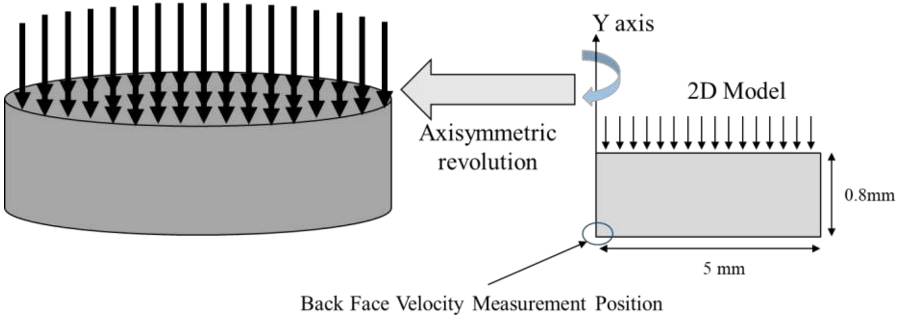

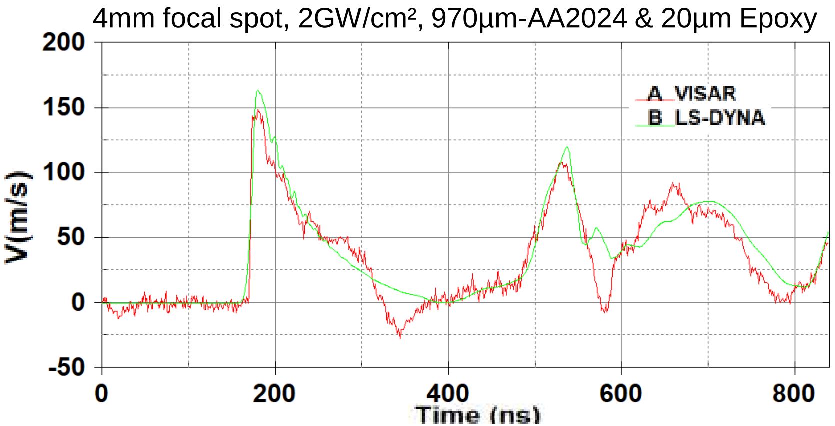

Epoxy primer CA7049

MAT_ELASTIC_PLASTIC_HYDRO

Parameters	Values
$\rho(\mathrm{kg/m^3})$	1700
G (MPa)	1600
C (m/s)	2000
S	1.493
γ_0	1.13
σ_{yy} (MPa)	5
EH (MPa)	10

Numerical modeling using LS-DYNA

PT1=0,24GW/cm² + PT2=0,52 GW/cm² - 48 µm d'epoxy+970 µm AA-2024

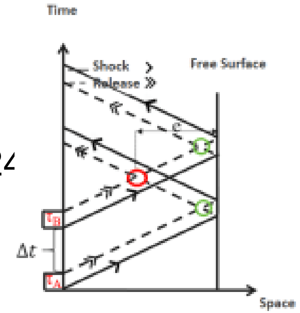

4mm focal spot+28µm Al tape

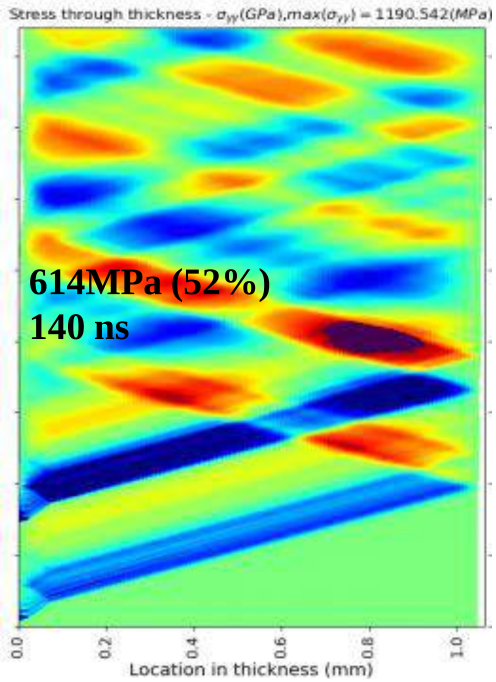

4mm focal spot+0µm Al tape

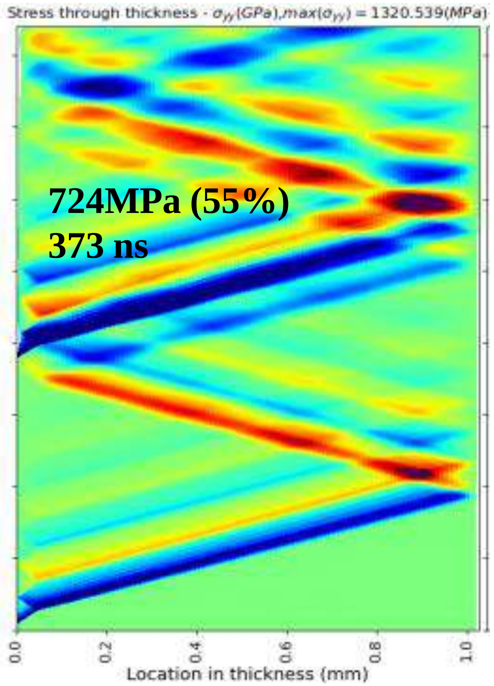

3mm focal spot+28µm AL tape

680MPa (54%)
160 ns

3mm focal spot+0µm AL tape

732MPa (55%)
373 ns

The negligable thickness of Al tape (< 3µm) is providing bigger tensile stress at the interface, it can be done using thin film deposition techniques (ion sputtering) which is not feasible for industrial applications

Numerical modeling using LS-DYNA

CertBond
COST Action CA18120

PT1=0,24GW/cm²+PT2=0,52 GW/cm²-4mm focal spot-48µm epoxy-28 µm AL tape

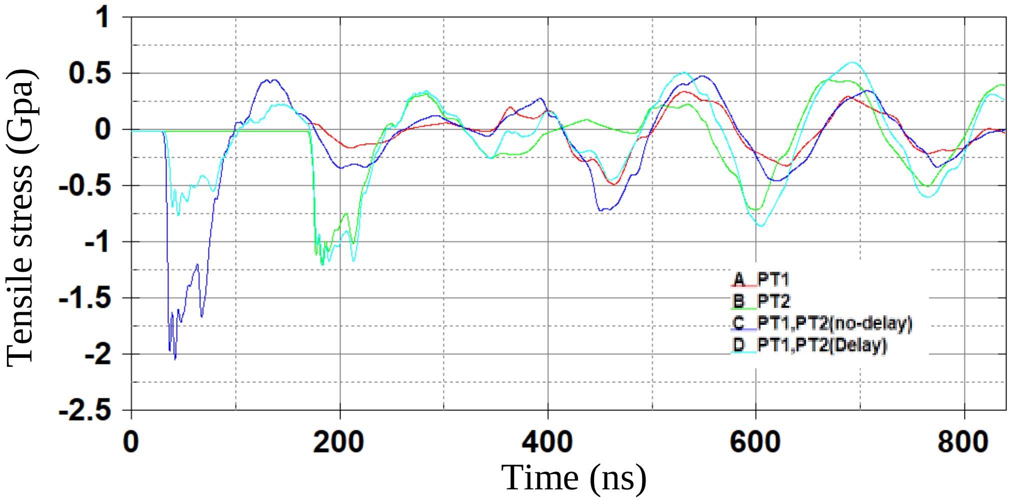

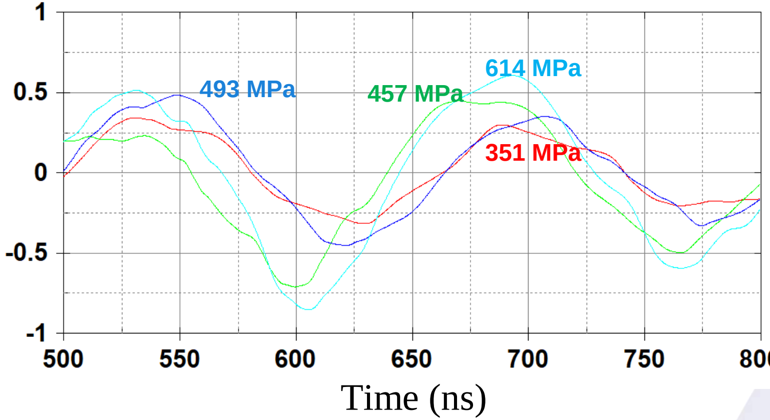

- By increasing the thickness of the aluminum tape the value of the stress at the interface decreases
- For some configurations we do not need the delay between the two beams

Symmetrical laser shock

50 µm AL tape with 6mm of pure AL plate

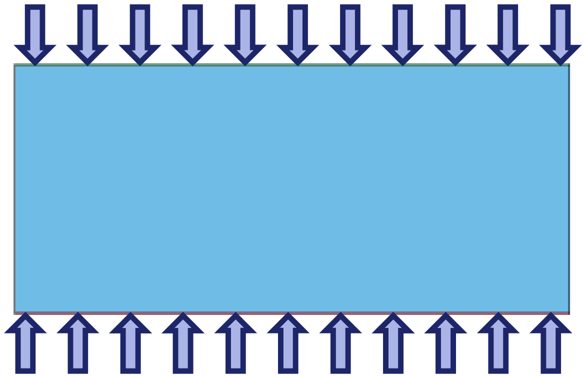

JOHNSON-COOK

Pure-AL

MID	RO	G	E	PR	DTF	VP	RATEOP
1	2.699e-06	25.000000	0.0	0.0	0.0	1.0	0.0
A	**B**	**N**	**C**	**M**	**TM**	**TR**	**EPSO**
0.0900000	0.2000000	0.3000000	0.0350000	1.0000000	775.00000	298.00000	0.0010000
CP	**PC**	**SPALL**	**IT**	**D1**	**D2**	**D3**	**D4**
875.00000	0.0	2.0	0.0	0.0	0.0	0.0	0.0
D5	**C2/P**	**EROD**	**EFMIN**	**NUMINT**			
0.0	0.0	0	1.000e-06	0.0			

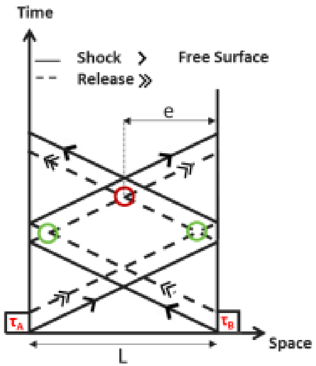

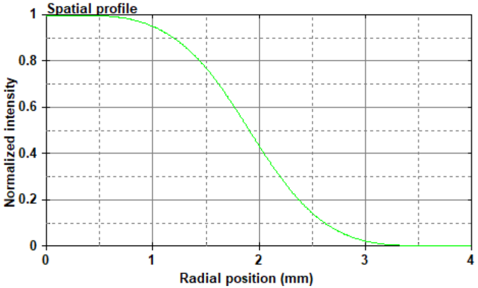

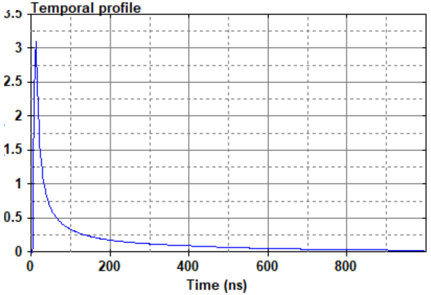

Equation of State

EOSID	C	S1	S2	S3	GAMAO
1	5328.0000	1.3380001	0.0	0.0	2.0000000
V0	**-**	**LCID**			
0.0	0.0	0			

Symmetrical laser shock

CertBond
COST Action CA18120

6mm-AL (1500 kg/m³) – 50 µm AL tape (2700 kg/m³) - 4mm focal spot

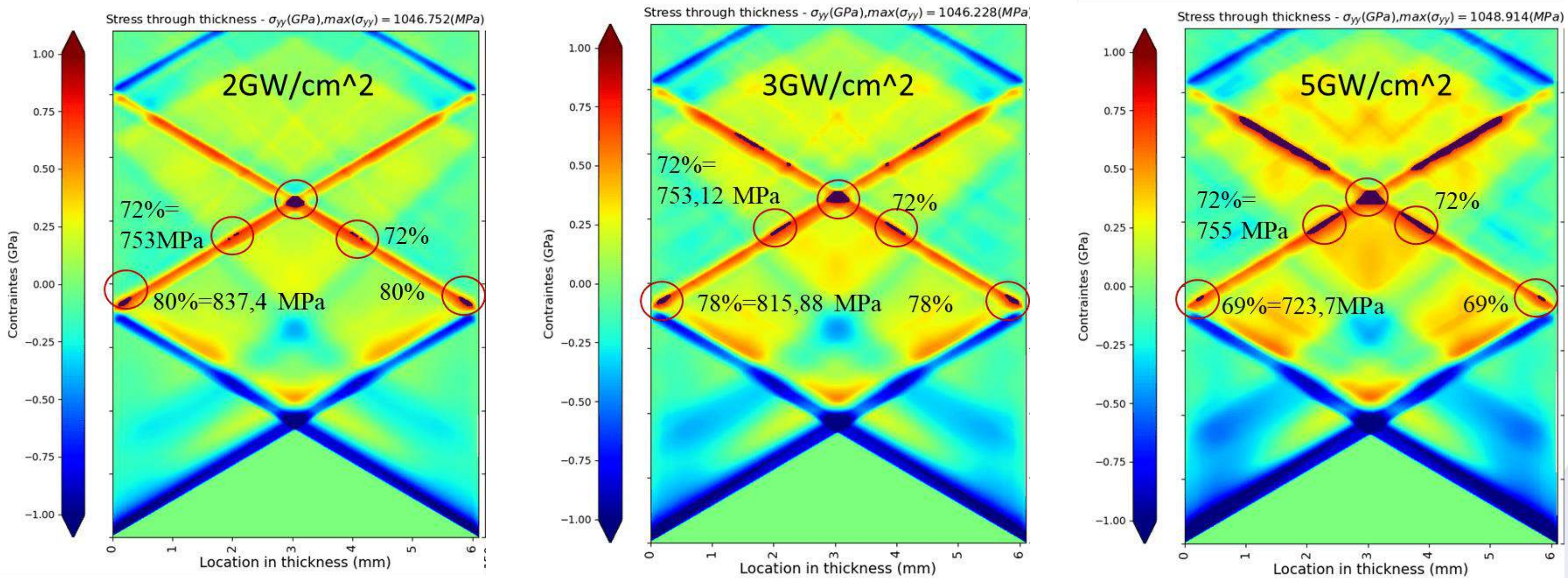

Important created tensile zones proved to be sensible to laser intensities, tape thickness, laser focal spot and for sure the delay between beams

CertBond
COST Action CA18120

Conclusion & Perspectives

EUROPEAN COOPERATION
IN SCIENCE & TECHNOLOGY

Funded by the Horizon 2020 Framework Programme
of the European Union

CONCLUSION

- Monopulse for very weak bonds
- Symetrical (and double pulses) impacts detect all weak bonds
- Adhesion level sensitivity (thickness,ageing,type) of External Aircraft Coatings has been proved.
- For each configuration of selective stripping for external aircraft coatings, laser parameters will be optimized numerically for experimental work.

PERSPECTIVES

2022 : Rescoll - demonstration at representative scale

The effect of pulse duration to locate the tensile stresses on the stack of Aluminium+Epoxy, will be studied in detail both numerically and experimentally.

Scientific issues : Predictive models for laser interaction and damage in collaboration with University Patras.

Acknowledgments

Researchers (PIMM): Y.Rouchausse, M.Gervais, B. Fayole, N. Mechbal, Emmanuel Richaud

Researchers (Collaborations): K.Tserpes (U.Patras), L.Videau (CEA), F. Touchard (PPrime), M. Boustie (PPrime), K. Brune (IFAM), Alexandra Karanika (HAI)

Phd's: S. Ünaldı, C. Le Bras, A.Rondepierre, M. Scius-Bertrand, M.Guerbois

Post-Doctorates: Mohammad Ayad

Projects:

- Compochoc: Rescoll, Airbus, Safran, Thales, IDIL, PIMM, CEA, Kuka
- Monarque : Safran, Airbus, Dassault, Thales, Imagine Optic, CEA, PIMM
- Forglaser : Airbus, Thales, PIMM, I2M, Imagine Optic, CEA
- Vulcan: Rescoll, HAI, PIMM, Fraunhofer, Dassault, Akzo Nobel
- Vanesse: RESCOLL-Dyna LS+

Funded by the Horizon 2020 Framework Programme of the European Union

REFERENCES

[1] S. Unaldi, K. Papadopoulos, A. Rondepierre, Y. Rouchausse, A. Karanika, F. Deliane, K. Tserpes, G. Floros, E. Richaud, and L. Berthe. Towards selective laser paint stripping using shockwaves produced by laser-plasma interaction for aeronautical applications on AA 2024 based substrates. 2021

[2] K. Tserpes, K. Papadopoulos, S. Unaldi, and L. Berthe. Development of a Numerical Model to Simulate Laser-Shock Paint Stripping on Aluminum Substrates. Aerospace, 2021.

[3] Rondepierre, S. Unaldi, Y. Rouchausse, L. Videau, R. Fabbro, O. Casagrande, C. Simon-Boisson, O. Besauc´ele, H.and Castelnau,L. Berthe, Beam size dependency of a laser-induced plasma in confined regime: Shortening of the plasma release. influence on pressureand thermal loading, Optics & Laser Technology 135 (2021) 3. doi:10.1016/j.optlastec.2020.106689.

[4] M. Scius-Bertrand, L. Videau, A. Rondepierre, E. Lescoute, Y. Rouchausse, J. Kaufman, D. Rostohar, J. Brajer, L. Berthe, Laser inducedplasma characterization in direct and water confined regimes: new advances in experimental studies and numerical modelling, Journal of Physics D: Applied Physics 54 (5) (2020). doi:10.1088/1361-6463/abc040.

[5] R. Fabbro, J. Fournier, P. Ballard, D. Devaux, and J. Virmont, “Physical study of laser-produced plasma in confined geometry,” J. Appl. Phys., vol. 68, no. 2, pp. 775–784, 1990.

[6] L. Berthe, R. Fabbro, P. Peyre, L. Tollier, and E. Bartnicki, “Shock waves from a water-confined laser-generated plasma,” J. Appl. Phys., vol. 82, no. 1997, pp. 2826–2832, 1997.

[7] L. Berthe et al., “State-of-the-art laser adhesion test (LASAT),” Nondestruct. Test. Eval., vol. 26, no. 3–4, pp. 303–317, Sep. 2011.

[8] Maxime Sagnard. Detection of Weak Bonds in Bond CFRP Assemblies using Symmetrical LAser Shock Adhesion Test (S-LASAT). PhD thesis, 2019. Thèse de doctorat dirigée par Berthe, Laurent , Mécanique-matériaux (AM) Paris, ENSAM 2019.

Thank You!

www.certbond.eu

Funded by the Horizon 2020 Framework Programme
of the European Union

CertBond
COST Action CA18120

Adhesive bonding in glass construction

Prof. Dr. ir. Christian Louter & Dr.-Ing. Christiane Kothe
Institute of Building Construction – Technische Universität Dresden

cost
EUROPEAN COOPERATION IN SCIENCE & TECHNOLOGY

Funded by the Horizon 2020 Framework Programme of the European Union

Presenters

Prof. Dr. ir. **Christian Louter**
christian.louter@tudresden.de

Dr.-Ing. **Christiane Kothe**
christiane.kothe@tu-dresden.de

Institute of Building Construction

Technische Universität Dresden

Outline

CertBond
COST Action CA18120

- What is glass construction?
- Why adhesive bonding in glass construction?
- Three common uses of bonding in glass construction
- Adhesive types, bond surfaces, and adhesive joining
- Examples
- Announcements

CertBond
COST Action CA18120

What is glass construction?

COST EUROPEAN COOPERATION IN SCIENCE & TECHNOLOGY

Funded by the Horizon 2020 Framework Programme of the European Union

Glass Construction

Wolfson Building, Glasgow, Schotland, ARUP
Photo: C. Louter

Material Behaviour

CertBond
COST Action CA18120

Glass exhibits brittle failure

- Glass breaks suddenly without warning

Glass

- Strong in compression
- Relatively weak in tension
- High scatter in (tensile) strength

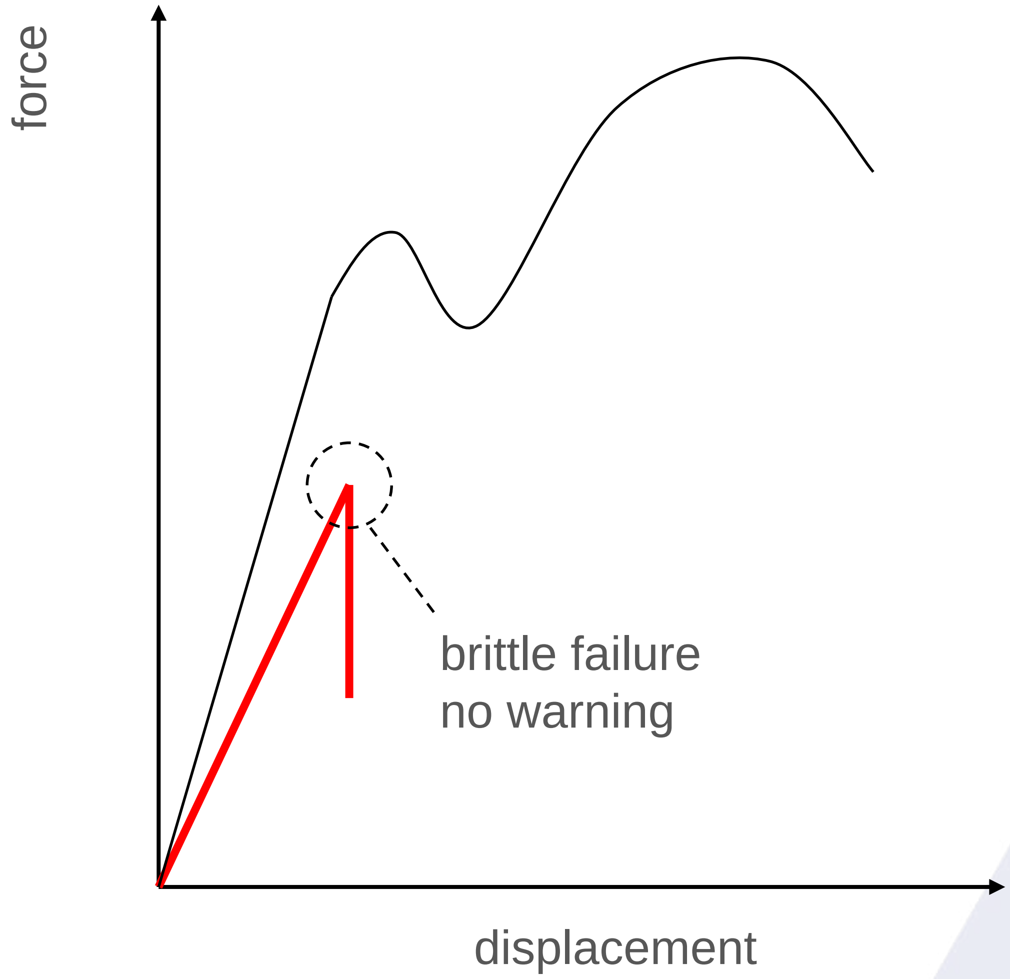

CertBond
COST Action CA18120

Why adhesive bonding in glass construction?

EUROPEAN COOPERATION IN SCIENCE & TECHNOLOGY

Funded by the Horizon 2020 Framework Programme of the European Union

Mechanical Connections

SADEV

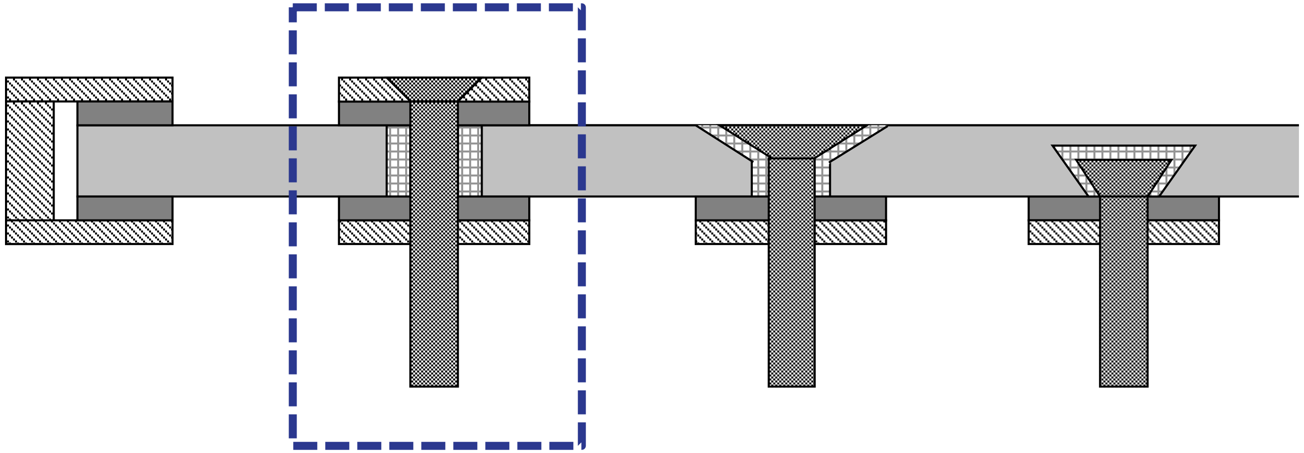

SADEV

Mechanical Connections

Centro Brasileiro Britânico, Sâo Paulo, Brazil:
Single skin façade with RODAN Spider System from DORMA

Mechanical vs. Adhesive Connections

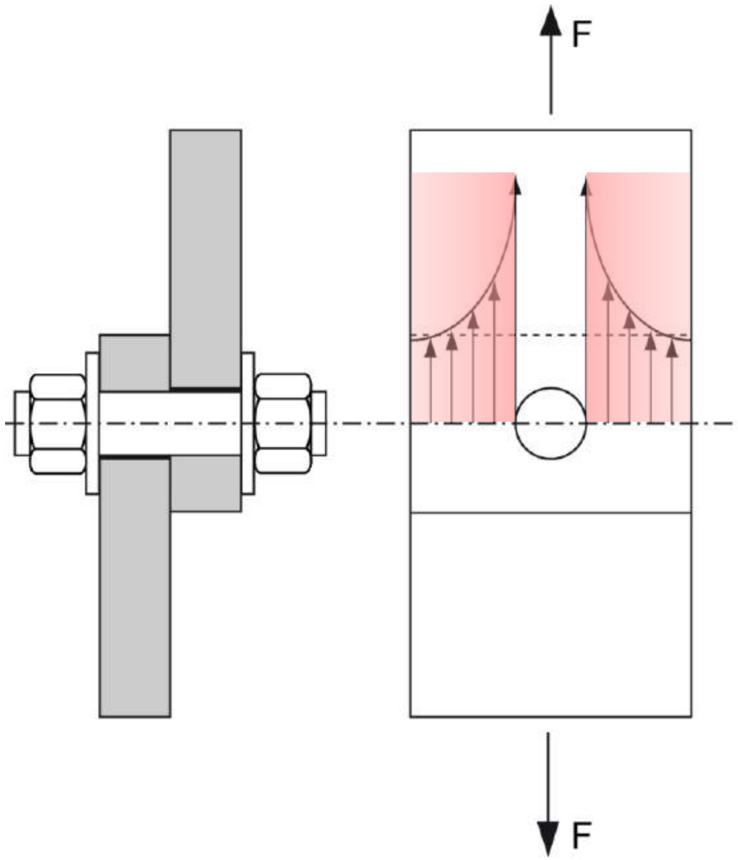

Bolted connection

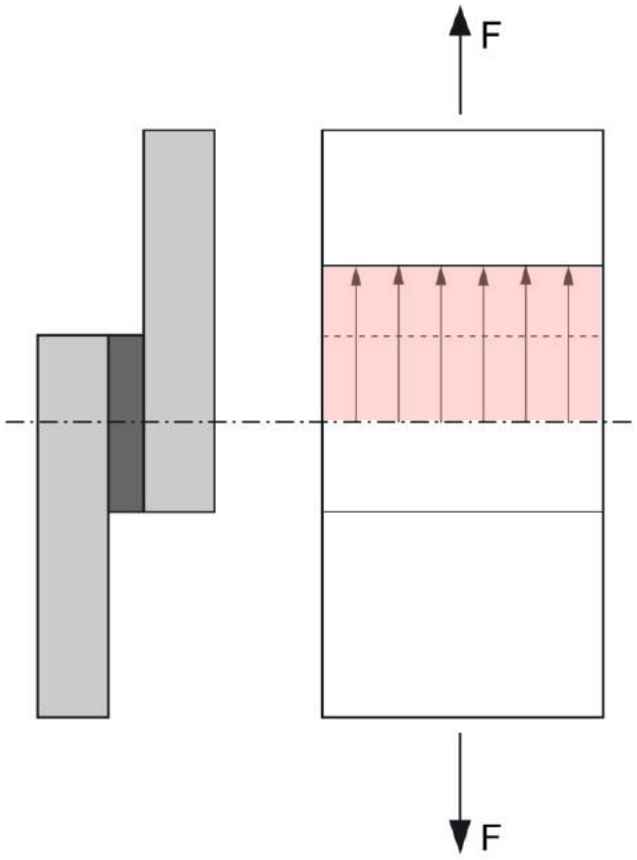

Adhesive connection

Three common uses of bondings in glass construction

CertBond
COST Action CA18120
EUROPEAN COOPERATION IN SCIENCE & TECHNOLOGY
Funded by the Horizon 2020 Framework Programme of the European Union

Laminated Glass

CertBond
COST Action CA18120

interlayers

Seele / SEDAK

Insulating Glass Units

CertBond
COST Action CA18120

Definition
An insulating glass unit (IGU) is a mechanically stable assembly of at least two glass panes separated by an edge spacer which provides a structural bond between the individual panes and hermetically seals the cavity.

Cavity
air-filled or gas-filled (argon, krypton, xenon)

Purpose of IGU
Significantly reduces the thermal transmittance (U-value) of glazed elements due to the enclosed gas volume.

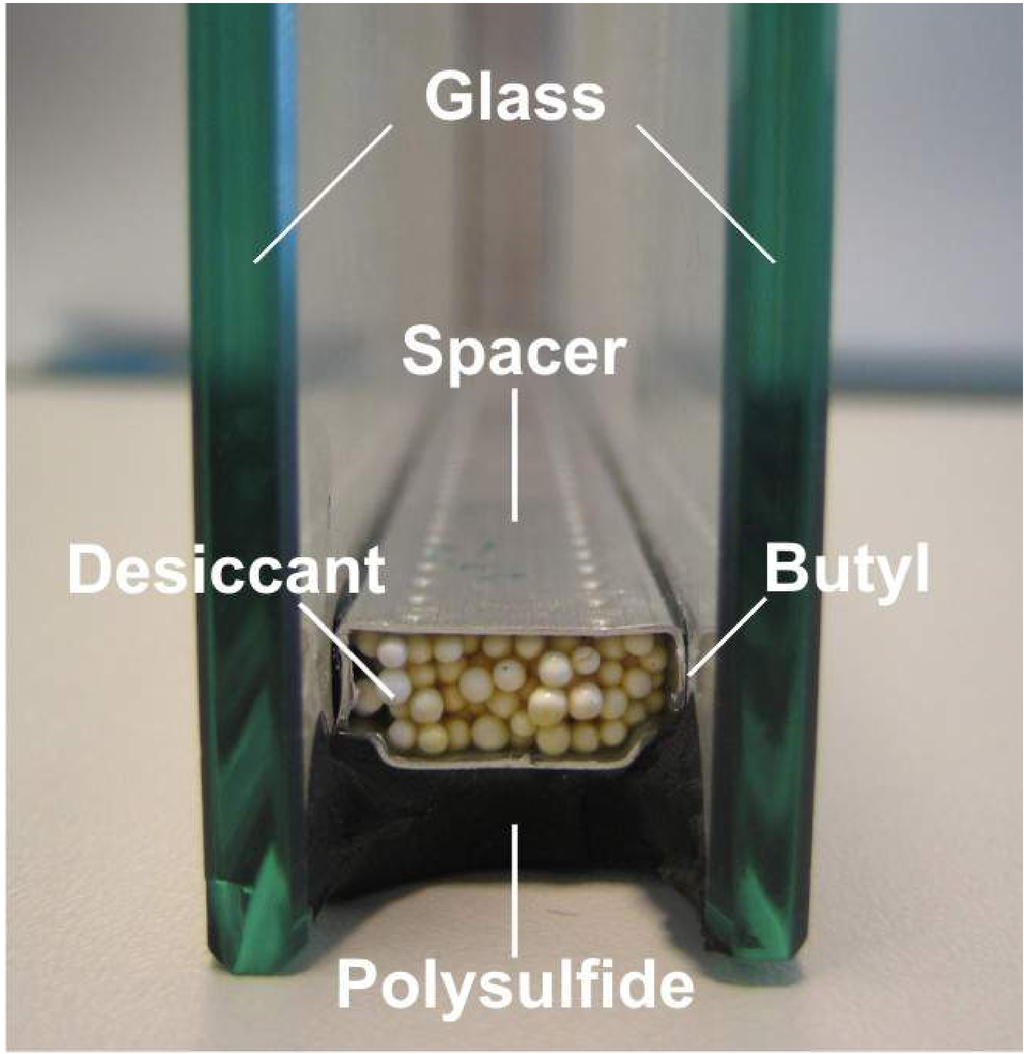

https://jhglass.en.made-in-china.com/product/QBgxJUIboYRE/China-3mm-6A-3mm-Ford-Blue-Float-Insulated-Glass.html

Structural Sealant Glazing

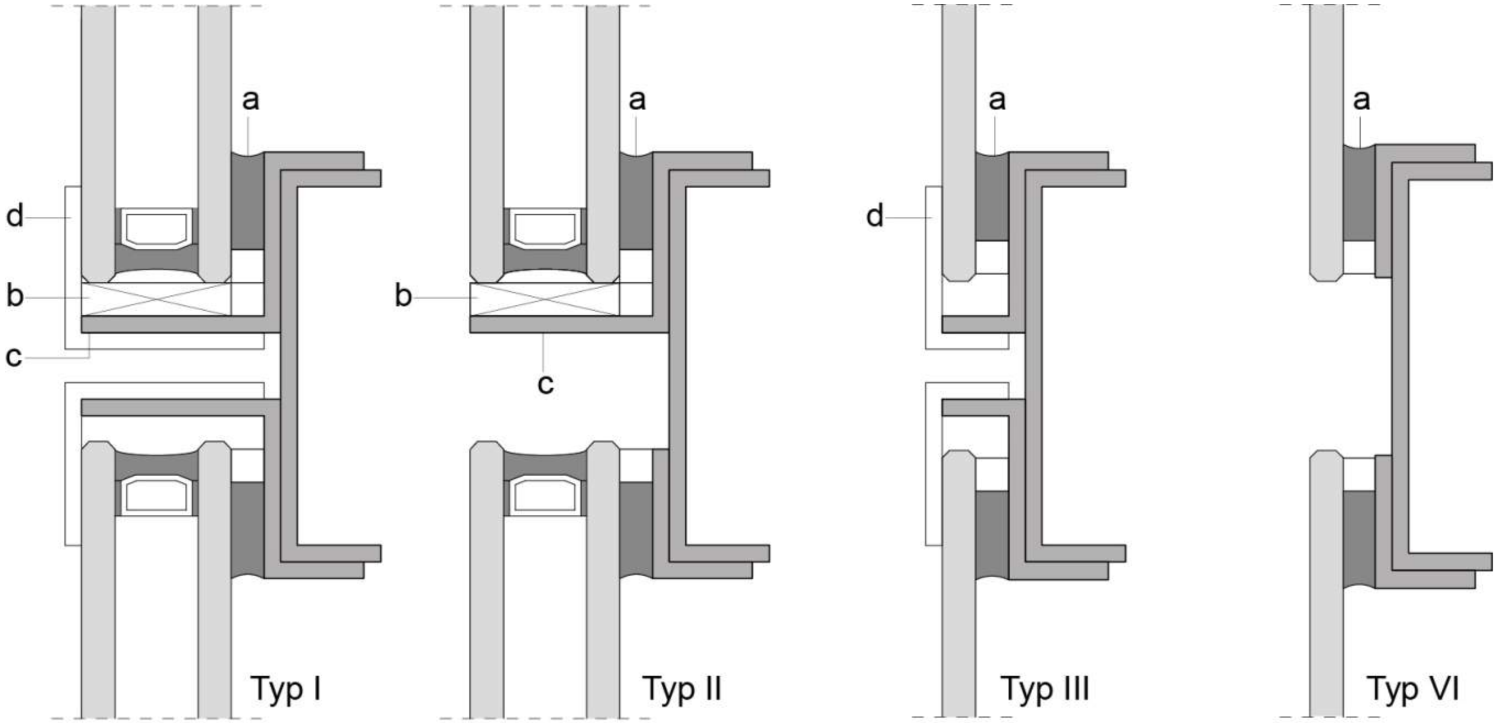

General types of joint detail design according to **ETAG 002**

Type I:	Self-weight carried on mechanical support
Type III & IV:	Self-weight of glazing carried by adhesive
Type I & III:	Additional retaining device to reduce danger in case of bond failure
Type II & IV:	No retaining device

a Adhesive
b Setting block
c Mechanical self-weight support
d Retaining device

EOTA ETAG 002

Adhesive types, laboratory testing, bond surfaces and adhesive joining

CertBond
COST Action CA18120

EUROPEAN COOPERATION IN SCIENCE & TECHNOLOGY

Funded by the Horizon 2020 Framework Programme of the European Union

Definition of adhesives

Adhesive:

ASTM D907-06 → an adhesive is "a substance capable of holding materials together by surface attachment"

DIN EN 923 → an adhesive is defined as a “non-metallic binder that acts via adhesion and cohesion”

Adhesion:

bonding of one material to another, namely an adhesive to a substrate, due to a variety of possible interactions

Cohesion:

internal strength of an adhesive as a result of a variety of interactions within the adhesive

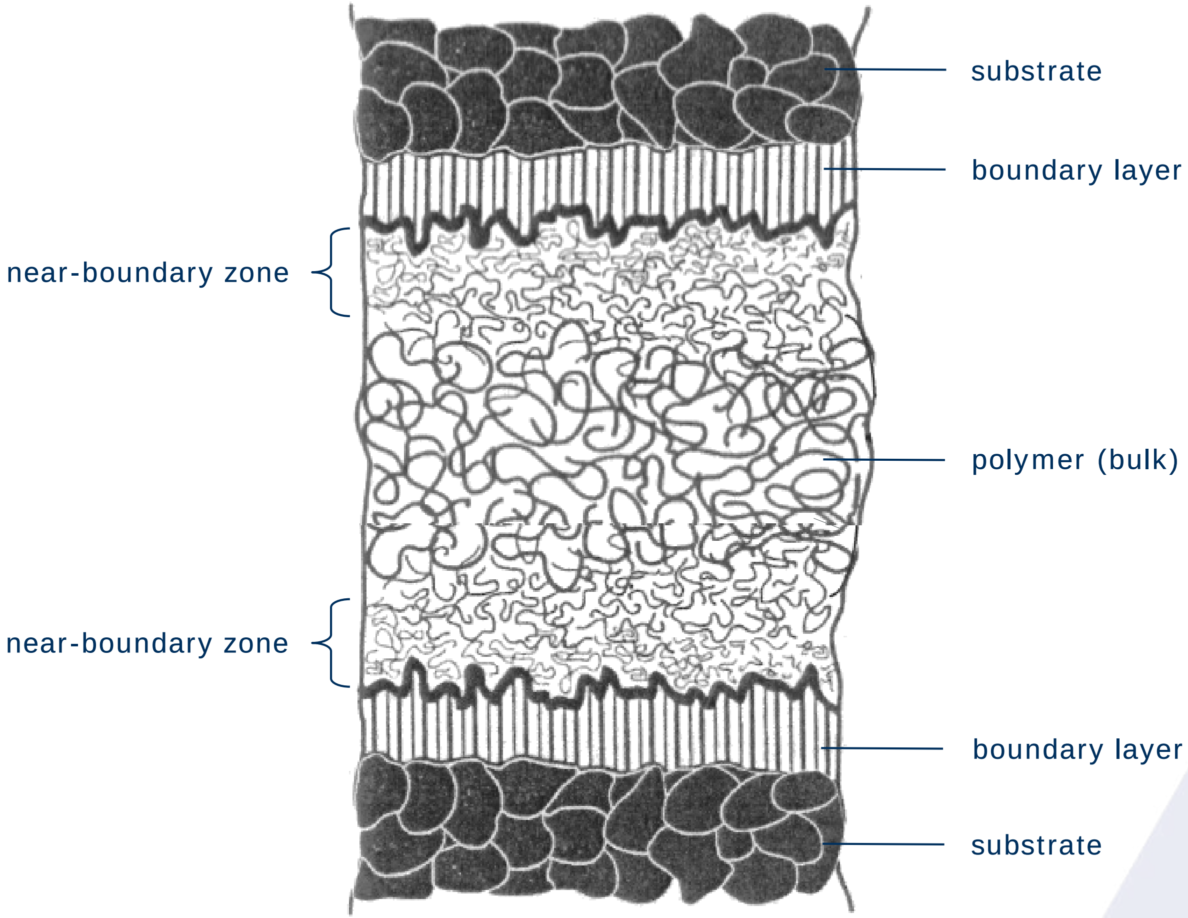

Properties of adhesive connections

CertBond
COST Action CA18120

Advantages:

- joining of different materials
- low thermal impact on the substrate materials (joining temperature-sensitive materials)
- no mechanical weakening of the substrates (e.g. no boreholes)
- homogeneous load-transfer
- sealing of the joint (reduced corrosion)
- joining of thin components (lamination)
- lightweight constructions
- transparent constructions
- additional functions (conductivity, insulation)

Disadvantages:

- additional surface preparation (cleaning/treatment)
- scheduling of curing time in production and storage
- limited resistances, temperature dependences, degradation (aging), compatibility problems
- careful process monitoring
- complex control measures
- testing methods mostly destructive
- complex strength calculations / proofs
- restricted repair options
- disassembly not non-destructive
- special measures for occupational safety, environmental protection, disposal management

Failure pattern according to EN ISO 10365

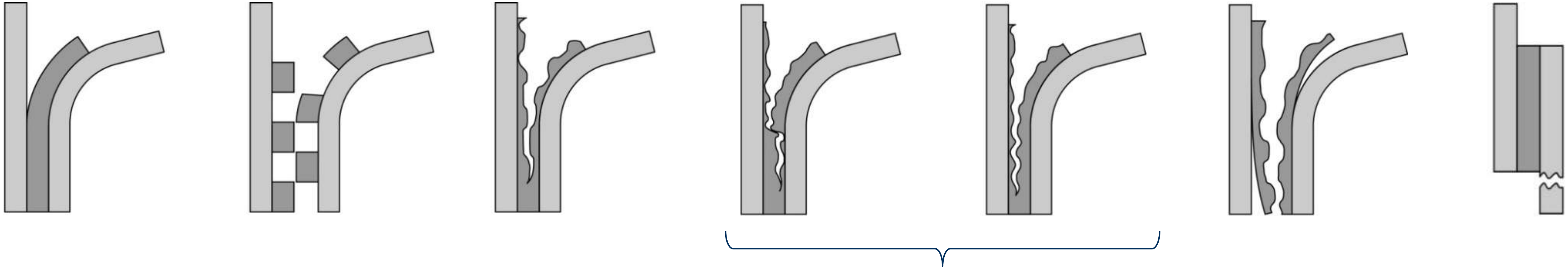

Adhesive failure (AF)

Adhesive failure on both substrates (AF)

Cohesive failure (CF)

Substrate-near cohesive failure (SCF)

Adhesive-cohesive failure with peeling (ACFP)

Substrate failure (SF)

Adhesive Classifications

Components	Chemical base	Strength class	Hardening
1-component	organic	structural bonding	chemical
2-component	inorganic	elastic bonding	physical
3-component			
 ritter-cartridges.de	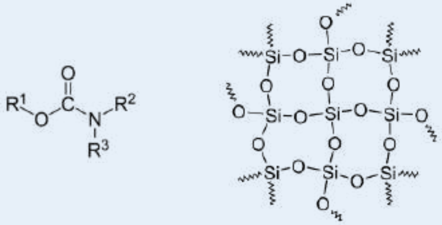	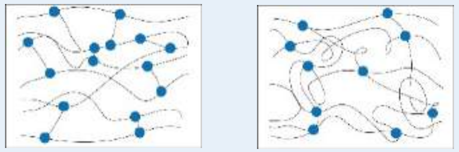 chemgapedia.de	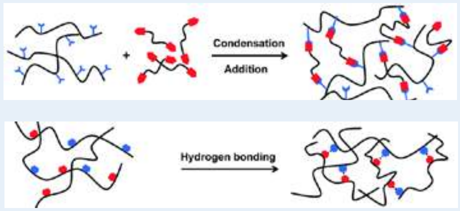 pubs.rsc.org

Chemical base

organic (carbon)		inorganic (silicon)	
natural	synthetic	siloxane	silicates and oxides
proteins (glutine, casein) carbohydrates (starch) plant resins	epoxy resins polyurethane acrylates polyester	silicones	water glass cement

Strength class

Adhesives used in glass construction

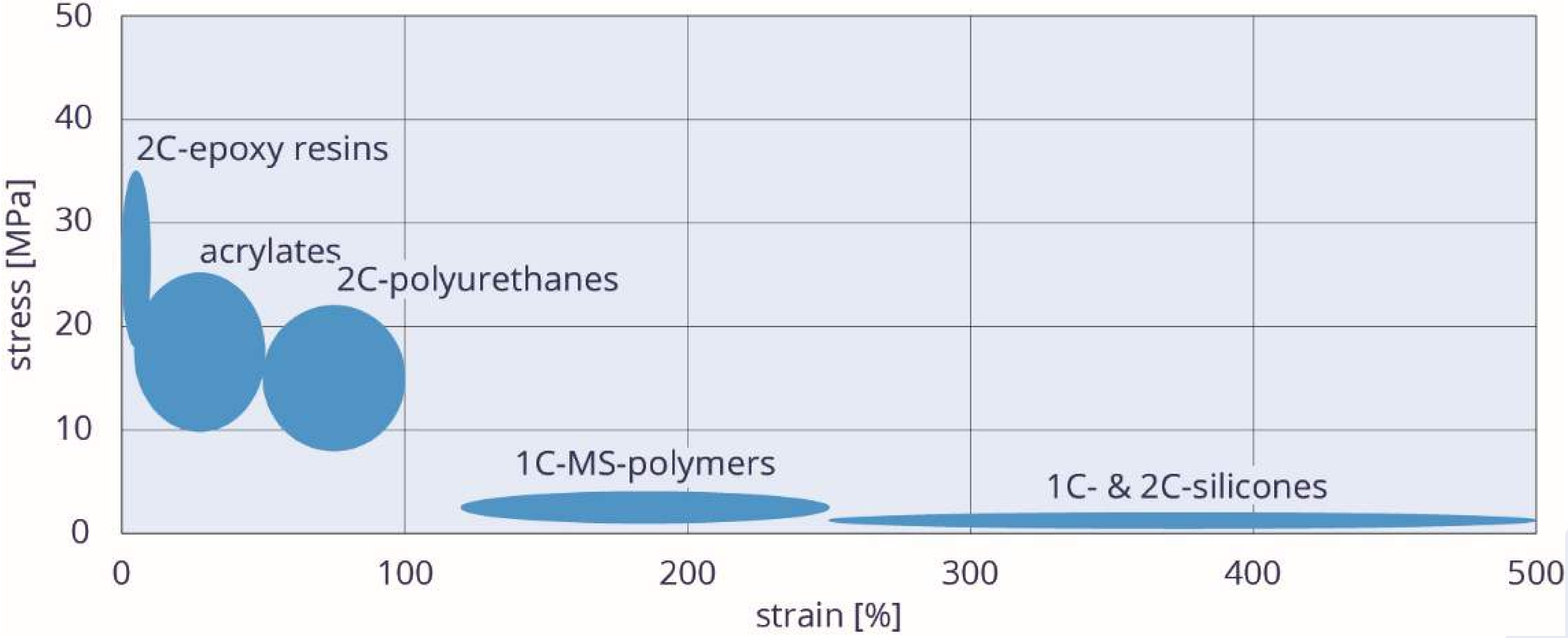

Curing mechanism

CertBond
COST Action CA18120

chemical	physical
monomers ⇩ chemical reaction uncrosslinked or crosslinked polymers	dissolved or meltable polymers ⇩ physical setting solidified polymers
polyaddition polycondensation polymerization	evaporation solidification gelling pressure sensitive adhesives

Chemical curing adhesives - reaction types

polymerization reactions	
step growth	chain growth
polyaddition polycondensation	polymerization (radical, anionic, cationic, coordinative)

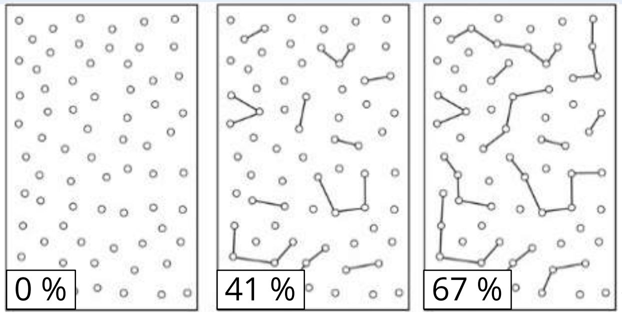

wikipedia.de

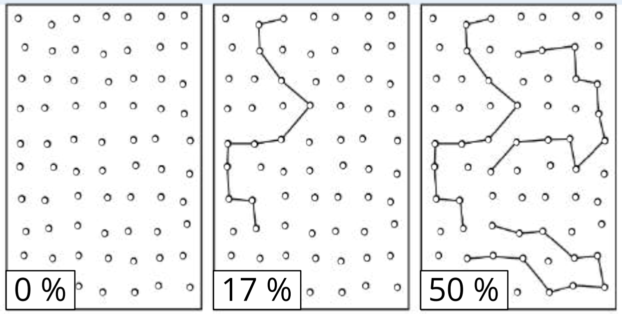

Bernd Tieke
Makromolekulare Chemie
Eine Einführung

Physical setting polymers - mechanisms

Evaporation	Solidification	Gelling	PSA
Solvent-based Polymer dispersion Contact adhesives	Hot-melt adhesives	Plastisols	Adhesive tape Butyl rubber
Polymers dissolved in solvents	Polymers in solid state	Polymers dispersed in plasticizer	Permanently sticky products

Laboratory analysis

Dynamic-mechanical analysis

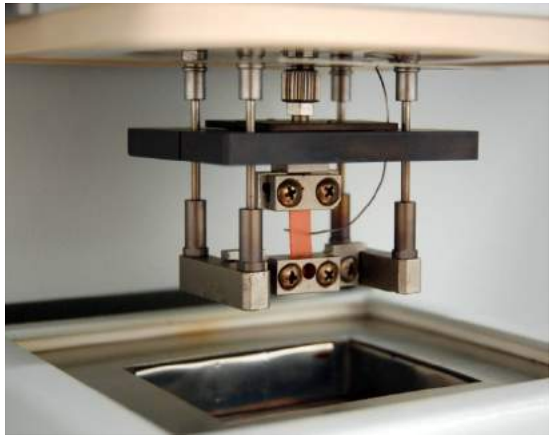

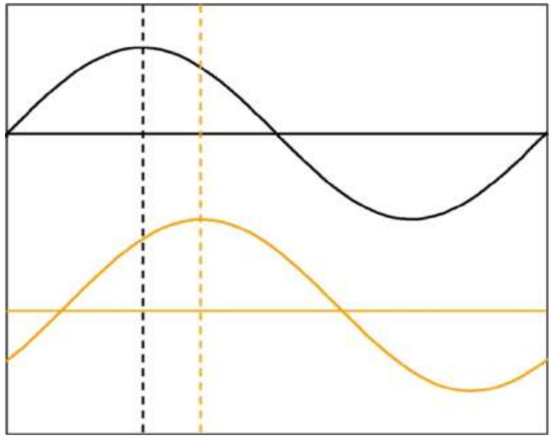

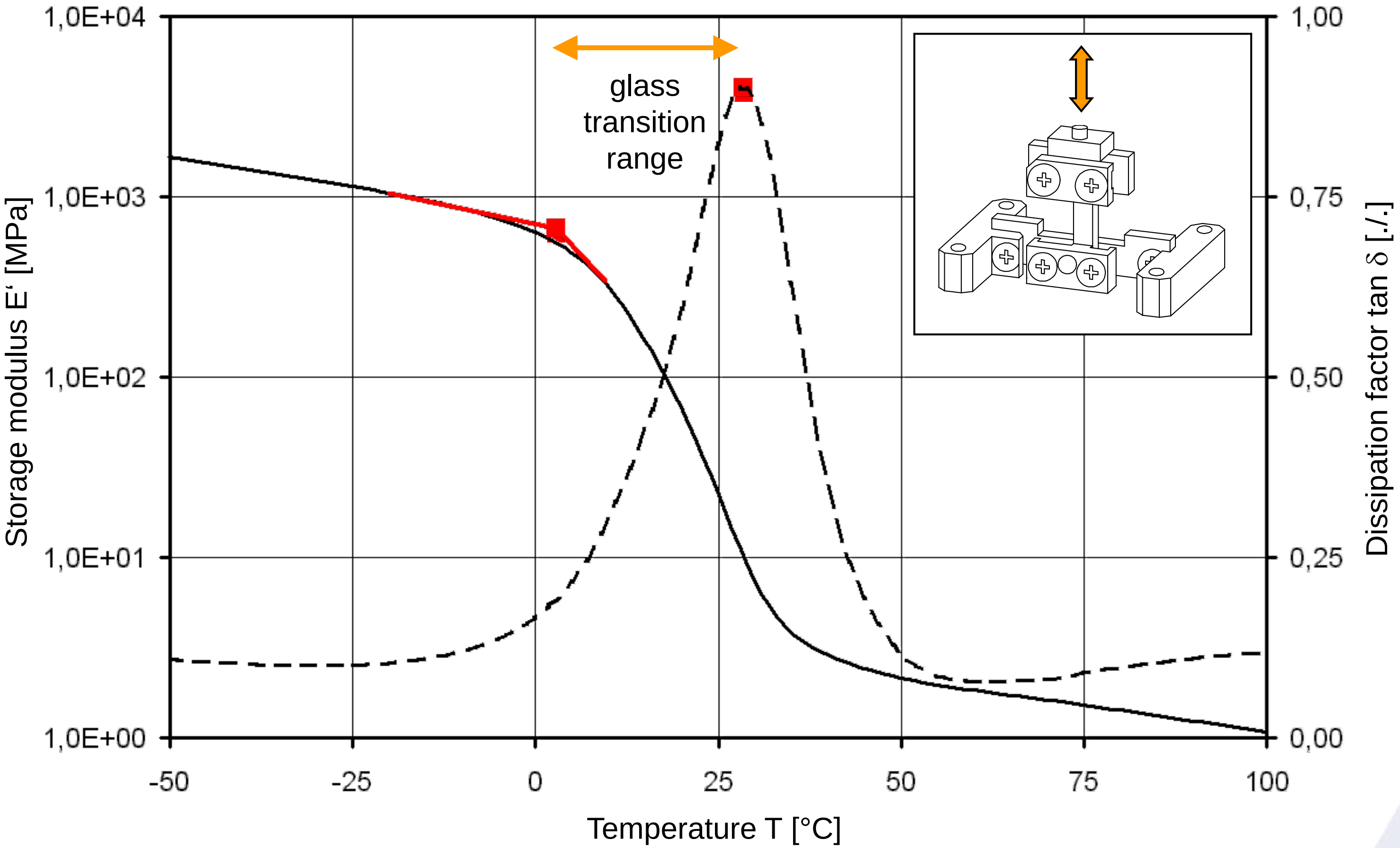

Differential scanning analysis

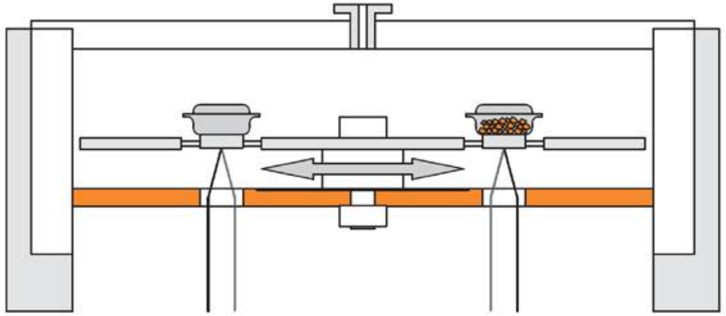

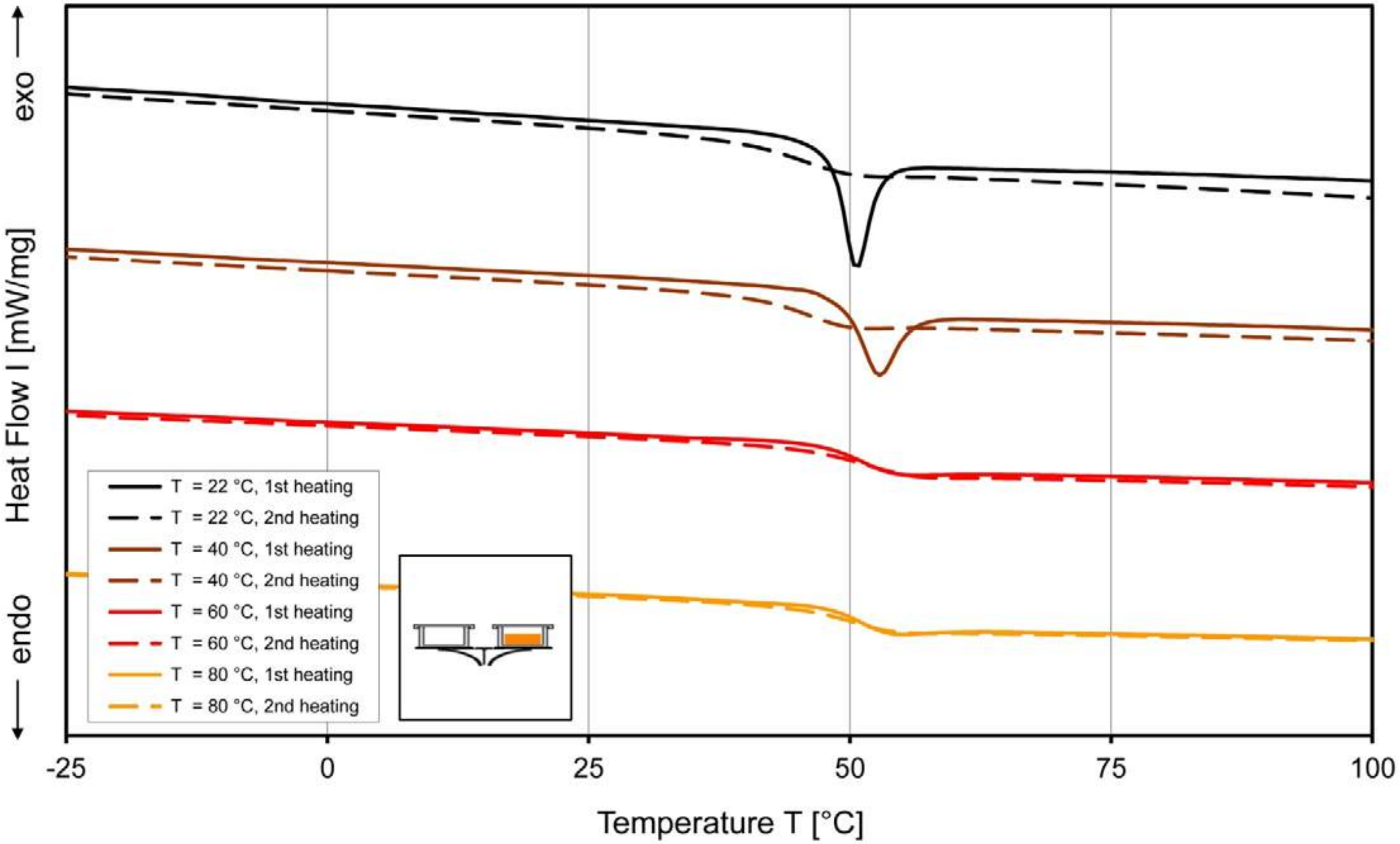

Fourier-transform infrared spectroscopy

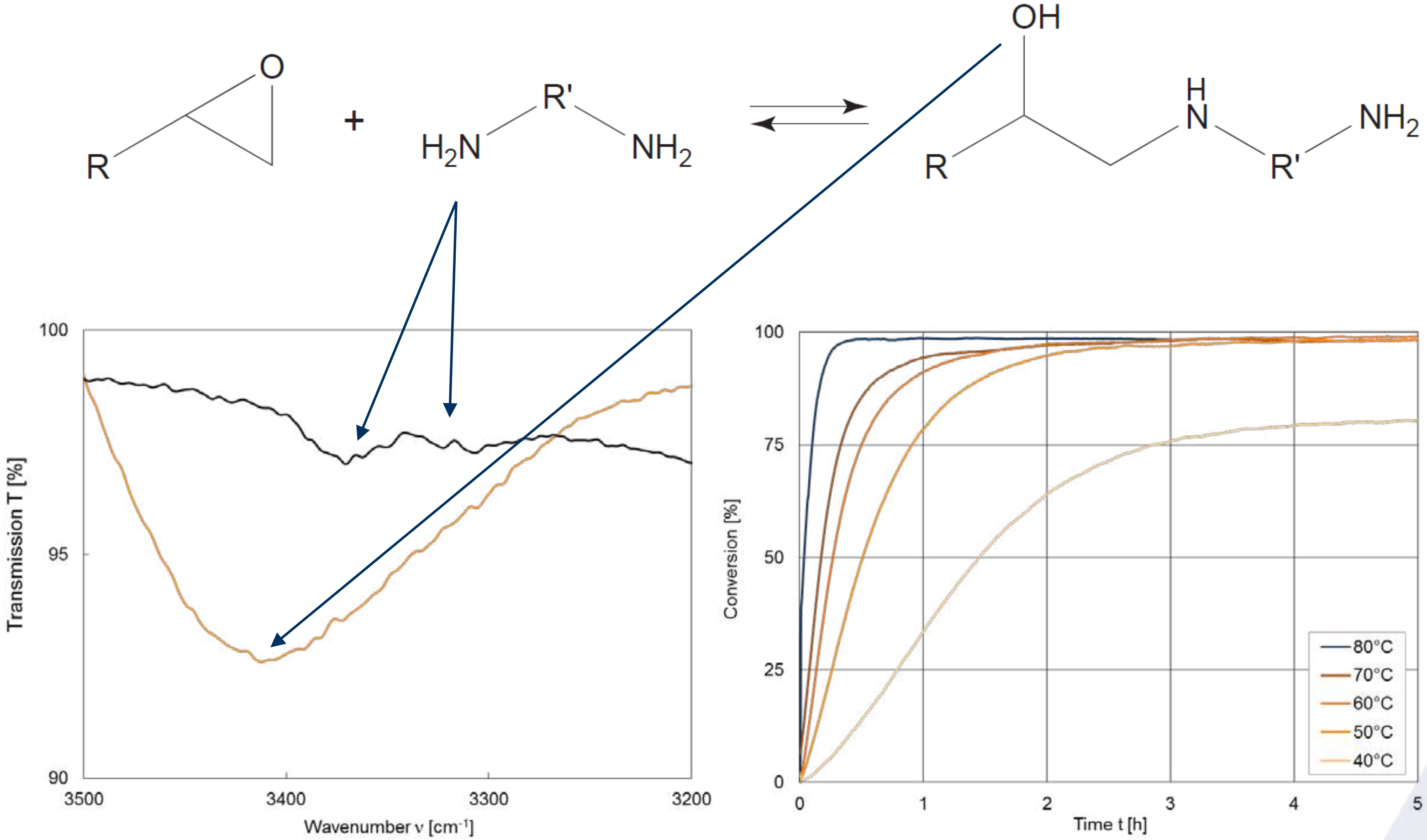

Thermogravimetric analysis

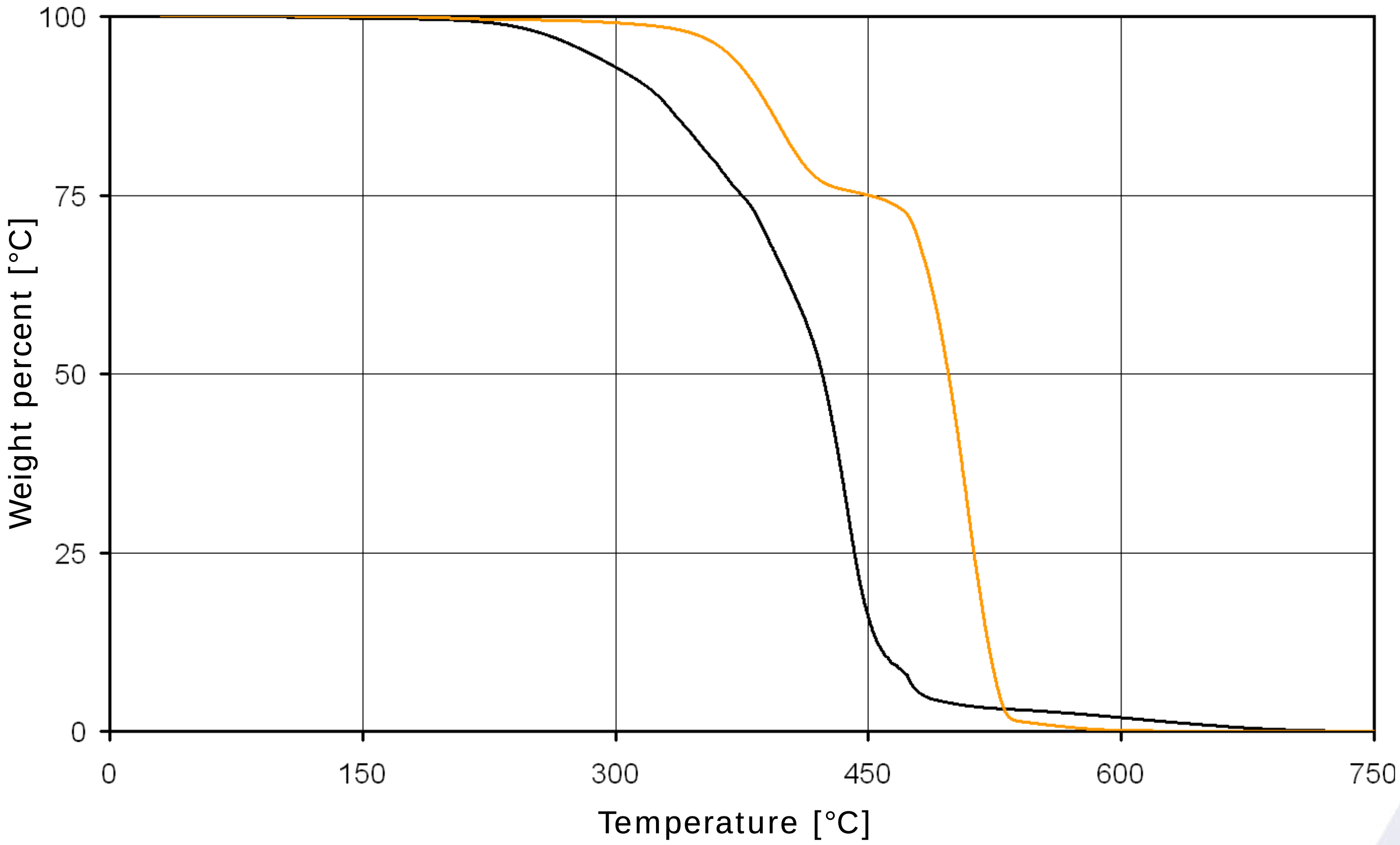

Microscopic analysis

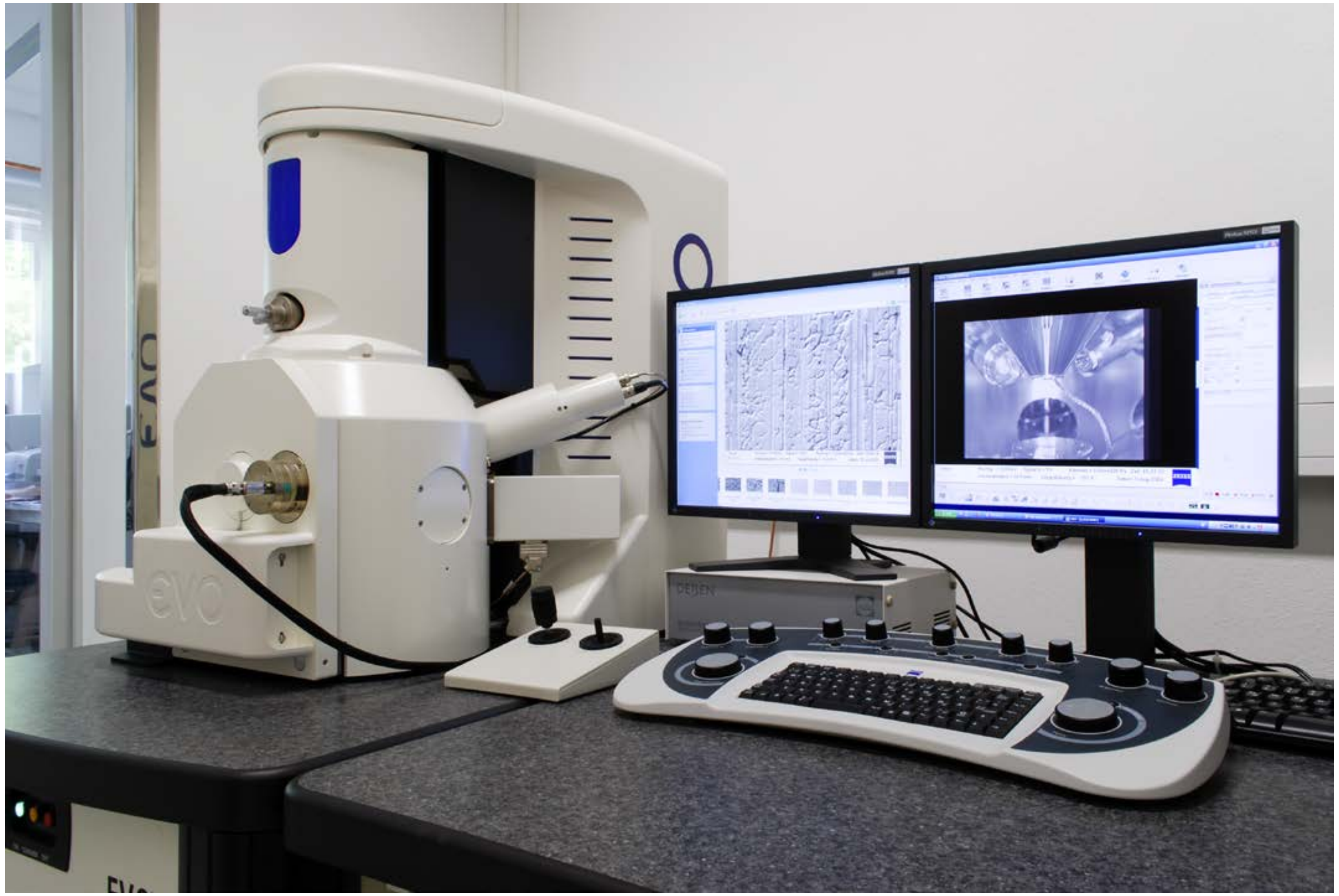

Ultraviolet-visible spectroscopy

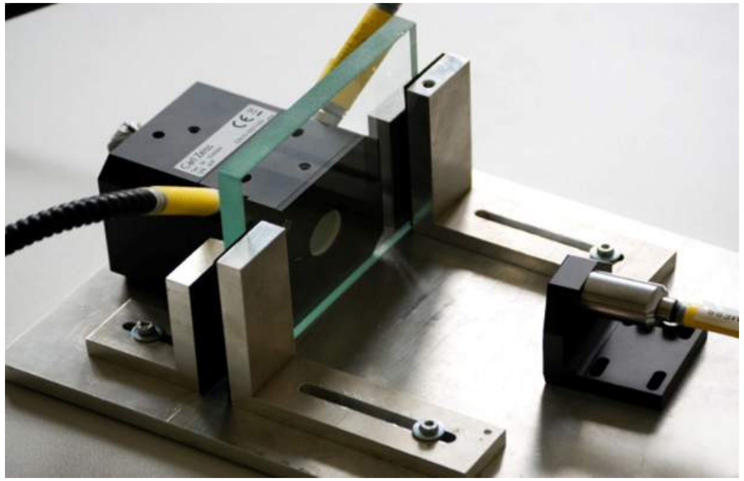

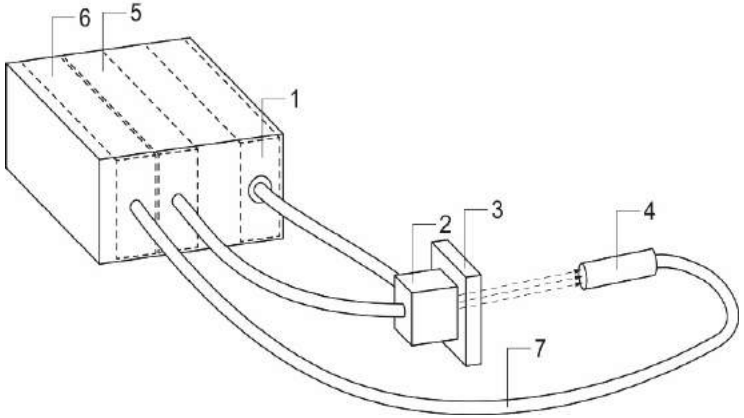

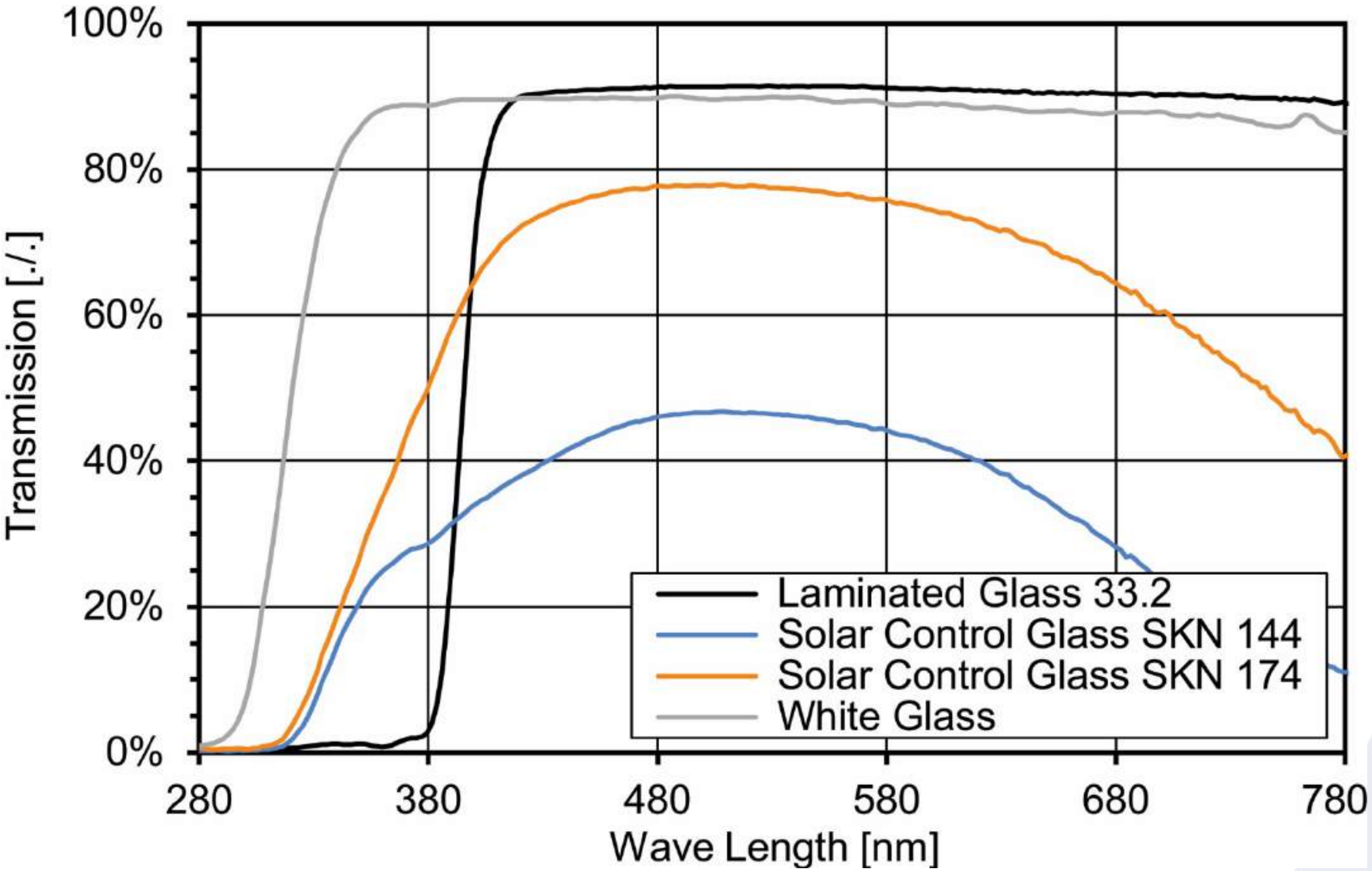

Mechanical testing

CertBond
COST Action CA18120

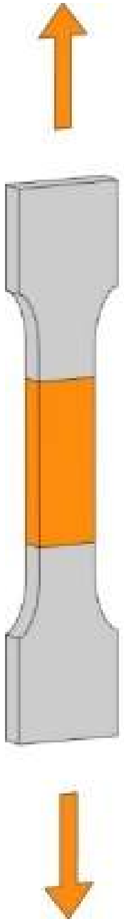

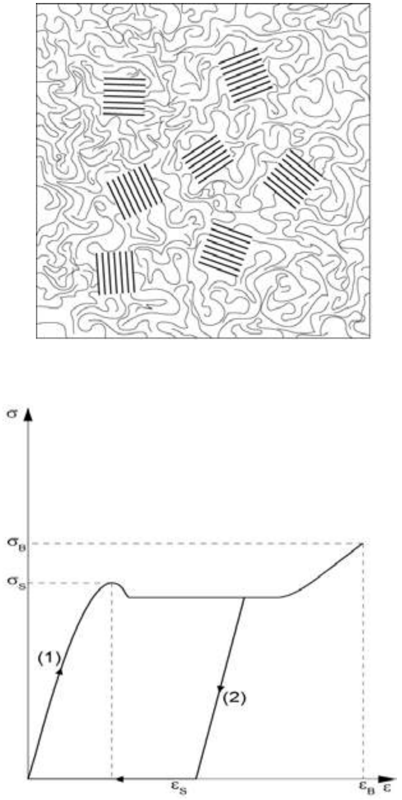

thermoplastic

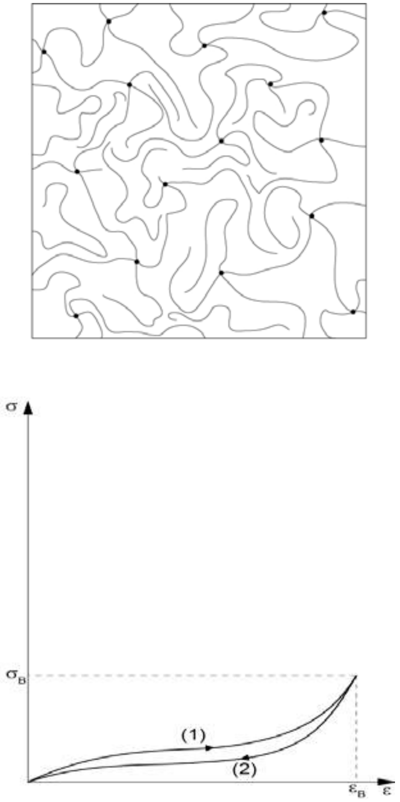

cross-linked elastomer

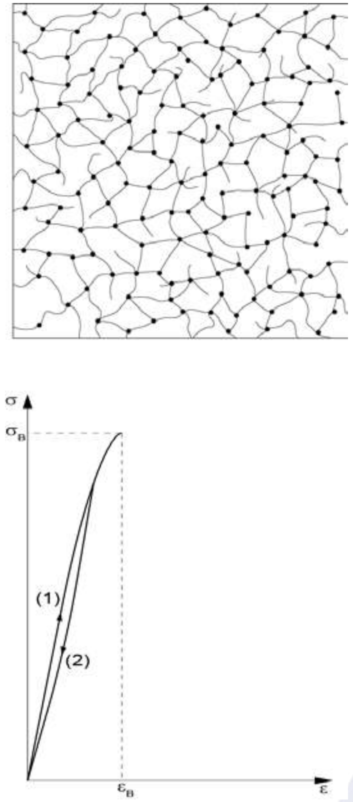

cross-linked thermoset

Adhesion and cohesion mechanisms

CertBond
COST Action CA18120

physical interactions:

- hydrogen bond
- van der Waals forces

⇨ electrostatically
weaker than chemical bonds (1/10 to 1/100)
long range (0.2 … 0.5 nm)

chemical bonds:

- covalent
- ionic
- koordinative
- (metallic)

⇨ strong bond
short range (0.1 … 0.2 nm)

mechanical adhesion:

- interlocking

⇨ covalent bonds in the adhesion zone between adhesive and substrate:

silicone	⟷	glass
epoxy resin	⟷	aluminum
polyurethane	⟷	wood

Substrate surfaces

metal

glass

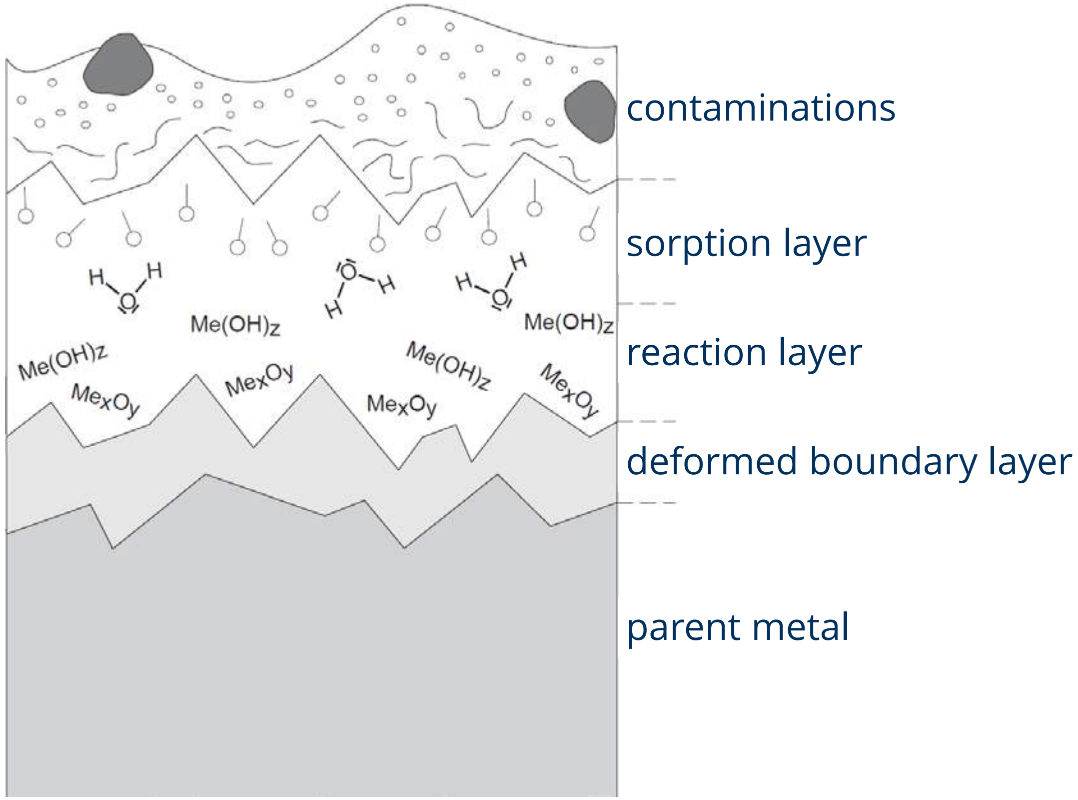

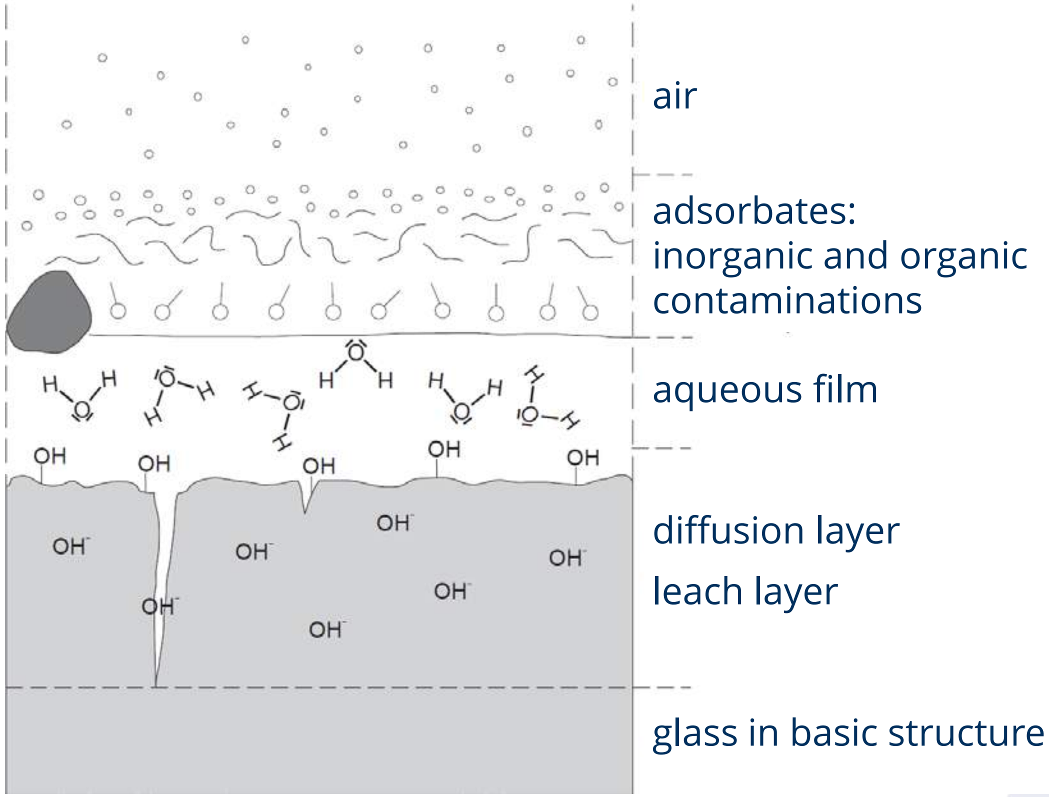

Wettability

- necessary condition for formation of adhesion forces

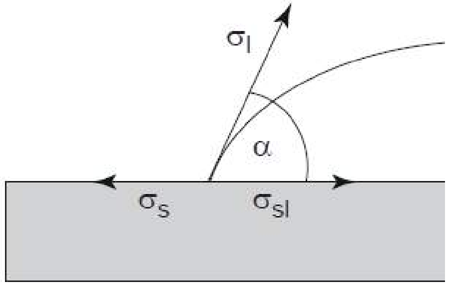

liquid drop

solid

$$\cos\alpha = \frac{\sigma_s - \sigma_{sl}}{\sigma_l}$$

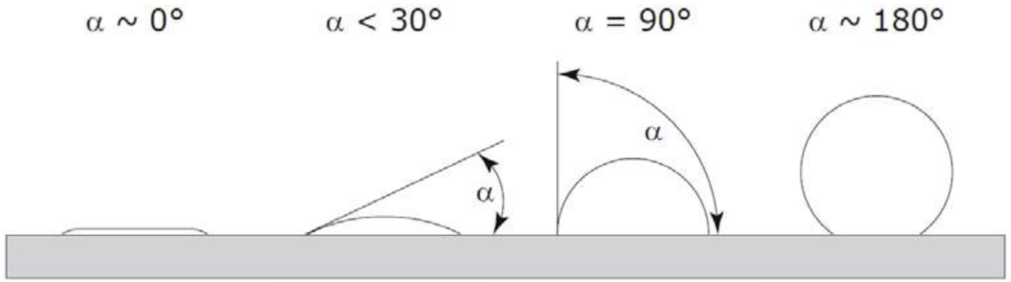

very good wettability | good wettability | insufficient wettability | no wettability

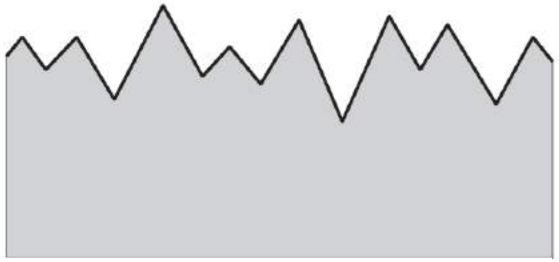

true surface

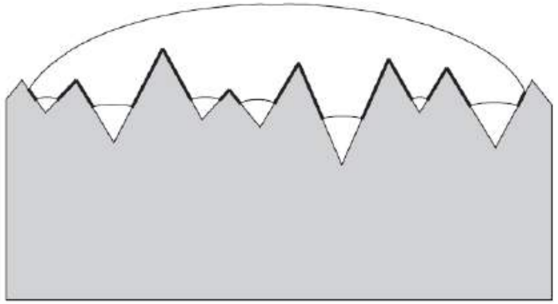

wetted, effective surface

Analysis of wettability

- recommended surface energy > 60 mN/m (Kothe, C., PhD-Thesis, TU Dresden, 2013)
- analysis with contact angle measurement or test inks

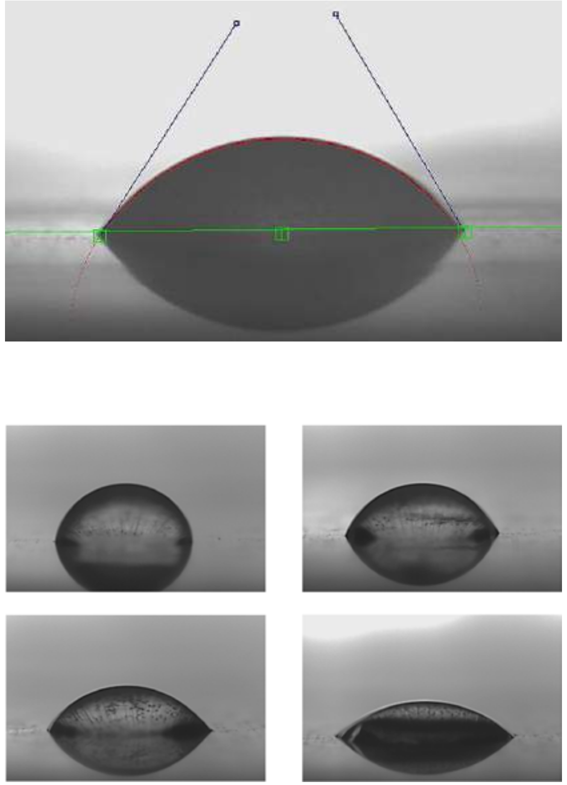

Surface pretreatments

Preparation	Pretreatment	Follow-up treatment
Shape	Mechanical	Maintenance
Preparing the parts to be joined Adjust the surfaces	Brushing Sandblasting Grinding, polishing	Conditioning Primer application
Area	Physical	Increase
Removing oxides Cleaning and degreasing	Flaming Corona discharge Low pressure plasma Atmospheric pressure plasma	Applying of adhesion promoters
selection of the cleaning agent / process according to contamination	Chemical	reaction times and ambient conditions (temperature, humidity)
	Pickling Anodizing Flame silicatization Sandblast-Coating	

Flame silicatization

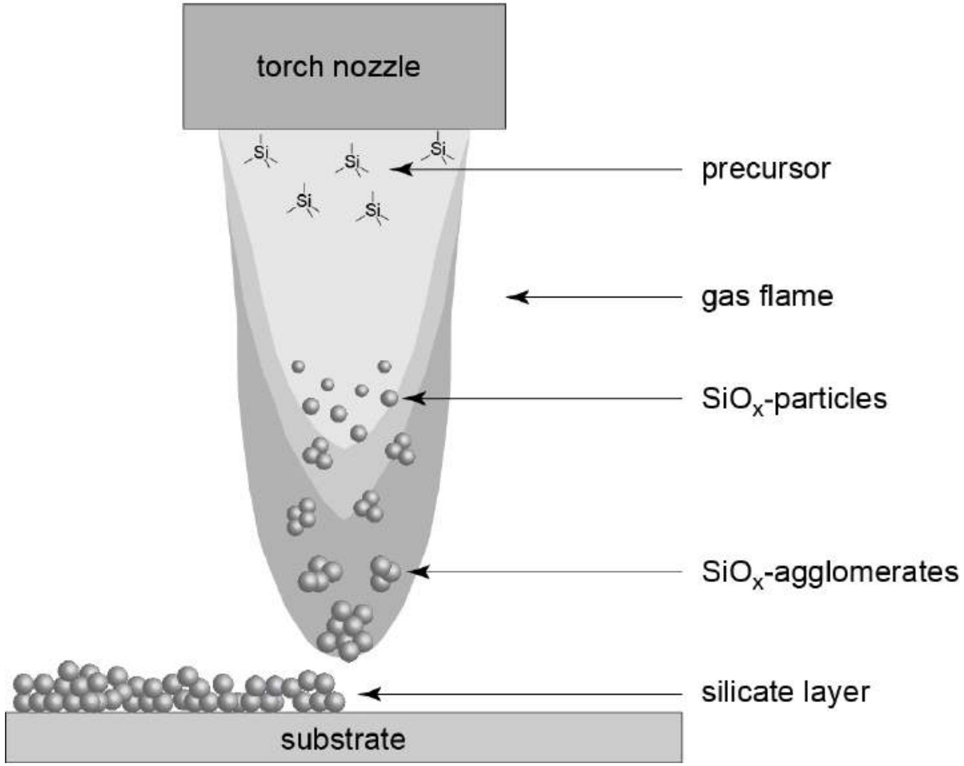

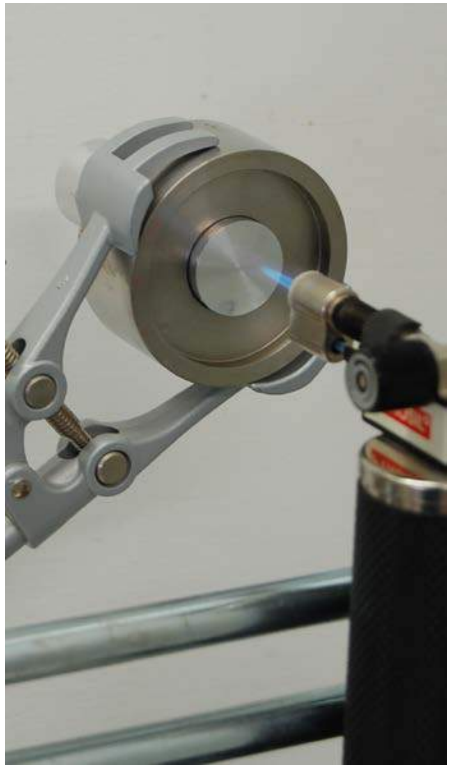

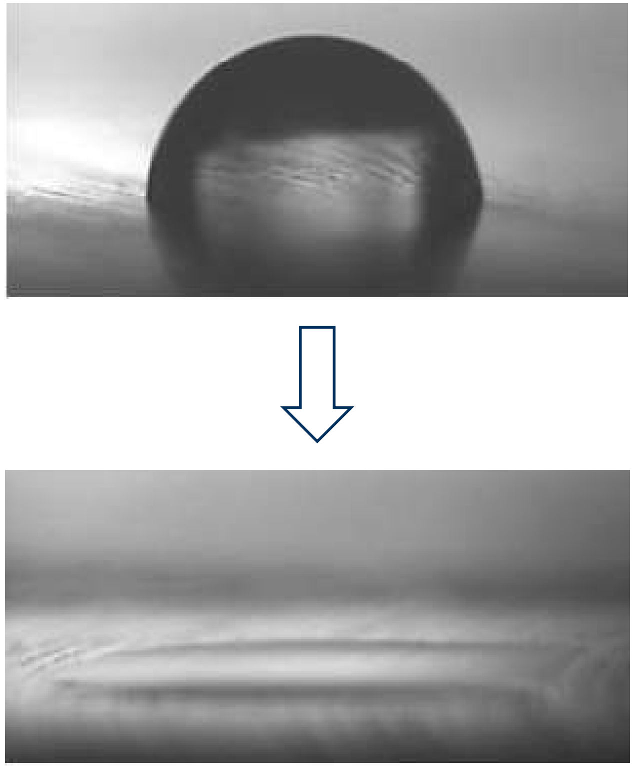

$$Si(CH_3)_4\,(g) + 8\,O_2 \longrightarrow SiO_2\,(s)\downarrow + 4\,CO_2\,(g)\uparrow + 6\,H_2O\,(g)\uparrow$$

Tetramethylsilane — Silicon dioxide

Kothe, C., PhD-Thesis, TU Dresden, 2013

Surface reactivity

$$SiO_2 + 2\,H_2O \longrightarrow Si(OH)_4$$

Silicon dioxide — Silica

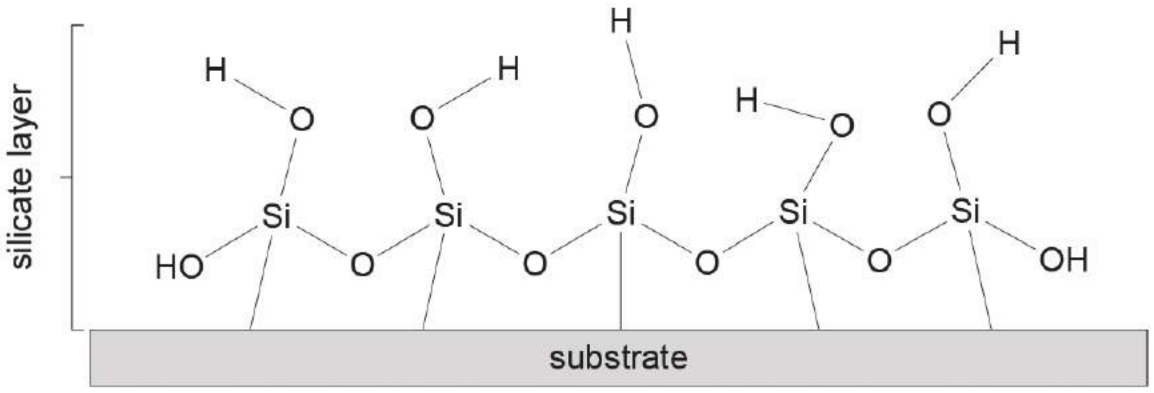

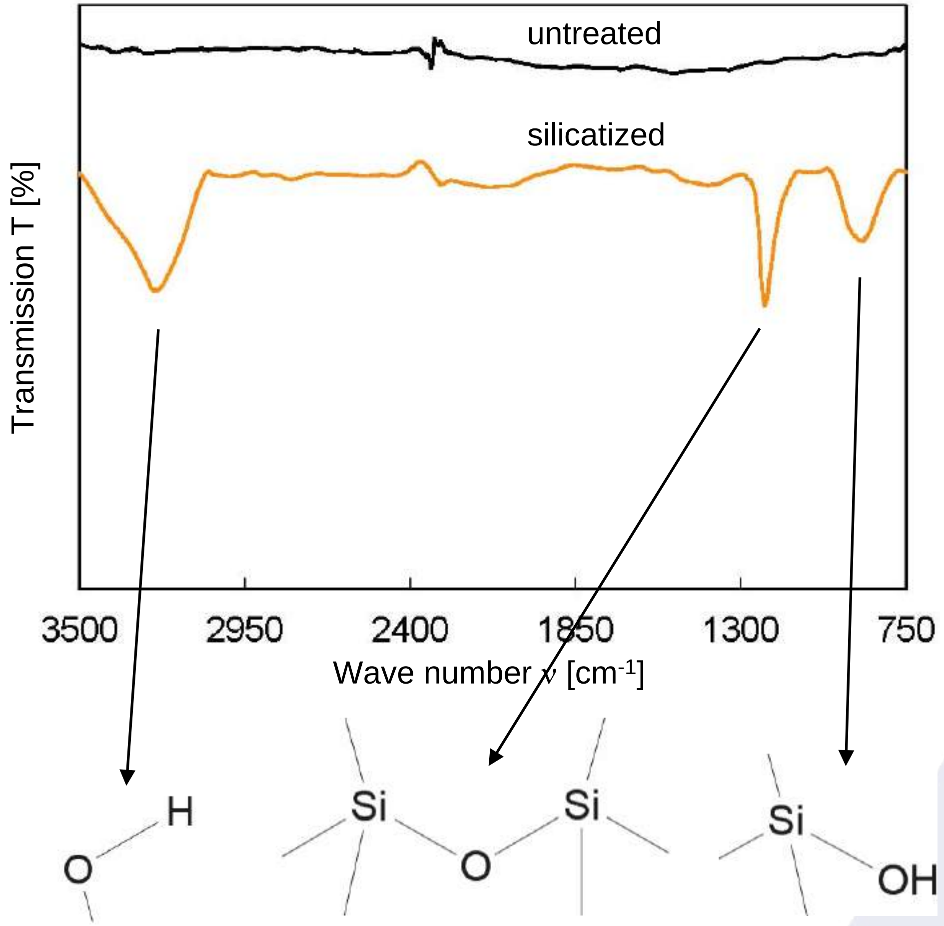

Kothe, C., PhD-Thesis, TU Dresden, 2013

Analysis of surface reactivity

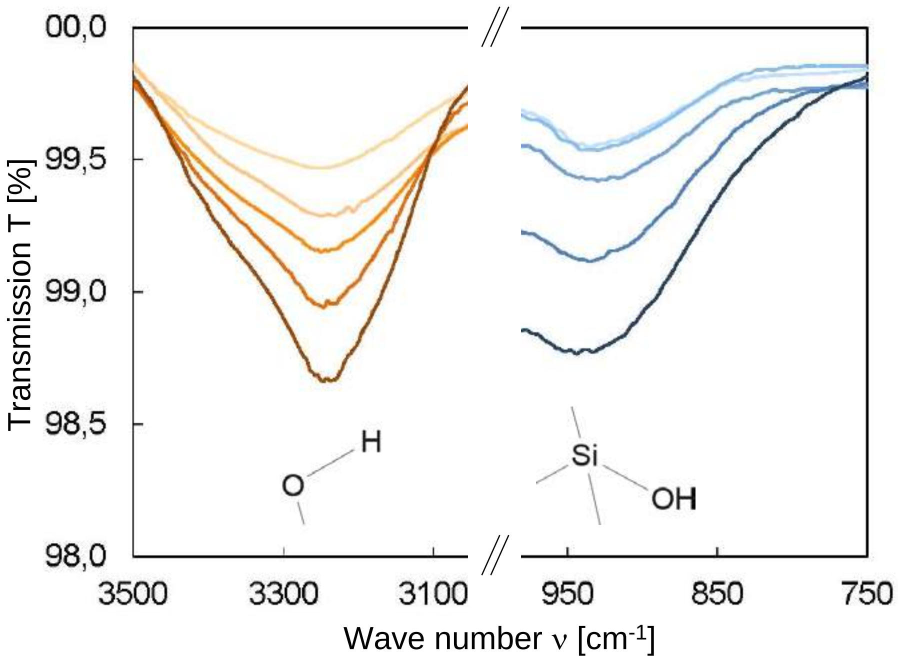

5 minutes
10 minutes
15 minutes
30 minutes
60 minutes

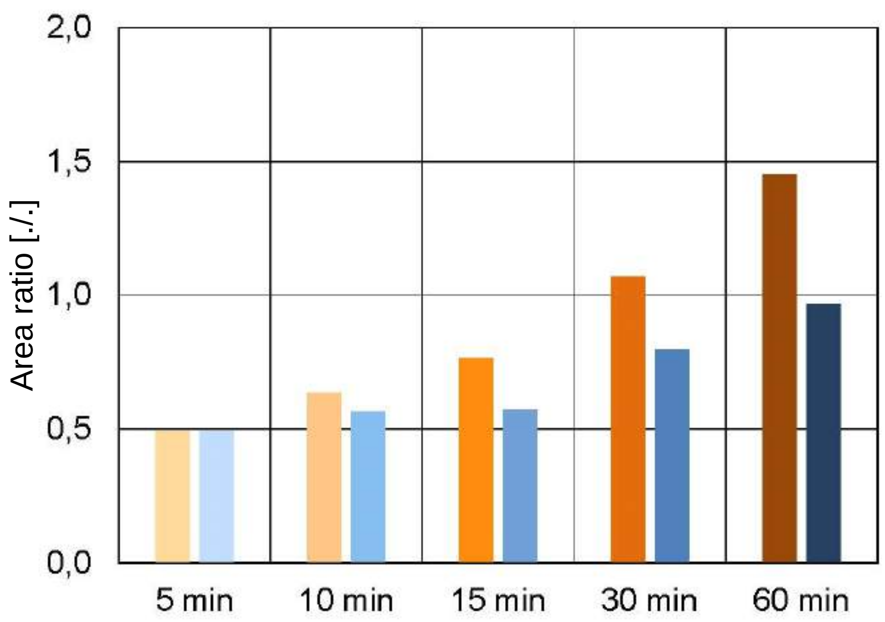

Hydroxylation (silanol formation)
+
Hydration (water retention)

Hydroxylation (silanol formation)

Kothe, C., PhD-Thesis, TU Dresden, 2013

Atmospheric pressure plasma

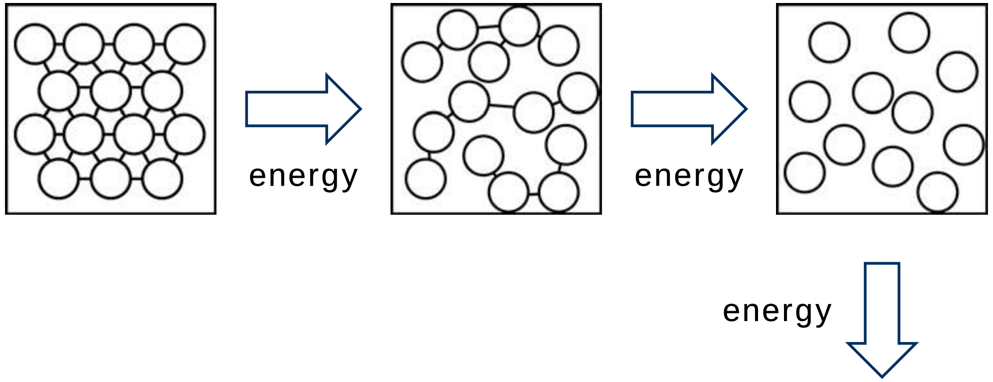

High voltage discharge

- Ions
- Electrons
- Excited molecules
- Radicales

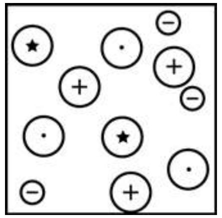

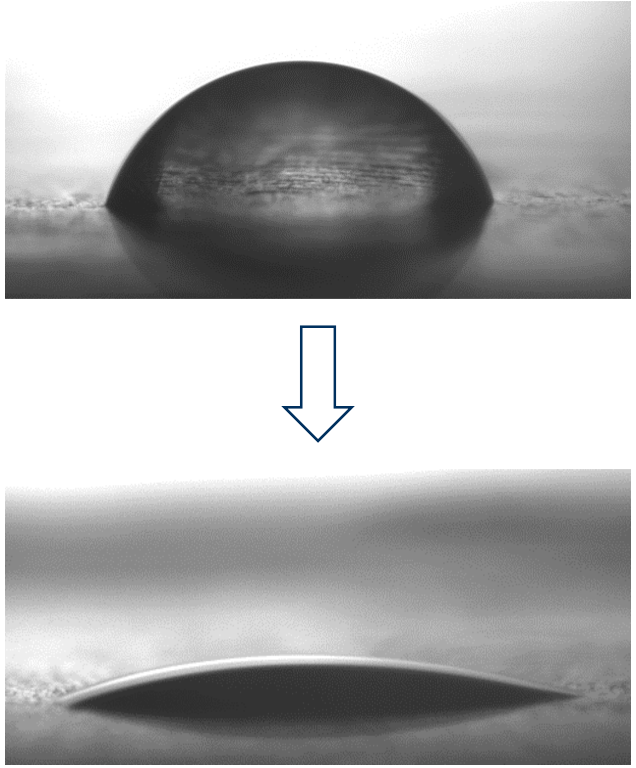

Kothe, C., PhD-Thesis, TU Dresden, 2013

Cleaning effect

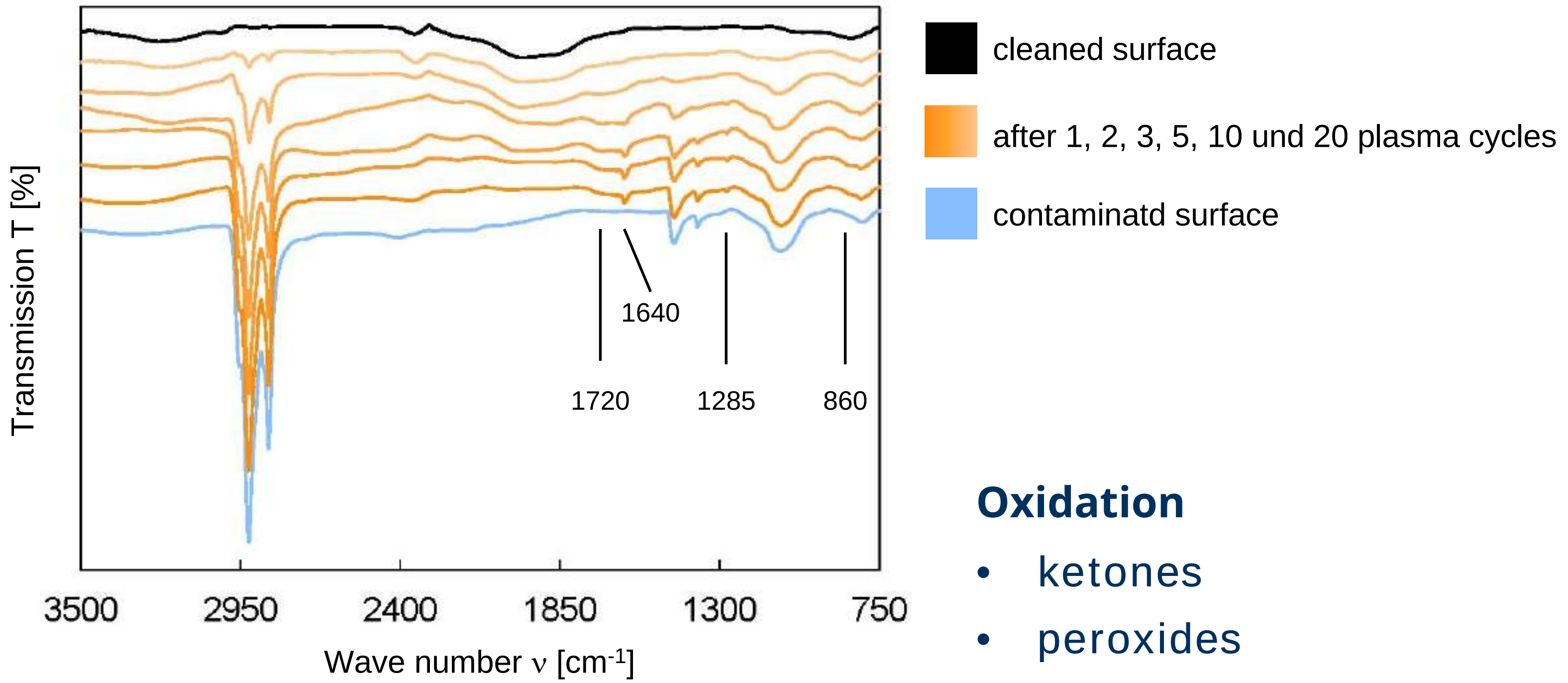

Oxidation

- ketones
- peroxides

→ CO_2, H_2O
→ → → micro cleaning

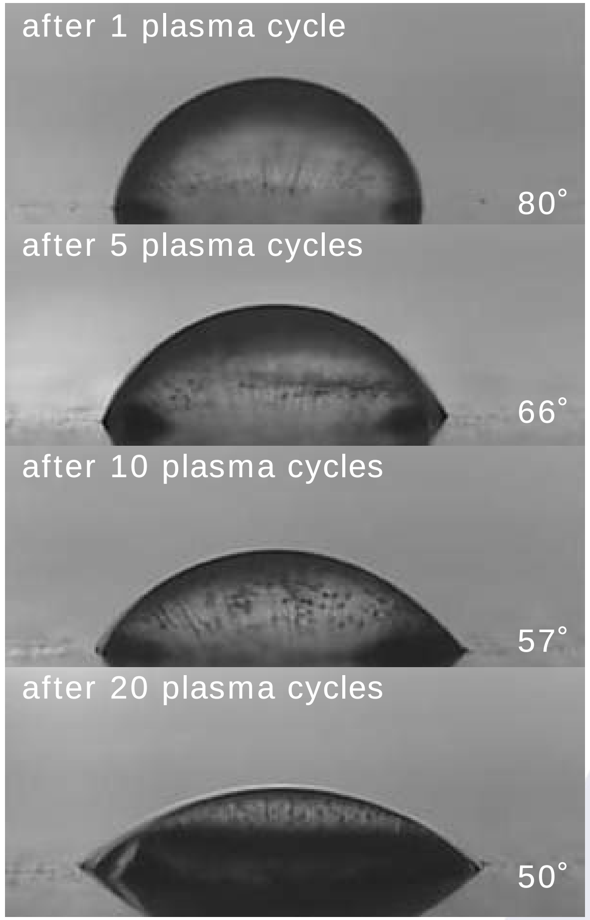

Kothe, C., PhD-Thesis, TU Dresden, 2013

Stability of plasma pretreatment

CertBond
COST Action CA18120

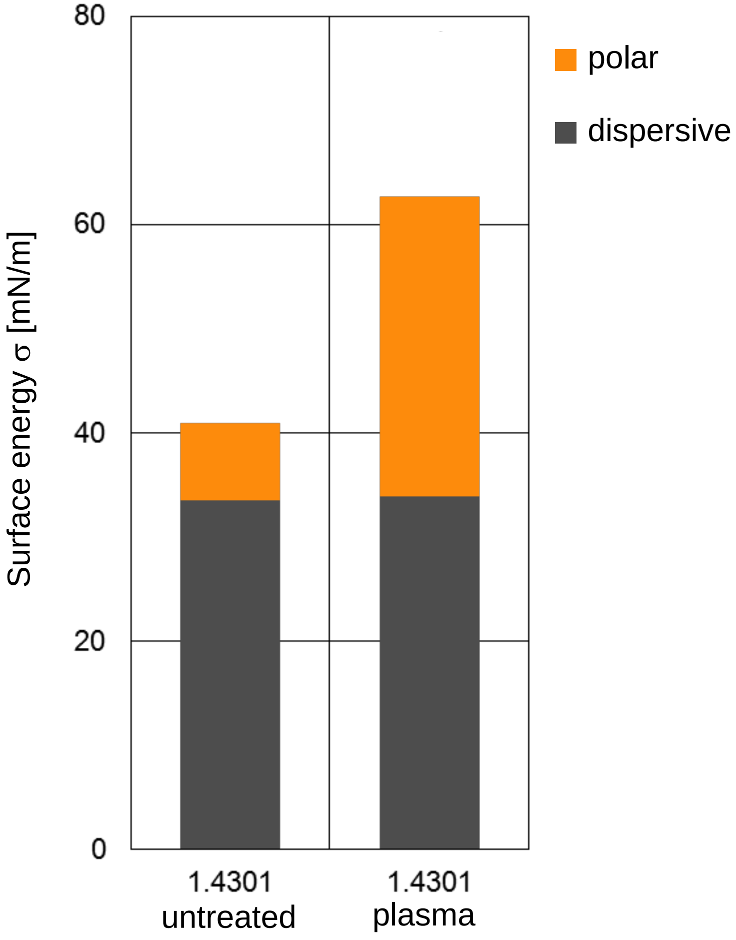

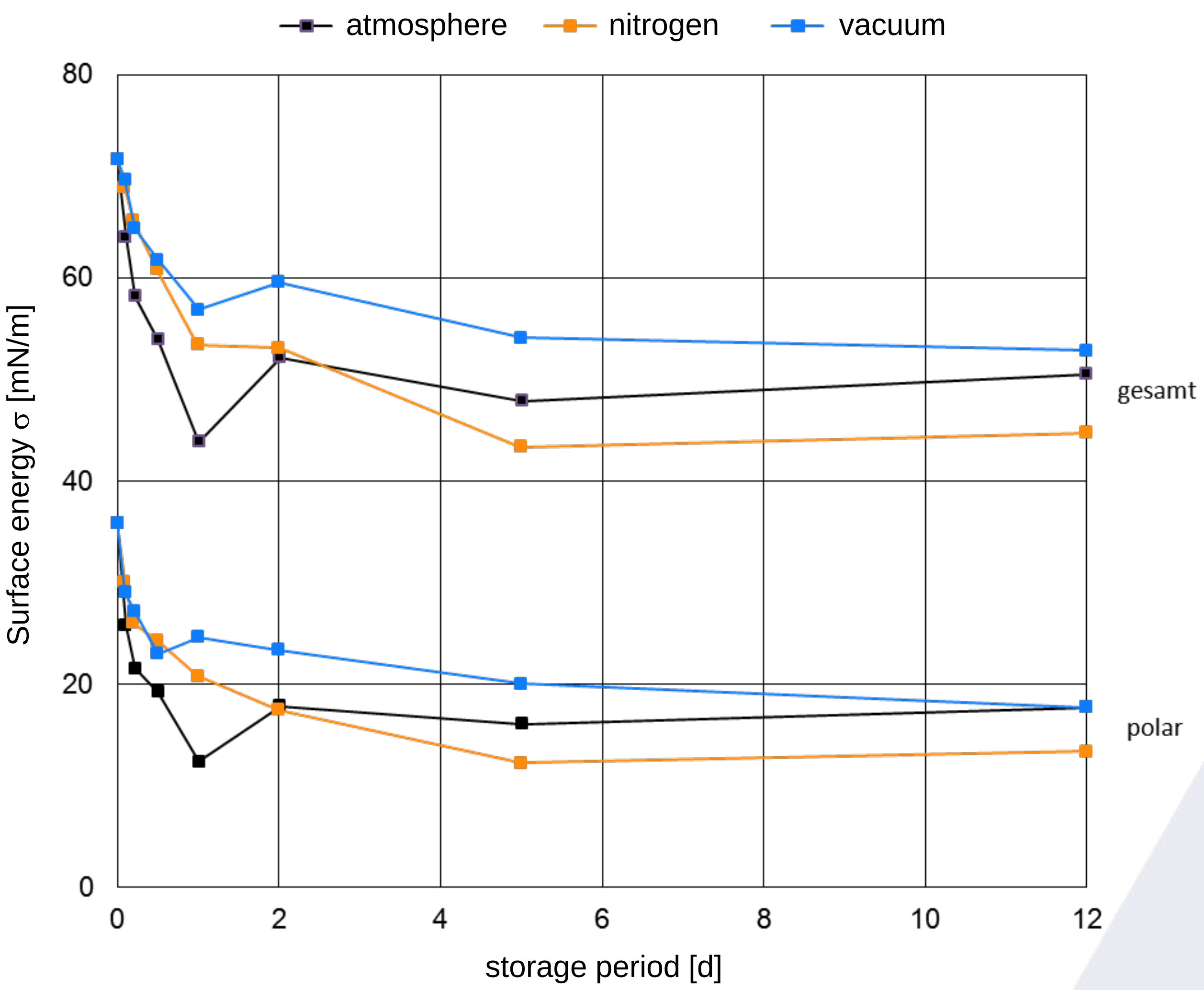

Weller, B., Kothe, C., Wünsch, J., EURADH 2014

Plasmapolymerisation

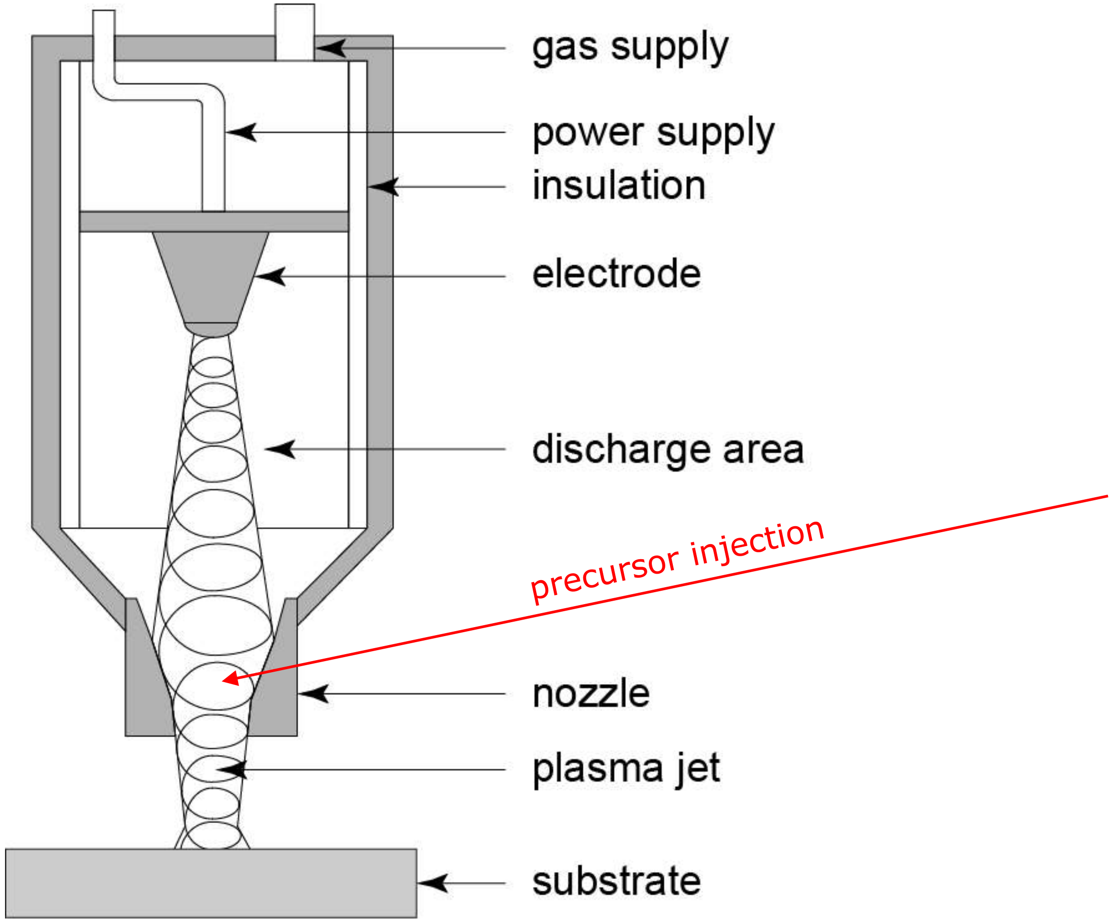

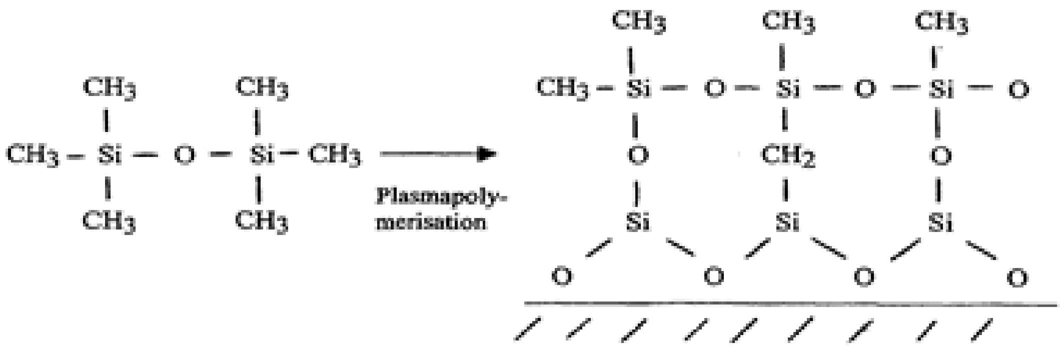

Primer

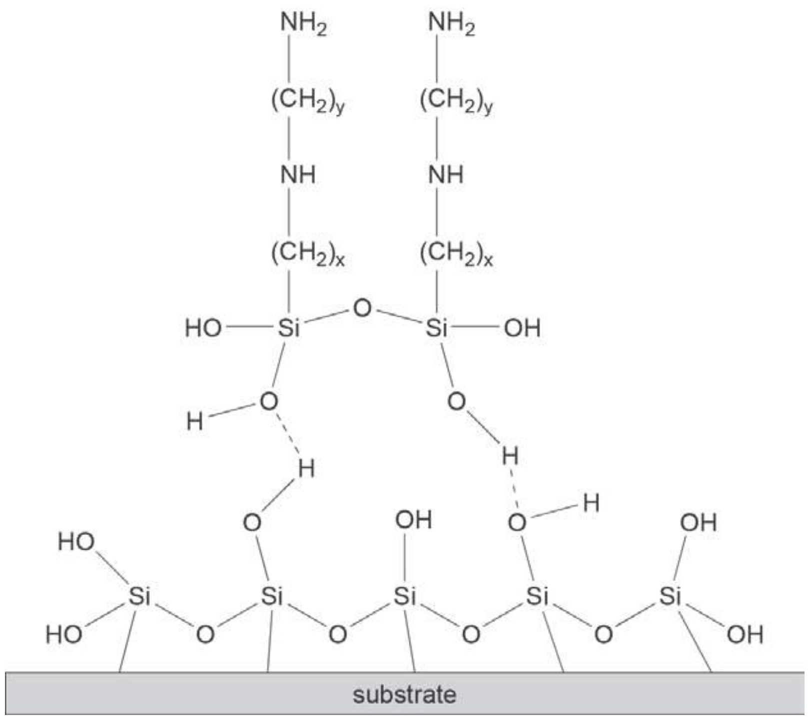

Silane primer

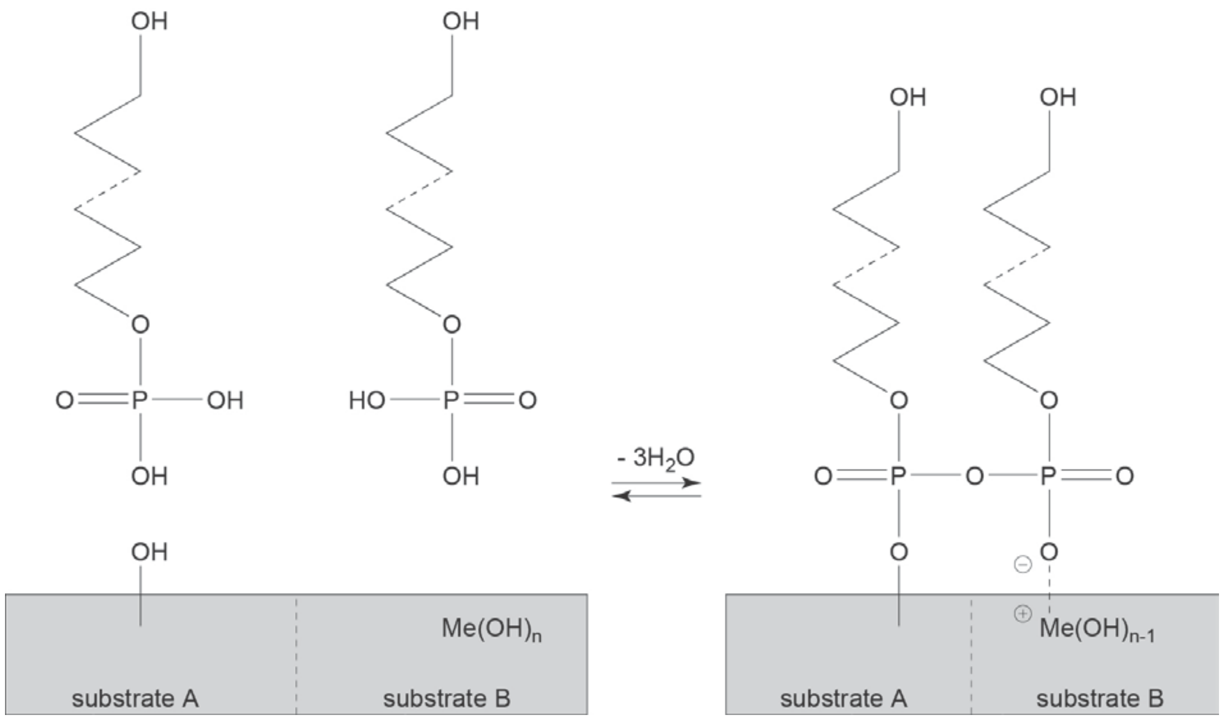

Phosphate primer

Glass bonding - selection criteria for the adhesive

- service temperature -20 °C to +80 °C

- adequate shear and tensile strength

- high stiffness for point fixings
- intermediate stiffness/flexibility for load-bearing joints
- high flexibility for linear or large planar joints

- compensation of CTE mismatches

- reduced tendency to creep

- durability (UV, corrosive media, moisture, cleaning agents)

- color/transparency

- processing properties (viscosity, open time, curing conditions, …)

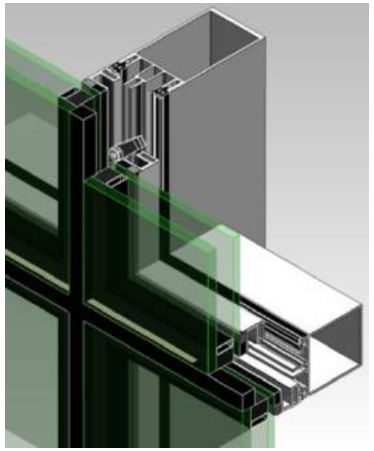

Development of a glass metal point fixing

Dynamic mechanical analysis

- storage modulus E‘
- temperature-dependent material behaviour
- initial temperature of the glass transition in the range of -5 °C to +47 °C

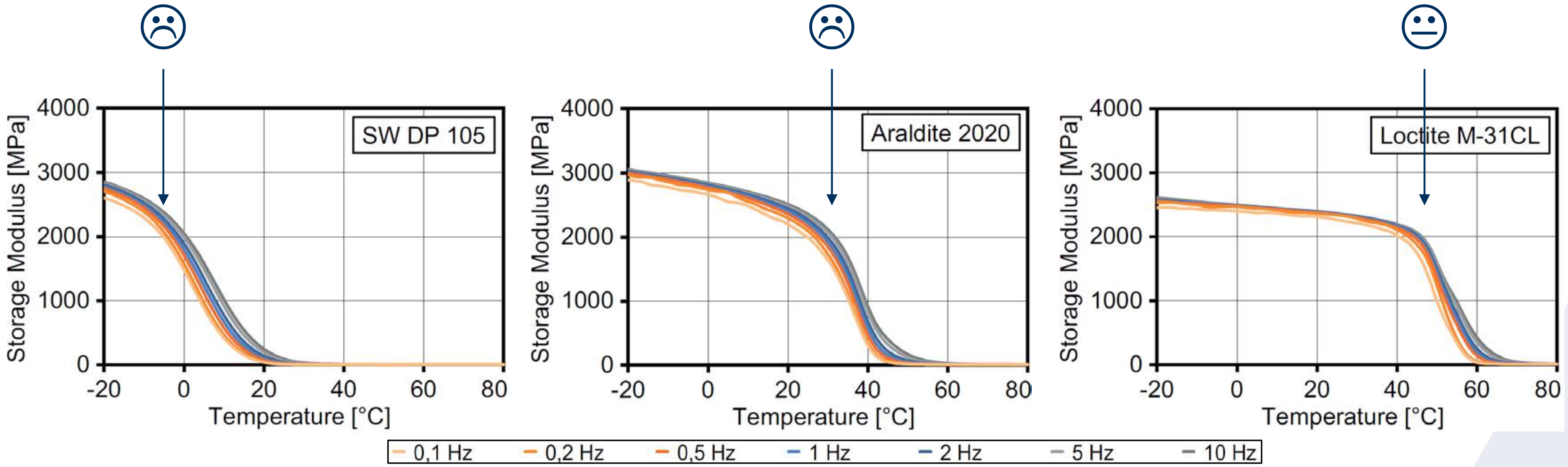

Wünsch, J., PhD-Thesis, TU Dresden, 2017

Tensile Tests

CertBond
COST Action CA18120

- deformation and fracture behaviour
- temperature-dependent
  - low temperatures → high modulus and high strength
  - within glass transition area → properties change significantly
  - high temperature →low modulus of elasticity, low strength and higher elongation at break

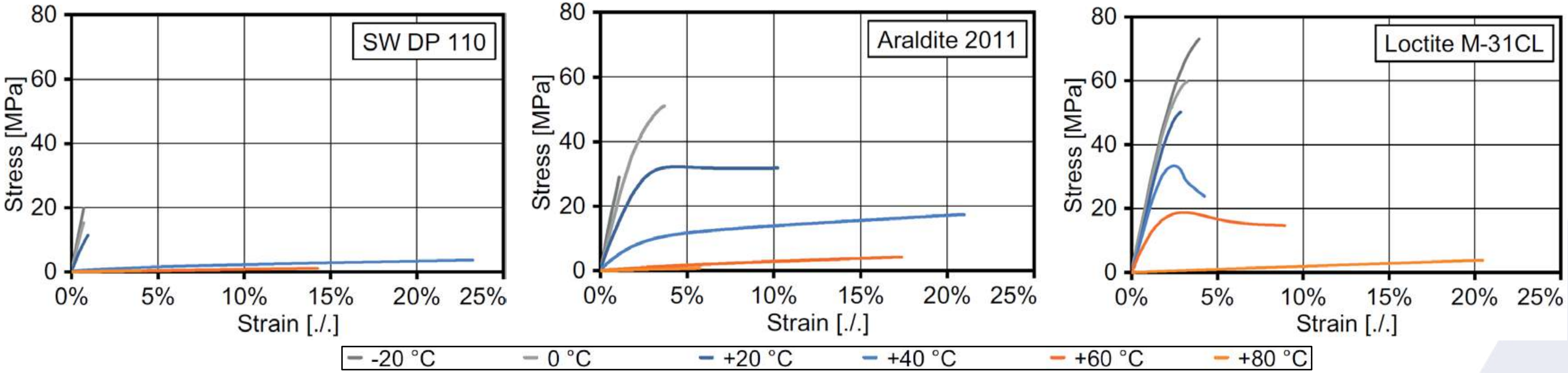

Wünsch, J., PhD-Thesis, TU Dresden, 2017

Small specimens

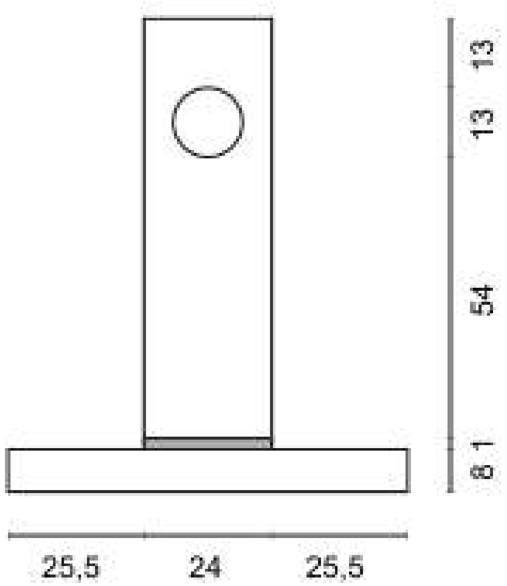

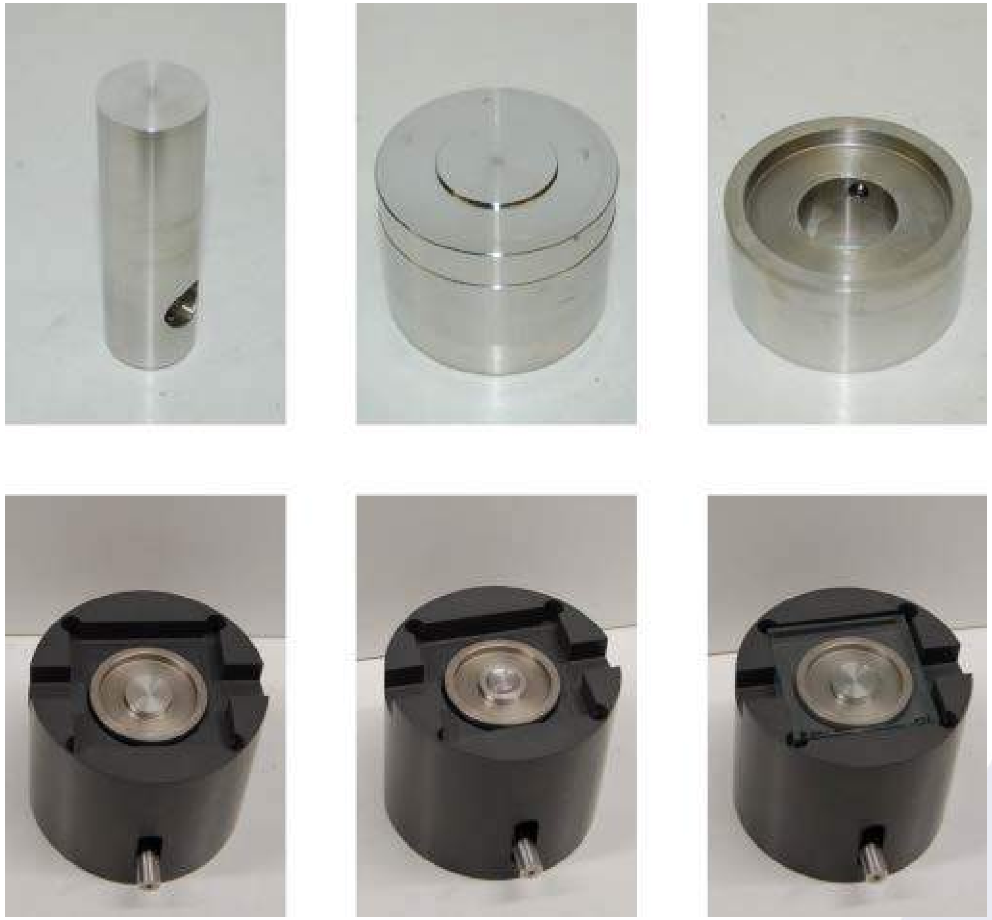

Kothe, C., PhD-Thesis, TU Dresden, 2013

Accelerated Weathering

CertBond
COST Action CA18120

Ageing	Description
FEU	Continuous exposure to condensed water for 500 h
GEM	Storage in demineralized water with addition of 0.1 % detergent at 45 °C for 500 h
KLI	Variable climate test for 500 h
KOR	Corrosion test with sodium chloride for 500 h
REI	Storage in façade cleaning solution at 45 °C for 500 h
SO2	Exposure to humid atmospheres containing sulfur dioxide for 480 h
SUN	Combined exposure to temperature, demineralized water and artificial light for 500 h
TEM	Exposure to increased temperature of 80 °C for 500 h
UV	Exposure to artificial light for 2000 h
WAS	Storage in demineralized water at 45 °C for 500 h

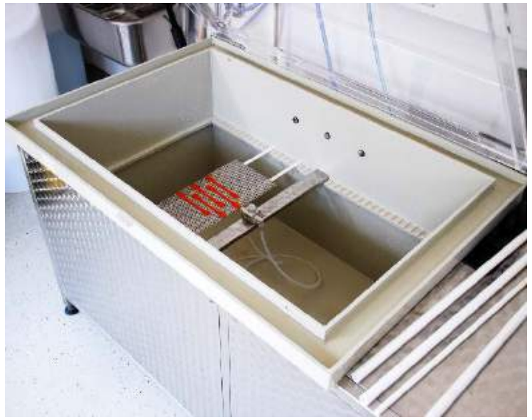

Testing of small specimens

CertBond
COST Action CA18120

- determination of adhesive strength between glass and stainless steel

- metal cylinder bonded to glass plate
- specimen subjected to accelerated weathering
- cylinder tensile test with constant strain rate 0.1 mm/min

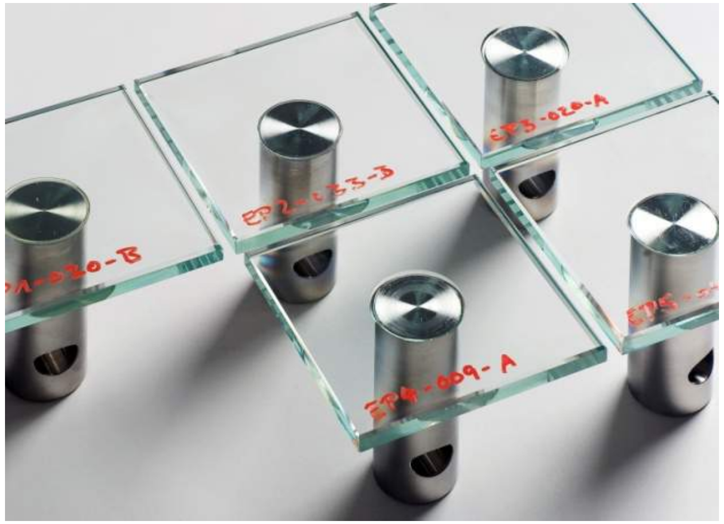

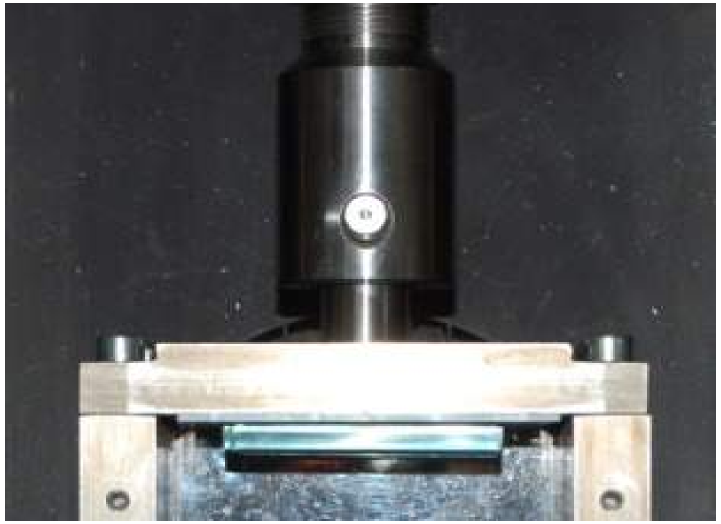

Tensile test

- reference strength → 5 % fractile in the range of 5 MPa and 15 MPa
- water or harmful media → strength reductions
- irradiation or exposure to high temperatures → little effects on the strength

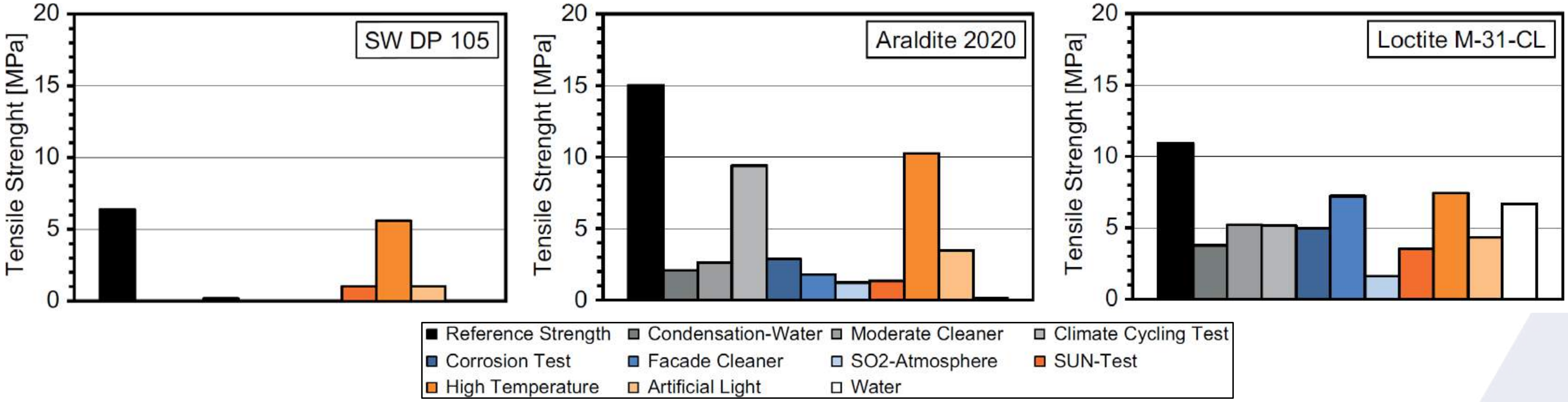

Wünsch, J., PhD-Thesis, TU Dresden, 2017

Acknowledgement

CertBond
COST Action CA18120

EUROPEAN COOPERATION
IN SCIENCE & TECHNOLOGY

Funded by the Horizon 2020 Framework Programme
of the European Union

Thank You!

www.certbond.eu

Funded by the Horizon 2020 Framework Programme of the European Union

CertBond
COST Action CA18120

A critical review on test methods and simulation models for the characterization of adhesive joints

Assoc. Prof. Konstantinos Tserpes

cost
EUROPEAN COOPERATION IN SCIENCE & TECHNOLOGY

Funded by the Horizon 2020 Framework Programme of the European Union

Sources of the lecture:

CertBond
COST Action CA18120

THE JOURNAL OF ADHESION
2021, AHEAD-OF-PRINT, 1-77
https://doi.org/10.1080/00218464.2021.1953479

Taylor & Francis
Taylor & Francis Group

Open access

Testing mechanical performance of adhesively bonded composite joints in engineering applications: an overview

Michal K. Budzik[a], Markus Wolfahrt[b], Paulo Reis[c], Marcin Kozłowski[d], José Sena-Cruz[e], Loucas Papadakis[f], Mohamed Nasr Saleh[g], Klara V. Machalicka[h], Sofia Teixeira de Freitas[g], and Anastasios P. Vassilopoulos[i]

[a] Department of Mechanical and Production Engineering, Aarhus University, Aarhus, Denmark [b] Polymer Competence Center Leoben, Leoben, Austria [c] Department of Electromechanical Engineering, University of Beira Interior, Covilhã, Portugal [d] Faculty of Civil Engineering, Department of Structural Engineering, Silesian University of Technology, Gliwice, Poland [e] Department of Civil Engineering, University of Minho, Guimarães, Portugal [f] Department Mechanical Engineering, Frederick University, Nicosia, Cyprus [g] Department of Aerospace Structures and Materials, Delft University of Technology, Delft, The Netherlands [h] Klokner Institute, Czech Technical University in Prague, Klokner Institute, Prague, Czechia [i] Composite Construction Laboratory (Cclab), Ecole Polytechnique Fédérale De Lausanne (EPFL), Lausanne, Switzerland

THE JOURNAL OF ADHESION
2021, AHEAD-OF-PRINT, 1-61
https://doi.org/10.1080/00218464.2021.1941903

Taylor & Francis
Taylor & Francis Group

Open access

A review on failure theories and simulation models for adhesive joints

Konstantinos Tserpes[a], Alberto Barroso-Caro[b], Paolo Andrea Carraro[c], Vinicius Carrillo Beber[d], Ioannis Floros[a], Wojciech Gamon[e], Marcin Kozłowski[f], Fabio Santandrea[g], Moslem Shahverdi[h], Davor Skejić[i], Chiara Bedon[j], and Vlatka Rajčić[i]

[a] Laboratory of Technology & Strength of Materials, Department of Mechanical Engineering & Aeronautics, University of Patras, Patras, Greece [b] Group of Elasticity and Strength of Materials, University of Seville, Seville, Spain [c] Department of Management and Engineering, University of Padova, Padova, Italy [d] Polymeric Materials and Mechanical Engineering, Fraunhofer Institute for Manufacturing Technology and Advanced Materials IFAM, Bremen, Germany [e] Faculty of Transport and Aviation Engineering, Silesian University of Technology, Silesian, Poland [f] Faculty of Civil Engineering, Silesian University of Technology, Silesian, Poland [g] Department of Applied Mechanics, RISE, Research Institutes of Sweden, Sweden [h] Empa, Swiss Federal Laboratories for Materials Science and Technology, Dübendorf, Switzerland [i] Faculty of Civil Engineering, University of Zagreb, Zagreb, Croatia [j] Department of Engineering and Architecture, University of Trieste, Trieste, Italy

Outline

- Methodologies to achieve certification
- Test Methods
- Conclusions
- Simulation Models
- Conclusion

CertBond
COST Action CA18120

Methodologies to achieve certification

EUROPEAN COOPERATION IN SCIENCE & TECHNOLOGY

Funded by the Horizon 2020 Framework Programme of the European Union

Mechanical testing

Test pyramid

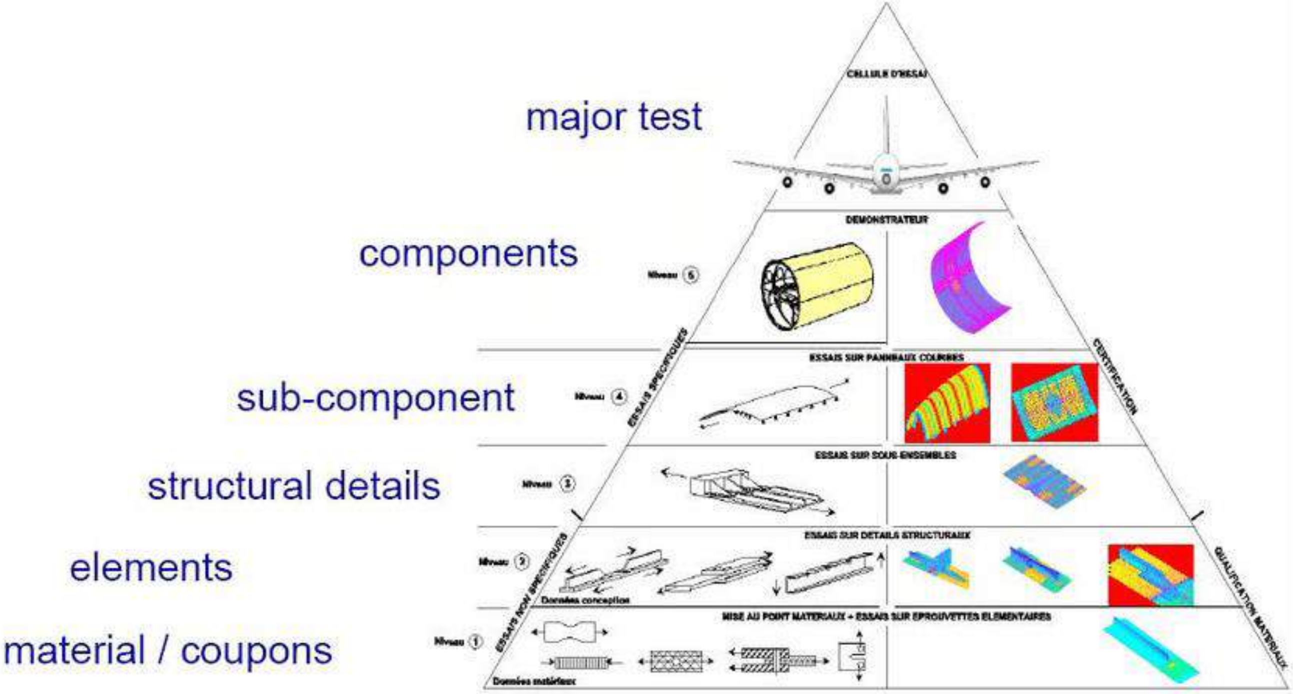

Simulation (Virtual Testing)

CertBond
COST Action CA18120

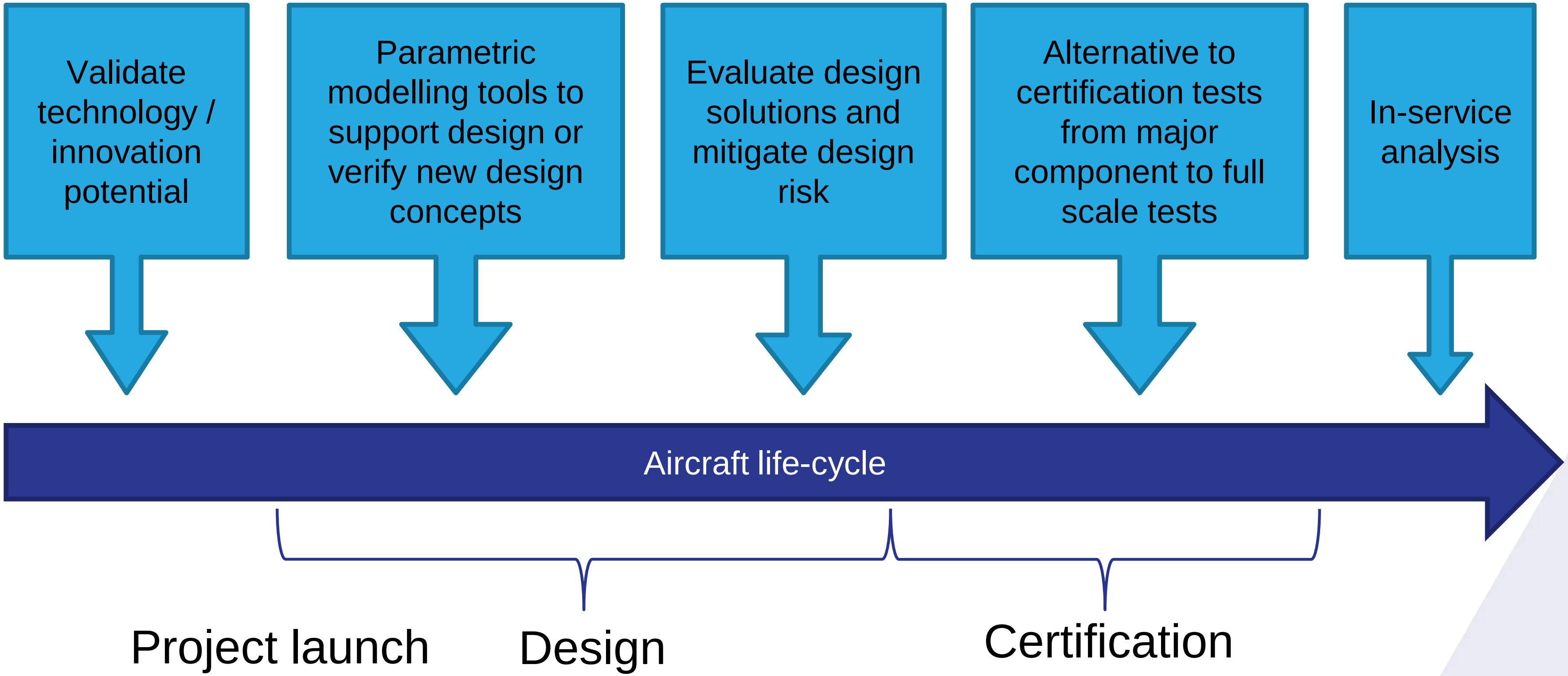

Test Methods

CertBond
COST Action CA18120

EUROPEAN COOPERATION IN SCIENCE & TECHNOLOGY
Funded by the Horizon 2020 Framework Programme of the European Union

Contents

CertBond
COST Action CA18120

Coupon-level:

- Strength-based approach (evolution of ultimate failure stresses and strains)
- Fracture mechanics, toughness approach (evaluation of crack growth)

Structural part level:

- Applications from the Aerospace, Wind Energy, Civil Engineering, Automotive

Strength analysis

CertBond
COST Action CA18120

- Assessment of bonded structures in terms of strength characterization is customarily done by performing **lap-shear** and **peel tests**.

- Single lap type joints are commonly used in the aerospace and automotive industries due to the fact that the adherend thickness is comparatively thin.

- Peel tests are carried out to assess the bond quality between a rigid and a flexible joining part. The test is mainly used for the comparative evaluation of adhesives and surface treatment methods.

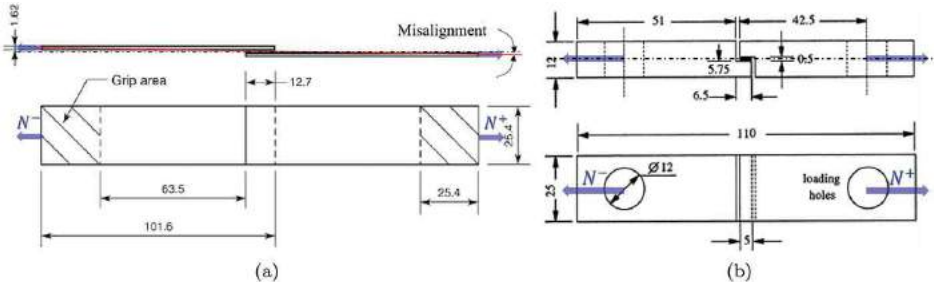

Lap joints specimens under axial loading *N*. (a) The Single Lap Joint (SLJ) geometry. (b) The Thick-Adherend Shear Test (TAST) geometry.

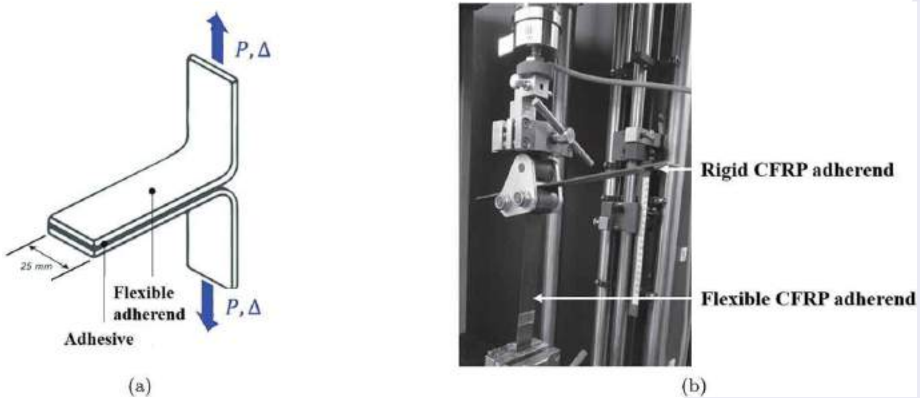

Peel testing configurations. (a) The T-peel test geometry. (b) The Composite Peel Test (CPT) set-up.

Fracture analysis

CertBond
COST Action CA18120

- The fracture-mechanical approach assumes the **presence of cracks (defects)** in the material, which in combination with external mechanical loading lead to fracture initiation, growth of a main crack and finally to critical failure.

- Introduction of **fracture mechanics** to bonded materials has revolutionized the field leading to more reliable structures by introducing new design criteria and predictive tools.

- Wide acceptance and use of fracture-mechanics-based approaches originate from the fact that bonded joints are regarded as **intrinsically and extrinsically heterogeneous**. The heterogeneities originate from both the geometrical features like corners, layer drops, edges as well as dissimilarities between material properties, e.g. different properties of laminas, or between the laminate and the adhesive. Also, adhesive joints are very sensitive to manufacturing defects, which are hard to avoid due to multistep technological processes.

- Since the early days, a number of test protocols and data reduction schemes have been proposed with only a relatively small amount of such being followed by a standard.

Fracture analysis

CertBond
COST Action CA18120

Fracture modes:

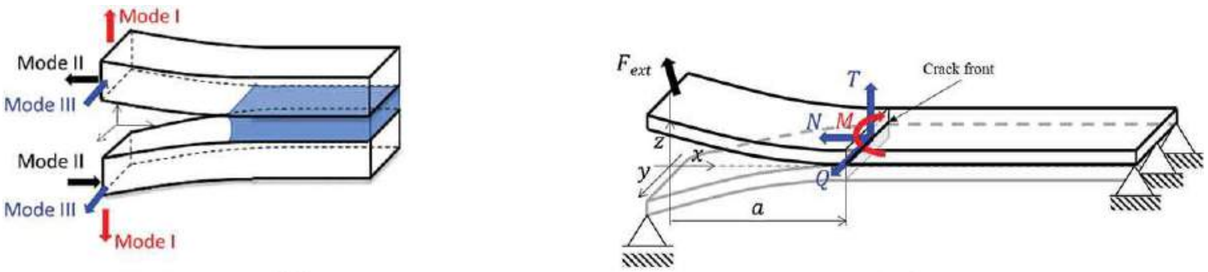

(a) (b)

- the mode I – opening or cleavage mode and followed by notation K_I, G_I, J_I
- the mode II–in-plane shear and followed by notation K_{II}, G_{II}, J_{II}
- the mode III – anti-plane shear and followed by notation K_{III}, G_{III}, J_{III}

- ❑ The existing crack growth criteria are congruent and indicate mode I as the most critical loading case. Hence, the joints are designed to carry the loads corresponding to mode II and mode III loading directions and such conditions are frequently encountered in real structures.

- ❑ Under an arbitrary external loading, for a prismatic, rectangular cross-section adherend (usually beam), using the effective crack tip forces approach, modes I, II and III can be combined through:

$$G = \frac{1}{2Eb^2h^3}\left(12M^2 + h^2N\right) + \frac{1}{2\mu hb^2}\left(T^2 + Q^2\right)$$

where E, μ, h, and b are the adherend Young's and shear modulus, adherend thickness and width, respectively. M, N and T are the bending (cleavage) moment, axial/membrane/in-plane force and transverse/out-of-the-plane shear force per unit width, respectively, and Q is the transverse/anti-plane shear force.

Fracture analysis

CertBond
COST Action CA18120

Mode I:

In this case, $N = Q \to 0$ *and* $F_{ext} = M$, leading to: $G = G_I = 6\frac{M^2}{Eb^2h}$

where M is the edge applied bending moment or the effective bending moment defined as $M=Pa/b$ with P being the projected on z-axis component of F_{ext} and a is the current crack length.

- Both, M and P could be applied to the tip of the adherends and both such loading conditions are now frequently in use with the latter case being subject of standardized method with the data reduction following bending of a cantilever beam.

- The family of methods is known under the name of Double Cantilever Beam tests (DCB), which forms the most widely used testing framework. Here, three types of loading boundary conditions are usually considered:
  i. loading with the bending moment M
  ii. loading with the transverse force T
  iii. constant displacement rate, i.e. Δ=const.),
  iv. loading by imposed constant displacement Δ where T can be regarded as reaction.

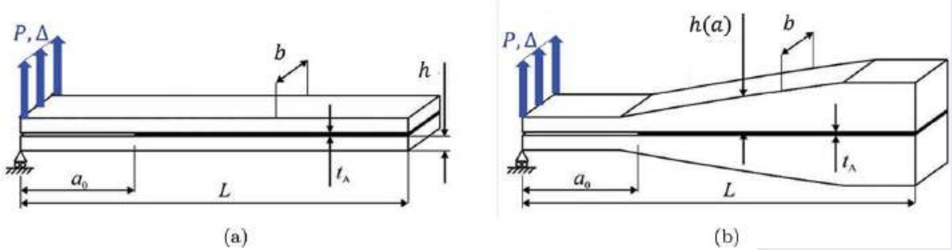

Schematic representation of the DCB (a) and the TDCB (b) specimens with initial crack of length α_0, under transverse force, P, or displacement, Δ loading

Fracture analysis

CertBond
COST Action CA18120

Mode II:

- **Introduction of pure mode II requires the crack tip force coming solely from the horizontal projection, along the *x*-axis. Direct application of such boundary condition rarely takes place and is a domain of 'stress' testing, incl. shear lap joints.**

- The fracture mechanics implementation is based on the beam bending configurations applied to bonded joints. For instance, the three-point bending test on bonded joints with an edge crack corresponds to the End Notched Flexure (ENF) experiment, the cantilever beam test applied to the edge crack specimen corresponds to the End Loaded Split (ELS) experiment or inverted version of such (iELS).

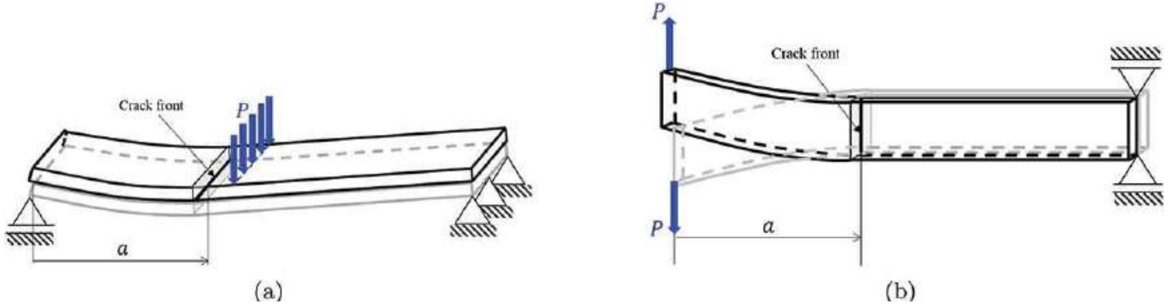

(a) ENF mode II testing configuration and (b) Split Cantilever Beam for mode III testing

Fracture analysis

Mode III:

- Compared to the other fracture modes, a relatively small amount of works considered mode III. The importance, specifically from the applied perspective, is indisputable.

- Several test methods were examined as ways to measure interlaminar mode III fracture toughness. Tests on short-fiber composites using a single notched plate arrangement have been conducted. Such configuration, under the name Edge Crack Torsion has been applied to the bonded joints to study rate effects in mode III. Main drawback these tests is the distortion due to the relatively low torsional rigidity of plates geometries. To address this issue, a modified DCB arrangement under with the loads applied in the crack plane but in transverse direction (thus anti-plane shear mode) was used.

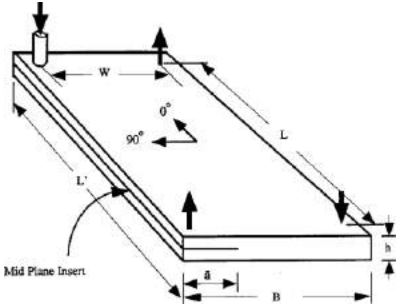

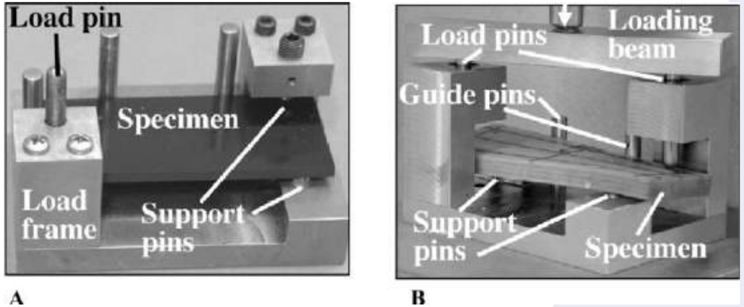

Fracture analysis

Mixed Mode:

- **Strive for more reliable design tools, more robust failure criteria, and experimental campaigns simulating as close as possible actual loading conditions, led academia and industry towards mixed-mode fracture testing.** The need for such an approach comes from the fact that, usually, structures experience complex loading scenarios during operations and life-time. In addition, even predominantly pure fracture loading lead to mixed-mode conditions at the crack tip.

- Combination of the DCB and the ENF produces a mixed-mode bending (MMB) test. The test gains significant importance and is one of the standards in the aerospace industry. Advantages here are easiness of producing different modes G_{II}/G_{I} ratios, which together with the DCB and the ENF can form the so-called fracture envelope.

Effect of adhesive's thickness

CertBond
COST Action CA18120

- The thickness of the bondline is one of the crucial geometrical parameters of an adhesively bonded joint.
- Application of adhesive joints in marine, civil engineering, or wind energy industries requires use of thick adhesive layers, up to several centimeters for which excluding adhesive thickness seems inappropriate.
- Historically, bondline thickness was often assumed as negligible when compared to other important length scale parameters; thus, for analysis the effect of the bondline thickness could be omitted – such case is present on the left side of the figure. Application of adhesive joints in marine, civil engineering, or wind energy industries requires use of thick adhesive layers, up to several centimeters for which excluding adhesive thickness seems inappropriate – such case can be seen on the right side of the figure.

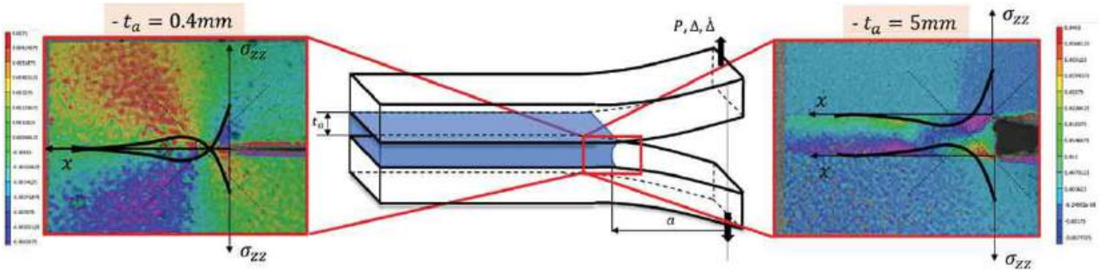

Adhesive thickness t_a affects the local, crack front, stress/strain field. The color map corresponds to the strain tensor shear component (ε_{xz}) captured using the digital image correlation. Predicted distribution of the crack opening stresses σ_{zz} is also presented

Dissimilar adherends

- Bonding and evaluation of structures and materials made of dissimilar adherends is gaining nowadays significant attention. **It is well recognized that once a bimaterial is loaded, a stress gradient exists at the interface between the two materials. Under such circumstances, the structure, or material, is likely to fail under apparent loading being lower than the failure load calculated for any of the two materials separately.**

- The adhesive thickness may play here a significant role, as the adhesive itself can form the ‘dissimilar’ interface, providing it is thick enough or it can be treated as a line which accommodates the stress gradient between the two joined materials. The latter problem received attention from the theoretical standpoint and led to the nascent of the interface fracture mechanics. The data here were often supported by the experimental investigations using so-called Brazilian disc test.

- Composite patching of aluminium fuselages or concrete bridges or attaching composite superstructures to steel decks are examples of bonding between two dissimilar adherends.

Applications

CertBond
COST Action CA18120

EUROPEAN COOPERATION IN SCIENCE & TECHNOLOGY
Funded by the Horizon 2020 Framework Programme of the European Union

Aerospace Engineering

Trends in Testing:

Thus, the real challenge is always to develop element/sub-component test set-ups which mimic the geometrical constraints and the load transfer in full-scale structures. These sub-component elements generally consist of a section taken through a single or multiple stiffeners and can be tested in fairly large numbers.

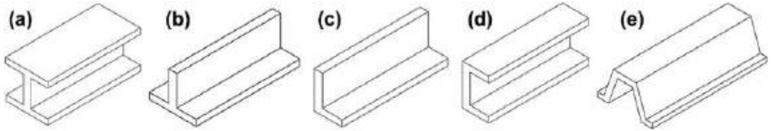

Typical stiffener profiles used to reinforce panels of aerospace structures

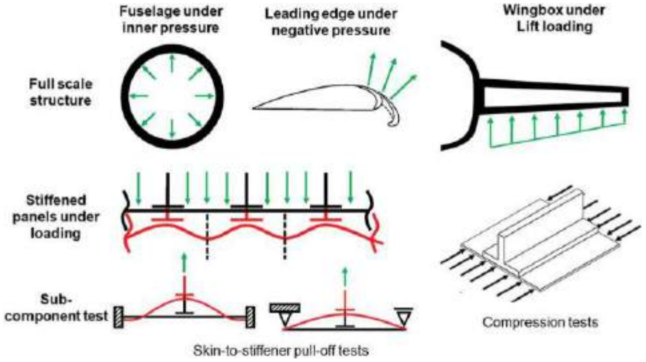

Sub-component tests representing the loads and boundary condition of the full-scale aerospace structures under service

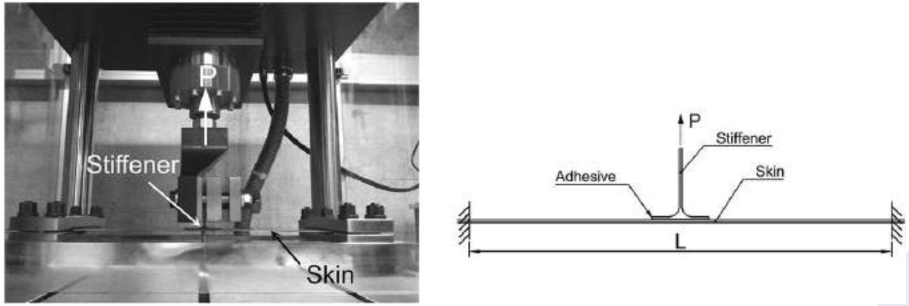

Pull-off test setup: Fiber Metal Laminate skin bonded to a CFRP T-stiffener

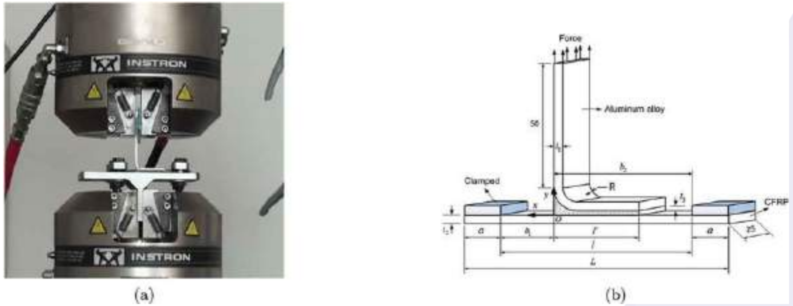

Pull-off test setup with CFRP skin bonded to an aluminium L-type stiffener

Aerospace Engineering

Trends in Testing:

- As far as the compression testing is concerned, these tests are used to evaluate the effectiveness of the adhesively-bonded joints, in maintaining the structural integrity, in the case of buckling and post-buckling. This serves one of the main objectives of attaching stringers/stiffeners to the skin of fuselage or wing structures, aiming to provide the required strength against buckling loads in service.

(a)

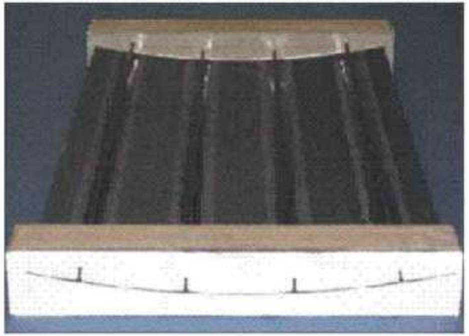

(b)

Specimens for compression tests with single (a) and multiple stiffeners (b)

✓ **Effect of design and manufacturing parameters**
✓ **Effects of defects**

Wind Energy

Potentials and Challenges:

- Blade issues contribute substantially to the failure rate.
- The thickness of adhesive bondline in large wind turbine rotor blades can reach or exceed 20–30 mm. Thus, the resulted bondline contain a significant number of fabrication defects (voids).
- Full scale physical blade testing is the ultimate tool for the certification/validation of the blade design and manufacture. Nevertheless, current experiments performed on full scale Mega Watts wind turbine blades are very time consuming and expensive.
- Bulk adhesive behavior becomes more important with thickness and in such cases fatigue data on bulk adhesives might be more reliable than those from joints.

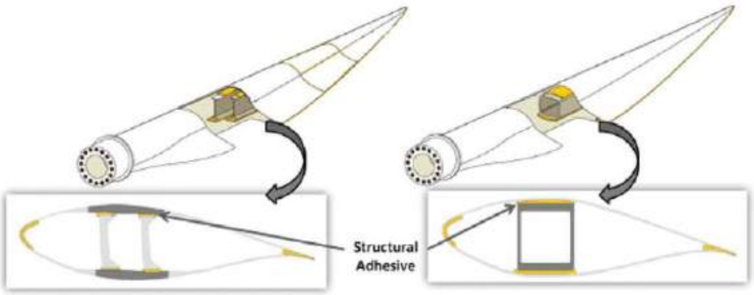

Voids in the bonding lines of composite wind turbine blades

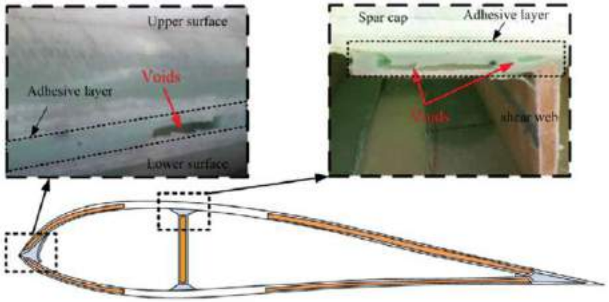

Voids in the bonding lines of composite wind turbine blades

Wind Energy

Sub-component (beam) during a cyclic loading.

Sub-component (beam) during a cyclic loading.

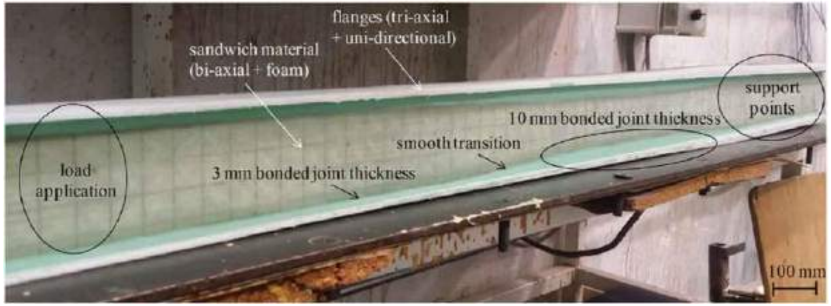

Characteristics of the sub-component.

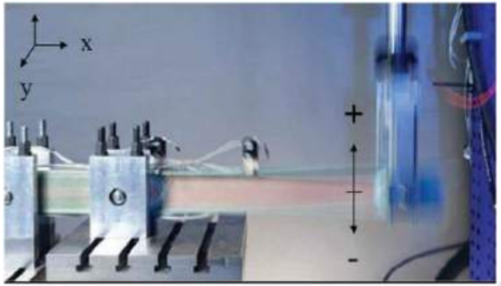

(a)

Experimental set-up used for fatigue loading experiment.

(a)

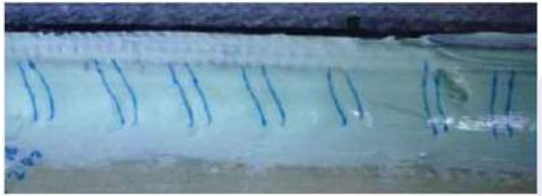

(b)

Transverse cracks in the beam adhesive bond line (left) and in a WTRB spar to shear web bondline (right) – not in scale.

Civil Engineering

Potentials and Challenges:

- In case of **strengthening of existing structures with FRPs**, mainly two strengthening techniques are used: (i) the externally bonded reinforcement (EBR) technique and (ii) near surface mounted (NSM) reinforcement technique. The EBR involves bonding the FRP material (in form of laminate or textile) onto the surface of a structural element to be strengthened, while the NSM the FRP reinforcement is placed into pre-cut groves in the element. Typically, both techniques use high-strength adhesives (or resins) to bond the FRP reinforcement to the substrate, e.g. epoxy adhesives.

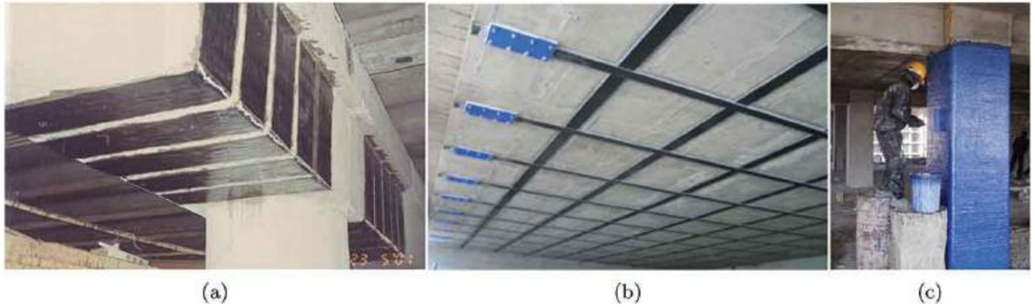

Examples of FRP strengthening of structural concrete elements in civil engineering: (a) shear strengthening, (b) flexural strengthening, (c) confinement

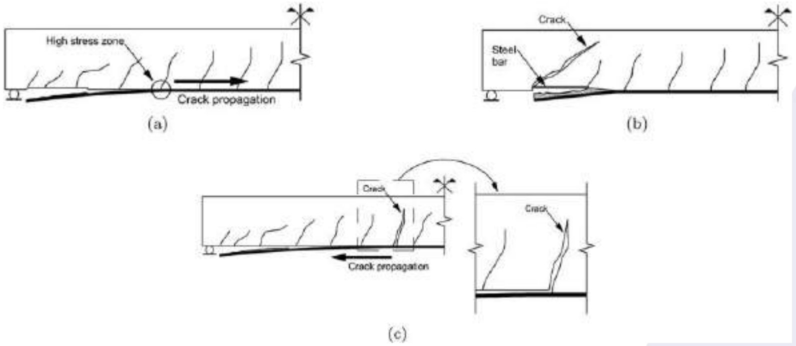

Different types of FRP deboning: (a) Interfacial debonding due to combined effects of shear and normal stress at the extremities of the FRP. (b) Debonding by concrete cover separation induced by a critical diagonal crack close to the FRP extremity. (c) Debonding at an intermediate flexural crack.

Civil Engineering

Trends in Testing:

- Common experimental setups for adhesively bonded composite joints reported in literature (that applies for both EBR and NSM) can be divided into two main groups: (i) direct pullout test and (ii) flexural beam test.

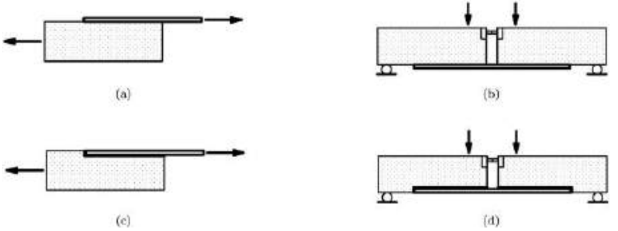

Schematic representation test setups for characterizing the bond of FRP concrete systems: (a-b) EBR and (c-d) NSM

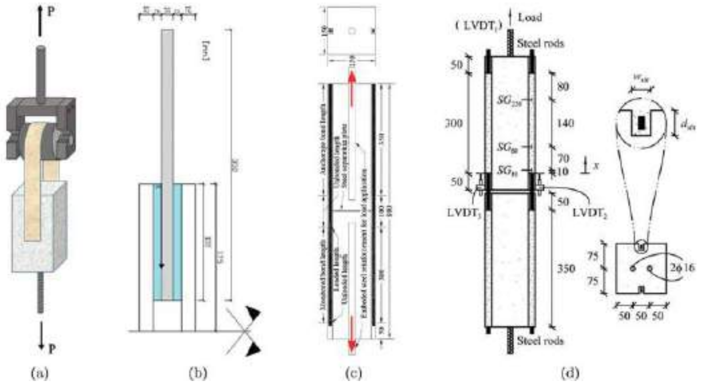

Examples of double-shear test of bond of FRP: (a) EBR concrete, (b) EBR glass, (c) NSM concrete, (d) NSM concrete.

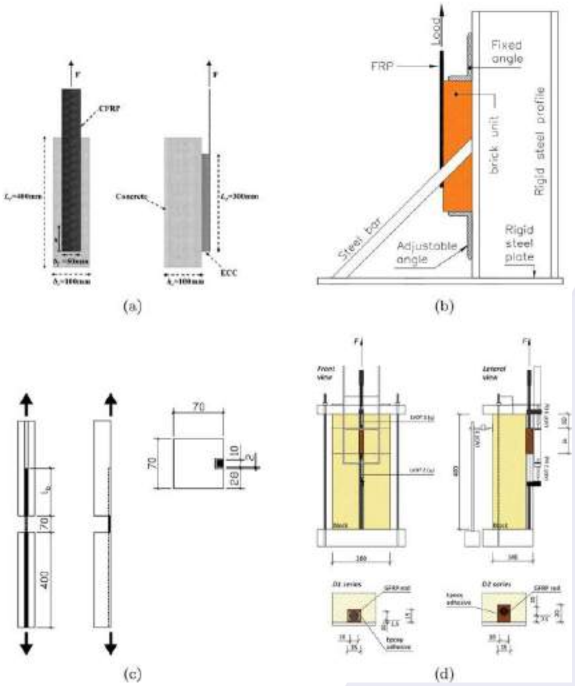

Examples of single-shear test of bond of FRP: (a) EBR concrete (b) EBR brick, (c) and (d) NSM timber.

Automotive Engineering

CertBond
COST Action CA18120

Potentials and Challenges:

- Fatigue strength of lightweight materials and joints in automotive structures as well as occupant' protection during crash are key requirements, which drive automotive manufacturers to improve their final products in order to satisfy the highly demanding market.
- Simultaneously, the introduction of novel materials and manufacturing and joining techniques is strongly correlated with quality and certification issues, which should be analysed and quantified by means of experimental investigations in terms of strength and endurance, in order to ensure the sustainability of such design solutions in automotive production.

Joining method	Multi-material design	Body stiffness	Crash resistance	Operation resistance	Corrosion resistance	Acoustics
Adhesive bonding	+++	+++	+++	+++	++	+
Spot welding	–	0	0	0	–	–
Clinching	–	–	–	+	0	–
Riveting	0	0	–	+	–	–
Joining with screws	0	0	0	0	–	–
Laser welding	–	++	++	++	0	0

Automotive Engineering

CertBond
COST Action CA18120

Trends in Testing:

- A major application in automotive structures in which structural adhesive bonding is involved is the joining of the glass windshield on the automotive bodywork by means of two-component polyurethane adhesive. This solution has motivated automotive manufactures to enhance further dissimilar attachments on automotive body such as composite reinforced plastic roof and hood.

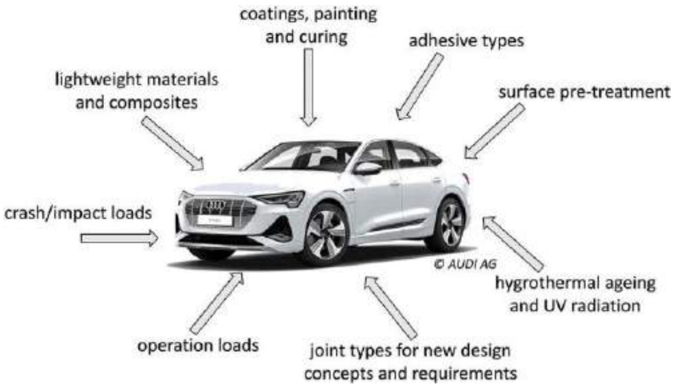

Overview of influencing parameters related to adhesive bonding applications in automotive structures reproduced based on Quattro Daily.

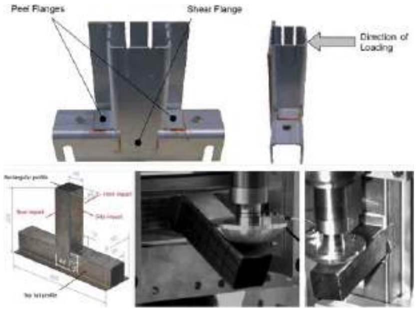

Automotive related applications of T-shaped specimens for experimental testing with purely adhesive bonded flanges under crash loads.

Conclusions

- Regardless of the various tests standardized by several international organizations, such as International Standard Organization (ISO), European Standard (EN), British Standards Institution (BSI) and American Society for Testing and Materials (ASTM), there is still controversy in terms of applied loads and respective adhesive properties obtained.

- In terms of strength characterization, for example, lap-shear and peeling tests are suggested and duly supported by international standards. Most of them were developed for the aerospace industry and are essentially optimized for thin adhesive joints involving, mainly, metallic adherends.

- So far, few standard test procedures for either fatigue or fracture behavior of adhesively bonded joints made from FRP composites have been established.

- Although several testing methods are available to characterize stiffened panels under tension, compression, bending, buckling and post-buckling loading conditions, only two typical tests are suggested for sub-components involving adhesive joints: skin-to-stiffener pull off-tests and compression tests of stiffened panels.

Conclusions

CertBond
COST Action CA18120

- To ensure continuous growth of the adhesive bonding field the new international standards, focusing on actual adhesive joints' performance rather than on specific application of adhesive joints are necessary. Principal damage onset locations for skin-to-stiffener joints – stiffener core or noddle and stiffener tip.

CertBond
COST Action CA18120

Failure Simulation Models

cost
EUROPEAN COOPERATION IN SCIENCE & TECHNOLOGY

Funded by the Horizon 2020 Framework Programme of the European Union

Contents

Classical Analytical Methods

CertBond
COST Action CA18120

- Most of the analytical models for adhesively bonded joints are 2D
- SLS: Volkesen's model and Golland & Reissner's model
- After the so-called classical works, some authors tried to obtain more general closed-form solutions by including, for example, adherends with dissimilar thickness and material properties or composite adherends
- Most analytical methods indicate that the strength of adhesive joints is enhanced by thicker bondline. However, in practice, the adhesive lap joint strength decreases as the bondline gets thicker.
- In order to realistically predict failure loads, analytical models should include the variation of stress through the adhesive thickness, including the interface stresses.

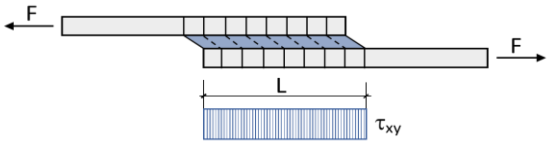

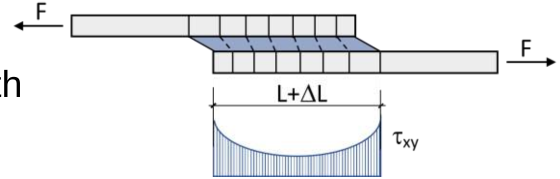

$$\tau_{xy} = \frac{F}{bL}$$

Process Zone Methods

- In the modelling of adhesive joints, **the consideration of only the peak (i.e. maximum) value of stress (or strain)**, has shown to produce over-conservative predictions.

- **Based on the concept that failure takes place within a process zone, process zone models (i.e. averaging methods), have been developed to address the effect of stress concentration on the mechanical behaviour of the joints.**

- Process zone methods rely on a length parameter (i.e. critical distance) which defines the size of the zone. This process length can be defined using calibration techniques.

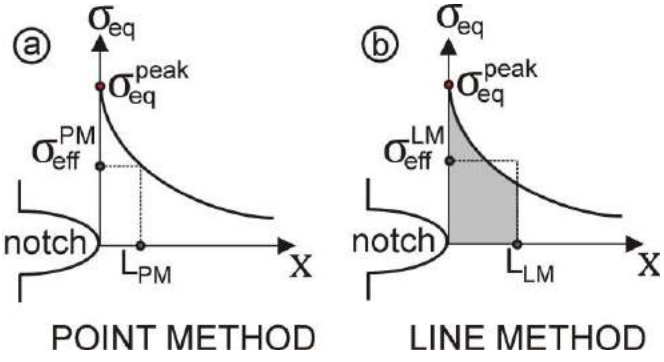

- Then, the defined failure criterion (stress or strain) can be considered as an average value in a point, in a line, in an area or in a volume. For instance, by averaging an equivalent stress σ_{eq} within a critical distance L, an effective stress σ_{eff} is obtained which can be used for prediction purposes.

- The TCD comprises several methods that consider the averaged stress in a point, in a line, in an area or in a volume.

$$Point\ method:\ \sigma_{eff,PM} = \sigma_{eq}(L_{PM}) \qquad Line\ method:\ \sigma_{eff,LM} = \frac{1}{L_{LM}}\int_0^{L_{LM}} \sigma_{eq}(x).dx$$

Linear Elastic Fracture Mechanics

- This method is used **to predict the critical load that leads to the propagation of an existing crack under a static load or the crack growth rate under cyclic loadings.** It can be applied when the material behaves in a linear-elastic manner and the fracture process zone is included in the singularity region.

- The LEFM was extended to interface cracks, so that is could be adopted for predicting, for instance, the propagation of cracks in bonded connections.

- Under fatigue loading, the G_{IC} is calculated by the Paris-law.

- Despite the complexities and difficulties, the LEFM was successfully applied to predict the crack propagation in bonded connections (see, for instance, some of the applications listed in the next section, as the VCCT technique is often adopted for the calculation of the ERR).

- **Special care must be taken when using the LEFM approach in bonded joints. Indeed, the fracture process zone can overcome the singularity region, leading to a significant dependence of the critical ERR on the adhesive thickness, under mode I and, mainly, mode II loadings.** As a final remark, it can be said that LEFM can be adopted to predict the static or fatigue crack propagation in bonded joints, provided that the fracture process zone is small, which is typically the case when the adhesive is sufficiently brittle

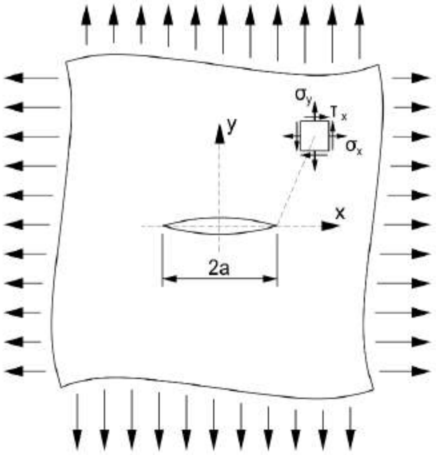

$$\sigma_c = \sqrt{\frac{E G_{Ic}}{\pi a}}$$

G_{Ic} is the mode I critical Energy Release Rate (ERR) and E is the Young's modulus

Virtual Crack Closure Technique (VCCT)

CertBond
COST Action CA18120

- Virtual Crack Closure Technique (VCCT) is a linear elastic fracture mechanics-based method used to compute the strain energy release rate based on 2D and solid 3D FEA which provide the mode separation required when using the mixed-mode fracture criterion.

- The key input parameters of the method are the critical mode-I strain energy release rate G_{IC} and critical mode-II strain energy release rate GIIC, which have to be determined experimentally. The VCCT method is usually applied through the FE method.

- In the last decade, VCCT method has been implemented into commercial FE codes such as ANSYS and Abaqus. Initially, the method has been widely used to simulate delamination growth in CFRP composites and in the last decade it has found many applications to adhesive joints together with the Cohesive Zone Modelling method.

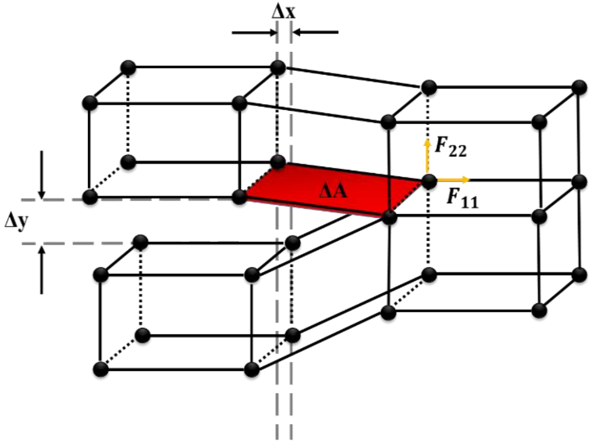

$$G_i = \frac{K_i^2}{E}\beta(i = 1,2,3)$$

$$G_I = -\frac{1}{2\Delta c}F_{22}\Delta y$$

$$G_{II} = -\frac{1}{2\Delta c}F_{11}\Delta x$$

$$G_{III} = -\frac{1}{2\Delta c}F_{33}\Delta z$$

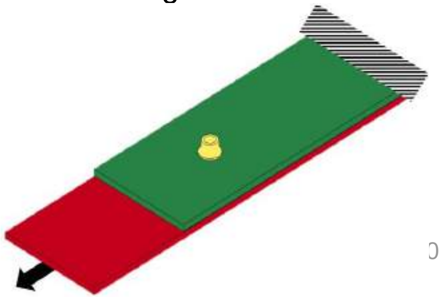

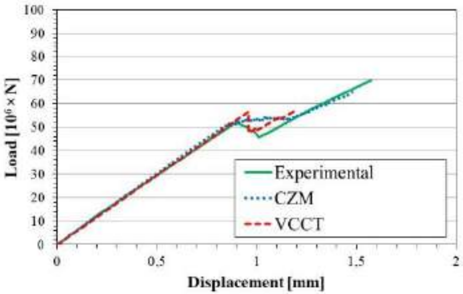

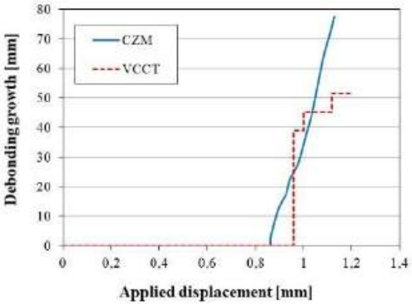

Stress Singularity Approach

- The use of failure initiation criteria based on nominal stresses is not a viable strategy to predict failure, whereas the use of singularity parameters to characterize the stress state is a feasible alternative, which is consistent with the principles of Linear Elastic Fracture Mechanics.

- In the early 20th century, analytical solutions of 2-dimensional elasticity problems with stress singularities were first derived.

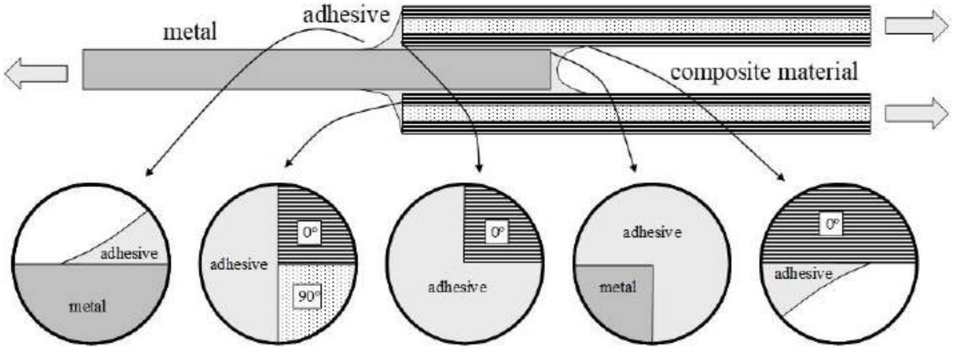

- **One of the first proposals to predict the failure initiation in adhesive joints defines a generalized stress intensity factor and compared it with a critical allowable value (the so-called generalized toughness) for the failure to initiate**.

- The growing adoption of composite materials, mainly in aeronautic lightweight structures, and the use of adhesive bonding with other materials complicate the analytical modelling of these singularity stress fields.

Finite Fracture Mechanics

- **Finite Fracture Mechanics is a mathematical framework designed to predict crack initiation in presence of stress concentrations. FFM is based on the idea that failure does not initiate at a single point through the generation of a crack of infinitesimal length, but rather with the formation of a finite-size crack appears, characterized by a length a_c and a critical load, P_c , which are both unknowns of the problem.**

- In the context of bonded joints, the principles of FFM can be illustrated by considering a bi-material corner with a remote applied load *P*.

- These two unknowns can be calculated by: $f(\sigma, \tau, \sigma_R, \tau_R) = 1 - \frac{\Delta \Pi_p}{\Delta A} = G_c(W_p)$

- All the examples reported so far considered 2D problems, which can be considered acceptable for simple geometries such as single or double lap joints. Extensions of the FFM to 3D problems were formulated. The stress fields and the ERR were calculated by FE analyses and the shape of the interface crack was chosen based on the iso-stress contour lines obtained from the analysis of the joint in the pristine condition. The 3D formulation was shown to slightly improve the failure predictions for scarf joints.

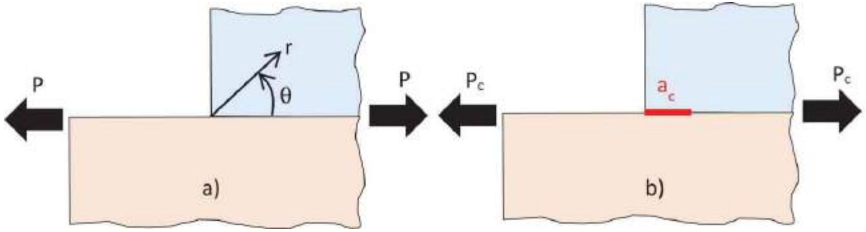

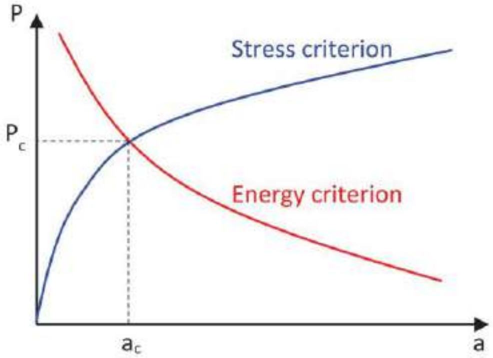

The Cohesive Zone Method (1/3)

- Cohesive Zone Modelling (CZM) is a damage mechanics-based numerical approach suitable for modelling crack initiation and propagation.

- Initially, the idea of a cohesion zone in front of the top of a crack was proposed. Later, it was numerically implemented and a numerical model which defines a function between traction and crack separation was proposed.

- During the last decades CZM has evolved and it has eventually achieved the status of method of choice for simulating delamination of composite materials and onset and debonding growth of adhesive joints. The method can be implemented either through spring elements or by using cohesive elements between the adherends in 2-D or 3-D problems.

- CZM approach has been successfully used by numerous authors for the simulation of delamination of CFRP materials as well as the debonding initiation and growth of joints with metal and/or composite adherents.

- For the most widely used bilinear traction-separation law, the main required inputs for the CZM approach are the initial stiffness of the joint, the maximum peak tractions and the critical energy release rate for normal and tangential directions.

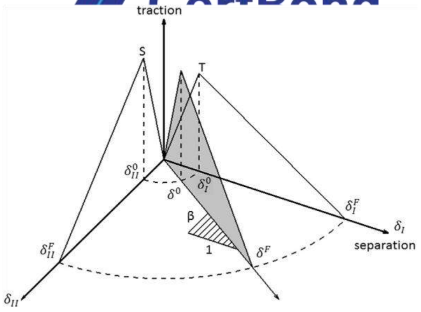

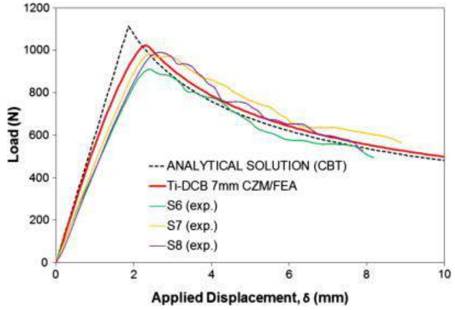

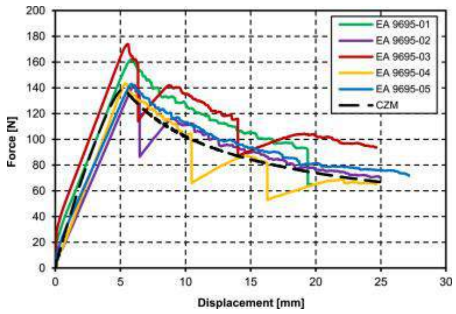

The Cohesive Zone Method (2/3)

- Apart from simulating delamination and debonding under pseudo-static loading, CZM has also been used to simulate fatigue crack growth, which has been the subject of intense research in the last decade.
- The general idea which underpins the simulation of fatigue debonding growth is the modification of the bilinear traction-separation law by degrading the strength, as well as the stiffness and fracture energy of the cohesive elements as a function of the applied load cycles.
- Numerical simulation of adhesive joints under fatigue loading takes place by means of simulating the debonding growth or creating a Paris-like law. In most cases the numerical models are validated by comparing the numerical to the experimental results. Researchers have simulated Mode I fatigue loading, high cycle fatigue growth and, Mode II fatigue loading, fatigue debonding under Mixed-Mode I+II loading using Compact Tension-Shear (CTS) specimen, the Short Beam Shear (SBS) specimen, a Mixed-Mode I+II bending apparatus and the Cracked Lap Shear (CLS).

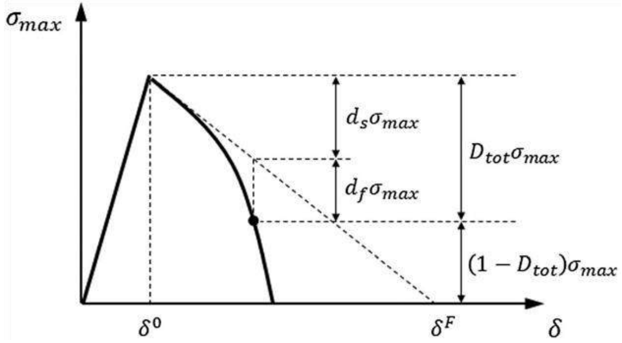

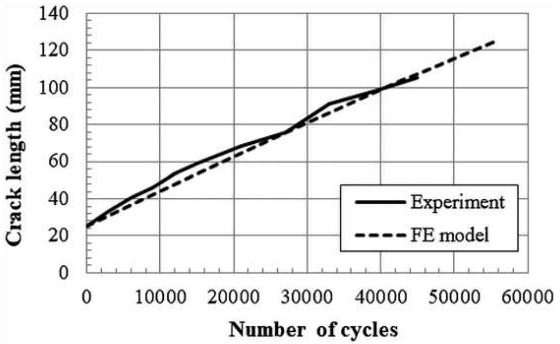

The Cohesive Zone Method (3/3)

CertBond
COST Action CA18120

Application of the CZM method to glued-in rods in cross laminated timber

- The basic modelling approach follows earlier applications of the CZM strategy to timber joints, and it is further adapted to include the bonding effect of the interposed glue.

- The CZM interaction takes place at the interface of the solid steel rod and the adjacent wooden elements, that are all described in the form of brick elements from the ABAQUS library.

- The numerical results prove that the use of CZM for the structural assessment of building structural elements can be efficient and accurate.

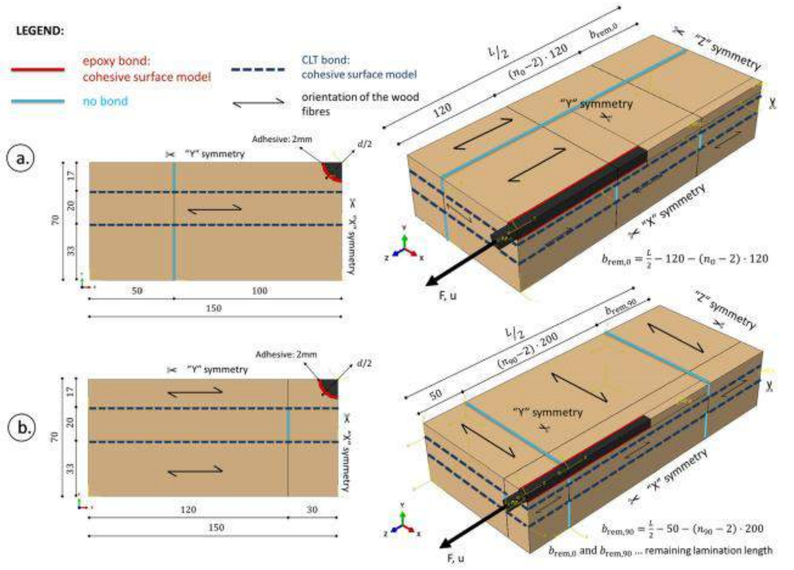

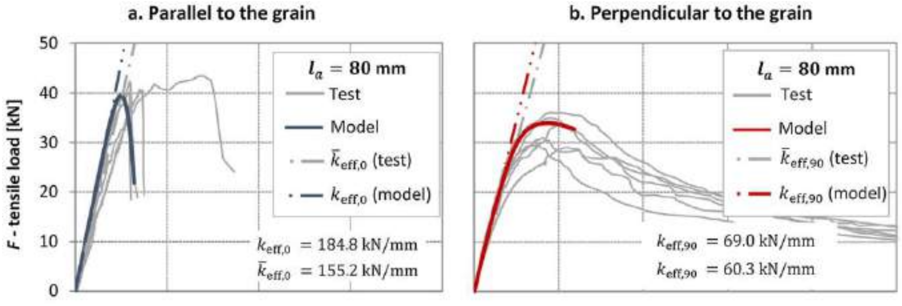

Progressive Damage Modeling

CertBond
COST Action CA18120

- Progressive damage modeling (PDM) is a widely used technique for predicting the fatigue/breakage behavior and strength of bonded joints based on their damage state's evolution. Several approaches for the simulation of damage progression in bonded joints have been introduced over the last decades. These approaches mainly focus on the prediction of the static strength of bonded joints based on different concepts, such as stress/strain-based failure criteria, continuum mechanics, cohesive zone models, and fracture mechanics.

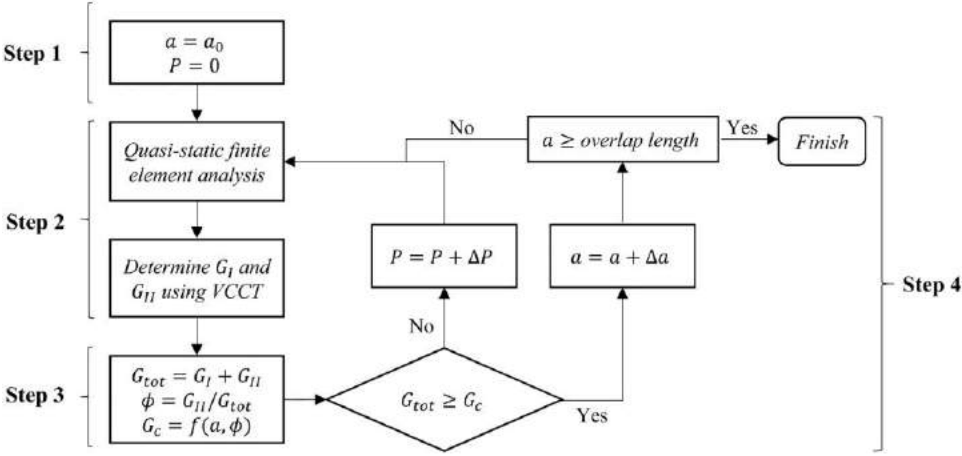

- One of the main challenges of PDM is its dependency on the experimental input. The second main challenge is its need for proper calibration of the method.

- The algorithmic implementation of PDM is straightforward, and it usually gives accurate results. Once the method is verified and validated, it can be calibrated for different joint configurations with minimum effort to predict such joints' behavior.

Probabilistic Methods

CertBond
COST Action CA18120

- Although deterministic analysis might suggest that performance requirements are fulfilled, **the inclusion of uncertainty in input variables and modelling assumptions might reveal that the probability of failure is yet significant.** The limitations of experimental and deterministic numerical methods motivate the introduction of probabilistic methods for the assessment of the structural performance of adhesively bonded joints.

- The problem of quantifying the effects of uncertainty in the analysis of the mechanical behaviour of adhesive joints has been addressed in various forms. We identified three categories of approaches to facilitate the navigation throughout the existing literature:
  1. statistical modelling (primarily, data-driven)
  2. structural reliability
  3. stochastic structural mechanics (primarily, physics-based).

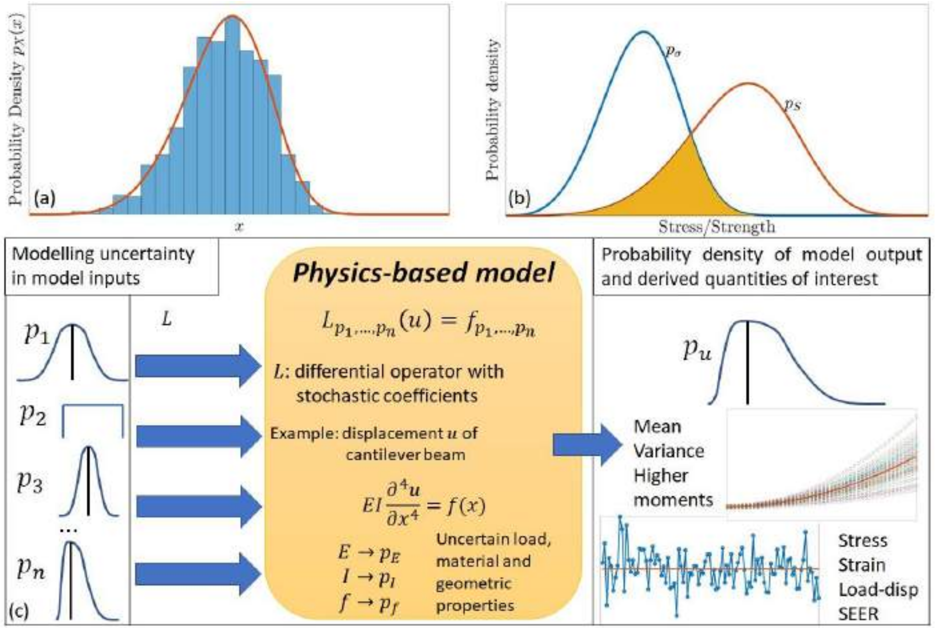

Conclusions

Modelling approach	Material input data	Results/application		Advantages	Limitations
		CI-CP-FF*	S-F-D**		
Classical Analytical Methods	- Elastic or elastic/plastic properties - Critical peel and shear stress values	CI	S+F	- Simple and fast calculations - Estimation of the effect of the macro-scale geometry - Account for material non-linearity (only some models)	- No through-the-thickness stress distribution - Neglects the effects of local corner geometry
Process Zone Methods	- Materials' constitutive laws. - Adhesive/interface strength - Adhesive/interface S-N curve (fatigue) - Critical length	CI or CP	S+F	- Simple application through FE analysis - No mesh convergence issues - Valid also for non-LE behaviour	- Non-trivial definition of the critical length - No damage evolution prediction when conceived for CI
LEFM	- Elastic properties - Critical ERR/SIF - Paris-like law (fatigue)	CP+FF	S+F+D	- Simple and fast calculations - Simple evaluation of the structural load bearing capability in the presence of detected damage - Once coupled with a crack initiation criterion, allows the development of a comprehensive predictive framework	- Applicable for LE behaviour only, with small process zones - Requires the calibration of the fracture parameters for a specific adhesive thickness
VCCT	- Elastic properties - Critical ERR/SIF - Paris-like law (fatigue)	CP+FF	S+F+D	- It does not require too fine meshes - Same advantages as LEFM	- Same as LEFM

* CI = Crack Initiation, CP = Crack Propagation, FF = Final Failure

** S = Static, F = Fatigue, D = Dynamic loading

Conclusions

CertBond
COST Action CA18120

Stress Singularity Approach	- Elastic properties - Critical GSIF or GSIF-life curves	CI	S+F	- Accounts for corner stress singularity and, thus, the effect of local corner geometry and adhesive thickness	- Different critical GSIFs for different corner geometry - Complex stress fields calculation - Limited to linear elastic behaviour
Finite Fracture Mechanics	- Elastic properties - Interface strength and fracture toughness	CI	S	- It predicts the influence of the global and corner local geometry, adhesive thickness and elastic properties - Useful in a preliminary design phase and for comparing different solutions. - It requires LE analyses only, though with significant local mesh refinements	- LE behaviour only - The input interface strength is of non-trivial characterisation - Labour intensive, mainly for complex components/geometries
CZM	- Materials' constitutive laws - Mode I and II cohesive laws - Mode I and II Paris-like laws	CI+CP+FF	S+F+D	- Applicable in case of non-LE behaviour and in case of large process zone - Available in most commercial FE codes, at least for static loadings	- Challenging identification of the cohesive laws - Dependence on the cohesive law type - Mesh dependence issues - Computationally expensive
Statistical modelling	Parameters of probability distribution, e.g. for Weibull model: α, γ and x_0	FF	S+F+D	Flexible to fit different types and moderately large of failure datasets Safety factors for design variables can be derived from the reliability function of the joint	Limited insights about the physics of failure
Structural reliability	Limit state function g(S,L"/„ σ), where S is the capacity of an adhesively bonded joint to resist the external load L/internal stress σ. The g function depends on material and geometric properties which might be deterministic or random with assigned probability distributions	FF	S+F+D	No assumptions about the statistical properties of key variables for failure Safety factors for design variables can be derived from the reliability function of the joint	Trade-off between accuracy and computational resources to evaluate the failure probability integral (e.g. via Monte Carlo simulations)
Stochastic structural mechanics	Varying with specific models. All or part of material and geometric properties (bulk and interface) are modelled as random variables with assigned probability distributions	CP, FF	S+F+D	Detailed insights into failure mechanisms Potentially high predictive power	Substantial modelling expertise, computational resources, model calibration and validation to secure reliability of the predictions

* CI = Crack Initiation, CP = Crack Propagation, FF = Final Failure

** S = Static, F = Fatigue, D = Dynamic loading

Acknowledgment

CertBond
COST Action CA18120

This STSM was developed under the COST Action CA18120 (CERTBOND) and supported by COST (European Cooperation in Science and Technology).

EUROPEAN COOPERATION IN SCIENCE & TECHNOLOGY

Funded by the Horizon 2020 Framework Programme of the European Union

CertBond
COST Action CA18120

Thank You!

www.certbond.eu

EUROPEAN COOPERATION IN SCIENCE & TECHNOLOGY

Funded by the Horizon 2020 Framework Programme of the European Union

CertBond
COST Action CA18120

https://certbond.eu/

Funded by the Horizon 2020
Framework Programme of the
European Union

EUROPEAN COOPERATION
IN SCIENCE & TECHNOLOGY